



UNIVERSITAT_{DE}
BARCELONA

Microbial Biochemistry of Emerging Contaminants and Anthropogenic Organic Matter in the Atlantic and Southern Oceans

Jon Iriarte Martinez



Aquesta tesi doctoral està subjecta a la llicència **Reconeixement- NoComercial – Compartir Igual 4.0. Espanya de Creative Commons**.

Esta tesis doctoral está sujeta a la licencia **Reconocimiento - NoComercial – Compartir Igual 4.0. España de Creative Commons**.

This doctoral thesis is licensed under the **Creative Commons Attribution-NonCommercial-ShareAlike 4.0. Spain License**.

MICROBIAL BIOGEOCHEMISTRY OF EMERGING CONTAMINANTS AND ANTHROPOGENIC ORGANIC MATTER IN THE ATLANTIC AND SOUTHERN OCEANS

Jon Iriarte Martinez



Programa de doctorat:
Química Analítica i Medi Ambient

Microbial Biogeochemistry of Emerging Contaminants and Anthropogenic Organic Matter in the Atlantic and Southern Oceans

Biogeoquímica Microbiana dels Contaminants Emergents i la Matèria Orgànica Antropogènica en els Oceans Atlàntic i Austral

Memòria presentada per optar al grau de Doctor per la Universitat de
Barcelona

Jon Iriarte Martinez

Co-Directora

Dra. Maria Vila-Costa

Investigadora científica
Institut de Diagnòstic
Ambiental i Estudis de
l'Aigua-CSIC

Co-Director

Dr. Jordi Dachs

Professor d'investigació
Institut de Diagnòstic
Ambiental i Estudis de
l'Aigua-CSIC

Tutora

Dra. Anna Rigol

Professora titular
Universitat de Barcelona

Barcelona, febrer del 2025



UNIVERSITAT DE
BARCELONA



CSIC
CONSEJO SUPERIOR DE INVESTIGACIONES CIENTÍFICAS

idæ^a



“Prometemos una vida de derroche y despilfarro, que en el fondo constituye una cuenta regresiva contra la naturaleza y contra la humanidad como futuro. [...] huimos de nuestra biología que defiende la vida por la vida misma, como causa superior, y la suplantamos por el consumismo funcional a la acumulación.”

*José “Pepe” Mújica,
expresidente de la República Oriental del Uruguay
discurso en la 68° Asamblea General de Naciones Unidas*

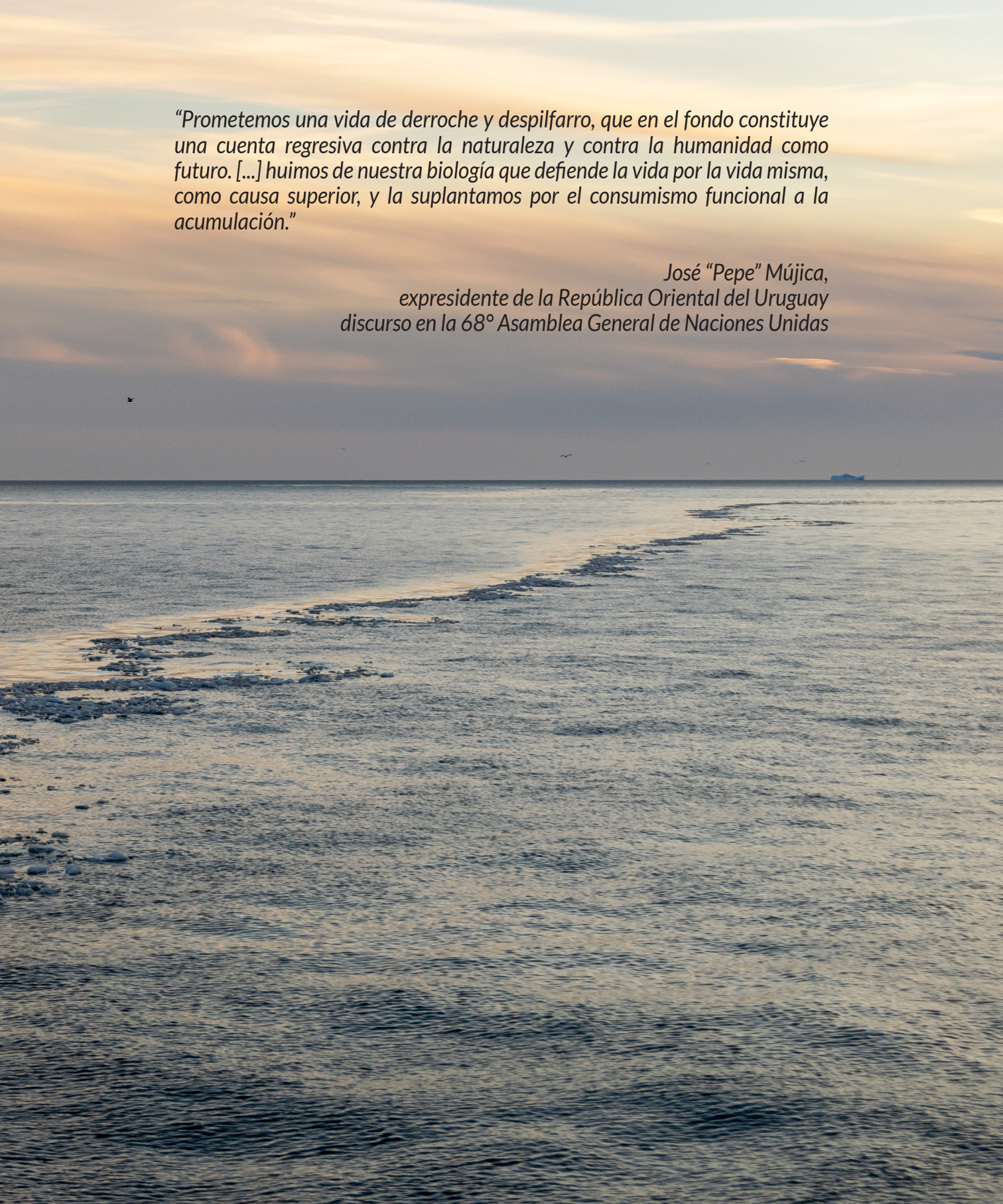


TABLE OF CONTENTS

List of abbreviations and acronyms	1
Abstract/Resum/Laburpena.....	3/6/9
Thesis structure.....	13
Chapter 1. General Introduction.....	16
1.1 Impact of human activities on the Earth system	18
1.2 Anthropogenic chemical pollution	21
1.2.1 Organic contaminants: properties and regulation	24
1.2.2 Organic contaminants selected for this thesis	32
1.3 Organic contaminants in the global ocean.....	45
1.3.1 Sources and transport	47
1.3.2 Fate and sinks	51
1.4 Marine microbial communities	52
1.4.1 Role of marine microbes in contaminant fate.....	55
1.4.2 Potential impact of ADOC on marine microbes	62
1.5 References	65
Chapter 2. Objectives	78
Chapter 3. Brief Overview of the Methodological Approaches	84
3.1 Sampling	86
3.1.1 Study area	86
3.1.2 Contamination control.....	88
3.1.3 Sampling methodologies.....	89
3.2 Sample treatment and analysis.....	91
3.2.1 Analytical chemistry methodologies	91
3.2.2 Molecular biology methodologies.....	94
3.2.3 Bioinformatic tools and software	96
3.3 References	99

Chapter 4. Biogeochemical Processes of PAHs and PFAAs in Maritime Antarctica	102
4.1 Why Antarctica matters for environmental chemistry	104
4.2 References	107
4.3 Publication I: Snow-Dependent Biogeochemical Cycling of Polycyclic Aromatic Hydrocarbons at Coastal Antarctica	110
4.4 Publication II: Inputs, Amplification and Sinks of Perfluoroalkyl Substances at Coastal Antarctica	160
 Chapter 5. Assessment of OPE Biodegradation Across the Atlantic and Southern Oceans.....	 210
5.1 Publication III: Bacterial Production Modulates the Persistence of Organophosphate Ester Flame Retardants and Plasticizers in the Ocean	212
 Chapter 6. Occurrence of Aromatic Hydrocarbon-degrading Genes in the Temperate and Tropical Ocean	 264
6.1 Publication IV: Entanglement of Hydrocarbon-Degrading Bacteria and Polycyclic Aromatic Hydrocarbons in the Ocean.....	268
 Chapter 7. General Discussion	 320
7.1 Main discussion	322
7.1.1 Advancing knowledge on marine pollution	322
7.1.2 Integrating disciplines to explore microbial biogeochemistry.....	325
7.1.3 Methodological approaches: A comparative analysis of benefits and limitations	329
7.2 Unresolved questions and future research needs.....	335
7.3 Perspectives for future research	338
7.4 References	343
 Chapter 8. Conclusions.....	 350
 Acknowledgements.....	 356

LIST OF ABBREVIATIONS AND ACRONYMS

ADOC	Anthropogenic Dissolved Organic Carbon
AH	Aromatic Hydrocarbon
ARHD	Aromatic Ring Hydroxylating Dioxygenase
ASV	Amplicon Sequence Variant
BA	Bacterial Abundance
BCF	Bioconcentration Factor
BP	Bacterial Production
CAS	Chemical Abstracts Service
C_B	Concentration in biota
CECs	Contaminants of Emerging Concern
CFCs	Chlorofluorocarbons
CHI	Cumulative Human Impact
C_O	Concentration in octanol
C_P	Concentration in particulate phase
C_{Plankton}	Concentration in plankton
CSIC	Consejo Superior de Investigaciones Científicas (Spanish National Research Council)
CTD	Conductivity, Temperature and Depth
C_W	Concentration in water
DCM	Deep Chlorophyll Maximum
DDT	Dichlorodiphenyltrichloroethane
DOC	Dissolved Organic Carbon
DOM	Dissolved Organic Matter
ECHA	European Chemicals Agency
EPA	Environmental Protection Agency
EU	European Union
FL	Free Living
GC	Gas Chromatography
GTDB	Genome Taxonomy Database
H	Henry's law constant
H'	Dimensionless Henry's law constant
HCB	Hydrocarbonoclastic Bacteria
HCHs	Hexachlorocyclohexanes
HMM	Hidden Markov Model
HMW	High Molecular Weight
HNA	High Nucleic Acid
IDAEA	Institute of Environmental Assessment and Water Research
IPCC	Intergovernmental Panel on Climate Change
K_{AW}	Air-water partition coefficient
K_{OA}	Octanol-air partition coefficient
K_{OW}	Octanol-water partition coefficient
LC	Liquid Chromatography
LC₅₀	Lethal Concentration 50
LIR	Leucine Incorporation Rate
LMW	Low Molecular Weight
LNA	Low Nucleic Acid
LOEC	Lowest Observed Effects Concentration

LRAT	Long-range Atmospheric Transport
MAG	Metagenome-assembled Genome
MS	Mass Spectrometer
MW	Molecular Weight
NADS	Nucleic Acid Double Staining
NOEC	No Observed Effects Concentration
OCPs	Organochlorine pesticides
OPEs	Organophosphate Esters
PA	Particle Attached
PAHs	Polycyclic Aromatic Hydrocarbons
PBDEs	Polybrominated diphenyl ethers
PBT	Persistent, Bioaccumulative, and Toxic
PCBs	Polychlorinated Biphenyls
PCDDs	Polychlorinated dibenzo-p-dioxins
PCDFs	Polychlorinated dibenzofurans
PDE	Phosphodiesterase
PI	Propidium Iodide
PME	Phosphomonoesterase
PFAS	Per- and polyfluoroalkyl substances
PFAAs	Perfluoroalkyl acids
PFCAs	Perfluoroalkyl carboxylic acids
PFSAs	Perfluoroalkyl sulfonic acids
PFOA	Perfluorooctanoic acid
PFOS	Perfluorooctane sulfonic acid
POPs	Persistent Organic Pollutants
PTE	Phosphotriesterase
R	Universal gas constant
RDA	Redundancy Analysis
REACH	Registration, Evaluation, Authorization, and restriction of Chemicals
SALCs	Semivolatile Aromatic-like Compounds
SML	Surface Microlayer
SPE	Solid Phase Extraction
SPP	Science-Policy Panel
SSA	Sea Spray Aerosol
SSL	Sub-surface layer
S_w	Water solubility
T	Temperature
TCA	Trichloroacetic acid
TPM	Transcripts per Million
UNEA	United Nations Environment Assembly
UNEP	United Nations Environment Programme
UPLC	Ultra Performance Liquid Chromatography
V_p	Vapor pressure

ABSTRACT

Since the Industrial Revolution, the intensity of human activities has increased exponentially, particularly during the Great Acceleration, which began approximately in 1950. This unprecedented growth has led to observable perturbations in the Earth system, which have been grouped and quantified in nine planetary boundaries that delimit “a safe operating space for humanity”. The introduction of novel entities – contaminants released due to anthropogenic activities– into the environment is one of the most recently quantified boundaries, though still with significant uncertainties. Anthropogenic organic chemicals are arguably the most concerning among the novel entities. Due to their particular physicochemical properties, these compounds may exhibit persistence, bioaccumulation, potential for long-range transport, and toxicity; properties that define persistent organic pollutants (POPs) and are commonly used as criteria for their risk assessment and regulation. Their ubiquitous presence in the environment poses a threat to the well-being of all organisms, a threat that has long been insufficiently acknowledged.

The global ocean is often the main sink of these contaminants. As a vital component of the Earth system, it sustains life through numerous processes, which may be compromised by the presence of anthropogenic pollutants. In the marine environment, classic pollutants such as polychlorinated biphenyls (PCBs) or polycyclic aromatic hydrocarbons (PAHs), have been intensively studied, whereas the same cannot be said for emerging contaminants, such as the organophosphate esters (OPEs) or per- and polyfluoroalkyl substances (PFAS). Nevertheless, several knowledge gaps remain for both cases, particularly regarding their persistence and fate in the often poorly addressed remote regions, where more field measurements are urgently needed.

The interaction between marine microorganisms and organic contaminants under oceanic conditions has been particularly overlooked. Marine bacteria play a key role in carbon and nutrient cycling, sustaining marine biogeochemical cycles and the food web. Their high metabolic activity makes them important drivers of the fate of organic contaminants composing the anthropogenic dissolved organic carbon (ADOC), as demonstrated in highly polluted sites like oil spills. However, their role in processing background contaminant concentrations in the open ocean remains poorly studied. More field-based research is needed to understand the implications of this two-way interaction, where microbes might influence the fate of organic contaminants, while anthropogenic contaminants may shape microbial communities. Such insights are essential for proper risk assessment of organic contaminants in the global ocean.

The central working hypothesis of this thesis is that background concentrations of organic contaminants, which are ubiquitously present in the oceans, significantly affect the composition and functioning of marine microbial communities, while the microbial loop modulates ADOC pool concentrations through biodegradation. To explore this, the general objective was to investigate the microbial biogeochemistry of key families of organic contaminants relevant to the global ocean, such as PAHs, OPEs, and PFAS, ensuring that the obtained results were as representative as possible of real oceanic conditions. A particular focus was placed on remote areas, such as the coastal Antarctica and the open ocean.

To achieve this, data was obtained from field measurements and field experiments, combining the direct measurement of contaminant concentrations with metagenomic data of microbial communities and, when feasible, data for other environmentally relevant physicochemical and biological parameters. More specifically, two time series analyses were performed using field data on environmental concentrations of PAHs and PFAS over three austral summers (from 2014 to 2018) on two Antarctic Peninsula islands, Livingston and Deception. Additionally, data on microbial community composition by 16S rRNA gene amplicon sequencing was analyzed, and multivariate approaches and other statistical tests were applied to assess the potential interactions between environmental concentrations of contaminants and microbial community composition. Furthermore, a similar approach was applied in another study using already published data on PAH concentrations and 16S amplicon sequencing from the Malaspina circumnavigation expedition, which covered the tropical and temperate oceans. This study also included the identification of an aromatic hydrocarbon-degrading gene in metagenomic datasets and its use as a biomarker for PAH biodegradation at background environmental levels, employing a bioinformatics approach we developed for this purpose. Lastly, the potential for OPE biodegradation in the Atlantic and Southern Oceans was addressed through a study in which six field experiments were conducted during two oceanographic campaigns carried out during this thesis. OPE concentrations were measured, alongside bacterial production rates and other parameters to gain insights into the role of biodegradation as an oceanic sink for OPEs in the surface ocean.

The results of this thesis provide the largest database of concentrations of PAHs and PFAS in coastal Antarctica, showing a large temporal and spatial variability that was partially attributed to inputs from snowmelt and geographical features of the Livingston and Deception Islands. The assessment of PAH biogeochemical features revealed increased biodegradation following large snowmelt inputs, suggesting that bacterial activity – and consequently, the extent of PAH biodegradation –, depended on snowmelt input. Regarding PFAS, a preferential decrease of sulfonated compounds was observed, suggesting a potential role of microbial-mediated desulfurization as a PFAS sink. The concurrent assessment of contaminant concentrations and microbial communities revealed significant correlations between amplicon sequence variants (ASVs) and chemical compounds for PAHs and PFAS, further highlighting the potential mutual interaction even at background concentrations. However, results also indicated that other environmental factors play an important role, evidencing the complexity of biogeochemical controls under low concentrations of contaminants.

The identification of the aromatic ring hydroxylating dioxygenase gene in the Genome Taxonomy Database (GTDB) and the Malaspina Vertical Profiles Gene Database showed that the potential for aromatic hydrocarbon degradation is distributed across multiple branches of the bacterial and archaeal phylogenomic trees and is present throughout the temperate and tropical ocean. Results showed a negative correlation between gene abundance and the concentration of the low molecular weight fraction of the PAHs, as well as a higher gene abundance in the particle-attached fraction associated with lower PAH concentrations in plankton. Furthermore, background concentration levels of PAHs were found to be significant factors in explaining the variation in the bacterial community composition, together with other previously described environmental factors such as temperature, nutrient concentrations, and planktonic biomass.

Field experiments on OPE exposure revealed a significant decrease related to biodegradation for two highly hydrophobic OPEs with aromatic moieties in the Atlantic Ocean after 48 hours. Moreover, the increase in protein production activity of heterotrophic bacteria significantly correlated with greater OPE depletion, highlighting the role of a biological process behind this observation. Overall, the results of this study represent the first report of OPE biodegradation field experiments conducted in the open ocean, where naturally occurring microbial communities were challenged to environmentally relevant concentrations of OPEs. These findings pave the way for future research on the fate and microbial biogeochemistry of these compounds in the surface ocean under real environmental conditions.

Overall, this thesis evidences that the concurrent characterization of contaminants and microbial communities through field-based measurements is a powerful approach for obtaining results that accurately represent real environmental conditions. Our findings suggest that environmental levels of organic contaminants, although not having the same driving force as other environmental factors, should still be considered as a relevant factor significantly influencing marine microbial communities. Similarly, microbial-mediated degradation was found to be a potential oceanic sink for emerging contaminants. These results raise new questions regarding the extent of biodegradation and the potential effects of organic contaminants on marine biogeochemical cycles, which future research must address. Understanding the complex biogeochemistry of these contaminants is crucial for conducting accurate risk assessments, particularly in the current and future context of increasing production and release of anthropogenic compounds, and the intensification of other environmental stressors derived from climate change.

RESUM

Des de la Revolució Industrial, la intensitat de les activitats humanes ha augmentat exponencialment, particularment durant la Gran Acceleració, que va començar aproximadament el 1950. Aquest creixement sense precedents ha portat a pertorbacions observables en el sistema terrestre, que s'han agrupat i quantificat en nou límits planetaris que delimiten “un espai operatiu segur per a la humanitat”. La introducció de noves entitats –contaminants alliberats a causa d'activitats antropogèniques– al medi ambient és un dels límits quantificats més recentment, encara que amb incerteses significatives. Els productes químics orgànics antropogènics són sens dubte els més preocupants entre les noves entitats. A causa de les seves propietats fisicoquímiques particulars, aquests compostos poden presentar persistència, bioacumulació, potencial de transport de llarga distància i toxicitat; propietats que defineixen als contaminants orgànics persistents (COPs) i s'utilitzen comunament com a criteris per a la seva avaluació i regulació de riscos. La seva presència omnipresent en el medi ambient suposa una amenaça per al benestar de tots els organismes, una amenaça que durant molt de temps ha estat insuficientment reconeguda.

L'oceà global és sovint el principal embornal d'aquests contaminants. Com a component vital del sistema terrestre, sosté la vida a través de nombrosos processos, que poden veure's compromesos per la presència de contaminants antropogènics. En el medi marí s'han estudiat intensament contaminants clàssics com els bifenils policlorats (PCBs) o els hidrocarburs aromàtics policíclics (PAHs), mentre que no es pot dir el mateix dels contaminants emergents, com els èsters organofosforats (OPEs) o les substàncies per- i polifluoroalquilades (PFAS). No obstant això, queden diverses llacunes de coneixement per a tots dos casos, en particular pel que fa a la seva persistència i el seu destí en les regions remotes, sovint mal abordades, on es necessiten urgentment més mesures de camp.

La interacció entre els microorganismes marins i els contaminants orgànics en condicions oceàniques ha estat especialment ignorada. Els bacteris marins tenen un paper clau en el cicle del carboni i els nutrients, sostenint els cicles biogeoquímics marins i la xarxa alimentària. La seva alta activitat metabòlica els converteix en importants impulsors del destí dels contaminants orgànics que componen el carboni orgànic dissolt antropogènic (ADOC), com es demostra en llocs altament contaminats com els vessaments de petroli. No obstant això, el seu paper en el processament de les concentracions de contaminants de fons a l'oceà obert segueix sent poc estudiat. Es necessita més investigació basada en el camp per comprendre les implicacions d'aquesta interacció bidireccional, on els microbis poden influir en el destí dels contaminants orgànics, mentre que els contaminants antropogènics poden donar forma a les comunitats microbianes. Aquests coneixements són essencials per a una avaluació adequada del risc dels contaminants orgànics en l'oceà global.

La hipòtesi de treball central d'aquesta tesi és que les concentracions de fons de contaminants orgànics, els quals es troben de manera omnipresent en els oceans, afecten significativament la composició i el funcionament de les comunitats microbianes marines, mentre que el bucle microbià modula les concentracions dels compostos que componen el ADOC a través de la biodegradació. Per explorar-ho, l'objectiu general era investigar la biogeoquímica microbiana de famílies clau de contaminants orgànics rellevants per a l'oceà global, com els PAHs,

OPEs i PFAS, assegurant que els resultats obtinguts fossin el més representatius possible de les condicions oceàniques reals. Es va posar un focus particular en àrees remotes, com l'Antàrtida costanera i l'oceà obert.

Per aconseguir-ho, es van obtenir dades a partir de mesures de camp i experiments de camp, combinant la mesura directa de concentracions de contaminants amb dades metagenòmiques de comunitats microbianes i, quan fos factible, dades per a altres paràmetres fisicoquímics i biològics rellevants ambientalment. Més específicament, es van realitzar dues anàlisis de sèries temporals utilitzant dades de camp sobre les concentracions ambientals de PAH i PFAS durant tres estius australs (de 2014 a 2018) en dues illes de la Península Antàrtica, Livingston i Deception. A més, es van analitzar dades sobre la composició de la comunitat microbiana per seqüenciació d'amplicon gen 16S rRNA, i es van aplicar enfocaments multivariants i altres proves estadístiques per avaluar les interaccions potencials entre les concentracions ambientals de contaminants i la composició de la comunitat microbiana. A més, es va aplicar un enfocament similar en un altre estudi utilitzant dades ja publicades sobre les concentracions de PAHs i la seqüenciació d'amplicon 16S de l'expedició de circumnavegació de Malaspina, que cobria els oceans tropicals i temperats. Aquest estudi també va incloure la identificació d'un gen de degradació d'hidrocarburs aromàtics en conjunts de dades metagenòmiques i el seu ús com a biomarcador per a la biodegradació de PAHs a nivells ambientals de fons, utilitzant un enfocament bioinformàtic que hem desenvolupat per a aquest propòsit. Finalment, es va abordar el potencial de la biodegradació dels OPE als oceans Atlàntic i Austral mitjançant un estudi en el qual es van realitzar sis experiments de camp durant dues campanyes oceanogràfiques realitzades durant aquesta tesi. Es van mesurar les concentracions d'OPEs, juntament amb les taxes de producció bacteriana i altres paràmetres per obtenir informació sobre el paper de la biodegradació com a embornal oceànic per a les OPEs en l'oceà superficial.

Els resultats d'aquesta tesi proporcionen la base de dades més gran de concentracions de PAHs i PFAS a l'Antàrtida costanera, mostrant una gran variabilitat temporal i espacial que es va atribuir parcialment a les entrades de fosa de neu i característiques geogràfiques de les illes Livingston i Deception. L'avaluació de les característiques biogeoquímiques dels PAHs va revelar un augment de la biodegradació després de grans entrades de fosa de neu, el que suggereix que l'activitat bacteriana - i en conseqüència, l'extensió de la biodegradació dels PAHs -, depenia de l'entrada de fosa de neu. Pel que fa als PFAS, es va observar una disminució preferencial dels compostos sulfonats, suggerint un paper potencial de la desulfuració mediada per microbis com a embornal de PFAS. L'avaluació concurrent de concentracions de contaminants i comunitats microbianes va revelar correlacions significatives entre les variants de seqüència d'amplicon (ASVs) i els compostos químics per als PAHs i PFAS, destacant encara més la interacció mútua potencial fins i tot en concentracions de fons. No obstant això, els resultats també van indicar que altres factors ambientals tenen un paper important, evidenciant la complexitat dels controls biogeoquímics sota baixes concentracions de contaminants.

La identificació del gen dioxigenasa hidroxilant de l'anell aromàtic a la base de dades *Genome Taxonomy Database* (GTDB) i la base de dades de gens de Perfils Verticals de Malaspina va mostrar que el potencial de degradació d'hidrocarburs aromàtics es distribueix a través de

múltiples branques dels arbres filogenòmics bacterians i arqueobacterians i està present a tot l'oceà temperat i tropical. Els resultats van mostrar una correlació negativa entre l'abundància del gen i la concentració de la fracció de baix pes molecular de les PAHs, així com una major abundància del gen en la fracció particulada associada amb concentracions més baixes de PAH en el plàncton. A més, es va trobar que els nivells de concentració de fons dels PAHs eren factors significatius per explicar la variació en la composició de la comunitat bacteriana, juntament amb altres factors ambientals descrits anteriorment com la temperatura, les concentracions de nutrients i la biomassa planctònica.

Els experiments de camp sobre l'exposició a OPEs van revelar una disminució significativa relacionada amb la biodegradació per a dues OPEs altament hidròfobes i amb substituents aromàtics a l'Oceà Atlàntic després de 48 hores. A més, l'augment de l'activitat de producció de proteïnes de bacteris heteròtrofs es va correlacionar significativament amb un major esgotament dels OPEs, destacant el paper d'un procés biològic darrere d'aquesta observació. En general, els resultats d'aquest estudi representen el primer informe d'experiments de camp de biodegradació d'OPEs realitzats en l'oceà obert, on les comunitats microbianes d'origen natural van ser desafiades a concentracions ambientalment rellevants d'aquets compostos. Aquests resultats aplanen el camí per a futures investigacions sobre el destí i la biogeoquímica microbiana d'aquets compostos en l'oceà superficial sota condicions ambientals reals.

En general, aquesta tesi evidencia que la caracterització concurrent de contaminants i comunitats microbianes a través de mesures basades en el camp és un enfocament potent per obtenir resultats que representen amb precisió condicions ambientals reals. Els nostres resultats suggereixen que els nivells ambientals de contaminants orgànics, encara que no tinguin la mateixa força impulsora que altres factors ambientals, han de considerar-se com un factor rellevant que influeix significativament en les comunitats microbianes marines. De la mateixa manera, es va trobar que la degradació mediada per microbis era un possible embornal oceànic per als contaminants emergents. Aquests resultats plantegen noves preguntes sobre l'abast de la biodegradació i els possibles efectes dels contaminants orgànics en els cicles biogeoquímics marins, que la recerca futura ha d'abordar. La comprensió de la biogeoquímica complexa d'aquests contaminants és crucial per dur a terme avaluacions de risc precises, particularment en el context actual i futur d'augment de la producció i alliberament de compostos antropogènics, i la intensificació d'altres factors d'estrès ambiental derivats del canvi climàtic.

LABURPENA

Industria Iraultzaz geroztik, giza jardueren intentsitatea esponentzialki handitu da, batez ere Azelerazio Handian, gutxi gorabehera 1950ean hasi zena. Aurrekaririk gabeko hazkunde horrek perturbazio behagarriak eragin ditu Lur sisteman, bederatzi muga planetariotan bildu eta kuantifikatu egin direnak «gizateriarentzako operazio-espazio seguru bat» ezarriz. Entitate berrien –jarduera antropogenikoen ondorioz askatutako kutsatzaileak– sarrera ingurumenara berriki kuantifikatutako mugetako bat da, oraindik ziurgabetasun handiak dituen bere inguruan. Produktu kimiko organiko antropogenikoak dira, zalantzarik gabe, entitate berrien artean kezkarrienak. Bere propietate fisiko-kimiko berezien ondorioz, konposatu horiek iraunkortasuna, biometaketa, irismen luzeko garraiorako ahalmena eta toxikotasuna erakuts dezakete. Propietate horiek poluitzaile organiko iraunkorrak (POP) definitzen dituzte, eta, eskuarki, arriskuak ebaluatzeko eta erregulazio irizpide gisa erabiltzen dira. Propietate horietaz gain, kutsatzaile hauek ingurumenean nonahiko presentzia izatea arrisku bat da organismo guztien ongizaterako, eta arrisku hori aspaldi ez da behar bezala aitortu.

Ozeano globala izan ohi da kutsatzaile horien harraska nagusia. Lur sistemaren ezinbesteko osagai honek bizitzari eusten dio prozesu ugariaren bidez, kutsatzaile antropogenikoen presentziak kolokan jar ditzakeenak. Itsas ingurunean, kutsatzaile klasikoak, hala nola poliklorobifeniloak (PCB) edo hidrokarburo aromatiko poliziklikoak (PAH), modu intentsiboan aztertu dira; aldiz, ezin da gauza bera esan kutsatzaile emergentei dagokienez, hala nola organofosfatoen esterrak (OPEak) edo per- eta polifluoroalkiloak (PFAS). Hala ere, bi kasuetarako hainbat ezagutza-hutsune geratzen dira, batez ere beren iraunkortasunari eta patuari dagokienez gutxi ikertutako urruneko eskualdeetan, non landa-neurketa gehiago premiazkoak diren.

Baldintza ozeanikoetan itsas mikroorganismoen eta kutsatzaile organikoen arteko elkarrekintza bereziki alde batera utzi da. Itsas bakterioek funtsezko zeregina dute karbonoaren eta mantenugaien ziklaketan, itsas ziklo biogeokimikoei eta elikadura sareari eusten baitiete. Jarduera metaboliko handia dutenez, karbono organiko disolbatu antropogenikoa (ADOC) konposatzen duten poluitzaile organikoen patuaren eragile garrantzitsuak dira, oso poluituta dauden lekuetan frogatzen den bezala, petrolio-isuriak kasu. Hala ere, ozeano irekian poluitzaileen hondoko kontzentrazioen prozesamenduan duten eginkizuna gutxi aztertuta dago oraindik. Alorrean oinarritutako ikerketa gehiago behar dira bi norabideko elkarrekintza horren ondorioak ulertzeko, non mikrobioek kutsatzaile organikoen patuan eragin lezaketen, kutsatzaile antropogenikoek mikrobio-komunitateak molda ditzaketen bitartean. Ezagutza horiek funtsezkoak dira ozeano globaleko kutsatzaile organikoen arriskuak behar bezala ebaluatzeko.

Tesi honen lan-hipotesi nagusia da kutsatzaile organikoen hondo-kontzentrazioek, ozeanoetan nonahi daudenek, nabarmen eragiten dutela itsasoko mikrobio-komunitateen osaera eta funtzionamenduan, eta mikrobio-begiztak, berriz, ADOC poolaren kontzentrazioak modulatzeko dituela biodegradazioaren bidez. Hau esploratzeko, helburu orokorra ozeano globalerako garrantzitsuak diren kutsatzaile organikoen funtsezko familien biogeokimika mikrobiarra ikertzea izan zen, hala nola PAHak, OPEak, eta PFASak, lortutako emaitzak benetako baldintza ozeanikoen ahalik eta adierazgarrienak zirela ziurtatuz. Arreta berezia jarri zen urruneko eremuetan, hala nola kostaldeko Antartikan eta ozeano irekian.

Hori lortzeko, datuak lortu ziren landa-neurketa eta landa-esperimentuen bitartez, kutsatzaileen kontzentrazioen zuzeneko neurketa mikrobio-komunitateen datu metagenomikoekin eta, bideragarria zenean, ingurumenerako garrantzitsuak diren beste parametro fisiko-kimiko eta biologiko batzuetarako datuekin konbinatuz. Zehatzago esanda, denboran-zeharreko bi analisi egin ziren, Antartikako penintsulako bi uhartetan, Livingston eta Deception, PAHen eta PFASen hiru austral udatan (2014tik 2018ra) izandako ingurumen-kontzentrazioei buruzko landa-datuak erabiliz. Horrez gain, 16S rRNA genearen aplikoiaren sekuentziazioaren bidezko mikrobio-komunitatearen konposizioari buruzko datuak aztertu ziren, eta aldagai anitzeko ikuspegiak eta beste proba estatistiko batzuk aplikatu ziren, kutsatzaileen ingurumen-kontzentrazioen eta mikrobio-komunitatearen konposizioaren arteko elkarrekintza potentzialak ebaluatzeko. Gainera, antzeko ikuspegiak aplikatu zen beste ikerketa batean, Malaspina zirkumnabigazio espedizioaren PAH kontzentrazioei eta 16S aplikoi sekuentziazioari buruz jada argitaratutako datuak erabiliz, ozeano tropikalak eta epelak aztertu zituenak. Ikerketa horretan, datu multzo metagenomikoetan hidrokarburo aromatikoak degradatzen dituen gene baten identifikazioa egin zen, eta biomarkatzaile gisa erabili zen hondoko ingurumen-mailetan ematen den PAHen biodegradazioarako, horretarako garatu genuen ikuspegi bioinformatiko bat erabiliz. Azkenik, Ozeano Atlantikoan eta Hegoaldeko Ozeanoan OPEak biodegradatzeko potentziala aztertu zen, bi kanpaina ozeanografikotan egindako sei landa-esperimentuen bidez. OPE kontzentrazioak neurtu ziren, bakterioen ekoizpen-tasekin eta beste parametro batzuekin batera, biodegradazioak gainazaleko ozeanoko OPEetarako harraska ozeaniko gisa duen paperari buruzko ezagutzak lortzeko.

Tesi honen emaitzek kostaldeko Antartikako PAHen eta PFASen kontzentrazioen datu-base handiena ematen dute. Datu hauek denbora- eta espazio-aldakortasun handia erakutsi zuten, elur-urteen sarrerei eta Livingston eta Deception uharteetako ezaugarri geografikoei partzialki egotzi zitzaizena. PAHen ezaugarri biogeokimikoen ebaluazioak elur-urte sarrera handien ondorengo biodegradazioa handitu zela agerian utzi zuen, bakterioen jardura –eta, ondorioz, PAHen biodegradazioaren hedadura–, elur-urte sarreraren arabera zela iradokiz. PFASari dagokionez, konposatu sulfonatuen lehentasunezko jaitiera ikusi zen, PFASen hustuleku gisa mikrobio-bidezko desulfurazioaren rol potentziala iradokiz. Poluitzaile-kontzentrazioen eta mikrobio-komunitateen ebaluazio konkurrenteak korrelazio esanguratsuak aurkitu zituen aplikoi-sekuentziako aldaeren (ASV) eta PAHetarako eta PFASetarako konposatu kimikoen artean, eta are gehiago nabarmendu zuen elkarrekiko interakzio potentziala, baita hondo-kontzentrazioetan ere. Hala ere, emaitzek beste ingurumen-faktore batzuek ere zeregin garrantzitsua dutela adierazi zuten, poluitzaile-kontzentrazio baxuen gain eragiten duten kontrol biogeokimikoen konplexutasuna agerian utziz.

Genomaren Taxonomiaren Datu-Basean (GTDB) eta Malaspina profil bertikalen gene-datu-basean egindako eraztun aromatikoko dioxigenasa hidroxilatzaile genearen identifikazioek erakutsi zuten hidrokarburo aromatikoak degradatzeko ahalmena zuhaitz filogenomiko bakteriano eta arkeoen adar ugaritan banatzen dela eta ozeano epel eta tropikal osoan dagoela. Emaitzek korrelazio negatiboa erakutsi zuten gene-ugaritasunaren eta PAHen pisu molekular txikiko frakzioaren kontzentrazioaren artean, baita gene-ugaritasun handiagoa ere planktonean PAH kontzentrazio txikiagoekin lotutako partikulari lotutako frakzioan. Gainera, PAHen hondoko

kontzentrazio-mailak bakterio-komunitatearen konposizioaren aldaketa azaltzeko faktore esanguratsuak zirela ikusi zen, aurretik deskribatutako beste ingurumen-faktore batzuekin batera, hala nola tenperatura, mantenugaien kontzentrazioak eta biomasa planktonikoa.

OPEen esposizioari buruzko landa-esperimentuek biodegradazioarekin lotutako beherakada nabarmena azaleratu zuten Ozeano Atlantikoan 48 orduren ondoren ordezkatzailerik aromatikoak dituzten bi OPE oso hidrofoborentzat. Bestalde, bakterio heterotrofoen proteina-ekoizpenaren jardueraren handitzeak korrelazio nabarmena agertu zuen OPEen agortze handiagoarekin, agortze horren atzean prozesu biologiko baten eginkizuna dagoela nabarmenduz. Oro har, ikerketa honek ozeano irekian egindako OPEen biodegradazioaren lehen emaitzak adierazten ditu, non jatorri naturaleko mikrobio-komunitateak ingurumen mailako OPE-kontzentrazio esanguratsupean inkubatu ziren. Aurkikuntza horiek bidea errazten dute etorkizunean konposatu horien patuari eta biogeokimika mikrobiarrari buruzko ikerketak egiteko, benetako ingurumen-baldintza ozeanikoetan.

Oro har, tesi honek agerian uzten du kutsatzaileen eta mikrobio-komunitateen karakterizazio konkurrentea, lekuan oinarritutako neurketen bidez, ikuspegi indartsua dela benetako ingurumen-baldintzak zehaztasunez adierazten dituzten emaitzak lortzeko. Gure aurkikuntzek iradokitzen dute kutsatzaile organikoen ingurumen-mailak, nahiz eta beste ingurumen-faktore batzuen indar eragile bera ez izan, oraindik ere faktore garrantzitsutzat hartu behar direla, itsas mikrobio-komunitateetan eragin nabarmena baitute. Era berean, ikusi zen mikrobio-bidezko degradazioa harraska ozeaniko potentziala zela kutsatzaile emergenteentzat. Emaitza horiek galdera berriak sortzen dituzte biodegradazioaren hedadurari eta kutsatzaile organikoek itsas ziklo biogeokimikoetan izan ditzaketen ondorioei buruz, eta etorkizuneko ikerketek horiei heldu behar diete. Kutsatzaile horien biogeokimika konplexua ulertzea funtsezkoa da arriskuen ebaluazio zehatzak egiteko, batez ere konposatu antropogenikoen ekoizpena eta askapena areagotzen ari den egungo eta etorkizuneko testuinguruari begira, are eta gehiago klima-aldaketatik eratorritako beste ingurumen-faktore estresagarri batzuen intentsifikazioa kontutan hartzen badugu.

THESIS STRUCTURE

The present thesis is structured into 8 chapters. **Chapter 1** provides a general introduction on biogeochemistry of marine pollution, summarizing existing knowledge on the current levels, biogeochemical cycling, and effects and interactions of organic contaminants with marine microbial communities. It starts addressing the global concern of anthropogenic chemical pollution in the Earth system, with a particular focus on organic contaminants in the global ocean. It includes an overview of the properties and current regulations, as well as sources, transport, and fate of Persistent Organic Pollutants and Contaminants of Emerging Concern, emphasizing on the selected families of contaminants. Finally, it provides various background aspects of marine microbial communities and their role in marine biogeochemical cycles, reviews microbial-mediated biodegradation of organic contaminants, and examines the potential influence of these compounds on microbial communities. This chapter highlights the need of field evidences to assess persistence of contaminants in the marine environment, and the lack of studies on the linkages between background concentrations of organic contaminants and marine microbial communities in large oceanic regions such as the open ocean and remote areas such as polar environments.

Chapter 2 presents the main objectives of the thesis.

Chapter 3 contains an overview of the sampling and analysis methodologies employed in this thesis.

The main body of the thesis is presented in **Chapters 4, 5** and **6**, which compile the obtained results and their discussion. It is structured as scientific publications completed within the framework of the doctoral thesis. **Chapter 4** examines the biogeochemical processes driving the occurrence of PAHs and PFAS in the coastal environments of two Antarctic islands. **Chapters 5** and **6** are related to the open ocean, where **Chapter 5** focuses on the assessment of OPE biodegradation through field experiments performed in the Atlantic and Southern Oceans, while **Chapter 6** explores the potential for PAH biodegradation in the ocean by analyzing the occurrence of biomarker genes using bioinformatic approaches.

Finally, **Chapter 7** presents a general discussion of all the obtained results, including thoughts on future research perspectives, while **Chapter 8** summarizes the overall conclusions derived from the work conducted during this doctoral thesis. Importantly, at the end of each chapter a list of the bibliographic references cited within that chapter is given.





CHAPTER 1

General Introduction

1.1 Impact of human activities on the Earth system

1.2 Anthropogenic chemical pollution

1.2.1 Organic contaminants: properties and regulation

Physicochemical properties

Regulation

1.2.2 Organic contaminants selected for this thesis

Polycyclic aromatic hydrocarbons

Organophosphate esters: flame retardants and plasticizers

Per- and polyfluoroalkyl substances

1.3 Organic contaminants in the global ocean

1.3.1 Sources and transport

1.3.2 Fate and sinks

1.4 Marine microbial communities

1.4.1 Role of marine microbes in contaminant fate

1.4.2 Potential impact of ADOC on marine microbes

1.5 References

1.1 Impact of human activities on the Earth system

Since its formation as a planet, environmental conditions on Earth have undergone significant fluctuations. To delineate these periods in Earth's history, the geological time scale was created. This representation of time relies on rock records to define the events that demarcate the boundaries between geological eras. The most recent of these geological eras is the Holocene, which began approximately 10,000 years ago and has been recognized as an unusually long period of stable environmental conditions (Petit et al., 1999). During this era of constancy, human civilizations have progressed and flourished (Rockström et al., 2009). This progressive development throughout human history has allowed them to interact and modify the landscape and surrounding environment.

For virtually all of human existence, human activities have been an insignificant force in the dynamics of the physical, chemical, and biological global-scale cycles (Steffen et al., 2004). The complex and self-regulating system formed by the interaction of these cycles is referred to as the Earth system. However, the Industrial Revolution in the late eighteenth century changed the scale of the human imprint on the Earth system. The use of fossil fuels allowed human emancipation and transition from solar energy (understanding solar radiation as the primary source of energy for the processes of living organisms at or near the Earth's surface, including humans for the majority of their existence), to a novel cost-effective energy source with high calorific capacity (Hubbert, 1949). This energy source, along with the advances in technology (industrialization), provided the means for an unprecedented exponential growth in productivity, largely driven by the profit motive inherent in capitalism (Anderson, 2009; Lux, 2003; Nevile, 2016). This dramatic increase of human activities (Figure 1.1), especially during the Great Acceleration since 1950 (after World War II), has altered the magnitude of the human-induced, or anthropogenic, changes, to a level where they now exert measurable global-scale changes on the Earth system (Figure 1.2).

Socio-economic trends

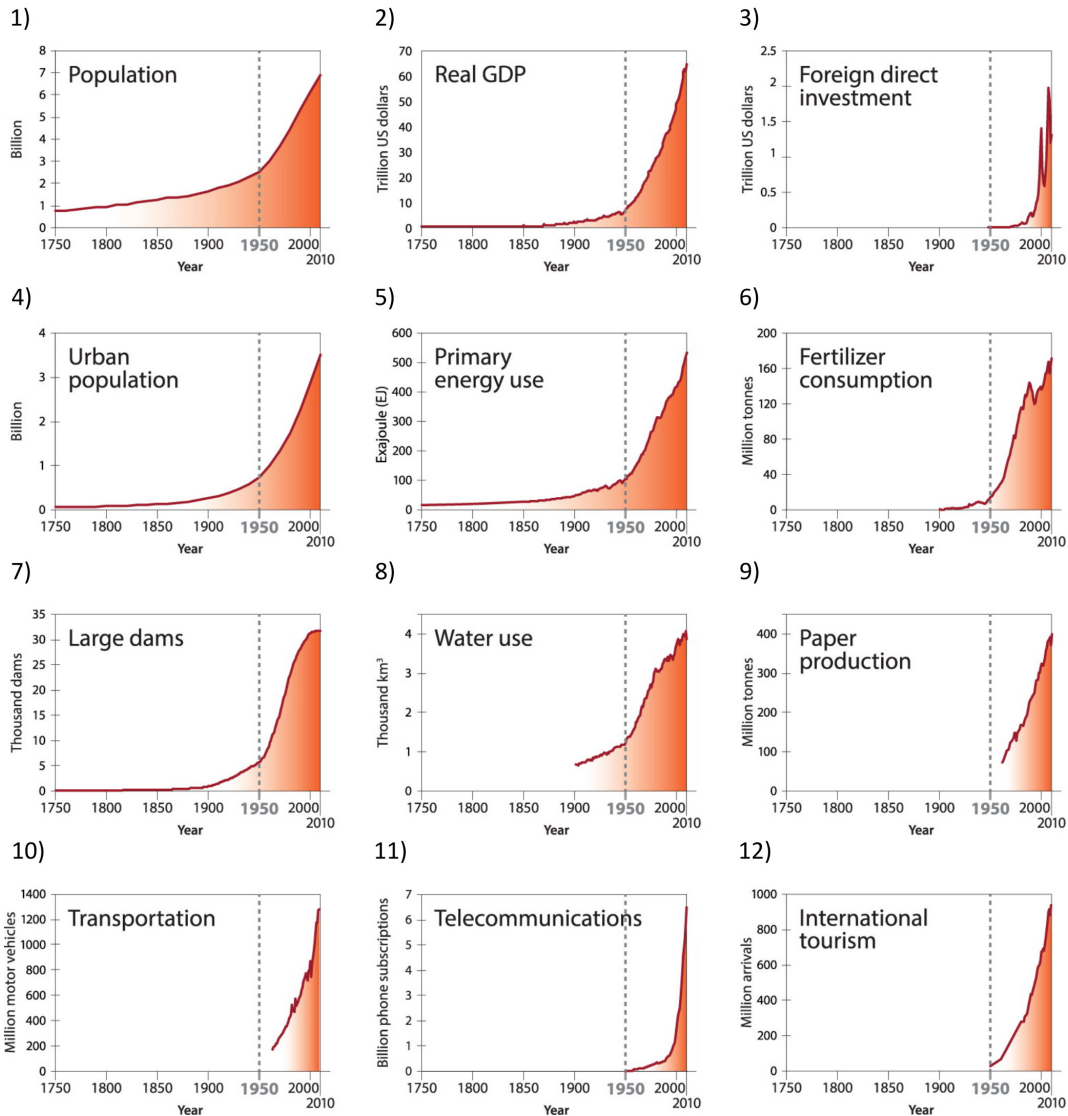


Figure 1.1 Trends from 1750 to 2010 in globally aggregated indicators for socio-economic development. (1) Global population data according to the HYDE (History Database of the Global Environment, 2013) database. Data before 1950 are modelled. (2) Global real GDP (Gross Domestic Product) in year 2010 US dollars. (3) Global foreign direct investment in current (accessed 2013) US dollars. (4) Global urban population data according to the HYDE database. Data before 1950 are modelled. (5) World primary energy use. (6) Global fertilizer (nitrogen, phosphate and potassium) consumption. (7) Global total number of existing large dams (15 m height above foundation). (8) Global water use is sum of irrigation, domestic, manufacturing and electricity water withdrawals and livestock water consumption from. (9) Global paper production from 1961 to 2010. (10) Global number of new motor vehicles per year. (11) Global sum of fixed landlines and mobile phone subscriptions. (12) Number of international arrivals per year for the period 1950–2010. From Steffen et al. (2015a). Copyright © 2015 by Sage Publications. Reprinted by permission of Sage Publications.

Earth system trends

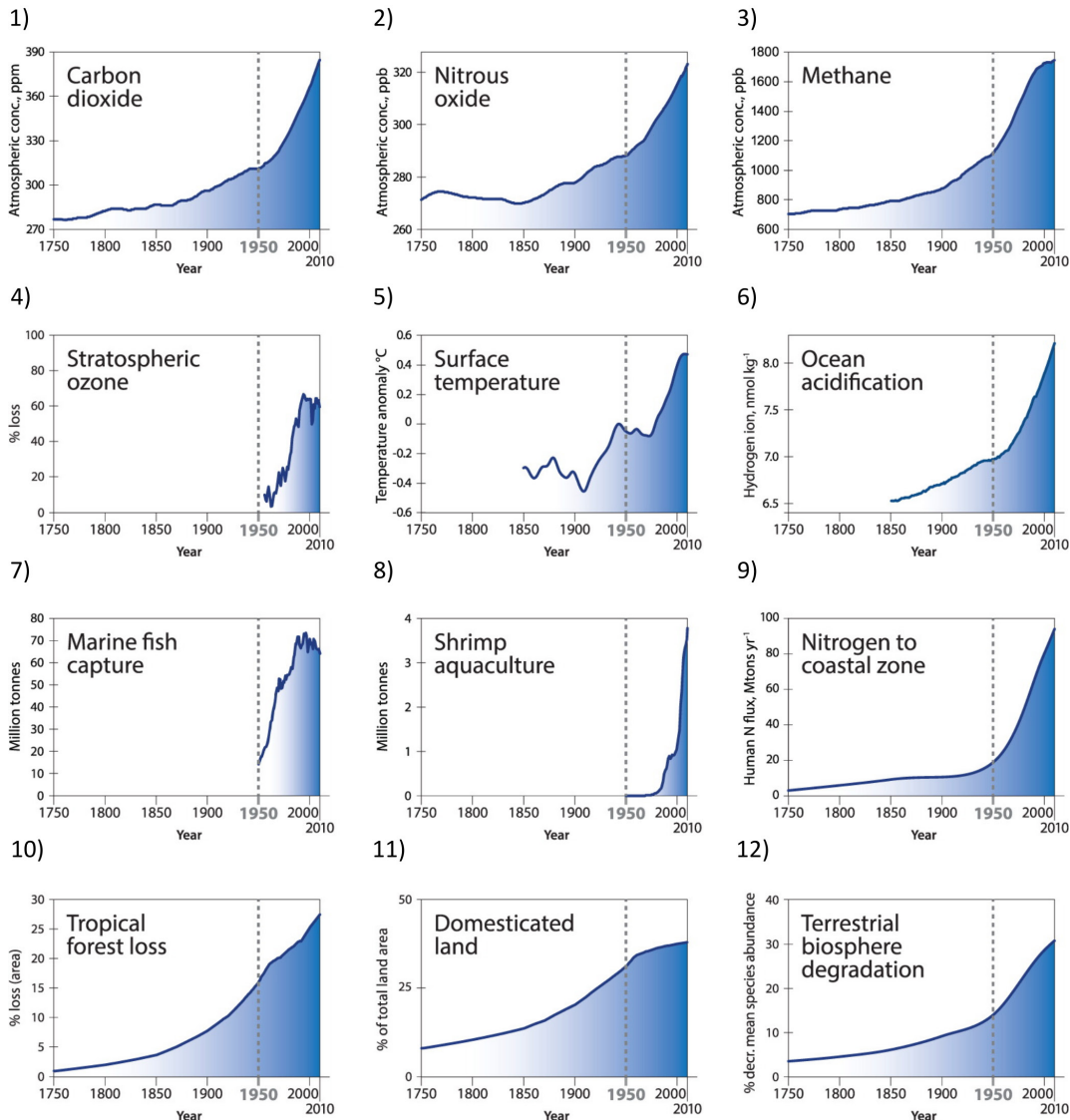


Figure 1.2 Trends from 1750 to 2010 in indicators for the structure and functioning of the Earth system. (1) Carbon dioxide, (2) nitrous oxide, and (3) methane from firn and ice core records (Law Dome, Antarctica) and Cape Grim, Australia. (4) Maximum percentage total column ozone decline (2-year moving average) over Halley, Antarctica. (5) Global surface temperature anomaly. (6) Ocean acidification expressed as global mean surface ocean hydrogen ion concentration. (7) Global marine fishes capture production (the sum of coastal, demersal and pelagic marine fish species only). (8) Global aquaculture shrimp production (the sum of 25 cultured shrimp species) as a proxy for coastal zone modification. (9) Model-calculated human-induced perturbation flux of nitrogen into the coastal margin. (10) Loss of tropical forests compared with 1700. (11) Increase in agricultural land area. (12) Percentage decrease in terrestrial mean species abundance relative to abundance in undisturbed ecosystems as an approximation for degradation of the terrestrial biosphere. From Steffen et al. (2015a). Copyright © 2015 by Sage Publications. Reprinted by permission of Sage Publications.

The concept of global change emerged to define these anthropogenic global-scale environmental changes, and even the proposition of a new geological era arose, termed the Anthropocene (Crutzen & Stoermer, 2021). It is important to note that global change encompasses not only climate change but also all alterations that influence the functioning of the Earth system (Casas, 2022). Furthermore, it signifies the global nature of the issue, wherein even localized activities affect the overall Earth system, either through repeated ubiquitous cumulative changes or via systemic alterations (Steffen et al., 2004).

The continuous and increasing pressure exerted by anthropogenic activities is pushing the Earth system beyond its normal operating range. In response to this observation, Rockström et al. (2009) investigated the Earth system's capacity to absorb this impact before experiencing an irreversible alteration of global environmental conditions, potentially marking the end of the Holocene. They proposed nine planetary boundaries, each of which would delineate the safe operating space for humanity before crossing thresholds that could shift into a new state with potentially disastrous consequences for humans. According to their estimations, three of the boundaries were already crossed, while others could not be quantified. Richardson et al. (2023) updated the planetary boundaries assessment framework and found that six of the nine boundaries are outside the safe operating space (Figure 1.3). The transgressed boundaries correspond to climate change, freshwater change, land system change, biogeochemical flows (phosphorus and nitrogen cycles), biosphere integrity, and novel entities; while ocean acidification is approaching the threshold of transgression. Quantifying the upper ends of the boundaries poses a great challenge, that in some cases hampers a precise determination of this upper edges. As a result, the upper edges of the wedges for the novel entities and the genetic diversity component of the biosphere integrity boundaries are blurred either because the upper end of the zone of increasing risk has not yet been quantitatively defined (novel entities) or because the current value is known only with great uncertainty (loss of genetic diversity). Both, however, are well outside of the safe operating space (Figure 1.3). This thesis will focus on the novel entities boundary, which was established to assess the potential that anthropogenic chemical pollution has to cause severe ecosystem and human health problems (Persson et al., 2022). The novel entities driver of global change, and its boundary, will be studied here for a large oceanic region, and several families of organic synthetic chemicals.

1.2 Anthropogenic chemical pollution

The novel entities boundary, originally named chemical pollution (Rockström et al., 2009), is defined as “new substances, new forms of existing substances and modified life forms”, including “chemicals and other new types of engineered materials or organisms not previously known to the Earth system as well as naturally occurring elements (for example, heavy metals) mobilized by anthropogenic activities” (Steffen et al., 2015b). This planetary boundary was established to address and evaluate what has long been largely overlooked regarding global change (Bernhardt et al., 2017; Rockström et al., 2009): the role of synthetic chemicals as agents of global change.

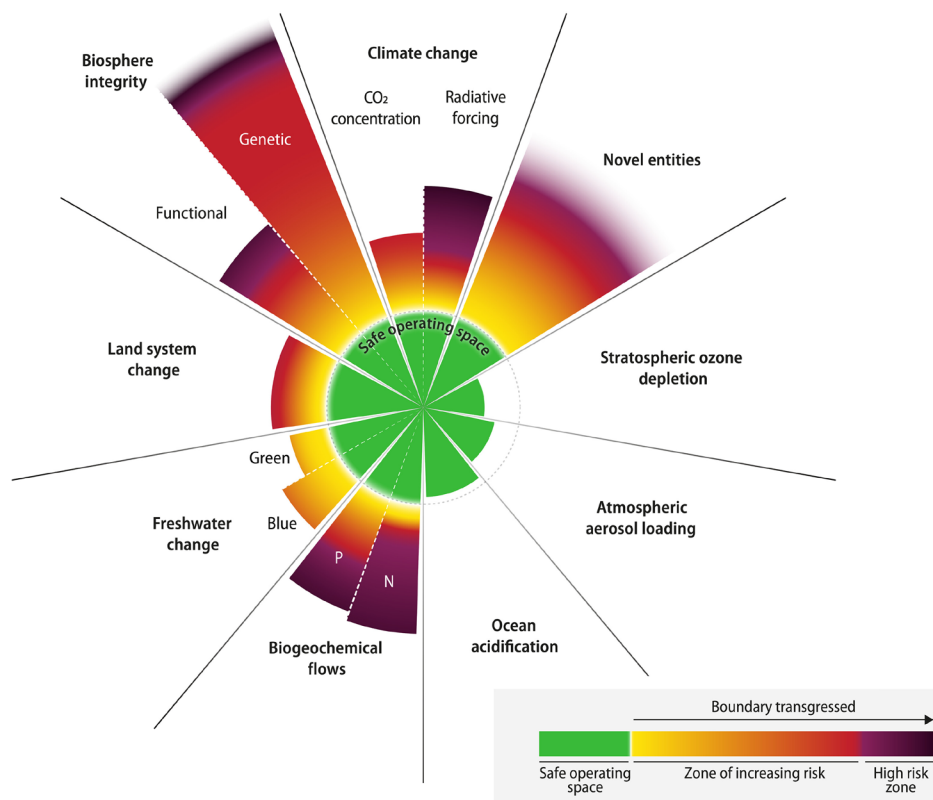


Figure 1.3 Status of control variables for all nine planetary boundaries as of 2023. The green zone is the safe operating space (below the boundary). Yellow to red represents the zone of increasing risk. Purple indicates the high-risk zone where interglacial Earth system conditions are transgressed with high confidence. Values for control variables are normalized so that the origin represents mean Holocene conditions and the planetary boundary (lower end of zone of increasing risk, dotted circle) lies at the same radius for all boundaries. Wedge lengths are scaled logarithmically. From Richardson et al. (2023). Licensed under CC BY-NC 4.0. <https://creativecommons.org/licenses/by-nc/4.0/>

As previously elucidated, during the last 200 years, particularly since 1950, human activities have increased significantly, resulting in an unprecedented exponential growth of the socio-economic trends (Figure 1.1). Throughout this period, chemical technologies have proven to be essential for human activities and production (Wang et al., 2020a). Consequently, this exponential growth has been mirrored in the chemical industry. Through an analysis of chemical reactions stored in the Reaxys database, Llanos et al. (2019) reported that the number of new chemicals has grown exponentially from 1800 to 2015, with an annual production rate of 4.4%. From all the synthesized chemicals, according to an analysis of 22 chemical inventories from 19 countries done by Wang et al. (2020a), the number of chemicals and chemical mixtures available in the market exceeds 350,000. Notably, of all the Chemical Abstracts Service registry numbers (CAS numbers) representing individual compounds they reported, approximately 87% corresponded to organic chemicals (carbon-based chemical substances). Similarly, in their attempt to quantify

the planetary boundary for novel entities, Persson et al. (2022) reported high growth rates over the last decades in the global trends of chemical industry production (Figure 1.4). The production of plastics, pesticide active ingredients, and several key monomers and solvents for the chemical industry has increased significantly in comparison to the global production values in 2000. This trend follows the pace of the great acceleration shown above for other anthropogenic activities (Figure 1.1) and changes in the Earth system (Figure 1.2).

Although chemicals provide benefits in certain areas (e.g., flame retardants), the intensive production and use of synthetic chemicals comes at a cost. During their lifecycle, many of these compounds are released and end up in the environment, where their potential effects on Earth system processes are usually not well known. Toxicological studies conducted under controlled laboratory conditions have demonstrated adverse effects on model organisms. However, these results are insufficient for comprehending and predicting the impact of complex mixtures of chemical contaminants under real environmental conditions. The large number of compounds released into the environment, the potential synergistic negative effects, the indirect effects mediated through species interactions, the interaction of chemicals with core ecosystem processes such as primary production, nutrient retention, carbon sequestration, ... All of these factors contribute additional layers of complexity to the comprehension of the environmental impacts of anthropogenic chemical pollution (Bernhardt et al., 2017). As Bernhardt et al. (2017) stated, “understanding the environmental impacts of synthetic chemicals in the real world requires ecological investigations in complex systems”. A better understanding of the biogeochemistry of synthetic chemicals is needed to effectively quantify their threat and implement corresponding regulations.

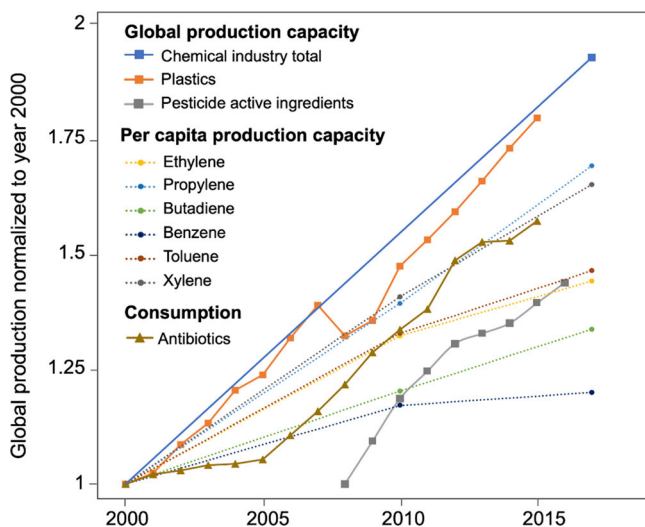


Figure 1.4 Current rising global trends of chemical industry production, expressed as the relative growth in some novel entities between 2000 and 2017 (for when comparable data are available): 1. Global production capacity for the chemical industry as a whole, plastics production and pesticide active ingredients (for which earliest data are from 2008); 2. Per capita production capacity in weight for key monomers and solvents: benzene, butadiene, ethylene, propylene, toluene, and xylene, 3: Global consumption of antibiotics. From Persson et al. (2022). Licensed under CC BY-NC-ND 4.0. <https://creativecommons.org/licenses/by-nc-nd/4.0/>

1.2.1 Organic contaminants: properties and regulation

Physicochemical properties

Various terms have been established to describe the introduction of novel entities into the environment. The term “contaminant” refers to a foreign and potentially toxic substance present in the environment above background levels. When a contaminant is demonstrated to exert adverse biological effects with empirical evidence, it is subsequently classified as a pollutant. According to Steffen et al. (2015b), the anthropogenic introduction of novel entities into the environment is of particular concern when these entities exhibit persistence, potential for long-range transport resulting in widespread distribution, accumulation in organisms and the environment, and potential adverse effects (e.g., toxicity) on critical Earth system processes. Various types of anthropogenic contaminants exhibit these characteristics and are considered of significant concern, such as plastic pollution. However, anthropogenic organic pollutants are arguably the most pertinent among the novel entities. The organic pollutants that show these four properties are known as Persistent Organic Pollutants (POPs), whereas those that show all except the potential for long-range transport are classified as Persistent, Bioaccumulative, and Toxic (PBT) chemicals. The inherent physicochemical characteristics of POPs and PBTs determine their environmental behavior. Consequently, the quantification of specific key properties and environmental parameters serves as a criterion for classifying organic chemicals as POPs or PBTs.

Persistence: It reflects the potential of a compound to last for long periods of time in the environment. It is usually attributed to extremely slow or nonexistent transformation through abiotic or biological processes. Since the environment lacks the capacity to effectively remove these contaminants, they can accumulate through various compartments and persist sufficiently to undergo long-range transport, potentially resulting in unexpected exposure and effects. The high persistence of organic chemicals alone presents numerous environmental and health risks, to the extent that recently, it has been proposed as a sufficient criterion for chemical regulation (Cousins et al., 2019). Persistence of organic chemicals is usually quantified by the determination of their degradation half-lives in individual environmental media (water, soil or sediment). Generally, chemicals with one degradation half-life exceeding 6 months are considered to be highly persistent (Cousins et al., 2019). However, under real environmental conditions, there are partitioning and transport processes that hamper the determination of persistence, by limiting their availability for abiotic or biotic degradation. Prediction on biodegradation could be improved by a better determination of the microbial consortia responsible for their transformations. However, very little is yet known about which microbial taxa, genes, and enzyme groups are key for the degradation of most of the chemicals, particularly in the marine environment.

Bioaccumulation and biomagnification (Figure 1.5): Bioaccumulation is defined as the increase in concentration of a chemical substance in a biological organism over time, whereas biomagnification refers to the increase in concentration of a chemical substance as it progresses up the food chain. Both result in elevated concentrations of contaminants in biota compared to their concentration in the environment. These phenomena are the consequence of the hydrophobic nature and high lipid solubility of many organic contaminants, indicating a significant propensity for the chemical to accumulate in organic matter, such as the tissues of living organisms. Evidence of bioaccumulation is determined by the bioconcentration factor (BCF), which quantifies the enrichment of a chemical in biota relative to the environmental water concentrations. It is defined as

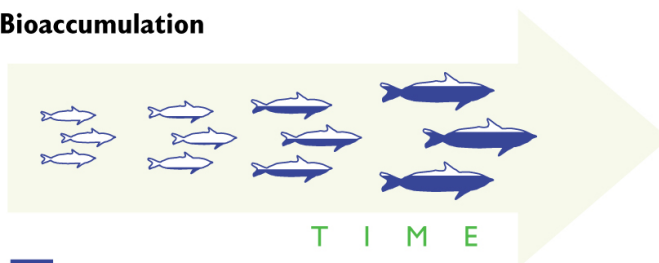
$$BCF = \frac{C_B}{C_W} \text{ (Eq. 1)}$$

where C_B and C_W are the chemical concentrations in the biota and water, respectively. Chemicals with a BCF greater than 5000 are classified as bioaccumulative (UNEP, 2023). In the absence of this data, octanol-water partition coefficient (K_{OW}) can also be used. This property is considered to be representative of the hydrophobicity, and it is defined as

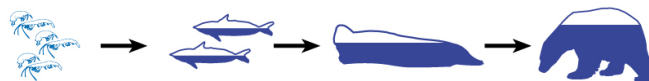
$$K_{OW} = \frac{C_O}{C_W} \text{ (Eq. 2)}$$

where C_O and C_W are the chemical concentrations in the octanol and water phase, respectively. Chemicals exhibiting $\log K_{OW}$ values greater than 5 are considered to bioaccumulate (UNEP, 2023).

Bioaccumulation



■ Contaminant levels



■ Contaminant levels

Biomagnification

Figure 1.5 Representations of bioaccumulation and biomagnification (Credit ©WWF).

Toxicity: Persistent organic pollutants can elicit toxic effects through acute or chronic toxicity. Although both are relevant, considering that exposure to POPs typically involves long-term exposure to low concentrations, researchers have emphasized the importance of assessing chronic toxicity (Vallack et al., 1998). Exposure to even low levels of POPs can lead to increased cancer risk, reproductive disorders, alterations of the immune system, neurobehavioral impairment, endocrine disruption, genotoxicity, and increased birth defects (World Health Organization. Regional Office for Europe, 2003). Acute toxicity data is usually reported as the median lethal concentration (LC_{50}), which is defined as the concentration of a chemical required to kill or significantly impair half of the exposed test organisms. Conversely, chronic toxicity experiments frequently assess sublethal effects, with results expressed in terms of no observed effects concentration (NOEC) or lowest observed effects concentration (LOEC). In recent years, the advancement and refinement of cellular and molecular experimental techniques have provided a means for measuring sublethal effects at the organism's cellular level, thereby expanding the potential to address chronic toxicity (Harmon, 2015). The toxic effects of mixtures, especially complex cocktails of synthetic chemicals is nowadays an emerging topic of research.

Potential for long-range transport: It describes the capacity of a compound to travel long distances due to its physicochemical properties. Either because of having a semi-volatile nature resulting in long-range atmospheric transport (LRAT) and subsequent deposition, or due to their high persistence allowing them enough time for global transport by other means (e.g., long-range oceanic transport), these contaminants are globally distributed (Figure 1.6). They even reach remote regions far from where they have been produced and used, such as polar environments. The potential for long-range transport has been assessed through modeling of environmental fate properties, but these models often struggle to accurately predict the real potential of organic compounds due to the complexity of the processes they undergo in the environment. Therefore, direct measurements of chemical concentrations in remote locations far from their sources remain the most straightforward and reliable way to demonstrate a chemical's ability to reach distant locations. Antarctica is of particular interest, as detection of chemicals in the most remote region can provide "the strongest evidence for persistence and mobility" (Bengtson Nash et al., 2023).

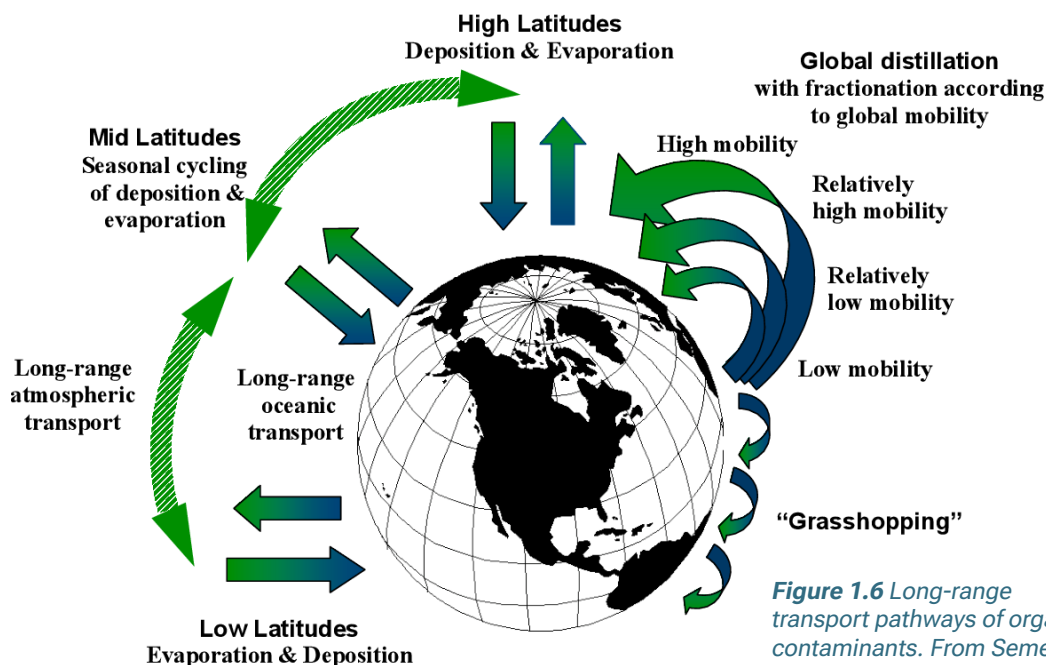


Figure 1.6 Long-range transport pathways of organic contaminants. From Semeena (2005).

Characterizing key physicochemical properties is important for understanding the environmental distribution of organic chemicals across different compartments and, consequently, predicting their fate. However, it is important to note that a complete understanding of a contaminant's fate cannot be achieved solely by examining its properties. Many other environmental factors influence the fate of contaminants, including atmospheric and oceanic currents as well as biogeochemical processes, among others. These factors must be considered together with the physicochemical properties to gain a more accurate understanding of the real situation. To achieve that level of understanding, direct measurements of chemicals in the environment are necessary, as they often provide the most reliable and strong evidence of a chemical's fate.

The main properties that need to be addressed to understand a contaminant's fate are vapor pressure, water solubility, the three partition coefficients between air, water, and octanol, and degradation rates or susceptibility to degradation in the different compartments. Additional properties utilized when relevant are the dissociation constant in water and the molecular weight, MW (Mackay et al., 2006; Semeena, 2005). Vapor pressure and water solubility are both measurements of the maximum capacity of a solvent phase to hold a dissolved chemical, with air and water serving as the solvents in these cases, respectively. Phase partition coefficients are defined as the equilibrium concentration ratio of a compound between two phases, characterizing its equilibrium distribution across those phases. For the concentration of a compound (C) in the phases i and j , the partition coefficient would be a dimensionless ratio given by this formula:

$$K_{ij} = \frac{C_i}{C_j} \text{ (Eq. 3)}$$

The three partition coefficients generally used in environmental chemistry are air-water partition coefficient (K_{AW}), octanol-water partition coefficient (K_{OW}), and octanol-air partition coefficient (K_{OA}) (Figure 1.7). K_{AW} can be estimated from vapor pressure and water solubility, representing a compound's propensity to migrate from water into air. However, when these parameters are challenging to measure, it is preferable to directly measure the K_{AW} , also known as the dimensionless Henry's law constant, H' (Mackay et al., 2006). This is done by directly calculating the ratio between the concentration in air and the concentration in water. Another approach to estimate K_{AW} is by using the Henry's law constant by:

$$K_{AW} = H' = \frac{H}{R\alpha T} \text{ (Eq. 4)}$$

where R is the universal gas constant ($8.314 \text{ Pa m}^3 \text{ K}^{-1} \text{ mol}^{-1}$), T is the absolute temperature (K), and H is the Henry's law constant ($\text{Pa m}^3 \text{ mol}^{-1}$). H defines the partitioning of a solute between the gas and water phases at equilibrium, and reflects the volatility of a solute in aqueous solution.

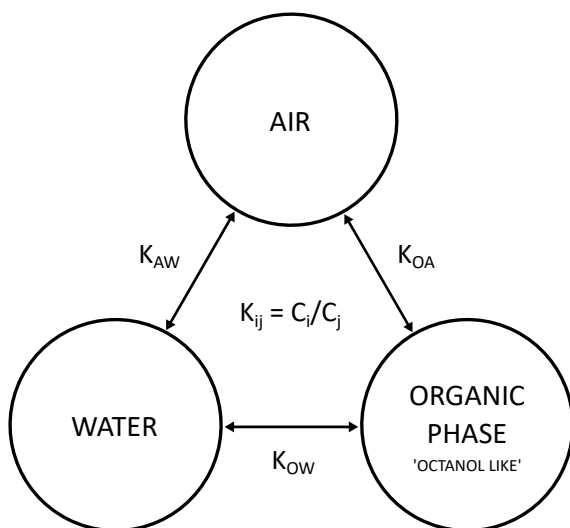


Figure 1.7 Diagram of the relationship between air, water, and organic phases (octanol is used as a surrogate of organic matter), and their partition coefficients.

K_{OW} offers a direct estimate of hydrophobicity or the tendency to distribute between water and organic substances such as lipids, waxes, and natural organic matter. Since octanol was found to be the most representative lipid-phase solvent for a variety of substances it has been used as a surrogate of organic matter (Baskaran & Wania, 2023). K_{OA} describes the partition of a chemical between air and the organic phase, and it has been used to describe the partitioning to vegetation, soil, aerosol particles, surfaces, materials, and animal tissue (Baskaran & Wania, 2023; Mackay et al., 2006).

The partition coefficients described above are directly related to the chemical structure of the organic contaminants. The majority of typical organic contaminants exhibit a significant hydrophobic nature (Mackay et al., 2006). As a general rule, an increase in MW is associated with enhanced hydrophobicity. Additionally, the nature of substituents plays a role in determining hydrophobicity. For instance, in the case of the polychlorinated biphenyls (PCBs), the degree of chlorine substitution directly correlates with the compound's hydrophobicity (Vallack et al., 1998). MW also affects volatility; typically, compounds with low molecular weight are more prone to volatilization and have a higher potential for LRTA. In contrast, heavier compounds are more likely to adhere to particles, soils, sediments, and organic matter. The chemical structure also significantly influences the persistence of organic contaminants, as it determines the reactivity of a compound to undergo degradation through abiotic (e.g., photodegradation) or biotic (e.g., biodegradation) processes. For example, anthropogenic organic contaminants with chemical structures that do not resemble any naturally occurring compound pose a challenge for the biochemical degradation mechanisms, which have not been evolutionarily adapted to break down such compounds (Manzetti et al., 2014).

Regulation of organic contaminants

Since the 1960s, when the ubiquitous presence of organic contaminants started to draw attention from researchers and scientists, ecotoxicological studies have identified various commercially utilized compounds as detrimental to the Earth system. The publication of Rachel Carson's book "Silent Spring" in 1962 is considered an important event that contributed to the establishment of the field of ecotoxicology and catalyzed the modern environmental movement by popularizing the concern about organic pollution (Bernhardt et al., 2017). In her book, she outlined the detrimental impacts that pesticides such as dichlorodiphenyltrichloroethane (DDT) were having on the environment. Additional examples of compounds that have been identified as detrimental include the chlorofluorocarbons (CFCs) and their role in the degradation of the stratospheric ozone layer (Adams & Halden, 2010), as well as the PCBs and their persistent toxic effects on the biosphere (Beyer & Biziuk, 2009).

These efforts screening organic contaminants resulted in the first local regulations to restrict or ban their production and use, such as the restrictions on organochlorine pesticides (OCPs) in the 1970s (Muir & Howard, 2006). Eventually, restrictions reached international levels and culminated with the United Nations Environment Programme (UNEP) Stockholm Convention on POPs in 2001, a global environmental treaty that aims to safeguard both human well-being

and the environment from the harmful impacts POPs (UNEP, 2023). The treaty initially listed 12 chemicals, colloquially referred to as the “dirty dozen” or legacy POPs, and included nine OCPs, PCBs used in industrial applications, and by-products such as polychlorinated dibenzo-p-dioxins and polychlorinated dibenzofurans (PCDD/PCDF). Since then, new chemicals have been proposed for listing under the convention, and nowadays, the list includes a total of 38 chemicals (Table 1.1). These recently identified POPs, often referred to as emerging POPs, include polybrominated diphenyl ethers (PBDEs), the perfluoroalkyl substances (PFAS) perfluorooctanoic acid (PFOA) and perfluorooctane sulfonic acid (PFOS), and insecticides such as the hexachlorocyclohexanes (HCHs), among others. The list will probably continue to increase, as “new” chemical contaminants continue to be reported and considered contaminants of emerging concern (CECs), such as the organophosphate esters (OPEs), other PFAS compounds, plastic additives, and others (Wang et al., 2024a).

The Stockholm Convention is not the only regulatory treaty currently addressing organic contaminants. The Environmental Protection Agency (EPA), an independent agency of the United States tasked with the mission to protect human health and the environment, developed the Priority Pollutant list in 1977 for water testing and regulatory purposes. The list currently includes 126 compounds that have been reported as toxic pollutants and detected in aquatic environments (USEPA, 1982). Among the listed compounds are numerous organochlorine compounds (some of which are also included in the Stockholm Convention), as well as other hazardous organic pollutants, such as the Polycyclic Aromatic Hydrocarbons (PAHs) and phthalates.

In the European Union (EU), the Water Framework Directive (European Commission, 2000) and the Marine Strategy Framework Directive (European Commission, 2008) are the main regulatory policies aimed at achieving a good environmental status of the EU's inland, coastal surface and marine waters. Pollution is among the qualitative descriptors they assess, with a designated list of pollutants and corresponding quality standard threshold concentrations. As an example, the Water Framework Directive includes OCPs, PBDEs, PAHs, and DDTs, along with metals, pharmaceuticals, and other industrial substances. In addition to these directives, the EU also has its regulatory agency, the European Chemicals Agency (ECHA), which is the organization responsible for assessing the potential risks of chemicals to human health and the environment. When a chemical compound is determined to be hazardous, it becomes subject to restrictions under the Registration, Evaluation, Authorization and Restriction of Chemicals (REACH) regulation, which is applicable throughout the European Union. Among the compounds they assess, the ECHA is currently developing regulations for flame retardants, for which they recently published the proposed regulatory strategy (ECHA, 2023). The aim is to implement restrictions on hazardous flame retardants, with implementation not anticipated before 2025. Examples of flame retardants include organohalogen flame retardants, among which PBDEs are already incorporated in the Stockholm Convention, and organophosphorus flame retardants, such as the OPEs (de Boer et al., 2024).

Table 1.1 POPs currently listed in the Stockholm Convention (UNEP, 2023), classified in three annexes. Keys: pesticide 🟢; industrial chemicals 🟡; unintentional by-products 🟣.

Annex A (Elimination): Parties are required to take action to stop the manufacture and application of the chemicals listed under Annex A.

Aldrin 🟢	Chlordane 🟢	Chlordecone 🟢
Decabromodiphenyl ether (commercial mixture, c-decaBDE) 🟡	Dechlorane plus 🟡	Dicofol 🟢
Dieldrin 🟢	Endrin 🟢	Heptachlor 🟢
Hexabromobiphenyl 🟡	Hexabromocyclododecane (HBCDD) 🟡	Hexabromodiphenyl ether and heptabromodiphenyl ether 🟡
Hexachlorobenzene (HCB) 🟢 🟡	Hexachlorobutadiene 🟡	Alpha hexachlorocyclohexane 🟢
Beta hexachlorocyclohexane 🟢	Lindane 🟢	Metoxychlor 🟢
Mirex 🟢	Pentachlorobenzene 🟢 🟡	Pentachlorophenol and its salts and esters 🟢
Polychlorinated biphenyls (PCB) 🟡	Polychlorinated naphthalenes 🟡	Perfluorooctanoic acid (PFOA), its salts and PFOA-related compounds 🟡
Perfluorohexane sulfonic acid (PFHxS), its salts and PFHxS-related compounds 🟡	Short-chain chlorinated paraffins (SCCPs) 🟡	Technical endosulfan and its related isomers 🟢
Tetrabromodiphenyl ether and pentabromodiphenyl ether 🟡	Toxaphene 🟢	UV-328 🟡

Annex B (Restriction): Parties are required to implement measures limiting the manufacture and application of chemicals listed under this annex, considering any applicable acceptable purposes and/or particular exemptions outlined in Annex B..

DDT 🟢	Perfluorooctane sulfonic acid (PFOS), its salts and perfluorooctane sulfonyl fluoride (PFOSF) 🟢 🟡
-------	---

Annex C (Unintentional production): Parties are required to implement strategies aimed at minimizing the unintentional release of chemicals listed under Annex C.

Hexachlorobenzene (HCB) 🟣	Hexachlorobutadiene 🟣	Pentachlorobenzene 🟣
Polychlorinated biphenyls (PCB) 🟣	Polychlorinated dibenzo-p-dioxins (PCDDs) 🟣	Polychlorinated dibenzofurans (PCDFs) 🟣
Polychlorinated naphthalenes 🟣		

Despite the existence of numerous regulations, the number of non-regulated chemical compounds in the market significantly surpasses that of regulated ones. Therefore, addressing the ecotoxicology and biogeochemistry of emerging contaminants entering the Earth system becomes crucial in order to improve regulatory policies. It is noteworthy that even compounds subject to restrictions, or even complete phase-out, will continue to pose long-term threats to the Earth system due to their persistence. Thus, a comprehensive understanding of the biogeochemical processes of these compounds is essential for their effective elimination from the environment. The regulation of a chemical compound does not necessarily entail the resolution of associated issues; rather, it constitutes the initial step towards addressing the problem.

1.2.2 Organic contaminants selected for this thesis

Polycyclic Aromatic Hydrocarbons (PAHs)

Polycyclic aromatic hydrocarbons (PAHs) are a large group of organic compounds containing two or more fused aromatic (benzene) rings. Depending on the number of rings, PAHs are categorized into low molecular weight PAHs (LMW PAHs; having two or three aromatic rings) and high molecular weight PAHs (HMW PAHs; having four or more aromatic rings). Naphthalene represents the most fundamental structure among the PAHs, comprising two aromatic rings, while benzo[*g,h,i*]perylene, consisting of six rings, is classified as one of the HMW PAHs. The aromatic rings can also incorporate substituents, as in the case of the methylated PAHs, or contain heteroatoms within the ring structures.

Due to their non-polar organic structure, PAHs are predominantly hydrophobic and lipophilic. The physicochemical properties of PAHs, and, consequently, their environmental fate, generally vary following their MW (Table 1.2). Vapor pressure and water solubility decrease when MW increases. As a result, compared to HMW PAHs, LMW PAHs are reasonably more volatile and more soluble in water, and consequently, more susceptible to degradation (Ghosal et al., 2016). On the other hand, the very low vapor pressure and water solubility of HMW PAHs cause them to adsorb strongly onto particles, such as soil and sediments, particularly to the organic matter and black carbon fractions. Due to their properties, PAHs are considered recalcitrant pollutants, especially HMW PAHs due to strong sorption to particles. The increased chemical stability and adsorption tendency conferred by additional aromatic rings make HMW PAHs particularly recalcitrant to degradation processes.

PAHs are naturally occurring organic compounds that originate from pyrogenic, petrogenic, or biogenic processes, with their emission sources divided as either natural or anthropogenic (Mojiri et al., 2019; Patel et al., 2020). Petrogenic PAHs result from direct inputs of petroleum, represented by accidental oil spills, and natural oil seeps. PAHs of biogenic origin include those synthesized by plants, algae, microorganisms, and phytoplankton, as well as those formed during gradual transformation of organic matter (Rocha & Palma, 2019). However, most PAHs are believed to originate from pyrogenic sources, which are the result of the incomplete combustion of fossil fuels, biomass, and other organic matter. Although natural sources such as volcanoes and

forest fires contribute to the formation of pyrogenic PAHs, they have been found to be marginal compared to the anthropogenic emission sources (Duran & Cravo-Laureau, 2016; Ghosal et al., 2016; Patel et al., 2020). PAH emitting anthropogenic activities include power production, waste incineration, fossil fuel-powered engines, coal tar production, iron, steel, and aluminum production, cement manufacturing, dye production, and rubber tire manufacturing, among others (Patel et al., 2020). The combination of the mentioned natural and anthropogenic sources, together with the subsequent global transport processes, has resulted in the widespread distribution of PAHs, which are now ubiquitously present across nearly all environmental compartments (air, water, soil, and sediment, Lawal, 2017).

Although PAHs are not included in the POPs list due to not fulfilling the high persistence criteria, they have been drawing attention for decades due to their ubiquitous presence, high concentrations in the environment, and toxicity. Data from toxicological and epidemiological studies have demonstrated the various mechanisms by which PAHs exert toxic effects on living organisms, such as humans or aquatic animals (Honda & Suzuki, 2020; Patel et al., 2020). The LMW PAHs are acutely toxic, and as MW increases, the acute toxicity decreases and carcinogenicity increases, making the HMW PAHs to be largely considered as genotoxic (Ghosal et al., 2016; Ravindra et al., 2008; Straif et al., 2005; Working Group on Polycyclic Aromatic Hydrocarbons, 2021). Due to being a widespread organic pollutant with potentially hazardous effects on human health, the U.S. EPA included 16 PAH compounds in their list of priority pollutants. Furthermore, the International Agency for Research on Cancer (IARC) classified the PAHs into four groups, regarding the strength of evidence for their carcinogenicity: not classifiable (Group 3), possible (Group 2B), probable (Group 2A) or human (Group 1) carcinogens (IARC Working Group on the Evaluation of Carcinogenic Risks to Humans, 2010; Working Group on Polycyclic Aromatic Hydrocarbons, 2021). In the EU, the European Commission has established regulations setting the maximum permissible limits for the sum of four PAHs in food (Regulation 2023/915, 2023) and defining the environmental quality standard concentrations for 11 PAHs listed in the Water Framework Directive (European Commission, 2000). Additionally, the ECHA has implemented restrictions on 8 PAH compounds in market products under the REACH regulation.

Organophosphate esters (OPEs): flame retardants and plasticizers

OPEs are a wide group of synthetic organic chemicals that share one basic common feature in their chemical structure: a central phosphate molecule and identical or different heterogeneous substituents (Greaves & Letcher, 2017). Three primary forms of OPEs exist: the organophosphate (OP) triesters, the OP diesters (degradation products of the triesters), and polyphosphates (Wang et al., 2020b). Among these, OP triesters are the most extensively used (X. Li, Zhao, et al., 2020). Henceforth, the term OPEs will specifically refer to the OP triesters. Depending on the substituents OPEs are classified as trialkyl derivatives, triaryl derivatives, and aryl-alkyl derivatives. Another important feature of the chemical structure of OPEs is the presence or absence of halogens (mainly chlorine) according to which the OPEs are categorized into two groups: halogenated or chlorinated OPEs, and non-halogenated OPEs.

As a consequence of the diverse substituent types, OPEs exhibit a broad spectrum of physicochemical properties (Table 1.3), ranging from very polar to very hydrophobic (Greaves & Letcher, 2017). As an example, log K_{OW} range from -9.8 to 10.6 (van der Veen & de Boer, 2012), although the most commonly used OPEs stay in the range between 1 and 5, indicating that they are more lipophilic than hydrophilic (Dou & Wang, 2023; Greaves & Letcher, 2017). Solubility tends to decrease with the increase of molecular weight, and the Henry's law constants and vapor pressure show a wide range of values, from high volatility to low volatility, indicating that the partitioning between air and environmental waters is highly variable (van der Veen & de Boer, 2012). This variability makes OPEs particularly challenging when attempting to assess their environmental behavior.

Generally, halogenated OPEs are used as flame-retardants, whereas non-halogenated OPEs are predominantly utilized as plasticizers and lubricants, though in some cases they are also used as flame-retardants (Andresen et al., 2004). OPEs are added to a large extent of industrial and household products, such as textiles, rubber, polyurethane foam, furniture, electronics, paints, polyvinyl chloride (PVC) plastics, lubricants and hydraulic fluids (European Chemicals Agency, 2023; van der Veen & de Boer, 2012; Wei et al., 2015). In most of these products, OPEs are present as additives rather than chemically bonded to the material, particularly when they are added to increase flame retardancy. As a result, these compounds are readily released into the surrounding environment from products through volatilization, leaching and abrasion, because they are merely mixed with the host material instead of chemically bonded to the other constituents (Dou & Wang, 2023; Wei et al., 2015).

In the last decades, there has been a massive increase in the use of OPEs, mainly due to the phase-out of PBDEs during the 2000s. OPEs have taken the place of PBDEs and other banned brominated flame retardants in the global market, a shift that has been reflected in their production volumes. In 1992 the global consumption was estimated in 100,000 tons/year, which by 2013 increased to 620,000 tons/year, accounting for a 30% of the total global flame retardants (Dou & Wang, 2023; Greaves & Letcher, 2017; Wang et al., 2021a; Xie et al., 2022). By 2017, the amount was estimated to be 760,000 tons/year, a 30% of the 2.53 million tonnes of flame retardants consumed globally (Chen & Ma, 2021; X. Wang et al., 2020b). This amount will presumably increase, as the global consumption of flame retardant chemicals is estimated to continue growing in the following years. The extensive utilization of OPEs was motivated by estimations suggesting that OPEs would exhibit lower persistence, reduced bioaccumulation, and a diminished potential for widespread distribution compared to PBDEs (Blum et al., 2019). Nevertheless, multiple research studies have demonstrated that OPEs exhibit greater mobility and persistence than initially anticipated (Fu et al., 2021; Rodgers et al., 2018; Sühring et al., 2020), and can even exert toxic effects on humans and biota (Antonopoulou et al., 2022; Blum et al., 2019; Dou & Wang, 2023; Hong et al., 2018; Hu et al., 2023; J.-X. Liu et al., 2022; Wang et al., 2020b). This unexpected persistency, together with their global utilization, has resulted in the widespread distribution of OPEs in the environment, where they have been detected in nearly all the compartments, even at remote areas (R. Li et al., 2023; Möller et al., 2012a; Wang et al., 2020b; Wei et al., 2015; Xie et al., 2022). These findings have collectively increased awareness regarding

OPEs, which are now classified as CECs. Nevertheless, there remains an absence of international regulations addressing this issue. The ECHA recently published its proposed regulatory strategy for flame retardants (ECHA, 2023); however, concerns have been raised regarding the potential efficacy of this regulation in meeting the necessary standards (de Boer et al., 2024).

Per- and polyfluoroalkyl substances (PFAS)

PFAS constitute a large group of thousands of synthetic chemicals that have been produced since the 1940s and are widely used in industrial applications and consumer products. Their surfactant properties, thermal and chemical stability, and water and oil repellency make them suitable for many applications, such as surfactants, fire-fighting foam, textiles, water-proof fabrics, non-sticking cooking pans, food packaging, paper products, personal care products, pharmaceuticals, and coating paints, among others (Glüge et al., 2020). PFAS consist of carbon atom-containing aliphatic substances on which the hydrogen atoms are fully (per-) or partially (poly-) substituted by fluorine atoms, attached with a functional group head, usually carboxylic or sulfonic acids (Zhang et al., 2022). The high stability of PFAS is attributed to the presence of numerous C-F bonds in the perfluoroalkyl moiety, which exhibit exceptionally low chemical reactivity and are highly resistant to cleavage. The perfluoroalkyl group's bonds contribute to enhanced molecular characteristics: strong acidity, reduced water surface tension, water and oil repellency, and high thermal, chemical, and biochemical stability (Wang et al., 2017).

Per- and polyfluoroalkyl substances (PFAS) encompass a diverse array of individual compounds and isomers that are categorized into distinct families. Among them, perfluoroalkyl acids (PFAAs) have gathered significant attention. This focus is attributed not only to the high persistence of PFAAs, their widespread application in various industries and products, and their direct emission into the environment; but also, to their indirect formation through the environmental degradation or metabolism of precursor substances (Buck et al., 2011). For the purpose of this thesis, perfluoroalkyl carboxylic acids (PFCAs) and perfluoroalkyl sulfonic acids (PFSAAs) will be the target compounds from the family of PFAAs (Table 1.4). They are mostly produced and present as linear carbon chains, and depending on the number of carbon atoms present in the chain they are divided as “short” or “long” chain compounds (Buck et al., 2011). These PFAS compounds exhibit high persistence and water solubility, characteristics that facilitate their long-range transport through water currents and aerosols (Ahrens et al., 2011; Prevedouros et al., 2006), complemented by the atmospheric transport and deposition of the (semi) volatile precursors (Young & Mabury, 2010), resulting in their global distribution in the environment (Ahrens & Bundschuh, 2014; Casas et al., 2020; González-Gaya et al., 2014; Nakayama et al., 2019).

The persistence, bioaccumulation, and toxicity of PFAS (Ahrens & Bundschuh, 2014; Fenton et al., 2021; Teaf et al., 2019; Xiang et al., 2019), in conjunction with their widespread distribution, have prompted increasing attention from the scientific community and policymakers, particularly regarding the ubiquitous PFOA and PFOS. For instance, data from the early 2000s indicated that PFOA was detected in blood samples from nearly the entire U.S. general population (>99%) (Teaf et al., 2019). The Stockholm Convention's Annex B was updated in 2009 to include PFOS and its salt, still allowing for specific exceptions in their production and use. However,

PFOA, its salts, and PFOA-related compounds were not added until 2019, when they were listed under the Annex A. Later, in 2022, perfluorohexane sulfonic acid (PFHxS), along with its salts and related compounds, were also included in Annex A (UNEP, 2023). PFAS levels in drinking waters have also been regulated by many countries, where the United States has taken the lead with the National Primary Drinking Water Regulation (NPDWR) for six PFAS that EPA announced on 2024 (USEPA, 2024a). Through this regulation, the EPA established unprecedented threshold levels for six PFAS compounds (which included PFOA, PFOS and PFHxS), which are more stringent than any current state standards for PFAS. Additionally, in 2024 the EPA has also published the Final Aquatic Life water Quality Criteria for PFOA and PFOS, which gather the latest scientific knowledge regarding the effects of these two compounds on freshwater organisms (USEPA, 2024b). These regulations seem to be promising for addressing the issue of PFAS pollution. However, (Wang et al., 2017) pointed out several flaws of the PFAS control measures. The extensive number of PFAS compounds involved renders it neither practical nor feasible to assess them individually, particularly considering that the predominant industrial practice of phasing out one PFAS is to substitute it with another similar PFAS. Furthermore, due to their persistence, the effectiveness of phasing-out alone is limited, and remediation strategies are necessary, wherein biodegradation presents novel possibilities.

Table 1.2 Physicochemical properties of the PAHs selected for this thesis. References: a Patel et al. 2020, b Joa et al. 2009, c LaGrega et al. 2001, d Lehndorff & Schwark 2009, e Finizio et al. 1997, f Burkhard 2000, g Mackay et al. 2006, h Odabasi et al. 2006, i Kang et al. 2016.

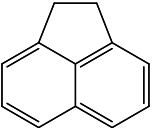
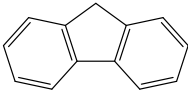
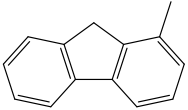
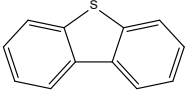
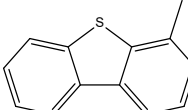
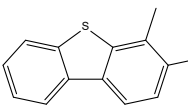
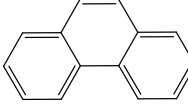
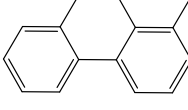
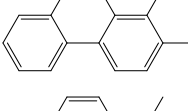
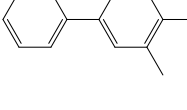
Compound	Abbreviation	Chemical structure	MW (g/mol)	S_w (mg/L)	V_p (Pa)	Log K_{ow}	Log K_{oa}
Acenaphthene	Ace		154	3.8 a	3.0×10^{-1} b	3.92 c	6.31 g
Fluorene	Flu		166	1.9 a	9.0×10^{-2} b	4.18 c	6.68 e
Methylfluorene	MFlu		180	1.09	4.0×10^{-4}	4.97	
Dibenzothiophene d	DBT		184	1.47	2.7×10^{-2}	4.38	7.24
Methyl- dibenzothiophene	MDBT		198				
Dimethyl- dibenzothiophene	DMDBT		212				
Phenanthrene	Phe		178	1.15 a	2.0×10^{-2} b	4.57 c	7.45 e
Methyl- phenanthrene d	MPhe		192	0.27	5.5×10^{-3}	4.99	7.49
Dimethyl- phenanthrene d	DMPhe		206	0.1	2.4×10^{-3}	5.44	8.03
Trimethyl- phenanthrene	TMPhe		220				

Table 1.2 Physicochemical properties of the PAHs selected for this thesis. References: a Patel et al. 2020, b Joa et al. 2009, c LaGrega et al. 2001, d Lehndorff & Schwark 2009, e Finizio et al. 1997, f Burkhard 2000, g Mackay et al. 2006, h Odabasi et al. 2006, i Kang et al. 2016 (continued).

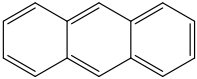
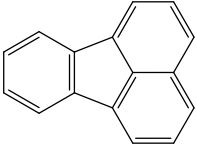
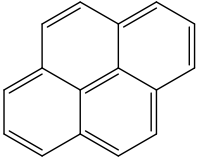
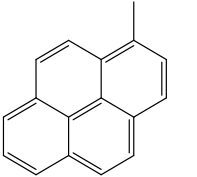
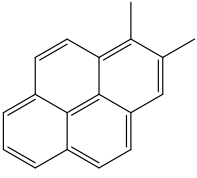
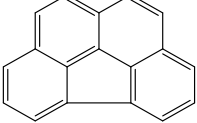
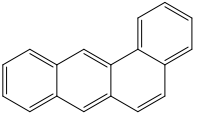
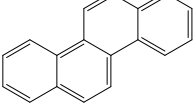
Compound	Abbreviation	Chemical structure	MW (g/mol)	S _w (mg/L)	V _p (Pa)	Log K _{ow}	Log K _{oa}
Anthracene	Ant		178	0.045 a	1.0x10 ⁻³ b	4.54 c	7.34 e
Fluoranthene	Flt		202	0.26 a	1.2x10 ⁻³ b	5.22 c	8.60 e
Pyrene	Pyr		202	0.13 a	6.0x10 ⁻⁴ b	5.18 c	8.61 e
Methyl-pyrene i	MPyr		216	0.10		5.48	
Dimethyl-pyrene	DMPyr		230				
Benzo[g,h,i] fluoranthene	B[g,h,i]f		226				
Benzo[a] anthracene	B[a]ant		228	0.011 a	2.8x10 ⁻⁵ b	5.91 c	9.56 e
Chrysene	Cry		228	1.5x10 ⁻³ a	5.7x10 ⁻⁷ b	5.65 c	10.44 e

Table 1.2 Physicochemical properties of the PAHs selected for this thesis. References: a Patel et al. 2020, b Joa et al. 2009, c LaGrega et al. 2001, d Lehndorff & Schwark 2009, e Finizio et al. 1997, f Burkhard 2000, g Mackay et al. 2006, h Odabasi et al. 2006, i Kang et al. 2016 (continued).

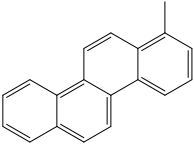
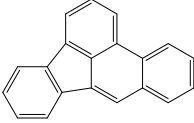
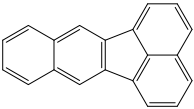
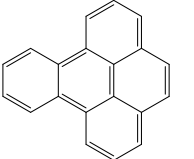
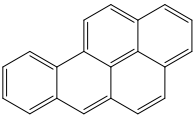
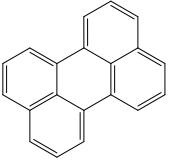
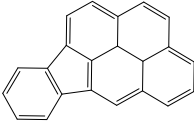
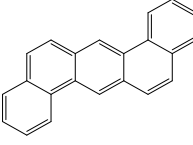
Compound	Abbreviation	Chemical structure	MW (g/mol)	S_w (mg/L)	V_p (Pa)	Log K_{ow}	Log K_{oa}
Methyl- chrysene	MCry		242				
Benzo[b] fluoranthene	B[b]f		252	1.5×10^{-3} a		6.20 f	11.19 e
Benzo[k] fluoranthene	B[k]f		252	8×10^{-4} a	5.2×10^{-8} b	6.11 f	11.19 e
Benzo[e] pyrene	B[e]pyr		252			6.12 f	11.13 e
Benzo[a] pyrene	B[a]pyr		252	3.8×10^{-3} a	7.0×10^{-7} b	6.13 f	11.56 h
Perylene	Pery		252			5.82 f	11.7
Indeno[1,2,3-cd] pyrene	In[1,2,3-cd] pyr		276	6.2×10^{-2} a		6.72 h	12.43 h
Dibenzo[a,h] anthracene	Dib[a,h]ant		278	5×10^{-4} a	3.7×10^{-10} b	6.50 h	12.59 h

Table 1.2 Physicochemical properties of the PAHs selected for this thesis. References: a Patel et al. 2020, b Joa et al. 2009, c LaGrega et al. 2001, d Lehdorff & Schwark 2009, e Finizio et al. 1997, f Burkhard 2000, g Mackay et al. 2006, h Odabasi et al. 2006, i Kang et al. 2016 (continued).

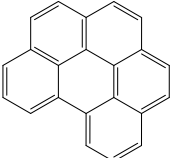
Compound	Abbreviation	Chemical structure	MW (g/mol)	S _w (mg/L)	V _p (Pa)	Log K _{ow}	Log K _{oa}
Benzo[g,h,i] perylene	B[g,h,i]pery		276	2.6x10 ⁻⁴ a	6x10 ⁻⁸ b	6.90 h	12.55 h

Table 1.3 Physicochemical properties of the OPEs selected for this thesis and other main OPEs found in the environment. Data from Brooke et al. 2009a, 2009b, ECHA 2018, Xie et al. 2022.

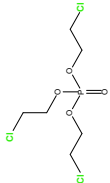
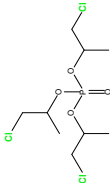
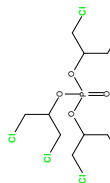
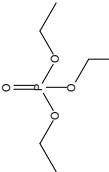
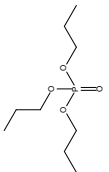
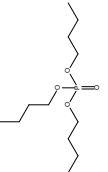
Compound	Abbreviation	CAS number	Formula	Chemical structure	MW (g/mol)	S _w (mg/L)	V _p (Pa)	Log K _{ow}	Log K _{oa}
Cl-OPEs									
Tris (2-chloroethyl) phosphate	TCEP	115-96-8	C ₆ H ₁₂ Cl ₃ O ₄ P		285.5	7.8x10 ³	1.1x10 ⁻³	1.8	5.3
Tris(1-chloro-2-propyl) phosphate	TCPP	13674-84-5	C ₉ H ₁₈ Cl ₃ O ₄ P		327.6	1.1x10 ³	1.4x10 ⁻³	2.7	8.2
Tris(1,3-dichloro-2-propyl) phosphate	TDCPP	13674-87-8	C ₉ H ₁₅ Cl ₆ O ₄ P		430.9	18.1	5.6x10 ⁻⁶	3.7	11
Alkyl-OPEs									
Triethyl phosphate	TEP	78-40-0	C ₆ H ₁₅ O ₄ P		182.2	1.1x10 ⁴	22	0.8	6.6
Tri-n-propyl phosphate	TnPP	513-08-6	C ₉ H ₂₁ O ₄ P		224.2	830	3.0	1.9	6.4
Tri-n-butyl phosphate	TnBP	126-73-8	C ₁₂ H ₂₇ O ₄ P		266.3	280	0.15	4.0	8.2

Table 1.3 Physicochemical properties of the OPEs selected for this thesis and other main OPEs found in the environment. Data from Brooke et al. 2009a, 2009b, ECHA 2018, Xie et al. 2022 (continued).

Compound	Abbreviation	CAS number	Formula	Chemical structure	MW (g/mol)	S _w (mg/L)	V _p (Pa)	Log K _{ow}	Log K _{oa}
Tri-isobutyl phosphate	TiBP	126-71-6	C ₁₂ H ₂₇ O ₄ P		266.3	16	1.7	3.6	7.5
Tris(2-butoxyethyl) phosphate	TBEP	78-51-3	C ₁₈ H ₃₉ O ₇ P		398.5	2.0	1.6x10 ⁻⁴	3.8	13
Tris(2-ethylhexyl) phosphate	TEHP	78-42-2	C ₂₄ H ₅₁ O ₄ P		434.6	1.5x10 ⁻⁵	1.1x10 ⁻⁵	9.5	15
Aryl-OPEs									
Triphenyl phosphate	TPhP	115-86-6	C ₁₈ H ₁₅ O ₄ P		326.3	1.9	8.5x10 ⁻⁴	4.6	8.5
2-Ethylhexyl diphenyl phosphate	EHDPP	1241-94-7	C ₂₀ H ₂₇ O ₄ P		362.4	0.051	3.5x10 ⁻⁴	5.7	8.4
Tri-m-cresyl phosphate	TmCP	563-04-2	C ₂₁ H ₂₁ O ₄ P		368.4	0.4	9.9x10 ⁻⁵	5.1	9.6
Tri-o-cresyl phosphate	ToCP	78-30-8	C ₂₁ H ₂₁ O ₄ P		368.4	0.4	5.5x10 ⁻⁵	5.1	9.6
Tri-p-cresyl phosphate	TpCPr	78-32-0	C ₂₁ H ₂₁ O ₄ P		368.4	0.4	4.4x10 ⁻⁵	5.1	9.6

Table 1.4 Physicochemical properties of the PFAS selected for this thesis. Data from ITRC 2023, Mudlaff et al. 2024.

Table 1-4 Physical/chemical properties of the PFAS selected for this thesis. Data from ITRC 2020, Mudrian et al. 2024.

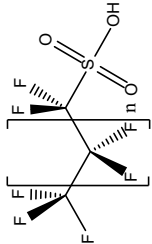
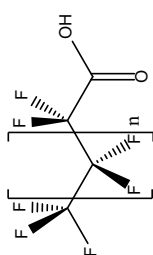
Compound	Abbreviation	CAS number	Formula	Chemical structure	MW (g/mol)	S _w (log mg/L)	V _p (log mmHg)	Log K _{ow}	Log K _{oa}	Log K _{aw}
Perfluoroalkyl sulfonic acids: PFSAs										
Perfluorobutane sulfonic acid	PFBS	375-73-5	C ₄ HF ₉ O ₃ S		300.12	3.05	-1.83	5.28	8.39	-3.12
Perfluoropentane sulfonic acid	PFPeS	2706-91-4	C ₅ HF ₁₁ O ₃ S		350.13	2.49	-2.17	5.93	9.34	-3.41
Perfluorohexane sulfonic acid	PFHxS	355-46-4	C ₆ HF ₁₃ O ₃ S		400.14	3.06	-2.56	6.51	9.02	-2.51
Perfluoroheptane sulfonic acid	PFHpS	375-92-8	C ₇ HF ₁₅ O ₃ S		450.15	1.44	-3.00	7.10	10.83	-3.73
Perfluorooctane sulfonic acid	PFOS	1763-23-1	C ₈ HF ₁₇ O ₃ S		500.16	0.92	-3.47	7.68	11.51	-3.83
Perfluorononane sulfonic acid	PFNS	68259-12-1	C ₉ HF ₁₉ O ₃ S		550.17	0.36	-3.97	8.28	12.20	-3.92
Perfluorodecane sulfonic acid	PFDS	335-77-3	C ₁₀ HF ₂₁ O ₃ S		600.18	-0.23	-4.50	8.92	12.95	-4.02
Perfluorododecane sulfonic acid	PFDoDS	79780-39-5	C ₁₂ HF ₂₅ O ₃ S		700.20	-1.59	-5.62	10.34	14.67	-4.33
Perfluoroalkyl carboxylic acids: PFCAs										
Perfluorobutanoic acid	PFBA	375-22-4	C ₄ HF ₇ O ₂	214.05	3.68	-0.30	4.37	8.24	-3.87	
Perfluoropentanoic acid	PFPeA	2706-90-3	C ₅ HF ₉ O ₂	264.06	3.00	-0.62	5.06	9.38	-4.32	
Perfluorohexanoic acid	PFHxA	307-24-4	C ₆ HF ₁₁ O ₂	314.07	2.41	-1.01	5.73	10.33	-4.60	
Perfluoroheptanoic acid	PFHpA	375-85-9	C ₇ HF ₁₃ O ₂	364.08	1.87	-1.47	6.33	11.08	-4.76	

Table 1.4 Physicochemical properties of the PFAS selected for this thesis. Data from ITRC 2023, Mudlaff et al. 2024 (continued).

Compound	Abbreviation	CAS number	Formula	Chemical structure	MW (g/mol)	S _w (log mg/L)	V _p (log mmHg)	Log K _{ow}	Log K _{oa}	Log K _{aw}
Perfluorooctanoic acid	PFOA	335-67-1	C ₈ HF ₁₅ O ₂		414.09	1.34	-1.95	6.96	11.80	-4.84
Perfluorononanoic acid	PFNA	375-95-1	C ₉ HF ₁₇ O ₂		464.10	0.81	-2.48	7.54	12.43	-4.89
Perfluorodecanoic acid	PFDA	335-76-2	C ₁₀ HF ₁₉ O ₂		514.11	0.26	-3.04	8.18	13.11	-4.93
Perfluoroundecanoic acid	PFUnDA	2058-94-8	C ₁₁ HF ₂₁ O ₂		564.12	-0.33	-3.61	8.82	13.81	-4.99
Perfluorododecanoic acid	PFDoDA	307-55-1	C ₁₂ HF ₂₃ O ₂		614.13	-0.98	-4.21	9.53	14.60	-5.10
Perfluorotridecanoic acid	PFTtDA	72629-94-8	C ₁₃ HF ₂₅ O ₂		664.14	-1.69	-4.81	10.26	15.48	-5.22
Perfluorotetradecanoic acid	PFTeDA	376-06-7	C ₁₄ HF ₂₇ O ₂		714.15	-2.47	-5.43	11.08	16.49	-5.41
Perfluorohexadecanoic acid	PFHxDA	67905-19-5	C ₁₆ HF ₃₁ O ₂		814.17	-4.30	-6.70	12.91	18.94	-6.03
Perfluorooctadecanoic acid	PFODA	16517-11-6	C ₁₈ HF ₃₅ O ₂		914.19					

1.3 Organic contaminants in the global ocean

The global ocean covers 71% of Earth's surface and includes all marine water. However, what makes the global ocean relevant is not just its vastness. It contains 97% of the world's water, and the marine biota inhabiting its diverse ecosystems constitute a critical food source supporting economies in numerous countries (IPCC (Intergovernmental Panel on Climate Change), 2019). It plays a crucial role in the global climate system, mitigating climate change and stabilizing global climate by absorbing 90% of the excess heat released into the environment, distributing the heat through oceanic currents, and sequestering nearly one-third of the anthropogenic carbon dioxide emissions (Gruber et al., 2019). Furthermore, marine microbial communities constitute a significant source of atmospheric oxygen, as it is estimated that approximately 70% is generated through the photosynthetic activity of phytoplankton (Echeveste et al., 2010; Sekerci & Petrovskii, 2015). Consequently, oceans are crucial for human health and the well-being of the Earth system (World Health Organization, 2019).

Nevertheless, human activities are having a significant negative impact on the global ocean. Halpern et al. (2019) assessed the pace of change of cumulative human impacts (CHI) by calculating and mapping the cumulative impact of 14 stressors related to human activities (including climate change, fishing, land-based pressures, and other commercial activities) on 21 different marine ecosystems globally for each of eleven years spanning 2003–2013. They found that almost 60% of the ocean is experiencing a significant increase of cumulative impact, particularly due to climate change, but also from pollution and fishing (Figure 1.8).

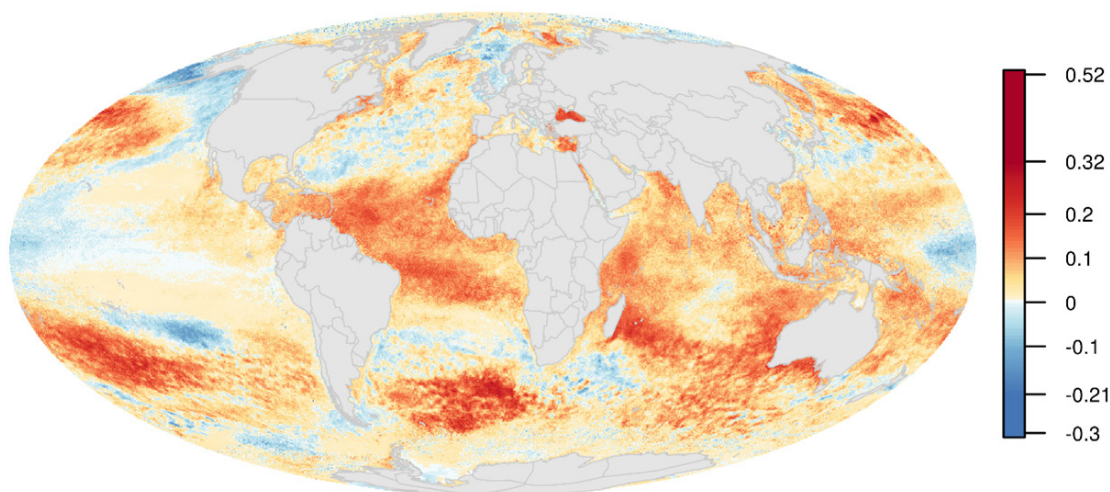


Figure 1.8 Annual change in CHI estimated using a linear regression model from 2003 to 2013. From Halpern et al. (2019). Licensed under CC BY 4.0. <https://creativecommons.org/licenses/by/4.0/>

Anthropogenic pollution of the global ocean is therefore a widespread existing problem. Human activities result in a complex mixture of contaminants entering the marine environment, such as plastics, manufactured chemicals, mercury, crude oil, pesticides, and nutrients (Figure 1.9). The major classes of marine chemical contaminants composing this complex mixture are the families of PAHs, OPEs, and PFAS, together with other halogenated hydrocarbons (e.g., PCBs, PBDEs), pesticides (e.g., DDT), and organometals. Oceans are the ultimate sink for these organic contaminants, which depending on their persistence, will remain there for long periods of time, posing a serious threat to marine ecosystems and human health (Landrigan et al., 2020; World Health Organization, 2019). However, ocean pollution remains inadequately recognized and insufficiently understood (Back to Blue, 2022; Hatje et al., 2022). Elucidating the interactions between organic contaminants and marine ecosystems will facilitate our comprehension of their environmental fate, ultimately enabling more effective approaches to address the issue of oceanic pollution.

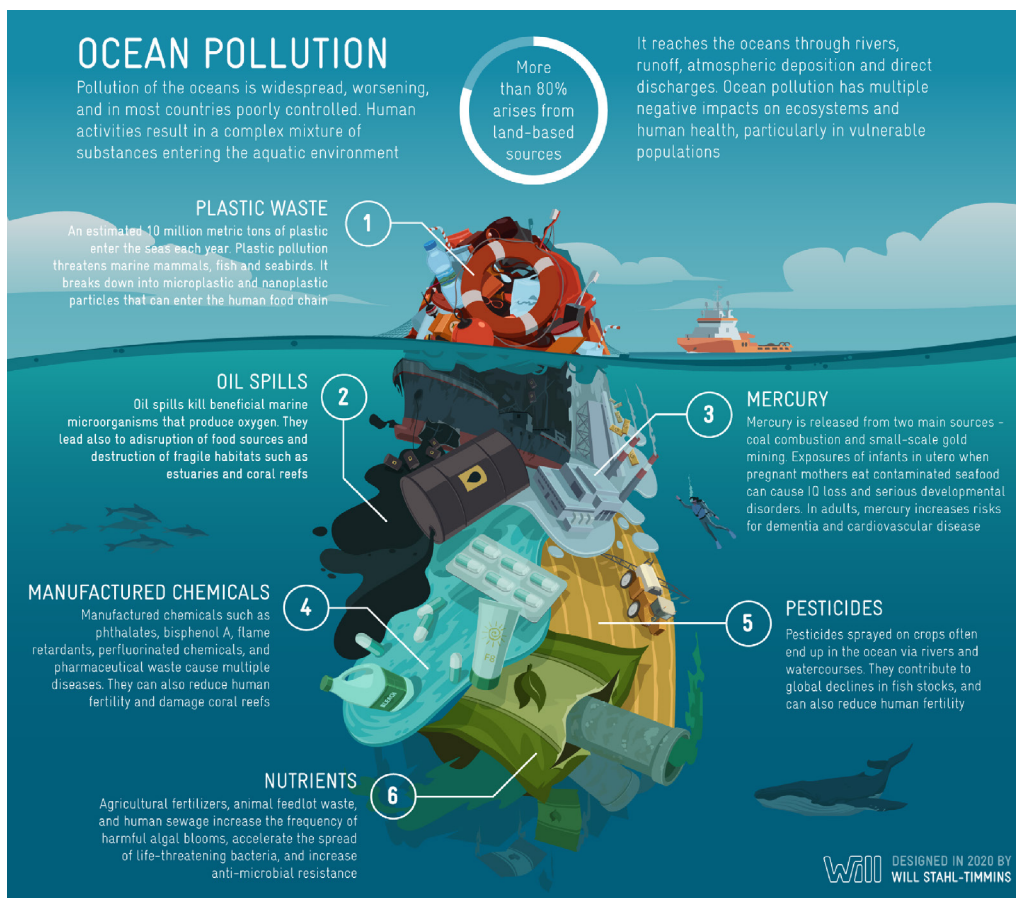


Figure 1.9 Representation of the complex mixture of anthropogenic pollutants that constitute oceanic pollution. From Landrigan et al. (2020). Licensed under CC BY 4.0. <https://creativecommons.org/licenses/by/4.0/>

1.3.1 Sources and transport

Organic contaminants (with the exception of crude oil spills, and ship's contamination) originate on terrestrial sources and enter the ocean through atmospheric or land-based inputs (see Figure 1.10). These terrestrial inputs include industrial discharges, agricultural and urban runoff, wastewater effluents, and other anthropogenic activities, which can directly enter the marine environment or arrive via riverine systems (Landrigan et al., 2020; Wang et al., 2024a). Three mechanisms of atmospheric deposition govern atmospheric inputs: dry deposition of particle-bound contaminants, wet deposition (which involves the washout of gas and particle-bound contaminants by rain or snow), and diffusive air-water exchange between the gaseous phase in the atmosphere and the dissolved marine phase. (Dachs & Méjanelle, 2010). Unlike the other mechanisms, diffusive exchange is a bidirectional and continuously occurring process. It is driven by the chemical equilibrium between the gas and the dissolved phase, where the contaminant will either volatilize or deposit to reach this equilibrium.

In the oceans, organic contaminant concentrations are in some regions influenced by proximity to source, with the highest concentrations typically occurring near population centers and industrial areas. This is evidenced by the observation of higher concentrations of organic contaminants and POPs in coastal areas close to the anthropogenic sources compared the open ocean and remote areas such as the poles (Gioia et al., 2011; Iwata et al., 1993). Despite exhibiting lower concentrations, the large volume of the oceans and their function as the ultimate sink implies that they play an important role as a global reservoir of organic contaminants (Jurado et al., 2004). However, the technical difficulties and the high costs associated with the use of research vessels and other types of specific infrastructure have resulted in less experimental data about the occurrence and fate of organic contaminants in the open ocean (Gioia et al., 2011).

Although rivers can be important sources of POPs to coastal areas, it is widely accepted that the atmosphere plays a dominant role in inputs to the open ocean, particularly for semi-volatile organic contaminants. Indeed, the atmosphere has been considered the most significant and rapid route of transport for POPs to surface waters (Atlas & Giam, 1981; Dachs & Méjanelle, 2010; Gioia et al., 2011). Among the mechanisms of atmospheric deposition, for those POPs present in the atmosphere predominantly in the gas phase (PCBs, HCHs, LWM PAHs), air-water diffusive exchange constitutes the main mechanism of deposition on a global scale compared to dry and wet deposition (Jurado et al., 2004, 2005). On the contrary, for other heavier compounds with higher affinity to aerosol particles, such as HMW PAHs, dry/wet deposition could be the dominant mechanism of removal from the atmosphere (Gioia et al., 2011; González-Gaya et al., 2014; Jurado et al., 2005). Furthermore, during precipitation events wet deposition is found to be the dominant deposition mechanism, probably due to the great efficiency of rain and snow when scavenging gas- and aerosol-phase organic contaminants (Casas et al., 2021; Jurado et al., 2005).

Regarding organic contaminants with lower volatility and hydrophobicity than traditional POPs, the transport mechanisms to open oceans are not as well elucidated. In the case of PFAS, particularly the ionic PFAAs and its two maximum exponents PFOA and PFOS, their main sources in the marine environment were thought to be mostly terrestrial by wastewater and riverine inputs (Pistocchi & Loos, 2009). However, later studies have highlighted the importance of atmospheric deposition, whose contribution was found to be even 1-2 orders of magnitude greater than that of wastewater treatment plant discharges in the Baltic Sea (Filipovic et al., 2013). The same study also found that riverine input was dominant, similar to reports from the Bohai Sea, where river inflow was the primary source of coastal PFAAs (Du et al., 2022). Once in the ocean, the water solubility of ionic PFAS enables them to be further transported by the oceanic currents (Casal et al., 2017; González-Gaya et al., 2014). Atmospheric transport is also suggested to significantly influence on the long-range transport of PFAS, particularly in remote areas where the influence of oceanic currents is limited (Casal et al., 2019), such as the Antarctic waters, where long-range oceanic transport is thought to be hindered by the Antarctic circumpolar current (Bengtson Nash et al., 2010). Among the atmospheric sources of PFAS, such as the formation in the atmosphere via degradation from volatile precursors, the enrichment of PFAAs in sea spray aerosols (SSA) has been demonstrated to be a significant mechanism of PFAAs remobilization from seawater to air (Sha et al., 2022, 2024). Notably, Casas et al. (2020) found PFAS to be enriched in sea spray aerosol relative to bulk seawater, based on simultaneous field measurements conducted in the Southern Ocean. Additionally, PFAS may undergo long-range atmospheric transport bound to other types of aerosols, such as organic and inorganic particles (Faust, 2023). Altogether, these processes facilitate the transport of PFAS to remote regions.

Regarding the OPEs, the diverse range of physicochemical properties within this class of compounds presents challenges in determining the predominance of one transport mechanism over others. The primary sources of OPEs in marine ecosystems are land-based (Wei et al., 2015). These include atmospheric release from man-made products (e.g., e-waste) and input from rivers. These terrestrial sources contribute to the presence of OPEs in coastal and offshore regions through atmospheric transport and deposition (Castro-Jiménez & Sempéré, 2018), as well as waterborne transport associated with oceanic currents (Schmidt et al., 2019). Furthermore, OPEs are potentially released in situ in marine environments by oceanic plastic debris, representing localized sources of OPEs and other organic plasticizers (Xie et al., 2022). Concerning long-range atmospheric transport and deposition, the atmospheric half-life of organophosphate esters (OPEs) was initially estimated to be insufficient for long-distance travel (Blum et al., 2019). However, several studies have reported environmental data showing occurrence of OPEs in the atmosphere, demonstrating that the most prevalent OPEs indeed undergo atmospheric long-range transport (Castro-Jiménez et al., 2016; J. Li et al., 2017; Möller et al., 2012b). Moreover, atmospheric deposition through air-water exchange has been proposed as the primary input route for OPEs into the environment (Marlina et al., 2024). Experimental data and subsequent estimations indicate that OPEs in the atmosphere have longer lifetimes than previously anticipated (Sührling et al., 2020); however, it remains uncertain whether this is attributable to the presence of atmospheric water or to partitioning to the particle phase (Fu et al., 2021). OPEs can also undergo long-range transport via oceanic currents, where chlorinated OPEs in particular are efficiently transported

due to their persistence, lower volatility, and higher solubility than the non-chlorinated OPEs (Xie et al., 2022). Consequently, a higher abundance of chlorinated-OPEs is commonly reported in the marine environments (Castro-Jiménez & Sempéré, 2018; Xie et al., 2022).

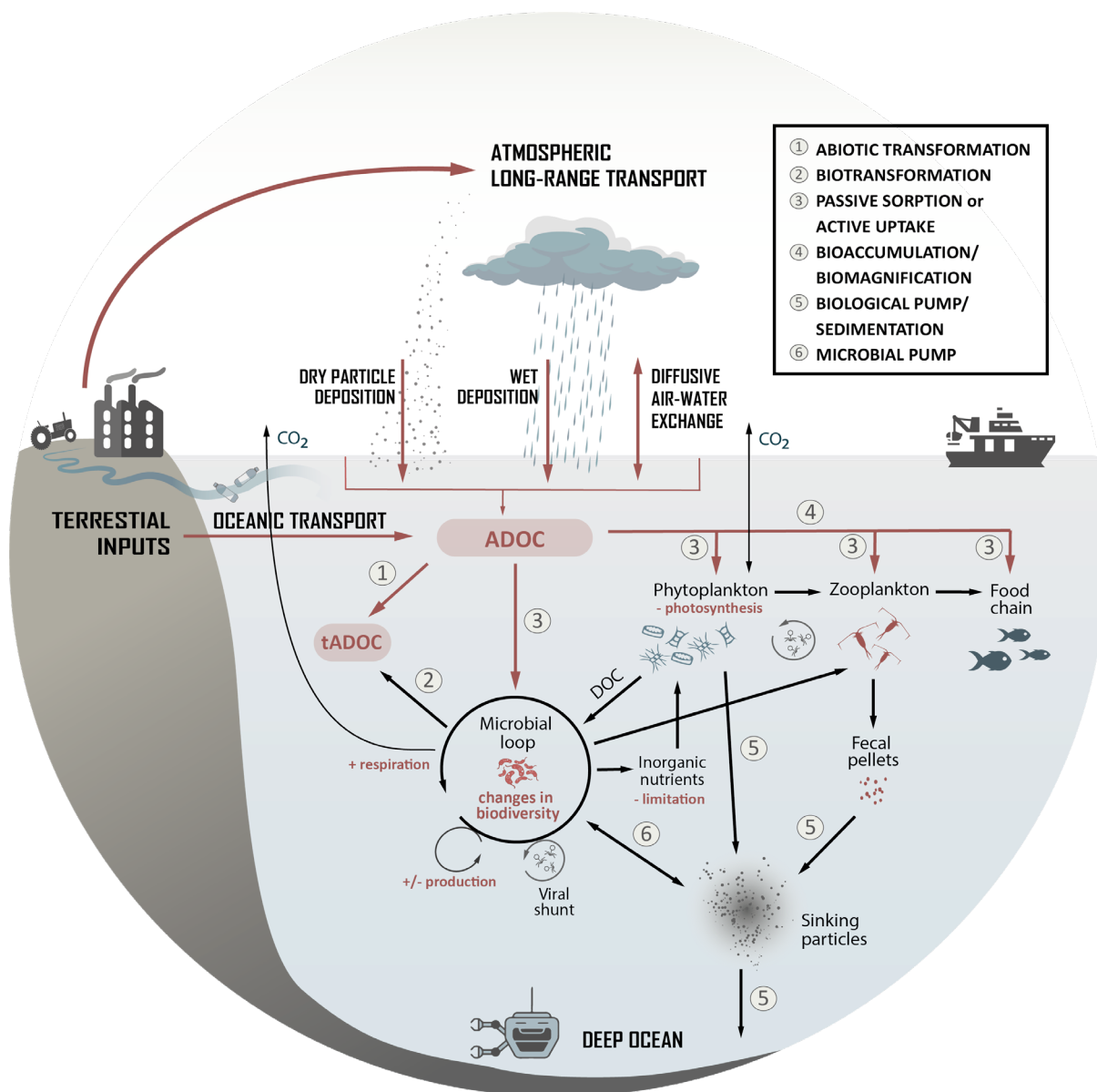


Figure 1.10 Cycling of the organic contaminant pool that comprises the Anthropogenic Dissolved Organic Carbon (ADOC) in the upper layer of the oceans. Red arrows indicate the sources, transport, and transformation processes that ADOC compounds undergo. The transformation products of ADOC resulting from abiotic or biotic processes are referred as tADOC. Black arrows indicate the transformation and sink processes that the overall dissolved organic carbon (DOC) pool, including ADOC, undergoes in the water column. The reported effects of ADOC on marine microbial communities are summarized.

1.3.2 Fate and sinks

Upon entering the ocean, organic contaminants undergo partitioning among various environmental compartments, specifically water, particulate matter, and biota. This partitioning will depend on sorption processes, partitioning coefficients, and additional physicochemical properties specific to each compound, as well as on environmental conditions, such as the amount of suspended particulate matter or water temperature (Galbán-Malagón et al., 2012). Generally, the environmental processes that organic contaminants undergo are linked to the oceanic carbon cycle. In fact, dissolved organic contaminants constitute what has been defined as the anthropogenic dissolved organic carbon (ADOC) pool (Vila-Costa et al., 2020). This complex mixture comprises both man-made synthetic organic chemicals and various organic compounds released into the environment as a consequence of anthropogenic activities.

ADOC compounds in the euphotic zone are depleted through transformation or other sinks, related to abiotic and biotic processes, depending on their persistence. The highly hydrophobic ADOC compounds, such as POPs and PAHs, will preferentially partition into organic matter. This organic matter is present in the particulate phase, either as particles and aggregates of different organic matrices, or as the cells of living organisms, such as phytoplankton (Gioia et al., 2011). Notably, the tendency of hydrophobic ADOC compounds to bioaccumulate in these marine primary producers serves as the principal pathway for ADOC entry into the marine food web, subsequently leading to amplification of concentrations towards higher trophic levels through biomagnification processes (Berrojalbiz et al., 2009; Jamieson et al., 2017; Romero-Romero et al., 2017). Once organic contaminants partition into suspended particles by sorption or passive uptake, they can be removed from the surface waters and delivered to the deep ocean by what is known as the biological pump. The biological pump is defined as the complex ensemble of biophysical processes through which phytoplankton fix carbon dioxide, and a fraction of the resultant organic matter is subsequently exported to the deep ocean by settling particles (e.g., phytoplankton dead cells, organic matter aggregates, zooplankton fecal pellets) (Galbán-Malagón et al., 2012; Sanganyado et al., 2021; Turner, 2015). This important process of the oceanic carbon cycle has the capacity to reduce the dissolved concentrations of organic contaminants in the surface ocean, thereby enhancing the air-to-water flux of pollutants by diffusive exchange, ultimately modulating the atmospheric transport and deposition of these compounds (Dachs et al., 2002; Galbán-Malagón et al., 2012; Gioia et al., 2011; Lohmann et al., 2007; Sanganyado et al., 2021).

However, processes other than the biological pump modulate ADOC concentrations. The less persistent and/or less hydrophobic ADOC compounds are susceptible to transformation and subsequent removal via abiotic processes, such as photodegradation or hydrolysis, and biotic processes, collectively referred to as biotransformation. Even though abiotic degradation, especially photodegradation, may play a role in surface waters, microbial degradation is the main marine sink for many contaminants (González-Gaya, Martínez-Varela, et al., 2019). Microbial communities mediate biotransformation and may result in the complete respiration of certain compounds to CO₂ by heterotrophic microorganisms. Biotransformation and respiration are integrated into the microbial loop, a complex trophic pathway where dissolved organic carbon

(DOC) and nutrients are cycled through bacteria, viruses, protozoa, and their interactions (Fenchel, 2008; Valiela, 2015). Not all the DOC is susceptible of remineralization, and the most recalcitrant fraction of DOC that resists biodegradation is sequestered to the deep ocean by the microbial carbon pump, analogous to the process observed in the biological pump (Buchan et al., 2014). Although the microbial loop is a ubiquitous feature of the global ocean and plays an important role in the marine carbon cycle, its role in the transformation and fate of the ADOC compounds remains poorly characterized, particularly for those CECs with limited environmental research conducted on them (González-Gaya, Casal, et al., 2019).

As Dachs and Méjanelle (2010) stated, “pollutants should be viewed as travelers that will be traveling, and affecting ecosystems during their journey until they are degraded and/or sequestered by the deep ocean”. Therefore, oceans play an important role in determining the transport, fate, and sinks of organic contaminants and their potential impact on the Earth system (Dachs et al., 2002). Acquiring comprehensive data regarding the biotic and abiotic potential of the ocean to modulate global organic contaminant concentrations is essential for conducting accurate modeling and risk assessment of these compounds in the environment. Unfortunately, many of the aspects of these complex issue remain understudied, including the potential of microbial communities to biotransform ADOC compounds, particularly for those CECs that have emerged in recent decades and in remote areas where experimental work is very demanding, such as the open ocean or the polar regions.

1.4 Marine microbial communities

Although they are invisible to the human eye, the huge number of marine microbes (bacteria, viruses, and protists) in the oceans far exceeds all multi-cellular metazoa in abundance, biomass, metabolic activity, and genetic and biochemical diversity (Pomeroy et al., 2007). A single liter of seawater is estimated to contain about one billion of these single-celled organisms, while the total amount of bacteria in the global ocean is estimated to be around 10^{29} (Whitman et al., 1998). The significance of bacteria extends beyond their biomass; their surface area plays a crucial role. While biomass (or volume) determines the maximum potential for metabolism and growth, the cell surface acts as the gateway for all organic and inorganic nutrients, oxygen, and waste products. Consequently, the rate of metabolism per unit of biomass is governed by the relationship between surface area and volume (Pomeroy et al., 2007). Regarding the surface area associated to bacteria in the euphotic zone of the oceans, it is far more overwhelming than their biomass (Figure 1.11). Considering surface area as an indicator of metabolic activity, this observation underscores the significant metabolic role of bacteria in oceanic ecosystems, emphasizing that the oceans are primarily a microbial environment.

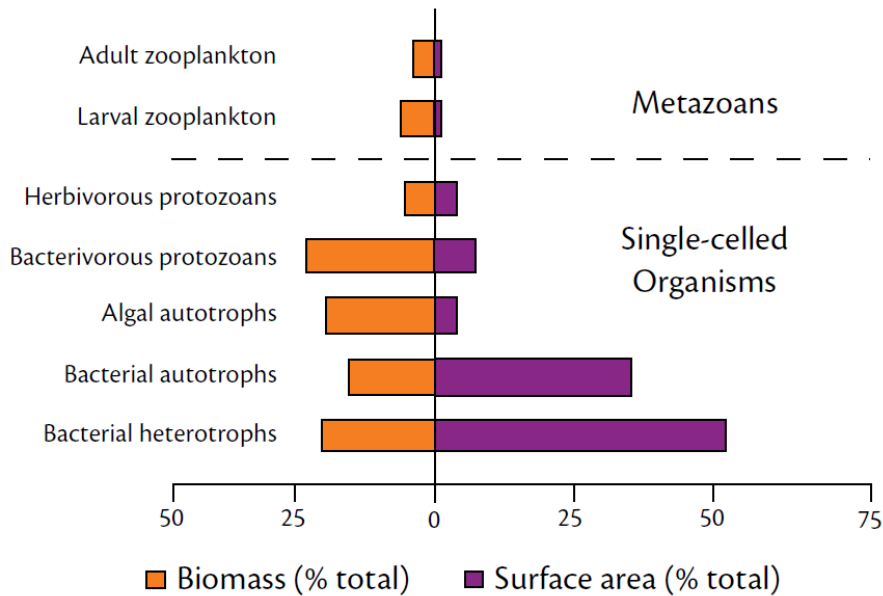


Figure 1.11 Distribution of biomass and calculated surface area (expressed as a percentage of total) for planktonic trophic groups in the euphotic zone of the oceans. The biomass value is a geometric mean of the data from various oceanic areas; surface area is calculated assuming simple spherical geometry. The total biomass for the plankton is 50 mg C m^{-3} and the total surface area is $1.2 \text{ m}^2 \text{ m}^{-3}$. From Pomeroy et al. (2007). Licensed under CC BY 4.0. <https://creativecommons.org/licenses/by/4.0/>

Marine microorganism can be classified depending on the energy and carbon sources they rely on. According to the carbon source, two main groups arise: autotrophs or primary producers, those organisms that rely on the conversion of CO_2 to organic compounds (CO_2 fixation); and heterotrophs or secondary producers, those unable to fix CO_2 that have to use organic carbon compounds. However, this division is not clear since the discovery of marine microorganism able to switch between trophic strategies, known as mixotrophs. These marine microorganisms and their interactions predominantly influence the flux of energy and biologically significant elements in the ocean, thereby maintaining the global ocean and Earth system equilibrium.

Phytoplankton in the photic layer of the ocean are estimated to produce more than 50% of the oxygen on Earth, while they simultaneously sustain the marine food webs by the primary production of organic matter from inorganic CO_2 . However, not all the produced organic matter enters the classic marine food web. Approximately one-half of the carbon fixed by photosynthetic primary producers is released as dissolved organic matter (DOM) and subsequently processed by heterotrophic bacteria (Buchan et al., 2014). These marine microorganisms play a central role in converting DOM and nutrients into particulate organic matter (POM), forms that can be utilized by other organisms in the food web, thus reincorporating them into the food web. This key process, referred to as the microbial loop, allows higher trophic levels to access the pool of organic matter

that was not available for them in the form of DOM, thus sustaining global biogeochemical cycles, ecosystems, and productivity (Y. Li et al., 2014; Okuda et al., 2014).

This microbial loop mediated recycling of DOM (and therefore of the DOC compounds within the DOM pool) and nutrients is the result of the interaction of microorganisms and DOM. Four possible mechanisms of interaction have been described (Kujawinski, 2011; Kujawinski et al., 2016). First, microorganisms can consume and incorporate whole or enzymatically modified molecules into metabolic pathways for biomass synthesis or energy production, resulting in subsequent transfer to higher trophic levels via predation or complete respiration to CO₂ (Kujawinski, 2011). Second, microorganisms can produce and release organic compounds that become part of the DOM as metabolic by-products, exudates (e.g., for nutrient acquisition or chemical defense), or during cell death caused by processes like viral shunt or grazing. This released DOM contains carbon and regenerated inorganic nutrients, such as nitrogen and phosphorus, which are then reutilized by phytoplankton and other bacteria (Pomeroy et al., 2007). Third, microorganisms can transform compounds by enzymatic activity, producing transformation products that remain in the DOM pool. As a result of this transformation, some of the compounds may become recalcitrant to further microbial transformation and be subjected to long-term carbon storage via the microbial carbon pump (Jiao et al., 2010). Lastly, microorganisms may ignore the compound if it has already become refractory due to prior abiotic or biotic alterations (Kujawinski, 2011) (Figure 1.10).

Among the large domain of prokaryotic microorganism that marine bacteria constitute, this thesis will focus on marine heterotrophic bacteria, due to their potential to transform ADOC compounds and their pivotal role in the C global cycling mediating the balance between the production and consumption of organic matter in the ocean (Kim et al., 2023). Depending on the availability of carbon and nutrients and their taxonomy, heterotrophic bacteria show different lifestyles. Those adapted to high-nutrient conditions are known as copiotrophs, whereas those that prefer low-nutrient concentrations are known as oligotrophs (Buchan et al., 2014). Copiotrophs are able to rapidly respond to high-nutrient availability and thrive due to the diverse metabolic capabilities they harbor, while oligotrophs rely on a simpler but less energetically demanding metabolism. Additionally, bacteria can also be divided as free-living (FL) or particle-attached (PA), taking also into account those able to shift between the two lifestyles. Although FL bacteria constitute the majority of marine bacteria in the epipelagic zone, PA bacteria exhibit higher per-cell activities and possess a more diverse metabolic capacity (Urvoy et al., 2022; Wang et al., 2024b). As a result, particles are regarded as hot spots of bacterial activity and organic matter biotransformation (Urvoy et al., 2022).

For many years, the sole method of investigating the biodiversity and metabolic capacities of marine microbes was through the culture and isolation of pure bacterial cultures. However, this approach was later recognized to have a significant bias due to the fact that the majority of marine bacteria are not cultivable (Yilmaz et al., 2016). It was not until the development of molecular techniques that allowed DNA sequencing that the diversity in the naturally occurring bacterial communities began to be understood. PCR amplification of the prokaryotic 16S ribosomal RNA (16S rRNA) gene and subsequent taxonomic classification through bioinformatic

tools is now a widely used approach. More recently, thanks to the drop of sequencing costs, direct DNA sequencing and complete reconstruction of bacterial genomes from metagenomic data, known as metagenome-assembled genomes (MAGs), is also used. This methodology is gaining relevance since it enables not only taxonomic classification but also facilitates the investigation of the potential metabolic capacity of bacterial communities.

Based on the accumulated data, current research indicates that the majority of known marine prokaryotic microorganisms are classified within approximately twelve broad phylogenetic divisions or phyla (Yilmaz et al., 2016). Regarding marine heterotrophic bacteria, bacteria belonging to the *Bacteroidota* phyla or to the *Alphaproteobacteria* or *Gammaproteobacteria* classes of the *Pseudomonadota* (previous *Proteobacteria*) phyla usually dominate bacterial communities (Ruiz-González et al., 2019; Sanz-Sáez et al., 2020). *Alpha*- and *Gammaproteobacteria* in particular encompass thousands of bacterial species, with very diverse metabolic capacities. Despite all the advances in marine microbiology, many unknown marine bacteria remain to be identified, and even for those taxonomically classified, there are still many questions regarding their potential metabolic capacities. Advancing research in this field is therefore essential to better understand the potential of marine microbial communities to interact with organic contaminants and the possible consequences of such interaction.

1.4.1 Role of marine microbes in contaminant fate

Whether because they obtain a metabolic advantage in the form of energy and nutrients, or due to the fortuitous transformation by promiscuous enzymes intended for the metabolic pathway of a different compound – a process known as co-metabolism (Benner et al., 2015; Nzila, 2013) –, biotransformation of organic contaminants by marine microorganisms is a relevant process occurring in the global ocean. Biotransformation does not always result in the complete degradation of a compound (biodegradation), as there are cases where it results in transformation products with higher toxicity and persistence than the original compound (bioactivation; Gerba, 2019). The potential for microbial loop-mediated biotransformation of anthropogenic organic contaminants has been assessed to different extents, depending on the specific chemical or chemical families under study. However, such assessments are usually limited to study acute exposition to high concentrations of contaminants, with the main objective of developing a suitable bioremediation method for heavily contaminated sites. Meanwhile, the potential biotransformation of the pool of compounds that compose ADOC at low background concentrations and under chronic exposure is underestimated, and information regarding the biodegradation rates under these realistic concentrations in the oceans is scarce. The following paragraphs summarize what is known about the environmental biodegradation of PAHs, OPEs, and PFAAs.

PAH biodegradation

PAHs represent an exemplary family of pollutants for which microbial degradation is quite well characterized, with established metabolic pathways and identified key genes (Mallick et al., 2011). This has been motivated by the increasing interest in biological remediation methods for

PAH-contaminated sites. As compounds that can originate from natural sources, or biomass combustion, PAHs have been part of the biogeochemical cycles for millions of years (Henner et al., 1997). As a result, marine microorganisms, predominantly bacteria and archaea, have developed diverse strategies to utilize PAHs as both an energy and carbon source. Predominantly, bacteria exhibit a preference for aerobic conditions in the degradation of PAHs. For the purposes of this thesis, the focus will be on reactions occurring under aerobic conditions.

In the presence of oxygen, PAHs are degraded via oxygenase-mediated metabolism by monooxygenase or dioxygenase enzymes (Ghosal et al., 2016; Patel et al., 2020). Generally, the initial and rate-limiting step is the incorporation of two oxygen molecules into an aromatic ring by the key aromatic ring hydroxylating dioxygenase (ARHD), forming a *cis*-dihydrodiol, which is then rearomatized to a diol intermediate by a dehydrogenase (Figure 1.12). These intermediates may then be cleaved by intradiol or extradiol ring-cleaving dioxygenases, such as the catechol dioxygenase (Duran & Cravo-Laureau, 2016; Ghosal et al., 2016; Mallick et al., 2011). The re-aromatization and ring cleavage reactions will alternate, ultimately leading to aliphatic products that enter the central metabolism via the tricarboxylic acid cycle (Ghosal et al., 2016; Walton & Buchan, 2024). Due to the high conservation and substrate specificity of the alpha subunit of the ARHD enzyme, it has been selected as an appropriate biomarker for investigating PAH degradation functionalities in environmental contexts, and it is frequently utilized (González-Gaya, Martínez-Varela, et al., 2019; S. Li et al., 2022; Walton & Buchan, 2024).

The taxonomic classification of the main bacterial players involved in the degradation of PAHs in the ocean is also quite well studied, particularly due to all the research that has been conducted after oil spills, both in field studies and under controlled laboratory conditions. (Gutierrez et al., 2013; Joye et al., 2014; Kimes et al., 2014). Bacteria with the metabolic capacity to degrade hydrocarbons and use them as substrates are known as hydrocarbonoclastic bacteria (HCB), and PAH degraders are among them (Yakimov et al., 2022). HCB are ubiquitously present in the marine environment, albeit in low abundance, as they are part of the rare biosphere (Kleindienst et al., 2016; Yakimov et al., 2022). However, this fast-growing opportunistic bacterium can bloom following an influx of PAHs or other hydrocarbons, becoming predominant until hydrocarbon exhaustion (Joye et al., 2014; Kimes et al., 2014; Kleindienst et al., 2016; Lozada et al., 2014). Almost all the marine PAH degraders fall within the *Gammaproteobacteria*, and *Alphaproteobacteria* classes, where several bacterial genera with PAH degrading capacity have been characterized, such as *Pseudomonas*, *Cycloclasticus* or *Burkholderia*, and *Sphingomonas*, *Rhodococcus* or *Hyphomonas*, respectively (Y. Huang et al., 2023; Krivoruchko et al., 2023; Q. Liu et al., 2024; Peng et al., 2020; Somee et al., 2022; Vaidya et al., 2017; Wang et al., 2018; Yagi & Madsen, 2009). ARHDs genes have actually been found to be very diverse and widespread among the bacterial tree (Iwai et al., 2010; Kaur et al., 2023; Yagi & Madsen, 2009). Furthermore, it is not common to find all the PAH degradation route genes in individual genomes (Góngora et al., 2024; Somee et al., 2022). Instead, several studies have shown that PAH and hydrocarbon degradation by bacterial consortia is more efficient, which suggests that the removal of these complex mixtures of compounds requires the metabolic capabilities of the whole microbial community (Gallego et al., 2014; Kumari et al., 2018; Vaidya et al., 2017). Consistent with this observation, numerous

genes involved in hydrocarbon degradation are frequently located on plasmids associated with horizontal gene transfer processes (DeBruyn et al., 2012; Q. Liu et al., 2024; Ma et al., 2006), which further enhances the cooperative nature of hydrocarbon degradation.

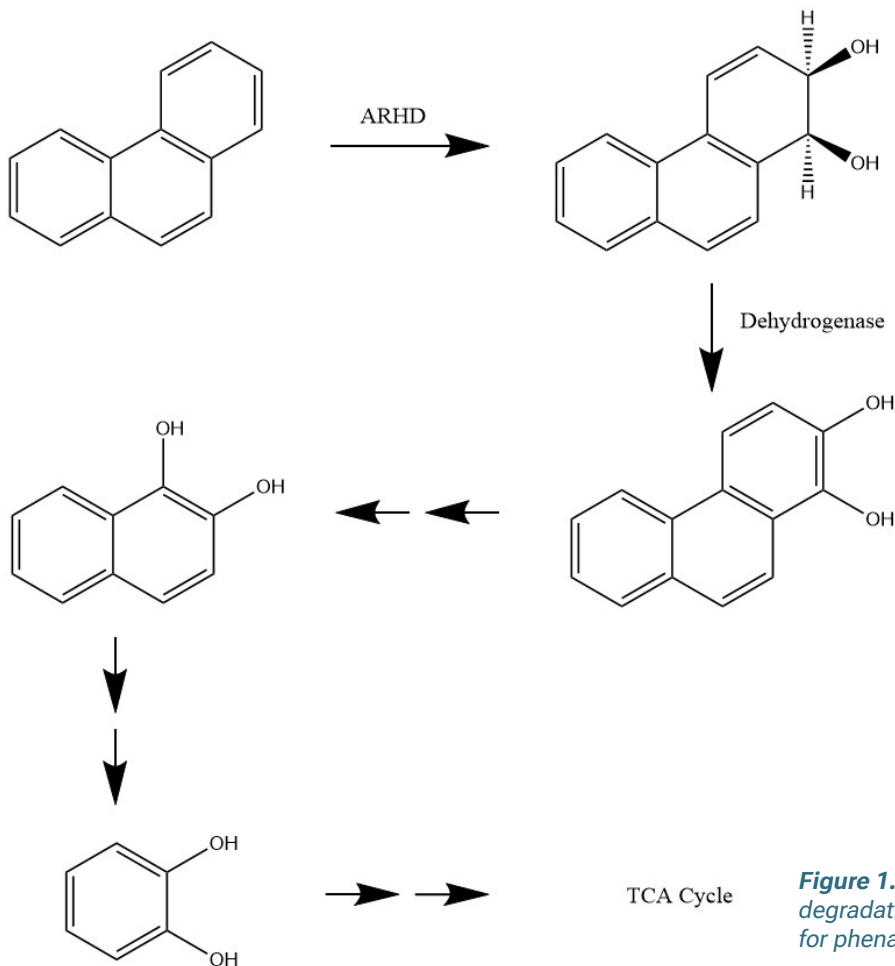


Figure 1.12 Simplified degradation pathway for phenanthrene.

HCB are not only important for PAH elimination after oil spills. González-Gaya et al. (2019) calculated that the integrated sinking flux of PAHs due to the biological pump was two orders of magnitude lower than the atmospheric input. The fact that 99% of the PAH do not settle to the deep ocean suggests that they are being removed by biotic or abiotic processes in the photic zone of the water column. However, after assessing PAH photodegradation by diagnostic ratios, results suggested that microbial degradation is the primary mechanism responsible for depleting the more abundant PAHs within the upper 200 m of the water column (González-Gaya et al., 2019). Microbial degradation is widely recognized as the primary process determining the fate of PAHs in

PAH-contaminated marine environments (Duran & Cravo-Laureau, 2016; Ghosal et al., 2016), and this phenomenon may also apply to the chronic background PAH pollution in the global ocean, or at least to the tropical and subtropical waters studied in (González-Gaya et al., 2019). However, the diversity of the microbial communities exposed to this background PAH concentrations remains poorly addressed. To comprehend how the intricate interplay among environmental factors, chemicals, and microbial communities determines the fate of PAHs in the world's oceans, it is essential to conduct on-site measurements of biodegradation rates, assess the presence of PAH-degrading microbes, and evaluate their metabolic capabilities under real-world conditions.

OPE biodegradation

Environmental degradation processes for OPEs are important since they determine the environmental fate and, thus the potential effects that OPEs will exert on the ecosystems (Xie et al., 2022). Abiotic processes such as hydrolysis and photodegradation in aquatic environments have been assessed, with different degrees of degradation depending on the compound structure, as well as on other environmental parameters, such as pH or dissolved oxygen (Cristale et al., 2017; Su et al., 2016). With respect to biodegradation processes in aquatic ecosystems, limited research has been conducted, particularly concerning the marine environment. Most of the work done regarding bacterial biodegradation has been centered on soil and sediments of highly polluted areas or activated sludge from wastewater treatment plants. Takahashi et al. (2013, 2010) isolated two bacterial strains, belonging to *Sphingobium* sp. and *Sphingomonas* sp., with the ability to remove the chlorinated OPEs TDCPP and TCEP. Regarding degradation of aryl-phosphates, a *Roseobacter* strain (Kawagoshi et al., 2004) and consortia of *Rhodococcus* and *Sphingopyxis* strains have been reported (Wang et al., 2019). Additionally, *Sphingomonas* and *Sphingobium* strains able to degrade the alkyl-OPE TBP have also been reported (J. Liu et al., 2019; Rangu et al., 2014).

Regarding the marine environment, few studies have attempted to address this issue, and all of them have been conducted in the Mediterranean Sea. (Castro-Jiménez et al., 2022) reported higher overall OPE degradation rates under biotic conditions for experiments conducted with coastal sediments from a site with high urban pressure. Biodegradation for seawater experiments has also been reported, where biodegradation of certain OPEs occurred under phosphorus-limited conditions, suggesting their utilization as phosphorus sources (Despotović et al., 2022; Vila-Costa et al., 2019).

The main OPE biodegradation route is thought to be by the cleavage of the ester bond and the formation of the corresponding phenols/alcohols and the ester metabolites (Figure 1.13). This initial step is catalyzed by a particular phosphoesterase, known as phosphotriesterase (PTE). The resulting di- and mono-esters can then be further hydrolyzed by the phosphodiesterases (PDE) and phosphomonoesterases or phosphatases (PME) (Takahashi et al., 2017). Phosphotriesterases capable of hydrolyzing various organophosphate compounds, such as those utilized in pesticides and nerve agents, are well-documented. Nevertheless, the substituents present in OPE flame

retardants and plasticizers exhibit poor leaving group characteristics, resulting in ester bonds that demonstrate resistance to hydrolysis by these common PTEs (Despotović et al., 2022; Wang et al., 2022). PTEs able to degrade OPE flame retardant and plasticizers have been isolated only in a handful of soil bacteria (X. Li, Reheman, et al., 2020; Rangu et al., 2014; Takahashi et al., 2017; Wang et al., 2021b, 2022), while (Despotović et al., 2022) have reported the sole PTE isolated from marine bacteria to date.

In the ocean phosphorus is an essential nutrient, and when inorganic phosphorus is limited, bacteria obtain this nutrient from other forms of dissolved organic phosphorus, mainly phosphomonoesters and diesters, by the use of the phosphatases and phosphodiesterases (Despotović et al., 2022). As a result, phosphatases such as the alkaline phosphatases PhoA and PhoX are widespread in the oceans (Sebastian & Ammerman, 2009; Srivastava et al., 2021). PhoA has even been suggested to be a promiscuous enzyme showing not only phosphatase activity, but also PDE and PTE activities (Srivastava et al., 2021). However, OPE degradation by this type of phosphatases has not been reported yet. The absence of reports regarding oceanic degradation of OPE flame retardants and plasticizers by either PTEs or other phosphatases raises the question of whether bacteria can degrade these anthropogenic compounds and utilize them as alternative phosphorus sources, or if they are unable to metabolize these exogenous compounds, particularly those microbial communities with no previous acute exposure to them.

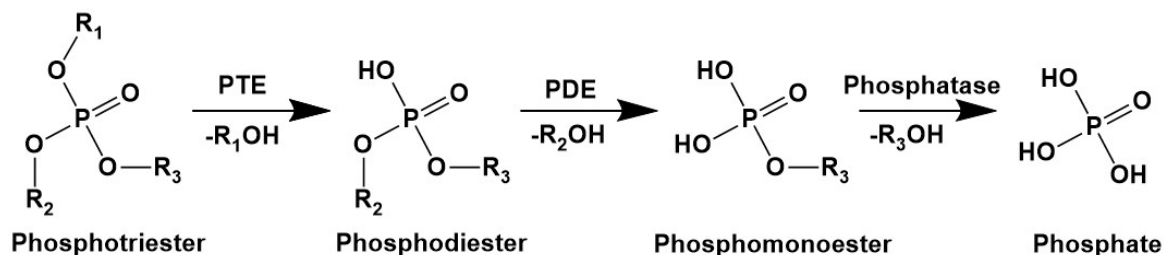


Figure 1.13 Simplified representation of the phosphoesterases-mediated degradation pathway of OPEs.

Alternatively, reactions occurring on the substituents of OPE compounds have been reported, such as methylation or hydroxylation (Yu et al., 2023). This observation raises the question to whether the direct degradation of the aromatic or aliphatic groups is feasible, particularly considering that the metabolic capacity to degrade hydrocarbons is widely distributed in the ocean (Q. Liu et al., 2024). However, despite some studies showing the occurrence of OPE diesters and hydroxylated OPE in marine sediments offshore China's East Coast (Gao et al., 2025; Liang et al., 2024), there is no evidence of such type of reactions occurring in marine environments. Further research is needed to assess the potential of microbial degradation as an oceanic sink of OPEs and to enhance our understanding of the fate of these contaminants in the global ocean.

PFAAs biodegradation

The strong biological and chemical resistance of the PFAS has resulted in their designation as “forever chemicals”. Biodegradation of completely fluorinated compounds such as the PFAAs is very rare, and there are several factors supporting this scarcity. In biology, fluorine is very rare compared to the other halogens. Thousands of chlorinated natural compounds have been identified, and bacteria have naturally developed organochloride metabolism, resulting in chloride that can be used to maintain the physiological chloride balance. On the contrary, only some dozen of fluorine-containing natural compounds are known, and they are singly fluorinated. On top of that, bacteria and other organisms do not use fluoride as they do with the other halogens, and fluoride is highly toxic for bacteria. So, while bacteria have evolved to obtain a physiological advantage of the chlorinated compounds, the metabolism of fluorinated compounds needs additional components without obtaining any cellular benefit from it. The lack of long-exposure to highly fluorinated natural compounds, the absence of selective benefit, and the particular chemistry of fluorine has resulted in PFAS degraders to be a very rare event in natural environments (Wackett, 2021, 2022).

However, there are some recent studies showing that biodegradation is possible, mainly on the heteroatoms of the molecule when present. Huang and Jaffé (2019) found defluorination and the subsequent shortening of the molecule for microbial incubation of PFOA and PFOS with an *Acidimicrobium* strain, and Yu et al. (2020) found defluorination of C₆ polyfluorinated compounds by a microbial consortium. The presence of functional groups in the most commercially abundant PFAS, such as carboxyl or sulfonyl groups in the PFAAs, offers a weaker point to attack than the C-F bonds, resulting in defluorination initiated by radical decarboxylation or radical desulfonation reactions (Figure 1.14; Wackett, 2022). Interestingly, after exposing naturally occurring microbial communities from a seawater flooded volcanic caldera, Cerro-Gálvez et al. (2020) found a significant decrease of PFOS and an increase of transcripts encoding for sulfur metabolism, suggesting desulfurization of PFOS molecules. Nevertheless, no evidence of defluorination was found. In general, the microbial metabolic degradation of heavily fluorinated compounds represents an uncommon phenotype, and, furthermore, the only successful evidence documented demonstrates relatively slow biodegradation rates (Wackett, 2022). Therefore, it seems unlikely that biodegradation plays an important role as an oceanic sink of PFAAs, compared to other vertical transport mechanisms proposed for their removal from the global surface oceans (Casal et al., 2017; González-Gaya, Casal, et al., 2019; Lohmann et al., 2013). Nevertheless, it has been emphasized that continued research into the natural biodegradation of PFAS is essential to identify, and potentially engineer, microorganisms capable of more efficient biodegradation (Wackett, 2022).

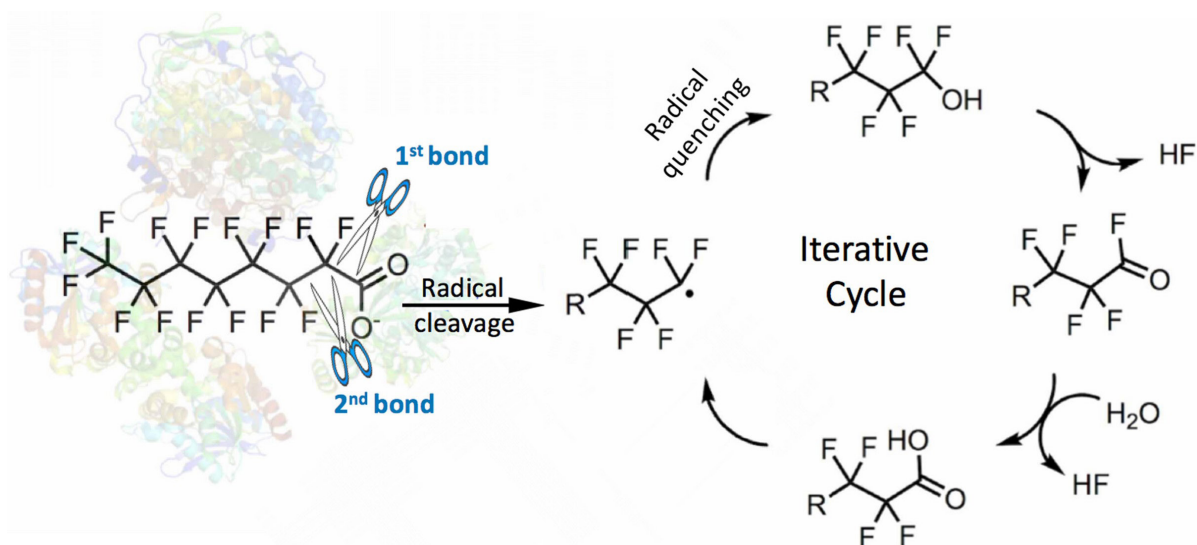


Figure 1.14 Radical decarboxylation proposed mechanism for the complete defluorination of perfluorooctanoate. From (Wackett, 2022). Licensed under CC BY 4.0. <https://creativecommons.org/licenses/by/4.0/>

1.4.2 Potential impact of ADOC on marine microbes

Marine microbial communities respond to changes in the availability, composition, and concentration of DOC and other essential nutrients, even when these variations are minimal (Hutchins & Fu, 2017). Although microbial responses associated with changes in DOC have been investigated (Moran et al., 2016), the potential effects of changes in the ADOC pool remain unexplored, as ADOC is generally considered an insignificant fraction of the DOC. However, despite ADOC concentrations usually being two orders of magnitude lower than DOC in the dissolved phase, the disproportionately hydrophobic nature of ADOC results in large ADOC bioaccumulation in cell membrane lipids, increasing its concentrations to the micromolar range in the particulate phase, at which it may exert potential toxic effects on microorganisms (Vila-Costa et al., 2020). Just by intercalating into the cell membranes, these organic contaminants already cause a baseline toxicity to the cells, termed narcosis. Cellular narcosis is the consequence of the perturbation that hydrophobic organic pollutants induce in the structure and functioning of cellular membranes, which, depending on the strength of the interaction with the membrane, can result in toxic effects that compromise organism viability (Escher et al., 2017; Wezel & Opperhuizen, 1995).

Among the negative impacts of ADOC compounds on marine bacteria, several studies have already addressed the toxic effects that they exert on marine phytoplankton. The observed effects include decrease of cell abundance, loss of viability, growth impairment, and dysregulation of photosynthetic genes, resulting in a reduction of productivity (Echeveste et al., 2010, 2016; Fernández-Pinos et al., 2017; Tetu et al., 2019). Furthermore, after performing a review of studies reporting effects of contaminants on marine ecosystems function, Johnston et al. (2015) concluded that up to 70% of the studies found negative impacts on primary production, reducing productivity and increasing respiration (Figure 1.10). However, most of the studies assessing the toxicity of organic contaminants are performed under experimental conditions that differ from realistic environmental conditions, by only testing isolated cell lines and neglecting the ecological interactions that would occur between the components of naturally occurring microbial communities, or by applying organic contaminants at concentrations significantly higher than those typically found in the environment.

In light of this limitation, a series of studies examined the responses of coastal microbial communities from diverse ecosystems exposed to environmentally relevant concentrations of ADOC, and reported the activation of detoxifying and cell-repair mechanism (Cerro-Gálvez et al., 2019; Cerro-Gálvez et al., 2019; Cerro-Gálvez et al., 2021). They also reported changes in microbial community composition after ADOC exposure, due to the stimulation of bacterial taxa belonging to the rare biosphere. While the presence of ADOC is detrimental for some organisms, those with the metabolic capacity to use them as substrates will obtain a metabolic advantage and thrive, resulting in the observed changes in the overall microbial community composition (Figure 1.15). Actually, ADOC compounds containing heteroatoms such as phosphorus, sulfur or nitrogen may provide an alternative source of these essential and often limited nutrients in addition to carbon and energy, which may result in the dysregulation of the marine trophic regimes and the marine

biogeochemical cycles (Vila-Costa et al., 2020). Although these compounds are generally not the preferred source of nutrients, existing studies report the potential use of ADOC compounds as a nutrient sources under specific conditions, such as OPEs and PFOS for phosphorus and sulfur, respectively (Cerro-Gálvez et al., 2020; Despotović et al., 2022; Vila-Costa et al., 2019).

Although the presence of some ADOC compounds in the marine environment is quite recent, their effects on the microbial communities are already arising. Regardless of the changes in concentrations of individual compounds, the concentrations of the total pool of ADOC compounds are expected to continue rising, subsequently increasing the intensity of ADOC modulation on microbial communities and biogeochemical cycles (Vila-Costa et al., 2020). Due to their chronic exposure it is plausible that given enough time some microbes will eventually develop the metabolic machinery to obtain advantage from them, resulting in the alteration of the biogeochemical cycles as we know. In this scenario, the collection of data regarding ADOC cycling in the environment and its interactions with marine microbial communities becomes imperative, in order to elucidate this vector of global change and implement appropriate risk assessment regulations.

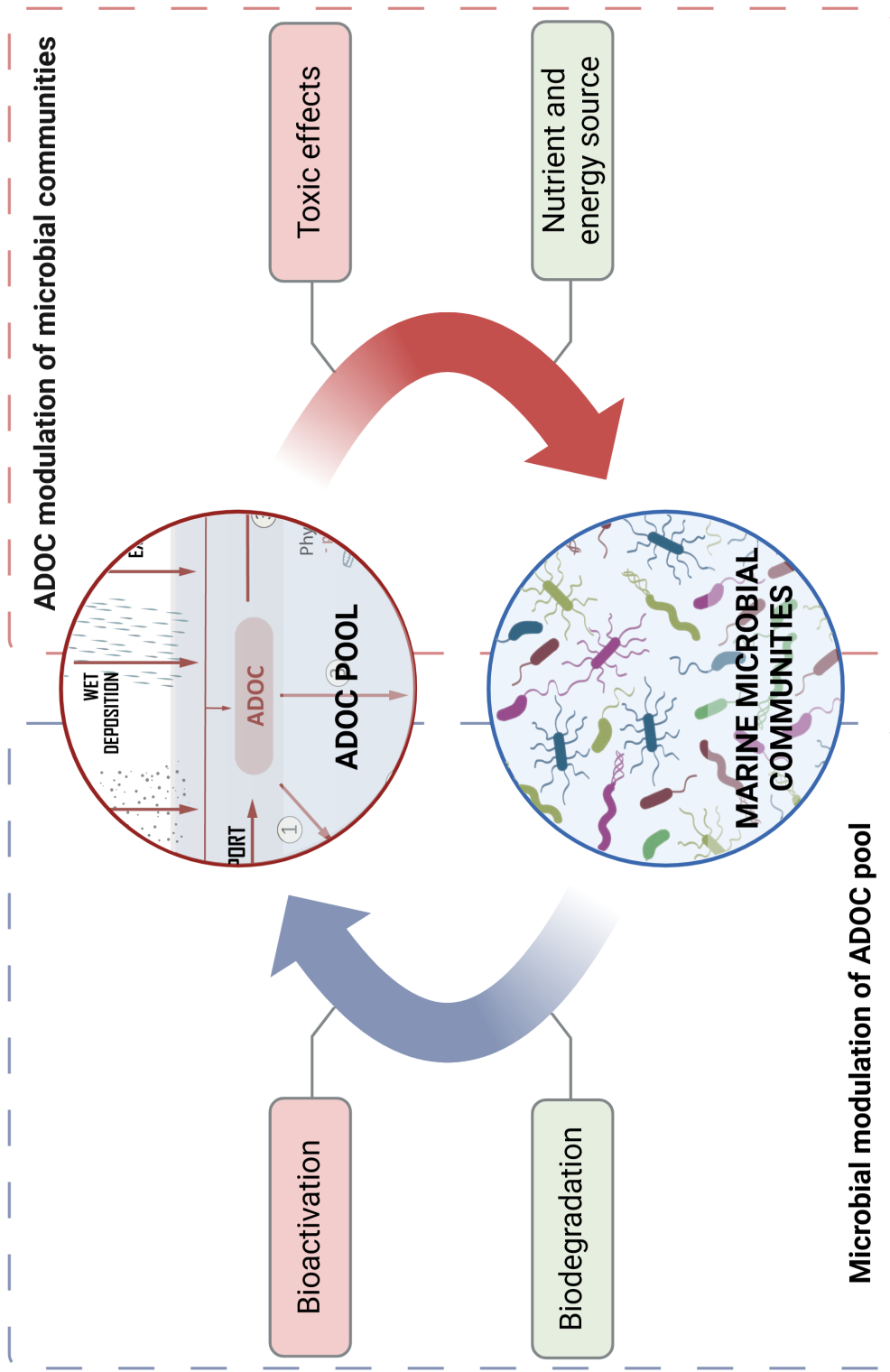


Figure 1.15 Bidirectional interactions between marine microbial communities and organic contaminants constituting the ADOC pool.

1.5 References

- Adams, D. E. C., & Halden, R. U. (2010). Fluorinated Chemicals and the Impacts of Anthropogenic Use (pp. 539–560).
- Ahrens, L., & Bundschuh, M. (2014). Fate and effects of poly- and perfluoroalkyl substances in the aquatic environment: A review. *Environ Toxicol Chem*, 33(9), 1921–1929.
- Ahrens, L., Shoeib, M., Harner, T., Lee, S. C., Guo, R., & Reiner, E. J. (2011). Wastewater Treatment Plant and Landfills as Sources of Polyfluoroalkyl Compounds to the Atmosphere. *Environ Sci Technol*, 45(19), 8098–8105.
- Anderson, D. (2009). Productivism and Ecologism: Changing Discourses in TVET. In *Work, Learning and Sustainable Development* (pp. 35–57). Springer Netherlands.
- Andresen, J. A., Grundmann, A., & Bester, K. (2004). Organophosphorus flame retardants and plasticisers in surface waters. *Science of The Total Environment*, 332(1–3), 155–166.
- Antonopoulou, M., Vlastos, D., Dormousoglou, M., Bouras, S., Varela-Athanasatou, M., & Bekakou, I.-E. (2022). Genotoxic and Toxic Effects of The Flame Retardant Tris(Chloropropyl) Phosphate (TCPP) in Human Lymphocytes, Microalgae and Bacteria. *Toxics*, 10(12), 736.
- Atlas, E., & Giam, C. S. (1981). Global Transport of Organic Pollutants: Ambient Concentrations in the Remote Marine Atmosphere. *Science* (1979), 211(4478), 163–165.
- Back to Blue. (2022). The zero-pollution ocean: A call to close the evidence gap.
- Baskaran, S., & Wania, F. (2023). Applications of the octanol–air partitioning ratio: a critical review. *Environmental Science: Atmospheres*, 3(7), 1045–1065.
- Bengtson Nash, S., Bohlin-Nizzetto, P., Galban-Malagon, C., Corsolini, S., Cincinelli, A., & Lohmann, R. (2023). Monitoring persistent organic chemicals in Antarctica in support of global chemical policy: a horizon scan of priority actions and challenges. *Lancet Planet Health*, 7(5), e435–e440.
- Bengtson Nash, S., Rintoul, S. R., Kawaguchi, S., Staniland, I., Hoff, J. van den, Tierney, M., & Bossi, R. (2010). Perfluorinated compounds in the Antarctic region: Ocean circulation provides prolonged protection from distant sources. *Environmental Pollution*, 158(9), 2985–2991.
- Benner, J., De Smet, D., Ho, A., Kerckhof, F.-M., Vanhaecke, L., Heylen, K., & Boon, N. (2015). Exploring methane-oxidizing communities for the co-metabolic degradation of organic micropollutants. *Appl Microbiol Biotechnol*, 99(8), 3609–3618.
- Bernhardt, E. S., Rosi, E. J., & Gessner, M. O. (2017). Synthetic chemicals as agents of global change. *Front Ecol Environ*, 15(2), 84–90.
- Berrojalbiz, N., Lacorte, S., Calbet, A., Saiz, E., Barata, C., & Dachs, J. (2009). Accumulation and Cycling of Polycyclic Aromatic Hydrocarbons in Zooplankton. *Environ Sci Technol*, 43(7), 2295–2301.
- Beyer, A., & Biziuk, M. (2009). Environmental Fate and Global Distribution of Polychlorinated Biphenyls (pp. 137–158).
- Blum, A., Behl, M., Birnbaum, L. S., Diamond, M. L., Phillips, A., Singla, V., Sipes, N. S., Stapleton, H. M., & Venier, M. (2019). Organophosphate Ester Flame Retardants: Are They a Regrettable Substitution for Polybrominated Diphenyl Ethers? In *Environmental Science and Technology Letters* (Vol. 6, Issue 11, pp. 638–649). American Chemical Society.
- Brooke, D. N., Crookes, M. J., Quarterman, P., & Burns, J. (2009a). Science Report-2-Ethylhexyl diphenyl phosphate. Environment Agency.
- Brooke, D. N., Crookes, M. J., Quarterman, P., & Burns, J. (2009b). Science Report-Tricresyl phosphate. Environment Agency.
- Buchan, A., LeClerc, G. R., Gulvik, C. A., & González, J. M. (2014). Master recyclers: features and functions of bacteria associated with phytoplankton blooms. *Nat Rev Microbiol*, 12(10), 686–698.
- Buck, R. C., Franklin, J., Berger, U., Conder, J. M., Cousins, I. T., de Voogt, P., Jensen, A. A., Kannan, K., Mabury, S. A., & van Leeuwen, S. P. (2011). Perfluoroalkyl and polyfluoroalkyl substances in the environment: Terminology, classification, and origins. *Integr Environ Assess Manag*, 7(4), 513–541.
- Burkhard, L. P. (2000). Estimating Dissolved

Organic Carbon Partition Coefficients for Nonionic Organic Chemicals. *Environ Sci Technol*, 34(22), 4663–4668.

Casal, P., Casas, G., Vila-Costa, M., Cabrerizo, A., Pizarro, M., Jiménez, B., & Dachs, J. (2019). Snow Amplification of Persistent Organic Pollutants at Coastal Antarctica. *Environ Sci Technol*, 53(15), 8872–8882.

Casal, P., González-Gaya, B., Zhang, Y., Reardon, A. J. F., Martin, J. W., Jiménez, B., & Dachs, J. (2017). Accumulation of Perfluoroalkylated Substances in Oceanic Plankton. *Environ Sci Technol*, 51(5), 2766–2775.

Casas, G. (2022). The Antarctic as Sentinel of Global Pollution [Universitat de Barcelona]. <http://hdl.handle.net/2445/188128>

Casas, G., Martínez-Varela, A., Roscales, J. L., Vila-Costa, M., Dachs, J., & Jiménez, B. (2020). Enrichment of perfluoroalkyl substances in the sea-surface microlayer and sea-spray aerosols in the Southern Ocean. *Environmental Pollution*, 267, 115512.

Casas, G., Martínez-Varela, A., Vila-Costa, M., Jiménez, B., & Dachs, J. (2021). Rain Amplification of Persistent Organic Pollutants. *Environ Sci Technol*, 55(19), acs.est.1c03295.

Castro-Jiménez, J., Cuny, P., Milton, C., Sylvi, L., Royer, F., Papillon, L., & Sempéré, R. (2022). Effective degradation of organophosphate ester flame retardants and plasticizers in coastal sediments under high urban pressure. *Sci Rep*, 12(1), 20228.

Castro-Jiménez, J., González-Gaya, B., Pizarro, M., Casal, P., Pizarro-Álvarez, C., & Dachs, J. (2016). Organophosphate Ester Flame Retardants and Plasticizers in the Global Oceanic Atmosphere. *Environ Sci Technol*, 50(23), 12831–12839.

Castro-Jiménez, J., & Sempéré, R. (2018). Atmospheric particle-bound organophosphate ester flame retardants and plasticizers in a North African Mediterranean coastal city (Bizerte, Tunisia). *Science of The Total Environment*, 642, 383–393.

Cerro-Gálvez, E., Casal, P., Lundin, D., Piña, B., Pinhassi, J., Dachs, J., & Vila-Costa, M. (2019). Microbial responses to anthropogenic dissolved organic carbon in the Arctic and Antarctic coastal seawaters. *Environ Microbiol*, 21(4), 1466–1481.

Cerro-Gálvez, E., Dachs, J., Lundin, D.,

Fernández-Pinos, M.-C., Sebastián, M., & Vila-Costa, M. (2021). Responses of Coastal Marine Microbiomes Exposed to Anthropogenic Dissolved Organic Carbon. *Environ Sci Technol*, 55(14), 9609–9621.

Cerro-Gálvez, E., Roscales, J. L., Jiménez, B., Sala, M. M., Dachs, J., & Vila-Costa, M. (2020). Microbial responses to perfluoroalkyl substances and perfluorooctanesulfonate (PFOS) desulfurization in the Antarctic marine environment. *Water Res*, 171, 115434.

Cerro-Gálvez, E., Sala, M. M., Marrasé, C., Gasol, J. M., Dachs, J., & Vila-Costa, M. (2019). Modulation of microbial growth and enzymatic activities in the marine environment due to exposure to organic contaminants of emerging concern and hydrocarbons. *Sci Total Environ*, 678, 486–498.

Chen, M.-H., & Ma, W.-L. (2021). A review on the occurrence of organophosphate flame retardants in the aquatic environment in China and implications for risk assessment. *Science of The Total Environment*, 783, 147064.

Cousins, I. T., Ng, C. A., Wang, Z., & Scheringer, M. (2019). Why is high persistence alone a major cause of concern? *Environ Sci Process Impacts*, 21(5), 781–792.

Cristale, J., Dantas, R. F., De Luca, A., Sans, C., Esplugas, S., & Lacorte, S. (2017). Role of oxygen and DOM in sunlight induced photodegradation of organophosphorous flame retardants in river water. *J Hazard Mater*, 323, 242–249.

Crutzen, P. J., & Stoermer, E. F. (2021). The ‘Anthropocene’ (2000) (pp. 19–21).

Dachs, J., Lohmann, R., Ockenden, W. A., Méjanelle, L., Eisenreich, S. J., & Jones, K. C. (2002). Oceanic Biogeochemical Controls on Global Dynamics of Persistent Organic Pollutants. *Environ Sci Technol*, 36(20), 4229–4237.

Dachs, J., & Méjanelle, L. (2010). Organic Pollutants in Coastal Waters, Sediments, and Biota: A Relevant Driver for Ecosystems During the Anthropocene? *Estuaries and Coasts*, 33(1), 1–14.

de Boer, J., Harrad, S., & Sharkey, M. (2024). The European Regulatory Strategy for flame retardants – The right direction but still a risk of getting lost. *Chemosphere*, 347, 140638.

DeBruyn, J. M., Mead, T. J., & Sayler, G. S. (2012). Horizontal Transfer of PAH Catabolism Genes

in *Mycobacterium*: Evidence from Comparative Genomics and Isolated Pyrene-Degrading Bacteria. *Environ Sci Technol*, 46(1), 99–106.

Despotović, D., Aharon, E., Trofimiyuk, O., Dubovetskiy, A., Cherukuri, K. P., Ashani, Y., Eliason, O., Sperfeld, M., Leader, H., Castelli, A., Fumagalli, L., Savidor, A., Levin, Y., Longo, L. M., Segev, E., & Tawfik, D. S. (2022). Utilization of diverse organophosphorus pollutants by marine bacteria. *Proceedings of the National Academy of Sciences*, 119(32).

Dou, M., & Wang, L. (2023). A review on organophosphate esters: Physiochemical properties, applications, and toxicities as well as occurrence and human exposure in dust environment. *J Environ Manage*, 325, 116601.

Du, D., Lu, Y., Zhou, Y., Zhang, M., Wang, C., Yu, M., Song, S., Cui, H., & Chen, C. (2022). Perfluoroalkyl acids (PFAAs) in water along the entire coastal line of China: Spatial distribution, mass loadings, and worldwide comparisons. *Environ Int*, 169, 107506.

Duran, R., & Cravo-Laureau, C. (2016). Role of environmental factors and microorganisms in determining the fate of polycyclic aromatic hydrocarbons in the marine environment. *FEMS Microbiol Rev*, 40(6), 814–830.

Echeveste, P., Dachs, J., Berrojalbiz, N., & Agustí, S. (2010). Decrease in the abundance and viability of oceanic phytoplankton due to trace levels of complex mixtures of organic pollutants. *Chemosphere*, 81(2), 161–168.

Echeveste, P., Galbán-Malagón, C., Dachs, J., Berrojalbiz, N., & Agustí, S. (2016). Toxicity of natural mixtures of organic pollutants in temperate and polar marine phytoplankton. *Science of The Total Environment*, 571, 34–41.

Escher, B. I., Baumer, A., Bittermann, K., Henneberger, L., König, M., Kühnert, C., & Klüver, N. (2017). General baseline toxicity QSAR for nonpolar, polar and ionisable chemicals and their mixtures in the bioluminescence inhibition assay with *Aliivibrio fischeri*. *Environ Sci Process Impacts*, 19(3), 414–428.

European Chemicals Agency. (2023). Regulatory strategy for flame retardants. European Chemicals Agency.

ECHA. (2018). ECHA Screening Report: an assessment of whether the use of TCEP, TCPP and

TDCP in articles should be restricted. https://echa.europa.eu/documents/10162/13641/screening_report_tcep_tcpp_td-cp_en.pdf/e0960aa7-f703-499c-24ff-fba627060698

European Commission. (2000). WFD (Water Framework Directive). Directive 2000/60/EC of the European Parliament and of the Council of 23 October 2000 establishing a framework for Community action in the field of water policy. *Official Journal of the European Communities*, 327(43), 1–72. <http://data.europa.eu/eli/dir/2000/60/oj>

European Commission. (2008). MSFD (Marine Strategy Framework Directive). Directive 2008/56/EC of the European Parliament and of the Council of 17 June 2008 establishing a framework for community action in the field of marine environmental policy. *Official Journal of the European Communities*. <http://data.europa.eu/eli/dir/2008/56/oj>

Faust, J. A. (2023). PFAS on atmospheric aerosol particles: a review. *Environ Sci Process Impacts*, 25(2), 133–150.

Fenchel, T. (2008). The microbial loop – 25 years later. *J Exp Mar Biol Ecol*, 366(1–2), 99–103.

Fenton, S. E., Ducatman, A., Boobis, A., DeWitt, J. C., Lau, C., Ng, C., Smith, J. S., & Roberts, S. M. (2021). Per- and Polyfluoroalkyl Substance Toxicity and Human Health Review: Current State of Knowledge and Strategies for Informing Future Research. *Environ Toxicol Chem*, 40(3), 606–630.

Fernández-Pinos, M.-C., Vila-Costa, M., Arrieta, J. M., Morales, L., González-Gaya, B., Piña, B., & Dachs, J. (2017). Dysregulation of photosynthetic genes in oceanic *Prochlorococcus* populations exposed to organic pollutants. *Sci Rep*, 7(1), 8029.

Filipovic, M., Berger, U., & McLachlan, M. S. (2013). Mass Balance of Perfluoroalkyl Acids in the Baltic Sea. *Environ Sci Technol*, 47(9), 4088–4095.

Finizio, A., Mackay, D., Bidleman, T., & Harner, T. (1997). Octanol-air partition coefficient as a predictor of partitioning of semi-volatile organic chemicals to aerosols. *Atmos Environ*, 31(15), 2289–2296.

Fu, J., Fu, K., Chen, Y., Li, X., Ye, T., Gao, K., Pan, W., Zhang, A., & Fu, J. (2021). Long-Range Transport, Trophic Transfer, and Ecological Risks of Organophosphate Esters in Remote Areas. *Environ Sci Technol*, 55(15), 10192–10209.

- Galbán-Malagón, C., Berrojalbiz, N., Ojeda, M.-J., & Dachs, J. (2012). The oceanic biological pump modulates the atmospheric transport of persistent organic pollutants to the Arctic. *Nat Commun*, 3(1), 862.
- Gallego, S., Vila, J., Tauler, M., Nieto, J. M., Breugelmans, P., Springael, D., & Grifoll, M. (2014). Community structure and PAH ring-hydroxylating dioxygenase genes of a marine pyrene-degrading microbial consortium. *Biodegradation*, 25(4), 543–556.
- Gao, M., Wang, Y., Wei, L., Li, S., Zhang, Q., Yang, Z., Bai, M., Yao, Y., Wang, L., & Sun, H. (2025). Novel organophosphate esters and their transformation products in offshore sediment from Eastern China: Occurrence, temporal trend, and risk assessment. *Environ Int*, 195, 109205.
- Gerba, C. P. (2019). Environmental Toxicology. In *Environmental and Pollution Science* (pp. 511–540). Elsevier.
- Ghosal, D., Ghosh, S., Dutta, T. K., & Ahn, Y. (2016). Current State of Knowledge in Microbial Degradation of Polycyclic Aromatic Hydrocarbons (PAHs): A Review. *Front Microbiol*, 7(AUG), 1369.
- Gioia, R., Dachs, J., Nizzetto, L., Berrojalbiz, N., Galbán, C., Del Vento, S., Méjanelle, L., & Jones, K. C. (2011). Sources, Transport and Fate of Organic Pollutants in the Oceanic Environment. In *Persistent Pollution – Past, Present and Future* (pp. 111–139). Springer Berlin Heidelberg.
- Glüge, J., Scheringer, M., Cousins, I. T., DeWitt, J. C., Goldenman, G., Herzke, D., Lohmann, R., Ng, C. A., Trier, X., & Wang, Z. (2020). An overview of the uses of per- and polyfluoroalkyl substances (PFAS). *Environ Sci Process Impacts*, 22(12), 2345–2373.
- Góngora, E., Lirette, A.-O., Freyria, N. J., Greer, C. W., & Whyte, L. G. (2024). Metagenomic survey reveals hydrocarbon biodegradation potential of Canadian high Arctic beaches. *Environ Microbiome*, 19(1), 72.
- González-Gaya, B., Casal, P., Jurado, E., Dachs, J., & Jiménez, B. (2019). Vertical transport and sinks of perfluoroalkyl substances in the global open ocean. *Environ Sci Process Impacts*, 21(11), 1957–1969.
- González-Gaya, B., Dachs, J., Roscales, J. L., Caballero, G., & Jiménez, B. (2014). Perfluoroalkylated Substances in the Global Tropical and Subtropical Surface Oceans. *Environ Sci Technol*, 48(22), 13076–13084.
- González-Gaya, B., Martínez-Varela, A., Vila-Costa, M., Casal, P., Cerro-Gálvez, E., Berrojalbiz, N., Lundin, D., Vidal, M., Mompeán, C., Bode, A., Jiménez, B., & Dachs, J. (2019). Biodegradation as an important sink of aromatic hydrocarbons in the oceans. *Nature Geoscience* 2019 12:2, 12(2), 119–125.
- Greaves, A. K., & Letcher, R. J. (2017). A Review of Organophosphate Esters in the Environment from Biological Effects to Distribution and Fate. *Bull Environ Contam Toxicol*, 98(1), 2–7.
- Gruber, N., Clement, D., Carter, B. R., Feely, R. A., van Heuven, S., Hoppema, M., Ishii, M., Key, R. M., Kozyr, A., Lauvset, S. K., Lo Monaco, C., Mathis, J. T., Murata, A., Olsen, A., Perez, F. F., Sabine, C. L., Tanhua, T., & Wanninkhof, R. (2019). The oceanic sink for anthropogenic CO₂ from 1994 to 2007. *Science* (1979), 363(6432), 1193–1199.
- Gutierrez, T., Singleton, D. R., Berry, D., Yang, T., Aitken, M. D., & Teske, A. (2013). Hydrocarbon-degrading bacteria enriched by the Deepwater Horizon oil spill identified by cultivation and DNA-SIP. *ISME J*, 7(11), 2091–2104.
- Halpern, B. S., Frazier, M., Afflerbach, J., Lowndes, J. S., Micheli, F., O'Hara, C., Scarborough, C., & Selkoe, K. A. (2019). Recent pace of change in human impact on the world's ocean. *Sci Rep*, 9(1), 11609.
- Harmon, S. M. (2015). The Toxicity of Persistent Organic Pollutants to Aquatic Organisms. In *Comprehensive Analytical Chemistry* (Vol. 67, pp. 587–613). Elsevier.
- Hatje, V., Sarin, M., Sander, S. G., Omanović, D., Ramachandran, P., Völker, C., Barra, R. O., & Tagliabue, A. (2022). Emergent interactive effects of climate change and contaminants in coastal and ocean ecosystems. *Front Mar Sci*, 9.
- Henner, P., Schiavon, M., Morel, J.-L., & Lichtfouse, E. (1997). Polycyclic aromatic hydrocarbon (PAH) occurrence and remediation methods. *Analisis*, 25(9–10), M56–M59.
- Honda, M., & Suzuki, N. (2020). Toxicities of Polycyclic Aromatic Hydrocarbons for Aquatic Animals. *Int J Environ Res Public Health*, 17(4), 1363.
- Hong, X., Chen, R., Hou, R., Yuan, L., & Zha,

- J. (2018). Triphenyl Phosphate (TPHP)-Induced Neurotoxicity in Adult Male Chinese Rare Minnows (*Gobiocypris rarus*). *Environ Sci Technol*, acs.est.8b04079.
- Hu, W., Gao, P., Wang, L., & Hu, J. (2023). Endocrine disrupting toxicity of aryl organophosphate esters and mode of action. In *Critical Reviews in Environmental Science and Technology* (Vol. 53, Issue 1, pp. 1–18). Taylor and Francis Ltd.
- Huang, S., & Jaffé, P. R. (2019). Defluorination of Perfluorooctanoic Acid (PFOA) and Perfluorooctane Sulfonate (PFOS) by *Acidimicrobium* sp. Strain A6. *Environ Sci Technol*, 53(19), 11410–11419.
- Huang, Y., Li, L., Yin, X., & Zhang, T. (2023). Polycyclic aromatic hydrocarbon (PAH) biodegradation capacity revealed by a genome-function relationship approach. *Environ Microbiome*, 18(1), 39.
- Hubbert, M. K. (1949). Energy from Fossil Fuels. *Science* (1979), 109(2823), 103–109.
- Hutchins, D. A., & Fu, F. (2017). Microorganisms and ocean global change. *Nat Microbiol*, 2(6), 17058.
- IARC Working Group on the Evaluation of Carcinogenic Risks to Humans. (2010). Some non-heterocyclic polycyclic aromatic hydrocarbons and some related exposures. *IARC Monogr Eval Carcinog Risks Hum*, 92, 1–853. <http://www.ncbi.nlm.nih.gov/pubmed/21141735>
- IPCC (Intergovernmental Panel on Climate Change). (2019). Special Report on the Ocean and Cryosphere in a Changing Climate. <https://www.ipcc.ch/srocc/>
- ITRC (Interstate Technology & Regulatory Council). (2023). PFAS Technical and Regulatory Guidance Document and Fact Sheets. <https://pfas-1.itrcweb.org/>
- Iwai, S., Chai, B., Sul, W. J., Cole, J. R., Hashsham, S. A., & Tiedje, J. M. (2010). Gene-targeted-metagenomics reveals extensive diversity of aromatic dioxygenase genes in the environment. *ISME J*, 4(2), 279–285.
- Iwata, H., Tanabe, S., Sakai, N., & Tatsukawa, R. (1993). Distribution of persistent organochlorines in the oceanic air and surface seawater and the role of ocean on their global transport and fate. *Environ Sci Technol*, 27(6), 1080–1098.
- Jamieson, A. J., Malkocs, T., Piertney, S. B., Fujii, T., & Zhang, Z. (2017). Bioaccumulation of persistent organic pollutants in the deepest ocean fauna. *Nat Ecol Evol*, 1(3), 0051.
- Jiao, N., Herndl, G. J., Hansell, D. A., Benner, R., Kattner, G., Wilhelm, S. W., Kirchman, D. L., Weinbauer, M. G., Luo, T., Chen, F., & Azam, F. (2010). Microbial production of recalcitrant dissolved organic matter: long-term carbon storage in the global ocean. *Nat Rev Microbiol*, 8(8), 593–599.
- Joa, K., Panova, E., Irha, N., Teinemaa, E., Lintelmann, J., & Kirso, U. (2009). Determination of polycyclic aromatic hydrocarbons (PAHs) in oil shale processing wastes: current practice and new trends. *Oil Shale*, 26(1), 59.
- Johnston, E. L., Mayer-Pinto, M., & Crowe, T. P. (2015). REVIEW: Chemical contaminant effects on marine ecosystem functioning. *Journal of Applied Ecology*, 52(1), 140–149.
- Joye, S. B., Teske, A. P., & Kostka, J. E. (2014). Microbial Dynamics Following the Macondo Oil Well Blowout across Gulf of Mexico Environments. *Bioscience*, 64(9), 766–777.
- Jurado, E., Jaward, F., Lohmann, R., Jones, K. C., Simó, R., & Dachs, J. (2005). Wet Deposition of Persistent Organic Pollutants to the Global Oceans. *Environ Sci Technol*, 39(8), 2426–2435.
- Jurado, E., Lohmann, R., Meijer, S., Jones, K. C., & Dachs, J. (2004). Latitudinal and seasonal capacity of the surface oceans as a reservoir of polychlorinated biphenyls. *Environmental Pollution*, 128(1–2), 149–162.
- Kang, H.-J., Lee, S.-Y., & Kwon, J.-H. (2016). Physico-chemical properties and toxicity of alkylated polycyclic aromatic hydrocarbons. *J Hazard Mater*, 312, 200–207.
- Kaur, T., Lakhawat, S. S., Kumar, V., Sharma, V., Neeraj, R. R. K., & Sharma, P. K. (2023). Polyaromatic Hydrocarbon Specific Ring Hydroxylating Dioxygenases: Diversity, Structure, Function, and Protein Engineering. *Curr Protein Pept Sci*, 24(1), 7–21.
- Kawagoshi, Y., Nakamura, S., Nishio, T., & Fukunaga, I. (2004). Isolation of Aryl-Phosphate Ester-Degrading Bacterium from Leachate of a Sea-Based Waste Disposal Site. In *JOURNAL OF BIOSCIENCE AND BIOENGINEERING* (Vol. 98, Issue 6).

- Kim, H. H., Laufkötter, C., Lovato, T., Doney, S. C., & Ducklow, H. W. (2023). Projected 21st-century changes in marine heterotrophic bacteria under climate change. *Front Microbiol*, 14.
- Kimes, N. E., Callaghan, A. V., Suflita, J. M., & Morris, P. J. (2014). Microbial transformation of the Deepwater Horizon oil spill—past, present, and future perspectives. *Front Microbiol*, 5, 603.
- Kleindienst, S., Grim, S., Sogin, M., Bracco, A., Crespo-Medina, M., & Joye, S. B. (2016). Diverse, rare microbial taxa responded to the Deepwater Horizon deep-sea hydrocarbon plume. *ISME J*, 10(2), 400–415.
- Krivoruchko, A., Kuyukina, M., Peshkur, T., Cunningham, C. J., & Ivshina, I. (2023). Rhodococcus Strains from the Specialized Collection of Alkanotrophs for Biodegradation of Aromatic Compounds. *Molecules*, 28(5), 2393.
- Kujawinski, E. B. (2011). The Impact of Microbial Metabolism on Marine Dissolved Organic Matter. *Ann Rev Mar Sci*, 3(1), 567–599.
- Kujawinski, E. B., Longnecker, K., Barott, K. L., Weber, R. J. M., & Kido Soule, M. C. (2016). Microbial Community Structure Affects Marine Dissolved Organic Matter Composition. *Front Mar Sci*, 3.
- Kumari, S., Regar, R. K., & Manickam, N. (2018). Improved polycyclic aromatic hydrocarbon degradation in a crude oil by individual and a consortium of bacteria. *Bioresour Technol*, 254, 174–179.
- LaGrega, M. D., Buckingham, P. L., & Evans, J. C. (2001). *Hazardous Waste Management* (2nd edition). McGraw-Hill.
- Landrigan, P. J., Stegeman, J. J., Fleming, L. E., Allemand, D., Anderson, D. M., Backer, L. C., Brucker-Davis, F., Chevalier, N., Corra, L., Czerucka, D., Bottein, M.-Y. D., Demeneix, B., Depledge, M., Deheyn, D. D., Dorman, C. J., Fénichel, P., Fisher, S., Gaill, F., Galgani, F., ... Rampal, P. (2020). Human Health and Ocean Pollution. *Ann Glob Health*, 86(1), 151.
- Lawal, A. T. (2017). Polycyclic aromatic hydrocarbons. A review. *Cogent Environ Sci*, 3(1), 1339841.
- Lehndorff, E., & Schwark, L. (2009). Biomonitoring airborne parent and alkylated three-ring PAHs in the Greater Cologne Conurbation I: Temporal accumulation patterns. *Environmental Pollution*, 157(4), 1323–1331.
- Li, J., Xie, Z., Mi, W., Lai, S., Tian, C., Emeis, K. C., & Ebinghaus, R. (2017). Organophosphate Esters in Air, Snow, and Seawater in the North Atlantic and the Arctic. *Environ Sci Technol*, 51(12), 6887–6896.
- Li, R., Gao, H., Hou, C., Fu, J., Shi, T., Wu, Z., Jin, S., Yao, Z., Na, G., & Ma, X. (2023). Occurrence, source, and transfer fluxes of organophosphate esters in the South Pacific and Fildes Peninsula, Antarctic. *Science of the Total Environment*, 894.
- Li, S., Shen, W., Lian, S., Wu, Y., Qu, Y., & Deng, Y. (2022). DARHD: A sequence database for aromatic ring-hydroxylating dioxygenase analysis and primer evaluation. *J Hazard Mater*, 436, 129230.
- Li, X., Reheman, A., Wu, W., Wang, D., Wang, J., Jia, Y., & Yan, Y. (2020). The genome analysis of halotolerant *Sphingobium yanoikuyae* YC-XJ2 with aryl organophosphorus flame retardants degrading capacity and characteristics of related phosphotriesterase. *Int Biodeterior Biodegradation*, 155, 105064.
- Li, X., Zhao, N., Fu, J., Liu, Y., Zhang, W., Dong, S., Wang, P., Su, X., & Fu, J. (2020). Organophosphate Diesters (Di-OPEs) Play a Critical Role in Understanding Global Organophosphate Esters (OPEs) in Fishmeal. *Environ Sci Technol*, 54(19), 12130–12141.
- Li, Y., Gal, G., Makler-Pick, V., Waite, A. M., Bruce, L. C., & Hipsey, M. R. (2014). Examination of the role of the microbial loop in regulating lake nutrient stoichiometry and phytoplankton dynamics. *Biogeosciences*, 11(11), 2939–2960.
- Liang, C., He, Y., Mo, X.-J., Guan, H.-X., & Liu, L.-Y. (2024). Universal occurrence of organophosphate tri-esters and di-esters in marine sediments: Evidence from the Okinawa Trough in the East China Sea. *Environ Res*, 248, 118308.
- Liu, J., Lin, H., Dong, Y., & Li, B. (2019). Elucidating the biodegradation mechanism of tributyl phosphate (TBP) by *Sphingomonas* sp. isolated from TBP-contaminated mine tailings. *Environmental Pollution*, 250, 284–291.
- Liu, J.-X., Cui, D.-L., Yang, D.-L., Li, J.-Y., Yang, Z.-Y., Su, J.-Z., Ren, C.-X., Niu, Y.-Y., & Xiang, P. (2022). Organophosphorus Flame Retardant TCPP Induces Cellular Senescence in Normal Human Skin Keratinocytes: Implication for Skin Aging. *Int J Mol Sci*, 23(22), 14306.

- Liu, Q., Peng, Y., Liao, J., Liu, X., Peng, J., Wang, J.-H., & Shao, Z. (2024). Broad-spectrum hydrocarbon-degrading microbes in the global ocean metagenomes. *Sci Total Environ*, 926, 171746.
- Llanos, E. J., Leal, W., Luu, D. H., Jost, J., Stadler, P. F., & Restrepo, G. (2019). Exploration of the chemical space and its three historical regimes. *Proceedings of the National Academy of Sciences*, 116(26), 12660–12665.
- Lohmann, R., Breivik, K., Dachs, J., & Muir, D. (2007). Global fate of POPs: Current and future research directions. *Environmental Pollution*, 150(1), 150–165.
- Lohmann, R., Jurado, E., Dijkstra, H. A., & Dachs, J. (2013). Vertical eddy diffusion as a key mechanism for removing perfluorooctanoic acid (PFOA) from the global surface oceans. *Environmental Pollution*, 179, 88–94.
- Lozada, M., Marcos, M. S., Commendatore, M. G., Gil, M. N., & Dionisi, H. M. (2014). The Bacterial Community Structure of Hydrocarbon-Polluted Marine Environments as the Basis for the Definition of an Ecological Index of Hydrocarbon Exposure. *Microbes Environ*, 29(3), 269–276.
- Lux, K. (2003). The failure of the profit motive. *Ecological Economics*, 44(1), 1–9.
- Ma, Y., Wang, L., & Shao, Z. (2006). *Pseudomonas*, the dominant polycyclic aromatic hydrocarbon-degrading bacteria isolated from Antarctic soils and the role of large plasmids in horizontal gene transfer. *Environ Microbiol*, 8(3), 455–465.
- Mackay, D., Shiu, W.-Y., Shiu, W.-Y., & Lee, S. C. (2006). *Handbook of Physical-Chemical Properties and Environmental Fate for Organic Chemicals*. CRC Press.
- Mallick, S., Chakraborty, J., & Dutta, T. K. (2011). Role of oxygenases in guiding diverse metabolic pathways in the bacterial degradation of low-molecular-weight polycyclic aromatic hydrocarbons: A review. *Crit Rev Microbiol*, 37(1), 64–90.
- Manzetti, S., van der Spoel, E. R., & van der Spoel, D. (2014). Chemical Properties, Environmental Fate, and Degradation of Seven Classes of Pollutants. *Chem Res Toxicol*, 27(5), 713–737.
- Marlina, N., Hassan, F., Chao, H.-R., Latif, M. T., Yeh, C.-F., Horie, Y., Shiu, R.-F., Hsieh, Y.-K., & Jiang, J.-J. (2024). Organophosphate esters in water and air: A minireview of their sources, occurrence, and air–water exchange. *Chemosphere*, 356, 141874.
- Mojiri, A., Zhou, J. L., Ohashi, A., Ozaki, N., & Kindaichi, T. (2019). Comprehensive review of polycyclic aromatic hydrocarbons in water sources, their effects and treatments. *Science of The Total Environment*, 696, 133971.
- Möller, A., Sturm, R., Xie, Z., Cai, M., He, J., & Ebinghaus, R. (2012a). Organophosphorus Flame Retardants and Plasticizers in Airborne Particles over the Northern Pacific and Indian Ocean toward the Polar Regions: Evidence for Global Occurrence. *Environ Sci Technol*, 46(6), 3127–3134.
- Möller, A., Sturm, R., Xie, Z., Cai, M., He, J., & Ebinghaus, R. (2012b). Organophosphorus Flame Retardants and Plasticizers in Airborne Particles over the Northern Pacific and Indian Ocean toward the Polar Regions: Evidence for Global Occurrence. *Environ Sci Technol*, 46(6), 3127–3134.
- Moran, M. A., Kujawinski, E. B., Stubbins, A., Fatland, R., Aluwihare, L. I., Buchan, A., Crump, B. C., Dorrestein, P. C., Dyhrman, S. T., Hess, N. J., Howe, B., Longnecker, K., Medeiros, P. M., Niggemann, J., Obernosterer, I., Repeta, D. J., & Waldbauer, J. R. (2016). Deciphering ocean carbon in a changing world. *Proceedings of the National Academy of Sciences*, 113(12), 3143–3151.
- Mudlaff, M., Sosnowska, A., Gorb, L., Bulawska, N., Jagiello, K., & Puzyn, T. (2024). Environmental impact of PFAS: Filling data gaps using theoretical quantum chemistry and QSPR modeling. *Environ Int*, 185, 108568.
- Muir, D. C. G., & Howard, P. H. (2006). Are There Other Persistent Organic Pollutants? A Challenge for Environmental Chemists. *Environ Sci Technol*, 40(23), 7157–7166.
- Nakayama, S. F., Yoshikane, M., Onoda, Y., Nishihama, Y., Iwai-Shimada, M., Takagi, M., Kobayashi, Y., & Isobe, T. (2019). Worldwide trends in tracing poly- and perfluoroalkyl substances (PFAS) in the environment. *TrAC Trends in Analytical Chemistry*, 121, 115410.
- Nevile, J. W. (2016). The Root of All Evil. In *Post-Keynesian Essays from Down Under Volume III: Essays on Ethics, Social Justice and Economics* (pp. 24–33). Palgrave Macmillan UK.
- Nzila, A. (2013). Update on the cometabolism

of organic pollutants by bacteria. *Environmental Pollution*, 178, 474–482.

Odabasi, M., Cetin, E., & Sofuoglu, A. (2006). Determination of octanol–air partition coefficients and supercooled liquid vapor pressures of PAHs as a function of temperature: Application to gas–particle partitioning in an urban atmosphere. *Atmos Environ*, 40(34), 6615–6625.

Okuda, N., Watanabe, K., Fukumori, K., Nakano, S., & Nakazawa, T. (2014). Biodiversity Researches on Microbial Loop in Aquatic Systems (pp. 51–67).

Patel, A. B., Shaikh, S., Jain, K. R., Desai, C., & Madamwar, D. (2020). Polycyclic Aromatic Hydrocarbons: Sources, Toxicity, and Remediation Approaches. *Front Microbiol*, 11(November).

Peng, T., Kan, J., Hu, J., & Hu, Z. (2020). Genes and novel sRNAs involved in PAHs degradation in marine bacteria *Rhodococcus* sp. P14 revealed by the genome and transcriptome analysis. *3 Biotech*, 10(3), 140.

Persson, L., Carney Almroth, B. M., Collins, C. D., Cornell, S., de Wit, C. A., Diamond, M. L., Fantke, P., Hassellöv, M., MacLeod, M., Ryberg, M. W., Søgaard Jørgensen, P., Villarrubia-Gómez, P., Wang, Z., & Hauschild, M. Z. (2022). Outside the Safe Operating Space of the Planetary Boundary for Novel Entities. *Environ Sci Technol*, 56(3), 1510–1521.

Petit, J. R., Jouzel, J., Raynaud, D., Barkov, N. I., Barnola, J.-M., Basile, I., Bender, M., Chappellaz, J., Davis, M., Delaygue, G., Delmotte, M., Kotlyakov, V. M., Legrand, M., Lipenkov, V. Y., Lorius, C., Pépin, L., Ritz, C., Saltzman, E., & Stievenard, M. (1999). Climate and atmospheric history of the past 420,000 years from the Vostok ice core, Antarctica. *Nature*, 399(6735), 429–436.

Pistocchi, A., & Loos, R. (2009). A Map of European Emissions and Concentrations of PFOS and PFOA. *Environ Sci Technol*, 43(24), 9237–9244.

Pomeroy, L. R., leB. Williams, P. J., Azam, F., & Hobbie, J. E. (2007). The Microbial Loop. *Oceanography*, 20(2), 28–33. <http://www.jstor.org/stable/24860040>

Prevedouros, K., Cousins, I. T., Buck, R. C., & Korzeniowski, S. H. (2006). Sources, Fate and Transport of Perfluorocarboxylates. *Environ Sci Technol*, 40(1), 32–44.

Rangu, S. S., Muralidharan, B., Tripathi,

S. C., & Apte, S. K. (2014). Tributyl phosphate biodegradation to butanol and phosphate and utilization by a novel bacterial isolate, *Sphingobium* sp. strain RSMS. *Appl Microbiol Biotechnol*, 98(5), 2289–2296.

Ravindra, K., Sokhi, R., & Van Grieken, R. (2008). Atmospheric polycyclic aromatic hydrocarbons: Source attribution, emission factors and regulation. *Atmos Environ*, 42(13), 2895–2921.

Regulation 2023/915. (2023). COMMISSION REGULATION (EU) 2023/915 on maximum levels for certain contaminants in food and repealing Regulation (EC) No 1881/2006. <http://data.europa.eu/eli/reg/2023/915/2024-07-22>

Richardson, K., Steffen, W., Lucht, W., Bendtsen, J., Cornell, S. E., Donges, J. F., Drüke, M., Fetzer, I., Bala, G., von Bloh, W., Feulner, G., Fiedler, S., Gerten, D., Gleeson, T., Hofmann, M., Huiskamp, W., Kumm, M., Mohan, C., Nogués-Bravo, D., ... Rockström, J. (2023). Earth beyond six of nine planetary boundaries. *Sci Adv*, 9(37).

Rocha, A. C., & Palma, C. (2019). Source identification of polycyclic aromatic hydrocarbons in soil sediments: Application of different methods. *Science of The Total Environment*, 652, 1077–1089.

Rockström, J., Steffen, W., Noone, K., Persson, Å., Chapin, F. S., Lambin, E. F., Lenton, T. M., Scheffer, M., Folke, C., Schellnhuber, H. J., Nykvist, B., de Wit, C. A., Hughes, T., van der Leeuw, S., Rodhe, H., Sörlin, S., Snyder, P. K., Costanza, R., Svedin, U., ... Foley, J. A. (2009). A safe operating space for humanity. *Nature*, 461(7263), 472–475.

Rodgers, T. F. M., Truong, J. W., Jantunen, L. M., Helm, P. A., & Diamond, M. L. (2018). Organophosphate Ester Transport, Fate, and Emissions in Toronto, Canada, Estimated Using an Updated Multimedia Urban Model. *Environ Sci Technol*, 52(21), 12465–12474.

Romero-Romero, S., Herrero, L., Fernández, M., Gómara, B., & Acuña, J. L. (2017). Biomagnification of persistent organic pollutants in a deep-sea, temperate food web. *Science of The Total Environment*, 605–606, 589–597.

Ruiz-González, C., Logares, R., Sebastián, M., Mestre, M., Rodríguez-Martínez, R., Galí, M., Sala, M. M., Acinas, S. G., Duarte, C. M., & Gasol, J. M. (2019). Higher contribution of globally rare bacterial taxa reflects environmental transitions across the surface ocean. *Mol Ecol*, 28(8), 1930–1945.

- Sanganyado, E., Chingono, K. E., Gwenzi, W., Chaukura, N., & Liu, W. (2021). Organic pollutants in deep sea: Occurrence, fate, and ecological implications. *Water Res*, 205, 117658.
- Sanz-Sáez, I., Salazar, G., Sánchez, P., Lara, E., Royo-Llonch, M., Sà, E. L., Lucena, T., Pujalte, M. J., Vaqué, D., Duarte, C. M., Gasol, J. M., Pedrós-Alió, C., Sánchez, O., & Acinas, S. G. (2020). Diversity and distribution of marine heterotrophic bacteria from a large culture collection. *BMC Microbiol*, 20(1), 207.
- Schmidt, N., Fauvelle, V., Ody, A., Castro-Jiménez, J., Jouanno, J., Changeux, T., Thibaut, T., & Sempéré, R. (2019). The Amazon River: A Major Source of Organic Plastic Additives to the Tropical North Atlantic? *Environ Sci Technol*, 53(13), 7513–7521.
- Sebastian, M., & Ammerman, J. W. (2009). The alkaline phosphatase PhoX is more widely distributed in marine bacteria than the classical PhoA. *ISME J*, 3(5), 563–572.
- Sekerci, Y., & Petrovskii, S. (2015). Mathematical Modelling of Plankton–Oxygen Dynamics Under the Climate Change. *Bull Math Biol*, 77(12), 2325–2353.
- Semeena, V. S. (2005). Long-range atmospheric transport and total environment fate of persistent organic pollutants: A study using a general circulation model. <https://api.semanticscholar.org/CorpusID:127737627>
- Sha, B., Johansson, J. H., Salter, M. E., Blichner, S. M., & Cousins, I. T. (2024). Constraining global transport of perfluoroalkyl acids on sea spray aerosol using field measurements. *Sci Adv*, 10(14).
- Sha, B., Johansson, J. H., Tunved, P., Bohlin-Nizzetto, P., Cousins, I. T., & Salter, M. E. (2022). Sea Spray Aerosol (SSA) as a Source of Perfluoroalkyl Acids (PFAAs) to the Atmosphere: Field Evidence from Long-Term Air Monitoring. *Environ Sci Technol*, 56(1), 228–238.
- Somee, M. R., Amoozegar, M. A., Dastgheib, S. M. M., Shavandi, M., Maman, L. G., Bertilsson, S., & Mehrshad, M. (2022). Genome-resolved analyses show an extensive diversification in key aerobic hydrocarbon-degrading enzymes across bacteria and archaea. *BMC Genomics*, 23(1), 690.
- Srivastava, A., Saavedra, D. E. M., Thomson, B., García, J. A. L., Zhao, Z., Patrick, W. M., Herndl, G. J., & Baltar, F. (2021). Enzyme promiscuity in natural environments: alkaline phosphatase in the ocean. *ISME Journal*, 15(11), 3375–3383.
- Steffen, W., Broadgate, W., Deutsch, L., Gaffney, O., & Ludwig, C. (2015). The trajectory of the Anthropocene: The Great Acceleration. *The Anthropocene Review*, 2(1), 81–98. Copyright © 2015 by Sage Publications. Reprinted by permission of Sage Publications.
- Steffen, W., Richardson, K., Rockström, J., Cornell, S. E., Fetzer, I., Bennett, E. M., Biggs, R., Carpenter, S. R., de Vries, W., de Wit, C. A., Folke, C., Gerten, D., Heinke, J., Mace, G. M., Persson, L. M., Ramanathan, V., Reyers, B., & Sörlin, S. (2015). Planetary boundaries: Guiding human development on a changing planet. *Science* (1979), 347(6223).
- Steffen, W., Sanderson, A., Tyson, P., Jäger, J., Matson, P., Moore, B., Oldfield, F., Richardson, K., Schellnhuber, H. J., Turner, B. L., & Wasson, R. J. (2004). *Global Change and the Earth System: A Planet Under Pressure*. Springer-Verlag.
- Straif, K., Baan, R., Grosse, Y., Secretan, B., El Ghissassi, F., & Coglianò, V. (2005). Carcinogenicity of polycyclic aromatic hydrocarbons. *Lancet Oncol*, 6(12), 931–932.
- Su, G., Letcher, R. J., & Yu, H. (2016). Organophosphate Flame Retardants and Plasticizers in Aqueous Solution: pH-Dependent Hydrolysis, Kinetics, and Pathways. *Environ Sci Technol*, 50(15), 8103–8111.
- Sühling, R., Scheringer, M., Rodgers, T. F. M., Jantunen, L. M., & Diamond, M. L. (2020). Evaluation of the OECD P OV and L RTP screening tool for estimating the long-range transport of organophosphate esters. *Environ Sci Process Impacts*, 22(1), 207–216.
- Takahashi, S., Abe, K., & Ker, Y. (2013). Microbial Degradation of Persistent Organophosphorus Flame Retardants. In *Environmental Biotechnology - New Approaches and Prospective Applications*. InTech.
- Takahashi, S., Katanuma, H., Abe, K., & Kera, Y. (2017). Identification of alkaline phosphatase genes for utilizing a flame retardant, tris(2-chloroethyl) phosphate, in *Sphingobium* sp. strain TCM1. *Appl Microbiol Biotechnol*, 101(5), 2153–2162.
- Takahashi, S., Satake, I., Konuma, I., Kawashima, K., Kawasaki, M., Mori, S., Morino, J., Mori, J., Xu, H., Abe, K., Yamada, R. H., & Kera, Y. (2010). Isolation and identification of persistent

- chlorinated organophosphorus flame retardant-degrading bacteria. *Appl Environ Microbiol*, 76(15), 5292–5296.
- Teaf, C. M., Garber, M. M., Covert, D. J., & Tuovila, B. J. (2019). Perfluorooctanoic Acid (PFOA): Environmental Sources, Chemistry, Toxicology, and Potential Risks. *Soil and Sediment Contamination: An International Journal*, 28(3), 258–273.
- Tetu, S. G., Sarker, I., Schrameyer, V., Pickford, R., Elbourne, L. D. H., Moore, L. R., & Paulsen, I. T. (2019). Plastic leachates impair growth and oxygen production in *Prochlorococcus*, the ocean's most abundant photosynthetic bacteria. *Commun Biol*, 2(1), 184.
- Turner, J. T. (2015). Zooplankton fecal pellets, marine snow, phytodetritus and the ocean's biological pump. *Prog Oceanogr*, 130, 205–248.
- UNEP. (2023). Stockholm Convention on Persistent Organic Pollutants (POPs). Text and Annexes (Revised in 2023). <https://www.pops.int/TheConvention/Overview/TextoftheConvention/tabid/2232>
- Urvoy, M., Gourmelon, M., Serghine, J., Rabiller, E., L'Helguen, S., & Labry, C. (2022). Free-living and particle-attached bacterial community composition, assembly processes and determinants across spatiotemporal scales in a macrotidal temperate estuary. *Sci Rep*, 12(1), 13897.
- USEPA. (1982). Appendix A to Part 423—126 Priority Pollutants. <https://www.ecfr.gov/current/title-40/part-423/appendix-Appendix A to Part 423>
- USEPA. (2024a). Per- and Polyfluoroalkyl Substances (PFAS). Final PFAS National Primary Drinking Water Regulation. <https://www.epa.gov/sdwa/and-polyfluoroalkyl-substances-pfas>
- USEPA. (2024b). PFAS and Aquatic Life. <https://www.epa.gov/wqc/pfas-and-aquatic-life>
- Vaidya, S., Jain, K., & Madamwar, D. (2017). Metabolism of pyrene through phthalic acid pathway by enriched bacterial consortium composed of *Pseudomonas*, *Burkholderia*, and *Rhodococcus* (PBR). *3 Biotech*, 7(1), 29.
- Valiela, I. (2015). *Marine Ecological Processes*. Springer New York.
- Vallack, H. W., Bakker, D. J., Brandt, I., Broström-Lundén, E., Brouwer, A., Bull, K. R., Gough, C., Guardans, R., Holoubek, I., Jansson, B., Koch, R., Kuylensstierna, J., Lecloux, A., Mackay, D., McCutcheon, P., Mocarelli, P., & Taalman, R. D. F. (1998). Controlling persistent organic pollutants—what next? *Environ Toxicol Pharmacol*, 6(3), 143–175.
- van der Veen, I., & de Boer, J. (2012). Phosphorus flame retardants: Properties, production, environmental occurrence, toxicity and analysis. *Chemosphere*, 88(10), 1119–1153.
- Vila-Costa, M., Cerro-Gálvez, E., Martínez-Varela, A., Casas, G., & Dachs, J. (2020). Anthropogenic dissolved organic carbon and marine microbiomes. *ISME J*, 14(10), 2646–2648.
- Vila-Costa, M., Sebastián, M., Pizarro, M., Cerro-Gálvez, E., Lundin, D., Gasol, J. M., & Dachs, J. (2019). Microbial consumption of organophosphate esters in seawater under phosphorus limited conditions. *Sci Rep*, 9(1), 233.
- Wackett, L. P. (2021). Why Is the Biodegradation of Polyfluorinated Compounds So Rare? *MSphere*, 6(5).
- Wackett, L. P. (2022). Nothing lasts forever: understanding microbial biodegradation of polyfluorinated compounds and perfluorinated alkyl substances. *Microb Biotechnol*, 15(3), 773–792.
- Walton, J. L., & Buchan, A. (2024). Evidence for novel polycyclic aromatic hydrocarbon degradation pathways in culturable marine isolates. *Microbiol Spectr*, 12(1).
- Wang, F., Xiang, L., Sze-Yin Leung, K., Elsner, M., Zhang, Y., Guo, Y., Pan, B., Sun, H., An, T., Ying, G., Brooks, B. W., Hou, D., Helbling, D. E., Sun, J., Qiu, H., Vogel, T. M., Zhang, W., Gao, Y., Simpson, M. J., ... Tiedje, J. M. (2024a). Emerging contaminants: A One Health perspective. *The Innovation*, 5(4), 100612.
- Wang, F.-Q., Bartosik, D., Sidhu, C., Siebers, R., Lu, D.-C., Trautwein-Schult, A., Becher, D., Huettel, B., Rick, J., Kirstein, I. V., Wiltshire, K. H., Schweder, T., Fuchs, B. M., Bengtsson, M. M., Teeling, H., & Amann, R. I. (2024b). Particle-attached bacteria act as gatekeepers in the decomposition of complex phytoplankton polysaccharides. *Microbiome*, 12(1), 32.
- Wang, J., Hlaing, T. S., Nwe, M. T., Aung, M. M., Ren, C., Wu, W., & Yan, Y. (2021b). Primary biodegradation and mineralization of aryl organophosphate flame retardants by *Rhodococcus-sphingopyxis* consortium. *J Hazard Mater*, 412, 125238.

- Wang, J., Khokhar, I., Ren, C., Li, X., Wang, J., Fan, S., Jia, Y., & Yan, Y. (2019). Characterization and 16S metagenomic analysis of organophosphorus flame retardants degrading consortia. *J Hazard Mater*, 380, 120881.
- Wang, J., Yuan, L., Wu, W., & Yan, Y. (2022). Characterization of the phosphotriesterase capable of hydrolyzing aryl-organophosphate flame retardants. *Appl Microbiol Biotechnol*, 106(19–20), 6493–6504.
- Wang, Q., Zhao, H., Bekele, T. G., Qu, B., & Chen, J. (2021a). Organophosphate esters (OPEs) in wetland soil and Suaeda salsa from intertidal Laizhou Bay, North China: Levels, distribution, and soil-plant transfer model. *Science of The Total Environment*, 764, 142891.
- Wang, W., Wang, L., & Shao, Z. (2018). Polycyclic Aromatic Hydrocarbon (PAH) Degradation Pathways of the Obligate Marine PAH Degradator *Cyclocloasticus* sp. Strain P1. *Appl Environ Microbiol*, 84(21).
- Wang, X., Zhu, Q., Yan, X., Wang, Y., Liao, C., & Jiang, G. (2020b). A review of organophosphate flame retardants and plasticizers in the environment: Analysis, occurrence and risk assessment. *Science of The Total Environment*, 731, 139071.
- Wang, Z., DeWitt, J. C., Higgins, C. P., & Cousins, I. T. (2017). A Never-Ending Story of Per- and Polyfluoroalkyl Substances (PFASs)? *Environ Sci Technol*, 51(5), 2508–2518.
- Wang, Z., Walker, G. W., Muir, D. C. G., & Nagatani-Yoshida, K. (2020a). Toward a Global Understanding of Chemical Pollution: A First Comprehensive Analysis of National and Regional Chemical Inventories. *Environ Sci Technol*, 54(5), 2575–2584.
- Wei, G.-L., Li, D.-Q., Zhuo, M.-N., Liao, Y.-S., Xie, Z.-Y., Guo, T.-L., Li, J.-J., Zhang, S.-Y., & Liang, Z.-Q. (2015). Organophosphorus flame retardants and plasticizers: Sources, occurrence, toxicity and human exposure. *Environmental Pollution*, 196, 29–46.
- Wezel, A. P. van, & Opperhuizen, A. (1995). Narcosis Due to Environmental Pollutants in Aquatic Organisms: Residue-Based Toxicity, Mechanisms, and Membrane Burdens. *Crit Rev Toxicol*, 25(3), 255–279.
- Whitman, W. B., Coleman, D. C., & Wiebe, W. J. (1998). Prokaryotes: The unseen majority. *Proceedings of the National Academy of Sciences*, 95(12), 6578–6583.
- Working Group on Polycyclic Aromatic Hydrocarbons. (2021). Human health effects of polycyclic aromatic hydrocarbons as ambient air pollutants: report of the Working Group on Polycyclic Aromatic Hydrocarbons of the Joint Task Force on the Health Aspects of Air Pollution.
- World Health Organization. (2019). Health, the global ocean and marine resources: policy brief. <https://iris.who.int/handle/10665/346832>
- World Health Organization. Regional Office for Europe. (2003). Health risks of persistent organic pollutants from long-range transboundary air pollution (p. EUR/03/5042687). Copenhagen : WHO Regional Office for Europe.
- Xiang, L., Li, Y.-W., Yu, P.-F., Feng, N.-X., Zhao, H.-M., Li, H., Cai, Q.-Y., Mo, C.-H., & Li, Q. X. (2019). Food Safety Concerns: Crop Breeding as a Potential Strategy to Address Issues Associated with the Recently Lowered Reference Doses for Perfluorooctanoic Acid and Perfluorooctane sulfonate. *J Agric Food Chem*, acs.jafc.9b04625.
- Xie, Z., Wang, P., Wang, X., Castro-Jiménez, J., Kallenborn, R., Liao, C., Mi, W., Lohmann, R., Vila-Costa, M., & Dachs, J. (2022). Organophosphate ester pollution in the oceans. *Nat Rev Earth Environ*, 3(5), 309–322.
- Yagi, J. M., & Madsen, E. L. (2009). Diversity, Abundance, and Consistency of Microbial Oxygenase Expression and Biodegradation in a Shallow Contaminated Aquifer. *Appl Environ Microbiol*, 75(20), 6478–6487.
- Yakimov, M. M., Bargiela, R., & Golyshin, P. N. (2022). Calm and Frenzy: marine obligate hydrocarbonoclastic bacteria sustain ocean wellness. *Curr Opin Biotechnol*, 73, 337–345.
- Yilmaz, P., Yarza, P., Rapp, J. Z., & Glöckner, F. O. (2016). Expanding the World of Marine Bacterial and Archaeal Clades. *Front Microbiol*, 6.
- Young, C. J., & Mabury, S. A. (2010). Atmospheric Perfluorinated Acid Precursors: Chemistry, Occurrence, and Impacts (pp. 1–109).
- Yu, Y., Yu, X., Zhang, D., Jin, L., Huang, J., Zhu, X., Sun, J., Yu, M., & Zhu, L. (2023). Biotransformation of Organophosphate Esters by Rice and Rhizosphere Microbiome: Multiple Metabolic Pathways, Mechanism, and Toxicity

Assessment. *Environ Sci Technol*, 57(4), 1776–1787.

Yu, Y., Zhang, K., Li, Z., Ren, C., Chen, J., Lin, Y.-H., Liu, J., & Men, Y. (2020). Microbial Cleavage of C–F Bonds in Two C 6 Per- and Polyfluorinated Compounds via Reductive Defluorination. *Environ Sci Technol*, 54(22), 14393–14402.

Zhang, Z., Sarkar, D., Biswas, J. K., & Datta, R. (2022). Biodegradation of per- and polyfluoroalkyl substances (PFAS): A review. *Bioresour Technol*, 344(Pt B), 126223.





CHAPTER 2

Objectives

Objectives

This thesis aimed to gain insights into the bidirectional interaction between marine microbial communities in the upper ocean and relevant families of organic contaminants that are part of the ADOC pool, particularly in less characterized remote areas such as the open ocean and Antarctic waters. Focus has been placed on the potential role of naturally occurring microbial communities in determining the fate of organic contaminants through biodegradation, as well as the capacity of these compounds to modulate microbial community composition and functionality.

The general working hypothesis of this thesis was that the background concentrations of organic contaminants with ubiquitous presence in the oceans significantly affect the composition and functioning of marine microbial communities, while the microbial loop modulates ADOC pool concentrations through biodegradation. However, both anthropogenic organic pollution and microbial pump-mediated biodegradation tend to be excluded or neglected as relevant factors in microbial ecology and environmental chemistry, respectively.

The following hypotheses were tested in this thesis:

- The presence of genes responsible for PAH degradation is a widespread feature in marine microbial communities that can be used to assess/predict/model the potential of naturally occurring microbial communities to degrade PAHs.
- The analysis of concurrent data on the occurrence of organic contaminants and marine microbial communities is a powerful and often unexplored approach to finding patterns and interactions.
- The biodegradation of contaminants of emerging concern, such as OPEs at environmentally relevant concentrations, is a relevant factor determining their fate in the open ocean.
- There are several methods that can be used in environmental chemistry when addressing biodegradation of organic contaminants, such as diagnostic ratios, historically used in organic geochemistry, experimental assessment of degradation by measured

depletion of the chemical in parallel to a suit of biological and chemical measurements, and bioinformatics approaches applied to extensive data sets. These three approaches can be used effectively, with their advantages and disadvantages depending on the contaminant family and the previous knowledge on their degradation potential.

Therefore, the general objective of this thesis was to assess the microbial biogeochemistry of certain families of organic contaminants that are relevant in the global ocean and constitute part of the anthropogenic organic carbon pool. To achieve this, data was obtained from field measurements and field experiments, combining the direct measurement of contaminant concentrations with metagenomic data of microbial communities and, when feasible, data for other environmentally relevant physicochemical and biological parameters. It is important to note that background knowledge regarding the biodegradation of organic contaminants varies depending on the chemical family. For well-established pollutants such as PAHs, biodegradation processes have been characterized, whereas for emerging contaminants such as OPEs and PFAAs, several unknowns remain regarding their biodegradation (i.e., identification of degradation genes, routes, taxa, etc.). Consequently, specific objectives were formulated based on the existing knowledge and limitations associated with each chemical family, in order to contribute to the overall understanding of the biodegradation processes.

The specific objectives of this thesis were to:

1. Provide the largest data set to date on PAH occurrence and seasonal variability in Antarctic coastal seawater and plankton, and the concurrent composition of the microbial community.
2. Explore the influence of environmental and biological factors, particularly bacterial communities, on the occurrence and variability of PAHs in the water column in coastal Antarctica.
3. Determine the potential of field biogeochemical assessments in identifying PAH biodegradation within the marine coastal Antarctic environment.
4. Evaluate the role of marine microbial communities and their promoted biodegradation as a potential sink for PFAAs in the marine coastal Antarctic environment.
5. Determine the occurrence of OPE biodegradation by marine microbial communities and quantify the extent of OPE losses attributable to biodegradation across diverse biogeochemical regions in the Atlantic and Southern Oceans. Explore biogeochemical controls on OPE's degradation.
6. Explore the responses of marine microbial communities to OPE exposure under oceanic conditions, focusing on community composition, bacterial production, and bacterial abundance.

7. Develop a new bioinformatic approach to identify aromatic hydrocarbon-degrading biomarker genes in metagenomic datasets that addresses the limitations of current methodologies.
8. Explore the use of aromatic hydrocarbon-degrading biomarker genes as a predictive tool to assess the potential of naturally occurring marine microbial communities to degrade PAH concentrations at background environmental levels in the tropical and temperate global ocean, as well the influence of PAHs on oceanic communities.

Objectives 1 to 3 are addressed in Publication I, where we created a dataset of PAH concentrations, with concurrent measurements of marine microbial communities from metagenomic data, comprising three time series of measurements during three austral summers in coastal Antarctica. We analyzed the data to find correlations between the fluctuations of PAH concentrations, the presence of hydrocarbonoclastic bacteria, and other environmental parameters, and to obtain a more comprehensive understanding of the cycling of PAHs in coastal Antarctica. Objective 4 is addressed in Publication II, where we employed a large multi-compartment dataset of PFAAs concentrations at coastal maritime Antarctica to study the trends of individual PFAAs compounds in seawater and explore the correlations between their concentrations and the composition of the bacterial communities during three austral summers. Objectives 5 and 6 are addressed in Publication III, where in a series of experiments carried out in situ across the Atlantic and Southern Oceans we exposed marine microbial communities to six OPEs under oceanic conditions, and we concurrently measured microbial community response and OPE concentrations. Objectives 7 and 8 are addressed in Publication IV, where we developed a new bioinformatic approach to find PAH-degrading genes in metagenomic datasets in a reliable way, and we performed an exploratory analysis of the occurrence of PAH degrading genes and concurrent measurements of PAH concentrations and other physicochemical parameters obtained from the Malaspina circumnavigation expedition.





CHAPTER 3

Brief Overview of Methodological Approaches

3.1 Sampling

3.1.1 Study area

3.1.2 Contamination control

3.1.3 Sampling methodologies

3.2 Sample treatment and analysis

3.2.1 Analytical chemistry methodologies

3.2.2 Molecular biology methodologies

3.2.3 Bioinformatic tools and software

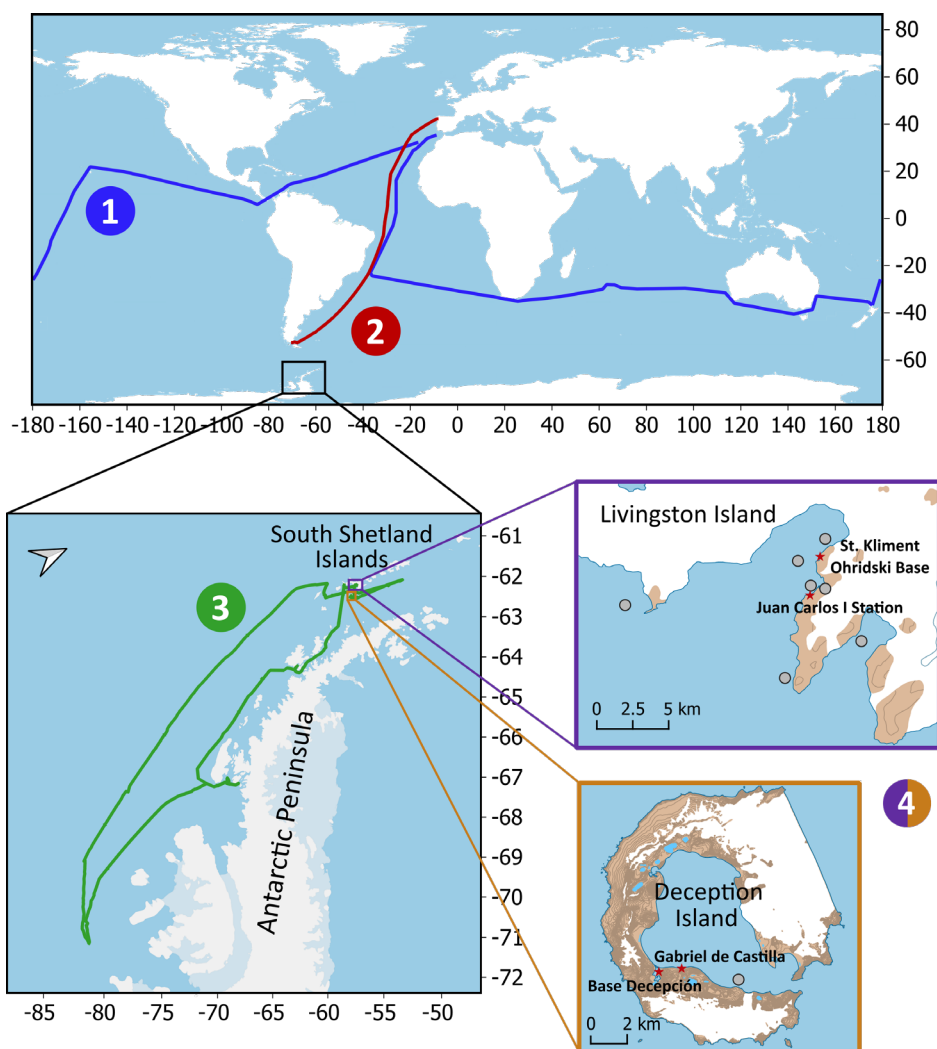
3.3 References

3.1 Sampling

3.1.1 Study area

To address the objectives of this thesis, field-based measurements and experiments were performed with seawater from remote areas. Remote areas in the context of this thesis refer to those marine regions distant from the main primary sources of anthropogenic organic chemical pollution, represented here either as sites located in the open ocean far from the coast or as coastal maritime areas in remote regions such as Antarctica. Sampling these sites is complex, as it is usually conducted during sampling campaigns that require specific infrastructure, such as oceanographic vessels and/or field-based research stations.

Chapter 4 encompasses the results of three Antarctic sampling campaigns carried out in the South Shetland Islands, Antarctic Peninsula. The first campaign was carried out during the austral summer of 2014-2015 (from December 1, 2014 to March 1, 2015) at Livingston Island (62°39'S, 60°23'W). Results from this campaign have been previously published and were incorporated into the analyses performed in this thesis. The second campaign took place in the austral summer of 2016-2017 (from January 22 to February 20, 2017) at Deception Island (62°59'S, 60°37'W). The last one was conducted during the austral summer of 2017-2018 (from January 8 to March 1, 2018) at Livingston Island. Both Livingston and Deception Islands host Antarctic stations operated by Spain: the Juan Carlos I and Gabriel de Castilla stations, respectively (Figure 3.1). Established in 1988, they have been operating during consecutive austral summers, which usually span from mid-November to March. Additionally, Livingston Island also hosts another scientific base, the St. Kliment Ohridski Base, managed by Bulgaria. Deception Island, in turn, hosts the Argentine base 'Decepción'.



- 1 Malaspina circumnavigation (Chapter 6)
 - 2 Atlantic Ocean, AN TOM-1 (Chapter 5)
 - 3 Bellingshausen Sea, Southern Ocean, AN TOM-2 (Chapter 5)
 - 4 Coastal Maritime Antarctica, South Shetland Islands (Chapter 4)
- Sampling site ★ Research station

Figure 3.1 Map depicting the oceanographic expeditions and Antarctic campaigns, illustrating the marine sampling regions pertinent to the fieldwork of this thesis.

Chapter 5 comprises samples taken during the AN TOM (Transport and biogeochemistry of emerging pollutants and ANThropogenic Organic Matter in the Southern Ocean), oceanographic campaigns. The research campaign was divided into two oceanographic cruises. The first expedition, AN TOM-1, consisted of a latitudinal transect that traversed the Atlantic Ocean, starting in Vigo, Spain, and ending in Punta Arenas, Chile. The cruise was conducted onboard the research vessel Sarmiento de Gamboa, from December 15, 2020, to January 15, 2021. The second expedition, AN TOM-2, took place in the Southern Ocean onboard RV Hespérides, between January 22 and February 8, 2022. During this cruise nearshore (Bransfield and Gerlache Straits) and offshore waters were sampled, covering a region of the Southern Ocean from the South Shetland Islands at 62°S to the Bellinghausen Sea at 71°S.

Chapter 6 is based on samples and data collected during the Malaspina 2010 expedition, an oceanographic campaign that circumnavigated the globe from December 13, 2010, to July 11, 2021, spanning a duration of 7 months and traversing the Atlantic, Indian, and Pacific Oceans (Duarte, 2015). The data re-analyzed and re-assessed for this study has been previously published in separate works (González-Gaya et al., 2016, 2019; Ruiz-González et al., 2019; Sánchez et al., 2024).

3.1.2 Contamination control

Environmental concentrations of organic contaminants are relatively low, often close to method detection limits. Therefore, rigorous quality control procedures are essential to avoid sample contamination and trace any potential incidents from sample collection through final analysis. Consequently, recipients, tubes and connections made of stainless steel, glass, or polytetrafluoroethylene (PTFE) were employed during the sampling for the determination OPEs and PAHs environmental concentrations, avoiding the use of any other type of plastic. In the context of PFAS analysis, equipment composed of stainless steel or polypropylene (PP) was utilized, with the exclusion of all fluoropolymer plastics and fluoroelastomer materials. Glassware was similarly excluded from PFAS analysis due to the potential for analyte loss. All sampling and laboratory materials were subjected to pre-cleaning with methanol and/or acetone prior to use in order to prevent potential contamination. Glassware and glass fiber filters were subjected to pre-combustion at 450°C for a duration of 4h prior to their utilization for sampling or sample treatment/analysis. To control potential contamination during sampling campaigns, field blank measurements were conducted. Field blanks were collected in a manner analogous to actual sample collection and were subsequently treated and processed using identical methodologies as the samples.

In the context of water sampling and treatment for microbiological protocols, the primary consideration is the maintenance of sterility. To achieve this goal, the labware employed to collect and/or handle water samples was pre-cleaned with 70% ethanol or 10% HCl, or subjected to UV-radiation. Additionally, the solutions and reagents employed in the protocols were autoclaved or filter-sterilized when necessary.

3.1.3 Sampling methodologies

Characterization of the water column

Prior to the collection of the water sample, a CTD (Conductivity, Temperature, and Depth) sensor was deployed at each sampling location to measure water temperature, salinity, turbidity, dissolved oxygen concentration, fluorescence, and photosynthetically active radiation (PAR) throughout the water column.

Water sampling

The water sampling methodology varied depending on the campaign (oceanographic or coastal Antarctica) and the intended measurements.

For determination of organic pollutants

At coastal Antarctica, sampling was conducted from a rigid inflatable boat. For the analysis of PAHs, between 100-120 L of surface seawater were collected in 20 L aluminum jerry cans and transported to the research stations for their immediate filtration and extraction. Briefly, the collected seawater was filtered through a pre-combusted and pre-weighed glass fiber filter ($0.7\ \mu\text{m}$, GF/F Whatmann) and then through a pre-cleaned XAD-2 adsorbent-packed stainless steel column. XAD-2 columns were stored at 4°C for refrigerated transport until further analysis in the ultraclean lab in Barcelona. The filtration and extraction was performed outdoors to avoid changes of temperature influencing particle-water re-partitioning. Regarding seawater for the analysis of PFAS, water samples were collected at different depths with a Niskin bottle and stored into 2 L PP bottles. Then, samples were extracted at the research station's laboratory using an established solid phase extraction (SPE) methodology (Casas et al., 2020).



Figure 3.2 Inflatable boat used for sampling.

At the oceanographic cruises sampling was conducted directly from the vessel. In the case of PAH analysis during the Malaspina expedition, subsurface water samples were collected at a depth of 4 m using the boat's built-in continuous water sampling systems. Briefly, particles were retained over pre-combusted and pre-weighed glass fiber filters ($0.7\ \mu\text{m}$ pore size, GF/F Whatmann) and contaminants in the filtrate were concentrated in XAD-2 adsorbent-packed



Figure 3.3 Rosette sampler coupled to CTD sensor.

stainless steel columns. The filters were stored at -20°C , while the XAD columns were kept refrigerated until they underwent further processing in the laboratory. Regarding OPE analysis in environmental samples and field experiments, surface seawater was collected using a rosette sampler filled with Niskin bottles and coupled to the CTD sensor. Subsequent OPE extraction was performed by filtering the water sample and preconcentrating the filtrate using a SPE methodology.

For microbial community characterization and other analysis

Additional water samples for the characterization of microbial communities by DNA sequencing approaches and measurements of physiological parameters such as prokaryotic abundances were also collected in parallel to the chemical samples. Environmental parameters such as inorganic nutrients, and other variables were measured using the same collected water. Generally, water samples for these purposes were collected utilizing Niskin bottles, directly deployed from the rigid inflatable boat (Coastal Antarctica), or mounted on

the rosette sampler (oceanographic cruises). Subsequent processing and analysis of these water samples were conducted utilizing previously sterilized equipment.

Plankton

Plankton samples were gathered by vertically dragging a $50\ \mu\text{m}$ mesh size net (Figure 3.4). The collected samples were then filtered through pre-combusted and pre-weighed filters ($2.7\ \mu\text{m}$ pore size, GF/D, Whatmann), using a filtration system. Filters were stored at -20°C until their analysis in the laboratory. The sampling depths ranged from 20 to 160 m in the Malaspina expedition, and from 12 to 60 m in Coastal Antarctica.

Figure 3.4 Plankton net



3.2 Sample treatment and analysis

This thesis employs two distinct approaches to get a better understanding of the microbially mediated biogeochemistry of organic contaminants in the ocean: statistical analysis of field-measured datasets on chemical concentrations and microbiological parameters from concurrent field samples, and field exposure experiments involving the addition of organic contaminants within environmental ranges. To achieve this, various analytical chemistry and molecular biology techniques have been applied, providing an interdisciplinary and comprehensive perspective on organic contaminant biogeochemistry through integrated data analysis. In the following section, a brief description of each applied technique will be given, as a general overview. Further details regarding materials and methods are elucidated in the corresponding methods section of each publication.

3.2.1 Analytical chemistry methodologies

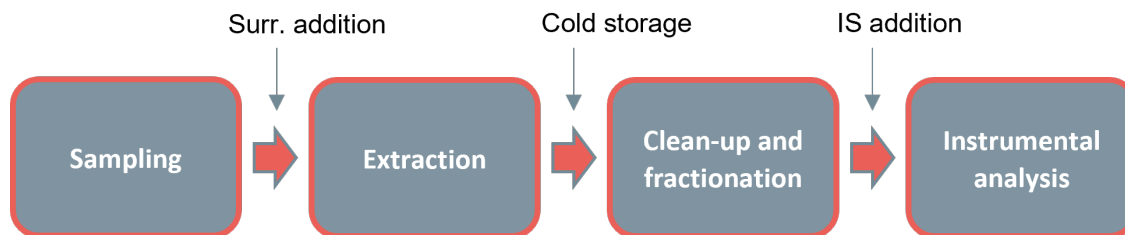


Figure 3.5 General steps of sample preparation for chemical analysis of organic compounds. 'Surr.' refers to surrogate, while 'IS' stands for Internal standard.

Prior to chemical analysis, all samples must undergo a sample preparation procedure (Figure 3.5). Generally, this procedure comprises a sample extraction step conducted in the field laboratory immediately following sample collection, which enables the concentration of large volumes of water samples into small volumes, facilitating storage and transport. In this thesis, the aforementioned XAD-2 packed stainless steel columns and SPE cartridges were employed. Specifically, XAD-2 columns were used for the analysis of PAHs, while OPEs and PFAS were extracted using Oasis HLB (6 cm³, 200 mg, Waters) and Oasis WAX (6 cm³, 150 mg, Waters) SPE cartridges, respectively. This extraction step typically involves the addition of a recovery standard, also called surrogates, to monitor potential analyte losses during sample treatment. These surrogates are generally deuterium-labeled versions of the target compounds or structurally similar to the target compounds. In the case of those samples concentrated on filters, such as plankton and water particulate phase, the filters were transported and then extracted using the Soxhlet extraction method in a clean lab. Once extracted, they were subjected to the same procedure as the water samples.

Ultraclean laboratory

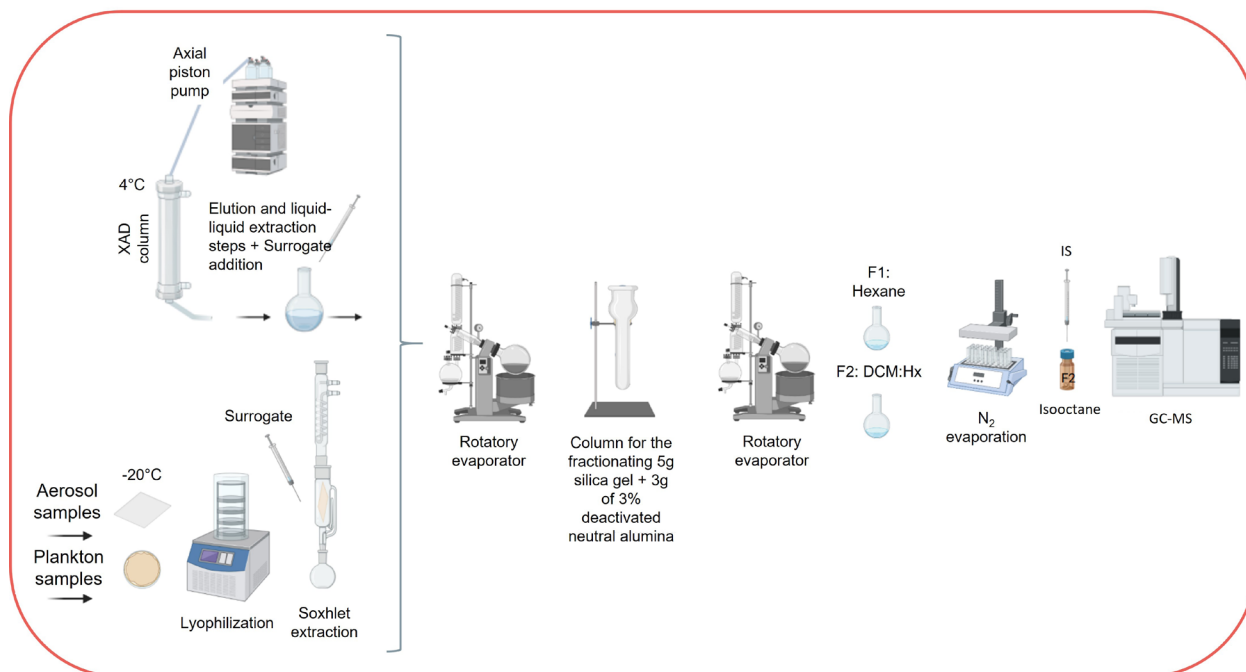


Figure 3.6 Sample preparation procedure for PAHs analysis using XAD and filters for water and plankton samples.

After the extraction step in the sampling campaign, the cold-stored concentrated samples are transported and processed in the home institution. In this case, samples were transported to Barcelona, where they were subjected to clean-up and fractionation steps in the ultraclean laboratory of the Institute of Environmental Assessment and Water Research (IDAEA-CSIC). These steps are intended for the isolation of the target analytes from potential interfering co-extractives, as well as the elimination of solvents used during sample elution and clean-up steps, and the preparation of the analytes in a chemical form suitable for their characterization and quantification (Fletouris, 2007). The specific steps and reagents used are therefore optimized, depending on the physicochemical properties of the target compounds, and the instrumental analysis to be used. The protocols used for the samples in this thesis are already established protocols described previously (Casal et al., 2018; Casas et al., 2020; Trilla-Prieto et al., 2024). Briefly, XAD-2 columns were sequentially eluted with solvents with different polarities. XAD-2 eluents, as well as Soxhlet extracts, were then subjected to evaporation to reduce the volume, before fractionating them on a 5 g of silica gel and 3 g of 3 % deactivated neutral alumina column with 25 mL of hexane and 40 mL of dichloromethane:hexane (1:3, v:v). The dichloromethane:hexane fraction containing the PAHs was concentrated and solvent exchanged to isooctane with a final volume of 100 μL (Figure 3.6). SPE cartridges were thawed and centrifuged to remove the remaining water. Regarding

elution, 12 mL methyl tert butyl ether:methanol (9:1; v/v) were used for the OPEs, while methanol followed by methanol with 0.1% of ammonia was employed for PFAS. Residual water was removed with baked sodium sulfate and eluents were concentrated under a gentle stream of N₂. Finally, OPE eluents were reconstituted with toluene, and PFAS eluents were reconstituted with 50:50 methanol/HPLC-grade water (Figure 3.7).

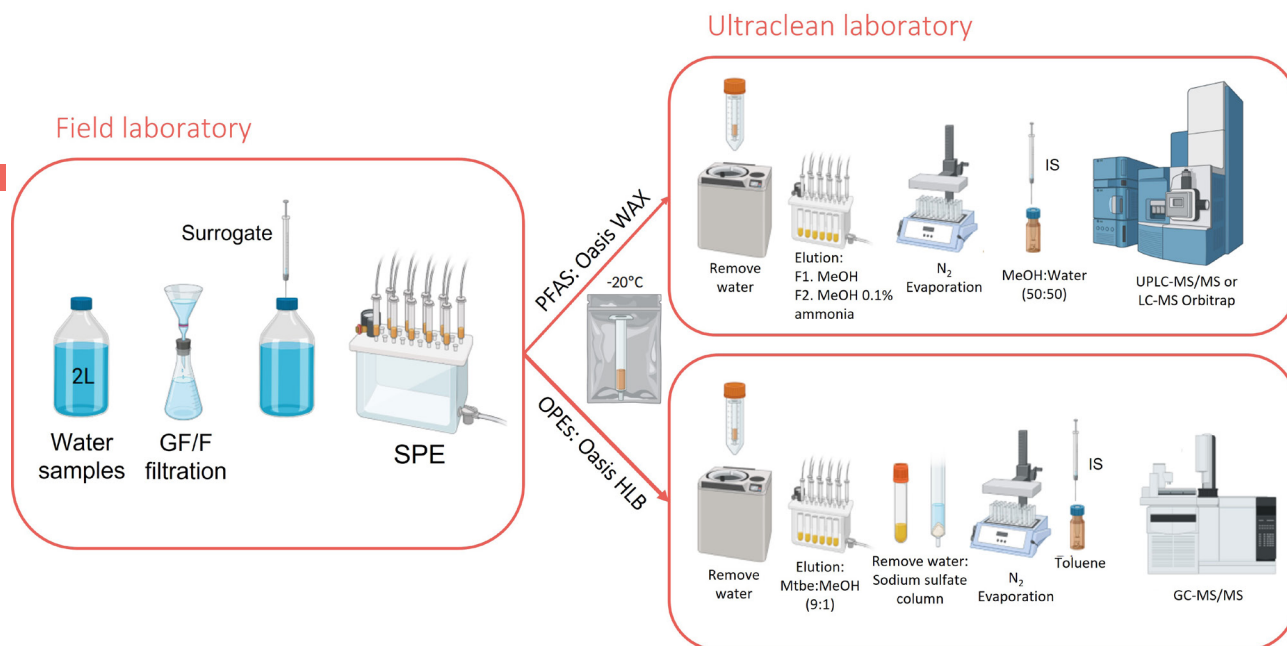


Figure 3.7 Sample preparation procedure for OPEs and PFAS analysis using SPE for water samples.

The last step is the instrumental analysis for the identification and quantification of the selected families of organic contaminants. In this thesis, it was performed by chromatographic techniques coupled to mass spectrometry. The chromatograph allows for the separation of the chemical compounds that form the pool of compounds in each sample, while the mass spectrometer acts as the detector, identifying the different analytes that sequentially come from the chromatograph by their mass spectrum. PAH analysis were conducted by gas chromatography coupled to a single quadrupole mass spectrometer (GC-MS), while OPEs were analyzed by gas chromatography coupled to a triple quadrupole mass spectrometer (GC-MS/MS) (González-Gaya et al., 2014; Trilla-Prieto et al., 2024). Regarding the analysis of PFAS, Ultra Performance Liquid Chromatography coupled to a triple quadrupole mass spectrometer (UPLC-MS/MS) and LC-MS Orbitrap were used (Casas et al., 2020; González-Gaya, Dachs, et al., 2014). Internal standards were added before instrumental analysis to correct for variability in the analytical instruments.

3.2.2 Molecular biology methodologies

The use of techniques based on molecular biology allows studying the microbiological aspects of the environmental samples. The development of culture-independent techniques, such as amplicon sequencing of the 16S rRNA gene and various omics approaches, has significantly enhanced our understanding of microbial diversity by overcoming the limitations imposed by reliance on a restricted number of culturable isolates. In this thesis, this culture-independent approach has been applied to study naturally occurring microbial communities in their full environmental complexity. The following techniques were used for the characterization of microbial community composition and community functionality:

Community composition

Amplicon sequencing of the 16S rRNA gene

The 16S rRNA gene encoding the small subunit of the ribosomal RNA molecules is highly conserved in most bacteria and archaea, and, consequently, it is widely used as a biomarker gene for the identification and taxonomic classification of prokaryotes in environmental samples. Through the extraction of DNA from environmental samples, amplification and sequencing of the 16S rRNA gene can be performed on the environmental DNA to characterize microbial community composition. Briefly, samples were incubated with lysozyme, proteinase K, and sodium dodecyl sulfate (SDS), and nucleic acids were extracted using the standard phenol-chloroform protocol (Vila-Costa et al., 2019). Regarding 16S amplicon sequencing, the V4–V5 region of the 16S rRNA gene was amplified with the primers 515F-Y and 926R (Parada et al., 2016). Sequencing was conducted by external services utilizing Illumina MiSeq platforms.

Metagenomics

Instead of targeting a single biomarker gene, through metagenomics a comprehensive analysis of total DNA isolated from environmental samples is performed. In this approach, the entire collection of genes and genomes within a community, known as the metagenome, is sequenced using next-generation sequencing platforms. The resulting sequences are then taxonomically/functionally classified using publicly available reference databases, providing insights into the taxonomy and functional potential of microbial communities. For the purpose of this thesis, a gene catalog constructed from metagenomic sequencing of DNA samples obtained from the Malaspina expedition was analyzed (Sánchez et al., 2024).

Flow cytometry

Flow cytometry is a technique that allows the quantification of cell abundances of aquatic microbial populations. In this thesis, it was used to determine prokaryotic cell abundances, as well as to differentiate between prokaryote cells with low nucleic acid and high nucleic acid content (LNA and HNA, respectively) (Gasol & Morán, 2015). Briefly, subsamples of 1.8 ml were fixed with 1% buffered paraformaldehyde solution (pH 7.0) plus 0.05% glutaraldehyde, and left

at room temperature in the dark for 10 minutes. 400 μL of the fixed samples were placed in flow cytometric tubes, 4 μL of SYBR Green I working solution (previously diluted in DMSO) were added, and tubes were let at room temperature for 10 minutes. Finally, samples were run on the flow cytometer, such as the BD Accuri C6 Plus.

Community functionality

Leucine Incorporation Rates (LIR)

This technique allows the estimation of heterotrophic bacterial production measured as leucine incorporation rates. It consists of incubating microbial communities with a certain added amount of radiolabelled leucine (L-[3,4,5- $^3\text{H}(\text{N})$] leucine), and then measuring the amount of labelled leucine incorporated into the newly synthesized bacterial proteins over time (Smith & Azam, 1992). Briefly, 1.2 ml triplicate live and one killed (5% trichloroacetic acid, TCA) subsamples were incubated with 3H-leucine (40 nM) for 4-5 hours at controlled temperature in the dark. Incubations were stopped by the addition of 120 μl of cold TCA 50% and then frozen ($-20\text{ }^{\circ}\text{C}$) until further processing by centrifugation and TCA rinsing. DPM counts were measured using a Tri-carb 3100TR liquid scintillation analyzer (Perkin Elmer), and converted to leucine incorporation rates.



Figure 3.7 Performing the leucine incorporation protocol onboard.

NADS (Nucleic Acid Double Staining)

The NADS viability protocol is based on the combination of the cell-permanent nucleic acid stain SYBR Green I and the cell-impermeant Propidium Iodide (PI) fluorescent probe. It is used to quantify the percentage of cells with intact membranes (termed as “viable” or live) versus the cells with damaged membranes (termed as “non-viable” or dead) by flow cytometry (Falcioni et al., 2008). Briefly, 400 μL of water sample were dispensed in flow cytometric tubes. Then, 4 μL of SYBR Green I working solution (previously diluted in DMSO) and 4 μL of PI solution were added. Tubes were incubated for 15 minutes at room temperature before running the samples using a BD Accuri C6 Plus flow cytometer.

3.2.3 Bioinformatic tools and software

Computational methodologies are essential for data processing, analysis, and visualization, particularly in the context of large databases, where the utilization of specialized software becomes necessary. For this thesis, the following bioinformatic tools and software were employed:

DNA sequencing data processing

Processing the vast amount of data generated by DNA sequencing techniques requires significant computational capacity and the use of bioinformatics tools in order to translate it into analyzable data. The specific procedures vary depending on the sequencing approach.

Ampliseq, a 16S amplicon sequencing analysis workflow

The Ampliseq pipeline (<https://nf-co.re/ampliseq/2.6.1/>) from nf-core (<https://nf-co.re/>) was used to process 16S rRNA raw amplicon sequences and characterize prokaryotic community composition (Straub et al., 2020). This bioinformatic analysis pipeline, developed for amplicon sequencing, automatically executes a multistep process using multiple bioinformatic tools, ultimately producing data on amplicon sequence variants (ASVs) and their abundances or counts for each sample through the implementation of the DADA2 software (Callahan et al., 2016). The taxonomic classification of the inferred ASVs is performed with reference taxonomic databases such as the SILVA high quality ribosomal RNA database, or the Genome Taxonomy Database (GTDB).

Metagenomic data

Sequencing the whole collection of genes and genomes present in a sample provides access to the functional gene composition of microbial communities, thus giving more information than the taxonomic analysis of the 16S rRNA gene sequencing. However, this comes at a cost, with higher sequencing expenses and increased computational resources required for data processing. The processing of metagenomic sequencing raw data typically involves assembling clean reads into larger DNA fragments called contigs. These contigs can then be used to reconstruct individual genomes, the so-called metagenome-assembled genomes or MAGs, or can be functionally and taxonomically annotated and used to build a gene catalog. In this thesis, a gene catalog (the Malaspina Vertical Profiles Gene Database, Sánchez et al., 2024) built from a set of metagenomes from the Malaspina expedition was used to survey specific biomarker genes related to aromatic hydrocarbon degradation.

Data analysis, visualization and statistics

R software

R is a programming language and free software used for statistical computing and creation of graphics (R Core Team, 2024). In this thesis R was used through RStudio, an integrated development environment for R, to prepare and normalize chemical and biological data, perform statistical analysis and tests, and generate the corresponding plots and graphics with the results.

Anvi'o

Anvi'o is an advanced analysis and visualization platform for 'omics data (Eren et al., 2015). It was used to generate plots illustrating the distribution of identified biomarker genes within the GTDB database in the phylogenomic trees of Bacteria and Archaea (Publication IV).

HMMER and phylogenetic placement with Phyloplace

HMMER is a sequence bioanalysis tool used for searching sequence databases for sequence homologs (Eddy, 2011). To do so it uses probabilistic models called profile Hidden Markov Models (HMMs). Profile HMMs comprise the evolutionary changes that have occurred in a set of related sequences, by performing a multiple sequence alignment and capturing position-specific information about how conserved each amino acid is in each column of the alignment. HMMER is often used with a profile database, such as the Pfam protein family database (Finn et al., 2007), where each Pfam profile represents a protein family or domain. Each of these Pfam profiles consist of a collection of multiple sequence alignments and profile HMMs. In this thesis, HMMER was used to query the Pfam profile of a biomarker gene associated with aromatic hydrocarbon degradation across different sequence datasets.

In order to improve the identification of genes coding for that specific Pfam profile, an additional step was implemented, based on phylogenetic placement of the sequences obtained from the HMMER search on a reference phylogenetic tree. To do so, a reference phylogeny for the protein family was estimated, in which clans containing manually curated aromatic hydrocarbon degrading enzymes with experimental evidence were identified. The query sequences classified in one of these specific clans in the reference by the Phyloplace tool were finally selected as positive hits (Lundin, 2023).

3.3 References

- Callahan, B. J., McMurdie, P. J., Rosen, M. J., Han, A. W., Johnson, A. J. A., & Holmes, S. P. (2016). DADA2: High-resolution sample inference from Illumina amplicon data. *Nat Methods*, 13(7), 581–583.
- Casal, P., Cabrerizo, A., Vila-Costa, M., Pizarro, M., Jiménez, B., & Dachs, J. (2018). Pivotal Role of Snow Deposition and Melting Driving Fluxes of Polycyclic Aromatic Hydrocarbons at Coastal Livingston Island (Antarctica). *Environ Sci Technol*, 52(21), 12327–12337.
- Casas, G., Martínez-Varela, A., Roscales, J. L., Vila-Costa, M., Dachs, J., & Jiménez, B. (2020). Enrichment of perfluoroalkyl substances in the sea-surface microlayer and sea-spray aerosols in the Southern Ocean. *Environmental Pollution*, 267, 115512.
- Duarte, C. M. (2015). Seafaring in the 21st Century: The Malaspina 2010 Circumnavigation Expedition. *Limnol Oceanogr Bull*, 24(1), 11–14.
- Eddy, S. R. (2011). Accelerated Profile HMM Searches. *PLoS Comput Biol*, 7(10), e1002195.
- Eren, A. M., Esen, Ö. C., Quince, C., Vineis, J. H., Morrison, H. G., Sogin, M. L., & Delmont, T. O. (2015). Anvi'o: an advanced analysis and visualization platform for 'omics data. *PeerJ*, 3, e1319.
- Falcioni, T., Papa, S., & Gasol, J. M. (2008). Evaluating the Flow-Cytometric Nucleic Acid Double-Staining Protocol in Realistic Situations of Planktonic Bacterial Death. *Appl Environ Microbiol*, 74(6), 1767–1779.
- Finn, R. D., Tate, J., Mistry, J., Coghill, P. C., Sammut, S. J., Hotz, H.-R., Ceric, G., Forslund, K., Eddy, S. R., Sonnenhammer, E. L. L., & Bateman, A. (2007). The Pfam protein families database. *Nucleic Acids Res*, 36(Database), D281–D288.
- Fletouris, D. J. (2007). Clean-up and fractionation methods. In *Food Toxicants Analysis* (pp. 299–348). Elsevier.
- Gasol, J. M., & Morán, X. A. G. (2015). Flow Cytometric Determination of Microbial Abundances and Its Use to Obtain Indices of Community Structure and Relative Activity (pp. 159–187).
- González-Gaya, B., Dachs, J., Roscales, J. L., Caballero, G., & Jiménez, B. (2014). Perfluoroalkylated Substances in the Global Tropical and Subtropical Surface Oceans. *Environ Sci Technol*, 48(22), 13076–13084.
- González-Gaya, B., Fernández-Pinos, M.-C., Morales, L., Méjanelle, L., Abad, E., Piña, B., Duarte, C. M., Jiménez, B., & Dachs, J. (2016). High atmosphere–ocean exchange of semivolatile aromatic hydrocarbons. *Nat Geosci*, 9(6), 438–442.
- González-Gaya, B., Martínez-Varela, A., Vila-Costa, M., Casal, P., Cerro-Gálvez, E., Berrojalbiz, N., Lundin, D., Vidal, M., Mompeán, C., Bode, A., Jiménez, B., & Dachs, J. (2019). Biodegradation as an important sink of aromatic hydrocarbons in the oceans. *Nature Geoscience* 2019 12:2, 12(2), 119–125.
- González-Gaya, B., Zúñiga-Rival, J., Ojeda, M.-J., Jiménez, B., & Dachs, J. (2014). Field Measurements of the Atmospheric Dry Deposition Fluxes and Velocities of Polycyclic Aromatic Hydrocarbons to the Global Oceans. *Environ Sci Technol*, 48(10), 5583–5592.
- Lundin, D. (2023). nf-core/phyloplace: First release (1.0.0). Zenodo.
- Parada, A. E., Needham, D. M., & Fuhrman, J. A. (2016). Every base matters: Assessing small subunit rRNA primers for marine microbiomes with mock communities, time series and global field samples. *Environ Microbiol*, 18(5), 1403–1414.
- R Core Team. (2024). R: A Language and Environment for Statistical Computing. <https://www.R-project.org/>
- Ruiz-González, C., Logares, R., Sebastián, M., Mestre, M., Rodríguez-Martínez, R., Galí, M., Sala, M. M., Acinas, S. G., Duarte, C. M., & Gasol, J. M. (2019). Higher contribution of globally rare bacterial taxa reflects environmental transitions across the surface ocean. *Mol Ecol*, 28(8), 1930–1945.
- Sánchez, P., Coutinho, F. H., Sebastián, M., Pernice, M. C., Rodríguez-Martínez, R., Salazar, G., Cornejo-Castillo, F. M., Pesant, S., López-Alforja, X., López-García, E. M., Agustí, S., Gojobori, T., Logares, R., Sala, M. M., Vaqué, D., Massana, R., Duarte, C. M., Acinas, S. G., & Gasol, J. M. (2024). Marine picoplankton metagenomes and MAGs from eleven vertical profiles obtained by the Malaspina Expedition. *Sci Data*, 11(1), 154.

Smith, D. C., & Azam, F. (1992). A simple, economical method for measuring bacterial protein synthesis rates in seawater using ³H-leucine. <https://api.semanticscholar.org/CorpusID:89585101>

Straub, D., Blackwell, N., Langarica-Fuentes, A., Peltzer, A., Nahnsen, S., & Kleindienst, S. (2020). Interpretations of Environmental Microbial Community Studies Are Biased by the Selected 16S rRNA (Gene) Amplicon Sequencing Pipeline. *Front Microbiol*, 11.

Trilla-Prieto, N., Iriarte, J., Berrojalbiz, N., Casas, G., Sobrino, C., Vila-Costa, M., Jiménez, B., & Dachs, J. (2024). Enrichment of Organophosphate Esters in the Sea Surface Microlayer from the Atlantic and Southern Oceans. *Environ Sci Technol Lett*.

Vila-Costa, M., Sebastián, M., Pizarro, M., Cerro-Gálvez, E., Lundin, D., Gasol, J. M., & Dachs, J. (2019). Microbial consumption of organophosphate esters in seawater under phosphorus limited conditions. *Sci Rep*, 9(1), 233.





CHAPTER 4

Biogeochemical Processes of PAHs and PFAAs in Maritime Antarctica

4.1 Why Antarctica matters for environmental chemistry

4.2 References

4.3 Publication I: Snow-Dependent Biogeochemical Cycling of Polycyclic Aromatic Hydrocarbons at Coastal Antarctica

4.4 Publication II: Inputs, Amplification and Sinks of Perfluoroalkyl Substances at Coastal Antarctica

4.1 Why Antarctica matters for environmental chemistry

Antarctica is considered the most remote region on Earth. Distant from the contamination sources arising from human activities, with sparse populations and low number of local contamination sources (Bengtson Nash et al., 2023), surrounded by the Southern Ocean, and protected by the Antarctic Circumpolar Current (Figure 4.1), which forms a physical barrier inhibiting effective north–south transport of surface waters of the surrounding oceans (Bengtson Nash, 2011), it is often termed as a pristine environment. Furthermore, all human activities on Antarctica are governed by the Antarctic Treaty system, which designates the continent as a zone of peace and science. More specifically, the Protocol on Environmental Protection to the Antarctic Treaty, signed in 1991 and in force since 1998, establishes Antarctica as a natural reserve. It applies to tourism, non-governmental, and governmental activities within the Antarctic Treaty Area, ensuring that they do not adversely impact the Antarctic environment or its scientific and aesthetic values. Altogether, its unique characteristics and unprecedented international regulation render Antarctica a huge natural laboratory.

In the field of environmental chemistry, detecting anthropogenic substances in Antarctica's ecosystem is crucial for highlighting the potential worldwide occurrence and impacts of concerning chemicals. While persistence and mobility criteria are often evaluated via theoretical modeling approaches, these predictions carry significant uncertainty without the support of environmental occurrence datasets. Determining the presence of a chemical in Antarctic environmental samples provides compelling evidence of its persistence and capacity for long-range transport, which is crucial for regulatory purposes by minimizing or eliminating such uncertainty. (Bengtson Nash et al., 2023). In this context, Antarctica has been proposed as a Sentinel of global pollution (Casas, 2022), comparable to how polar regions are considered as “early warning” regions for the manifestations of environmental effects of global change, particularly climate change (IPCC, 2019).

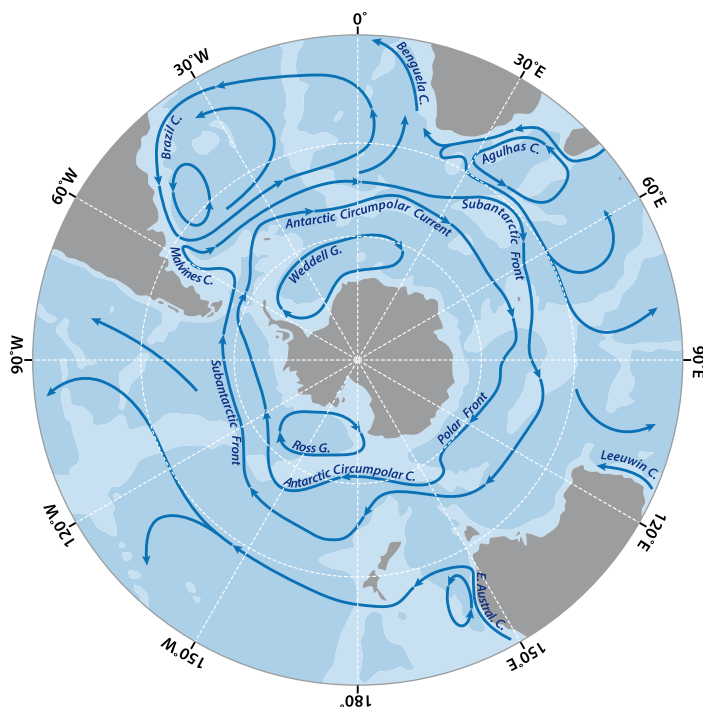


Figure 4.1 The Antarctic Circumpolar Current, surrounded by the Subantarctic Front and other oceanic currents from adjacent oceans. Abbreviations: C = Current, G = Gyre. Image from Adobe Stock (135050870).

The occurrence of POPs in Antarctica has been already documented, detecting POPs in different abiotic and biotic components (Bhardwaj et al., 2018; Fuoco et al., 2009; Galbán-Malagón et al., 2018; Khairy et al., 2016; Mwangi et al., 2016; Vecchiato et al., 2015), as well as many other anthropogenic organic contaminants (Cabrerizo et al., 2014; Casal et al., 2019; Trilla-Prieto et al., 2024; Xie et al., 2020). Atmospheric long-range transport is considered the main delivery pathway, although some entrance from the ocean through upwelling waters or by the formation of sea-spray aerosols has also been proposed for certain chemicals (Bengtson Nash, 2011; Bengtson Nash et al., 2010; Casas et al., 2020; Sha et al., 2024). Additionally, local sources originating from scientific stations have also been reported (Hale et al., 2008; Khairy et al., 2016; Wild et al., 2015). Concentrations of organic contaminants are generally low compared to temperate regions; however, certain Antarctic regions are more susceptible to the influx of contaminants, such as the Antarctic Peninsula. This region is more exposed to air masses from northern latitudes carrying organic chemicals and resulting in higher atmospheric concentrations than the rest of maritime Antarctica (Casal et al., 2017; Galbán-Malagón et al., 2013). Furthermore, Coastal Antarctica and the Antarctic Peninsula, in particular, receive greater precipitation than Continental Antarctica (Dalaiden et al., 2020; Turner et al., 2019; Vignon et al., 2021), which contributes to the input of chemicals through rain and snow-driven wet deposition (Casal et al., 2017; Casas et al., 2021; Khairy et al., 2016), subsequently leading to the entrance of contaminants to the marine environment from snowmelt (Casal et al., 2018; Khairy et al., 2016).

Despite the gathered knowledge, the field of Antarctic research on organic contaminants faces several challenges. The challenging working conditions in the Antarctic and Southern Ocean result in studies on organic contaminants often being limited to a small number of samples, which constrains the possibility of compound monitoring over time and on a large spatial scale (Bengtson Nash et al., 2023). Furthermore, very little is known about the capabilities of Antarctic organisms to respond to the background exposure of organic contaminants. It has been hypothesized that due to the low level of historical exposure to anthropogenic organic chemicals Antarctic phylogenies have not developed detoxification mechanisms comparable to those of temperate and tropical counterparts (Bengtson Nash, 2011). Cerro-Gálvez et al., (2019) reported responses of microbial communities in polar coastal seawaters to exposure of ADOC at environmentally relevant concentrations, where they detected changes in microbial communities and expression of cellular adaptation and detoxifying mechanisms. However, more research is needed in order to gain insights into the potential effects that organic contaminants exert on the Antarctic ecosystems, particularly over those microorganisms that sustain the Antarctic food webs. Similarly, assessing the metabolic potential of local microbial communities to transform anthropogenic contaminants is crucial to understand the biogeochemistry and fate of these compounds in maritime Antarctica.

The effects of climate change on the Antarctic ecosystems also pose a challenge, as all major drivers of organic chemical behavior and fate are likely to be affected, such as air and sea temperature, precipitation events, organic carbon cycling, ... (Bengtson Nash et al., 2023). For example, modeling results predict an increase in precipitation, particularly in the Antarctic coastal region (Turner et al., 2014). Furthermore, rainfall is expected to contribute more significantly to total precipitation, especially in the Antarctic Peninsula (Vignon et al., 2021). The coupling of increased wet deposition (with the consequent snow and rain-driven amplification of organic contaminants), and increased inputs of snowmelt due to rainfall and warming temperatures (Jones et al., 2019), will likely result in an increased input of chemicals into coastal seawaters. Consequently, the potential of the Antarctic Peninsula region to become not only a sentinel of pollution, but a net sink of organic contaminants may increase in the coming decades (Casas, 2022). Since these cold regions act as traps for organic chemicals, understanding the fate of these compounds is essential, especially in the context of climate change and increasing anthropogenic impacts. Gathering data on the occurrence of organic contaminants across different environmental compartments, tracking their concentrations over time, and studying their biogeochemistry and coupling with the local microbial communities are therefore some of the aspects that need to be addressed for a proper risk assessment of organic chemicals. These aspects are investigated in this thesis.

4.2 References

- Bengtson Nash, S. (2011). Persistent organic pollutants in Antarctica: current and future research priorities. *Journal of Environmental Monitoring*, 13(3), 497.
- Bengtson Nash, S., Bohlin-Nizzetto, P., Galban-Malagon, C., Corsolini, S., Cincinelli, A., & Lohmann, R. (2023). Monitoring persistent organic chemicals in Antarctica in support of global chemical policy: a horizon scan of priority actions and challenges. *Lancet Planet Health*, 7(5), e435–e440.
- Bengtson Nash, S., Rintoul, S. R., Kawaguchi, S., Staniland, I., Hoff, J. van den, Tierney, M., & Bossi, R. (2010). Perfluorinated compounds in the Antarctic region: Ocean circulation provides prolonged protection from distant sources. *Environmental Pollution*, 158(9), 2985–2991.
- Bhardwaj, L., Chauhan, A., Ranjan, A., & Jindal, T. (2018). Persistent Organic Pollutants in Biotic and Abiotic Components of Antarctic Pristine Environment. *Earth Systems and Environment*, 2(1), 35–54.
- Cabrerizo, A., Galbán-Malagón, C., Del Vento, S., & Dachs, J. (2014). Sources and fate of polycyclic aromatic hydrocarbons in the Antarctic and Southern Ocean atmosphere. *Global Biogeochem Cycles*, 28(12), 1424–1436.
- Casal, P., Cabrerizo, A., Vila-Costa, M., Pizarro, M., Jiménez, B., & Dachs, J. (2018). Pivotal Role of Snow Deposition and Melting Driving Fluxes of Polycyclic Aromatic Hydrocarbons at Coastal Livingston Island (Antarctica). *Environ Sci Technol*, 52(21), 12327–12337.
- Casal, P., Casas, G., Vila-Costa, M., Cabrerizo, A., Pizarro, M., Jiménez, B., & Dachs, J. (2019). Snow Amplification of Persistent Organic Pollutants at Coastal Antarctica. *Environ Sci Technol*, 53(15), 8872–8882.
- Casal, P., Zhang, Y., Martin, J. W., Pizarro, M., Jiménez, B., & Dachs, J. (2017). Role of Snow Deposition of Perfluoroalkylated Substances at Coastal Livingston Island (Maritime Antarctica). *Environ Sci Technol*, 51(15), 8460–8470.
- Casas, G. (2022). The Antarctic as Sentinel of Global Pollution [Universitat de Barcelona]. <http://hdl.handle.net/2445/188128>
- Casas, G., Martínez-Varela, A., Roscales, J. L., Vila-Costa, M., Dachs, J., & Jiménez, B. (2020). Enrichment of perfluoroalkyl substances in the sea-surface microlayer and sea-spray aerosols in the Southern Ocean. *Environmental Pollution*, 267, 115512.
- Casas, G., Martínez-Varela, A., Vila-Costa, M., Jiménez, B., & Dachs, J. (2021). Rain Amplification of Persistent Organic Pollutants. *Environ Sci Technol*, 55(19), acs.est.1c03295.
- Cerro-Gálvez, E., Casal, P., Lundin, D., Piña, B., Pinhassi, J., Dachs, J., & Vila-Costa, M. (2019). Microbial responses to anthropogenic dissolved organic carbon in the Arctic and Antarctic coastal seawaters. *Environ Microbiol*, 21(4), 1466–1481.
- Dalaiden, Q., Goosse, H., Lenaerts, J. T. M., Cavitte, M. G. P., & Henderson, N. (2020). Future Antarctic snow accumulation trend is dominated by atmospheric synoptic-scale events. *Commun Earth Environ*, 1(1), 62.
- Fuoco, R., Capodaglio, G., Muscatello, B., & Radaelli, M. (2009). Persistent Organic Pollutants (POPs) in the Antarctic Environment. A Review of Findings. <https://api.semanticscholar.org/CorpusID:130532029>
- Galbán-Malagón, C., Cabrerizo, A., Caballero, G., & Dachs, J. (2013). Atmospheric occurrence and deposition of hexachlorobenzene and hexachlorocyclohexanes in the Southern Ocean and Antarctic Peninsula. *Atmos Environ*, 80, 41–49.
- Galbán-Malagón, C. J., Hernán, G., Abad, E., & Dachs, J. (2018). Persistent organic pollutants in krill from the Bellingshausen, South Scotia, and Weddell Seas. *Science of The Total Environment*, 610–611, 1487–1495.
- Hale, R. C., Kim, S. L., Harvey, E., La Guardia, M. J., Mainor, T. M., Bush, E. O., & Jacobs, E. M. (2008). Antarctic Research Bases: Local Sources of Polybrominated Diphenyl Ether (PBDE) Flame Retardants. *Environ Sci Technol*, 42(5), 1452–1457.
- IPCC (Intergovernmental Panel on Climate Change). (2019). Special Report on the Ocean and Cryosphere in a Changing Climate. <https://www.ipcc.ch/srocc/>
- Jones, M. E., Bromwich, D. H., Nicolas, J. P., Carrasco, J., Plavcová, E., Zou, X., & Wang, S.-

H. (2019). Sixty Years of Widespread Warming in the Southern Middle and High Latitudes (1957–2016). *J Clim*, 32(20), 6875–6898.

Khairy, M. A., Luek, J. L., Dickhut, R., & Lohmann, R. (2016). Levels, sources and chemical fate of persistent organic pollutants in the atmosphere and snow along the western Antarctic Peninsula. *Environmental Pollution*, 216, 304–313.

Mwangi, J. K., Lee, W.-J., Wang, L.-C., Sung, P.-J., Fang, L.-S., Lee, Y.-Y., & Chang-Chien, G.-P. (2016). Persistent organic pollutants in the Antarctic coastal environment and their bioaccumulation in penguins. *Environmental Pollution*, 216, 924–934.

Sha, B., Johansson, J. H., Salter, M. E., Blichner, S. M., & Cousins, I. T. (2024). Constraining global transport of perfluoroalkyl acids on sea spray aerosol using field measurements. *Sci Adv*, 10(14).

Trilla-Prieto, N., Iriarte, J., Berrojalbiz, N., Casas, G., Sobrino, C., Vila-Costa, M., Jiménez, B., & Dachs, J. (2024). Enrichment of Organophosphate Esters in the Sea Surface Microlayer from the Atlantic and Southern Oceans. *Environ Sci Technol Lett*.

Turner, J., Barrand, N. E., Bracegirdle, T. J., Convey, P., Hodgson, D. A., Jarvis, M., Jenkins, A., Marshall, G., Meredith, M. P., Roscoe, H., Shanklin, J., French, J., Goosse, H., Guglielmin, M., Gutt, J., Jacobs, S., Kennicutt, M. C., Masson-Delmotte, V., Mayewski, P., ... Klepikov, A. (2014). Antarctic climate change and the environment: an update. *Polar Record*, 50(3), 237–259.

Turner, J., Phillips, T., Thamban, M., Rahaman, W., Marshall, G. J., Wille, J. D., Favier, V., Winton, V. H. L., Thomas, E., Wang, Z., van den Broeke, M., Hosking, J. S., & Lachlan-Cope, T. (2019). The Dominant Role of Extreme Precipitation Events in Antarctic Snowfall Variability. *Geophys Res Lett*, 46(6), 3502–3511.

Vecchiato, M., Argiriadis, E., Zambon, S., Barbante, C., Toscano, G., Gambaro, A., & Piazza, R. (2015). Persistent Organic Pollutants (POPs) in Antarctica: Occurrence in continental and coastal surface snow. *Microchemical Journal*, 119, 75–82.

Vignon, É., Roussel, M. -L., Gorodetskaya, I. V., Genthon, C., & Berne, A. (2021). Present and Future of Rainfall in Antarctica. *Geophys Res Lett*, 48(8).

Wild, S., McLagan, D., Schlabach, M., Bossi, R., Hawker, D., Cropp, R., King, C. K., Stark, J. S., Mondon, J., & Nash, S. B. (2015). An Antarctic

Research Station as a Source of Brominated and Perfluorinated Persistent Organic Pollutants to the Local Environment. *Environ Sci Technol*, 49(1), 103–112.

Xie, Z., Wang, Z., Magand, O., Thollot, A., Ebinghaus, R., Mi, W., & Dommergue, A. (2020). Occurrence of legacy and emerging organic contaminants in snow at Dome C in the Antarctic. *Science of The Total Environment*, 741, 140200.





4.3 PUBLICATION I

Snow-Dependent Biogeochemical Cycling of Polycyclic Aromatic Hydrocarbons at Coastal Antarctica

Jon Iriarte
Jordi Dachs
Gemma Casas
Alicia Martínez-Varela
Naiara Berrojalbiz
Maria Vila-Costa

Environmental Science & Technology. 2023,
57(4), 1625-1636.
<https://doi.org/10.1021/acs.est.2c05583>

Snow-Dependent Biogeochemical Cycling of Polycyclic Aromatic Hydrocarbons at Coastal Antarctica

Jon Iriarte, Jordi Dachs,* Gemma Casas, Alicia Martínez-Varela, Naiara Berrojalbiz, and Maria Vila-Costa*



Cite This: *Environ. Sci. Technol.* 2023, 57, 1625–1636



Read Online

ACCESS |



Metrics & More



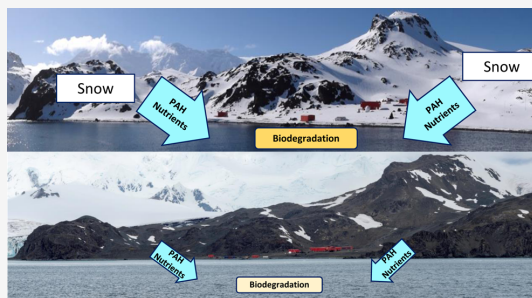
Article Recommendations



Supporting Information

ABSTRACT: The temporal trend of polycyclic aromatic hydrocarbons (PAHs) in coastal waters with highly dynamic sources and sinks is largely unknown, especially for polar regions. Here, we show the concurrent measurements of 73 individual PAHs and environmental data, including the composition of the bacterial community, during three austral summers at coastal Livingston (2015 and 2018) and Deception (2017) islands (Antarctica). The Livingston 2015 campaign was characterized by a larger snow melting input of PAHs and nutrients. The assessment of PAH diagnostic ratios, such as parent to alkyl-PAHs or LMW to HMW PAHs, showed that there was a larger biodegradation during the Livingston 2015 campaign than in the Deception 2017 and Livingston 2018 campaigns. The biogeochemical cycling, including microbial degradation, was thus yearly dependent on snow-derived inputs of matter, including PAHs, consistent with the microbial community significantly different between the different campaigns. The bivariate correlations between bacterial taxa and PAH concentrations showed that a decrease in PAH concentrations was concurrent with the higher abundance of some bacterial taxa, specifically the order *Pseudomonadales* in the class *Gammaproteobacteria*, known facultative hydrocarbonoclastic bacteria previously reported in degradation studies of oil spills. The work shows the potential for elucidation of biogeochemical processes by intensive field-derived time series, even in the harsh and highly variable Antarctic environment.

KEYWORDS: polycyclic aromatic hydrocarbons, PAH, coastal Antarctica, biodegradation, biogeochemical processes, marine bacterial communities



INTRODUCTION

Polycyclic aromatic hydrocarbons (PAHs) are ubiquitous in the oceans and polar regions.^{1–4} Even though most emissions of PAHs are land-based due to the use of fossil fuels and biomass burning,⁵ PAHs can reach remote regions, such as Antarctica, through long-range atmospheric transport and deposition.^{1,6} Diffusive air–water exchange is the main input of PAHs for most oceanic regions.^{3,4,7} However, for maritime Antarctica, snow scavenging of atmospheric PAHs and the subsequent melting of the snowpack play a key role as a pollutant input to coastal seawater.⁶ Indeed, PAH concentrations in seawater have been shown to increase gradually during the austral summer due to the melting of the snowpack accumulated during the preceding winter–spring, which, when melted, flashed-out pollutants from land to the sea.⁶ Nevertheless, this was described for the 2014–2015 austral summer, after an important snowpack was accumulated and melted. The extent of the snow events and snowpack is highly variable yearly, and thus there is a dearth of understanding of the variability of PAH cycling depending on snow accumulation, which in turn depends on the weather patterns in the Antarctic

Peninsula region.^{8,9} The understanding of the sources and dynamics of PAHs in coastal areas, especially in polar regions, is especially important for PAHs. PAHs and other semivolatile aromatic-like compounds are among the main families of anthropogenic organic chemicals entering the ocean and account for a relevant fraction of the anthropogenic dissolved organic carbon in the marine environment.^{10,11} Furthermore, together with other families of pollutants, they form complex mixtures of organic pollutants that are toxic to marine phytoplankton.¹²

Once in the water column, the fate of PAHs is dominated by the biological pump and degradation.¹¹ The biological pump is the settling of organic matter-bound PAHs into deep waters and sediments. This is the sinking of PAHs that have been

Received: August 2, 2022

Revised: January 5, 2023

Accepted: January 6, 2023

Published: January 19, 2023



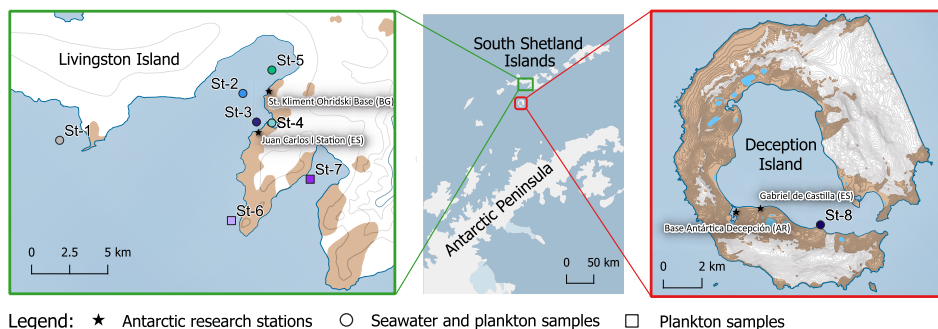


Figure 1. Location of the sampling sites for water and plankton samples at coastal Livingston Island (left panel) and Deception Islands (right panel) in the South Shetlands Islands (Antarctica). Figure created using Quantarctica version 3.2.³⁰

incorporated in phytoplankton or partitioned to detritus and other organic carbon pools driven by PAH hydrophobicity. However, the biological pump removes only 1% of the atmospheric inputs of PAHs.¹¹ The vast majority of PAHs entering the ocean are degraded in the photic zone. Even though photodegradation can occur, the overall PAH sink is dominated by microbial degradation.^{11,13} Despite this relevance, the study of microbial degradation of PAHs under field conditions has been mainly centered under scenarios of high concentrations, such as those found in oil spills,^{14,15} with few field studies addressing the degradation of PAHs when these occur at their background levels.¹⁶

Hydrocarbon-degrading bacteria are known as hydrocarbonoclastic bacteria (HCB), which include obligate HCB, that is, bacteria that only grow using hydrocarbons as carbon and energy sources, and facultative HCB, those able to grow with alternative carbon sources.¹⁷ HCB are naturally found at low abundances but can become predominant shortly after pulses of hydrocarbons (both aliphatic and aromatic).^{18–20} HCB are also ubiquitous in remote environments such as polar sea ice, the surface microlayer, or deep marine nonpolluted seawater.^{21–25} HCB belong to different phylogenetic groups, including members in the most common marine dominant classes, *Gammaproteobacteria*, *Alphaproteobacteria*, and *Flavobacteria*. In polar environments, there is a suite of microbial responses, including biodegradation, due to exposure to mixtures of anthropogenic dissolved organic carbon (ADOC).^{16,26} Other works assessing the influence of ADOC on polar bacteria at ultratrace concentrations have reported the growth of the rare biosphere, in some cases, HCB.^{26,27} Nevertheless, studies attempting to compare HCB presence to the occurrence of PAH in seawater and assess their mutual interactions are still scarce at background environmental levels, despite the reported HCB and PAH co-occurrence under scenarios of oil spills.^{16,28,29} In addition, the interactions of HCB and PAHs have never been reported for time series of measurements. Dynamics of PAHs over the austral summer may depend on the highly variable snow deposition events, glacier melting, and other environmental conditions. Characterizing potential consumers might provide hints toward a better elucidation of the biogeochemistry of PAHs, and especially biodegradation, in these ecosystems.

The objectives of this work were (i) to contribute with the largest data set to date on PAHs in Antarctic seawater and plankton as well as HCB communities, comprising three-time series of measurements in maritime Antarctica during three

austral summers, (ii) to explore the influence of environmental factors, and especially microbial communities including HCB, on the occurrence and variability of PAHs in the water column under scenarios of variable strength of snow melting, (iii) explore the potential of *in situ* field biogeochemical assessments to identify the role of HCB in the PAH degradation in the marine environment.

MATERIALS AND METHODS

Site Description. This study comprises samples collected during three different sampling campaigns performed during the austral summer. Two of the campaigns took place at South and False Bays of Livingston Island (62° 39' S, 60° 23' W) from December 1st, 2014, to March 1st, 2015, and from January 8th to March 1st, 2018, respectively. The third campaign took place at the inner bay of Deception Island (62° 59' S, 60° 37' W) from January 22nd to February 20th, 2017. Both islands are part of the South Shetland Archipelago, lying 150 km north of the Antarctic Peninsula. Livingston Island has a surface area of 850 km² and it is mostly covered by glaciers. The only two research stations on the island are located at South Bay: the Spanish Antarctic research station Juan Carlos I and the Bulgarian research station Saint Kliment Ohridski. Both stations operate only during the summer months, accounting for a maximum population of 50 people. Deception Island, which has a surface area of 72 km², is a volcanic island where over half of the area is covered by glaciers, with Port Foster in the caldera. Currently, there are two research stations that are only operative during the summer months: the Spanish Antarctic research station Gabriel de Castilla and the Argentinian Antarctic station Deception. The conditions at coastal Livingston are representative of the maritime sector of the Antarctic Peninsula and other Antarctic sectors receiving important snow inputs and under the influence of glaciers. In contrast, Port Foster at Deception is a particular site that may not be fully representative of other Antarctic coastal sites due to the geometry and influence of the volcano.

Sampling. Simultaneous plankton and seawater samples were taken from a rigid inflatable boat at 8 different locations (Figure 1, Table S1).³⁰ Station 1 (St-1) was located off-shore Punta Hanna at the eastern side of South Bay. Stations 2–5 (St-2–St-5) were located at different locations in South Bay and at different distances from the Pimpirev and Johnsons glaciers. In fact, St-4 is located in a small bay only 200 m from the Johnsons glacier. All five stations for Livingston Island were sampled during the 2018 campaign (Livingston 2018), while

only St-3 and St-4 were sampled during the 2014–2015 campaign (Livingston 2015). Additional plankton samples were taken at stations 6 and 7, next to Miers Bluff and inside False Bay, respectively. Conversely, Station 8 (St-8) is located inside Port Foster Bay at Deception Island and was sampled during the 2016–2017 campaign (Deception 2017).

Concurrently with water sampling, CTD depth profiles were taken to evaluate water temperature, salinity, turbidity, fluorescence, and photosynthetic active radiation (PAR) (Table S2).

In total, 46 surface seawater samples were collected. Twenty-six, seven, and thirteen during the Livingston 2015, Deception 2017, and Livingston 2018 sampling campaigns, respectively. Up to 100–120 L of seawater at 0.5–1 m depth was collected in 20 L aluminum jerry cans and transported to the research stations for their immediate filtration and extraction. This took place outside of the research stations to keep the temperature at ambient levels (1–4 °C), so no repartitioning between dissolved and particle phases occurred during sample manipulation. This also avoided any potential contamination from indoor air. Briefly, seawater was filtered through a precombusted and preweighed glass fiber filter (140 mm, GF/F Whatman) and then through a precleaned XAD-2 adsorbent (50 g, Supelco), packed in stainless steel columns. XAD-2 columns were stored at 4 °C for refrigerated transport until further analysis in a clean lab in Barcelona. GF/F filters were wrapped in precombusted aluminum foil and stored at –20 °C in air-tight plastic bags. The GF/F filters corresponding to surface particles were not analyzed for this study.

Fifty plankton samples were collected using a conical plankton net with a 50 μ m mesh size by three vertical hauls from the bottom to the surface. The sampling depths ranged from 12 m to 60 m (Table S1). The samples were collected at 8 different sampling stations (St-1–St-8) (Figure 1 and Table S1). Samples were filtered through precombusted and preweighed glass fiber filters (47 mm, GF/D Whatman). The filters containing plankton samples were wrapped in precombusted aluminum foil and stored at –20 °C in air-tight plastic bags until further analysis in a clean lab in Barcelona.

Fifteen milliliters of the water samples was taken and kept at –20 °C for analyzing dissolved inorganic nutrients: nitrate + nitrite ($\text{NO}_3^- + \text{NO}_2^-$), ammonium (NH_4^+), and phosphate (PO_4^{3-}). For the absolute quantification of bacterial abundance (BA) by flow cytometry, 1.8 mL of the water sample was fixed with a 1% buffered paraformaldehyde solution (pH 7.0) plus 0.05% glutaraldehyde (P + G), left at room temperature in the dark for 10 min, and frozen and stored at –80 °C until further processing.

Samples for 16S rDNA library construction were collected from surface water and analyzed as reported elsewhere.²⁴ Four liters of each sample was prefiltered through 3 μ m pore size 47 mm diameter polytetrafluoroethylene filters (Millipore, Billerica, MA) to remove grazers and the particle-attached living fraction and sequentially onto 0.2 μ m pore size 47 mm PTFE (Millipore, Billerica, MA) filters to capture the free-living bacteria fraction, using a peristaltic pump with a flow of <50 mL min^{–1}. Each filter was placed in 1 mL of the lysis buffer (50 mM Tris HCl, 40 mM EDTA, 0.75 M sucrose). All filters were stored at –20 °C until further processing.

Analytical Procedures for PAH Determination. The procedures followed for the extraction, identification, and quantification of PAHs are described in Annex S1 in the

Supporting Information and were the same for the three campaigns. Quality assurance and quality control are reported in Annex S2 in the Supporting Information. Briefly, strict measures were taken to clean the material used during sampling and analysis. Field blanks consisted of GF/D filters and XAD-2 columns that followed the same process as the samples, albeit without the pass of plankton or water. Recoveries and limits of quantification are summarized in Tables S3 and S4 in the Supporting Information. Recoveries ranged between 41 and 100% and between 19 and 100% for the plankton and water-dissolved phases, respectively. Concentrations were corrected for surrogate recoveries to account for the different recoveries of the lighter surrogates for the 2017–2018 water sampling.

The following parent and alkylated PAHs were analyzed: phenanthrene (Phe), anthracene (Ant), dibenzothiophene (DBT), fluoranthene (Flt), pyrene (Pyr), benzo[a]anthracene (B[a]ant), chrysene (Cry), benzo[b]fluoranthene (B[b]f), benzo[k]fluoranthene (B[k]f), benzo[e]pyrene (B[e]pyr), benzo[a]pyrene (B[a]pyr), perylene (Pery), dibenzo[a,h]-anthracene (Dib[a,h]ant), benzo[ghi]perylene (B[ghi]per), indeno[1,2,3-cd]pyrene (In[1,2,3-cd]pyr), benzo[ghi]-fluoranthene (B[ghi]f), methylfluorene (Σ MFlu, sum of 4 isomers), methylphenanthrenes (Σ MPhe, sum of 5 isomers), dimethylphenanthrenes (Σ DMPhe, sum of 10 isomers), trimethylphenanthrenes (Σ TMPhe, sum of 12 isomers), methyl-dibenzothiophenes (Σ MDBT, sum of 3 isomers), dimethyl-dibenzothiophenes (Σ DMDBT, sum of 6 isomers), methylpyrenes (Σ MPyr, sum of 5 isomers), dimethylpyrenes (Σ DMPyr, sum of 8 isomers), and methylchrysenes (Σ MCry, sum of 4 isomers).

PAH concentrations in the water-dissolved and plankton phases for the Livingston 2015 campaign have been reported in a companion publication and are used here when needed.⁶

Bacterial Abundance and Nutrient Quantification.

Bacterial abundance was estimated by flow cytometry as described elsewhere.³¹ Dissolved inorganic nutrients were analyzed by standard segmented flow with colorimetric detection using a SEAL Analyzer AA3 HR.³² Detection limits (defined as three times the standard deviation of 10 replicates at 50% diluted samples) were 0.006 μ M for NO_3^- , 0.003 μ M for NO_2^- , 0.003 μ M for NH_4^+ , and 0.01 μ M for PO_4^{3-} (Table S5).

Nucleic Acids Extraction and Sequencing. After thawing, samples were incubated with lysozyme, proteinase K, and sodium dodecyl sulfate (SDS), and nucleic acids were extracted simultaneously with phenol/chloroform/isoamyl alcohol (25:24:1) and chloroform/isoamyl alcohol (24:1).³³ The resulting solution was concentrated to 200 μ L using an Amicon Ultra 10-kDa filter unit (Millipore). Partial bacterial 16S gene fragments of both DNA were amplified using primers 515F-Y and 926R³⁴ plus adapters for Illumina MiSeq sequencing. The PCR reaction mixture was thermocycled at 95 °C for 3 min, 30 cycles at 95 °C for 45 s, 50 °C for 45 s, and 68 °C for 90 s, followed by a final extension of 5 min at 68 °C. PCR amplicon sizes were checked in tris-acetate-EDTA (TAE) agarose gels. Illumina MiSeq sequencing was conducted at the Pompeu Fabra University Sequencing Service. The complete nucleotide sequence data set generated and analyzed in this study was deposited in the sequence read archive (SRA) under the bioproject accession # PRJNA739708 and SUB9892364.

Bioinformatics. DADA2 v1.4 was used to differentiate the 16S V4-5 amplicon sequence variants (ASVs) and remove

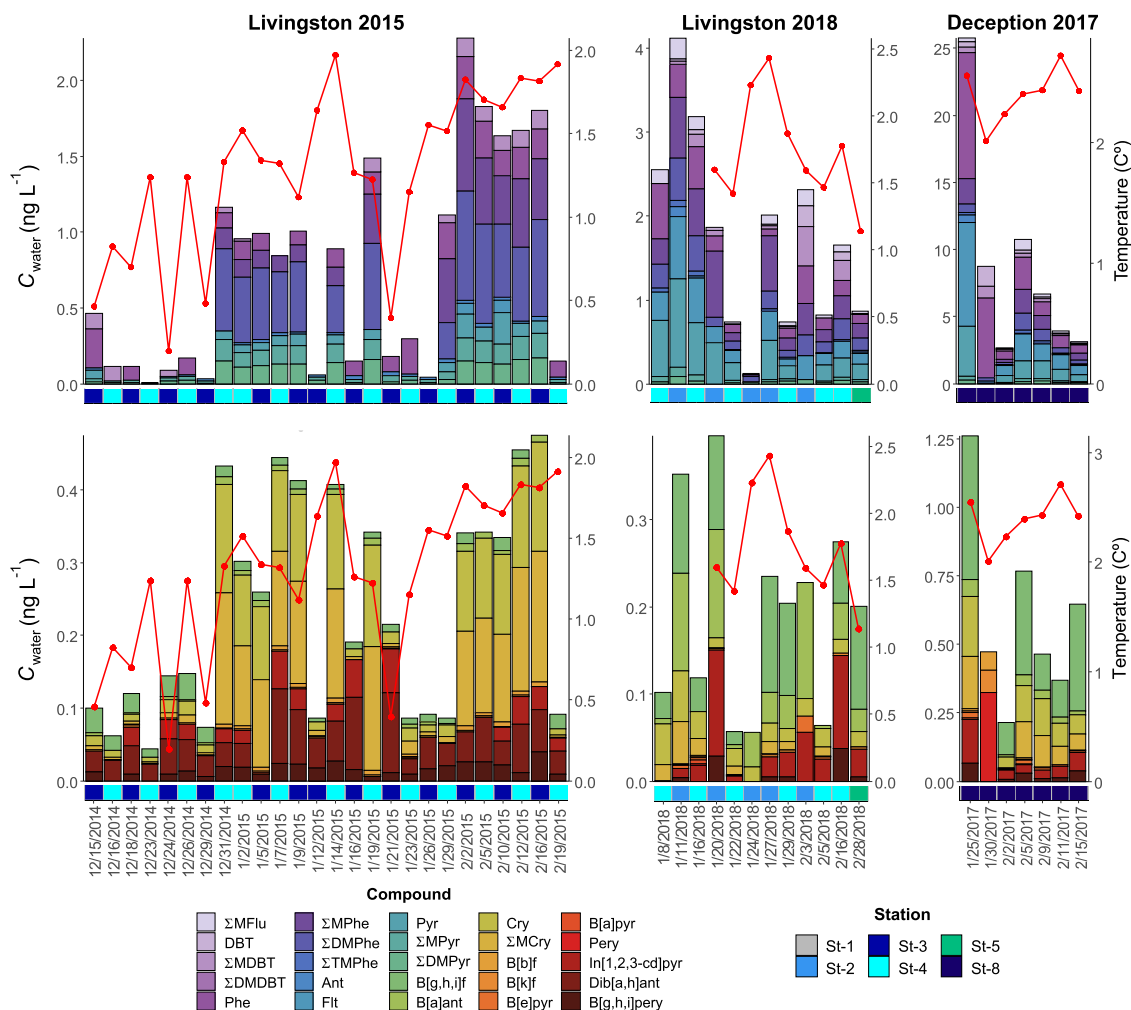


Figure 2. Concentrations of low MW PAHs (upper panels) and high MW PAHs (lower panels) in the water-dissolved phase for the three sampling campaigns at Livingston and Deception Islands. The red line indicates the seawater temperature.

chimeras (parameters: maxN = 0, maxEE = 2,4, truncLen = 227,210).³⁵ DADA2 resolves ASVs by modeling the errors in Illumina-sequenced amplicon reads. The approach is threshold-free, inferring exact variants up to 1 nucleotide difference using the quality score distribution in a probability model. Previously, spurious sequences and primers were trimmed using cutadapt v.1.16.³⁶ Taxonomic assignment of the ASVs was performed with the SILVA algorithm classifier against SILVA database release 138 (Quast et al., 2013). Taxonomic assignment of the ASVs was performed with the RDP algorithm classifier against RDP database release 11.5.³⁷ ASVs classified as Mitochondria or Chloroplast were removed. The final ASV table contained 69 samples, obtaining for the entire sample set 7359 ASVs from 16S rRNA gene V4-5 fragments, from which 1844 were unique. The maximum and minimum number of unique ASVs per sample was 425 and 49, respectively, with an average of 153.3 ± 76.4 . To allow for comparisons between samples, samples below 5000 reads/sample were filtered, and rarefaction was done to the minimum

sequencing depth (6131 reads/sample) with the rarefy() function from package vegan v2.5-7 in the R environment.³⁸ The identification of HCB was performed following the same approach reported elsewhere.¹⁶ The list of HCB genera includes genera either collected from hydrocarbon-polluted environments, usually oil spills, observed to have stimulated growth following hydrocarbon exposure (both aromatic and aliphatic hydrocarbons), or showing hydrocarbon catabolic activity, both from isolates and from marine environments, after metagenome-assembled genomes reconstruction.

Validation of 16S Sequencing Data by Quantitative PCR (qPCR). The relative abundances assessed by 16S sequencing were validated using qPCR to estimate the abundances of 16S rRNA of one group of HCB, the genera Colwellia, psychrophilic genera of obligate HCB.²⁵ Quantitative PCR was performed using a LightCycler 480 SYBR Green I Master (A F. Hoffmann–La Roche AG, Inc) in a LightCycler 480 II (A F. Hoffmann–La Roche AG, Inc), in 20 μ L reaction volumes on 96-well plates. PCR conditions were reproduced

using the Colwellia-specific primers pair COL134 and COL209³⁹ following Krolicka et al.⁴⁰ All samples were run as technical duplicates along with the quantification curve to reduce variability between assays. The plasmid used for the quantification curves was pNORM conjugative plasmid.⁴¹ Quantification limits (LOQ) were established as the minimum amount of plasmid that could be detected without interference from the negative control. The quality criteria within the standard curve were $R^2 > 0.99$, and a slope between -3.1 and -3.4 . The accepted efficiency of the reactions ranged from 97 to 100%. Melting curves were obtained to confirm amplification specificity. The amplification protocol was performed following the manufacturer's guidelines.

Statistical Analysis. All statistical analyses were carried out with R v4.1.0 software (<http://www.r-project.org/>). Analysis of variance (ANOVA) followed by a post-hoc Tukey HSD was used to test significant differences among samples, using the *stat* v4.1.0 and *agricolae* v1.3.5 packages in R. Package *ggpubr* v0.4.0 was used for Pearson correlations ($p \leq 0.05$). A nonmetric multidimensional scaling (NMDS) approach was used to assess the clustering of the samples based on their ASV composition using function *metaMDS* from *vegan* v2.5-7 package in R.³⁸ PERmutational Multivariate ANOVA⁴² was used with function *Adonis* from package *vegan* to elucidate the factors (i.e., campaign, site, date) that significantly structured the microbial communities. Heatmaps (*heatmap.2* function from the *gplots* v3.1.1 package) were used to visualize Pearson correlations between bacterial taxa and environmental data among the different samples, whereas *PLS2* (*plsdepot* v0.1.17 package) was used to explore the correlation between the relative bacterial taxa abundance (predictive, X-matrix) and the environmental data in each sample. Further graphs were plotted using package *ggplot* v3.3.5, also in the R environment.⁴³

RESULTS AND DISCUSSION

Occurrence of PAHs in Seawater and Plankton. The concentrations of the 73 targeted parent and alkylated PAHs in the water-dissolved phase and plankton phases at coastal Livingston and Deception Islands are reported in Tables S6 and S7 and shown in Figures 2 and S2. Dissolved-phase concentrations of Σ_{73} PAHs at coastal Deception and Livingston Islands averaged 9.4 (2.9 – 27.0) ng L^{-1} and 1.9 (0.2 – 4.5) ng L^{-1} , respectively. These concentrations are within the range of those reported in the open oceans and the Arctic Ocean.^{3,4,44,45} However, these coastal concentrations are significantly lower than those reported in other coastal regions such as the coastal eastern Indian Ocean (West Australia coast),⁴ coastal Mediterranean,^{46,47} or Eastern Asia (Eastern China coast).^{48–50} This is consistent with the small population in the research stations at South Bay and Port Foster (Livingston and Deception Islands, respectively) and the remoteness to populated regions. The Antarctic circumpolar current acts as a barrier for the North–South transport of organic pollutants by oceanic currents;⁵¹ therefore, PAHs reaching coastal Antarctica are driven by long-range atmospheric transport followed by air–water diffusive exchange or wet deposition.^{1,4,6,52}

The water-dissolved-phase PAH profile was dominated by 3–4 ring PAHs such as phenanthrene, methylphenanthrenes, pyrene, and fluoranthene, among others, consistent with previous works of PAHs in remote oceanic regions, including Antarctica.^{3,4,11,44,45} For the most abundant PAHs, concen-

trations at Deception were significantly higher than in Livingston (Figure S3). Concentrations between the latter were not significantly different. Even though the dissolved-phase concentrations were sampled at South Bay during two austral summers, there are some differences between the two years. The Livingston 2015 campaign summer was characterized by an important snowpack accumulated during the previous winter and spring, which melted during the summer. On the contrary, snow deposition was lower in the winter before the Livingston 2018 campaign, with less snow cover and thus lower snowmelt inputs during the summer (see pictures in Figure S1). It has been shown that snow amplification of concentrations and melting is an important input of PAHs during the austral summer, increasing the coastal seawater concentrations of PAHs and other pollutants.^{6,53,54} The concentrations at the end of the Livingston 2015 campaign were slightly higher than those in the 2018 campaign for some alkyl-PAHs, such as dimethylphenanthrenes. During the austral summer of 2015, dissolved- and gas-phase concentrations were close to equilibrium, with a net deposition and net volatilization in the early and late summer, respectively.⁶ During the Livingston 2018 campaign, there were probably, as well, close to equilibrium air and water phase concentrations, as dissolved-phase concentrations were similar in both campaigns. Therefore, the differences in atmospheric deposition between Livingston 2015 and 2018 were due to the wet deposition of snow. Nevertheless, despite these differences in inputs due to snow melting, the overall PAH concentrations in 2015 and 2018 were not different, suggesting that the removal processes of dissolved-phase PAHs could have mitigated differences in the source strength. This mitigation can be caused by the biological pump (sorption to phytoplankton, zooplankton, bacteria, and organic detritus followed by the sinking of particles) or abiotic or biotic degradation. Both processes will affect high and low MW PAHs, respectively (Table S8).

Plankton-phase concentrations of Σ_{73} PAHs at coastal Deception and Livingston Islands averaged 495 (72 – 2005) ng g^{-1} and 102 (15 – 479) ng g^{-1} , respectively. These concentrations are comparable to those reported in the south Atlantic or south Pacific oceans but slightly lower than those reported for the Indian Ocean or the Mediterranean Sea.^{11,44} The PAH profile is similar to that found in the water-dissolved phase, consistent with dynamic plankton–water partitioning, and is dominated by 3–4 ring PAHs, with high abundances of alkyl-PAHs (Figure S2). There is high variability in plankton-phase concentrations, consistent with previous studies,^{11,44} which is probably the result not only of the intrinsic variability of plankton biomass but also of different strengths of sources and degradation processes affecting the PAH concentrations (see below). The comparison of PAH concentrations in plankton for the three campaigns shows that for most PAHs with 3–5 aromatic rings, the levels at Deception Island were significantly higher than those at Livingston Island (Figure S4). For most compounds, there are no significant differences between the two campaigns performed at Livingston Island, despite the higher PAH fluxes from snow melting during the Livingston 2015 campaign.

Geochemical Evidences for PAH Biodegradation.

There are a number of trends and patterns that provide geochemical insights into the biodegradation of PAHs. These include PAH patterns in seawater and plankton, partitioning among the different phases, and the ratios of individual PAHs

that can be used to identify either the source of PAHs or the extent of weathering (photo- and biodegradation). First, biodegradation is faster for parent PAHs than alkyl-PAHs.⁵⁵ We found that $\text{Phe}/(\sum \text{MPhe} + \sum \text{DMPhe} + \sum \text{TMPhe})$, $\text{DBT}/(\sum \text{MDBT} + \sum \text{DMDBT})$, and $\text{Pyr}/(\sum \text{MPyr} + \sum \text{DMPyr})$ ratios in the water-dissolved phase were significantly lower for the Livingston 2015 campaign than in the other two campaigns. While these ratios were kept consistently low during the Livingston 2015 campaign, the ratios decreased over the austral summer for the other two campaigns, but these never reached the low levels of the Livingston 2015 campaign (Figures S5). Second, generally, LMW PAHs (having 3–4 aromatic rings) are mainly found in the dissolved phase, are more bio-available for degradation, and show higher degradation rates.^{56–58} Thus, the ratios between LMW and HMW PAH are good indicators of the degree of biodegradation of PAH.¹¹ These were lower for the Livingston 2015 campaign than for the other two campaigns, even though a decrease in this ratio during the Livingston 2018 campaign was observed (Figure S6).

Third, photodegradation could occur in surface waters. Photolysis of B[a]Ant has been shown to be faster than that of Cry, and thus the ratio B[a]Ant/Cry can be tentatively used for photodegradation.⁵⁹ The B[a]Ant/Cry ratio in the dissolved-phase samples from the surface was lower as well during the 2015 campaign than the other two campaigns, also consistent with a higher degree of photodegradation. However, the extent of photodegradation was discernible only at the surface since such a trend of the B[a]Ant/Cry ratio was not observed for the plankton-phase PAHs integrating the water column. A larger sink due to biodegradation than photodegradation has also been reported before for other oceanic regions.¹¹

Finally, an assessment of partitioning also provides additional clues on the relevance of biodegradation. The PAH partition between the dissolved phase and the organic matter pools due to their hydrophobicity. Compound-specific bioconcentration factors (BCF, L kg^{-1}) in all of the samples were calculated by

$$\text{BCF} = \frac{C_{\text{plankton}} 10^3}{C_{\text{water}}} \quad (1)$$

where C_{plankton} is the concentration in the plankton phase (ng g^{-1}) and C_{water} is the concentration in the water-dissolved phase (ng L^{-1}).

There were significant linear correlations between the BCFs and the octanol–water partition coefficient (K_{OW}) for both the Deception 2017 and Livingston 2018 campaigns ($p < 0.05$), explaining 28 and 39% of the variability in BCFs. However, for the Livingston 2015 campaign, even significantly, it only explained 4% of the variability. Such differences can be due to various factors, such as faster growth rates of the microbial communities favored by snow inputs, thus inducing lower C_{plankton} by dilution. Alternatively, a larger degradation of dissolved-phase compounds (lower C_{water}) can increase the BCF of the less hydrophobic chemicals, resulting in shallower slopes during the 2015 campaign and thus driving a lower degree of equilibrium between the dissolved and plankton phases. (Figure S7).

Further evidence of PAH degradation from partitioning comes from a multicompartimental work comprising atmospheric, snow, soil, and seawater samples for the Livingston

2015 campaign.⁵⁴ In this companion work, it was observed that the fugacity ratios between seawater and air for alkylated PAHs were higher, closer to the predicted values due to inputs from snow amplification than for parent PAHs. Such differences between parent and alkyl-PAHs are also indicative of microbial degradation of PAH. In addition, a comprehensive assessment of the variability of plankton-phase PAHs from various oceans (including the Livingston 2015 concentrations)¹¹ showed that biodegradation was the main sink for 3–4 ring PAHs.

All of these geochemical pieces of evidence show a key role of biodegradation explaining the occurrence of PAHs, but with different strengths for different austral summers and of larger magnitude during the Livingston 2015 campaign. Whereas the increasing trend in PAH concentrations for the 2015 campaign (Figure 2) was driven by the large PAH inputs from snow melting, geochemical evidence suggests that biodegradation was more active during this austral summer (2015) than for the other campaigns (2017, 2018). The importance of biodegradation on the PAH occurrence is hidden under the increase of PAH due to snowmelt inputs. Conversely, for the 2017 and 2018 campaigns, when the snow had already melted at the beginning of the campaign (smaller snowpack), the decrease of the PAH concentrations was apparent (Figure 2), consistent with biodegradation, even if it was of lower magnitude than during the 2015 campaign. This suggests that the biogeochemistry of PAHs in coastal Antarctica is not only due to different magnitudes of snow-related inputs but also to different extents of biodegradation driven by potential differences in the HCB community, which in turn would also be dependent on the snow- and glacier-derived inputs of nutrients or organic matter.⁶⁰ In fact, the concentrations of inorganic nutrients during the Livingston 2015 campaign were significantly higher than the other two campaigns (Figure S8).

Microbial Structure and Hydrocarbonoclastic Bacteria Abundance. Characterization of the free-living microbial communities was performed for concurrent samples to those of PAHs and for the three sampling campaigns and is reported here for the first time. The microbial community composition was significantly different in each campaign (Permanova test, $p < 0.05$), and samples clustered together according to the campaigns (Figure S9). In general, microbial communities in all three campaigns were dominated by the classes *Bacteroidia* (ranging from 10 to 53% of relative contribution to the total 16S rDNA pool, mean $38 \pm 9\%$), *Gammaproteobacteria* (9–71, $30 \pm 11\%$), and *Alphaproteobacteria* (15–60%, mean $31 \pm 11\%$) (Figure S10). *Bacteroidia* was mostly accounted for by the order *Flavobacteriales*, *Gammaproteobacteria* by orders *Enterobacterales* and *Pseudomonadales*, and *Alphaproteobacteria* by *SAR11* and *Rhodobacterales*, consistent with previous reports in this region.^{24,61,62} Within *Alphaproteobacteria*, *SAR11* had a significantly higher contribution in Deception 2017, where the lowest nutrient concentrations were measured, consistent with the *SAR11* frugal lifestyle and their success in nutrient-poor environments.⁶³ Within *Gammaproteobacteria*, *Enterobacterales* and *Pseudomonadales* had a significantly higher contribution in Livingston 2015 site with the highest concentrations of nutrients, whereas *Gammaproteobacteria* other than *Pseudomonadales* and *Enterobacterales* showed the opposite pattern. This is consistent with their copiotroph lifestyle already observed in other marine environments.⁶⁴ Within *Bacteroidia*, *Flavobacteriales* was the main taxa for the three campaigns, with a decrease

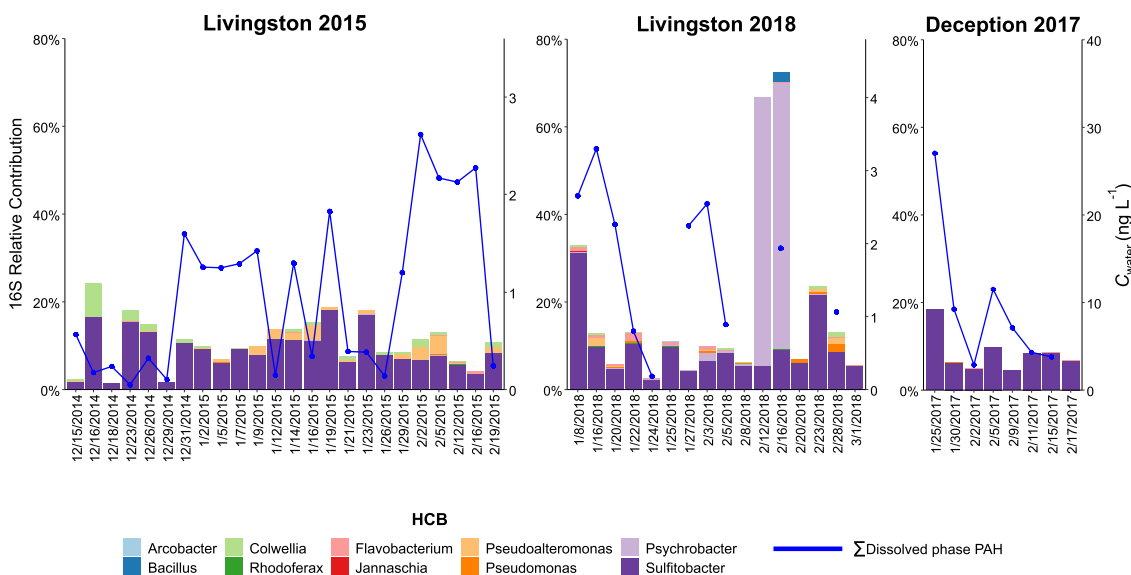


Figure 3. Relative contributions of the top 10 more abundant hydrocarbonoclastic bacteria (HCB) found in coastal waters of Livingston and Deception Islands for the three sampling campaigns.

in Deception 2017 in favor of *SAR11* compared to the other campaigns.

Bacterial taxa identified as HCB contributed to the total pool of 16S ASV reads on average $13 \pm 13\%$, ranging from 2 to 30% (except for 2 days at Livingston 2018 when a bloom of *Psychrobacter* reached a contribution of 58%) (Figure 3). The lowest diversity of HCB taxa was detected at Deception 2017, whereas the HCB community in Livingston Island was richer and more diverse (Table S9). HCB was mostly accounted for by *Sulfitobacter* at the genus level at all of the campaigns, with relative abundances ranging from 0.015 to 30%, with mean values of $9 \pm 6\%$. The presence of *Sulfitobacter* in the Antarctic Peninsula has also been reported previously at similar relative abundances.^{65,66} Other major contributors were facultative HCB such as *Psychrobacter*, *Pseudoalteromonas*, *Alkanindiges*, and *Acinetobacter*. Obligate HCB (*Oleispira*, *Colwellia*)²⁵ and other facultative HCB such as *Marinomonas*, *Glaciecola*, and *Pseudomonas* were present at lower relative abundances (Table S9). These HCB taxa have been previously found in Antarctic waters and sediments, and in some manipulative experiments at low temperatures, their role in PAH degradation has been reported.^{16,40,67}

The relative abundances of 16S rDNA ASV reads calculated using 16S amplicon sequencing data were validated for genus *Colwellia* by qPCR using taxonomical specific primers. A significant correlation between the relative abundances of *Colwellia* in the 16S rDNA ASV pool vs. absolute concentrations of *Colwellia* assessed by qPCR was observed ($p < 0.05$) in samples obtained at Johnsons Dock during the Livingston 2015 campaign (Figure S11). These results provide a quantitative validation of the relative abundances assessed by 16S sequencing.

Role of Bacteria on the Fate and Occurrence of PAHs.

As discussed above, the temporal trends of PAHs in water and plankton, as well as the diagnostic ratios, showed evidence of the influence of varying snow-associated inputs of PAHs and

degradation. Benchmarking allows blocking such variability in PAH abundances due to processes (inputs or sinks) different than biodegradation. Such an approach has been used before for assessing persistence in field and laboratory works.^{68,69} Here, we used chrysene as a reference chemical for the benchmarking; since it is not within the 3–4 aromatic ring PAHs, which are efficiently biodegraded, it is degraded by photolysis at a slower pace than other PAHs, and it is still not very hydrophobic, so it does not settle fast to sediments. Conversely, chrysene is also abundant in snow inputs,^{6,11} and benchmarking by chrysene allows blocking the variable yearly influence of snow inputs. The temporal trends of relative abundances of PAHs in the water-dissolved phase (as those derived by normalizing to chrysene) showed that the increase of concentrations during the Livingston 2015 campaign due to snow inputs was not apparent anymore (Figure 4). The lower relative abundances of chrysene-normalized LMW PAH concentrations during Livingston 2015 support a higher PAH biodegradation in that period. The potential for biodegradation was assessed by the presence of HCB that was, however, not significantly higher in Livingston 2015 than in the other 2 campaigns (Figure 3), suggesting that activity is not directly uniquely linked to HCB abundances but to other environmental parameters such as temperature and nutrient availabilities,⁷⁰ factors that are related to snow/glacier inputs, which can induce a different composition of HCB in different years.

To get insights into taxa in the HCB group with a potential relevance on PAH fate, Pearson correlations between the relative abundances of specific taxa and the chrysene-normalized PAH concentrations in the water-dissolved phase were calculated. These correlations were significantly positive and negative for several taxa (Figure 5). The significant positive correlations may be related to common factors driving the occurrence of both abundances (for example, glacier/snow melting inputs) and do not offer evidence for causation

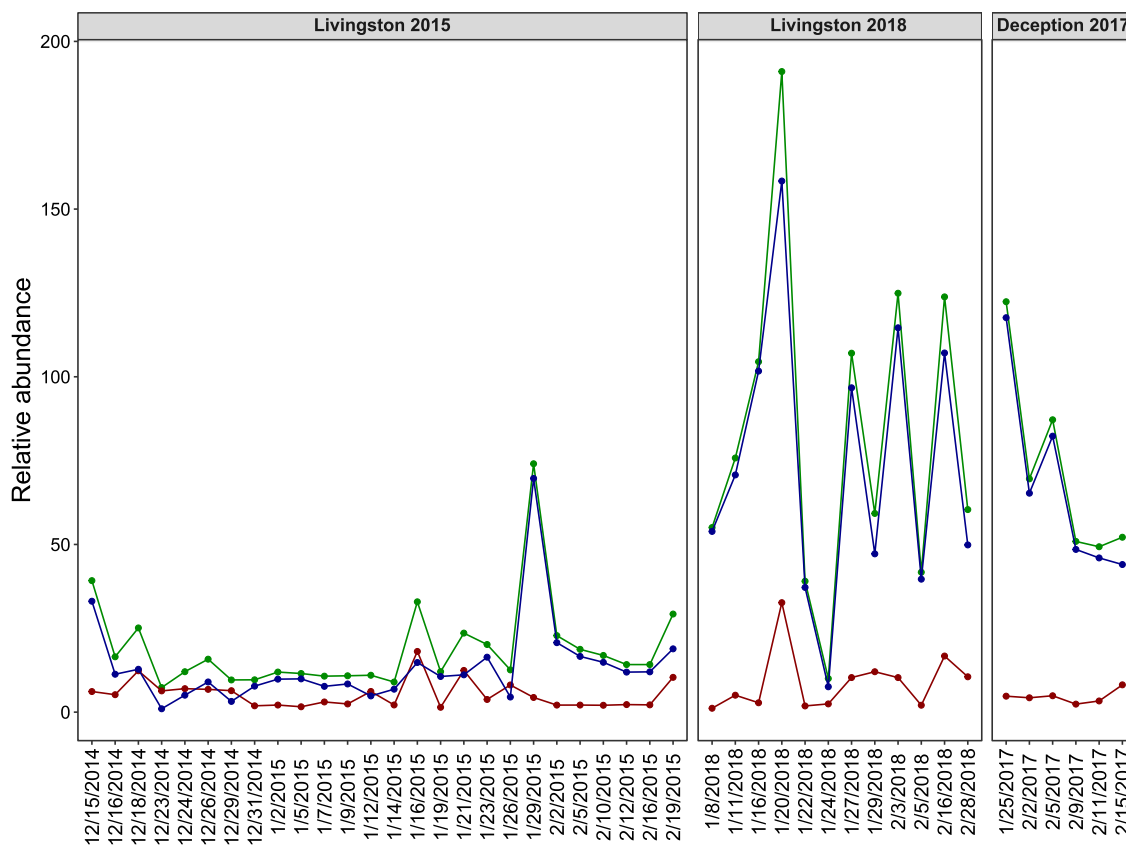


Figure 4. Temporal trends of relative abundances of PAHs in the water-dissolved phase after normalizing to chrysene for the three campaigns. The benchmarking using chrysene blocks the influence of different inputs such as snow, allowing us to compare the different degradation for the three campaigns, with lower relative contributions at Livingston 2015 consistent with larger biodegradation. The green line shows the sum of the relative abundances of all of the PAHs, the blue line is the sum of LMW PAHs, and the red line is the sum of HMW PAHs.

between bacterial abundances and PAHs in either direction. On the other hand, there were significant negative correlations between the abundance of LMW PAHs (and thus total PAHs) and that of 6 specific ASV, four of which belonged to *Pseudomonadales*. This group is described as facultative HCB in many studies and they bloom after pulses of PAH in the early stages of oil spill accidents in seawater at low temperatures.^{71–73} At low “background” concentrations of PAH, *Pseudomonadales* have been found to play a role in degrading PAH at the surface microlayer of coastal Antarctica.¹⁶ That the 3–4 aromatic ring PAHs decrease when the abundances of *Pseudomonadales* increase is consistent with their microbial degradation. Interestingly, water-dissolved-phase HMW PAHs did not show any significant negative correlations with the 16S amplicon sequencing data, probably because these included free-living bacteria but not the particle-associated bacteria which may interact with particle-bound HMW PAHs.¹⁶ PLS analysis showed that members of *Pseudomonadales* and *Flavobacteriales* orders were key contributors to principal component 1 (Figures S12 and S13), which separated the Livingston 2015 campaign from the others. It is noteworthy that these same ASV of *Pseudomonadales* and *Flavobacteriales* were those correlating negatively with PAH concentrations.

The degradation of PAHs during this campaign was maximal, as discerned above from geochemical evidence including the PAH diagnostic ratios. High nutrient conditions, maybe due to a stronger glacier/snow melting, may have favored the higher abundances of these taxa. If true, this would mean that snow melting triggers a higher PAH input but also a larger biodegradation potential of the microbial community.

The concurrent assessment of PAHs during three austral summers shows a large yearly variability in the occurrence of certain PAHs. The importance of snow inputs was highly variable, with a clear influence on the temporal trends of PAHs. However, biodegradation was also maximal for the same year with large inputs of melting snow. There was a covariability of certain bacteria and PAHs that would need further research to confirm their role as keystone taxa of microbiomes degrading PAHs in polar environments. The concurrent characterization of pollutants and microbial communities in field-derived time series of measurements is a powerful approach and provides important tools to discern the complexity of biogeochemistry and thus the fate and sinks for pollutants in the environment.

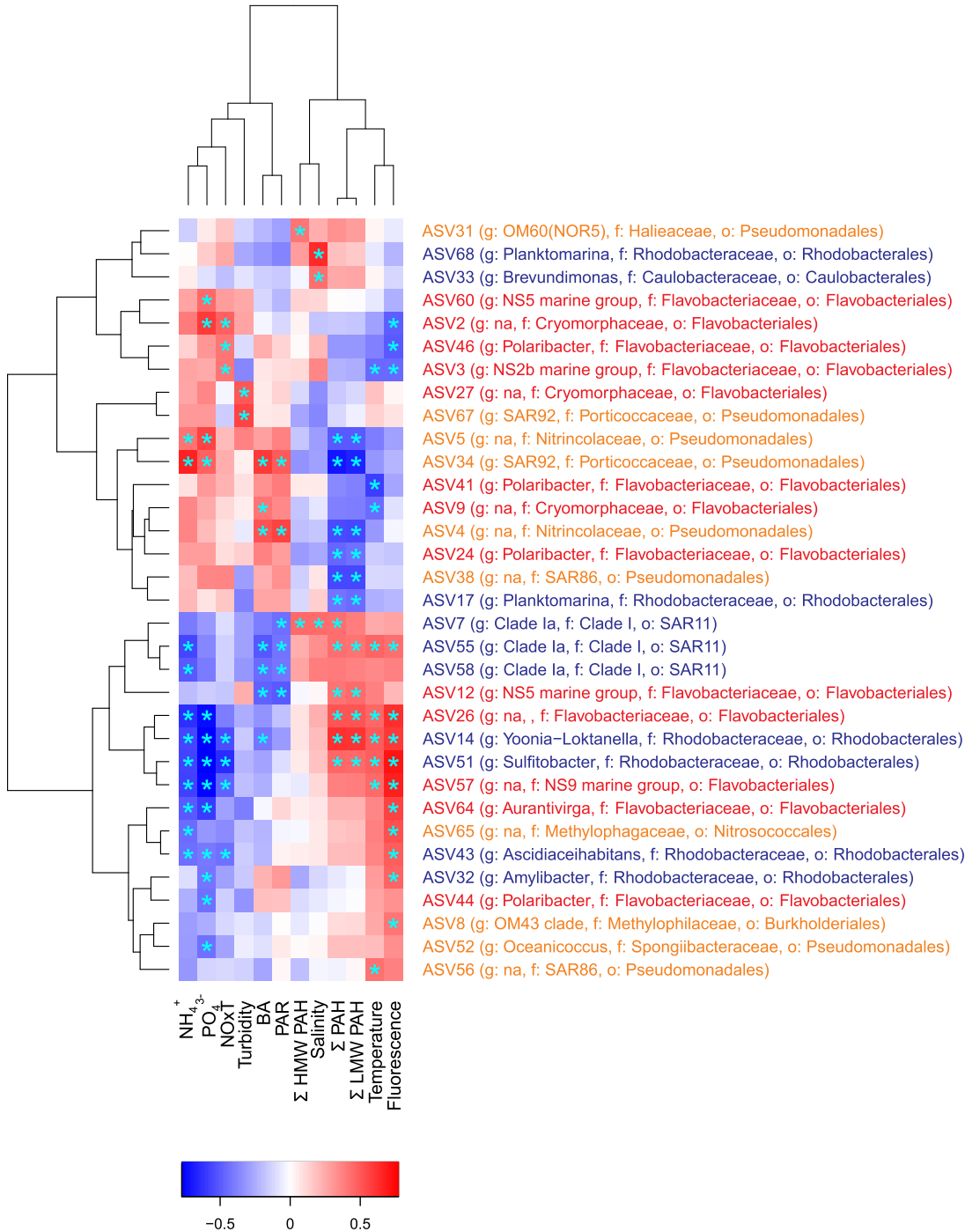


Figure 5. Correlation heatmap between ASV relative abundances and environmental variables. PAH concentrations in the water-dissolved phase were benchmarked for chrysene. Positive and negative correlations are indicated with red and blue colors, respectively. Significant correlations ($p < 0.05$) are represented with a blue asterisk. NH_4^+ , PO_4^{3-} , NO_3^- : Inorganic nutrients. BA: Bacterial abundance. PAR: Photosynthetically active radiation. Colors on the ASV taxonomy indicate the class (Gammaproteobacteria in yellow, Alphaproteobacteria in blue, and Bacteroidia in red).

■ ASSOCIATED CONTENT

SI Supporting Information

The Supporting Information is available free of charge at <https://pubs.acs.org/doi/10.1021/acs.est.2c05583>.

Analytical procedures for PAH determination; quality assurance/quality control for PAH analysis; description and coordinates of the sampling stations; ancillary data for the seawater samples; recoveries of PAH surrogates for each sampling campaign; limits of quantification for PAHs for seawater and plankton samples; nutrient concentrations and bacterial abundances for the water samples; individual PAH concentrations in the dissolved- and plankton-phase concentrations; classification of the analyzed PAHs as low molecular weight and high molecular weight; relative abundances of hydrocarbonoclastic taxa; picture of South Bay for the 2015, 2017, and 2018 campaigns (January) showing the difference in snow cover; occurrence of individual PAHs in plankton for the three sampling campaigns; differences in individual PAH concentrations in the water-dissolved phase and in plankton for the three sampling campaigns assessed by ANOVA followed by a Tukey test; temporal series of the parent/alkyl-PAHs concentration ratios and LMW/HMW ratios in the water-dissolved phase for the three campaigns; data on bioconcentrations factors versus octanol–water partition coefficients; concentrations of *in situ* inorganic nutrients; nonmetric multidimensional scaling (NMDS) of the microbial communities composition; correlation plots between amplicon sequencing relative abundance and qPCR relative abundance for the genus *Colwellia* at Jhonsons Dock; and partial least squares regression (PLS) and weight of the VIP *x* variables (individual ASV) over components 1 and 2 of the PLS (PDF)

■ AUTHOR INFORMATION

Corresponding Authors

Jordi Dachs – Department of Environmental Chemistry, Institute of Environmental Assessment and Water Research, IDAEA-CSIC, 08034 Barcelona, Spain; orcid.org/0000-0002-4237-169X; Email: jordi.dachs@idaea.csic.es

Maria Vila-Costa – Department of Environmental Chemistry, Institute of Environmental Assessment and Water Research, IDAEA-CSIC, 08034 Barcelona, Spain; orcid.org/0000-0003-1730-8418; Email: maria.vila@idaea.csic.es

Authors

Jon Iriarte – Department of Environmental Chemistry, Institute of Environmental Assessment and Water Research, IDAEA-CSIC, 08034 Barcelona, Spain; orcid.org/0000-0003-2315-1920

Gemma Casas – Department of Environmental Chemistry, Institute of Environmental Assessment and Water Research, IDAEA-CSIC, 08034 Barcelona, Spain

Alicia Martínez-Varela – Department of Environmental Chemistry, Institute of Environmental Assessment and Water Research, IDAEA-CSIC, 08034 Barcelona, Spain

Naiara Berrojalbiz – Department of Environmental Chemistry, Institute of Environmental Assessment and Water Research, IDAEA-CSIC, 08034 Barcelona, Spain

Complete contact information is available at: <https://pubs.acs.org/doi/10.1021/acs.est.2c05583>

Notes

The authors declare no competing financial interest.

■ ACKNOWLEDGMENTS

This work has been supported by the Spanish Ministry of Science and Innovation (MCIN) through projects REMARCA (CTM2012-34673), SENTINEL (CTM2015-70535), ANTOM (PGC2018-096612-B-I00), MIQAS (PID2021-128084OB-I00), and PANTOC (PID2021-127769NB-I00). J. Iriarte acknowledges the predoctoral FPU fellowship (FPU19/02782) funded by the Spanish Ministry of Universities. Dr. Daniel Lundin is acknowledged for his support in bioinformatic analyses. The research group of Global Change and Genomic Biogeochemistry receives support from the Catalan Government (2017SGR800). IDAEA-CSIC is a Centre of Excellence Severo Ochoa (Spanish Ministry of Science and Innovation, Project CEX2018-000794-S).

■ REFERENCES

- (1) Cabrerizo, A.; Galbán-Malagón, C.; del Vento, S.; Dachs, J. Sources and Fate of Polycyclic Aromatic Hydrocarbons in the Antarctic and Southern Ocean Atmosphere. *Global Biogeochem. Cycles* **2014**, *28*, 1424–1436.
- (2) Nizzetto, L.; Lohmann, R.; Gioia, R.; Jahnke, A.; Temme, C.; Dachs, J.; Herckes, P.; di Guardo, A.; Jones, K. C. PAHs in Air and Seawater along a North-South Atlantic Transect: Trends, Processes and Possible Sources. *Environ. Sci. Technol.* **2008**, *42*, 1580–1585.
- (3) González-Gaya, B.; Fernández-Pinos, M.-C.; Morales, L.; Méjanelle, L.; Abad, E.; Piña, B.; Duarte, C. M.; Jiménez, B.; Dachs, J. High Atmosphere–Ocean Exchange of Semivolatile Aromatic Hydrocarbons. *Nat. Geosci.* **2016**, *9*, 438–442.
- (4) Cai, M.; Liu, M.; Hong, Q.; Lin, J.; Huang, P.; Hong, J.; Wang, J.; Zhao, W.; Chen, M.; Cai, M.; Ye, J. Fate of Polycyclic Aromatic Hydrocarbons in Seawater from the Western Pacific to the Southern Ocean (17.5°N to 69.2°S) and Their Inventories on the Antarctic Shelf. *Environ. Sci. Technol.* **2016**, *50*, 9161–9168.
- (5) Wang, X. W.; Zhong, N. N.; Hu, D. M.; Uu, Z. Z.; Zhang, Z. H. Polycyclic Aromatic Hydrocarbon (PAHs) Pollutants in Groundwater from Coal Gangue Stack Area: Characteristics and Origin. *Water Sci. Technol.* **2009**, *59*, 1043–1051.
- (6) Casal, P.; Cabrerizo, A.; Vila-Costa, M.; Pizarro, M.; Jiménez, B.; Dachs, J. Pivotal Role of Snow Deposition and Melting Driving Fluxes of Polycyclic Aromatic Hydrocarbons at Coastal Livingston Island (Antarctica). *Environ. Sci. Technol.* **2018**, *52*, 12327–12337.
- (7) Lohmann, R.; Breivik, K.; Dachs, J.; Muir, D. Global Fate of POPs: Current and Future Research Directions. *Environ. Pollut.* **2007**, *150*, 150–165.
- (8) Thomas, E. R.; Marshall, G. J.; McConnell, J. R. A Doubling in Snow Accumulation in the Western Antarctic Peninsula since 1850. *Geophys. Res. Lett.* **2008**, *35*, No. L01706.
- (9) Miles, G. M.; Marshall, G. J.; McConnell, J. R.; Aristarain, A. J. Recent Accumulation Variability and Change on the Antarctic Peninsula from the ERA40 Reanalysis. *Int. J. Climatol.* **2008**, *28*, 1409–1422.
- (10) Vila-Costa, M.; Cerro-Gálvez, E.; Martínez-Varela, A.; Casas, G.; Dachs, J. Anthropogenic Dissolved Organic Carbon and Marine Microbiomes. *ISME J.* **2020**, *14*, 2646–2648.
- (11) González-Gaya, B.; Martínez-Varela, A.; Vila-Costa, M.; Casal, P.; Cerro-Gálvez, E.; Berrojalbiz, N.; Lundin, D.; Vidal, M.; Mompeán, C.; Bode, A.; Jiménez, B.; Dachs, J. Biodegradation as an Important Sink of Aromatic Hydrocarbons in the Oceans. *Nat. Geosci.* **2019**, *12*, 119–125.
- (12) Echeveste, P.; Galbán-Malagón, C.; Dachs, J.; Berrojalbiz, N.; Agustí, S. Toxicity of Natural Mixtures of Organic Pollutants in Temperate and Polar Marine Phytoplankton. *Sci. Total Environ.* **2016**, *571*, 34–41.

- (13) Trilla-Prieto, N.; Vila-Costa, M.; Casas, G.; Jiménez, B.; Dachs, J. Dissolved Black Carbon and Semivolatile Aromatic Hydrocarbons in the Ocean: Two Entangled Biogeochemical Cycles? *Environ. Sci. Technol. Lett.* **2021**, *8*, 918–923.
- (14) Dombrowski, N.; Donaho, J. A.; Gutierrez, T.; Seitz, K. W.; Teske, A. P.; Baker, B. J. Reconstructing Metabolic Pathways of Hydrocarbon-Degrading Bacteria from the Deepwater Horizon Oil Spill. *Nat. Microbiol.* **2016**, *1*, 16057.
- (15) Joye, S. B.; Kleindienst, S.; Gilbert, J. A.; Handley, K. M.; Weisenhorn, P.; Overholt, W. A.; Kostka, J. E. Responses of Microbial Communities to Hydrocarbon Exposures. *Oceanography* **2016**, *29*, 136–149.
- (16) Martinez-Varela, A.; Casas, G.; Berrojalbiz, N.; Piña, B.; Dachs, J.; Vila-Costa, M. Polycyclic Aromatic Hydrocarbon Degradation in the Sea-Surface Microlayer at Coastal Antarctica. *Front. Microbiol.* **2022**, *13*, No. 907265.
- (17) Nikolova, C.; Gutierrez, T. Marine Hydrocarbon-Degrading Bacteria: Their Role and Application in Oil-Spill Response and Enhanced Oil Recovery. In *Microbial Biodegradation and Bioremediation*; Elsevier, 2022; pp 591–600.
- (18) Head, I. M.; Jones, D. M.; Röling, W. F. M. Marine Microorganisms Make a Meal of Oil. *Nat. Rev. Microbiol.* **2006**, *4*, 173–182.
- (19) Lozada, M.; Marcos, M. S.; Commendatore, M. G.; Gil, M. N.; Dionisi, H. M. The Bacterial Community Structure of Hydrocarbon-Polluted Marine Environments as the Basis for the Definition of an Ecological Index of Hydrocarbon Exposure. *Microbes Environ.* **2014**, *29*, 269–276.
- (20) Teramoto, M.; Queck, S. Y.; Ohnishi, K. Specialized Hydrocarbonoclastic Bacteria Prevailing in Seawater around a Port in the Strait of Malacca. *PLoS One* **2013**, *8*, No. e66594.
- (21) Garneau, M. É.; Michel, C.; Meisterhans, G.; Fortin, N.; King, T. L.; Greer, C. W.; Lee, K. Hydrocarbon Biodegradation by Arctic Sea-Ice and Sub-Ice Microbial Communities during Microcosm Experiments, Northwest Passage (Nunavut, Canada). *FEMS Microbiol. Ecol.* **2016**, *92*, No. fiw130.
- (22) Yuan, J.; Lai, Q.; Sun, F.; Zheng, T.; Shao, Z. The Diversity of PAH-Degrading Bacteria in a Deep-Sea Water Column above the Southwest Indian Ridge. *Front. Microbiol.* **2015**, *6*, 853.
- (23) McFarlin, K. M.; Perkins, M. J.; Field, J. A.; Leigh, M. B. Biodegradation of Crude Oil and Corexit 9500 in Arctic Seawater. *Front. Microbiol.* **2018**, *9*, 1788.
- (24) Martinez-Varela, A.; Casas, G.; Piña, B.; Dachs, J.; Vila-Costa, M. Large Enrichment of Anthropogenic Organic Matter Degrading Bacteria in the Sea-Surface Microlayer at Coastal Livingston Island (Antarctica). *Front. Microbiol.* **2020**, *11*, No. 571983.
- (25) Yakimov, M. M.; Bargiela, R.; Golyshin, P. N. Calm and Frenzy: Marine Obligate Hydrocarbonoclastic Bacteria Sustain Ocean Wellness. *Curr. Opin. Biotechnol.* **2022**, *73*, 337–345.
- (26) Cerro-Gálvez, E.; Casal, P.; Lundin, D.; Piña, B.; Pinhassi, J.; Dachs, J.; Vila-Costa, M. Microbial Responses to Anthropogenic Dissolved Organic Carbon in the Arctic and Antarctic Coastal Seawaters. *Environ. Microbiol.* **2019**, *21*, 1466–1481.
- (27) Cerro-Gálvez, E.; Dachs, J.; Lundin, D.; Fernández-Pinos, M. C.; Sebastián, M.; Vila-Costa, M. Responses of Coastal Marine Microbiomes Exposed to Anthropogenic Dissolved Organic Carbon. *Environ. Sci. Technol.* **2021**, *55*, 9601–9621.
- (28) Gutierrez, T. Occurrence and Roles of the Obligate Hydrocarbonoclastic Bacteria in the Ocean When There Is No Obvious Hydrocarbon Contamination. In *Taxonomy, Genomics and Ecophysiology of Hydrocarbon-Degrading Microbes*; Springer: Cham, 2019; pp 337–352.
- (29) Xu, X.; Liu, W.; Tian, S.; Wang, W.; Qi, Q.; Jiang, P.; Gao, X.; Li, F.; Li, H.; Yu, H. Petroleum Hydrocarbon-Degrading Bacteria for the Remediation of Oil Pollution Under Aerobic Conditions: A Perspective Analysis. *Front. Microbiol.* **2018**, *9*, 2885.
- (30) Matsuoka, K.; Skoglund, A.; Roth, G.; de Pomereu, J.; Griffiths, H.; Headland, R.; Herried, B.; Katsumata, K.; le Brocq, A.; Licht, K.; Morgan, F.; Neff, P. D.; Ritz, C.; Scheinert, M.; Tamura, T.; van de Putte, A.; van den Broeke, M.; von Deschanden, A.; Deschamps-Berger, C.; Liefvering, B. van.; Tronstad, S.; Melvaer, Y. Quantarctica, an Integrated Mapping Environment for Antarctica, the Southern Ocean, and Sub-Antarctic Islands. *Environ. Model. Softw.* **2021**, *140*, No. 105015.
- (31) Gasol, J. M.; Morán, X. A. G. Flow Cytometric Determination of Microbial Abundances and Its Use to Obtain Indices of Community Structure and Relative Activity. In *Hydrocarbon and Lipid Microbiology Protocols*; Springer Protocols Handbooks; Springer, 2015; pp 159–187.
- (32) Hansen, H. P.; Koroleff, F. Determination of Nutrients. In *Methods of Seawater Analysis*; Wiley-VCH Verlag GmbH: Weinheim, Germany, 1999; pp 159–228.
- (33) Vila-Costa, M.; Sebastián, M.; Pizarro, M.; Cerro-Gálvez, E.; Lundin, D.; Gasol, J. M.; Dachs, J. Microbial Consumption of Organophosphate Esters in Seawater under Phosphorus Limited Conditions. *Sci. Rep.* **2019**, *9*, No. 233.
- (34) Parada, A. E.; Needham, D. M.; Fuhrman, J. A. Every Base Matters: Assessing Small Subunit rRNA Primers for Marine Microbiomes with Mock Communities, Time Series and Global Field Samples. *Environ. Microbiol.* **2016**, *18*, 1403–1414.
- (35) Callahan, B. J.; McMurdie, P. J.; Rosen, M. J.; Han, A. W.; Johnson, A. J. A.; Holmes, S. P. DADA2: High-Resolution Sample Inference from Illumina Amplicon Data. *Nat. Methods* **2016**, *13*, 581–583.
- (36) Martin, M. Cutadapt Removes Adapter Sequences from High-Throughput Sequencing Reads. *EMBnet J.* **2011**, *17*, 10.
- (37) Cole, J. R.; Wang, Q.; Fish, J. A.; Chai, B.; McGarrell, D. M.; Sun, Y.; Brown, C. T.; Porras-Alfaro, A.; Kuske, C. R.; Tiedje, J. M. Ribosomal Database Project: Data and Tools for High Throughput RNA Analysis. *Nucleic Acids Res.* **2014**, *42*, D633–D642 DOI: 10.1093/nar/gkt1244.
- (38) Oksanen, J.; Simpson, G. L.; Blanchet, F. G.; Kindt, R.; Legendre, P.; Minchin, P. R.; O'Hara, R. B.; Solymos, P.; Stevens, M. H. H.; Szoecs, E.; Wagner, H.; Barbour, M.; Bedward, M.; Bolker, B.; Bolcard, D.; Carvalho, G.; Chirico, M.; De Caceres, M.; Durand, S.; Evangelista, H. B. A.; FitzJohn, R.; Friendly, M.; Furneaux, B.; Hannigan, G.; Hill, M. O.; Lahti, L.; McGlinn, D.; Ouellette, M. H.; Ribeiro Cunha, E.; Smith, T.; Stier, A.; Ter Braak, C. J. F.; Weedon, J. *Vegan: Community Ecology Package*, 2020. R package version 2.5-7; <https://CRAN.R-project.org/package=vegan>.
- (39) Króllicka, A.; Boccadoro, C.; Møland, M.; Preston, C. M.; Birch, J.; Scholin, C.; Baussant, T. In *Detection of Oil Leaks by Quantifying Hydrocarbonoclastic Bacteria in Cold Marine Environments Using the Environmental Sample Processor*, Proceedings of the 37th AMOP Technical Seminar on Environmental Contamination and Response, 2014; pp 791–807.
- (40) Króllicka, A.; Boccadoro, C.; Nilsen, M. M.; Demir-Hilton, E.; Birch, J.; Preston, C.; Scholin, C.; Baussant, T. Identification of Microbial Key-Indicators of Oil Contamination at Sea through Tracking of Oil Biotransformation: An Arctic Field and Laboratory Study. *Sci. Total Environ.* **2019**, *696*, No. 133715.
- (41) Gat, D.; Mazar, Y.; Cytryn, E.; Rudich, Y. Origin-Dependent Variations in the Atmospheric Microbiome Community in Eastern Mediterranean Dust Storms. *Environ. Sci. Technol.* **2017**, *51*, 6709–6718.
- (42) Mardale, B. H.; Anderson, M. J. Fitting multivariate models to community data: a comment on distance-based redundancy analysis. *Ecology* **2001**, *82*, 290–297.
- (43) Wickham, H. A Layered Grammar of Graphics. *J. Comput. Graph. Stat.* **2010**, *19*, 3–28.
- (44) Berrojalbiz, N.; Dachs, J.; Ojeda, M. J.; Valle, M. C.; Castro-Jiménez, J.; Wollgast, J.; Ghiani, M.; Hanke, G.; Zaldivar, J. M. Biogeochemical and Physical Controls on Concentrations of Polycyclic Aromatic Hydrocarbons in Water and Plankton of the Mediterranean and Black Seas. *Global Biogeochem. Cycles* **2011**, *25*, No. GB4003.
- (45) Liu, M.; Cai, M.; Duan, M.; Chen, M.; Lohmann, R.; Lin, Y.; Liang, J.; Ke, H.; Zhang, K. PAHs in the North Atlantic Ocean and

the Arctic Ocean: Spatial Distribution and Water Mass Transport. *J. Geophys. Res.: Oceans* **2022**, 127, No. e2021JC018389.

(46) Guitart, C.; García-Flor, N.; Bayona, J. M.; Albaigés, J. Occurrence and Fate of Polycyclic Aromatic Hydrocarbons in the Coastal Surface Microlayer. *Mar. Pollut. Bull.* **2007**, 54, 186–194.

(47) Guigüe, C.; Tedetti, M.; Ferretto, N.; García, N.; Méjanelle, L.; Goutx, M. Spatial and Seasonal Variabilities of Dissolved Hydrocarbons in Surface Waters from the Northwestern Mediterranean Sea: Results from One Year Intensive Sampling. *Sci. Total Environ.* **2014**, 466–467, 650–662.

(48) Hong, W. J.; Jia, H.; Li, Y. F.; Sun, Y.; Liu, X.; Wang, L. Polycyclic Aromatic Hydrocarbons (PAHs) and Alkylated PAHs in the Coastal Seawater, Surface Sediment and Oyster from Dalian, Northeast China. *Ecotox. Environ. Saf.* **2016**, 128, 11–20.

(49) Ya, M.; Xu, L.; Wu, Y.; Li, Y.; Zhao, S.; Wang, X. Fossil Fuel-Derived Polycyclic Aromatic Hydrocarbons in the Taiwan Strait, China, and Fluxes across the Air-Water Interface. *Environ. Sci. Technol.* **2018**, 52, 7307–7316.

(50) Zheng, H.; Cai, M.; Zhao, W.; Khairy, M.; Chen, M.; Deng, H.; Lohmann, R. Net Volatilization of PAHs from the North Pacific to the Arctic Ocean Observed by Passive Sampling. *Environ. Pollut.* **2021**, 276, No. 116728.

(51) Bengtson Nash, S. Persistent Organic Pollutants in Antarctica: Current and Future Research Priorities. *J. Environ. Monit.* **2011**, 13, 497–504.

(52) Casas, G.; Martínez-Varela, A.; Vila-Costa, M.; Jiménez, B.; Dachs, J. Rain Amplification of Persistent Organic Pollutants. *Environ. Sci. Technol.* **2021**, 55, 12961–12972.

(53) Casal, P.; Zhang, Y.; Martin, J. W.; Pizarro, M.; Jiménez, B.; Dachs, J. Role of Snow Deposition of Perfluoroalkylated Substances at Coastal Livingston Island (Maritime Antarctica). *Environ. Sci. Technol.* **2017**, 51, 8460–8470.

(54) Casal, P.; Casas, G.; Vila-Costa, M.; Cabrerizo, A.; Pizarro, M.; Jiménez, B.; Dachs, J. Snow Amplification of Persistent Organic Pollutants at Coastal Antarctica. *Environ. Sci. Technol.* **2019**, 53, 8872–8882.

(55) Bagby, S. C.; Reddy, C. M.; Aeppli, C.; Fisher, G. B.; Valentine, D. L. Persistence and Biodegradation of Oil at the Ocean Floor Following Deepwater Horizon. *Proc. Natl. Acad. Sci. U.S.A.* **2017**, 114, E9–E18.

(56) Shuttleworth, K. L.; Cerniglia, C. E. Environmental Aspects of PAH Biodegradation. *Appl. Biochem. Biotechnol.* **1995**, 54, 291–302.

(57) Amodu, O.S.; Ntwampe, S.K.O.; Ojumu, T. V. *Bioavailability of High Molecular Weight Polycyclic Aromatic Hydrocarbons Using Renewable Resources*; INTECH Open Access Publisher, 2013.

(58) Crampon, M.; Bureau, F.; Akpa-Vincelas, M.; Bodilis, J.; Machour, N.; le Derf, F.; Portet-Koltalo, F. Correlations between PAH Bioavailability, Degrading Bacteria, and Soil Characteristics during PAH Biodegradation in Five Diffusely Contaminated Dissimilar Soils. *Environ. Sci. Pollut. Res.* **2014**, 21, 8133–8145.

(59) Behymer, T. D.; Hites, R. A. Photolysis of Polycyclic Aromatic Hydrocarbons Adsorbed on Simulated Atmospheric Particulates. *Environ. Sci. Technol.* **1985**, 19, 1004–1006.

(60) Olund, S.; Lyons, W. B.; Welch, S. A.; Welch, K. A. Fe and nutrients in coastal Antarctic streams: Implications for primary production in the Ross Sea. *J. Geophys. Res.-Biogeosci.* **2018**, 123, 3507–3522.

(61) Signori, C. N.; Pellizari, V. H.; Enrich-Prast, A.; Sievert, S. M. Spatiotemporal Dynamics of Marine Bacterial and Archaeal Communities in Surface Waters off the Northern Antarctic Peninsula. *Deep Sea Res., Part II* **2018**, 149, 150–160.

(62) Ozturk, R. C.; Feyzioglu, A. M.; Altinok, I. Prokaryotic Community and Diversity in Coastal Surface Waters along the Western Antarctic Peninsula. *Polar Sci.* **2022**, 31, No. 100764.

(63) Giovannoni, S. J. SAR11 Bacteria: The Most Abundant Plankton in the Oceans. *Annu. Rev. Mar. Sci.* **2017**, 9, 231–255.

(64) Auladell, A.; Barberán, A.; Logares, R.; Garcés, E.; Gasol, J. M.; Ferrera, I. Seasonal Niche Differentiation among Closely Related Marine Bacteria. *ISME J.* **2022**, 16, 178–189.

(65) Cao, S.; He, J.; Zhang, F.; Lin, L.; Gao, Y.; Zhou, Q. Diversity and Community Structure of Bacterioplankton in Surface Waters off the Northern Tip of the Antarctic Peninsula. *Polar Res.* **2019**, 38, 3941.

(66) Alcamán-Arias, M. E.; Fuentes-Alburquenque, S.; Vergara-Barros, P.; Cifuentes-Anticevic, J.; Verdugo, J.; Polz, M.; Farias, L.; Pedrós-Alió, C.; Díez, B. Coastal Bacterial Community Response to Glacier Melting in the Western Antarctic Peninsula. *Microorganisms* **2021**, 9, 88.

(67) Gontikaki, E.; Potts, L. D.; Anderson, J. A.; Witte, U. Hydrocarbon-Degrading Bacteria in Deep-Water Subarctic Sediments (Faroe-Shetland Channel). *J. Appl. Microbiol.* **2018**, 125, 1040–1053.

(68) McLachlan, M. S.; Zou, H.; Gouin, T. Using Benchmarking to Strengthen the Assessment of Persistence. *Environ. Sci. Technol.* **2017**, 51, 4–11.

(69) Cerro-Gálvez, E.; Roscales, J. L.; Jiménez, B.; Sala, M. M.; Dachs, J.; Vila-Costa, M. Microbial Responses to Perfluoroalkyl Substances and Perfluorooctanesulfonate (PFOS) Desulfurization in the Antarctic Marine Environment. *Water Res.* **2020**, 171, No. 115434.

(70) Vergeynst, L.; Kjeldsen, K.; Lassen, P.; Rysgaard, S. Bacterial Community Succession and Degradation Patterns of Hydrocarbons in Seawater at Low Temperature. *J. Hazard. Mater.* **2018**, 353, 127–134.

(71) Dubinsky, E. A.; Conrad, M. E.; Chakraborty, R.; Bill, M.; Borglin, S. E.; Hollibaugh, J. T.; Mason, O. U.; M Piceno, Y.; Reid, F. C.; Stringfellow, W. T.; Tom, L. M.; Hazen, T. C.; Andersen, G. L. Succession of Hydrocarbon-Degrading Bacteria in the Aftermath of the Deepwater Horizon Oil Spill in the Gulf of Mexico. *Environ. Sci. Technol.* **2013**, 47, 10860–10867.

(72) Gutierrez, T.; Morris, G.; Ellis, D.; Bowler, B.; Jones, M.; Salek, K.; Mulloy, B.; Teske, A. Hydrocarbon-Degradation and MOS-Formation Capabilities of the Dominant Bacteria Enriched in Sea Surface Oil Slicks during the Deepwater Horizon Oil Spill. *Mar. Pollut. Bull.* **2018**, 135, 205–215.

(73) Krolicka, A.; Boccadoro, C.; Nilsen, M. M.; Baussant, T. Capturing Early Changes in the Marine Bacterial Community as a Result of Crude Oil Pollution in a Mesocosm Experiment. *Microbes Environ.* **2017**, 32, 358–366.

SUPPORTING INFORMATION

Snow-Dependent Biogeochemical Cycling of Polycyclic Aromatic Hydrocarbons at Coastal Antarctica

Jon Iriarte, Jordi Dachs*, Gemma Casas, Alicia Martínez-Varela, Naiara Berrojalbiz and Maria Vila-Costa*

Department of Environmental Chemistry, Institute of Environmental Assessment and Water Research, IDAEA-CSIC; 08034 Barcelona, Catalunya, Spain

Corresponding authors: jordi.dachs@idaea.csic.es & maria.vila@idaea.csic.es

Summary: 39 pages. 2 annexes, 9 tables, 13 figures

Table of Contents

Annex S1. Analytical Procedures for PAH determination

Annex S2. Quality Assurance/Quality Control for PAH analysis

Table S1. Description and coordinates of the sampling stations.

Table S2. Ancillary data for the seawater samples (average between 0.2 to 5 m depth) obtained from the CTD cast.

Table S3. Recoveries of PAH surrogates for each sampling campaign.

Table S4. Limits of quantification for PAHs for seawater and plankton samples for Deception 2017 and Livingston 2018.

Table S5. Nutrient concentrations and bacterial abundances for the water samples.

Table S6. Individual PAH concentrations in the dissolved phase (ng L^{-1}) for the Deception 2017 and Livingston 2018 campaigns.

Table S7. Individual PAH Plankton phase concentrations ($\text{ng g}_{\text{dw}}^{-1}$) for the Deception 2017 and Livingston 2018 campaigns.

Table S8. Classification of the PAHs analyzed in this study as low molecular weight (LMW) PAH or high molecular weight (HMW) PAH.

Table S9. Relative abundances (%) of HCB taxa, expressed as the mean, standard deviation, maximum and minimum of each taxa for each campaign.

Figure S1. Picture of South bay for the 2015, 2017 and 2018 campaigns (January) showing the difference in snow cover.

Figure S2: Occurrence of individual PAHs in plankton for the three sampling campaigns.

Figure S3: Differences in individual PAH concentrations in the water dissolved phase for the three sampling campaigns assessed by an ANOVA followed by a Tukey test.

Figure S4: Differences in individual PAH concentrations in the plankton phase for the three sampling campaigns assessed by an ANOVA followed by a Tukey test.

Figure S5: Temporal series of the parent/alkyl-PAHs concentration ratios in the water dissolved phase for the three campaigns.

Figure S6: Temporal series of the LMW/HMW ratios in the water dissolved phase for the three campaigns.

Figure S7: Bioconcentration factors (Log BCF) versus octanol-water partition coefficients (Log K_{ow}) for the three sampling campaigns.

Figure S8: Boxplot of inorganic nutrient concentrations for the three campaigns.

Figure S9: Non-metric Multidimensional Scaling (NMDS) plot for clustering samples according to their ASV composition.

Figure S10: Structure of the bacterial community for the three sampling campaigns.

Figure S11: Correlation between amplicon sequencing relative abundance and qPCR relative abundance for the genus *Colwellia* at Jhonsons dock.

Figure S12: Partial least squares regression (PLS).

Figure S13: Plot showing the weight of the VIP x variables (individual ASV) over the components 1 and 2 of the PLS.

References

Annex S1. Analytical Procedures for PAH determination

Sample handling (filtrations and elution through the XAD-2 column) was performed outside the Antarctic stations to avoid potential contamination from the in-side laboratory. Further processing of the samples was performed in a clean lab (ISO 5). The analytical methodology has been reported elsewhere.¹ Briefly, XAD-2 columns were eluted with 200 mL of methanol, followed by 200 mL of dichloromethane and 100 mL of hexane at a flow rate of 2 mL min⁻¹ using an axial piston pump. The methanol fraction was concentrated and liquid-liquid extracted with 50 mL of hexane for three times. The hexane extracts were dried over anhydrous sodium sulphate and combined with the dichloromethane and hexane fractions. After reducing the volume with a rotatory evaporator, the extracts were fractionated with 25 mL of hexane, 40 mL of dichloromethane:hexane (1:3, v:v) and 20 mL dichloromethane:acetone (70:30, v:v) on a 5 g of a silica gel column (silica 60-200 mesh, activated at 250 °C for 24 h) and 3 g of 3 % deactivated neutral alumina column (aluminum oxide 90, activated at 250 °C for 12 h). Plankton samples were lyophilized during 5 h and Soxhlet-extracted with dichloromethane:hexane (1:1, v:v) during 24 h, and fractionated using the same procedure than for the dissolved phase. The perdeuterated standards acenaphthene-d10, phenanthrene-d10, crysene-d12 and perylene-d12 were added before extraction for recovery control.

Before the injection, the vials were spiked with 50 ng of the perdeuterated standards anthracene-d10, pyrene-d10 and benzo[b]fluoranthrene-d12 that were used as injection (internal) standards. PAH quantification was performed with an Agilent 6890 Series gas chromatograph coupled to a mass spectrometer Agilent 5973 (GCMS) operating in selected ion monitoring (SIM) and electron impact mode (EI). A 30 m capillary column (HP-5MS, 0.25mm x 0.25µm film thickness) was used. The oven temperature was increased to 90 °C (held for 1 min), then increased to 175 °C at 6 °C/min (held for 4 min), increased to 235 °C at 3 °C/min, increased to 300 °C at 8 °C/min (held for 8 min), and finally to 315 °C for 5 min (held for 8 min). Injector and transfer line temperatures were 280 and 300 °C, respectively. 2 µL of sample were injected in split less mode.

Annex S2. Quality Assurance/Quality Control for PAH analysis

All containers, tubes and connections used during sampling and chemical analysis were of stainless steel, glass or PTFE, and they had been pre-cleaned with acetone prior use in order to avoid contamination.

Field blanks consisted of GF/D filters and XAD-2 columns that followed the same process as the samples albeit without the pass of plankton or water. Procedural and/or field blanks were analyzed with each batch of 4-6 samples to monitor potential contamination during sampling and extraction. The limits of quantification (LOQs) were defined as the mean concentration of field or procedural blanks, whichever higher, plus three times the standard deviation of the blank response. For the analytes which were not found in procedural blanks, LOQ were derived from the lowest standard in the calibration curve (three times the signal-to-noise ratio of the lowest standard in the calibration curve). Surrogate recoveries are resumed in Table S3 and limits of quantification are listed in Table S4.

Table S1. Description and coordinates of the sampling stations.

Sampling station	Campaign	Sample type	S	W	Sampling name	Plankton net depth
St-1	Livingston 2018	Seawater and plankton	62° 38.792'	60° 38.411'	Hannah Point	30 m
St-2	Livingston 2018	Seawater and plankton	62° 38.346'	60° 23.912'	South Bay	30 m
St-3	Livingston 2015	Seawater and plankton	62° 39.425'	60° 23.277'	Raquelia Rocks	30 m
St-4	Livingston 2015 & 2018	Seawater and plankton	62°39,556'	60° 22,132'	Johnsons Dock	13-14 m
St-5	Livingston 2018	Seawater and plankton	62° 37.718'	60° 21.400'	Emona Anchor-age	30 m
St-6	Livingston 2018	Plankton	62° 42.694'	60° 26.547'	Miers Bluff	60 m
St-7	Livingston 2018	Plankton	62° 41.757'	60° 20.008'	False Bay	40 m
St-8	Deception 2017	Seawater and plankton	62° 59.386'	60° 37.115'	Colatinas Point	15 m

Table S2. Ancillary data for the seawater samples (average between 0.2 to 5 m depth) obtained from the CTD cast. PAR means photosynthetic active radiation and n.d. means no-data available.

Date	Sampling station	Campaign	Temperature (°C)	Salinity (PSU)	Fluorescence (RFU)	PAR	Turbidity (NTU)
15/12/2014	St-3	Livingston 2015	0.46	34.01	0.52	129.51	4.86
16/12/2014	St-4	Livingston 2015	0.82	33.68	0.33	161.21	5.97
18/12/2014	St-3	Livingston 2015	0.70	33.81	0.68	207.84	5.50
23/12/2014	St-4	Livingston 2015	1.24	33.70	0.50	203.10	3.90
24/12/2014	St-3	Livingston 2015	0.20	34.00	0.22	367.00	3.17
26/12/2014	St-4	Livingston 2015	1.24	33.70	0.50	203.10	3.90
29/12/2014	St-3	Livingston 2015	0.48	33.99	0.41	295.60	3.59
31/12/2014	St-4	Livingston 2015	1.33	33.84	0.28	431.20	3.92
02/01/2015	St-4	Livingston 2015	1.52	33.77	0.25	294.90	2.65
05/01/2015	St-3	Livingston 2015	1.34	33.55	0.59	259.30	4.87
07/01/2015	St-4	Livingston 2015	1.32	33.59	0.43	550.20	4.92
09/01/2015	St-3	Livingston 2015	1.12	33.95	0.57	126.04	2.27
12/01/2015	St-3	Livingston 2015	1.64	33.81	0.43	307.60	3.13
14/01/2015	St-4	Livingston 2015	1.97	33.36	1.21	154.07	3.68
16/01/2015	St-3	Livingston 2015	1.26	33.91	1.91	68.30	3.02
19/01/2015	St-4	Livingston 2015	1.23	33.69	1.01	176.72	5.95
21/01/2015	St-3	Livingston 2015	0.40	33.55	0.91	179.76	5.70
23/01/2015	St-4	Livingston 2015	1.15	33.34	1.57	49.63	6.65
26/01/2015	St-3	Livingston 2015	1.55	33.55	1.12	81.98	5.79
29/01/2015	St-4	Livingston 2015	1.51	33.29	1.63	29.66	10.55
02/02/2015	St-3	Livingston 2015	1.82	33.73	1.21	67.37	5.07
05/02/2015	St-4	Livingston 2015	1.71	33.19	1.04	67.40	12.38
10/02/2015	St-3	Livingston 2015	1.66	33.58	1.62	46.30	7.24
12/02/2015	St-4	Livingston 2015	1.83	33.33	1.52	42.01	10.46
16/02/2015	St-3	Livingston 2015	1.82	33.52	0.68	305.40	6.15
19/02/2015	St-4	Livingston 2015	1.91	33.39	0.92	137.83	8.23
25/01/2017	St-8	Deception 2017	2.55	34.00	5.32	10.22	3.96
30/01/2017	St-8	Deception 2017	2.01	34.02	1.27	267.22	3.66
02/02/2017	St-8	Deception 2017	2.23	33.48	1.03	236.03	3.64
05/02/2017	St-8	Deception 2017	2.40	33.73	4.21	102.64	4.35
09/02/2017	St-8	Deception 2017	2.43	33.74	4.31	17.63	3.68
11/02/2017	St-8	Deception 2017	2.71	33.68	5.46	52.19	4.13
15/02/2017	St-8	Deception 2017	2.43	33.81	2.36	57.16	3.67
17/02/2017	St-8	Deception 2017	2.50	33.90	1.29	202.91	3.67
08/01/2018	St-4	Livingston 2018	n.d	n.d	n.d	n.d	n.d
11/01/2018	St-2	Livingston 2018	n.d	n.d	n.d	n.d	n.d
16/01/2018	St-4	Livingston 2018	n.d	n.d	n.d	n.d	n.d
20/01/2018	St-2	Livingston 2018	1.60	34.14	0.66	0.27	3.56
22/01/2018	St-4	Livingston 2018	1.42	33.30	0.40	0.27	7.84
23/01/2018	St-6	Livingston 2018	0.68	33.63	0.29	0.27	7.17
23/01/2018	St-7	Livingston 2018	1.99	33.96	0.59	0.27	3.74
24/01/2018	St-2	Livingston 2018	2.23	33.94	0.88	0.27	3.66
25/01/2018	St-4	Livingston 2018	1.71	33.46	0.27	0.27	5.85
27/01/2018	St-2	Livingston 2018	2.43	33.68	0.31	0.27	4.86
29/01/2018	St-4	Livingston 2018	1.87	33.49	0.58	0.27	6.04
03/02/2018	St-2	Livingston 2018	1.59	34.75	0.15	0.27	3.55
05/02/2018	St-4	Livingston 2018	1.47	33.61	0.44	0.27	6.41
08/02/2018	St-1	Livingston 2018	2.25	33.82	0.19	0.27	8.56
12/02/2018	St-2	Livingston 2018	1.76	33.67	0.18	0.27	7.11
16/02/2018	St-4	Livingston 2018	1.78	33.26	0.23	0.27	7.44
20/02/2018	St-2	Livingston 2018	2.93	33.86	0.23	0.27	3.87
23/02/2018	St-4	Livingston 2018	1.82	33.16	0.19	0.27	9.83
28/02/2018	St-5	Livingston 2018	1.14	33.63	0.28	0.27	5.44

28/02/2018	St-2	Livingston 2018	n.d	n.d	n.d	n.d	n.d
01/03/2018	St-1	Livingston 2018	1.73	33.94	0.30	0.27	4.08

Table S3. Recoveries of PAH surrogates for each sampling campaign.

Livingston 2015		
Surrogate	Seawater	Plankton
acenaphthene-d10	63±9.5%	65±18%
phenanthrene-d10	96±17%	72±12%
crysene-d12	85±25%	85±14%
perylene-d12	100±17%	100±25%
Livingston 2018		
Surrogate	Seawater	Plankton
phenanthrene-d10	19±12%	51±5.7%
perylene-d12	67±33%	77±23%
Deception 2017		
Surrogate	Seawater	Plankton
phenanthrene-d10	20±11%	31±4.8%
perylene-d12	64±32%	66±7.5%

Table S4. Limits of quantification for PAHs for seawater and plankton samples for Deception 2017 and Livingston 2018. The limits of quantification (LOQs, ng) were defined as the mean concentration of field blanks plus three times the standard deviation of the blank response. For the analytes not detected in blanks, LOQs were derived from the lowest standard in calibration curve (three times the signal-to-noise ratio of the lowest standard in the calibration curve).

PAH	Liv. 2018 sea-water (ng)	Dec. 2017 sea-water (ng)	Liv. 2018 plank-ton (ng)	Dec. 2017 plank-ton (ng)
MFlu(1)	0.005	0.005	0.005	0.018
MFlu(2)	0.005	0.005	0.005	0.021
MFlu(3)	0.005	0.005	0.018	0.038
MFlu(4)	0.058	0.005	0.040	0.066
DBT	0.069	0.086	0.077	0.011
MDBT(1)	0.068	0.137	0.020	0.011
MDBT(2)	0.034	0.101	0.009	0.005
MDBT(3)	0.005	0.043	0.010	0.005
DMDBT(1)	0.005	0.085	0.005	0.005
DMDBT(2)	0.005	0.044	0.005	0.005
DMDBT(3)	0.042	0.189	0.005	0.005
DMDBT(4)	0.005	0.095	0.005	0.005
DMDBT(5)	0.005	0.037	0.005	0.005
Phe	0.632	0.941	0.244	0.364
MPhe(1)	0.065	0.108	0.024	0.047
MPhe(2)	0.084	0.157	0.035	0.064
MPhe(5)	1.017	1.085	0.009	0.005
MPhe(3)	0.085	0.136	0.034	0.087
MPhe(4)	0.045	0.131	0.028	0.057
DMPhe(1)	0.016	0.051	0.005	0.005
DMPhe(2)	0.017	0.039	0.005	0.005
DMPhe(3)	0.005	0.005	0.005	0.005
DMPhe(4)	0.047	0.129	0.005	0.005
DMPhe(5)	0.029	0.070	0.005	0.005
DMDBT(6)	0.005	0.005	0.005	0.005
DMPhe(6)	0.023	0.065	0.005	0.022
DMPhe(7)	0.005	0.005	0.005	0.005
DMPhe(8)	0.005	0.005	0.005	0.005
DMPhe(9)	0.009	0.005	0.005	0.005
DMPhe(10)	0.005	0.005	0.005	0.005
TMPhe(1)	0.005	0.005	0.005	0.005
TMPhe(2)	0.005	0.005	0.005	0.005
TMPhe(3)	0.005	0.005	0.005	0.005
TMPhe(4)	0.005	0.005	0.005	0.005
TMPhe(5)	0.005	0.005	0.005	0.005

TMPhe(6)	0.005	0.005	0.005	0.005
TMPhe(7)	0.005	0.005	0.005	0.005
TMPhe(8)	0.005	0.005	0.005	0.005
TMPhe(9)	0.005	0.005	0.005	0.005
TMPhe(10)	0.005	0.005	0.005	0.005
TMPhe(11)	0.005	0.005	0.005	0.005
TMPhe(12)	0.005	0.005	0.005	0.005
Ant	0.580	0.049	0.019	0.026
Flt	0.581	1.761	0.036	0.253
Pyr	0.981	1.085	0.031	0.079
MPyr(1)	0.005	0.005	0.005	0.005
MPyr(2)	0.092	0.124	0.005	0.005
MPyr(3)	0.063	0.037	0.005	0.005
MPyr(4)	0.087	0.093	0.005	0.005
MPyr(5)	0.064	0.005	0.005	0.005
DMPyr(1)	0.005	0.005	0.005	0.005
DMPyr(2)	0.005	0.005	0.005	0.005
DMPyr(3)	0.005	0.005	0.005	0.005
DMPyr(4)	0.005	0.005	0.005	0.005
DMPyr(5)	0.005	0.033	0.005	0.005
DMPyr(6)	0.005	0.035	0.005	0.005
DMPyr(7)	0.005	0.055	0.005	0.005
DMPyr(8)	0.005	0.147	0.005	0.005
B[g,h,i]f	1.263	1.466	0.160	0.160
B[a]ant	0.160	0.160	0.160	0.160
Cry	0.160	0.160	0.160	0.160
MCry(1)	0.160	0.160	0.160	0.160
MCry(3)	0.160	0.160	0.160	0.160
MCry(4)	0.160	0.160	0.160	0.160
MCry(2)	0.160	0.160	0.160	0.160
B[b]f	0.035	0.090	0.134	0.010
B[k]f	0.072	0.118	0.010	0.010
B[e]pyr	0.160	0.160	0.160	0.160
B[a]pyr	0.160	0.160	0.160	0.160
Pery	0.160	0.160	0.160	0.160
In[1,2,3- cd]pyr	0.160	0.430	0.160	0.160
Dib[a,h]ant	0.160	0.160	0.160	0.160
B[g,h,i]per	0.160	0.160	0.160	0.160

Table S5: Nutrient concentrations and bacterial abundances for the water samples. Bacterial abundances were measured by flow cytometry for the Deception 2017 and Livingston 2018 campaigns, but by counts of the 16S for the Livingston 2015 campaign. Those measured by flow cytometry are multiplied by 1000 to transform the units from cells/mL to copies of 16S/L, assuming that each cell has 1 copy of the 16S gene.

Date	Station	Campaign	NO ₃ ⁻ + NO ₂ ⁻ (μmol L ⁻¹)	N-NH ₄ ⁺ (μmol L ⁻¹)	P-PO ₄ ³⁻ (μmol L ⁻¹)	Bacterial abundance (copies 16S L ⁻¹)
15/12/2014	St-3	Livingston 2015	29.13	1.34	2.03	2.08E+09
16/12/2014	St-4	Livingston 2015	24.84	3.77	1.74	3.54E+09
18/12/2014	St-3	Livingston 2015	16.18	2.07	1.44	1.25E+09
23/12/2014	St-4	Livingston 2015	23.46	3.94	1.78	6.86E+09
24/12/2014	St-3	Livingston 2015	24.02	4.68	1.65	6.60E+09
26/12/2014	St-4	Livingston 2015	18.49	12.60	1.46	5.09E+09
29/12/2014	St-3	Livingston 2015	27.67	22.62	1.83	6.34E+09
31/12/2014	St-4	Livingston 2015	24.00	22.40	1.77	1.09E+10
02/01/2015	St-4	Livingston 2015	23.83	10.65	1.86	5.78E+08
05/01/2015	St-3	Livingston 2015	15.39	22.75	1.35	8.08E+09
07/01/2015	St-4	Livingston 2015	17.27	22.48	1.64	5.73E+09
09/01/2015	St-3	Livingston 2015	15.46	22.51	1.35	2.00E+10
12/01/2015	St-3	Livingston 2015	21.49	7.95	1.61	1.23E+10
14/01/2015	St-4	Livingston 2015	14.87	21.41	1.36	1.42E+10
16/01/2015	St-3	Livingston 2015	22.88	8.84	1.64	4.21E+09
19/01/2015	St-4	Livingston 2015	19.51	22.95	1.72	1.64E+10
21/01/2015	St-3	Livingston 2015	25.82	22.64	1.81	5.90E+09
23/01/2015	St-4	Livingston 2015	21.41	1.66	1.75	7.27E+09
26/01/2015	St-3	Livingston 2015	20.18	23.21	1.66	5.70E+09
29/01/2015	St-4	Livingston 2015	14.16	21.76	1.75	1.34E+09
02/02/2015	St-3	Livingston 2015	12.00	22.77	1.72	1.15E+09
05/02/2015	St-4	Livingston 2015	18.36	8.59	1.87	1.33E+09
10/02/2015	St-3	Livingston 2015	21.87	23.15	1.95	4.78E+10
12/02/2015	St-4	Livingston 2015	12.97	22.83	2.19	7.85E+09
16/02/2015	St-3	Livingston 2015	23.92	22.86	1.96	2.98E+09
19/02/2015	St-4	Livingston 2015	20.66	14.48	2.11	1.29E+09
25/01/2017	St-8	Deception 2017	7.65	0.56	0.46	5.12E+08
30/01/2017	St-8	Deception 2017	20.40	0.27	1.08	4.57E+08
02/02/2017	St-8	Deception 2017	18.93	0.11	1.04	4.97E+08
05/02/2017	St-8	Deception 2017	10.13	0.05	0.58	6.85E+08
09/02/2017	St-8	Deception 2017	16.14	0.40	1.20	6.24E+08
11/02/2017	St-8	Deception 2017	14.34	0.06	0.93	4.48E+08
15/02/2017	St-8	Deception 2017	8.50	0.73	1.12	3.80E+08

17/02/2017	St-8	Deception 2017	13.20	0.11	0.91	3.47E+08
08/01/2018	St-4	Livingston 2018	9.58	7.65	1.06	n.d
11/01/2018	St-2	Livingston 2018	n.d	n.d	n.d	n.d
16/01/2018	St-4	Livingston 2018	19.83	10.80	2.12	2.22E+08
20/01/2018	St-2	Livingston 2018	26.15	1.97	1.69	1.89E+08
22/01/2018	St-4	Livingston 2018	19.36	20.91	1.53	2.37E+08
23/01/2018	St-6	Livingston 2018	n.d	n.d	n.d	n.d
23/01/2018	St-7	Livingston 2018	n.d	n.d	n.d	n.d
24/01/2018	St-2	Livingston 2018	26.83	2.65	1.87	2.15E+08
25/01/2018	St-4	Livingston 2018	18.31	2.84	1.42	1.98E+08
27/01/2018	St-2	Livingston 2018	23.27	2.52	1.40	1.47E+08
29/01/2018	St-4	Livingston 2018	n.d	n.d	n.d	1.54E+08
03/02/2018	St-2	Livingston 2018	18.82	10.80	1.65	9.50E+07
05/02/2018	St-4	Livingston 2018	15.32	5.08	1.46	1.50E+08
08/02/2018	St-1	Livingston 2018	23.36	3.07	1.62	1.43E+08
12/02/2018	St-2	Livingston 2018	20.70	13.05	1.33	4.57E+07
16/02/2018	St-4	Livingston 2018	17.75	9.76	1.32	1.68E+08
20/02/2018	St-2	Livingston 2018	20.78	6.97	1.38	n.d
23/02/2018	St-4	Livingston 2018	14.53	8.51	1.26	3.69E+08
28/02/2018	St-5	Livingston 2018	24.25	5.32	1.39	n.d
28/02/2018	St-2	Livingston 2018	18.45	4.72	1.23	n.d
01/03/2018	St-1	Livingston 2018	10.59	1.12	1.16	1.81E+08

Table S6: Individual PAH concentrations in the water dissolved phase (ng L^{-1}) for the Deception 2017 and Livingston 2018 campaigns.

Date	25-1- 17	30-1- 17	2-2- 17	5-2- 17	9-2- 17	11-2- 17	15-2- 17	8-1-18	11-1- 18	16-1- 18	20-1- 18	22-1- 18	24-1- 18	27-1- 18	29-1- 18	3-2- 18	5-2- 18	16-2- 18	28-2- 18
Station	St-8	St-8	St-8	St-8	St-8	St-8	St-8	St-4	St-2	St-4	St-2	St-4	St-2	St-2	St-4	St-2	St-4	St-4	St-5
Σ MFlu	0.26	n.q.	0.07	0.82	0.21	0.15	0.08	0.16	0.25	0.15	n.q.	0.03	0.01	0.11	0.05	0.19	0.04	0.09	0.03
DBT	0.44	1.49	0.05	0.19	0.11	0.09	0.07	<loq	0.02	0.05	0.04	<loq	<loq	0.02	0.01	0.24	<loq	0.10	0.004
Σ MDBT	0.41	0.85	0.06	0.30	0.25	0.10	0.09	0.0003	0.04	0.15	0.06	0.0003	0.004	0.04	0.02	0.47	<loq	0.23	0.01
Phe	9.37	6.01	0.66	2.40	1.04	0.92	0.62	0.66	0.39	0.50	0.19	0.11	<loq	0.09	0.11	0.45	0.14	0.19	0.11
Σ MPhe	1.90	<loq	0.21	1.80	0.98	n.q.	0.53	0.31	0.73	0.57	0.79	0.10	0.02	0.66	0.15	0.38	0.14	0.27	0.17
Σ DMPhe	0.66	0.17	0.16	1.27	0.88	0.37	0.26	0.28	0.50	0.42	0.11	0.10	0.06	0.22	0.08	0.24	0.13	0.24	0.15
Σ TMPh	0.14	n.q.	0.03	0.18	0.18	0.09	0.07	0.05	0.08	0.05	n.q.	0.01	0.01	0.02	0.02	n.q.	0.02	0.02	0.02
Ant	0.59	0.21	0.03	0.10	0.04	0.03	0.04	<loq	0.11	0.03	<loq	<loq	<loq	<loq	<loq	<loq	<loq	<loq	0.02
Flt	7.72	<loq	0.79	1.99	1.30	1.12	0.67	0.35	0.74	0.53	0.20	0.14	<loq	0.35	0.09	0.28	0.13	0.20	0.13
Pyr	3.72	<loq	0.50	1.33	1.27	0.84	0.52	0.67	1.06	0.63	0.49	0.22	<loq	0.46	0.15	<loq	0.19	0.23	0.18
Σ MPyr	0.28	0.03	0.04	0.21	0.21	0.11	0.09	0.06	0.11	0.08	n.q.	0.03	n.q.	0.03	0.03	n.q.	0.02	0.04	0.03
Σ DMPyr	0.28	<loq	0.04	0.15	0.19	0.09	0.08	0.02	0.09	0.03	n.q.	0.01	0.01	0.02	0.03	0.05	0.01	0.04	0.02
B[g,h,j]f	0.53	<loq	0.12	0.38	0.13	0.13	0.39	0.03	0.11	0.04	0.11	0.01	<loq	0.13	0.11	<loq	<loq	0.07	0.12
B[a]ant	0.06	<loq	0.01	0.04	0.03	0.02	0.02	0.01	0.11	<loq	0.12	0.00	0.04	0.04	0.04	0.13	0.003	0.04	0.03
Cry	0.22	<loq	0.04	0.13	0.14	0.09	0.07	0.05	0.06	0.03	0.01	0.02	0.02	0.02	0.02	0.02	0.02	0.02	0.02
Σ MCry	0.19	n.q.	n.q.	0.13	0.11	0.07	0.06	0.02	0.05	0.02	n.q.	0.01	n.q.	0.01	0.01	<loq	0.01	n.q.	n.q.
B[b]f	0.01	0.07	0.002	0.01	0.002	<loq	0.003	0.001	0.001	0.001	0.001	0.001	<loq	0.001	0.001	<loq	0.001	<loq	0.001
B[k]f	0.01	0.08	<loq	0.004	<loq	<loq	<loq	<loq	0.001	0.001	0.002	0.001	<loq	0.002	0.003	<loq	<loq	0.003	0.003
B[e]pyr	0.02	n.q.	<loq	0.003	0.01	0.01	0.01	<loq	0.004	0.002	<loq	<loq	n.q.	<loq	<loq	0.02	0.002	<loq	<loq
B[a]pyr	0.005	n.q.	<loq	0.002	<loq	<loq	<loq	<loq	<loq	0.005	<loq	<loq	n.q.	<loq	<loq	<loq	<loq	n.q.	<loq
Pery	n.q.	0.32	0.003	n.q.	<loq	<loq	<loq	<loq	n.q.	0.002	n.q.	<loq	n.q.	n.q.	n.q.	n.q.	n.q.	n.q.	n.q.
In[1,2,3- cd]pyr	0.16	n.q.	0.03	0.03	0.03	0.04	0.07	<loq	0.01	0.02	0.12	0.01	<loq	0.02	0.03	0.06	0.03	0.11	0.03
Dib[a,h]ant	n.q.	n.q.	n.q.	n.q.	n.q.	n.q.	n.q.	n.q.	n.q.	n.q.	n.q.	<loq	n.q.	n.q.	n.q.	n.q.	n.q.	n.q.	n.q.
B[g,h,i]pery	0.06	n.q.	0.01	0.03	0.01	0.01	0.04	<loq	0.004	<loq	0.03	<loq	<loq	0.005	0.005	<loq	<loq	0.04	0.005

Table S7: Individual PAH Plankton phase concentrations (ng g_{dw}⁻¹) for the Deception 2017 and Livingston 2018 campaigns.

Date	25-1-17	30-1-17	2-2-17	5-2-17	9-2-17	11-2-17	15-2-17	17-2-17	8-1-18	11-1-18	16-1-18	20-1-18	22-1-18
Station	St-8	St-8	St-8	St-8	St-8	St-8	St-8	St-8	St-4	St-2	St-4	St-2	St-4
ΣMFlu	9.2	1.7	<loq	<loq	<loq	24	<loq	24	2.0	10	0.44	4.0	0.56
DBT	6.0	4.5	0.97	1.8	<loq	1.2	4.5	17	<loq	<loq	<loq	<loq	<loq
ΣMDBT	12	12	2.9	4.7	<loq	2.3	3.6	1.9	<loq	0.84	<loq	<loq	<loq
Phe	127	75	21	<loq	33	102	146	822	6.1	26	<loq	15	<loq
ΣMPhe	25	27	10	25	26	35	27	182	13	48	7.1	22	6.3
ΣDMPhe	17	26	15	41	39	29	23	42	19	69	10	26	6.9
ΣTMPhe	5.9	11	7.3	9.3	24	12	9.3	8.0	11	45	30	8.7	1.6
Ant	10	6.4	<loq	3.5	3.2	4.3	6.2	21	0.36	2.8	<loq	0.66	<loq
Flt	151	56	<loq	30	29	61	21	622	4.3	25	2.8	7.0	3.2
Pyr	91	16	6.7	21	21	59	16	227	4.1	46	4.2	11	4.2
ΣMPyr	10	5.3	2.8	3.3	8.3	4.0	4.2	17	4.2	19	9.3	3.3	0.9
ΣDMPyr	3.2	5.5	2.0	4.9	15	4.5	8.1	4.3	3.8	30	10	3.8	0.2
B[g,h,i]f	5.4	<loq	<loq	<loq	<loq	<loq	<loq	<loq	0.89	20	<loq	<loq	<loq
B[a]ant	34	<loq	<loq	<loq	<loq	<loq	<loq	<loq	1.8	4.7	<loq	n.q.	n.q.
Cry	34	<loq	<loq	<loq	11	6.2	4.8	11	3.5	17	12	4.5	1.6
ΣMCry	3.6	<loq	<loq	<loq	7.7	<loq	4.1	<loq	5.3	30	14	5.5	1.2
B[b]f	16	1.0	4.0	0.7	1.8	2.1	1.0	2.4	0.8	7.2	3.0	1.5	0.4
B[k]f	18	n.q.	n.q.	3.6	1.5	1.6	0.75	1.5	0.29	2.3	2.3	0.39	0.23
B[e]pyr	19	n.q.	n.q.	<loq	<loq	<loq	<loq	<loq	2.0	16	4.7	2.4	0.51
B[a]pyr	14	n.q.	n.q.	n.q.	n.q.	n.q.	n.q.	<loq	0.59	7.0	2.0	0.72	0.33
Pery	6.3	<loq	<loq	<loq	<loq	<loq	<loq	<loq	0.69	1.4	<loq	0.85	0.34
In[1,2,3-cd]pyr	12	<loq	<loq	<loq	<loq	<loq	n.q.	<loq	0.90	10	3.1	1.1	0.47
Dib[a,h]ant	<loq	n.q.	n.q.	n.q.	n.q.	n.q.	n.q.	n.q.	0.16	0.84	0.30	0.14	0.03
B[g,h,i]pery	13	<loq	<loq	<loq	<loq	<loq	<loq	<loq	1.4	39	5.3	2.1	1.2

Date																						
Station	23-1-18	23-1-18	24-1-18	27-1-18	29-1-18	3-2-18	5-2-18	8-2-18	16-2-18	23-2-18	28-2-18	23-1-18	23-1-18	24-1-18	27-1-18	29-1-18	3-2-18	5-2-18	8-2-18	16-2-18	23-2-18	28-2-18
Station	St-6	St-7	St-2	St-2	St-4	St-2	St-4	St-1	St-4	St-4	St-5	St-6	St-7	St-2	St-2	St-4	St-2	St-4	St-1	St-4	St-4	St-5
ΣMFlu	3.2	0.30	3.1	2.8	0.48	1.9	0.66	3.4	0.9	1.0	1.2	3.2	0.30	<loq	<loq	<loq	<loq	<loq	<loq	<loq	<loq	<loq
DBT	<loq	<loq	<loq	<loq	<loq	<loq	<loq	<loq	<loq	<loq	<loq	<loq	<loq	<loq	<loq	<loq	<loq	<loq	<loq	<loq	<loq	<loq
ΣMDBT	<loq	<loq	<loq	<loq	<loq	<loq	<loq	<loq	<loq	<loq	<loq	<loq	<loq	<loq	<loq	<loq	<loq	<loq	<loq	<loq	<loq	<loq
Phe	11	3.4	17	12	<loq	5.5	<loq	14	6.9	7.0	5.3	15	3.4	17	12	<loq	5.5	<loq	14	6.9	7.0	5.3
ΣMPhe	15	2.9	19	15	8.1	9.5	8.9	18	6.5	12	8.1	22	3.0	25	18	10	9.2	12	27	6.5	16	9.3
ΣDMPhe	12	1.4	11	7.3	5.3	5.1	6.5	22	3.3	20	5.3	12	1.4	11	7.3	5.3	5.1	6.5	22	3.3	20	5.3
ΣTMPhe	0.75	<loq	0.76	1.4	0.86	0.32	0.76	1.1	0.49	0.72	0.28	4.2	1.0	6.3	3.4	2.3	2.0	3.3	10	5.1	5.1	5.5
Ant	4.2	1.0	6.3	3.4	2.3	2.0	3.3	10	5.1	5.1	5.5	6.4	1.7	8.5	4.5	3.0	1.8	5.5	11	5.4	4.5	7.1
Pyr	5.8	0.9	4.8	3.2	2.5	2.5	2.8	8.1	2.0	9.5	2.6	4.8	0.5	3.0	2.6	1.6	1.7	1.5	6.6	0.9	6.0	1.5
ΣMPyr	4.8	0.5	3.0	2.6	1.6	1.7	1.5	6.6	0.9	6.0	1.5	<loq	<loq	<loq	<loq	<loq	<loq	<loq	<loq	<loq	<loq	<loq
ΣDMPyr	<loq	<loq	<loq	<loq	<loq	<loq	<loq	<loq	<loq	<loq	<loq	<loq	<loq	<loq	<loq	<loq	<loq	<loq	<loq	<loq	<loq	<loq
B[g,h,i]f	2.3	n.q.	<loq	<loq	<loq	<loq	n.q.	7.9	n.q.	<loq	<loq	2.3	n.q.	<loq	<loq	<loq	<loq	n.q.	7.9	<loq	<loq	<loq
B[a]ant	4.3	<loq	5.7	3.0	<loq	1.8	<loq	13	<loq	5.8	2.8	4.3	<loq	5.7	3.0	<loq	1.8	<loq	13	<loq	5.8	2.8
Cry	3.2	<loq	2.7	<loq	<loq	1.1	<loq	10	<loq	<loq	<loq	3.2	<loq	2.7	<loq	<loq	1.1	<loq	10	<loq	<loq	<loq
ΣMCry	<loq	<loq	<loq	<loq	<loq	<loq	<loq	5.5	<loq	<loq	<loq	<loq	<loq	<loq	<loq	<loq	<loq	<loq	5.5	<loq	<loq	<loq
B[b]f	0.59	0.18	0.56	0.66	0.44	0.17	0.82	3.9	0.19	1.4	0.32	0.59	0.18	0.56	0.66	0.44	0.17	0.82	3.9	0.19	1.4	0.32
B[k]f	2.6	<loq	2.1	<loq	<loq	<loq	<loq	10	<loq	<loq	<loq	2.6	<loq	2.1	<loq	<loq	<loq	<loq	10	<loq	<loq	<loq
B[e]pyr	<loq	n.q.	<loq	<loq	<loq	<loq	<loq	4.2	<loq	<loq	<loq	<loq	<loq	<loq	<loq	<loq	<loq	<loq	4.2	<loq	<loq	<loq
B[a]pyr	<loq	<loq	<loq	<loq	<loq	<loq	<loq	2.0	<loq	<loq	<loq	<loq	<loq	<loq	<loq	<loq	<loq	<loq	2.0	<loq	<loq	<loq
Pery	<loq	<loq	<loq	<loq	<loq	<loq	<loq	3.6	<loq	<loq	<loq	<loq	<loq	<loq	<loq	<loq	<loq	<loq	3.6	<loq	<loq	<loq
In[1,2,3-cd]pyr	<loq	n.q.	<loq	<loq	<loq	<loq	<loq	<loq	<loq	<loq	<loq	<loq	<loq	<loq	<loq	<loq	<loq	<loq	<loq	<loq	<loq	<loq
Dib[a,h]ant	<loq	n.q.	<loq	<loq	<loq	<loq	<loq	<loq	<loq	<loq	<loq	<loq	<loq	<loq	<loq	<loq	<loq	<loq	<loq	<loq	<loq	<loq
B[g,h,i]pery	4.4	<loq	2.2	<loq	<loq	<loq	<loq	5.0	<loq	<loq	<loq	4.4	<loq	2.2	<loq	<loq	<loq	<loq	5.0	<loq	<loq	<loq

Table S8: Classification of the PAHs analyzed in this study as low molecular weight (LMW) PAH or high molecular weight (HMW) PAH according to the number of aromatic rings and molecular weight.

LMW	HMW
ΣMFlu	B[g,h,i]f
DBT	B[a]ant
ΣMDBT	Cry
Phe	ΣMCry
ΣMPhe	B[b]f
ΣDMPhe	B[k]f
ΣTMPhe	B[e]pyr
Ant	B[a]pyr
Flt	Pery
Pyr	In[1,2,3-cd]pyr
ΣMPyr	Dib[a,h]ant
ΣDMPyr	B[g,h,i]pery

Table S9: Relative abundances (%) of HCB taxa, expressed as the mean, standard deviation, maximum and minimum of each taxa for each campaign.

HCB	Livingston 2015				Deception 2017				Livingston 2018			
	Mean	Sd	Max.	Min.	Mean	Sd	Max.	Min.	Mean	Sd	Max.	Min.
HCB_Sulfitobacter	3.78	5.17	17.40	0.01	3.20	2.97	11.60	0.02	4.23	6.15	29.61	0.03
HCB_Psychrobacter	0.06	0.06	0.20	0.02	0.03	0.00	0.03	0.03	4.20	14.28	58.07	0.02
HCB_Bacillus									0.49	0.83	1.95	0.03
HCB_Pseudoalteromonas	1.03	1.09	3.49	0.02	0.02	0.01	0.03	0.02	0.24	0.41	1.64	0.02
HCB_Marinomonas	0.07	0.06	0.11	0.03					0.12	0.22	0.52	0.02
HCB_Flavobacterium	0.09	0.06	0.21	0.02	0.07	0.08	0.20	0.02	0.12	0.14	0.82	0.02
HCB_Pseudomonas	0.06	0.04	0.11	0.03	0.09	0.08	0.18	0.02	0.11	0.21	1.13	0.02
HCB_Rhodferax	0.15		0.15	0.15					0.10	0.07	0.26	0.03
HCB_Nocardioides	0.02		0.02	0.02					0.09	0.16	0.46	0.02
HCB_Sphingobium									0.07	0.04	0.15	0.02
HCB_Colwellia	0.22	0.82	7.58	0.02	0.05	0.02	0.08	0.04	0.07	0.13	0.90	0.02
HCB_Alkanindiges	0.07		0.07	0.07	0.12	0.05	0.16	0.07	0.07	0.05	0.17	0.02
HCB_Shewanella	0.13	0.19	0.70	0.02	0.07		0.07	0.07	0.07	0.05	0.14	0.02
HCB_Jannaschia									0.07	0.09	0.17	0.02
HCB_Arcobacter	0.22	0.13	0.31	0.13					0.07		0.07	0.07
HCB_Sulfuricurvum	0.15	0.09	0.21	0.05					0.05	0.04	0.13	0.02
HCB_Sphingomonas									0.05	0.06	0.21	0.02
HCB_Arenimonas									0.05	0.00	0.05	0.05
HCB_Polaromonas	0.07	0.03	0.11	0.02					0.05	0.02	0.08	0.02
HCB_Novosphingobium									0.05	0.03	0.08	0.02
HCB_Arthrobacter									0.05	0.04	0.08	0.02
HCB_Thiobacillus	0.05	0.03	0.08	0.02					0.04	0.02	0.07	0.02
HCB_Rhodococcus									0.04	0.02	0.08	0.02
HCB_Woeseia	0.06		0.06	0.06					0.04	0.02	0.05	0.02
HCB_Ralstonia									0.03		0.03	0.03
HCB_Glaciecola	0.03		0.03	0.03					0.03	0.00	0.03	0.03
HCB_Psychrilyobacter	0.03	0.02	0.06	0.02					0.03	0.02	0.05	0.02
HCB_Bacteroides	0.04	0.02	0.07	0.02					0.03	0.02	0.08	0.02
HCB_Thalassotalea	0.04	0.03	0.08	0.02					0.03	0.01	0.05	0.02
HCB_Acinetobacter	0.25	0.05	0.29	0.20					0.03	0.01	0.05	0.02
HCB_Nonlabens	0.09	0.03	0.11	0.07					0.03	0.02	0.05	0.02
HCB_Faecalibacterium									0.03	0.01	0.05	0.02
HCB_Paludibacter	0.02		0.02	0.02					0.02	0.01	0.03	0.02
HCB_Lachnoclostridium									0.02		0.02	0.02
HCB_Proteiniphilum									0.02		0.02	0.02
HCB_Desulfobacterium	0.02		0.02	0.02					0.02		0.02	0.02
HCB_Bdellovibrio									0.02	0.00	0.02	0.02

HCb_Geobacter					0.02	0.02	0.02
HCb_Cutibacterium	0.14		0.14	0.14			
HCb_Vibrio	0.10	0.10	0.21	0.03			
HCb_Oleispira	0.10	0.05	0.13	0.07			
HCb_Halomonas	0.03		0.03	0.03			
HCb_Cytophaga	0.02		0.02	0.02			
HCb_Marinobacter	0.02		0.02	0.02			
HCb_Thauera	0.02		0.02	0.02			

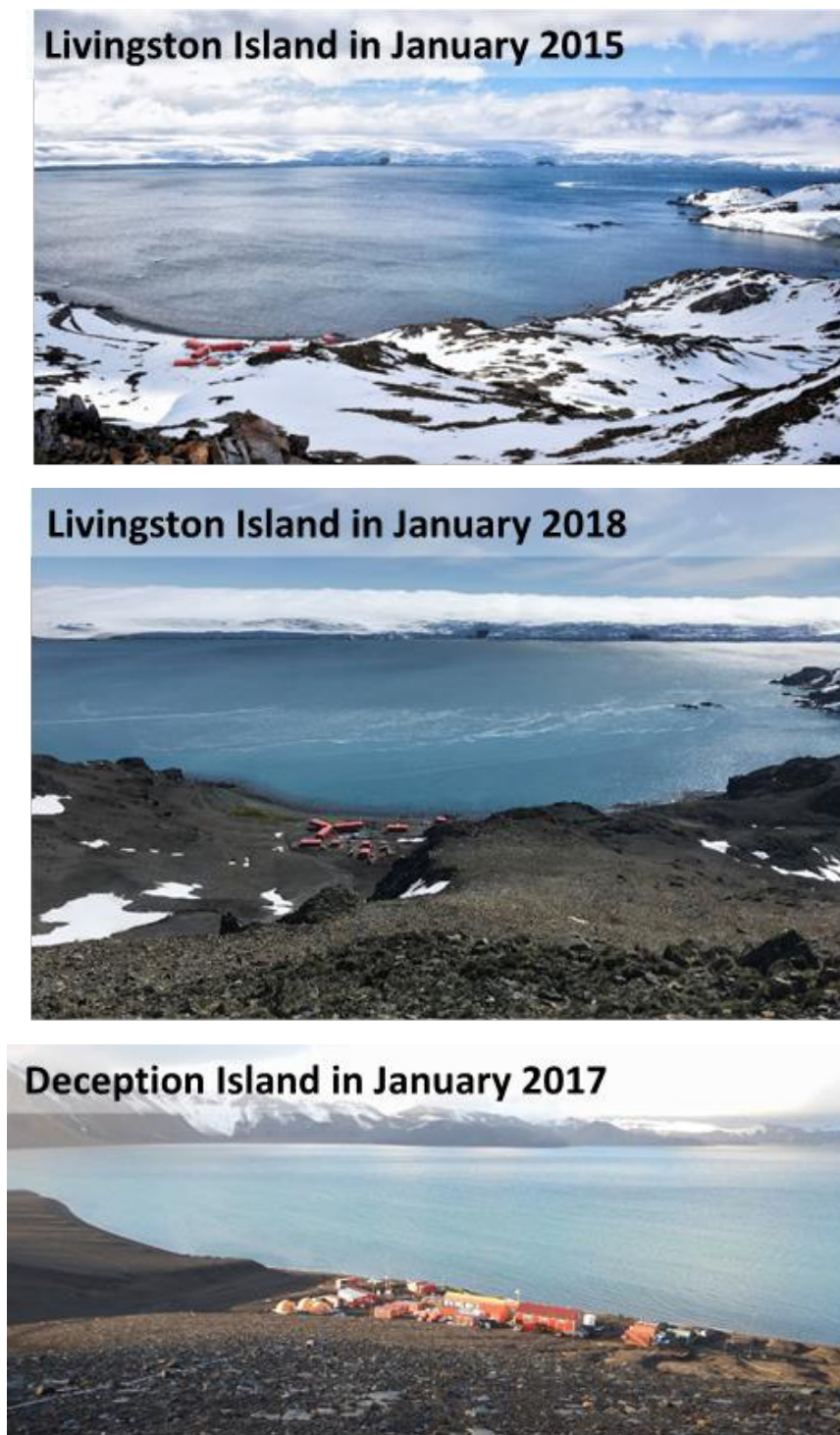


Figure S1: Picture of South bay for the 2015, 2017 and 2018 campaigns (January) showing the difference in snow cover.

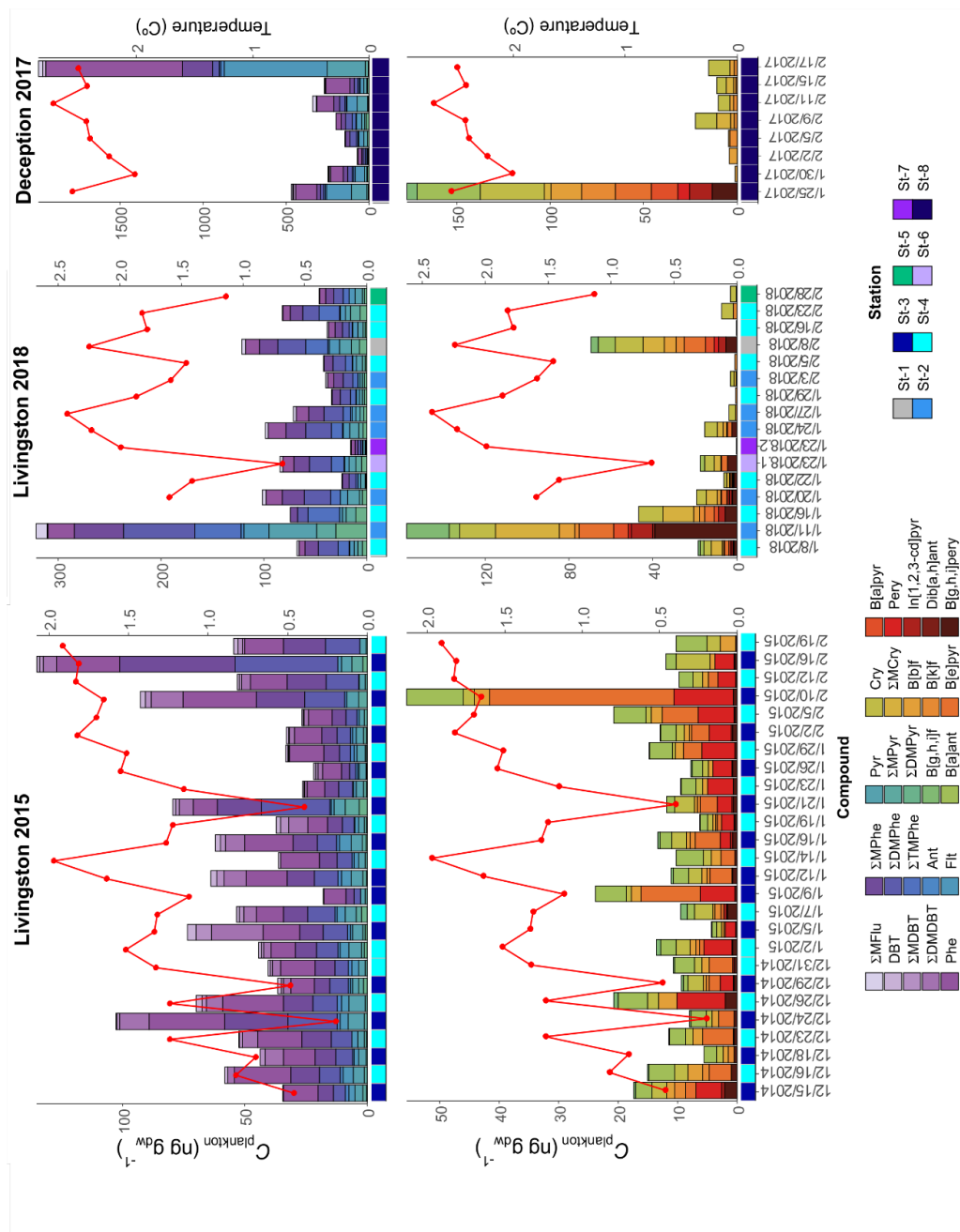


Figure S2: Occurrence of individual low MW PAHs (upper panels) and high MW PAHs (lower panels) in the plankton phase for the three sampling campaigns. Red line indicates seawater temperature.

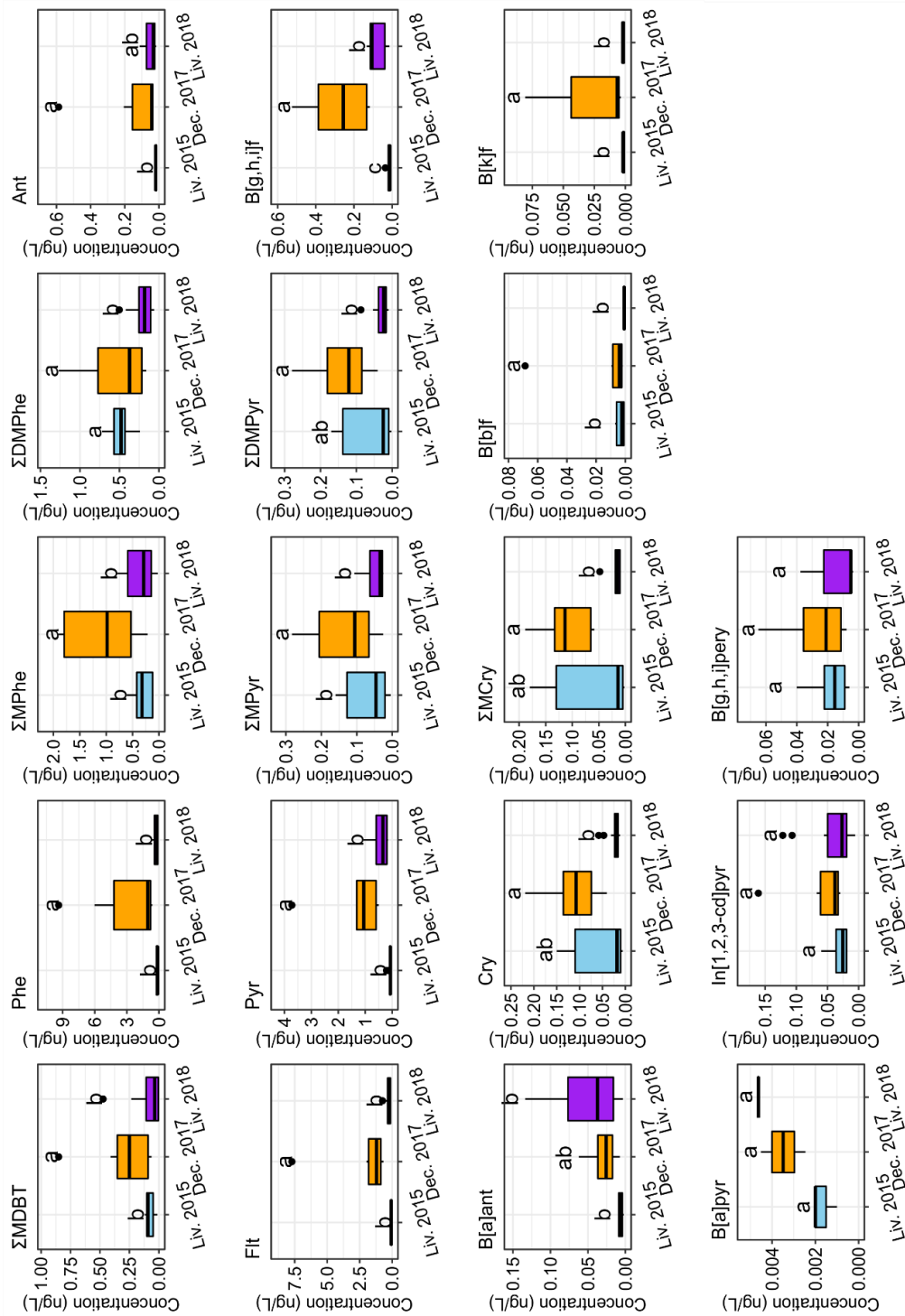


Figure S3: Differences in individual PAH concentrations in the water dissolved phase for the three sampling campaigns assessed by an ANOVA followed by a Tukey test. Significant differences ($p < 0.05$) are indicated with different letters.

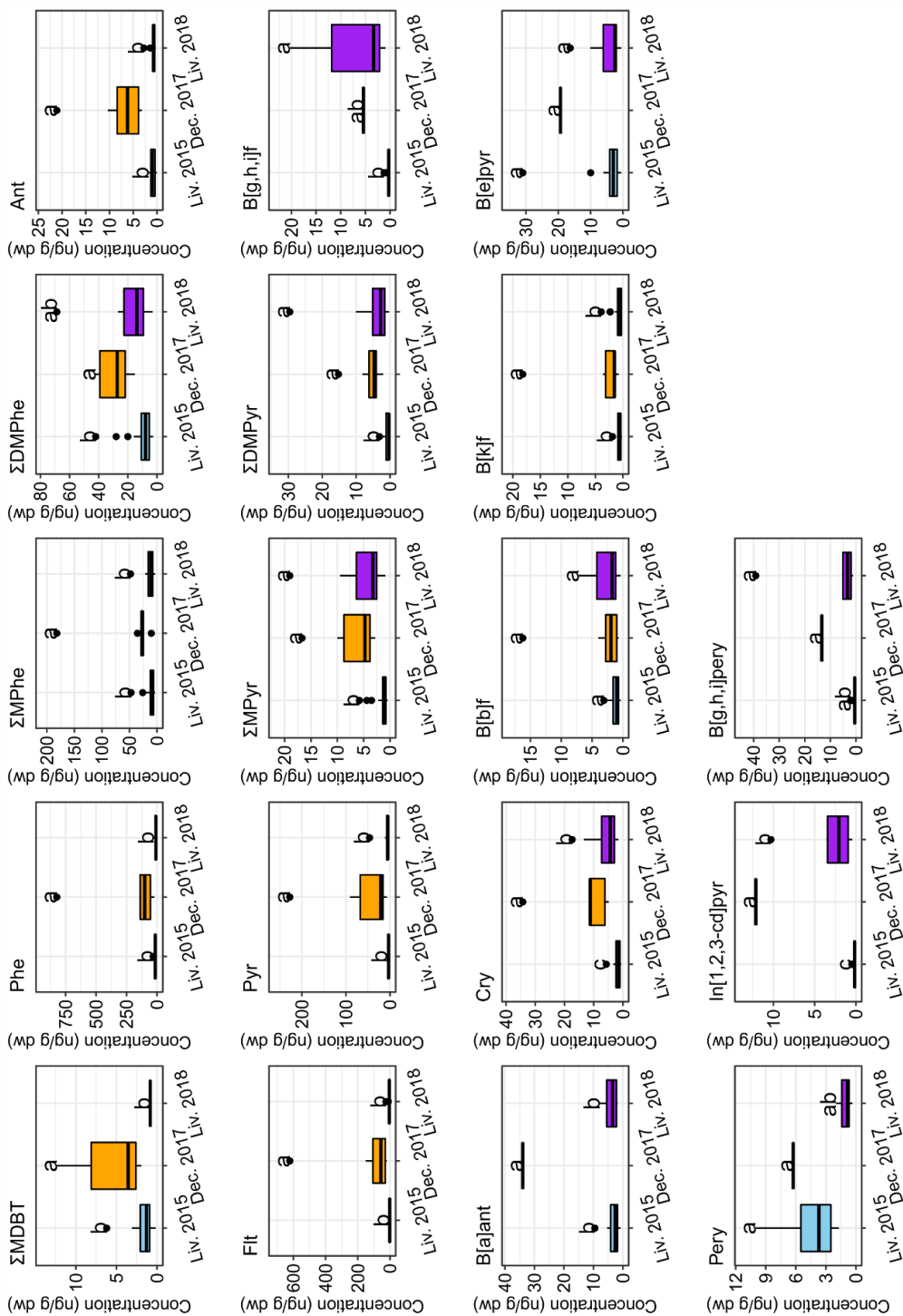


Figure S4: Differences in individual PAH concentrations in the plankton phase for the three sampling campaigns assessed by an ANOVA followed by a Tukey test. Significant differences ($p < 0.05$) are indicated with different letters.

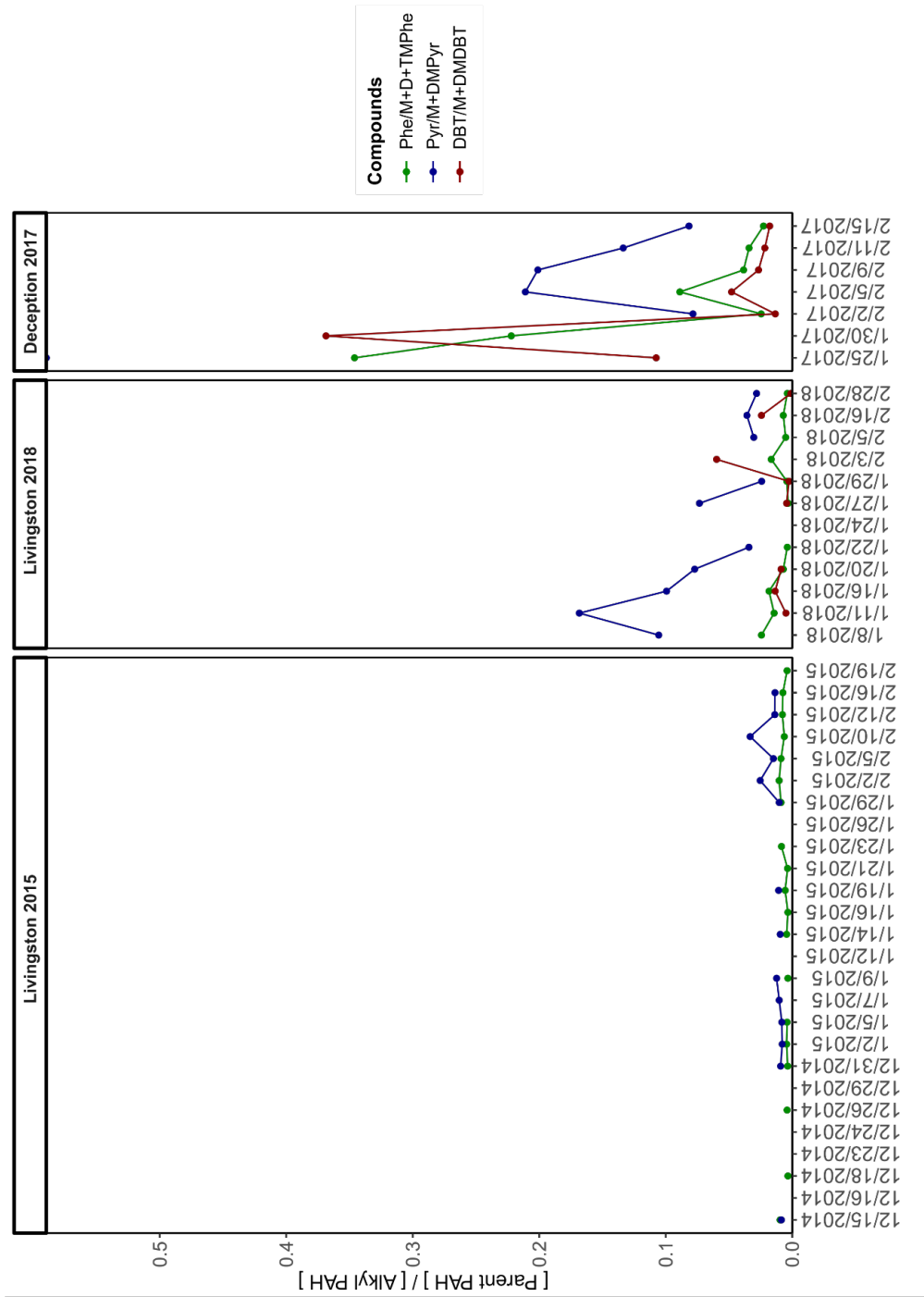


Figure S5: Temporal series of the parent/alkyl-PAHs concentration ratios in the water dissolved phase for the three campaigns. The ratios for the phenanthrene, pyrene and dibenzothiophene and their methylated forms are shown in green, blue and red, respectively.

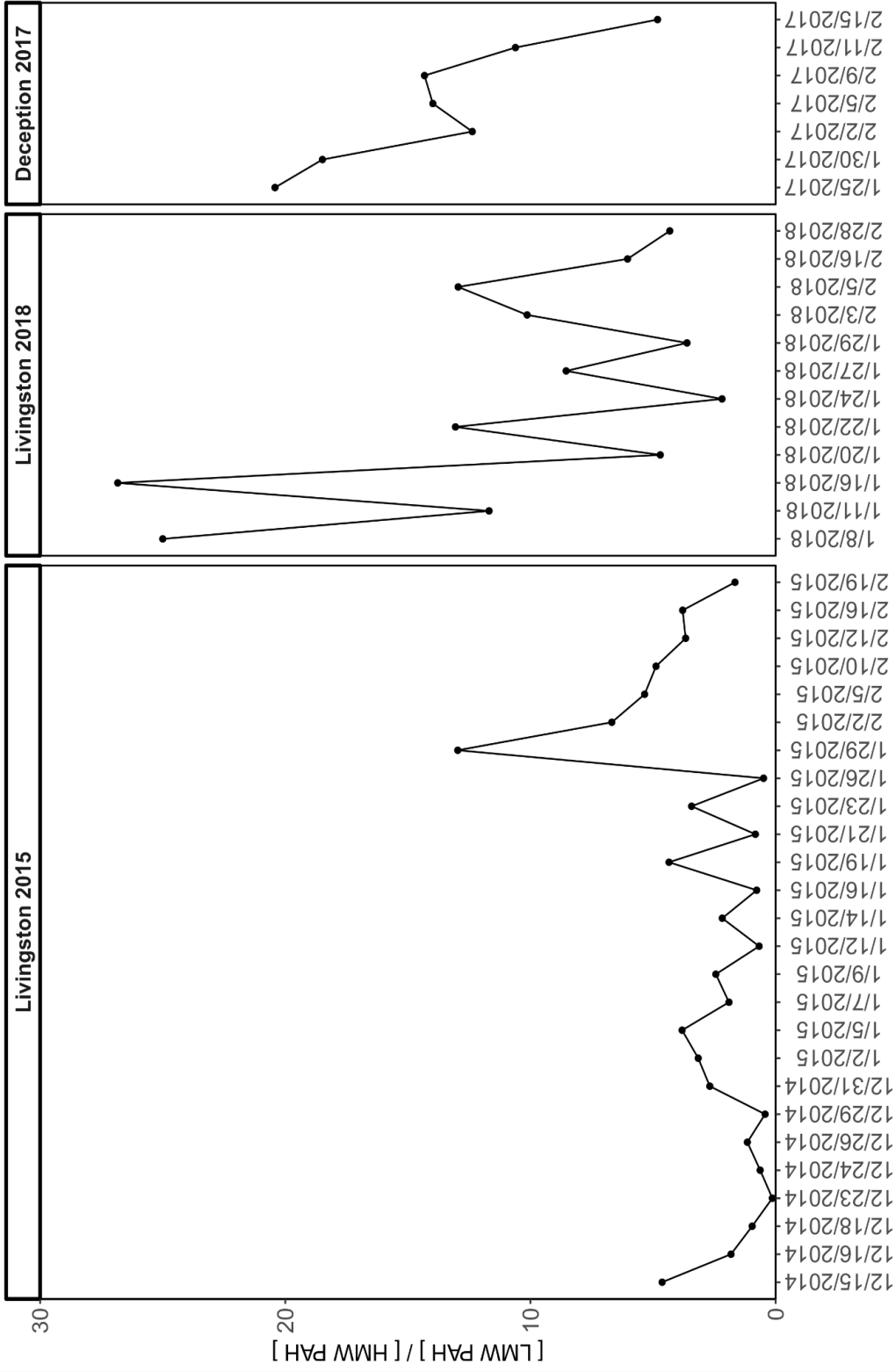


Figure S6: Temporal series of the LMW/HMW ratios in the water dissolved phase for the three campaigns.

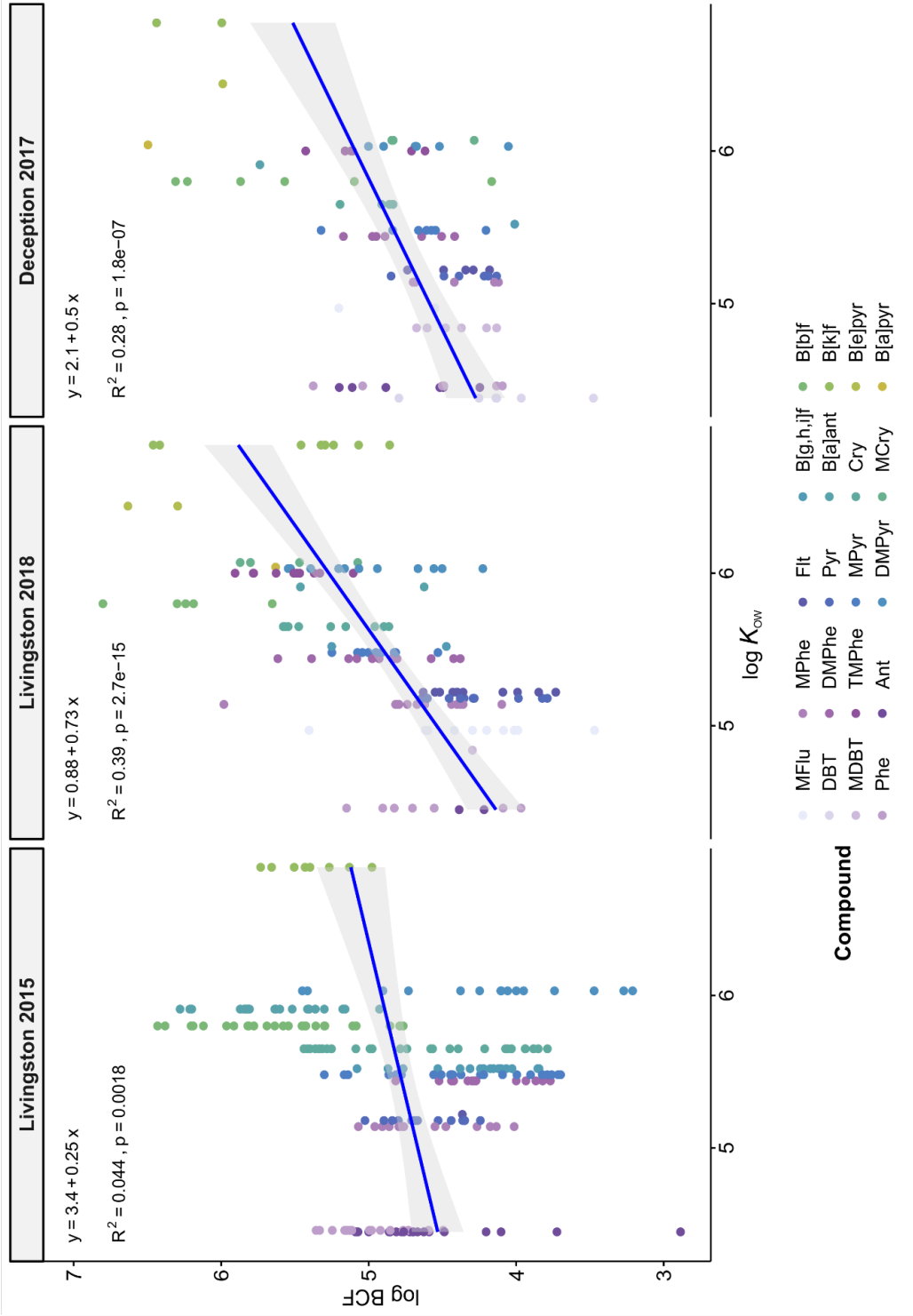


Figure S7: Bioconcentration factors ($\log BCF$) versus octanol-water partition coefficients ($\log K_{ow}$) for the three sampling campaigns.

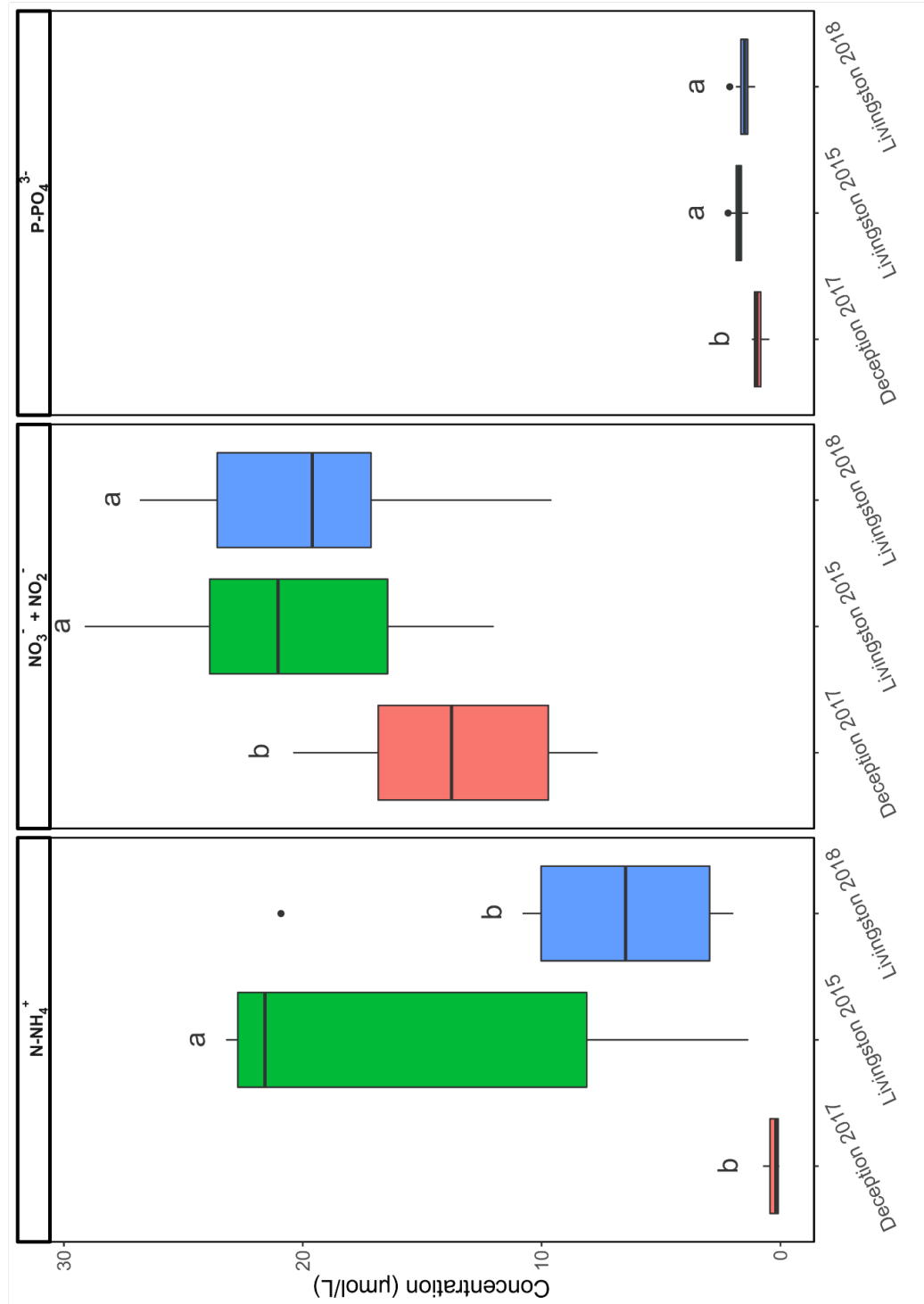


Figure S8: Boxplot of inorganic nutrient concentrations for the three campaigns. Letters indicate significant differences ($p < 0.05$) obtained with an ANOVA test followed by a Tukey test.

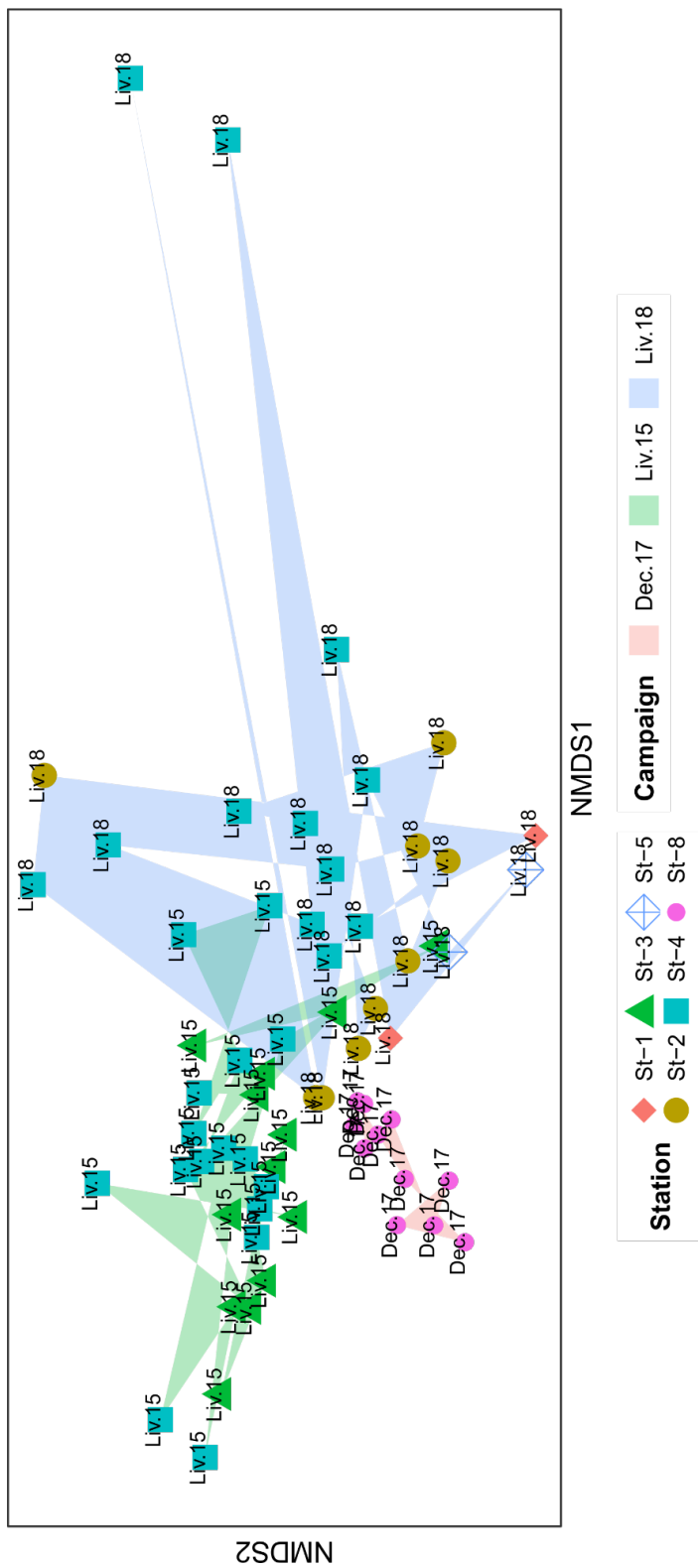


Figure S9: Non-metric Multidimensional Scaling (NMDS) plot for clustering samples according to their ASV composition. Background colors represent each of the sampling campaigns (Livingston 2015 in green, Livingston 2018 in blue and Deception 2017 in red), while colored shapes represent different sampling stations.

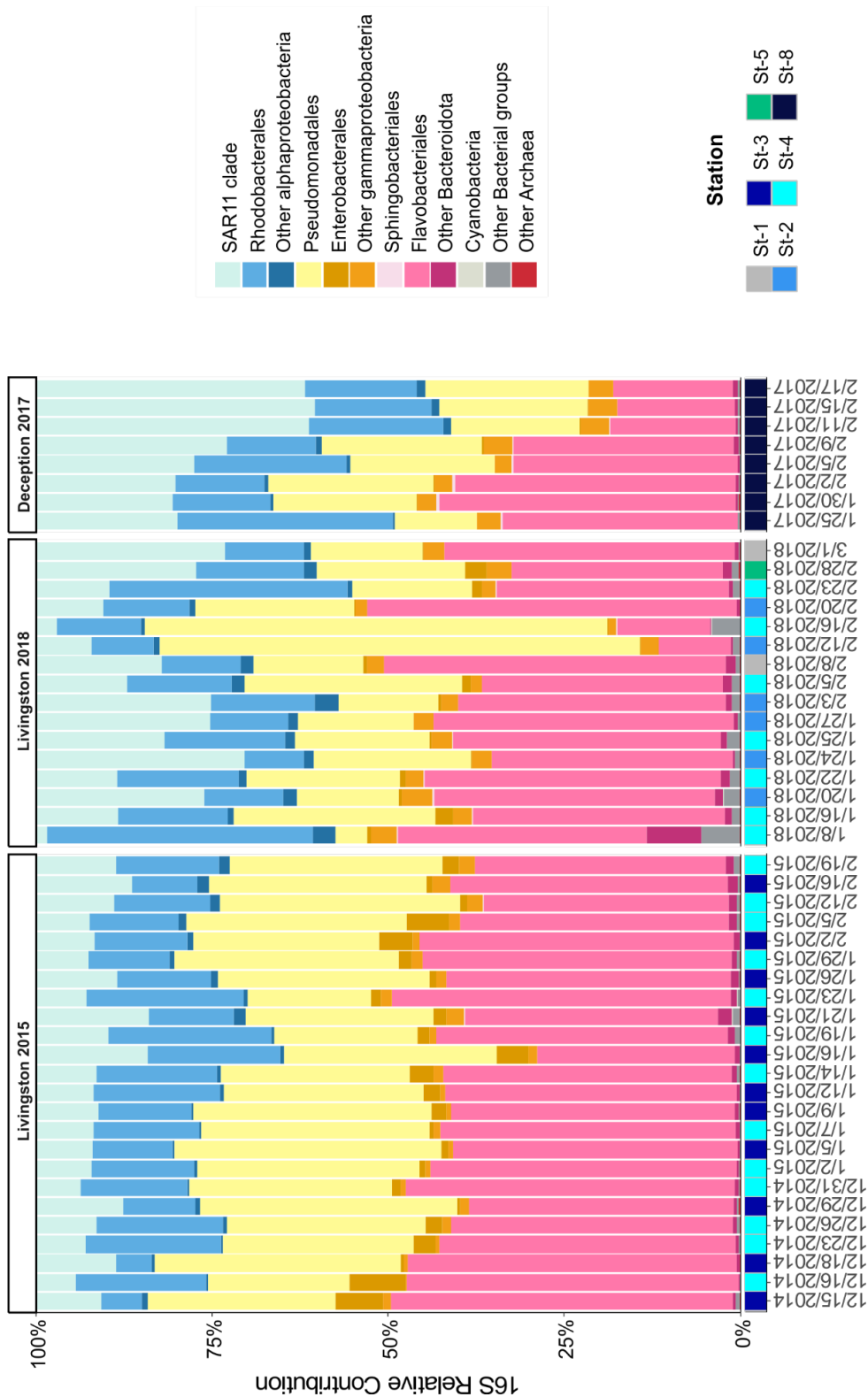


Figure S10: Structure of the bacterial community for the three sampling campaigns.

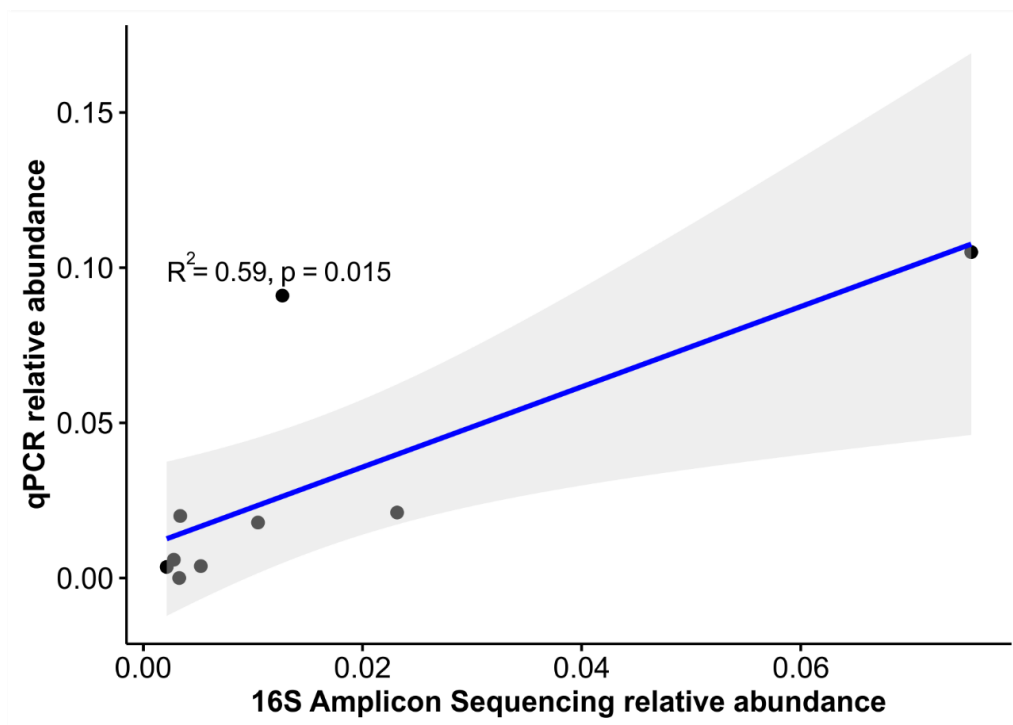


Figure S11: Correlation between amplicon sequencing relative abundance and qPCR relative abundance for the genus *Colwellia* at Jhonsons dock.

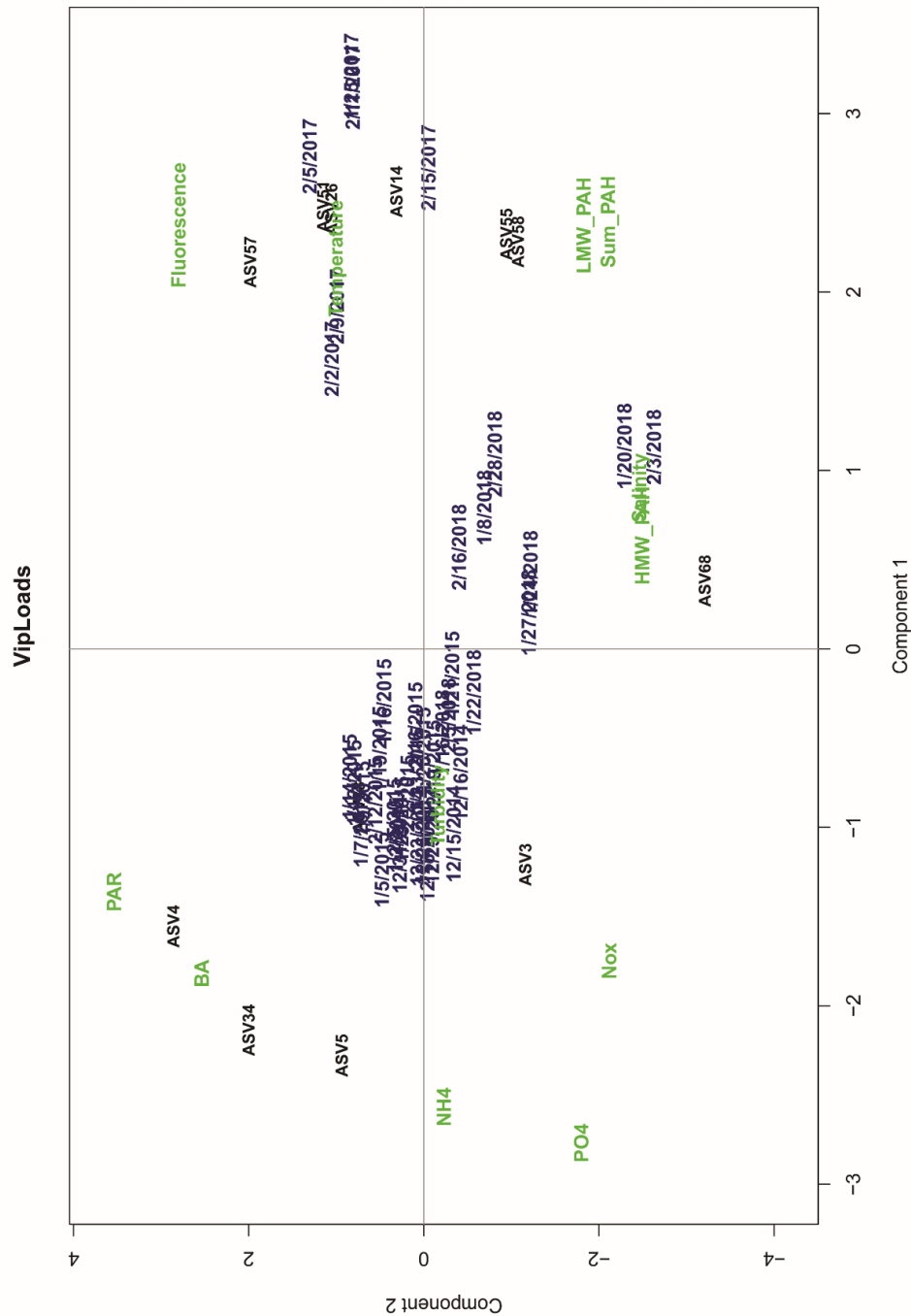


Figure S12: Partial least squares regression (PLS): In black: VIP X loadings from a matrix of ASV abundances. In blue: x scores plot showing the distribution of water samples according to the bacterial community composition. In green: VIP y loadings of PAH concentrations and other environmental variables.

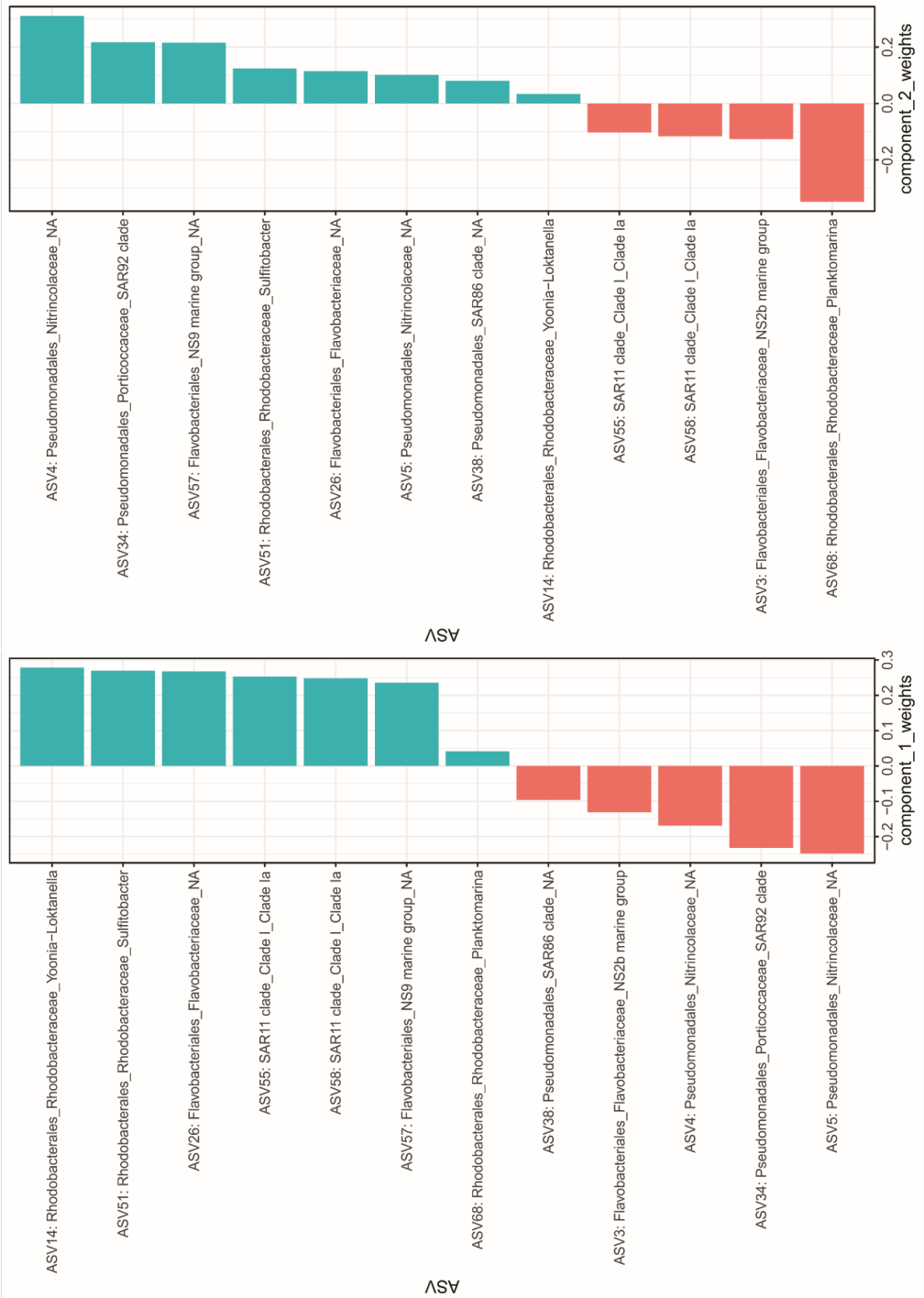


Figure S13: Plot showing the weight of the VIP x variables (individual ASV) over the components 1 and 2 of the PLS.

References

- (1) Casal, P.; Cabrerizo, A.; Vila-Costa, M.; Pizarro, M.; Jiménez, B.; Dachs, J. Pivotal Role of Snow Deposition and Melting Driving Fluxes of Polycyclic Aromatic Hydrocarbons at Coastal Livingston Island (Antarctica). *Environmental Science & Technology* **2018**, 52 (21), 12327–12337.





4.4 PUBLICATION II

Inputs, Amplification and Sinks of Perfluoroalkyl Substances at Coastal Antarctica

Gemma Casas
Jon Iriarte
Lisa A. D'Agostino
Jose L. Roscales
Alicia Martínez-Varela
Maria Vila-Costa
Jonathan W. Martin
Begoña Jiménez
Jordi Dachs

Environmental Pollution.
2023, 338, 122608.
[https://doi.org/10.1016/
j.envpol.2023.122608](https://doi.org/10.1016/j.envpol.2023.122608)



Contents lists available at ScienceDirect

Environmental Pollution

journal homepage: www.elsevier.com/locate/envpolInputs, amplification and sinks of perfluoroalkyl substances at coastal Antarctica[☆]Gemma Casas^{a,b,d}, Jon Iriarte^a, Lisa A. D'Agostino^c, Jose L. Roscales^b, Alicia Martinez-Varela^a, Maria Vila-Costa^a, Jonathan W. Martin^c, Begoña Jiménez^b, Jordi Dachs^{a,*}^a Institute of Environmental Assessment and Water Research, Spanish National Research Council (IDAEA-CSIC), Catalonia, Barcelona, Spain^b Department of Instrumental Analysis and Environmental Chemistry, Institute of Organic Chemistry, Spanish National Research Council (IQOG-CSIC), Madrid, Spain^c Department of Environmental Science (ACES, Exposure & Effects), Science for Life Laboratory, Stockholm University, Stockholm, 106 91, Sweden^d BETA Tech Center, University of Vic, Catalonia, Vic, Spain

ARTICLE INFO

Keywords:

PFAS
PFAAs
PFOA
PFOS
POPs
Southern ocean
Coastal
Antarctica
Long-range transport
Lakes
Snow
Seawater
Amplification
Degradation
Marine bacteria

ABSTRACT

The sources, biogeochemical controls and sinks of perfluoroalkyl substances, such as perfluoroalkyl acids (PFAAs), in polar coastal regions are largely unknown. These were evaluated by measuring a large multi-compartment dataset of PFAAs concentrations at coastal Livingston and Deception Islands (maritime Antarctica) during three austral summers. PFAAs were abundant in atmospheric-derived samples (aerosols, rain, snow), consistent with the importance of atmospheric deposition as an input of PFAAs to Antarctica. Such PFAAs deposition was unequivocally demonstrated by the occurrence of PFAAs in small Antarctic lakes. Several lines of evidence supported the relevant amplification of PFAAs concentrations in surface waters driven by snow scavenging of sea-spray aerosol-bound PFAAs followed by snow-melting. For example, vertical profiles showed higher PFAAs concentrations at lower-salinity surface seawaters, and PFAAs concentrations in snow were significantly higher than in seawater. The higher levels of PFAAs at Deception Island than at Livingston Island are consistent with the semi-enclosed nature of the bay. Concentrations of PFOS decreased from 2014 to 2018, consistent with observations in other oceans. The sink of PFAAs due to the biological pump, transfer to the food web, and losses due to sea-spray aerosols alone are unlikely to have driven the decrease in PFOS concentrations. An exploratory assessment of the potential sinks of PFAAs suggests that microbial degradation of perfluoroalkyl sulfonates should be a research priority for the evaluation of PFAAs persistence in the coming decade.

1. Introduction

Per- and polyfluoroalkyl substances (PFAS) are an ever-increasing family of synthetic chemicals widely used in industrial and consumer applications, since the late 1940s (Lindstrom et al., 2011; Oliaei et al., 2012). Many PFAS, particularly perfluoroalkyl acids (PFAAs), bioaccumulate and biomagnify, are toxic to biota and humans, are extremely persistent in the environment, and can be transported over long distances to reach remote regions (Casas et al., 2020; Del Vento et al., 2012; MacInnis et al., 2019a; Young et al., 2007). Numerous efforts and societal resources have been invested to investigate, regulate the use, and reduce the occurrence of these contaminants in the environment. Perfluorooctanoic acid (PFOA) and perfluorooctanesulfonic acid (PFOS) are the two PFAAs that have been most widely assessed in

terms of occurrence and impacts. In 2006, the U.S. Environmental Protection Agency (EPA) launched the PFOA Stewardship program on the elimination of PFOA and its precursors (U.S. Environmental Protection Agency, EPA.). Later, PFOS and its salts were added in Annex B of the Stockholm Convention on Persistent Organic Pollutants in 2009, and PFOA and its salts were listed under the Annex A, as persistent organic pollutants (POPs), calling for the worldwide restriction on their use.

PFAAs are ubiquitous in all the oceans (Ahrens et al., 2010; González-Gaya et al., 2019, 2014; Muir and Miaz, 2021), and for many years, oceanic currents were thought to be the main global transport mechanism of ionic PFAAs (Armitage et al., 2009; Stemmler and Lamme, 2010; Yamashita et al., 2008). However, PFAAs have been reported in land areas far away from the coast (Rankin et al., 2016) and in remote regions (Young et al., 2007). This is the case of Antarctica and parts of

[☆] This paper has been recommended for acceptance by Jiayin Dai.

* Corresponding author.

E-mail address: jordi.dachs@idaea.csic.es (J. Dachs).<https://doi.org/10.1016/j.envpol.2023.122608>

Received 25 July 2023; Received in revised form 20 September 2023; Accepted 22 September 2023

Available online 22 September 2023

0269-7491/© 2023 Elsevier Ltd. All rights reserved.

the Southern Ocean, where maritime transport from the Atlantic, Pacific and Indian oceans is restricted by the Antarctic Circumpolar Current (ACC), which acts as a barrier for north-south exchange (Bengtson Nash et al., 2010; P. Benskin et al., 2012; Yamashita et al., 2008). Despite this, perfluoroalkyl carboxylates and perfluoroalkyl sulfonates (PFCA and PFSA) have been found in coastal Antarctic waters at concentrations of few to hundreds pg L^{-1} (Cai et al., 2012a; Casal et al., 2017b; Casas et al., 2020; Wei et al., 2007; Wild et al., 2015; Zhao et al., 2012). This suggests that marine currents may not be the main transport mechanism accounting for the PFAAs occurrence in the maritime Antarctica. Atmospheric concentrations of neutral PFAS (i.e. precursors of ionic PFAS) have been shown to be ubiquitous in the oceanic atmosphere, including the Southern ocean (Del Vento et al., 2012; Martin et al., 2006; Wang et al., 2015; Young and Mabury, 2010), which is consistent with the arrival of PFAAs to the Antarctic coast by atmospheric transport and subsequent atmospheric oxidation and deposition, rather than direct transport by ocean currents (Casal et al., 2017b). Therefore, like for semivolatile POPs (Casal et al., 2019, 2018; Casas et al., 2021; Khairy et al., 2016; Zhang et al., 2015), wet deposition may play an important role on neutral and ionic PFAS transport, not only for polar regions, but across different climatic zones.

Previous studies have measured high concentrations of $\Sigma\text{PFCA} + \Sigma\text{PFSA}$ in Antarctic snow ($760\text{--}3600 \text{ pg L}^{-1}$) (Casal et al., 2017b; Wang et al., 2015) and rain ($400\text{--}8400 \text{ pg L}^{-1}$) (Casas et al., 2021), pointing out the importance of wet deposition on their occurrence. These deposition processes can lead to significant PFAAs concentrations in water and soils, a process named amplification, (Casal et al., 2019; Casas et al., 2021). These concentrations are many orders of magnitude higher than those derived from air-surface partitioning, which is negligible for PFCAs and PFSA. Amplification processes can also occur in the sea-surface microlayer (SML) and during the formation of sea-spray aerosols (SSA). SML is the layer between 1 and 1000 μm thick at the surface of the ocean and presents an enrichment of organic matter (OM) and of the microorganisms that live in this layer (Martinez-Varela et al., 2020). The SML is also characterized by its hydrophobic character caused by the enrichment of OM and surfactants, enhancing the surface enrichment of hydrophobic and amphiphilic substances such as PFAAs (Casas et al., 2020). SSA are formed from the SML via bubble bursting which are entrained by the wind (Guieu et al., 2017; Lewis and Schwartz, 2004), and by this mechanism PFAAs can be transferred to the atmosphere. The enrichment factor of PFAAs at coastal Antarctic ranged between 1.2 and 5, and between 522 and 4690, in the SML and SSA, respectively, when compared to underlying waters. The atmospheric transport of PFAAs associated with the SSA (Casal et al., 2017b; Casas et al., 2020; Johansson et al., 2019; Sha et al., 2021) and their subsequent deposition by wet deposition (snow and rain) (Casal et al., 2017b; Casas et al., 2021) are an important transport mechanism contributing to PFAAs occurrence in the maritime Antarctica.

Other processes driving the amplification of PFAAs concentrations in Antarctic coastal seawaters include melting glaciers (Bogdal et al., 2009), and remobilization by flushing of stored PFAAs due to snow-melting (Casal et al., 2017b). In addition, studies have identified penguin feces (guano) as an amplification process of POP concentrations in coastal Antarctica (Cabrero et al., 2012; Huang et al., 2014; Roossens et al., 2007), but little attention has been paid to the dynamics of PFAAs entering the coastal environment through guano. Generally, little is known about the drivers of variability of PFAAs occurrence in the highly dynamic coastal Antarctica, as well as their sources and sinks.

The objectives of this work were (i) to develop a large multi-compartment data set for PFAAs in the western Antarctic coast, by assessing their occurrence in relevant environmental matrices (seawater, snow deposition, snowmelt, lake water) at Livingston and Deception Islands (South Shetland Islands, Antarctica), (ii) to determine the drivers of variability of PFAAs occurrence and amplification processes at coastal Antarctica, and (iii) to explore the potential sinks of PFAAs in the maritime Antarctica.

2. Materials and methods

2.1. Study area

The sampling was conducted at Livingston Island ($62^\circ 39' \text{ S}$, $60^\circ 23' \text{ W}$) and Deception Island ($62^\circ 58' \text{ S}$, $60^\circ 39' \text{ W}$) (Figure S1, in the Supplementary Information, SI). These two islands belong to the South Shetland Archipelago in the Antarctic Peninsula. Samples from Deception Island were collected during the 2017 austral summer (January 23 - February 17), while samples from Livingston Island were collected in 2018 (January 02 - March 01). The average air temperature during the sampling campaign was $1.6 \pm 1.7^\circ \text{C}$, ranging from -2.9 to 5.1°C , at Deception Island, and $2.1 \pm 1.8^\circ \text{C}$, ranging from -5.4 to 10.2 , at Livingston Island. The sampling stations (st) are shown in Figures S2 and S3, and ancillary information is given in Table S1. Livingston Island has an area of 850 km^2 and is mostly covered by glaciers (Temniskova-Topalova, D., & Chipev, 2001). Only about 10% of the area of the island is free of snow and ice during the austral summer, and the highest elevation is 1700 m. The Spanish Antarctic research station Juan Carlos I (JCI) and the Bulgarian research station Saint Kliment Ohridski (St.KO) are situated in South Bay, in the western Hurd Peninsula. With only two research stations, this area is less populated and less visited by cruise tourism than Deception Island. Deception Island is a volcanic island and has an area of 72 km^2 , with a highest elevation of 542 m and over half of the island is covered by glaciers. The caldera, named Port Foster, is connected to the open ocean through a 550 m wide channel in the caldera wall; therefore, it is a unique natural harbor that is well protected from the open ocean. The only research stations currently active are the Argentine summer research station Deception (Dec) and the Spanish research station Gabriel de Castilla (GC), both located in Port Foster.

2.2. Sampling methodology

Seawater sampling was conducted from a rigid inflatable boat at different sampling sites (Figure S2-S3A), and collected in 2 L polypropylene (PP) bottles. The seawater samples were collected at different depths between surface and 30 m depth, with a Niskin bottle and poured into 2 L PP bottles after their collection. Before seawater collection, CTD (Conductivity, Temperature, Depth) profiles were taken to evaluate water temperature, salinity, turbidity, fluorescence and photosynthetic active radiation (Table S2). After collection, samples were transported to the research station and were filtered through pre-combusted GF/F glass fiber filters (47 mm diameter, Whatmann $0.7 \mu\text{m}$ mesh size) on a glass filtration unit, then spiked with 50 pg of nine recovery standards (Table S3).

Surface snow samples, snowmelt and lake water samples were collected with a stainless steel shovel into PP bottles from different sampling sites (Figure S2-S3B). Snowmelt samples were collected from stream unequivocally originating from snow or ice melting. For snow samples, only the top 2–3 cm of snow was collected. After collection, snow samples were left to melt at $4\text{--}6^\circ \text{C}$ for 24–48 h at the research station in sealed PP bottles. Snow, snowmelt collected from streams, and lake water samples were also filtered and spiked like seawater samples.

PFAAs were extracted using an established solid phase extraction (SPE) method with OASIS WAX cartridges (6 cm^3 , 150 mg; Waters) with minor modifications (Casas et al., 2020; Yamashita et al., 2005).

Fifteen mL of sample were taken and kept at -20°C for analyzing nutrients: nitrogen (NO_x), ammonium (NH_4^+) and phosphate (PO_4^{3-}). For bacterial abundance (BA), 1.8 mL of the water samples were fixed with 1% buffered paraformaldehyde solution (pH 7.0) plus 0.05% glutaraldehyde (P + G), left at room temperature in the dark for 10 min, and frozen and stored at -80°C until further processing.

Samples for bacterial taxonomy 16S rDNA library construction were collected from surface seawater. Four liters of each sample were pre-filtered through $3 \mu\text{m}$ pore size 47 mm diameter polytetrafluoroethylene

filters (Millipore, Bellerica, MA) to remove grazers and the particle-attached living fraction, and sequentially onto 0.2 μm pore-size 47 mm Teflon (Millipore, Bellerica, MA) under filters to capture the free-living bacteria cells fraction, using a peristaltic pump with flow of $<50 \text{ mL min}^{-1}$. Each filter was placed in 1 mL lysis buffer (50 mM Tris HCl, 40 mM EDTA, 0.75 M sucrose) and stored at -20°C until further processing.

The detailed procedure followed for the elution, identification and quantification of PFAAs, the nutrients and bacterial taxonomy 16S rDNA analysis are described in the Annex S1 in SI.

2.3. Quality assurance and quality control (QA/QC)

All containers used were made of stainless steel or polypropylene and all sampling materials were rinsed with methanol before sample collection or use to avoid contamination. All filters were precombusted at 450°C for 4h. Procedural blank SPE cartridges were also analyzed to monitor potential contamination during sample treatment. In addition, field blanks consisted of SPE cartridges that were transported to sampling sites, shipped back to the laboratory together with the samples, and processed in the same manner as samples; albeit without the extraction of 2L of water. Levels of PFAAs in the field and procedural blanks are given in Table S4. Recovery of surrogate standards spiked before the SPE extraction are presented in Table S5. Concentrations were not corrected for surrogates (Casal et al., 2017b; Casas et al., 2021; González-Gaya et al., 2019). The limits of quantification (LODs) were defined as the mean concentration of field blanks plus three times the standard deviation (SD) of the blank value. For the analytes not detected in blanks, LOD was derived from the lowest standard in the calibration curves (Table S6). Table S7 shows the detection frequency in each matrix analyzed in this study. Bioinformatics annotation and statistical analyses are described in Annex S2 in SI.

3. Results and discussion

3.1. Overall PFAAs multi-compartmental occurrence at coastal Antarctica

The targeted PFAAs were analyzed in surface seawater, deep seawater, fresh snow, and snowmelt from both Livingston and Deception Islands. In addition, at Deception Island, PFAAs were also analyzed in lake water. Compound specific concentrations are shown in Tables S7–S10. Aerosol and rain PFCAs and PFSAs concentrations have been reported and discussed elsewhere (Casas et al., 2021), and are used here when needed. Considering all matrices (Fig. 1 and S4), the most frequently detected PFCAs were PFOA (average detection frequency for all matrices, 91%) and PFNA (90%), and for PFSAs was PFBS (83%). PFBA had the highest average concentrations of all target analytes in all matrices, with a detection frequency of 88%. A large number of targeted PFAAs were detected in atmospheric samples, including the aerosol-phase (total particulates) and in wet deposition samples of rain and snow.

3.2. PFAAs in coastal seawater

Concentrations of ΣPFAAs in surface seawater from Livingston Island ($n = 40$) averaged $250 \pm 210 \text{ pg L}^{-1}$, ranging from 25 to 1020 pg L^{-1} (Fig. 2, Table S7). The average ΣPFAAs concentrations at Johnson glacier station (st-28) from the 2018 austral summer ($190 \pm 140 \text{ pg L}^{-1}$) were in the same range as those reported at the same sampling station during the 2014–2015 austral summer ($190 \pm 100 \text{ pg L}^{-1}$) (Casal et al., 2017b). This previous assessment was centered on sampling in front of the Johnson glacier at Livingston Island. A key difference, and novel contribution of this work, is that here we assess PFAAs occurrence covering a large coastal region, as five spatial transects were examined covering large areas around South and False Bays in Livingston Island

(Figure S3 and S5), in addition to the sampling at Deception Island.

The pattern of concentrations of individual PFAAs and the ΣPFAAs did not show significant spatial differences in South and False bays (ANOVA test, $p > 0.05$), but coastal waters from st-25 and st-26 were those with higher PFAAs levels (Figure S5 and S6), with average ΣPFAAs concentrations of $610 \pm 580 \text{ pg L}^{-1}$ and $500 \pm 500 \text{ pg L}^{-1}$, respectively. These stations are located close to two different penguin colonies in South Bay, east of Hurd Peninsula (Figure S3). St-29 also had high concentrations ($377 \pm 203 \text{ pg L}^{-1}$), and to minor extend in St-30, in comparison with other sample locations. Likely because this station is located close to a large penguin colony at Hannah Point (Figure S3). These peaks in concentrations, however, show a factor of 2 differences for different sampling dates (Figure S5), indicating a high variability in these seawater masses in the proximity of local coastal sources. These high concentrations are consistent with the hypothesis that penguin guano could act as an amplifier of concentrations in coastal Antarctica facilitated by penguins foraging in regional waters and defecating at the colony or its adjacent waters. Run-off of guano-bound PFAAs by melting snow transfers the amplified PFAAs signal in guano to adjacent waters. It is unlikely that this potential influence of guano is confounded with that from snow/ice melting due to different locations of major glacier inputs and penguin colonies. Profiles of PFAAs concentrations in the samples also agree with the penguin amplification hypothesis. Specifically, the PFAAs with higher concentrations in the penguin's influenced stations were PFPeA, PFBA and PFHxA. PFOA, PNA, PFUDa and PFTrDA were also detected in these samples. High concentrations of PFHxA, PFPeA, PFOA and PFNA have been reported in penguin guano from Tierra del Fuego (Patagonia, south America), and PFOS, PFHxA and PFBS were reported in penguin guano from Antarctica (Llorca et al., 2012). Roscales and coworkers (2019) also detected high concentrations and a high contribution of PFHxA and PFOS in plasma from Gentoo penguins in Livingston Island (Roscales et al., 2019).

PFBA and PFPeA were the main PFAAs in seawater around Livingston Island, with an average contribution of 21% and 20% to ΣPFAAs , respectively (Figure S7), whereas the C9–14 PFAAs accounted for a smaller contribution, always below 10% of ΣPFAAs . PFOS contributed on average less than 10% to ΣPFAAs , consistent with previous studies in the Arctic (Zhao et al., 2012), but in the lower range of previous works in these and other Antarctic coastal sites (Cai et al., 2012b; Casal et al., 2017b). C4–C7 PFCA were generally significantly inter-correlated in surface seawater at Livingston Island (r^2 0.17–0.99, Figure S8), while PFOA was correlated with PFOS and long chain PFCAs. Such correlations are consistent with similar sources and biogeochemistry.

In this study, concentrations of PFAAs from Livingston Island were not significantly correlated with water salinity and temperature when all stations were considered. Only PFOS concentrations in surface seawater showed a significant positive correlation with turbidity ($r_p^2 = 0.82$, $p < 0.05$) (Figure S9), as glaciers/snow inputs are associated with larger turbidity due to erosion and increased primary production, it suggests that freshwater inputs could be a source of PFOS. PFUnDA concentrations in surface seawater were positively correlated with NO_3T ($r_p^2 = 0.95$, $p < 0.05$), PFNA was positively correlated with P-PO_4^{3-} ($r_p^2 = 0.42$, $p < 0.05$), and only PFOA was positively correlated with bacterial abundance ($r_p^2 = 0.31$, $p < 0.05$). These correlations are consistent with the role of snowmelt and glacier melting contributing to PFAAs in coastal Antarctica (Casal et al., 2017b), and its associated nutrient inputs increasing the microbial abundances.

Vertical PFAAs profiles from 1.5 m to 30 m depth were measured at a number of seawater sampling stations (Figure S3 and S10), and the maximum concentrations were present near the surface, from 1.5 m to 5 m depth. For the vertical profiles at False Bay and Hannah Point, PFAAs concentrations showed a significant negative correlation with salinity ($p < 0.05$) and a significant positive correlation with turbidity ($p < 0.05$) (False Bay, st-25 and Hannah Point, st-29, Fig. 3 and Figure S11), consistent with significant inputs of snowmelt to coastal seawater PFAAs concentrations.

Concentrations of Σ PFAAs in surface seawater from Deception Island ($n = 11$) averaged $1200 \pm 610 \text{ pg L}^{-1}$, ranging from 240 to 2100 pg L^{-1} (Fig. 2, Table S7), which was an order of magnitude higher than at Livingston Island. However, the maximum concentrations measured were still one order of magnitude lower than the Σ PFAAs concentrations reported for King George Island, also in the South Shetland archipelago (Cai et al., 2012a). The difference in Σ PFAAs concentrations between Livingston and Deception islands is explained by the high

concentrations of PFBA ($1300 \pm 320 \text{ pg L}^{-1}$) and PFHxA ($400 \pm 75 \text{ pg L}^{-1}$) at Deception island, which dominated the PFAS profile (Figure S12) contributing more than 95%. PFOS concentrations at Deception ($30 \pm 5.7 \text{ pg L}^{-1}$) were also one order of magnitude higher than in Livingston Island ($1.1 \pm 0.5 \text{ pg L}^{-1}$). PFNA was significantly correlated with PFOA and PFDA in Deception surface seawater, but there were no other significant correlations among PFAAs. None of the concentrations of PFAAs from Deception Island were significantly correlated with water CTD,

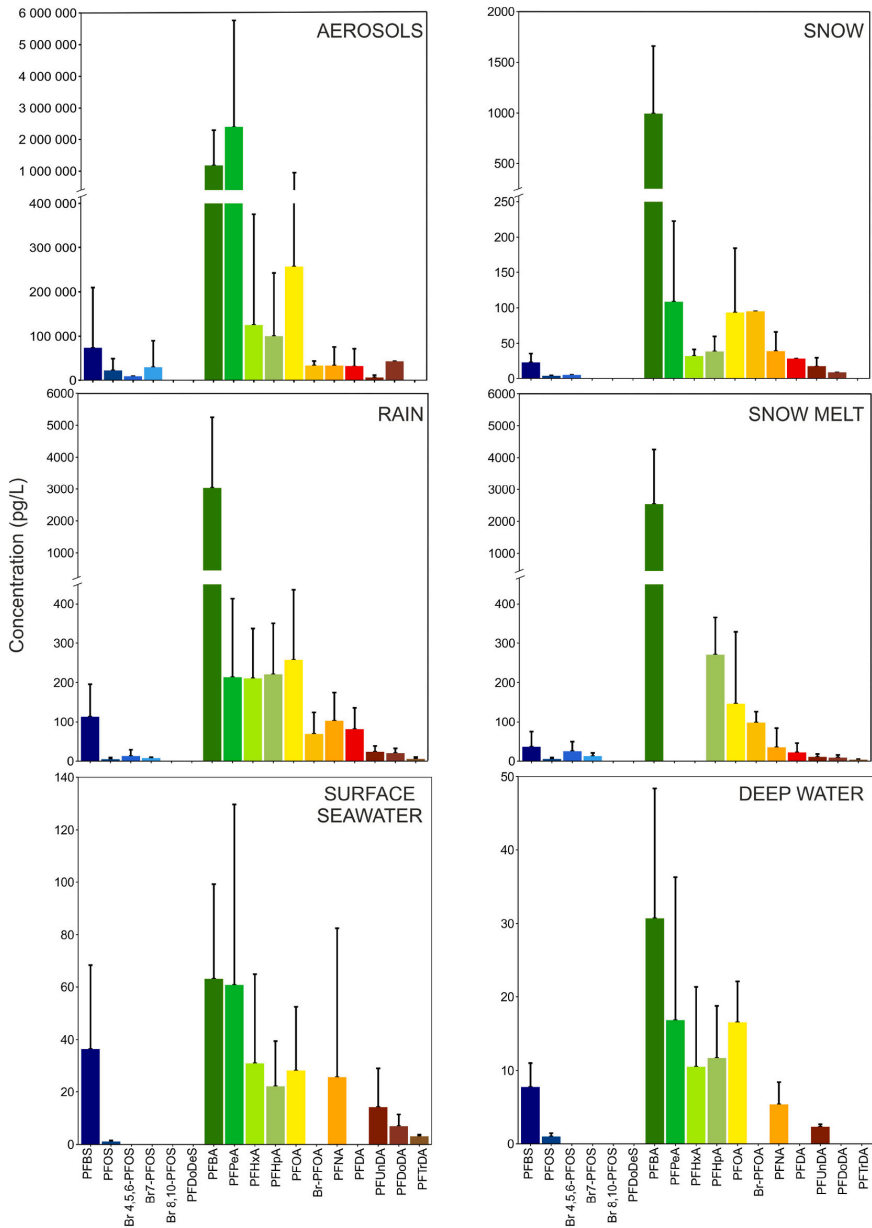


Fig. 1. Concentrations of individual PFAAs (pg/L, mean and +2 SD) in aerosol, snow, rain, snowmelt, surface seawater and depth seawater from Livingston Island (2018).

nutrients or BA abundances.

3.3. PFAS in snow, rain, snowmelt and lake water

Atmospheric wet deposition of PFAS in snow and rain are key inputs in maritime Antarctica, with potential for amplification of seawater concentrations (Casal et al., 2019; Casas et al., 2021). Σ PFAAs in snow samples from Deception Island ranged from 240 to 20000 pg L^{-1} (Figure S13, Table S8), with the profile dominated by PFBA, which contributed more than 50% to Σ PFAAs on average. This was followed by PFOA (13%) and PFOS (8%). Σ PFSAs contribution in snow samples from Deception Island was less than 15% of Σ PFAAs. On Deception Island, near-field surface snow collected close to GC research station (st-1, Figure S2) showed the highest concentrations (Σ PFAAs of 10000 pg L^{-1}).

Only three samples of fresh snow were collected at Livingston Island due to the few snow events occurring during the 3-month campaign (Figure S13). However, the sample that presented the highest concentration (st-20) was also located within the perimeter of the JCI research station with a Σ PFAAs concentration of 2500 pg L^{-1} (Figure S3B, Figure S13, Table S8). The PFAAs concentrations in snow were comparable, but two-fold higher than reported before at Livingston Island when the Σ PFAAs average was 1300 pg L^{-1} for surface snow samples from the JCI transited areas (Casal et al., 2017b); the increase may be related to the research station enlargement between the two campaigns. PFBA was the PFCA with the highest concentration, contributing on average to more than 70% in all snow samples from Livingston Island, followed by PFPeA and PFOA. PFSAs had a small contribution to Σ PFAAs (<1% of Σ PFAAs). Wet deposition samples (snow and rain) and aerosols were the matrices with the highest number of individual PFAS detected (Fig. 1, Figure S1 and Table S6), consistent with the important role of long-range atmospheric transport as a source of PFAS in this region (Casal et al., 2019; Casas et al., 2021).

Average Σ PFAAs concentrations in snowmelt ranged from 1200 to 6700 pg L^{-1} at Livingston Island, and between 1200 and 4400 pg L^{-1} at Deception Island (Table S9; Figure S14). PFBA was again the compound with the highest concentrations and highest contribution (>80% in Livingston Island and >60% in Deception Island), followed by PFOS and PFOA. Sampling site st-02 was inside a penguin colony, with high concentrations of PFPeA (99%), followed by PFBA and PFOA. We calculated the ratio between average concentrations of individual PFCA in snow deposition (C_{SD}) to the average concentration in snowmelt (C_{SM}). The C_{SD}/C_{SM} ratios were generally around 1 or higher for all individual

PFCA, (Table S10, SI), with significant positive correlation between C_{SD}/C_{SM} ratios and the number of carbons in the PFCA alkylated chain (#C) (Figure S15), consistent with a higher proportion of long-chain PFCA in fresh snow than snow-melt as reported elsewhere (Casal et al., 2017b).

The small lakes on these Antarctic islands receive water from atmospheric deposition only. Therefore, these are interesting as unequivocal confirmation of the potential of atmospheric inputs to support aquatic concentrations of PFAAs, an approach that has been used historically in temperate regions to demonstrate the relevance of atmospheric inputs of POPs (Swackhamer et al., 1988). Regarding lake water samples from Deception Island, Σ PFAAs ranged between 280 and 3900 pg L^{-1} , with a mean concentration of 1800 pg L^{-1} (Table S11; Figure S16), being lower than those concentrations reported in snow-melt. These concentrations are in a lower range than those in lakes from King George Island (2100–4800 pg L^{-1}) (Cai et al., 2012a). The most abundant compound and with higher concentrations in lake water was PFBA, accounting for more than 80% of Σ PFAAs and with an average concentration of 1500 pg L^{-1} (Figure S4).

3.4. The role of amplification processes as drivers of concentrations in coastal Antarctica

In the environment, there are a number of transport and partitioning processes that lead to amplification of concentrations and fugacities (Casal et al., 2019; Casas et al., 2021, 2020; Macdonald et al., 2002). In the polar environment, these are especially relevant due to the low temperatures and high biomass of phytoplankton and bacteria which can exacerbate these processes. These include enhanced bioaccumulation and persistence at low temperatures,⁴⁷ snow and rain as effective scavengers of atmospheric pollutants,^{30–31} and partitioning at the surface microlayer.⁶ The latter may be favored by exudation of surfactant-like organic chemicals by the abundant phytoplankton, with implications to transfer to sea-spray aerosol.

A number of laboratory-based studies have shown a strong enrichment of long-chain perfluoroalkyl acids (PFAA) in SSA in comparison to seawater (Johansson et al., 2019; McMurdo et al., 2008; Reth et al., 2011; Sha et al., 2021). Modelling approaches estimate an important emission of PFAAs associated with SSA in the Southern Ocean (Johansson et al., 2019). Moreover, field studies in coastal Antarctica (Casas et al., 2020) and in coastal Norway (Sha et al., 2022) show high enrichment factors of PFAAs in SSA, ranging between 522 and 4690 in coastal Antarctica (Casas et al., 2020). This shows the effective amplification of PFAAs in SSA, which can drive potential long-range

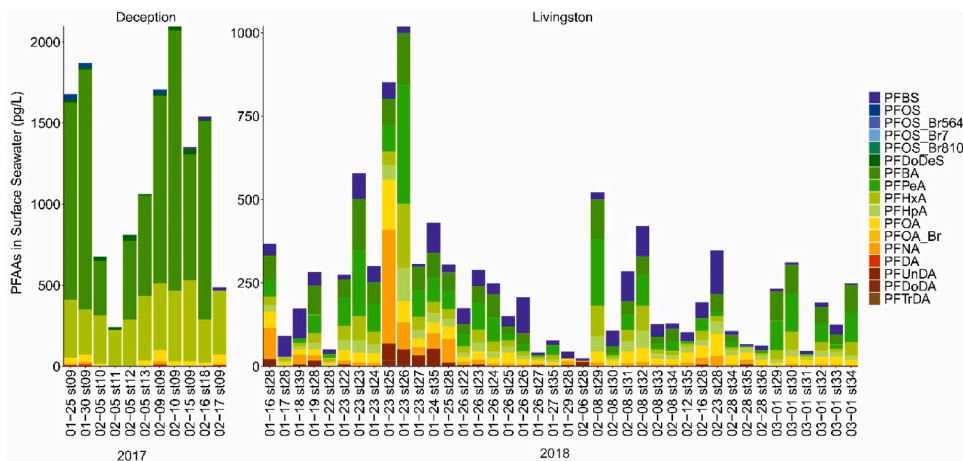


Fig. 2. Surface seawater PFAA concentrations in pg L^{-1} in Deception and Livingston Islands.

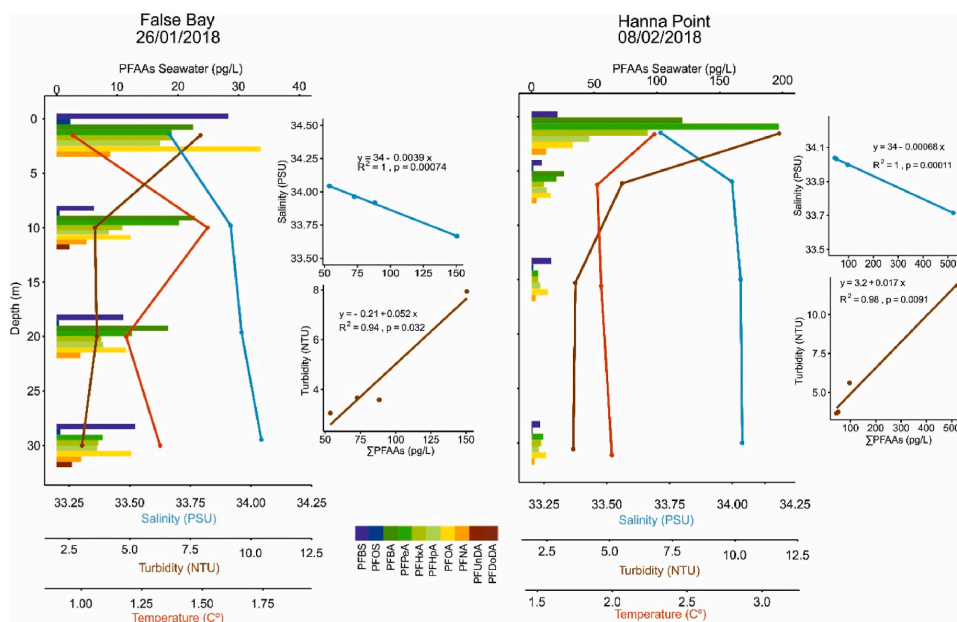


Fig. 3. Vertical profiles of PFAAs in seawater from Livingston Island (2018) and correlations between PFAAs concentrations and salinity and turbidity in seawater. Concentrations of PFAAs are in pg L^{-1} .

atmospheric transport and deposition of PFAS. Besides, wet deposition can amplify concentrations in coastal waters by scavenging of SSA-bound PFAAs by snow and rain (Casal et al., 2019; Casas et al., 2021). This is especially important in the maritime Antarctica because SSA are the dominant pool of aerosols in this region (Maskey et al., 2011). Snow has received more attention in polar environments as an amplification mechanism for PFAS than rain events, even though rainfall events are common during austral summer in the Antarctic Peninsula (Carrasco and Cordero, 2020), and rainfall occurrence is predicted to increase in the coming decades (Vignon et al., 2021). In this study, mean Σ PFAAs concentrations in rain (4000 pg L^{-1}) was higher than in snow (1400 pg L^{-1}) at Livingston Island, consistent with the recent meta-analysis of amplification potential of rain and snow (Casas et al., 2021).

The measurements of PFAAs in SSA, wet deposition (snow and rain) and snowmelt provide insights into long-range atmospheric transport and deposition to Deception Island lakes, and its bay (Port Foster). Several studies have shown evidence that glacial- and snow-melt can impact surface water concentrations of PFAAs (MacInnis et al., 2019b; Skaar et al., 2019; Veillette et al., 2012) and other POPs (Cabrerizo et al., 2019; Helm et al., 2002; Lafrenière et al., 2006). High PFAAs concentrations in glacial- and snowmelt-impacted surface waters from Lake Linnévatnet (Svalbard, Norway) in 2014 and 2015, dominated by PFBA (mean 0.6 ng/L) and PFOA (mean 0.3 pg L^{-1}) have been reported (Skaar et al., 2019). Elevated concentrations of PFCAs were also observed in the water column during snowmelt periods compared to ice-covered or ice-free periods in Lake Hazen in the Canadian High Arctic (MacInnis et al., 2019b). In this work, the correlations of some PFAAs in coastal seawater with turbidity and nutrients, as well vertical profiles with maximum PFAAs concentrations when salinity was lower (Fig. 3), support the hypothesis that coastal inputs from snowmelt and glaciers play a significant role in the local occurrence of PFAAs. The comparison of concentrations between snow, lake water and seawater provides further evidence. Fig. 4 shows the ratio between lake and surface seawater, as well as the ratio between snow and seawater for Deception Island. PFBA

and PFOA were enriched in lake and in snow when compared with seawater, confirming that PFAS were entering the lakes and surface seawater by atmospheric inputs. Foster Bay is semi-enclosed, with longer seawater residence time, when compared with South Bay at Livingston Island. Consequently, the higher concentrations in Foster Bay (Fig. 2) can be explained by the magnitude of the amplification processes or drivers explained in this study (wet deposition for example), as well as different residence times of the water mass inside Foster Bay. In addition, Deception Island is one of the most frequently visited location by tourists in Antarctica. In 2016/2017 season, 2470 visitors (tourists, staff and crew) visited Baily Head, at Deception Island (IAATO, 2019). This could also contribute to the high concentrations of PFAAs in Foster Bay. Such tourism is not relevant at Livingston Island. The magnitude of Tourism as a source of PFAAs cannot be quantified here, but the results suggest its influence is local. Figure S17 shows the ratio between the mean surface seawater concentrations of individual PFAAs in Deception Island versus Livingston Island. PFOS, PFBA, PFHxA and PFOA ratios above 1, indicating that these compounds are more enriched at Deception Island, consistent with the drivers mentioned above.

Rain and snow deposition is of larger magnitude in the Western peninsula region than other Antarctic regions, and the Southern Ocean receives larger wet deposition inputs than many oceanic regions such as the Southern Atlantic (Jurado et al., 2005). Therefore, the low, but sometimes higher concentrations than in other oceanic regions, reported here for coastal Antarctica are consistent with such an enhanced wet deposition of PFAAs.

Temporal comparisons of PFAAs concentrations at coastal Livingston, between austral summers of 2014–2015 and 2017–2018, show that concentrations of PFOS, PFOA and PFHxA have decreased (ANOVA $p < 0.05$), whereas PFNA, PFHxA, PFPeA, PFDoDA are not significantly different, and PFUnDA and PFTrDA concentrations have increased significantly (ANOVA, $p < 0.05$). The sampling and analysis followed the same methodology for both campaigns, and differences would be the result of different relevance of their sources, cycling and sinks. The inputs due to atmospheric deposition and currents have been commented

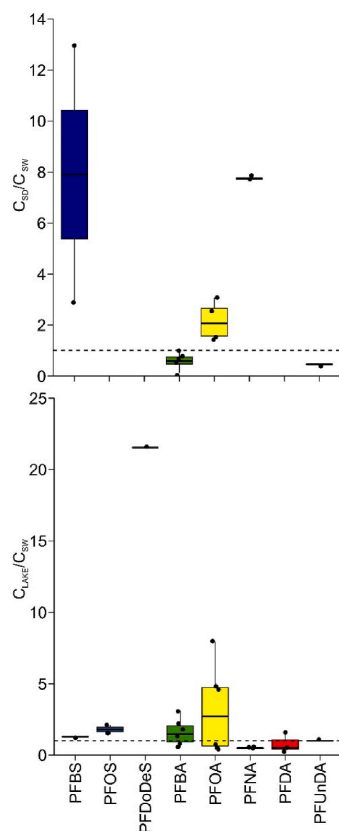


Fig. 4. Ratio between snow and surface seawater (C_{SD}/C_{SW}) and lake and surface seawater (C_{LAKE}/C_{SW}) at Deception Island. Results are shown as a box plot. The black horizontal line inside each box represents the median; the boxes represent the 25th and 75th percentiles of concentrations above the LOQ. The upper whisker extends from the hinge to the largest value (excluding outliers) no further than $1.5 \times$ IQR from the hinge (where IQR is the inter-quartile range, or distance between the first and third quartiles). The lower whisker extends (excluding outliers) from the hinge to the smallest value at most $1.5 \times$ IQR of the hinge. There are no outliers represented. Each dot is a measure. The dashed line marks 1.

above, as well as the amplification mechanism coupled with these PFAS sources. Even though the snow pack and melting was quantitatively more important in the 2015 campaign than that in 2018, PFOS is not enriched in snow (Casal et al. 2017a,b) so the snow input of PFOS were not higher in 2015 than in 2018. It is thus noteworthy to evaluate potential PFAAs sinks from the water column.

3.5. PFAS sinks at coastal Antarctica

The Antarctic circumpolar current acts as a barrier to the entrance of pollutants by ocean currents to the maritime Antarctica (Bengtson Nash et al., 2010), but for the same reason, it can also be a barrier for the export of pollutants from the region. Therefore, the potential outputs or sinks of PFAAs from the maritime Antarctica water column are settling fluxes due to the biological pump, eddy diffusion, aerosolization with sea-spray, and potential degradation. The extent of the biological pump as a PFAAs removal mechanism from the ocean surface has been evaluated before for the Southern ocean and elsewhere (Casal et al., 2017b,

2017a; González-Gaya et al., 2019), and it is of larger magnitude than that of the vertical flux due to eddy diffusivity (González-Gaya et al., 2019; Lohmann et al., 2013). The average residence time due to the settling in the water column due to the combined biological pump and diffusion sinks is of 360 and 32 years for PFOA and PFOS, respectively (González-Gaya et al., 2019). In Antarctic waters, these residence times could be significantly lower due to the higher primary productivity in comparison to the global oceans. Nevertheless, it is not plausible that the observed decrease of PFOS concentrations after few years in surface seawater was due to settling fluxes alone.

The concentrations of PFOS reported here for the years 2017–2018 are very low, in fact these were below LOQ for many sampling events. The ratio PFOS/PFOA for surface seawater ranged from 0 to 1.02, with a maximum PFOS/PFOA of 1 and 0.1 at Deception and Livingston Islands respectively, lower than those reported previously for the same Antarctic environment in 2014–15 (0–2.6) (Casal et al., 2017b), and for other oceans. For example, Muir and Miaz (2021) compiled previous reports of PFOS and PFOA with medians of the ratio PFOS/PFOA of 5.4, 2.5 and 0.2 for the maritime Antarctica during the periods 2000–2009, 2010–2014, and 2015–2019, respectively. These ratios are lower than those in the South Atlantic, which were 2.86, 15 and 1.36 for the same time periods 2000–2009, 2010–2014 and 2015–2019, respectively (Muir and Miaz, 2021). The apparent decrease of PFOS/PFOA ratio is noteworthy in many marine regions. The preferential decrease of PFOS in comparison to PFOA, cannot be due neither to losses by aerosolization, since enrichment factors of PFOS and PFOA during sea-spray formation are not significantly different (Casas et al., 2020).

PFAAs in general have been nicknamed “forever chemicals”, based on the strong C–F bond and multiples evidences of their persistence in the environment. Even though degradation of PFAAs has been reported under artificial-engineered systems (Lei et al., 2020; Lewis et al., 2020; Singh et al., 2019; Stonebridge et al., 2020; Trang et al., 2022) these evidences have been elusive for the natural environment. However, some recent reports suggest that microbial degradation could be feasible. For example, ether-PFAS, although with different structures of those targeted here, have been suggested to be degraded by soil microbiomes (Jiang et al., 2021). On the other hand, PFOS and PFOA have also been suggested to be degraded by an *Acidimicrobium* sp. strain under culture conditions (Huang 2019). With larger marine significance, a recent work has shown PFOS degradation by bacteria in seawater for the first time; precisely in Deception Island (Antarctica) (Cerro-G Alvez et al., 2020). This degradation was a desulfurization, and thus did not imply breaking the strong C–F bonds. Such desulfurization is feasible in the environment due to the fact that use of organic S is energetically favourable in comparison to the use of inorganic S. Therefore, it is noteworthy to further evaluate the occurrence of PFOS and other PFAAs and how it is related to the in-situ microbial populations, even though further experiments on the degradation of PFOS and other PFSA, which would have allowed demonstrating if any degradation occurred were not done.

3.6. PFAAs and microorganisms

We explored the correlations between PFAAs concentrations and other environmental parameters (nutrient concentrations, salinity, etc.) and the composition of the bacterial communities in the same samples. This analysis was done for the concentrations of PFCA and PFSA reported here for the 2016–2017 and 2017–18 austral summers, but also for the PFCA and PFSA concentrations during the 2014–2015 summer reported previously (Casal et al., 2017b), and for which the bacterial taxonomy has also been characterized using the analysis of 16S rDNA amplicons (Iriarte et al., 2023). Total number of reads per samples ranged from 6131 to 149614, with unique ASV per sample ranging from 49 to 384 (Figure S18, Text S2).

The composition of free living bacterial communities derived from the analysis of 16S rDNA amplicons showed a general dominance of the

classes *Flavobacteriia* (ranging from 10 to 53% of relative contribution to the total 16S rDNA pool, mean $38 \pm 9\%$), Gammaproteobacteria (9–71%, $30 \pm 11\%$) and Alphaproteobacteria (15–60%, $31 \pm 11\%$). Bacteroidia was mostly accounted by the order Flavobacteriales, Gammaproteobacteria by orders Enterobacteriales and Pseudomonadales, and Alphaproteobacteria by SAR11 and Rhodobacterales, consistent with previous reports (Martínez-Varela et al., 2020; Öztürk et al., 2022). We selected the most abundant taxa (>50 reads in at least one sample) to be correlated with physicochemical data. Bacterial taxa could be divided into two main groups according to the different correlation between their relative abundances and the concentrations of PFAAs (Fig. 5). One group of taxa, dominated by different genus in the Rhodobacteraceae and Flavobacteriaceae families, positively correlated with the Σ PFCA and temperature. These genera have a typical copiotrophic lifestyle (Landa et al., 2016; Ruiz-González et al., 2019), and this co-variability may be related to snow- and glacier-melt inputs that introduce PFAAs and organic and inorganic nutrients into surface waters. Oppositely, a

second group of specific taxa of Pseudomonadales and Flavobacteriales showed negative significant correlations with Σ PFCA and Σ PFSA concentrations, indicating potential taxa sensitive to PFAAs toxicities. The PFSA/PFCA ratio showed only one significant negative correlation with the abundance of Rhodobacteraceae, in the order Rhodobacteriales within the Alphaproteobacteria (Fig. 5). Rhodobacterales was the order that showed the highest contribution to the pool of transcripts of PFOS-degrading bacteria in coastal Antarctica and accounted for most of the desulfuring gene expression in PFOS-exposed communities (Cerro-G Alvez et al., 2020). Correlations do not demonstrate a causality, and further work is needed to demonstrate a relevant microbial degradation of PFSAs. Such degradation would be linked to the cycle of dissolved organic sulfur in the ocean, which contain biogenic sulfonates.

Nevertheless, these data are suggestive of a role for certain bacterial taxa in the biodegradation of some specific PFAAs, with a particular focus on to PFSA desulfuration in Antarctic seawater, a topic that deserves further exploration in the future. In addition, it is feasible that the

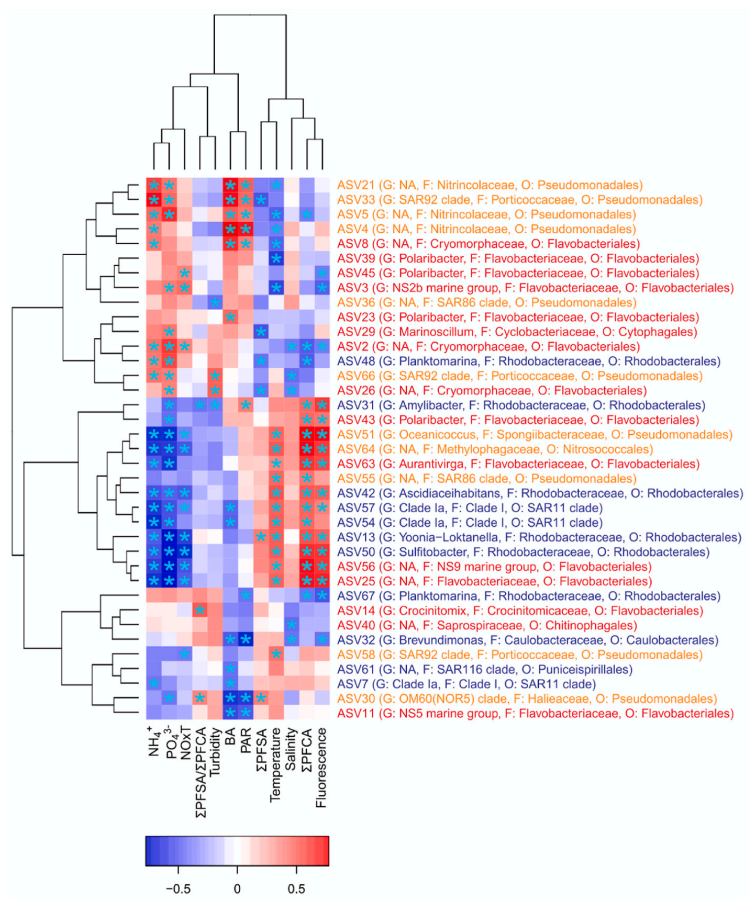


Fig. 5. Bivariate correlation map between environmental and bacterial composition variables, considering the surface seawater PFAAs concentrations from this study (2016–2017 and 2017–18 austral summers) and PFAAs concentrations during the 2014–2015 summer (Casal et al., 2017b). The environmental variables in the x axis: nutrients (Phosphate, PO_4^{3-} , ammonium, NH_4^+ , nitrogen, NO_3^-), CTD data (Turbidity, Temperature, Photosynthetically active radiation, PAR and Fluorescence) and bacterial abundance (BA). PFAAs concentrations in the x axis: sum of perfluoroalkyl carboxylic acids (Σ PFCA), sum of perfluoroalkyl sulfonic acids (Σ PFSA), ratio between the sum of PFSA and the sum of PFCA (Σ PFSA/ Σ PFCA). In the y axis: bacterial ASV (Amplicon Sequence Variant) and taxonomy. For each ASV genus (G), family (F), order (O) and class (Alphaproteobacteria in blue, Gammaproteobacteria in orange and Bacteroidia in red) are specified. Unidentified genus are expressed as “na”. Red and blue sectors represent positive and negative correlations, asterisks indicate significant correlations (Pearson correlation, $p \leq 0.05$).

international measures taken against PFOS in 2009 within the Stockholm Convention, have led to a decrease of their emissions and subsequent transport to Antarctica, and that the Antarctic ecosystem is slowly, within a time-frame of several years, removing PFOS from the environment. The microbial biodiversity in the ocean is huge, with a vast machinery able to multiple and surprising metabolisms. The study of these natural biodegradation processes, and how these relate to the different PFAS inputs, the bioavailable PFAAs, and biogeochemical variables is an urgent research need for the next decade.

4. Conclusions

The concentrations of PFAAs in seawater, snow, rain and plankton from a large sample set from Livingston and Deception islands (Southern Shetland, Antarctica), shows that PFAAs are ubiquitous in the maritime Antarctica, and with concentrations comparable to other oceanic regions. The enrichment of PFAS in snow and rain when compared with seawater, further confirms the important role of wet deposition as an input of PFAS to the Antarctic environment. This is further confirmed by higher concentrations of PFAS in vertical profiles related to low salinity, and the occurrence of PFAS in lakes with only atmospheric sources of PFAS. The PFOS/PFOA ratio shows that it has decreased during the last decade, as previously observed in other oceanic regions. The assessment of the potential sinks of PFAAs, suggest that in addition to the biological pump removing plankton associated PFAAs, the depletion of PFSA by microbial degradation linked to the organic sulfur cycle is feasible, and should receive further attention in future research efforts.

Author statement

GC, BJ and JD wrote the manuscript with contributions from all authors. GC, AM, BJ and JD participated in the sampling campaigns. GC, JR, LA, JM and BJ participated in the instrumental analysis. J.I and MV did the genomic work. GC, BJ and JD designed the work and conceived the manuscript.

Declaration of competing interest

The authors declare the following financial interests/personal relationships which may be considered as potential competing interests: Jordi Dachs reports financial support and administrative support were provided by Spanish Scientific Research Council. Jordi Dachs reports financial support was provided by Spanish agency for research.

Data availability

Data will be made available on request.

Acknowledgments

This work has been supported by the Spanish Ministry of Science and Innovation (MCIN) through projects REMARCA (CTM2012-34673), SENTINEL (CTM2015-70535) and ANATOM (PGC2018-096612-B-I00). The research group of Global Change and Genomic Biogeochemistry receives support from the Catalan Government (2017SGR800). IDAEA-CSIC is a Centre of Excellence Severo Ochoa (Spanish Ministry of Science and Innovation, Project CEX2018-000794-S).

Appendix A. Supplementary data

Supplementary data to this article can be found online at <https://doi.org/10.1016/j.envpol.2023.122608>.

References

- Ahrens, L., Xie, Z., Ebinghaus, R., 2010. Distribution of perfluoroalkyl compounds in seawater from northern Europe, Atlantic ocean, and Southern Ocean. *Chemosphere* 78, 1011–1016. <https://doi.org/10.1016/j.chemosphere.2009.11.038>.
- Armitage, J.M., Schenker, U., Scheringer, M., Martin, J.W., Macleod, M., Cousins, I.T., 2009. Modeling the global fate and transport of perfluorooctane sulfonate (PFOS) and precursor compounds in relation to temporal trends in wildlife exposure. *Environ. Sci. Technol.* 43, 9274–9280. https://doi.org/10.1021/ES901448P/SUPPL_FILE/ES901448P_SI_001.PDF.
- Bengtson Nash, S., Rintoul, S.R., Kawaguchi, S., Staniland, I., Hoff, J. van den, Tierney, M., Bossi, R., 2010. Perfluorinated compounds in the Antarctic region: ocean circulation provides prolonged protection from distant sources. *Environ. Pollut.* 158, 2985–2991. <https://doi.org/10.1016/j.envpol.2010.05.024>.
- Benskin, P., Muir, J.C.G., Scott, B.D.F., Spencer, C., O De Silva, A., Kylin, H.W., Martin, J., Morris, A., Lohmann, R., Tomy, G., Rosenberg, B., Taniyasu, S., Yamashita, N., 2012. Perfluoroalkyl acids in the Atlantic and Canadian Arctic oceans. *Environ. Sci. Technol.* 46, 5815–5823. <https://doi.org/10.1021/es300578x>.
- Bogdal, C., Schmid, P., Zennegg, M., Anselmetti, F.S., Scheringer, M., Hungerbühler, K., 2009. Blast from the past: melting glaciers as a relevant source for persistent organic pollutants. *Environ. Sci. Technol.* 43, 8173–8177. https://doi.org/10.1021/ES901628X/SUPPL_FILE/ES901628X_SI_001.PDF.
- Cabrero, A., Dachs, J., Barceló, D., Jones, K.C., 2012. Influence of organic matter content and human activities on the occurrence of organic pollutants in Antarctic soils, lichens, grass, and mosses. *Environ. Sci. Technol.* 46, 1396–1405. https://doi.org/10.1021/ES203425B/SUPPL_FILE/ES203425B_SI_001.PDF.
- Cabrero, A., Muir, D.C.G., Teixeira, C., Lamoureux, S.F., Lafreniere, M.J., 2019. Snow deposition and melting as drivers of polychlorinated biphenyls and organochlorine pesticides in Arctic rivers, lakes, and ocean. *Environ. Sci. Technol.* 53, 14377–14386. https://doi.org/10.1021/ACS.EST.9B05150/SUPPL_FILE/ES9B05150_SI_001.PDF.
- Cai, M., Yang, H., Xie, Z., Zhao, Z., Wang, F., Lu, Z., Sturm, R., Ebinghaus, R., 2012a. Per- and polyfluoroalkyl substances in snow, lake, surface runoff water and coastal seawater in Fildes Peninsula, King George Island, Antarctica. *J. Hazard Mater.* 209–210, 335–342. <https://doi.org/10.1016/j.jhazmat.2012.01.030>.
- Cai, M., Yang, H., Xie, Z., Zhao, Z., Wang, F., Lu, Z., Sturm, R., Ebinghaus, R., 2012b. Per- and polyfluoroalkyl substances in snow, lake, surface runoff water and coastal seawater in Fildes Peninsula, King George Island, Antarctica. *J. Hazard Mater.* 209–210, 335–342. <https://doi.org/10.1016/j.jhazmat.2012.01.030>.
- Carrasco, J.F., Cordero, R.R., 2020. Analyzing precipitation changes in the northern tip of the Antarctic peninsula during the 1970–2019 period. *Atmos.* 11 (1270–11270), 1270. <https://doi.org/10.3390/ATMOS11121270>.
- Casal, P., González-Gaya, B., Zhang, Y., Reardon, A.J.F., Martin, J.W., Jiménez, B., Dachs, J., 2017a. Accumulation of perfluoroalkylated substances in oceanic plankton. *Environ. Sci. Technol.* 51, 2766–2775. <https://doi.org/10.1021/acs.est.6b05821>.
- Casal, P., Zhang, Y., Martin, J.W., Pizarro, M., Jiménez, B., Dachs, J., 2017b. Role of snow deposition of perfluoroalkylated substances at coastal Livingston island (maritime Antarctica). *Environ. Sci. Technol.* 51, 8460–8470. <https://doi.org/10.1021/acs.est.7b02521>.
- Casal, P., Cabrerizo, A., Vila-Costa, M., Pizarro, M., Jiménez, B., Dachs, J., 2018. Pivotal role of snow deposition and melting driving fluxes of polycyclic aromatic hydrocarbons at coastal Livingston island (Antarctica). *Environ. Sci. Technol.* 52, 12327–12337. <https://doi.org/10.1021/acs.est.8b03640>.
- Casal, P., Casas, G., Vila-Costa, M., Cabrerizo, A., Pizarro, M., Jiménez, B., Dachs, J., 2019. Snow amplification of persistent organic pollutants at coastal Antarctica. *Environ. Sci. Technol.* 53, 8872–8882. <https://doi.org/10.1021/acs.est.9b03006>.
- Casas, G., Martínez-Varela, A., Roscales, J.L., Vila-Costa, M., Dachs, J., Jiménez, B., 2020. Enrichment of perfluoroalkyl substances in the sea-surface microlayer and sea-spray aerosols in the Southern Ocean. *Environ. Pollut.* 267, 115512. <https://doi.org/10.1016/j.envpol.2020.115512>.
- Casas, G., Martínez-Varela, A., Vila-Costa, M., Jiménez, B., Dachs, J., 2021. Rain amplification of persistent organic pollutants. *Environ. Sci. Technol.* 55, 12961–12972. <https://doi.org/10.1021/ACS.EST.1C03295>.
- Cerro-G Alvez, E., Roscales, J.L., Jim Enez, B., Montserrat Sala, M., Dachs, J., Vila-Costa, M., 2020. Microbial responses to perfluoroalkyl substances and perfluorooctanesulfonate (PFOS) desulfurization in the Antarctic marine environment. *Water Res.* 171, 115434. <https://doi.org/10.1016/j.watres.2019.115434>.
- Del Vento, S., Halsall, C., Gioia, R., Jones, K., Dachs, J., 2012. Volatile per- and polyfluoroalkyl compounds in the remote atmosphere of the western Antarctic Peninsula: an indirect source of perfluoroalkyl acids to Antarctic waters? *Atmos. Pollut. Res.* 3, 450–455. <https://doi.org/10.5094/APR.2012.051>.
- González-Gaya, B., Dachs, J., Roscales, J.L., Caballero, G., Jiménez, B., 2014. Perfluoroalkylated substances in the global tropical and subtropical surface oceans. *Environ. Sci. Technol.* 48, 13076–13084. <https://doi.org/10.1021/es503490z>.
- González-Gaya, B., Casal, P., Jurado, E., Dachs, J., Jiménez, B., 2019. Vertical transport and sinks of perfluoroalkyl substances in the global open ocean. *Environ. Sci. Process. Impacts* 21, 1957–1969. <https://doi.org/10.1039/C9EM00266A>.
- Guieu, C., Milosavljević, S.F., Engel, A., Bange, H.W., Cunliffe, M., Burrows, S.M., Friedrichs, G., Galgani, L., Herrmann, H., Hertkorn, N., Johnson, M., Liss, P.S., Quinn, P.K., Schartau, M., Soloviev, A., Stolle, C., Upstill-Goddard, R.C., Van Pinxteren, M., Zänker, B., 2017. The Ocean's vital skin: toward an integrated understanding of the sea surface microlayer. *Front. Mar. Sci.* 165. <https://doi.org/10.3389/fmars.2017.00165>.
- Helm, P.A., Diamond, M.L., Semkin, R., Strachan, W.M.J., Teixeira, C., Gregor, D., 2002. A mass balance model describing multiyear fate of organochlorine compounds in a

- high arctic lake. *Environ. Sci. Technol.* 36, 996–1003. <https://doi.org/10.1021/ES010952K>/SUPPL_FILE/ES010952K.S.PDF.
- Huang, S., Jaffé, P.R., 2019. Defluorination of Perfluorooctanoic Acid (PFOA) and Perfluorooctane Sulfonate (PFOS) by Acidimicrobium Sp. Strain A6. *Environ. Sci. Technol.* 53, 11410–11419. <https://doi.org/10.1021/acs.est.9b04047>.
- Huang, T., Sun, L., Wang, Y., Chu, Z., Qin, X., Yang, L., 2014. Transport of nutrients and contaminants from ocean to island by emperor penguins from Amanda Bay, East Antarctica. *Sci. Total Environ.* 468–469, 578–583. <https://doi.org/10.1016/J.SCITOTENV.2013.08.082>.
- IAATO, 2019. International Association of Antarctica Tour Operators. <https://iaato.org/information-resources/data-statistics/>.
- Iriarte, J., Dachs, J., Casas, G., Martínez-Varela, A., Berrojalbiz, N., Vila-Costa, M., 2023. Snow-dependent biogeochemical cycling of polycyclic aromatic hydrocarbons at coastal Antarctica. *Environ. Sci. Technol.* 57, 1625–1636. <https://doi.org/10.1021/ACS.EST.2C05583>/ASSET/IMAGES/LARGE/ES2C05583_0006.JPEG.
- Jiang, T., Geisler, M., Zhang, W., Liang, Y., 2021. Fluoroalkylether compounds affect microbial community structures and abundance of nitrogen cycle-related genes in soil-microbe-plant systems. *Ecotoxicol. Environ. Saf.* 228, 113033 <https://doi.org/10.1016/J.ECOENV.2021.113033>.
- Johansson, J.H., Salter, M.E., Acosta Navarro, J.C., Leck, C., Nilsson, E.D., Cousins, I.T., 2019. Global transport of perfluoroalkyl acids via sea spray aerosol. *Environ. Sci. Process. Impacts* 21, 635–649. <https://doi.org/10.1039/C8EM00525G>.
- Jurado, E., Jaward, F., Lohmann, R., Jones, K.C., Simó, R., Dachs, J., 2005. Wet deposition of persistent organic pollutants to the global oceans. *Environ. Sci. Technol.* 39, 2426–2435. <https://doi.org/10.1021/es048599g>.
- Khairi, M.A., Luek, J.L., Dickhut, R., Lohmann, R., 2016. Levels, sources and chemical fate of persistent organic pollutants in the atmosphere and snow along the western Antarctic Peninsula. *Environ. Pollut.* 216, 304–313. <https://doi.org/10.1016/J.ENVPOL.2016.05.092>.
- Lafrenière, M.J., Blais, J.M., Sharp, M.J., Schindler, D.W., 2006. Organochlorine pesticide and polychlorinated biphenyl concentrations in snow, snowmelt, and runoff at Bow Lake, Alberta. *Environ. Sci. Technol.* 40, 4909–4915. <https://doi.org/10.1021/ES060237G>.
- Landa, M., Blain, S., Christaki, U., Monchy, S., Obernosterer, I., 2016. Shifts in bacterial community composition associated with increased carbon cycling in a mosaic of phytoplankton blooms. *ISME J.* 10, 39–50. <https://doi.org/10.1038/ismej.2015.105>.
- Lei, Y.J., Tian, Y., Sobhani, Z., Naidu, R., Fang, C., 2020. Synergistic degradation of PFAS in water and soil by dual-frequency ultrasonic activated persulfate. *Chem. Eng. J.* 388, 124215 <https://doi.org/10.1016/J.CEJ.2020.124215>.
- Lewis, E.R., Schwartz, S.E., 2004. Sea salt aerosol production: mechanisms, methods, measurements and models—a critical review. In: *Geophysical Monograph Series*. American Geophysical Union, pp. 1–408. <https://doi.org/10.1029/152GM01>.
- Lewis, A.J., Joyce, T., Hadaya, M., Ebrahimi, F., Dragiev, I., Giardetti, N., Yang, J., Fridman, G., Rabinovich, A., Fridman, A.A., McKenzie, E.R., Sales, C.M., 2020. Rapid degradation of PFAS in aqueous solutions by reverse vortex flow gliding arc plasma. *Environ. Sci. Water Res. Technol.* 6, 1044–1057. <https://doi.org/10.1039/C9EW01050E>.
- Lindstrom, A.B., Strynar, M.J., Libelo, E.L., 2011. Polyfluorinated compounds: past, present, and future. *Environ. Sci. Technol.* 45, 7954–7961. https://doi.org/10.1021/ES2011622/ASSET/IMAGES/ES2011622_S000L1.JPG.V03.
- Lorca, M., Farré, M., Tavano, M.S., Alonso, B., Korembli, G., Barceló, D., 2012. Fate of a broad spectrum of perfluorinated compounds in soils and biota from Tierra del Fuego and Antarctica. *Environ. Pollut.* 163, 158–166. <https://doi.org/10.1016/J.ENVPOL.2011.10.027>.
- Lohmann, R., Jurado, E., Dijkstra, H.A., Dachs, J., 2013. Vertical eddy diffusion as a key mechanism for removing perfluorooctanoic acid (PFOA) from the global surface oceans. *Environ. Pollut.* 179, 88–94. <https://doi.org/10.1016/J.ENVPOL.2013.04.006>.
- Macdonald, R., Mackay, D., Hickie, B., 2002. Contaminant amplification in the environment. *Environ. Sci. Technol.* 36, 456A–462A. <https://doi.org/10.1021/ES022470U>.
- MacInnis, J.J., Lehnher, I., Muir, D.C.G., Quinlan, R., De Silva, A.O., 2019a. Characterization of perfluoroalkyl substances in sediment cores from High and Low Arctic lakes in Canada. *Sci. Total Environ.* 666, 414–422. <https://doi.org/10.1016/J.SCITOTENV.2019.02.210>.
- MacInnis, J.J., Lehnher, I., Muir, D.C.G., St Pierre, K.A., St Louis, V.L., Spencer, C., De Silva, A.O., 2019b. Fate and transport of perfluoroalkyl substances from snowpacks into a lake in the high arctic of Canada. *Environ. Sci. Technol.* 53, 10753–10762. <https://doi.org/10.1021/acs.est.9b03372>.
- Martin, J.W., Ellis, D.A., Mabury, S.A., Hurley, M.D., Wallington, T.J., 2006. Atmospheric chemistry of perfluoroalkanesulfonamides: kinetic and product studies of the OH radical and Cl atom initiated oxidation of N-ethyl perfluorobutanesulfonamide. *Environ. Sci. Technol.* 40, 864–872. <https://doi.org/10.1021/ES051362F>.
- Martínez-Varela, A., Casas, G., Piña, B., Dachs, J., Vila-Costa, M., 2020. Large enrichment of anthropogenic organic matter degrading bacteria in the sea-surface microlayer at coastal Livingston island (Antarctica). *Front. Microbiol.* 11, 2153. <https://doi.org/10.3389/FMICB.2020.571983/BIBTEX>.
- Maskey, S., Geng, H., Song, Y.C., Hwang, H., Yoon, Y.J., Ahn, K.H., Ro, C.U., 2011. Single-particle characterization of summertime antarctic aerosols collected at King George island using quantitative energy-dispersive electron probe X-ray microanalysis and attenuated total reflection Fourier transform-infrared imaging techniques. *Environ. Sci. Technol.* 45, 6275–6282. https://doi.org/10.1021/ES200936M/SUPPL_FILE/ES200936M.SI.001.PDF.
- McMurdo, C.J., Ellis, D.A., Webster, E., Butler, J., Christensen, R.D., Reid, L.K., 2008. Aerosol enrichment of the surfactant PFO and mediation of the Water–Air transport of gaseous PFOA. *Environ. Sci. Technol.* 42, 3969–3974. <https://doi.org/10.1021/es7032026>.
- Muir, D., Miaz, L.T., 2021. Spatial and temporal trends of perfluoroalkyl substances in global ocean and coastal waters. *Environ. Sci. Technol.* 55, 9527–9537. <https://doi.org/10.1021/ACS.EST.0C08035>.
- Oliaei, F., Kriens, D., Weber, R., Watson, A., 2012. PFOS and PFC releases and associated pollution from a PFC production plant in Minnesota (USA). *Environ. Sci. Pollut. Res.* 204 (20), 1977–1992. <https://doi.org/10.1007/S11356-012-1275-4>, 2012.
- Ozturk, R.C., Feyzioglu, A.M., Altinok, I., 2022. Prokaryotic community and diversity in coastal surface waters along the Western Antarctic Peninsula. *Pol. Sci.* 31, 100764. <https://doi.org/10.1016/J.POLAR.2021.100764>.
- Rankin, K., Mabury, S.A., Jenkins, T.M., Washington, J.W., 2016. A North American and global survey of perfluoroalkyl substances in surface soils: distribution patterns and mode of occurrence. *Chemosphere* 161, 333–341. <https://doi.org/10.1016/J.CHEMOSPHERE.2016.06.109>.
- Reth, M., Urs Berger, A., Dag Broman, A., Ian Cousins, A.T., Douglas Nilsson, A.A.E., McLachlan, A.M.S., 2011. Water-to-air transfer of perfluorinated carboxylates and sulfonates in a sea spray simulator. *Environ. Chem.* 8, 381–388. <https://doi.org/10.1071/EN11007.AC>.
- Roosens, L., Van Den Brink, N., Riddle, M., Blust, R., Neels, H., Covaci, A., 2007. Penguin colonies as secondary sources of contamination with persistent organic pollutants. *J. Environ. Monit.* 9, 822–825. <https://doi.org/10.1039/B708103K>.
- Roscales, J.L., Vicente, A., Ryan, P.G., González-Solis, J., Jiménez, B., 2019. Spatial and interspecies heterogeneity in concentrations of perfluoroalkyl substances (PFASs) in seabirds of the Southern Ocean. *Environ. Sci. Technol.* 53, 9855–9865. <https://doi.org/10.1021/ACS.EST.9B02677>/SUPPL_FILE/ES9B02677_SI.001.PDF.
- Ruiz-González, C., Logares, R., Sebastián, M., Mestre, M., Rodríguez-Martínez, R., Galí, M., Sala, M.M., Acinas, S.G., Duarte, C.M., Gasol, J.M., 2019. Higher contribution of globally rare bacterial taxa reflects environmental transitions across the surface ocean. *Mol. Ecol.* 28, 1930–1945. <https://doi.org/10.1111/MEC.15026>.
- Sha, B., Johansson, J.H., Benskin, J.P., Cousins, I.T., Salter, M.E., 2021. Influence of water concentrations of perfluoroalkyl acids (PFAAs) on their size-resolved enrichment in nascent sea spray aerosols. *Environ. Sci. Technol.* 55, 9489–9497. <https://doi.org/10.1021/ACS.EST.0C03804>.
- Sha, B., Johansson, J.H., Tunved, P., Bohlin-Nizzetto, P., Cousins, I.T., Salter, M.E., 2022. Sea spray aerosol (SSA) as a source of perfluoroalkyl acids (PFAAs) to the atmosphere: field evidence from long-term air monitoring. *Environ. Sci. Technol.* 56, 228–238. <https://doi.org/10.1021/ACS.EST.1C04277>/ASSET/IMAGES/MEDIUM/ES1C04277_M004.GIF.
- Singh, R.K., Fernando, S., Baygi, S.F., Multari, N., Thagard, S.M., Holsen, T.M., 2019. Breakdown products from perfluorinated alkyl substances (PFAS) degradation in a plasma-based water treatment process. *Environ. Sci. Technol.* 53, 2731–2738. <https://doi.org/10.1021/ACS.EST.8B07031>/SUPPL_FILE/ES8B07031_SI.001.PDF.
- Skaar, J.S., Røder, E.M., Lyche, J.L., Ahrens, L., Kallenborn, R., 2019. Elucidation of contamination sources for poly- and perfluoroalkyl substances (PFASs) on Svalbard (Norwegian Arctic). *Environ. Sci. Pollut. Res.* 26, 7356–7363. <https://doi.org/10.1007/S11356-018-2162-4>.
- Stemmler, I., Lammel, G., 2010. Atmospheric Chemistry and Physics Pathways of PFOA to the Arctic: variabilities and contributions of oceanic currents and atmospheric transport and chemistry sources. *Atmos. Chem. Phys.* 10, 9965–9980. <https://doi.org/10.5194/acp-10-9965-2010>.
- Stonebridge, J., Baldwin, R., Thomson, N.R., Pracek, C., 2020. Fluoride-selective electrode as a tool to evaluate the degradation of PFAS in groundwater: a bench-scale investigation. *Groundw. Monit. Remediat.* 40, 73–80. <https://doi.org/10.1111/GWMR.12374>.
- Swackhamer, D.L., McVeety, B.D., Hites, R.A., 1988. Deposition and evaporation of polychlorobiphenyl congeners to and from siskiwiit lake, Isle royale, lake superior. *Environ. Sci. Technol.* 22, 664–672. <https://doi.org/10.1021/ES00171A008>.
- Temniskova-Topalova, D., Chipev, N., 2001. Diatoms from Livingston island, the South-Shetland islands, Antarctica. In: Jahn, R., Kociolek, J.P., Witkowski, A., Compere, P. (Eds.), *Proc. 16th Int. Diatom Symp. Univ., Athens, Greece*, pp. 291–293.
- Trang, B., Li, Y., Xue, X.-S., Ateia, M., Houk, K.N., Dichtel, W.R., 2022. Low-temperature mineralization of perfluorocarboxylic acids. *Science* 377, 839–845. <https://doi.org/10.1126/SCIENCE.ABM8868>.
- U.S. Environmental Protection Agency.EPA. [WWW Document]. URL <https://www.epa.gov/>.
- Veillette, J., Muir, D.C.G., Antoniadis, D., Small, J.M., Spencer, C., Loewen, T.N., Babaluk, J.A., Reist, J.D., Vincent, W.F., 2012. Perfluorinated chemicals in meromictic lakes on the northern coast of Ellesmere Island, High Arctic Canada. *JSTOR* 65, 245–256.
- Vignon, Roussel, M.L., Gorodetskaya, I.V., Genthon, C., Berne, A., 2021. Present and future of rainfall in Antarctica. *Geophys. Res. Lett.* 48 <https://doi.org/10.1029/2020GL029281>.
- Wang, Z., Xie, Z., Mi, W., Möller, A., Wolschke, H., Ebinghaus, R., 2015. Neutral poly/per-fluoroalkyl substances in air from the atlantic to the Southern Ocean and in antarctic snow. *Environ. Sci. Technol.* 49, 7770–7775. <https://doi.org/10.1021/acs.est.5b00920>.
- Wei, S., Chen, L.Q., Taniyasu, S., So, M.K., Murphy, M.B., Yamashita, N., Yeung, L.W.Y., Lam, P.K.S., 2007. Distribution of perfluorinated compounds in surface seawaters between Asia and Antarctica. *Mar. Pollut. Bull.* 54, 1813–1818. <https://doi.org/10.1016/J.MARPOLBUL.2007.08.002>.
- Wild, S., McLagan, D., Schlabach, M., Bossi, R., Hawker, D., Cropp, R., King, C.K., Stark, J.S., Mondon, J., Nash, S.B., 2015. An antarctic research station as a source of brominated and perfluorinated persistent organic pollutants to the local

- environment. *Environ. Sci. Technol.* 49, 103–112. <https://doi.org/10.1021/es5048232>.
- Yamashita, N., Kannan, K., Taniyasu, S., Horii, Y., Petrick, G., Gamo, T., 2005. A global survey of perfluorinated acids in oceans. *Mar. Pollut. Bull.* 51, 658–668. <https://doi.org/10.1016/j.marpolbul.2005.04.026>.
- Yamashita, N., Taniyasu, S., Petrick, G., Wei, S., Gamo, T., Lam, P.K.S., Kannan, K., 2008. Perfluorinated acids as novel chemical tracers of global circulation of ocean waters. *Chemosphere* 70, 1247–1255. <https://doi.org/10.1016/j.chemosphere.2007.07.079>.
- Young, C.J., Mabury, S.A., 2010. Atmospheric perfluorinated acid precursors: chemistry, occurrence, and impacts. *Rev. Environ. Contam. Toxicol.* 208, 1–109. https://doi.org/10.1007/978-1-4419-6880-7_1.
- Young, C.J., Furdul, V.I., Franklin, J., Koerner, R.M., Muir, D.C.G., Mabury, S.A., 2007. Perfluorinated acids in arctic snow: new evidence for atmospheric formation. *Environ. Sci. Technol.* 41, 3455–3461. https://doi.org/10.1021/ES0626234/SUPPL_FILE/ES0626234SI20070203_021824.PDF.
- Zhang, L., Cheng, I., Muir, D., Charland, J.-P., 2015. Scavenging ratios of polycyclic aromatic compounds in rain and snow in the Athabasca oil sands region. *Atmos. Chem. Phys.* 15, 1421–1434. <https://doi.org/10.5194/acp-15-1421-2015>.
- Zhao, Z., Xie, Z., Möller, A., Sturm, R., Tang, J., Zhang, G., Ebinghaus, R., 2012. Distribution and long-range transport of polyfluoroalkyl substances in the Arctic, Atlantic Ocean and Antarctic coast. *Environ. Pollut.* 170, 71–77. <https://doi.org/10.1016/j.envpol.2012.06.004>.

Supporting Information

Inputs, Amplification and Sinks of Perfluoroalkyl Substances at Coastal Antarctica

Gemma Casas^{1,2,4}, Jon Iriarte¹, Lisa A. D'Agostino³, Jose L. Roscales², Alicia Martinez-Varela¹, Maria Vila-Costa¹, Jonathan W. Martin³, Begoña Jiménez², and Jordi Dachs^{1*}

¹Institute of Environmental Assessment and Water Research, Spanish National Research Council (IDAEA-CSIC), Barcelona, Catalonia 08034, Spain

²Department of Instrumental Analysis and Environmental Chemistry, Institute of Organic Chemistry, Spanish National Research Council (IQOG-CSIC), Madrid 28006, Spain ³Department of Environmental Science (ACES, Exposure & Effects), Science for Life Laboratory, Stockholm University, Stockholm 106 91, Sweden

⁴ BETA Tech Center, University of Vic, Vic, Catalonia, Spain

* Corresponding author email: jordi.dachs@idaea.csic.es

Summary

Pages: 35

Annexes: 2

Figures: 18

Tables: 12

References: 1

Table of Contents

Annex S1. Sample Analysis

Annex S2. Bioinformatic annotation and statistical analyses

Figure S1. Livingston and Deception (South Shetland, Antarctic Peninsula) location.

Figure S2. Sampling stations (st) in Deception Island.

Figure S3. Seawater sampling stations (st) in Livingston Island (A) and snow, snowmelt aerosol and rain sampling stations (B).

Figure S4. Concentrations of PFAS in Deception Island (pg/L) in aerosol, rain, snow, snow melt, lake and sea water samples.

Figure S5. PFAS concentrations in surface seawater from 5 different sampling transects in Livingston Island.

Figure S6. Average concentrations of Σ PFAS in surface seawater in pg/L from Livingston in different sampling locations.

Figure S7. Relative composition of PFAS in surface seawater (SW) samples from Livingston Island.

Figure S8. Correlations between individual PFAS in surface seawater samples from Livingston Island (a) and Deception Island (b).

Figure S9. Correlation plot with confidence interval at 95% of PFOS concentrations in surface seawater with Turbidity in Livingston Island.

Figure S10. Vertical profiles of PFAS in seawater from Livingston Island (from 1.5 m to 30 m depth). PFAS concentrations are pg L⁻¹.

Figure S11. Correlation plot with confidence interval at 95% of depth seawater profiles with salinity and turbidity for individual PFAS concentrations at False Bay and Hanna Point-2.

Figure S12. Relative composition (%) of PFAS in surface seawater (SW) samples from Deception Island.

Figure S13. Snow concentrations (pg/L) in Livingston and Deception Island.

Figure S14. PFAS snow melt concentrations (pg/L) in Livingston and Deception Island.

Figure S15. Comparison of average PFCAs concentrations in snow deposition (CSD) and snowmelt (CSM). Linear regression by least-squares (with confidence interval at 95%)

fitting between the CSD/CSM ratios for individual PFCAs versus the number of carbons in the PFCA alkylated chain (#C) in Livingston and in Deception Island.

Figure S16. PFAS lake water concentrations in Deception Island.

Figure S17. PFAS mean concentrations in SW for Deception Island versus concentrations in SW from Livingston Island. The dashed dotted line marks the number 1.

Figure S18. Sequencing of 16S amplicon for bacterial community characterization.

Table S1. Sampling stations information.

Table S2. Average CTD data from seawater sample stations.

Table S3. Target, recovery and internal standards PFAS and precursor and product ion from the UPLC-MS/MS and the exact mass used in the UHPLC-HRMS.

Table S4. Levels of PFAAs in the procedural and field blanks.

Table S5. Mean and standard deviation of the recovery (%) of recovery standards.

Table S6. Limits of detection (LOQs) in pg.

Table S7. PFAS detection frequency (%) for Livingston and Deception Island in different sample matrix analyzed in this study.

Table S8. Concentrations in seawater (pg/L).

Table S9. Concentrations in snow (pg/L). nd=not detected, nq= not quantified, < loq= lower than limits of quantification.

Table S10. Concentrations in snowmelt (pg/L). nd=not detected, nq= not quantified, < loq= lower than limits of quantification.

Table S11. Ratio between average concentrations of individual PFCA in snow deposition (CSD) to the average concentration in snowmelt (CSM): CSD/CSM for Livingston and Deception Islands.

Table S12. Concentrations in lake water (pg/L). nd=not detected, nq= not quantified, < loq= lower than limits of quantification.

References

ANNEXES

Annex S1. Sample Analysis

At the research station's laboratory, after the GF/F filtration of the samples, PFAS were extracted using an established solid phase extraction (SPE) method with OASIS WAX cartridges (6 cm³, 150 mg; Waters) with minor modifications (Casas et al., 2020). The cartridges were previously conditioned with 4 mL of methanol, 4 mL of methanol containing 0.1% ammonia and 4 mL of precleaned HPLC- grade water. After loading 2 L of water sample through the cartridges, these were washed with 4 mL of HPLC- grade water, dried under vacuum, and stored at -20°C in sealed bags. After the sampling campaign, the samples were eluted and concentrated in an ultraclean laboratory (ISO-5) at the Institute of Environmental Assessment and Water Research (IDAEA-CSIC). Briefly, OASIS WAX cartridges were pH washed with 4 mL of ammonium acetate buffer (25 mM pH 4) and centrifuged to remove the remaining water and then eluted with 4 mL methanol, followed by 8 mL of methanol containing 0.1% ammonia. The final eluents (8 mL of methanol containing 0.1% ammonia) were concentrated under N₂ and reconstituted in PP vials with 0.2 mL of a solution 50:50 methanol/HPLC-grade. Before the instrumental analysis, the vials were spiked with 10 pg of six internal standards (Table S3).

A total of 7 perfluoroalkyl sulfonic acids (PFSA) and 14 perfluoroalkyl carboxylic acids (PFCAs) were the target compounds, including C4-C16 and C18 PFCAs, and C4-C6, and C8 and C10-C12 PFSA; C# indicates the total number of carbon atoms (Table S3).

PFAS were analyzed by ultra-performance liquid chromatography coupled to a triple quadrupole mass spectrometer (UPLC-MS/MS, XEVO TQS, Waters, Milford, MA) based on an established method with minor modifications (Casas et al., 2021, 2020; González-Gaya et al., 2014). A PFAS isolator column (Isolator column Waters ACQUITY UPLC) was installed between the pump and injector and used to separate background contaminations from the sample to be analyzed. A guard column (Waters Acquity UPLC BEH C18 1.7 µm Vanguard 2,1 x 5 mm) was installed between the injector and the analytical column to remove

potential contamination in the mobile phase and minimize extra column volumes. Each ten microliter extract was loaded into a Waters Acquity UPLC BEH Shield RP18 analytical column (1.7 μm , 2.1 x 100 mm; Waters) maintained at 50 °C. Mobile phase consisted of water and methanol:acetonitrile (80:20) with a constant 2mM of ammonium acetate buffer at flow rate of 0.3 mL min⁻¹. Analytes were ionized with an electrospray ionization (ESI) source operating in negative ion mode. Multiple-reaction-monitoring (MRM) mode was used for data acquisition. Each sample was injected in duplicate. To eliminate any potential carryover, acetonitrile was injected in duplicate and passed through the system after every sample or calibration standard. Selected extracts were analyzed with ultra-high-pressure liquid chromatography (UHPLC, Ultimate 300) and HRMS (Q Exactive Orbitrap HF-X, Thermo Fisher Scientific) using electrospray ionization (ESI) in positive and negative mode. Extracts (20 μL) were injected to the column (Waters Acquity UPLC BEH C18). The mobile phase were 10mM ammonium acetate in water (A) and methanol (B). LC-HRMS was operated in HRMS full scan.

Nutrient (NO_x, N-NH₄⁺, PO₄³⁻) analyses were done by standard segmented flow with colorimetric detection⁴³ using a SEAL Analyzer AA3 HR. For the inorganic nutrients analysis, detection limits (defined as three times the standard deviation, SD, of 10 replicates at 50% diluted samples) were 0.006 μM for NO₃⁻, 0.003 μM for NO₂⁻, 0.003 μM for NH₄⁺, and 0.01 μM for PO₄³⁻. Bacterial abundance (BA) was determined by flow cytometry using a FACS Calibur (Becton Dickinson) flow cytometer, as described elsewhere (Gasol and Morán, 2015).

Filters for 16S rDNA sequencing were thawed and incubated with lysozyme, proteinase K and sodium dodecyl sulfate. Nucleic acids were extracted simultaneously with phenil/chloroform/isoamyl alcohol (25:24:1, v:v:v) and with chloroform/isoamyl alcohol (24:1, v:v)⁴⁴. The resulting solution was concentrated to 200 μL using an Amicon Ultra 10-kDa filter unit (Millipore). Partial bacterial 16S gene fragments of DNA were amplified using primers 515f/926r⁴⁵ plus adaptors for Illumina MiSeq sequencing. The PCR reaction mixture was thermocycled at 95°C for 3 min, 30 cycles at 95°C for 45 s, 50°C for 45 s, and 68°C for 90 s, followed by a final extension of 5 min at 68°C. PCR amplicon sizes were

checked in tris- acetate-EDTA (TAE) agarose gels. Illumina MiSeq sequencing (2 x 250 bp) was conducted at the Pompeu Fabra University Sequencing Service. The complete nucleotide sequences obtained in this study have been deposited in the European Nucleotide Archive under the accession number PRJEB52605.

ANNEX S2. Bioinformatic annotation and statistical analyses

Quality control, trimming of the reads, processing, inference of amplicon sequence variants (ASV), and taxonomical classification were done using the nf-core/amplicon 1.2.0dev. pipeline <https://github.com/nf-core/ampliseq>, settings: ‘truncclenl 225-truncclenr 180(Bedia et al., 2018; D.L. Massart, B.G.M.Vandeginste, S.N.Deming, Y. Michotte, n.d.). In short, nf-core/amplicon pipeline uses FastQC v.0.11.9 for quality control (Chemometrics: a textbook), primers are trimmed using Cutadapt v3.2(Parada et al., 2016), then data was imported to QIIME2 v2021.2.0(Straub et al., 2020) where chimeras were removed and ASVs generated using DADA2(Ewels et al., 2020) and classified against the SILVA v.138 database(Andrews, 2020). ASVs classified as Mitochondria or Chloroplast were removed. Normalization of library sizes to mitigate biases introduced by varying read counts in samples was accomplished through rarefaction using the vegan v2.6.2 package. Rarefaction resulted in 349467 reads, which clustered into 1916 unique ASVs

All statistical analyses were performed with R studio 1.4 or SPSS Statistics version 22.0 (IBM Corp.).

Significance was set to $p < 0.05$. Correlation analyses were performed by Pearson rank-order analysis and differences in PFAS concentrations among sampling sites were evaluated by means of one-way ANOVAs. Kruskal-Wallis and post-hoc Mann-Whitney U tests were used to evaluate differences in \sum PFAS concentrations between sampling stations as well between matrices (95% confidence interval). PFAS concentrations in the next sections are presented as mean \pm SD unless otherwise noted. Heatmaps were used to visualize correlations between environmental data including pollutant concentrations and relative abundance of taxonomical groups. In this case, only those ASV with 50 or more reads in at least one

sample were selected, resulting in a list of 68 unique ASVs. The number of unique ASVs per sample varied between 30 and 58, while the number of reads per sample fell within the range of 4871 to 5985. Further graphs were carried out using the “ggplots2” package, also in the R environment.

FIGURES

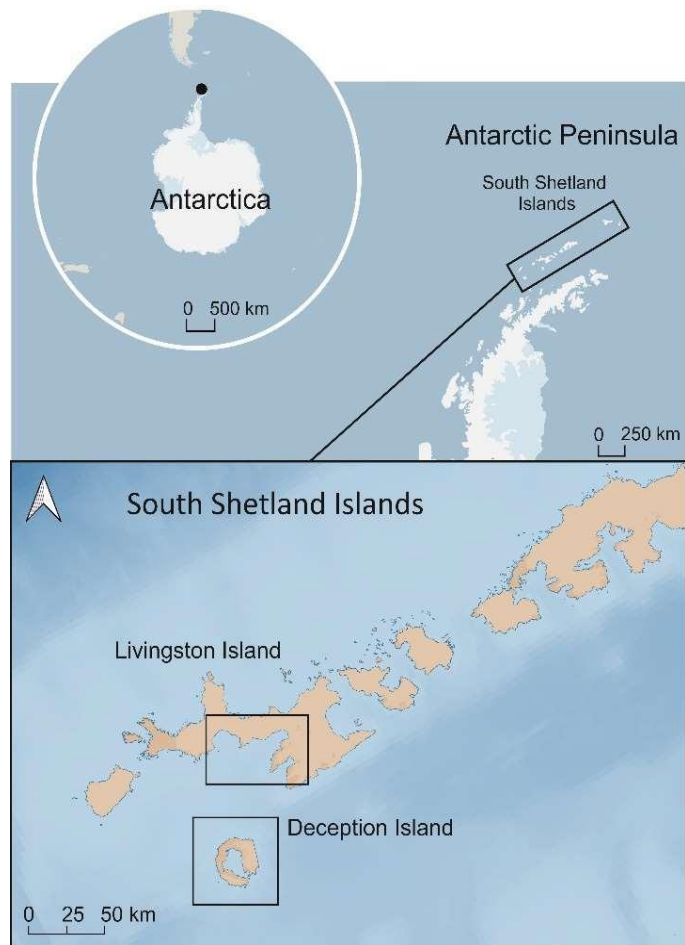


Figure S1. Livingston and Deception Islands (South Shetland, Antarctic Peninsula) location.

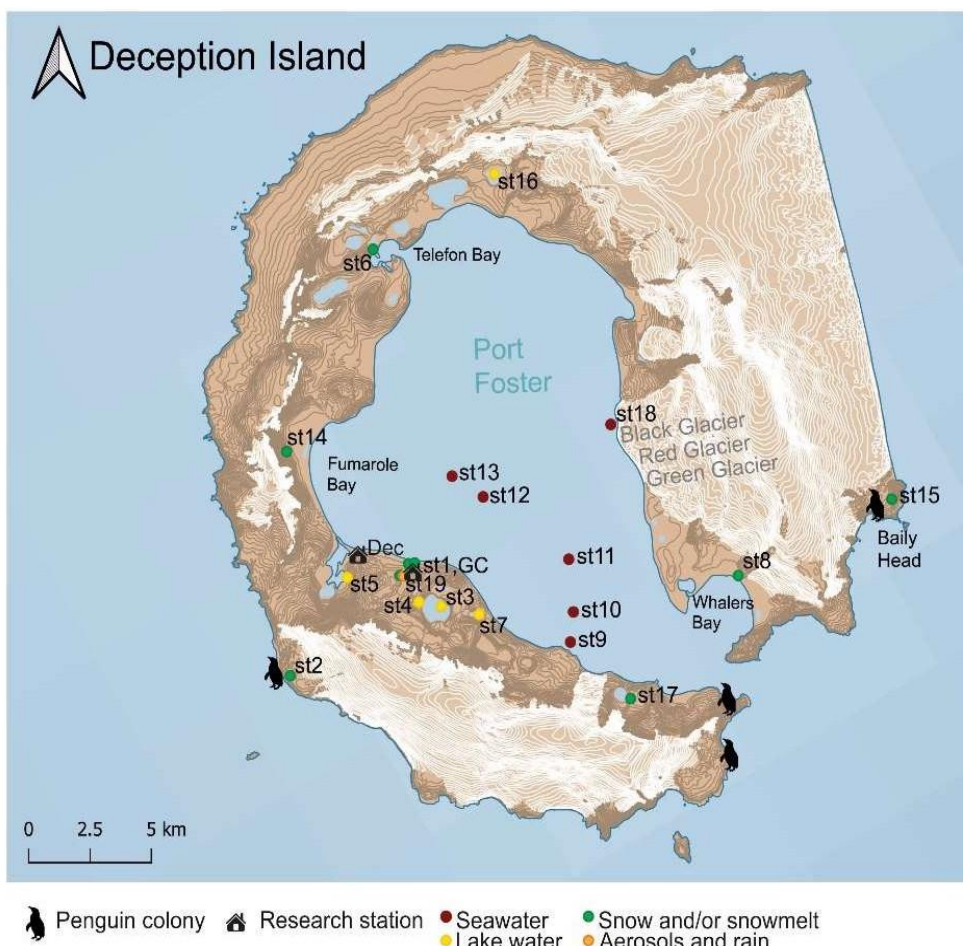
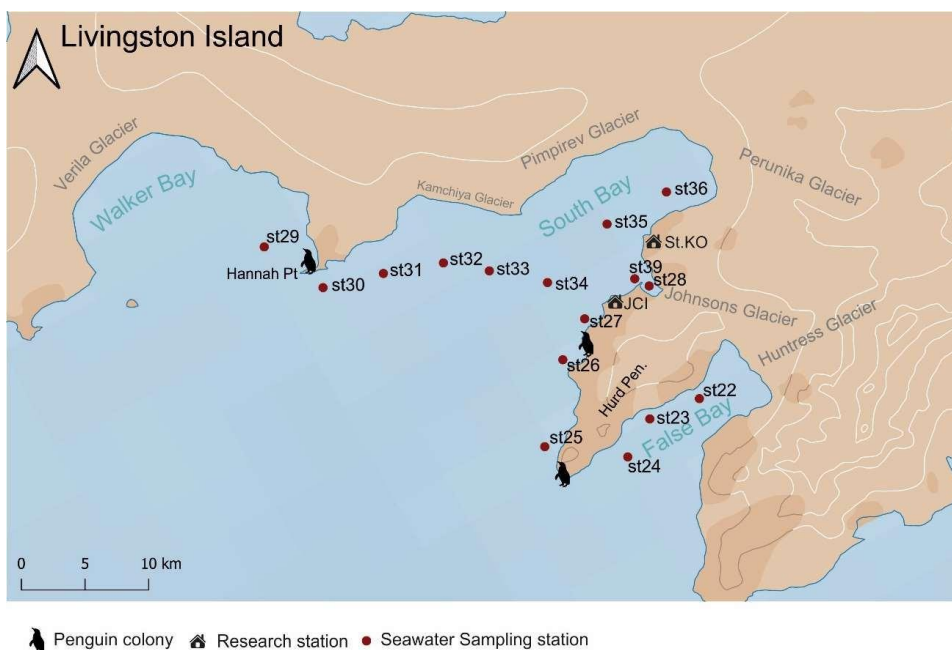


Figure S2. Sampling stations (st) in Deception Island.

A)



B)

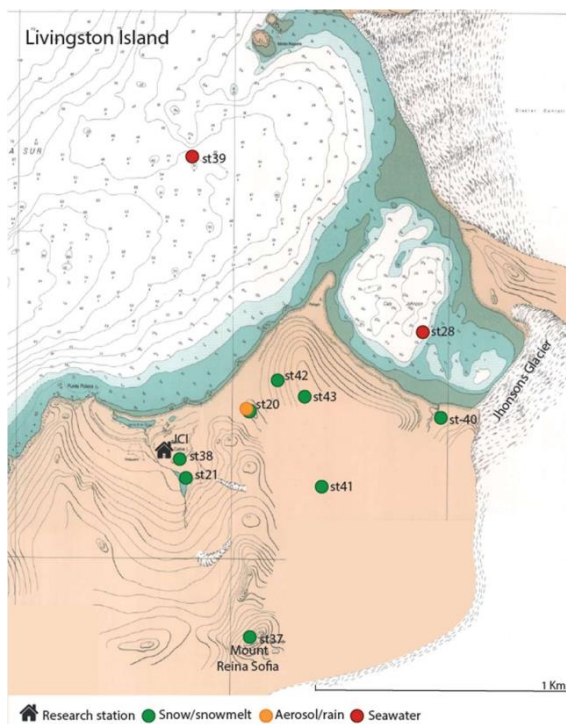


Figure S3. Seawater sampling stations (st) in Livingston Island (A) and snow, snowmelt aerosol and rain sampling stations (B).

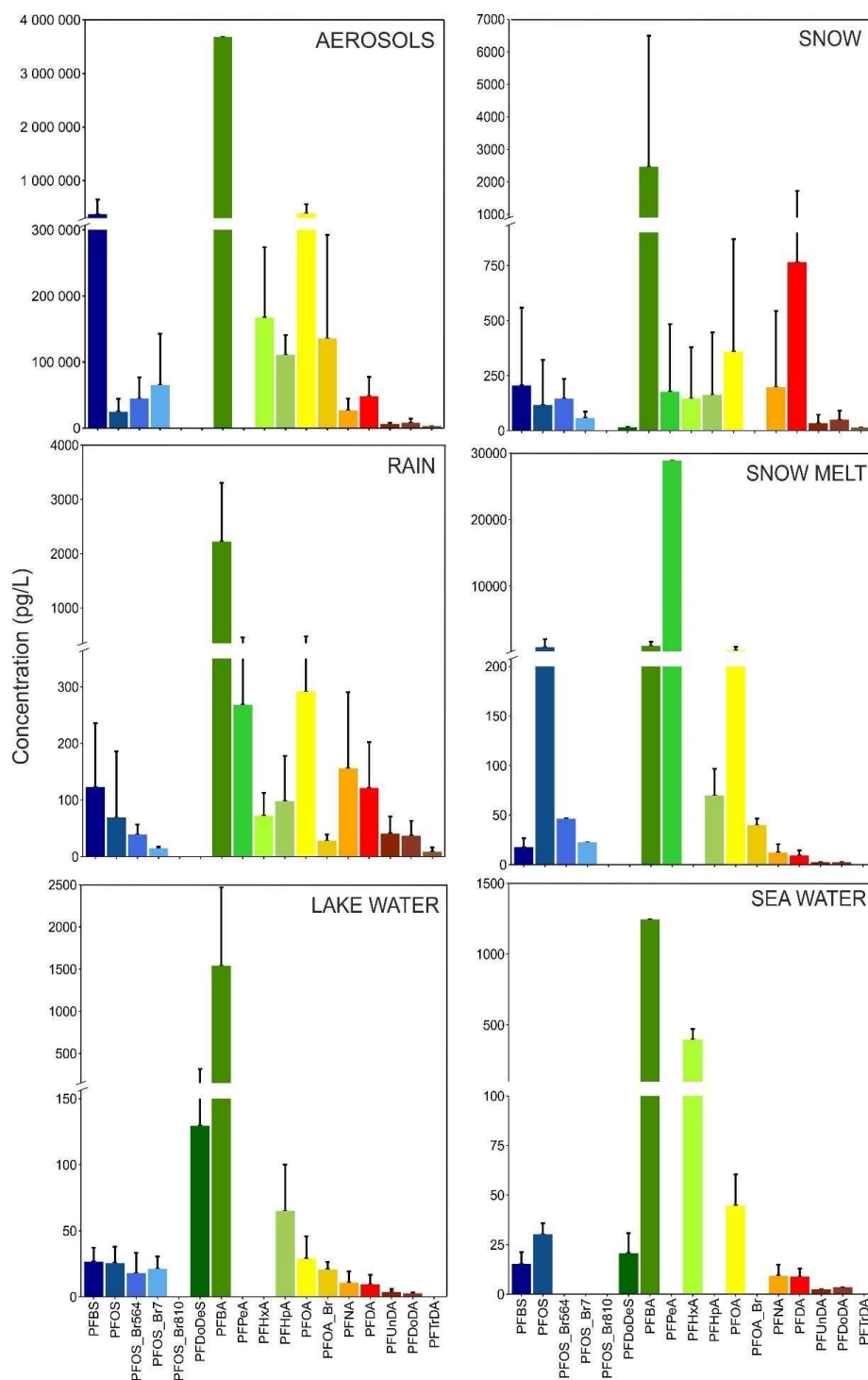


Figure S4. Concentrations of PFAS in Deception Island (pg/L, mean + 1SD) in aerosol, rain, snow, snow melt, lake water and seawater samples.

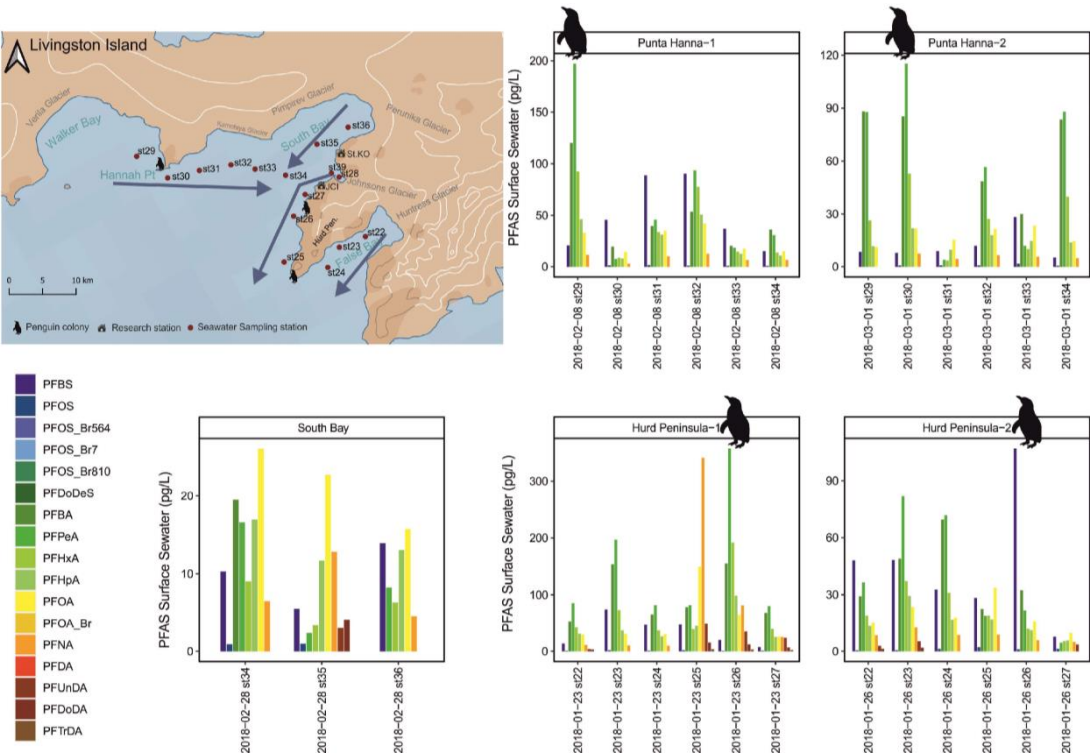


Figure S5. PFAS concentrations in surface seawater from 5 different sampling transects in Livingston Island.

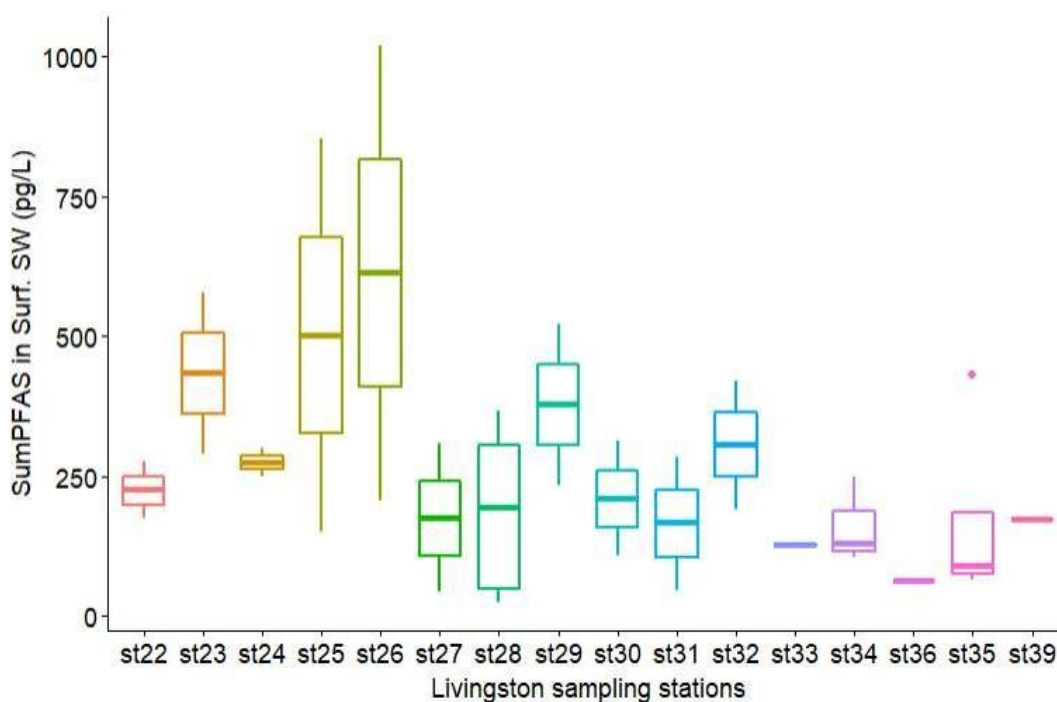


Figure S6. Average concentrations of Σ PFAS in surface seawater in pg/L from Livingston Island in different sampling locations. Results are shown as a box plot. The horizontal line inside each box represents the median, the boxes represent the 25th and 75th percentiles of concentrations above the LOQ. The upper whisker extends from the hinge to the largest value no further than $1.5 \times \text{IQR}$ from the hinge (where IQR is the inter-quartile range, or distance between the first and third quartiles). The lower whisker extends from the hinge to the smallest value at most $1.5 \times \text{IQR}$ of the hinge. The dots are outliers.

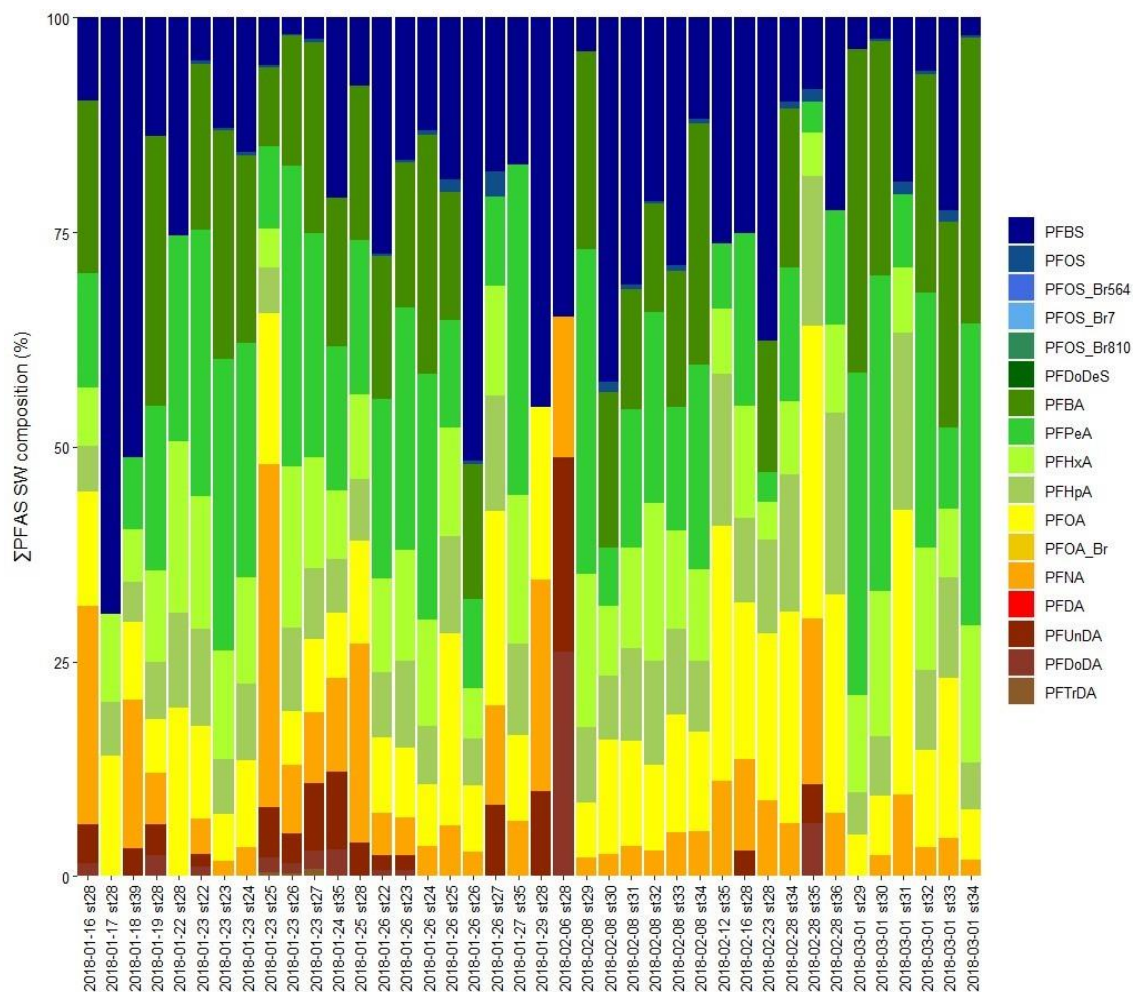


Figure S7. Relative composition of PFAS in surface seawater (SW) samples from Livingston Island.

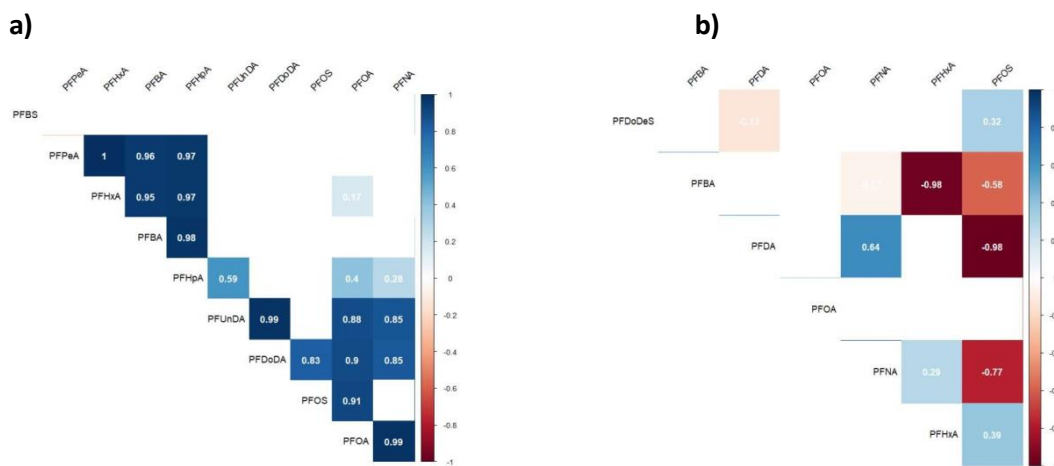


Figure S8. Correlations between individual PFAS in surface seawater samples from Livingston Island (a) and Deception Island (b). The color intensity and the numbers inside each square indicate the strength (r -value) of the Pearson correlation. Positive correlations are displayed in blue and negative correlations in red color. Only correlations with $p < 0.05$ are shown. In the right side of the correlogram, the legend color shows the correlation coefficients and the corresponding colors.

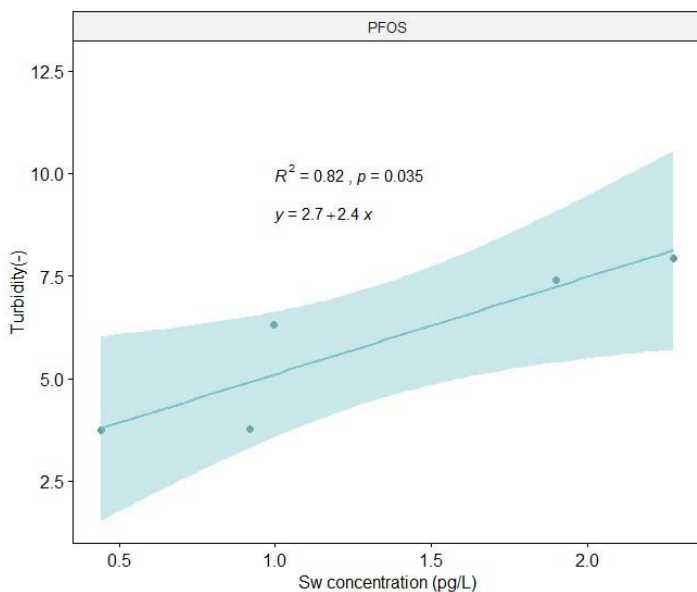


Figure S9. Correlation plot with confidence interval at 95% of PFOS concentrations in surface seawater with Turbidity in Livingston Island.

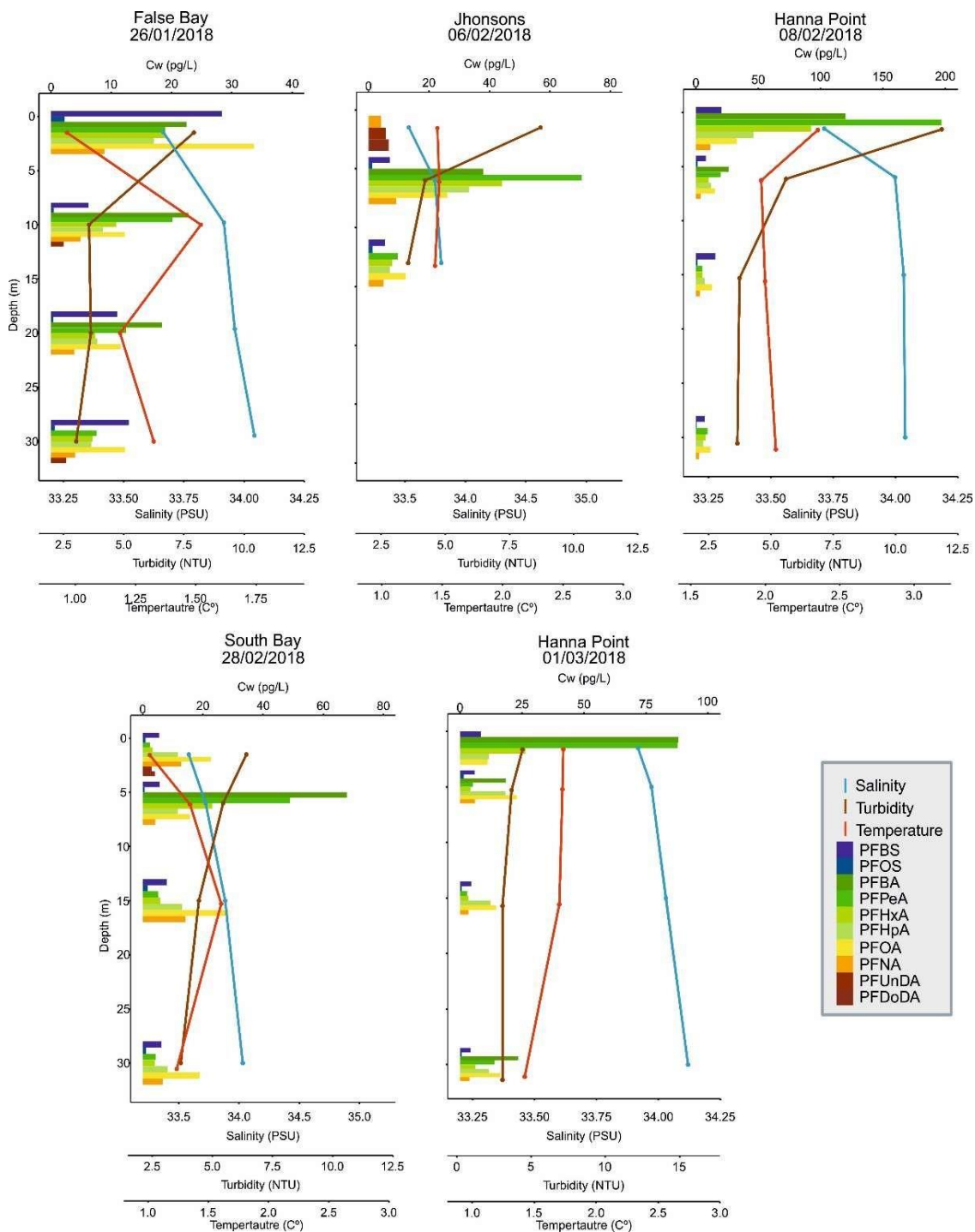
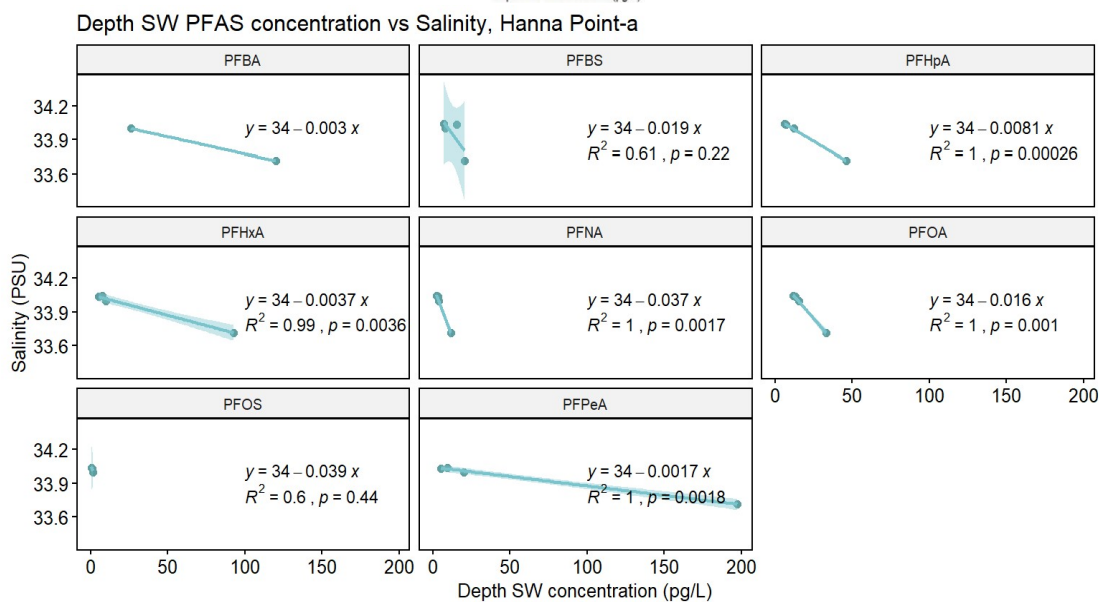
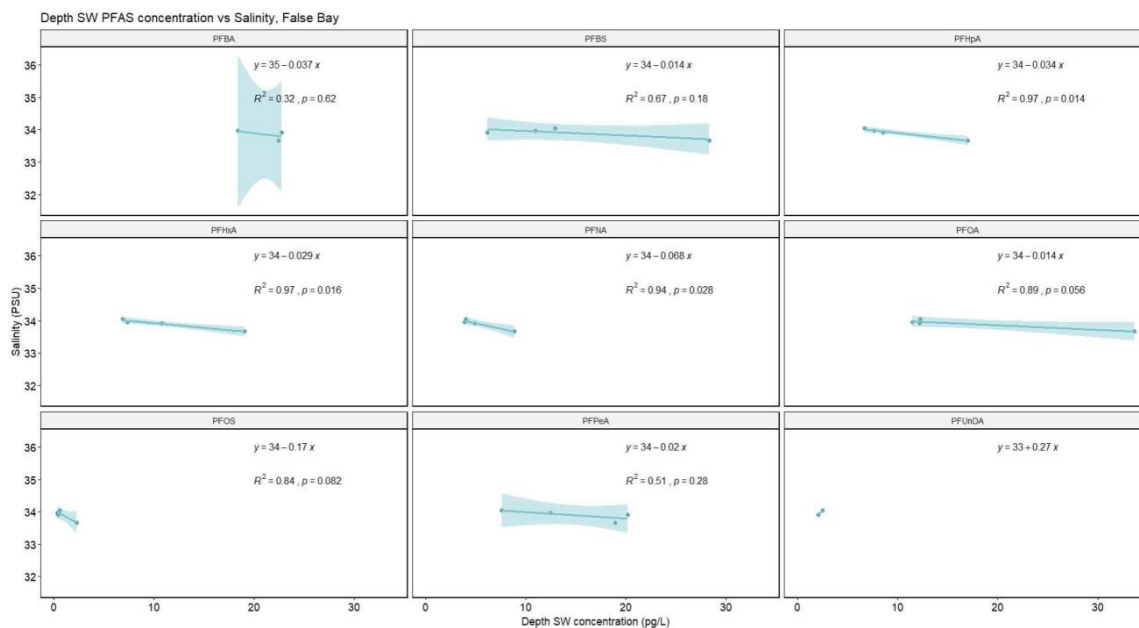


Figure S10. Vertical profiles of PFAS in seawater from Livingston Island (from 1.5 m to 30 m depth). PFAS concentrations are pg L^{-1} .



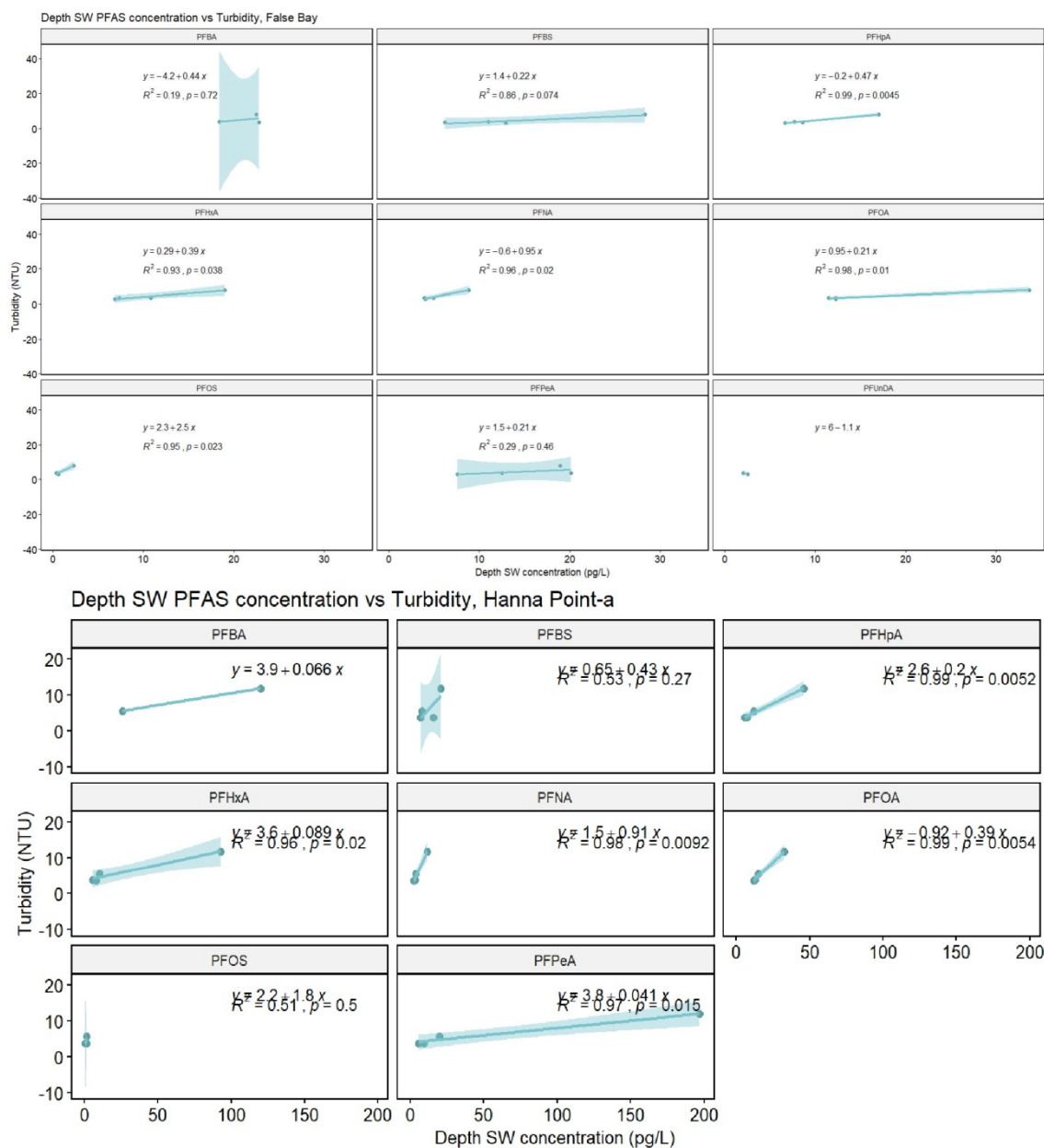


Figure S11. Correlation plot with confidence interval at 95% of depth seawater profiles with salinity and turbidity for individual PFAS concentrations at False Bay and Hanna Point-2.

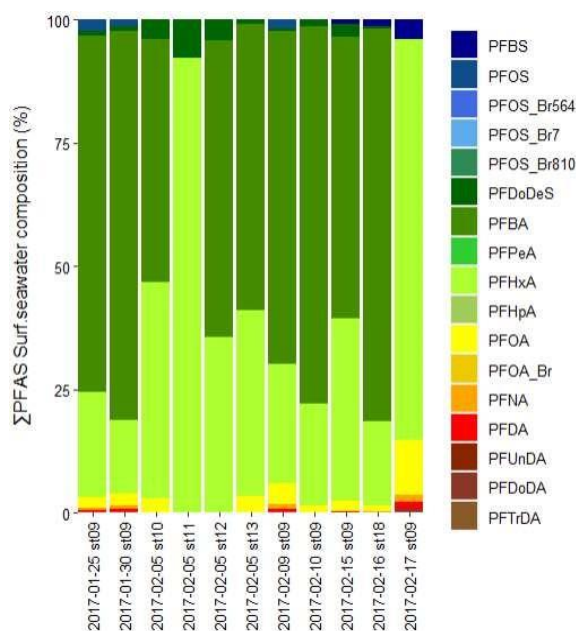


Figure S12. Relative composition (%) of PFAS in surface seawater (SW) samples from Deception Island.

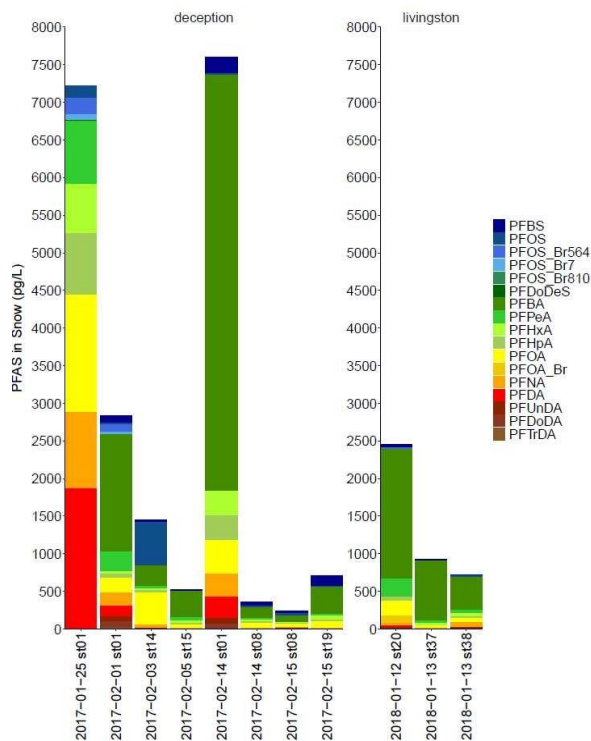


Figure S13. Snow concentrations (pg/L) in Livingston and Deception Islands.

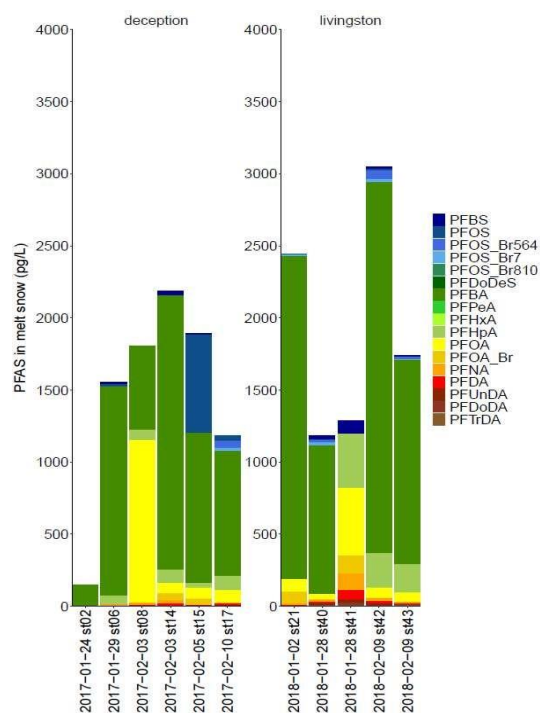


Figure S14. PFAS snowmelt concentrations (pg/L) in Livingston and Deception Islands.

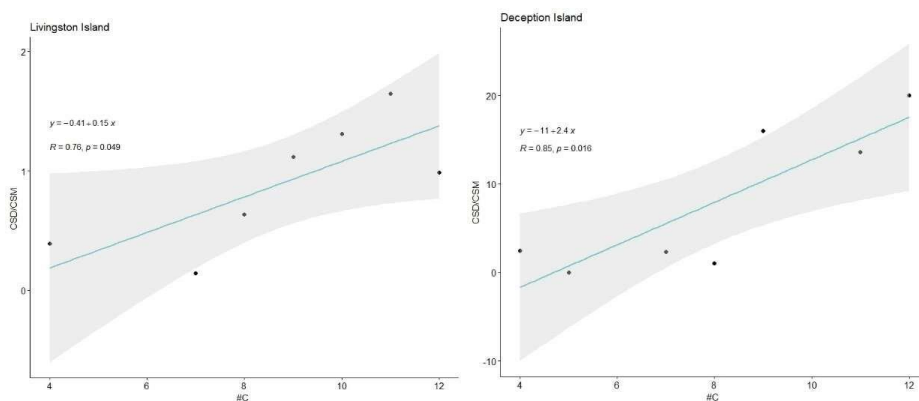


Figure S15. Comparison of average PFCA concentrations in snow deposition (C_{SD}) and snowmelt (C_{SM}). Linear regression by least-squares (with confidence interval at 95%) fitting between the C_{SD}/C_{SM} ratios for individual PFCA versus the number of carbons in the PFCA alkylated chain (#C) in Livingston and in Deception Island.

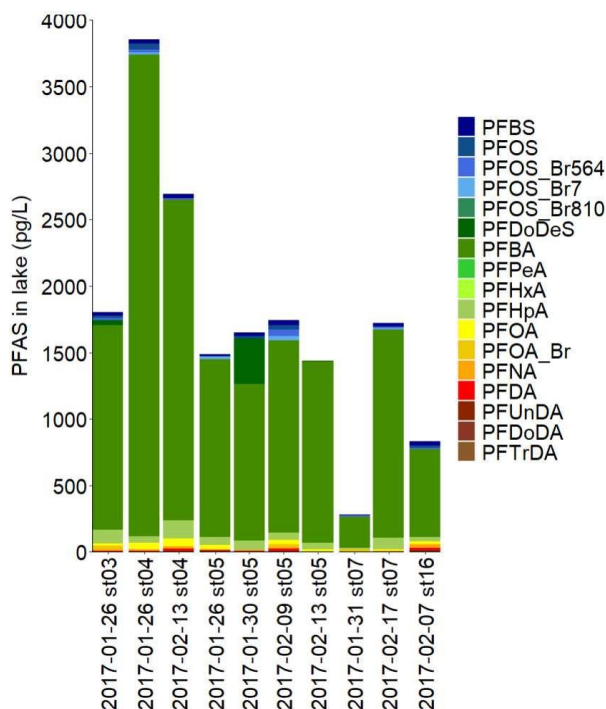


Figure S16. PFAS lake water concentrations in Deception Island.

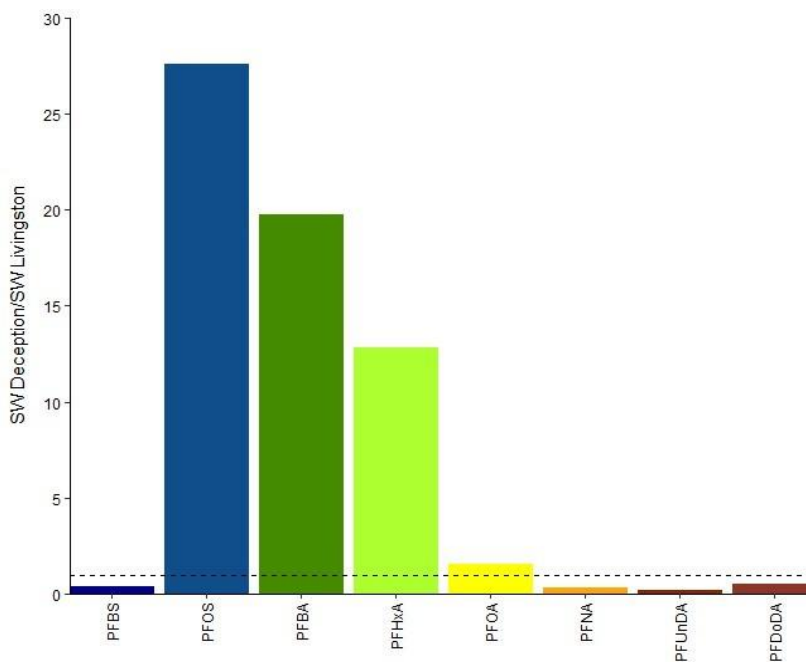


Figure S17. PFAS mean concentrations in SW for Deception Island versus concentrations in SW from Livingston Island. The dashed dotted line marks the number 1.

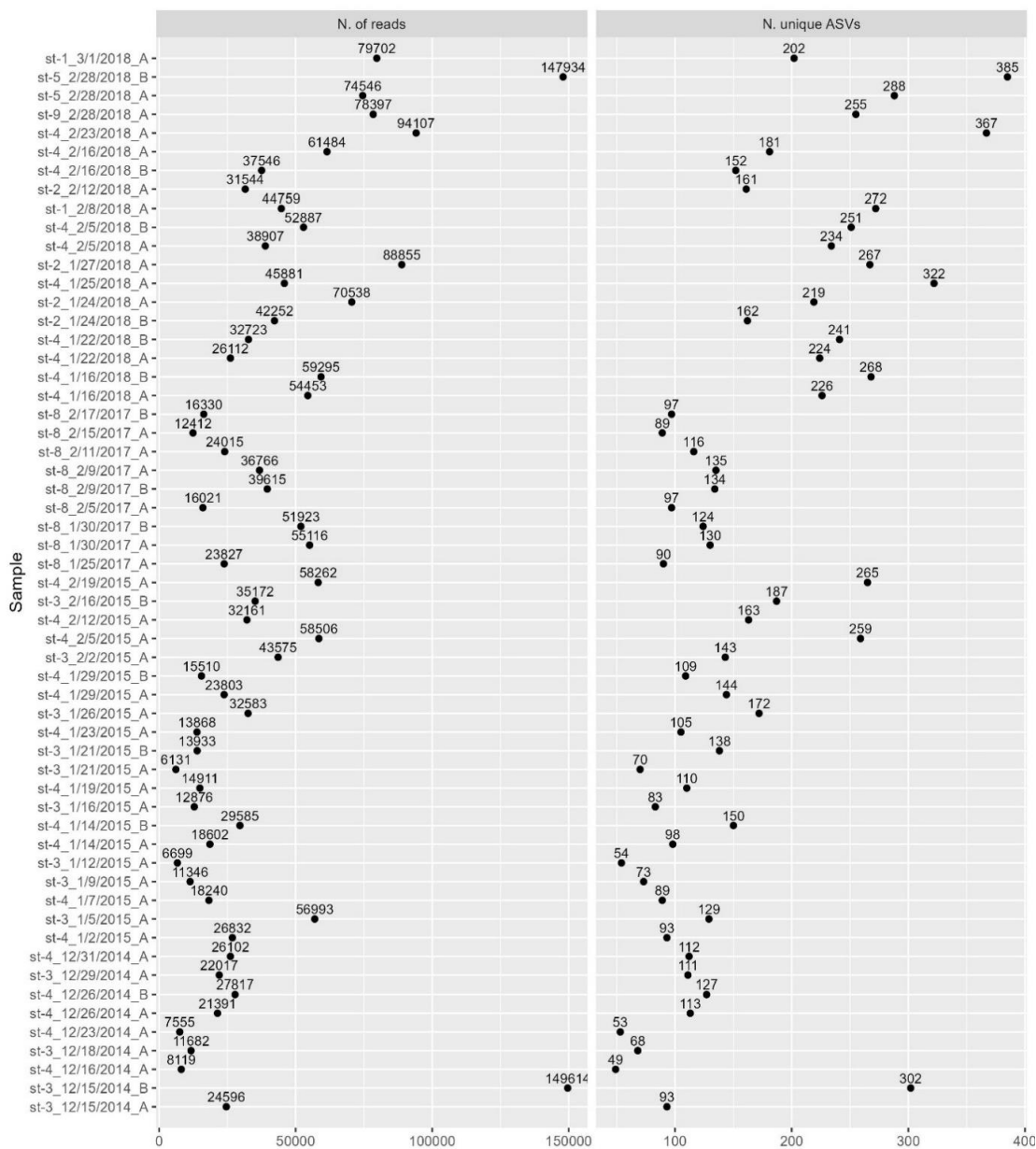


Figure S18. Sequencing of 16S amplicon for bacterial community characterization. Total number of 16S rRNA gene reads per library (left panel), and number of unique ASV per sample (right panel), before normalizing by sequencing depth.

TABLES

Table S1. Sampling stations information.

Station	Island	Location	Sample type
st01	Deception	Gabriel de Castilla research station	rain, snow
st02	Deception	Pinguinera Punta Descubierta	melt
st03	Deception	Crater lake	lake
st04	Deception	Zapatilla lake	lake
st05	Deception	Irizar lake	lake
st06	Deception	Telefon bay	melt
st07	Deception	Soto lake	lake
st08	Deception	Whalers bay	melt, snow
st09	Deception	Colatinas	sw
st10	Deception	Transect point 1	sw
st11	Deception	Transect point 2	sw
st12	Deception	Transect point 3	sw
st13	Deception	Transect point 4	sw
st14	Deception	Fumarole bay	melt, snow
st15	Deception	Baily Head	melt, snow
st16	Deception	Crater 70 lake	lake
st17	Deception	Collins point	melt
st18	Deception	Black glacier	sw
st19	Deception	Mecon point	aerosol,snow
st20	Livingston	Nautica	aerosol, rain, snow
st21	Livingston	Melt river near JCI	melt
st22	Livingston	False bay transect point1	sw
st23	Livingston	False bay transect point2	sw
st24	Livingston	False bay transect point3	sw
st25	Livingston	False bay Hurd Peninsula point1	sw, swd
st26	Livingston	False bay Hurd Peninsula point2	sw
st27	Livingston	False bay Hurd Peninsula point3	sw
st28	Livingston	Jhonsons glacier	sw,swd
st29	Livingston	Hanna point transect point6	sw,swd
st30	Livingston	Hanna point transect point5	sw
st31	Livingston	Hanna point transect point4	sw
st32	Livingston	Hanna point transect point3	sw
st33	Livingston	Hanna point transect point2	sw
st34	Livingston	Hanna point transect point1	sw
st35	Livingston	South bay	sw,swd
st36	Livingston	Emona encorage	sw
st37	Livingston	Mount Reina Sofia	snow
st38	Livingston	Juan Carlos I research station	snow
st39	Livingston	Raquelias Rocks	sw
st40	Livingston	Melt lake near Jhonsons glacier	melt
st41	Livingston	Melt lake near mount Reina Sofia	melt
st42	Livingston	Melt lake near Nautica	melt
st43	Livingston	Melt lake near Nautica	melt

Table S2. Average CTD data from seawater sample stations.

Station	Date	Depth (m)	Island	Temperature (°C)	Conductivity (S/m)	Salinity (PSU)	Fluorescence (RFU)	Turbidity (NTU)
st09	2017-01-25	1.5	Deception	2.55	3.05	34.00	5.03	3.76
st09	2017-01-30	1.5	Deception	2.04	3.00	33.99	0.97	3.66
st09	2017-02-09	1.5	Deception	2.45	3.02	33.74	4.15	3.72
st09	2017-02-10	1.5	Deception	2.68	3.04	33.79	4.27	4.21
st09	2017-02-15	1.5	Deception	2.49	3.02	33.79	2.45	3.66
st09	2017-02-17	1.5	Deception	2.51	3.03	33.90	0.96	3.66
st39	2018-01-18	1.5	Livingston	1.64	2.92	33.37	0.13	12.67
st28	2018-01-19	1.5	Livingston	1.64	2.92	33.37	0.13	12.67
st28	2018-01-22	1.5	Livingston	1.32	2.86	32.97	0.11	12.52
st22	2018-01-23	1.5	Livingston	1.93	2.99	33.93	0.04	3.76
st25	2018-01-23	1.5	Livingston	0.82	2.86	33.54	0.02	7.39
st35	2018-01-24	1.5	Livingston	2.14	3.00	33.91	0.09	3.66
st28	2018-01-25	1.5	Livingston	1.78	2.92	33.24	0.11	8.09
st22	2018-01-26	1.5	Livingston	1.93	2.99	33.97	0.04	3.75
st25	2018-01-26	1.5	Livingston	0.97	2.89	33.67	0.03	7.94
st25	2018-01-26	10	Livingston	1.52	2.95	33.92	0.08	3.59
st25	2018-01-26	20	Livingston	1.19	2.93	33.96	0.05	3.66
st25	2018-01-26	30	Livingston	1.33	2.95	34.04	0.05	3.05
st35	2018-01-27	1.5	Livingston	2.75	3.02	33.41	0.05	6.80
st28	2018-01-29	1.5	Livingston	1.90	2.94	33.42	0.04	8.49
st28	2018-02-06	1.5	Livingston	1.47	2.92	33.53	0.09	8.67
st28	2018-02-06	6	Livingston	1.48	2.93	33.75	0.10	4.17
st28	2018-02-06	13	Livingston	1.45	2.94	33.80	0.07	3.51
st35	2018-02-06	1.5	Livingston	1.47	2.92	33.53	0.09	8.67
st29	2018-02-08	1.5	Livingston	2.32	3.00	33.71	0.11	11.86
st29	2018-02-08	6	Livingston	1.94	2.99	34.00	0.13	5.62
st29	2018-02-08	15	Livingston	1.96	3.00	34.03	0.13	3.75
st29	2018-02-08	30	Livingston	2.03	3.01	34.04	0.14	3.66
st35	2018-02-12	1.5	Livingston	1.70	2.93	33.47	0.19	8.65
st28	2018-02-16	1.5	Livingston	1.75	2.92	33.22	0.31	8.45
st28	2018-02-23	1.5	Livingston	1.77	2.90	33.02	0.19	10.79
st36	2018-02-28	1.5	Livingston	0.96	2.87	33.58	0.12	6.31
st35	2018-02-28	1.5	Livingston	0.96	2.87	33.58	0.12	6.31
st35	2018-02-28	6	Livingston	1.29	2.92	33.72	0.27	5.34
st35	2018-02-28	15	Livingston	1.55	2.95	33.89	0.30	4.34
st35	2018-02-28	30	Livingston	1.18	2.93	34.03	0.12	3.59
st29	2018-03-01	1.5	Livingston	1.73	2.97	33.92	0.15	4.40
st29	2018-03-01	5	Livingston	1.73	2.97	33.97	0.29	3.66
st29	2018-03-01	15	Livingston	1.70	2.98	34.03	0.22	3.05
st29	2018-03-01	30	Livingston	1.42	2.96	34.12	0.16	3.05

Table S3. Target, recovery and internal standards used and precursor and product ion used in the UPLC-MS/MS and the exact mass used in the UHPLC-HRMS.

Compound	Acronym	Precursor ion	Product Ion	Exact mass
Perfluoroalkanesulfonic acids				
PFSA				
Perfluorobutane sulfonic acid	PFBS	299	80	298.943
Perfluoropentane sulfonic acid	PFPeS* ^b			348.939
Perfluorohexane sulfonic acid	PFHxS with Br- PFHxS ^a	399	80	398.936
Perfluorooctane sulfonic acid	PFOS with	499	80	498.930
	Br-PFOS ^a			
	Br 7-PFOS ^a			
	Br 5, 6, 4-PFOS ^a			
	Br 8, 10-PFOS* ^a			
Perfluorononane sulfonic acid	PFNS* ^b			572.120
Perfluorodecane sulfonic acid	PFDS*	599	80	598.924
Perfluorododecane sulfonic acid	PFDoDS*	699	80	698.917
Perfluoroethylcyclohexane sulfonate	PFECHS*	461	381	460.933
Perfluoroalkyl carboxylic acids				
PFCA				
Perfluorobutanoic acid	PFBA	213	169	212.979
Perfluoropentanoic acid	PFPeA	263	219	262.976
Perfluorohexanoic acid	PFHxA	313	269	312.973
Perfluoroheptanoic acid	PFHpA	363	319	362.970
Perfluorooctanoic acid	PFOA with Br-PFOA ^a	413	369	412.966
Perfluorononanoic acid	PFNA	463	419	462.963
Perfluorodecanoic acid	PFDA	513	469	512.960
Perfluoroundecanoic acid	PFUnDA	563	519	562.956
Perfluorododecanoic acid	PFDoDA	613	569	612.954
Perfluorotridecanoic acid	PFTrDA	663	619	662.950
Perfluorotetradecanoic acid	PFTeDA*	713	669	712.947
Perfluorohexadecanoic acid	PFHxDA*	813	769	812.941
Perfluorooctadecanoic acid	PFODA*	913	869	912.934

Recovery standard

Perfluoro-n-[¹³ C ₄]butanoic acid	PFBA ¹³ C ₄	217	172	216.993
Perfluoro-n-[1,2- ¹³ C ₂]hexanoic acid	PFHxA ¹³ C ₂	315	270	314.980
Perfluoro-n-[1,2,3,4- ¹³ C ₄]octanoic acid	PFOA ¹³ C ₄	417	372	416.980
Perfluoro-n-[1,2,3,4,5- ¹³ C ₅]nonanoic acid	PFNA ¹³ C ₅	468	423	467.980
Perfluoro-n-[1,2- ¹³ C ₂]decanoic acid	PFDA ¹³ C ₂	515	470	514.967
Perfluoro-n-[1,2- ¹³ C ₂]undecanoic acid	PFUnDA ¹³ C ₂	570	525	564.964
Perfluoro-n-[1,2- ¹³ C ₂]dodecanoic acid	PFDoDA ¹³ C ₂	615	570	614.960
Sodium perfluoro-1-hexane[¹⁸ O ₂]sulfonate	PFHxS ¹⁸ O ₂	403	84	402.945
Sodium perfluoro-1-[1,2,3,4- ¹³ C ₄]octanesulfonate	PFOS ¹³ C ₄	503	80	502.944

Internal standard

Perfluoro-n-[2,3,4- ¹³ C ₃]butanoic acid	PFBA ¹³ C ₃	216	172	215.989
Perfluoro-n-[¹³ C ₅]pentanoic acid	PFPeA ¹³ C ₅	268	223	
Sodium perfluoro-1-[¹³ C ₈]-octanesulfonate	PFOS ¹³ C ₈	507	80	506.957
Perfluoro-n-[¹³ C ₈]octanoic acid	PFOA ¹³ C ₈	421	376	420.993
Sodium perfluoro-1-[1,2,3- ¹³ C ₃]-hexanesulfonate	PFHxS ¹³ C ₃	402	99	401.947
Perfluoro-n-[1,2,3,4,5,6,7- ¹³ C ₇]undecanoic acid	PFUnDA ¹³ C ₇	570	525	569.980

Those compounds with * were not detected. ^a=only analyzed by UPLC-MS/MS. ^b= only analyzed by UHPLC-HRMS. All standards were supplied by Wellington Laboratories.

Table S4. Levels of PFAAs in the procedural and field blanks.

	Oasis WAX field blanks				Oasis WAX Procedural blanks	
	Water samples from from Livingston Island Island		Water samples Deception			
	Mean (pg)	Sd	Mean (pg)	Sd	Mean (pg)	Sd
PFBA	4.6	1.0	1.5	1.1	3.2	0.8
PFPeA	n.d		n.d		n.d	
PFBS	n.d		0.2		n.d	
PFHxA	n.d		n.d		n.d	
PFHpA	n.d		n.d		0.2	0.1
PFHxS	n.d		n.d		n.d	
PFOA	0.6	0.2	0.3	0.5	0.6	0.3
PFECHS	n.d		n.d		n.d	
PFNA	n.d		n.d		n.d	
PFOS	0.4	0.4	0.1		n.d	
PFDA	n.d		n.d		n.d	
PFUnDA	n.d		n.d		n.d	
PFDS	n.d		n.d		n.d	
PFDoDA	n.d		n.d		n.d	
PFTTrDA	n.d		n.d		n.d	
PFDoDeS	n.d		n.d		n.d	
PFTeDA	n.d		n.d		n.d	
PFHxDA	n.d		n.d		n.d	
PFODA	n.d		n.d		n.d	

Table S5. Mean and standard deviation of the recovery (%) of recovery standards.

	PFBA ¹³ C ₄		PFHxA ¹³ C ₂		PFHxS ¹³ C ₂		PFOA ¹³ C ₄		PFOS ¹³ C ₄		PFNA ¹³ C ₅		PFDA ¹³ C ₂		PFUnDA ¹³ C ₂		PFDoDA ¹³ C ₂	
	mean	sd (%)	mean	sd (%)	mean	sd (%)	mean	sd (%)	mean	sd (%)	mean	sd (%)	mean	sd (%)	mean	sd (%)	mean	sd (%)
UPLC-MS/MS	90		82		78		114		112		95		41		85		57	
UHPLC-HRMS	25		23		23		30		25		28		15		25		18	
	31		79		n.q.		92		53		69		53		38		35	
	19		15		n.q.		22		22		22		29		15		11	

Table S6. Limits of quantification (LOQs) in pg.

	PFBA	PFPeA	PFBS	PFHxA	PFHpA	PFHKS	PFOA	PFCHS	PFNA	PFOS	PFDA	PFUnDA	PFOS	PFDoDA	PFtDA	PFDoDS	PFtGD	PFHMDA	PFODA	PFDA-Br	PFOS Br7	PFOS Br5,6,4	PFOS Br6,10
UPLC-MS/MS	4.8	0.4	0.1	0.9	0.2	0.2	0.4	0.3	0.1	0.1	0.2	0.2	0.1	0.2	0.2	0.3	2.2	3.0	6.7	0.6	0.4	0.3	0.8
UHPLC-HRMS	3.7	0.2	0.3	0.3	0.5	n.q.	1.2	0.1	0.2	0.1	4.1	0.2	0.1	0.1	0.2	0.1	0.2	12.1	4.4	n.q.	n.q.	n.q.	

Table S7. PFAS detection frequency (%) for Livingston and Deception Islands in different sample matrices analyzed in this study.

Sample type	Island	S																					
		PFBA	PFPeA	PFBS	PFHxA	PFHpA	PFOA	PFCHS	PFNA	PFOS	PFDA	PFUnDA	PFOS	PFDoDA	PFtDA	PFDoDS	PFtGD	PFHMDA	PFODA	PFDA-Br	PFOS Br7	PFOS Br5,6,4	PFOS Br6,10
Seawater	Deception	82	0	27	100	0	82	55	27	45	27	9	0	91	0	0	0	0	0	0	0	0	0
Snow	Deception	100	88	100	100	100	100	100	88	38	63	38	13	13	0	25	25	0	0	0	0	0	0
Snowmelt	Deception	100	17	67	0	83	67	83	17	0	33	17	0	0	33	17	17	0	0	0	0	0	0
Lake water	Deception	100	0	90	0	100	80	90	50	90	60	40	0	30	30	40	70	0	0	0	0	0	0
Total mean	Deception	95	26	71	50	71	82	82	58	64	42	26	3	33	16	20	28	0	0	0	0	0	0
Seawater	Livingston	70	93	100	95	95	98	93	60	0	40	28	8	0	0	0	0	0	0	0	0	0	0
Depth seawater	Livingston	50	100	100	100	100	100	100	100	0	14	0	0	0	0	0	0	0	0	0	0	0	0
Snow	Livingston	100	100	100	67	67	100	100	67	33	67	33	0	0	33	0	33	0	33	0	33	0	0
Snowmelt	Livingston	100	0	80	0	60	100	100	80	100	80	80	80	0	40	80	60	0	0	0	0	0	0
Total mean	Livingston	80	73	95	65	80	99	98	77	33	50	35	22	0	18	20	23	0	0	0	0	0	0
Livingston																							
Total	Both	88	50	83	58	76	91	90	67	49	46	31	13	17	17	20	26	0	0	0	0	0	0

Table S8. Concentrations in seawater (pg/L). nd=not detected, nq= not quantified, < loq= lower than LOQ

Station	Date	Depth (m)	Island	PFBA	PFPeA	PFBS	PFHxA	PFHpA	PFOA	PFNA	PFOS	PFUnDA	PFDoDA	PFTrDA
st09	2017-01-25	1.5	Deception	1200	nd	nd	360	nd	36	8.0	37	nd	nd	nd
st09	2017-01-30	1.5	Deception	1500	nd	nd	280	nd	47	13	26	nd	nd	nd
st10	2017-02-05	1.5	Deception	340	nd	nd	300	nd	19	nd	<loq	nd	nd	nd
st11	2017-02-05	1.5	Deception	<loq	nd	nd	220	nd	<loq	nd	<loq	nd	nd	nd
st12	2017-02-05	1.5	Deception	490	nd	nd	290	nd	<loq	nd	nd	nd	nd	nd
st13	2017-02-05	1.5	Deception	620	nd	nd	400	nd	33	nd	<loq	2.0	nd	nd
st09	2017-02-09	1.5	Deception	1200	nd	nd	410	nd	70	17	29	2.5	nd	nd
st09	2017-02-10	1.5	Deception	1600	nd	nd	430	nd	33	nd	<loq	nd	nd	nd
st09	2017-02-15	1.5	Deception	770	nd	11	500	nd	28	2.0	<loq	<loq	nd	nd
st18	2017-02-16	1.5	Deception	1200	nd	19	260	nd	20	2.0	<loq	2.0	nd	nd
st09	2017-02-17	1.5	Deception	<loq	nd	20	400	nd	55	7.0	<loq	nd	3.5	nd
st28	2018-01-16	1.5	Livingston	74	49	36	25	20	49	94	<loq	17	5.7	nd
st28	2018-01-17	1.5	Livingston	<loq	<loq	64	9.4	5.7	13	<loq	<loq	nd	nd	nd
st39	2018-01-18	1.5	Livingston	<loq	14	89	11	7.9	16	30	<loq	5.7		
st28	2018-01-19	1.5	Livingston	89	54	39	30	19	18	17	<loq	10	6.9	nd
st28	2018-01-22	1.5	Livingston	<loq	12	13	10	5.6	10	<loq	<loq	nd	nd	nd
st22	2018-01-23	1.5	Livingston	53	86	14	43	31	30	11	0.9	3.8	3.2	nd
st23	2018-01-23	1.5	Livingston	150	200	74	73	37	31	11	1.7	nd	nd	nd
st24	2018-01-23	1.5	Livingston	66	82	47	37	27	30	10	1.0	nd	nd	nd
st25	2018-01-23	1.5	Livingston	78	82	47	39	45	150	340	1.9	49	15	3.6
st26	2018-01-23	1.5	Livingston	160	360	20	190	99	65	81	0.8	35	12	3.3
st27	2018-01-23	1.5	Livingston	68	80	7.7	40	25	26	25	1.0	24	6.7	2.4
st35	2018-01-24	1.5	Livingston	75	72	91	35	27	33	47	<loq	39	13	nd
st28	2018-01-25	1.5	Livingston	55	55	24	30	22	36	71	<loq	12	nd	nd
st22	2018-01-26	1.5	Livingston	29	37	48	19	13	15	8.5	0.4	3.0	1.3	nd

st23	2018-01-26	1.5	Livingston	49	82	48	37	29	24	13	0.6	5.3	1.9	nd
st24	2018-01-26	1.5	Livingston	69	72	33	31	17	18	8.7	1.4	nd	nd	nd
st25	2018-01-26	1.5	Livingston	22	19	28	19	17	34	8.9	2.3	nd	nd	nd
st25	2018-01-26	10	Livingston	23	20	6.2	11	8.6	12	4.9	0.5	2.1	nd	nd
st25	2018-01-26	20	Livingston	18	12	11	7.4	7.7	11	3.9	0.4	nd	nd	nd
st25	2018-01-26	30	Livingston	<loq	7.6	13	6.9	6.7	12	4.0	0.6	2.5	nd	nd
st26	2018-01-26	1.5	Livingston	32	22	100	12	11	16	5.9	1.0	nd	nd	nd
st27	2018-01-26	1.5	Livingston	<loq	4.5	7.7	5.5	5.8	10	5.0	1.3	3.6	nd	nd
st35	2018-01-27	1.5	Livingston	<loq	30	13	13	8.3	7.7	5.0	<loq	nd	nd	nd
st28	2018-01-29	1.5	Livingston	<loq	<loq	20	<loq	<loq	9.0	11	<loq	4.4	nd	nd
st28	2018-02-06	6	Livingston	38	71	7.1	44	33	26	9.1	1.2	nd	nd	nd
st28	2018-02-06	13	Livingston	<loq	10	5.4	7.9	7.0	12	5.0	1.3	nd	nd	nd
st28	2018-02-06	1.5	Livingston	<loq	<loq	8.9	<loq	<loq	<loq	4.1	<loq	5.8	6.6	nd
st29	2018-02-08	1.5	Livingston	120	200	21	93	46	33	12	<loq	nd	nd	nd
st29	2018-02-08	6	Livingston	26	20	8.0	10	12	15	3.8	1.5	nd	nd	nd
st29	2018-02-08	15	Livingston	<loq	5.4	16	5.4	7.2	13	3.2	1.3	nd	nd	nd
st29	2018-02-08	30	Livingston	<loq	9.4	7.0	7.8	6.0	12	2.4	0.7	nd	nd	nd
st30	2018-02-08	1.5	Livingston	19	7.4	46	8.6	8.0	14	2.8	1.2	nd	nd	nd
st31	2018-02-08	1.5	Livingston	40	46	89	34	31	35	10	1.7	nd	nd	nd
st32	2018-02-08	1.5	Livingston	54	94	90	78	51	42	13	0.9	nd	nd	nd
st33	2018-02-08	1.5	Livingston	20	18	37	15	13	17	6.6	0.9	nd	nd	nd
st34	2018-02-08	1.5	Livingston	36	31	15	14	11	15	6.7	0.8	nd	nd	nd
st35	2018-02-12	1.5	Livingston	<loq	7.8	27	7.8	18	31	11	<loq	nd	nd	nd
st28	2018-02-16	1.5	Livingston	<loq	39	48	25	19	35	21	<loq	5.6	nd	nd

st28	2018-02-23	1.5	Livingston	53	12	130	15	38	67	31	<loq	nd	nd	nd
st34	2018-02-28	1.5	Livingston	20	17	10	9.0	17	26	6.5	0.9	nd	nd	nd
st36	2018-02-28	1.5	Livingston	<loq	8.2	14	6.3	13	16	4.6	<loq	nd	nd	nd
st35	2018-02-28	1.5	Livingston	<loq	2.4	5.5	3.4	12	23	13	1.0	3.0	4.1	nd
st35	2018-02-28	6	Livingston	68	49	5.7	23	12	16	4.2	0.7	nd	nd	nd
st35	2018-02-28	15	Livingston	<loq	5.2	8.0	5.8	13	29	14	1.7	nd	nd	nd
st35	2018-02-28	30	Livingston	<loq	4.4	6.3	4.0	8.4	19	6.7	1.1	nd	nd	nd
st29	2018-03-01	5	Livingston	19	5.1	5.9	4.1	18	23	6.0	1.5	nd	nd	nd
st29	2018-03-01	15	Livingston	<loq	2.8	4.5	3.4	12	14	3.4	0.6	nd	nd	nd
st29	2018-03-01	30	Livingston	23	14	4.3	6.1	12	16	3.8	0.6	nd	nd	nd
st30	2018-03-01	1.5	Livingston	85	120	7.8	53	22	22	7.5	0.7	nd	nd	nd
st31	2018-03-01	1.5	Livingston	<loq	3.9	8.8	3.5	10	15	4.4	0.7	nd	nd	nd
st32	2018-03-01	1.5	Livingston	49	57	12	27	18	21	6.6	0.8	nd	nd	nd
st34	2018-03-01	1.5	Livingston	84	88	5.2	40	14	15	4.9	0.5	nd	nd	nd
st29	2018-03-01	1.5	Livingston	88	88	8.5	26	12	11	<loq	<loq	nd	nd	nd

Table S9. Concentrations in snow (pg/L). nd=not detected, nq= not quantified, < loq= lower than LOQ.

Station	Date	Island	PFBA	PFPeA	PFBS	PFHxA	PFHpA	PFOA	PFNA	PFOS	PFDA	PFUnDA	PFDoDA	PFTrDA	PFDoDes	PFOA_Br	PFOS_Br7	PFOS_Br564	PFOS_Br810
st14	2017-02-03	Deception	280	27	34	30	26	430	34	570	<loq	12	4.2	nd	nd	nq	nq	nq	nq
st15	2017-02-05	Deception	360	42	7.5	31	19	48	10	<loq	<loq	0.9	nd	nd	nd	nq	nq	nq	nq
st19	2017-02-15	Deception	370	27	140	48	19	86	16	9.2	<loq	nd	nd	nd	nd	nq	nq	nq	nq
st08	2017-02-15	Deception	91	6.2	31	8.9	7.9	45	15	25	<loq	7.1	nd	nd	nd	nq	nq	nq	nq
st08	2017-02-14	Deception	140	28	50	25	18	63	13	21	<loq	nd	nd	nd	nd	nq	nq	nq	nq
st01	2017-01-25	Deception	11000	840	1100	660	820	1600	1000	160	1900	nd	nd	nd	16	nd	79	210	nd
st01	2017-02-01	Deception	1600	270	97	29	63	190	170	27	150	64	85	15	nd	nd	37	82	nd
st01	2017-02-14	Deception	5500	nd	220	330	330	450	300	9.0	280	86	62	nd	nd	nd	<loq	<loq	nd
st37	2018-01-13	Livingston	810	35	15	26	<loq	33	13	<loq	<loq	nd	nd	nd	nd	nq	nq	nq	nq
st38	2018-01-13	Livingston	450	51	16	39	24	49	67	4.1	<loq	26	nd	nd	nd	nq	nq	nq	nq
st20	2018-01-12	Livingston	1700	240	38	nd	54	200	37	3.5	29	8.5	8.5	nd	nd	95	<loq	5.0	nd

Table S10. Concentrations in snowmelt (pg/L). nd=not detected, nq= not quantified, < loq= lower than LOQ.

Station	Date	Island	PFBA	PFPeA	PFBS	PFHxA	PFHpA	PFOA	PFNA	PFOS	PFDA	PFUnDA	PFDoDA	PFTrDA	PFDoDes	PFOA_Br	PFOS_Br7	PFOS_Br564	PFOS_Br810
st02	2017-01-24	Deception	150	29000	nd	nd	nd	<loq	nd	nd	nd	nd	nd	nd	nd	nd	nd	nd	nd
st06	2017-01-29	Deception	1500	nd	14	nd	59	<loq	6	10	3.5	<loq	<loq	nd	nd	nd	nd	nd	nd
st08	2017-02-03	Deception	600	nd	15	nd	71	1000	15	2600	8.5	<loq	nd	nd	nd	nd	nd	nd	nd
st14	2017-02-03	Deception	1900	nd	31	nd	95	69	26		17	<loq	<loq	nd	nd	45	nd	nd	nd
st15	2017-02-05	Deception	1100	nd	11	nd	30	80	6.5	680	6.5	<loq	nd	nd	nd	35	nd	nd	nd
st17	2017-02-10	Deception	870	nd	nd	nd	95	88	8.5	35	11	2.5	2.5	nd	nd	nd	23	47	nd
st21	2018-01-02	Livingston	2300	nd	nd	nd	nd	86	12	3	9	<loq	<loq	nd	nd	79	5.5	nd	nd
st40	2018-01-28	Livingston	1000	nd	25	nd	nd	37	15	6	14	8.5	4.0	3.5	nd	nd	18	13	nd
st41	2018-01-28	Livingston	5400	nd	93	nd	380	470	120	nd	64	21	19	5.0	nd	120	nd	nd	nd
st42	2018-02-09	Livingston	2600	nd	19	nd	240	73	18	10	17	11	5.5	2.0	nd	nd	21	53	nd
st43	2018-02-09	Livingston	1400	nd	8.5	nd	200	66	8	2.5	6.5	2.5	6.0	4.0	nd	nd	5.5	8.5	nd

Table S11. Ratio between average concentrations of individual PFCA in snow deposition (C_{SD}) to the average concentration in snowmelt (C_{SM}): C_{SD}/C_{SM} for Livingston and Deception Islands.

Compound	Livingston	Deception
	C_{SD}/C_{SM}	C_{SD}/C_{SM}
PFBA	0.4	2.5
PFPeA		0.01
PFHpA	0.1	2.3
PFOA	0.6	1.1
PFNA	1.1	16
PFDA	1.3	
PFUnDA	1.6	14
PFDoDA	1.0	20

Table S12. Concentrations in lake water (pg/L). nd=not detected, nq= not quantified, < loq= lower than limits of quantification.

Station	Date	Island	PFBA	PFPeA	PFBS	PFHxA	PFHpA	PFOA	PFNA	PFOS	PFDA	PFUnDA	PFDoDA	PFTrDA	PFDoDs	PFOA_Br	PFOS_Br	PFOS_Br7	PFOS_Br564PFOS_Br810
st03	2017-01-26	Deception	1500	nd	25	nd	100	17	11	19	6.5	2.5	nd	nd	36	25	<loq	17	nd
st04	2017-01-26	Deception	3600	nd	38	nd	50	47	11	44	6.0	2.0	nd	nd	nd	nd	17	17	nd
st05	2017-01-26	Deception	1300	nd	16	nd	62	31	7.5	<loq	5.5	3.0	3.5	nd	nd	nd	23	nd	nd
st05	2017-01-30	Deception	1200	nd	29	nd	70	<loq	6.5	13	4.0	nd	2.0	nd	350	nd	nd	nd	nd
st07	2017-01-31	Deception	240	nd	6.0	nd	13	<loq	3.0	<loq	<loq	nd	nd	nd	nd	15	<loq	10	nd
st16	2017-02-07	Deception	660	nd	32	nd	32	19	31	20	18	7.5	2.5	nd	nd	nd	<loq	9.5	nd
st05	2017-02-09	Deception	1400	nd	40	nd	57	31	9.0	32	19	2.5	3.0	nd	nd	23	34	53	nd
st05	2017-02-13	Deception	1400	nd	nd	nd	46	16	nd	<loq	3.0	<loq	nd	nd	8.5	nd	nd	nd	nd
st04	2017-02-13	Deception	2400	nd	32	nd	130	60	16	<loq	20	5.00	nd	nd	nd	nd	<loq	9.5	nd
st07	2017-02-17	Deception	1600	nd	25	nd	85	12	3.0	<loq	3.5	<loq	nd	nd	nd	nd	12	11	nd

References

- Andrews, S., 2020. FastQC: A quality control tool for high throughput sequence data. [WWW Document].
- Bedia, C., Cardoso, P., Dalmau, N., Garreta-Lara, E., Gómez-Canela, C., Gorrochategui, E., Navarro-Reig, M., Ortiz-Villanueva, E., Puig-Castellví, F., Tauler, R., 2018. Applications of Metabolomics Analysis in Environmental Research. *Compr. Anal. Chem.* 82, 533–582.
- Casas, G., Martínez-Varela, A., Roscales, J.L., Vila-Costa, M., Dachs, J., Jiménez, B., 2020. Enrichment of perfluoroalkyl substances in the sea-surface microlayer and sea-spray aerosols in the Southern Ocean. *Environ. Pollut.* 267, 115512.
- Casas, G., Martinez-Varela, A., Vila-Costa, M., Jiménez, B., Dachs, J., 2021. Rain Amplification of Persistent Organic Pollutants. *Environ. Sci. Technol.* 55, 12961–12972.
- D.L. Massart, B.G.M. Vandeginste, S.N. Deming, Y. Michotte, L.K., n.d. *Chemometrics: a textbook*, Elsevier, Data Handling in Science and Technology.
- Ewels, P.A., Peltzer, A., Fillinger, S., Patel, H., Alneberg, J., Wilm, A., Garcia, M.U., Di Tommaso, P., Nahnsen, S., 2020. The nf-core framework for community-curated bioinformatics pipelines. *Nat. Biotechnol.* 2020 383 38, 276–278.
- Gasol, J.M., Morán, X.A.G., 2015. Flow Cytometric Determination of Microbial Abundances and Its Use to Obtain Indices of Community Structure and Relative Activity 159–187.
- González-Gaya, B., Dachs, J., Roscales, J.L., Caballero, G., Jiménez, B., 2014. Perfluoroalkylated substances in the global tropical and subtropical surface oceans. *Environ. Sci. Technol.* 48, 13076–13084.
- Parada, A.E., Needham, D.M., Fuhrman, J.A., 2016. Every base matters: Assessing small subunit rRNA primers for marine microbiomes with mock communities, time series and global field samples. *Environ. Microbiol.* 18, 1403–1414.
- Straub, D., Blackwell, N., Langerica-Fuentes, A., Peltzer, A., Nahnsen, S., Kleindienst, S., 2020. Interpretations of Environmental Microbial Community Studies Are Biased by the Selected 16S rRNA (Gene) Amplicon Sequencing Pipeline. *Front. Microbiol.* 11, 2652.





CHAPTER 5

Assessment of OPE Biodegradation Across the Atlantic and Southern Oceans

5.1 Publication III: Bacterial Production Modulates the Persistence of Organophosphate Ester Flame Retardants and Plasticizers in the Ocean





5.1 PUBLICATION III

Bacterial Production Modulates the Persistence of Organophosphate Ester Flame Retardants and Plasticizers in the Ocean

Jon Iriarte
Núria Trilla-Prieto
Naiara Berrojalbiz
Maria Vila-Costa
Jordi Dachs

Environmental Science & Technology Letters.
2025, 12(2), 158-165.
<https://doi.org/10.1021/acs.estlett.4c01128>

Bacterial Production Modulates the Persistence of Organophosphate Ester Flame Retardants and Plasticizers in the Ocean

Jon Iriarte, Núria Trilla-Prieto, Naiara Berrojalbiz, Maria Vila-Costa,* and Jordi Dachs



Cite This: *Environ. Sci. Technol. Lett.* 2025, 12, 158–165



Read Online

ACCESS |

Metrics & More

Article Recommendations

Supporting Information

ABSTRACT: Understanding the biodegradation of organic pollutants is crucial for assessing the persistence and fate of these contaminants and improve their risk assessment, eventually drawing policy. The occurrence of organophosphate ester (OPE) flame retardants and plasticizers has been widely reported in the marine environment. However, few studies have assessed the potential of marine microorganisms to degrade them, particularly under oceanic conditions. Here, we report the results of six degradation experiments where in situ bacterial communities were challenged with environmentally relevant concentrations of OPEs in the Atlantic and Southern Oceans. Hydrophobic aryl-OPEs significantly decreased by 60% and 25% in the Atlantic and Southern Oceans, respectively. In Atlantic waters, up to 40% of OPE depletion was due to sorption to cells and close to 20% to biodegradation. The cold temperatures of the Southern Ocean resulted in a slower, nondetectable biodegradation, further confirmed by bacterial production results. Bacterial composition exposed to OPEs also showed a larger degree of changes in the Atlantic than in the Southern Ocean. Significant negative correlations were found between the fold changes in bacterial production and the decreases in OPE concentrations, suggesting that bacterial carbon demand is directly related to OPE biodegradation in the oceans.

KEYWORDS: organophosphate esters (OPEs), plasticizers, bacterial production, biodegradation, Atlantic Ocean, Southern Ocean

INTRODUCTION

Persistence is thought to be an extremely important property in the risk assessment and prioritization of contaminants.¹ However, degradation tests in idealized conditions do not reflect the real persistence of synthetic chemicals in the environment.^{2–4} At the global scale, the degradation of organic pollutants in the vast ocean is of great importance, even though field experiments in the open ocean have barely been performed before,^{5,6} and generally for legacy persistent organic pollutants or hydrocarbons.^{7–10}

Organophosphate esters (OPEs) are widely used as flame retardants and plasticizers in a myriad of products.^{11,12} OPEs are global pollutants and ubiquitous in all environments, also in the marine environment.^{13,14} Their widespread environmental occurrence has raised concerns, with toxicity studies indicating threats to human health and ecosystems.^{15–20} Despite the importance of biodegradation in determining the fate of organic pollutants, studies on OPE degradation by bacteria remain limited, primarily focusing on soils, sediments, and wastewater treatment plants.^{21–23} The interactions of OPEs and marine microbial communities, which are essential to food webs and biogeochemical cycles, remain largely unknown.¹³ OPEs, as phosphorus-containing compounds, may introduce a significant anthropogenic source of dissolved organic phosphorus (DOP) to marine ecosystems,^{24,25} potentially disrupting phosphorus and carbon biogeochemical cycles. In large nutrient-poor ocean regions, where P is often limited, marine microorganisms rely on alternative sources like DOP to meet their P demands.^{26–28} Marine bacteria might utilize OPEs under phosphorus-limited conditions as reported in coastal Mediterranean waters.²⁹ Several marine isolates show OPE degradation capacity,³⁰ with unknown environmental relevance. However, the biodegradation of OPEs in open oceans is unknown. Factors affecting biodegradation include compound properties (e.g., concentration, structure, bioavailability), microbial community traits (e.g., presence of degrading genes, metabolic flexibility), and environmental variables (e.g., temperature, pH, nutrient levels).^{31–33} For synthetic compounds like OPEs, degradation is particularly challenging

phorus (DOP) to marine ecosystems,^{24,25} potentially disrupting phosphorus and carbon biogeochemical cycles. In large nutrient-poor ocean regions, where P is often limited, marine microorganisms rely on alternative sources like DOP to meet their P demands.^{26–28} Marine bacteria might utilize OPEs under phosphorus-limited conditions as reported in coastal Mediterranean waters.²⁹ Several marine isolates show OPE degradation capacity,³⁰ with unknown environmental relevance. However, the biodegradation of OPEs in open oceans is unknown. Factors affecting biodegradation include compound properties (e.g., concentration, structure, bioavailability), microbial community traits (e.g., presence of degrading genes, metabolic flexibility), and environmental variables (e.g., temperature, pH, nutrient levels).^{31–33} For synthetic compounds like OPEs, degradation is particularly challenging

Received: December 20, 2024

Revised: January 14, 2025

Accepted: January 14, 2025

Published: January 17, 2025



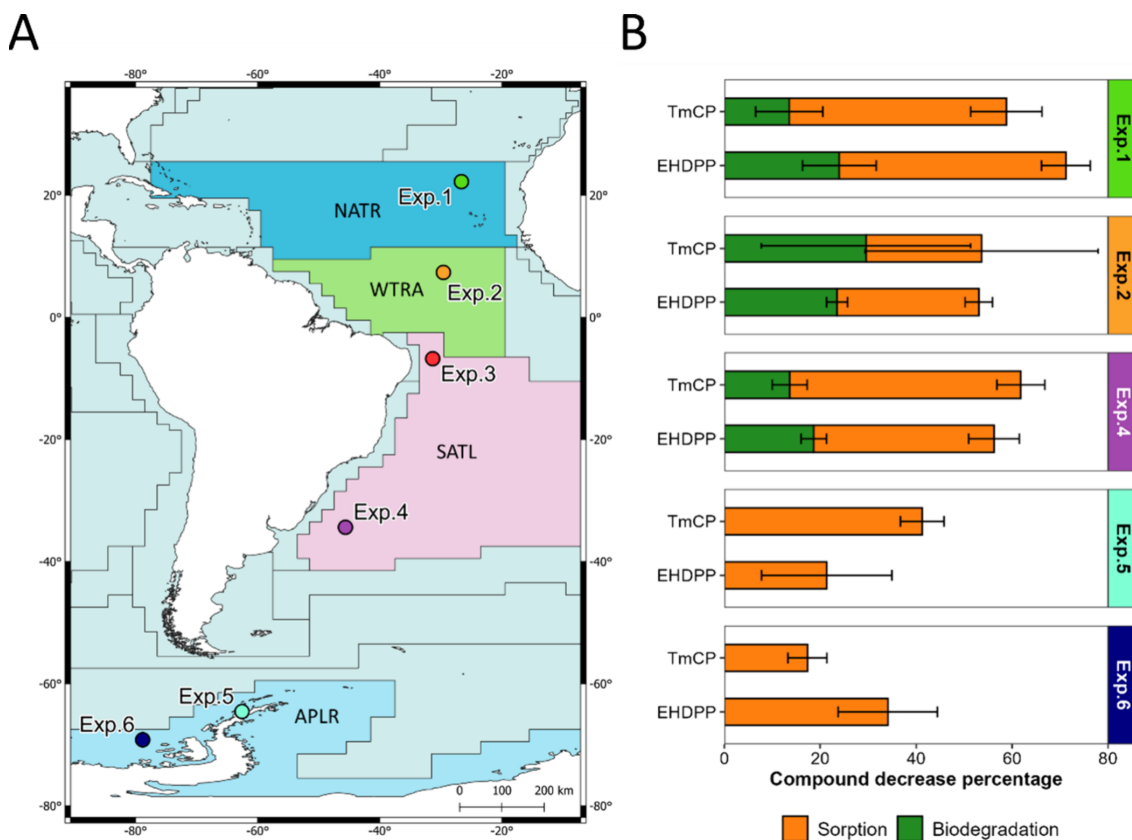


Figure 1. (A) Water sampling locations for each experiment done during AN TOM oceanographic campaigns. Longhurst biogeochemical provinces corresponding to each location are colored on the map: North Atlantic Tropical Gyral Province (NATR), Western Tropical Atlantic Province (WTRA), South Atlantic Gyral Province (SATL), and Austral Polar Province (APLR). Made with QGIS v.3.20. (B) OPEs compound decrease percentage due to sorption to cells and biodegradation, calculated using the 0.2-filtered control concentrations as baseline measurements. Results of experiment 3 could not be included due to limitations in the field experiment.

due to their lack of resemblance to natural biogenic molecules, making their role in marine phosphorus cycling uncertain.

This study aimed to assess the potential role of biodegradation of OPEs in the marine environment and to gain insight into bacteria-OPE interactions. This is the first time that microbial responses and degradation of OPEs are assessed *in situ*, under oceanic conditions.

METHODS AND MATERIALS

Six degradation experiments were performed, in which concentrations were quantified concurrently with the physiological response and changes in the taxonomic composition of the prokaryotic communities exposed to OPEs. These experiments were performed *in situ* during two oceanographic campaigns. The first, AN TOM-1, was a latitudinal (38°N–47°S) transect across the Atlantic Ocean (from Vigo, Spain, to Punta Arenas, Chile) onboard the research vessel Sarmiento de Gamboa, carried out between December 15, 2020 and January 15, 2021 (Figure 1A). The second, AN TOM-2, took place in the Southern Ocean onboard RV Hespérides, between January 22 and February 8, 2022. Coastal (Bransfield and Gerlache Straits) and offshore waters were sampled between the South Shetland Islands (62°S) and the Bellingshausen Sea (71°S)

(Figure 1A). The water column depth ranged from 4827 to 5382 m in the Atlantic Ocean, and around 250 m in the Antarctic continental shelf.

Seawater samples were taken 5 m below the surface at six locations (Figure 1A) using a rosette sampler coupled to a Conductivity, Temperature, and Depth (CTD) sensor (12 L Niskin bottles, Sea-Bird Scientific). Several physicochemical properties were measured at each sampling location: water temperature, salinity, turbidity, dissolved oxygen, total chlorophyll, bacterial abundance, heterotrophic bacterial production, and photosynthetically active radiation (PAR) (Table S1, Annex S1). Concurrent OPE concentrations in subsurface water from the Atlantic and Southern oceans were used as a proxy for field surface OPE concentrations.³⁴

Exposure experiments were performed with CTD-collected seawater filtered through a 200 μ m nylon mesh, and subsequently filtered through 3 μ m pore-size polycarbonate (PC) membrane filters (Isopore, Millipore) using a peristaltic pump at 40 rpm, to exclude grazers and particle-associated bacteria, thereby reducing variability. Exposure experiments comprised a 48-h incubation (T48) with OPE amendments at *in situ* temperature-controlled conditions in the dark ran in duplicate (Annex S2, Figure S1). Initial time point was

sampled after 30 min of OPE spike (T0). Sorption controls (SC hereafter) were prepared by inactivating cells through heating at 70 °C for 10 min.³⁵ and were used to assess OPE partitioning between dead cells and seawater, or losses during final filtration, which can deplete the dissolved phase concentration.³⁶ Controls to assess for OPEs losses due to abiotic factors (e.g., sorption to bottle walls, volatilization, and hydrolysis) were prepared by filtering the seawater through 0.2- μm polytetrafluoroethylene (PTFE) filters. All conditions were spiked with 100 μL of a 4 ng μL^{-1} OPE mix in acetone (TnBP, EHDPP, TCEP, TCPP, TPhP, and TmCP; Table S2), into precombusted (450 °C, 4 h) 2 L glass bottles, allowing acetone to evaporate for 30 min before adding seawater. These compounds were selected to cover a wide range of physicochemical properties, comprising halogenated-, aryl-, and alkyl-OPEs (Table S3), and are commonly found in seawater.¹⁴ The targeted nominal concentration was 200 ng L^{-1} (per compound).

After incubation, aliquots of seawater were taken from the biotic bottles for flow cytometric determination of prokaryotic cell abundance and membrane compromised cell abundance (NADS), and heterotrophic bacterial production. Biomass for 16S rRNA gene sequencing was collected by filtering the remaining volume onto 0.2 μm pore-size PTFE filters, while the filtrate was preconcentrated using a solid phase extraction (SPE) system for the determination of OPE concentrations (Annex S3).

Sorption controls were analyzed to determine cell viability by NADS, which confirmed that most of the cells were not viable (average nonviable cells >95%, Figure S2). Then, they were filtered and SPE extracted. 0.2-filtered control bottles were directly preconcentrated on SPE and analyzed for the determination of OPEs.

A nutrient limitation experiment was performed in parallel to each OPE incubation to assess the nutrient limitation regimes at each site. Briefly, previously baked (450 °C, 4 h) 100 mL glass bottles were filled with 3 μm prefiltered seawater to exclude grazers and particle-associated bacteria. Five different amendments were designed to cover different nutrient limitation regimes and the potential role of OPE compounds as carbon or phosphorus sources: controls (Ctrl.), nitrogen and phosphorus (N+Pi), phosphorus + carbon (Pi+C), nitrogen + carbon (N+C), and OPE + nitrogen (OPEs+N) (Figure S3). Glucose (10 μM final concentration), inorganic phosphate (0.25 μM final concentration), and ammonium (2 μM final concentration) were used as carbon, phosphorus, and nitrogen sources, respectively. OPEs were added to a final nominal concentration of 2000 ng L^{-1} to the bottles following the same spiking strategy reported above. This elevated concentration was intended to simulate a comparable P molar concentration to that of the inorganic phosphate treatment. Bottles were incubated in duplicate at the same conditions described previously for 24 h. Samples to quantify bacterial production and prokaryotic cell abundance were taken at the end of the incubation.

Procedures for the determination of bacterial abundance, NADS, bacterial production, and OPE concentrations have been reported before and are described in Supporting Information as well as the detailed QA-QC, and the statistical analyses (Annex S1, S3, and S4).

RESULTS AND DISCUSSION

Environmental Conditions Differentiate Sampling

Locations. Four different Longhurst biogeochemical provinces were covered by the six experiments performed, which included North Atlantic Tropical and the South Atlantic Gyres, the South Subtropical Convergence zone, and polar waters (Figure 1A). Whether the biogeochemical provinces were under different nutrient limitation regimes was tested by measuring bacterial heterotrophic production after nutrient additions in 24 h incubations. Results suggest that Exp.1 was colimited by N and Pi, Exp.2 was mainly limited by C, Exp.3 had no limitation, and Exp.4 was mainly limited by N with minor limitation by Pi. These results are in agreement with results from Browning and Moore (2023) showing primary limitation by N with co/serial limitation by P in the northern hemisphere subtropical waters.²⁷ In experiments 5 and 6 from the Southern Ocean none of the nutrient amendments triggered bacterial activity or growth. Previous studies have noted that in cold temperature conditions, the bacterial response time to nutrient amendments is prolonged compared to that in temperate waters.³⁷ The results are also consistent with observations of the Southern Ocean being generally not limited for N or P.

Dissimilarity between sampling locations was assessed by PCA of the environmental variables. Almost 70% of the total variance was explained by the first two principal components (48.8% PC1, 20.5% PC2). PC1 mainly separated the Atlantic and Southern Oceans, with temperature, turbidity, salinity, dissolved oxygen, bacterial abundance, and total chlorophyll strongly correlated with PC1 (Figure S4). The water temperature in the Atlantic Ocean ranged between 23.6 and 27.5 °C, while in Antarctica it was near 0 °C. Bacterial abundance (7.2×10^5 vs 2.3×10^5 cell mL^{-1}), salinity (36.4 vs 33.8 PSU), and turbidity (0.21 vs 0.17 NTU) were also higher in the Atlantic Ocean. On the other side, dissolved oxygen (6.5 vs 10.7 mg L^{-1}) and total chlorophyll α (0.1 vs 0.9 μg L^{-1}) were higher in the Southern Ocean (Table S1). In agreement with this, an NMDS analysis performed with the initial bacterial community compositions also separated the Atlantic and Southern Oceans. Both were dominated by *Cyanobacteriota*, but to different extents ($25.0 \pm 3.8\%$ and $38 \pm 6.5\%$, respectively, Figure S5). After them, *Alphaproteobacteria pelagibacterales* ($23.0 \pm 5.2\%$), *Gammaproteobacteria enterobacterales* ($8.7 \pm 5.7\%$), other *Alphaproteobacteria* ($8.0 \pm 1.7\%$), and *Gammaproteobacteria SAR86* ($6.5 \pm 1.8\%$) were the most abundant in the Atlantic Ocean; whereas *Gammaproteobacteria pseudomonadales* ($18.4 \pm 12.2\%$), *Alphaproteobacteria pelagibacterales* ($14.5 \pm 4.9\%$), *Alphaproteobacteria rhodobacterales* ($11.2 \pm 7.8\%$), and *Bacteroidota flavobacteriales* (9.5 ± 1.9) appeared in the Southern Ocean. Environmental factors such as temperature have been previously described as main drivers modulating microbial populations.^{38,39}

PC2 was mainly correlated with individual OPE concentrations at the sampling sites, based on published subsurface water OPE concentrations data from the Atlantic and Southern Oceans.³⁴ The OPE concentrations of the 6 compounds ranged from 6.8 ng L^{-1} at Exp.2 location to 26.2 at Exp.3 location in the Atlantic Ocean, and from 9.2 ng L^{-1} at Exp.5 location to 32.7 at Exp.6 location in the Southern Ocean. The mean \sum_{24} OPE concentrations were 12.7 ± 7.5 ng L^{-1} for the Atlantic Ocean, and 17.1 ± 9.1 ng L^{-1} for the Southern

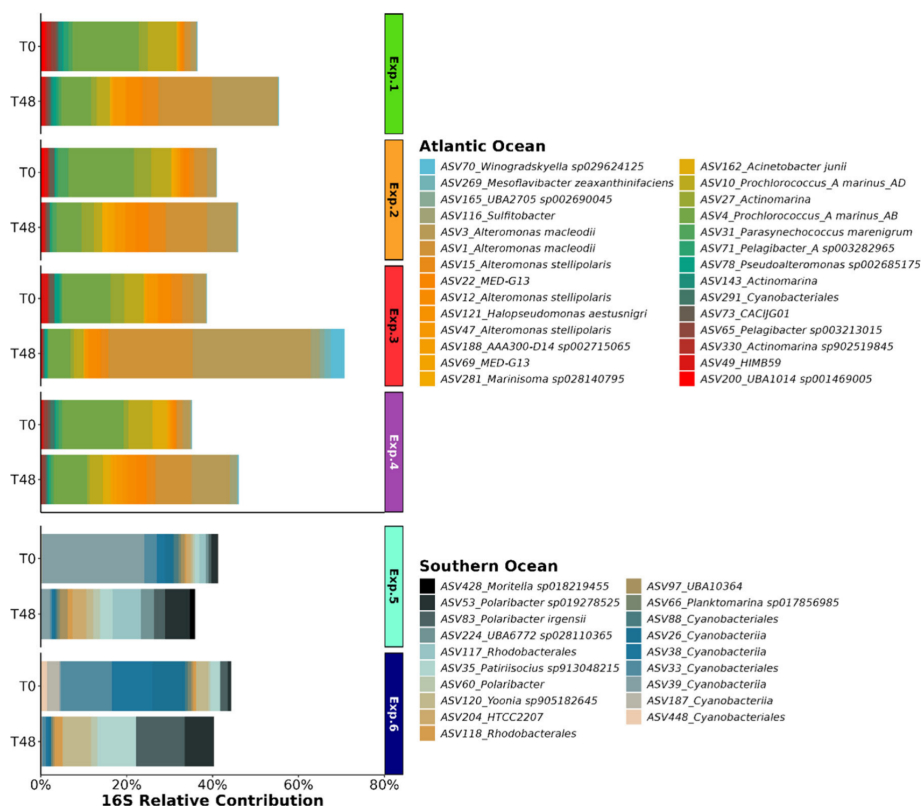


Figure 2. Barplot of the relative abundance of the 28 and 19 ASVs with the greatest fold change for the Atlantic and Southern Oceans, respectively. ASVs from the Atlantic Ocean experiments are at the top, while those from Southern Ocean experiments are at the bottom. Individual experiments and incubation times (T0, initial time viable bacteria treatment; T48, 48-h incubation viable bacteria treatment) are shown.

Ocean.³⁴ The exposure \sum_6 OPE concentrations ranged from 902 ng L⁻¹ to 1139 ng L⁻¹, which are below nominal concentration due to abiotic factors. These concentrations are higher than those in offshore marine environments.⁴⁰ However, it is still within the range of OPE concentrations found in coastal waters close to urban areas,¹³ and lower than in the Atlantic Ocean under the influence of the Amazon River plume.⁴¹

Decrease of the Most Hydrophobic OPEs. The comparison of the OPE concentrations in the 48h biotic incubation with the 0.2-filtered and sorption controls showed a significant decrease of TmCP and EHDPP in most of the experiments, while no clear trend was observed for the other OPEs (Figure S6, Table S4). Interestingly, these compounds were the most hydrophobic OPEs of the mixture, with $\log K_{OW} > 5$ (octanol–water partition coefficient). This decrease could be due to sorption to microbial cells, or to biodegradation.³⁶ The experiments conducted in the Atlantic Ocean revealed that the 48h biotic incubation ratios, when compared to 0.2-filtered or sorption controls (Figures S7 and S8), were below 1 for TmCP (ranging from 0.38 to 0.46, and 0.61 to 0.75, respectively) and EHDPP (ranging from 0.29 to 0.47, and 0.54 to 0.70, respectively), indicating the occurrence of both cell partitioning and biodegradation. Conversely, in the Southern Ocean experiments, the biotic incubation to sorption controls ratios were around 1 (ranging from 1.08 to 1.34 considering

both TmCP and EHDPP), implying that the observed decrease was due to cell partitioning, not biodegradation. The 48-h incubation period was likely insufficient to capture the degradation of other OPEs.

The experiments conducted in the Atlantic Ocean revealed that out of a 60% total decrease (with respect to 0.2-filtered concentrations) in TmCP and EHDPP concentrations, roughly 40% was attributed to sorption to cells, while the remaining 20% was potentially due to biodegradation (Figure 1B and Figure S9). The overall assessment of biodegradation in relation to $\log K_{OW}$ showed a step change for compounds with $\log K_{OW} > 5$ (Figure S9). Additional studies are necessary to determine whether increased hydrophobicity correlates with a potential underlying trend in enhanced biodegradation. In the Southern Ocean, sorption accounted for a 25–30% of TmCP and EHDPP decrease (Figure 1B and Figure S10). TmCP and EHDPP losses due to other abiotic factors were found to be minimal (Table S5). The occurrence of sorption to cells is consistent with the significant negative correlation between the concentration ratios in sorption and 0.2-filtered controls and $\log K_{OW}$ (Figure S11).

Changes in Bacterial Community Composition. Alpha diversity analyses revealed a significant reduction in Chao1 and Shannon diversity indexes (Wilcoxon, $p = 6 \times 10^{-4}$ and $p = 3 \times 10^{-4}$, respectively) for the Atlantic Ocean experiments following 48h incubations, whereas Southern Ocean experi-

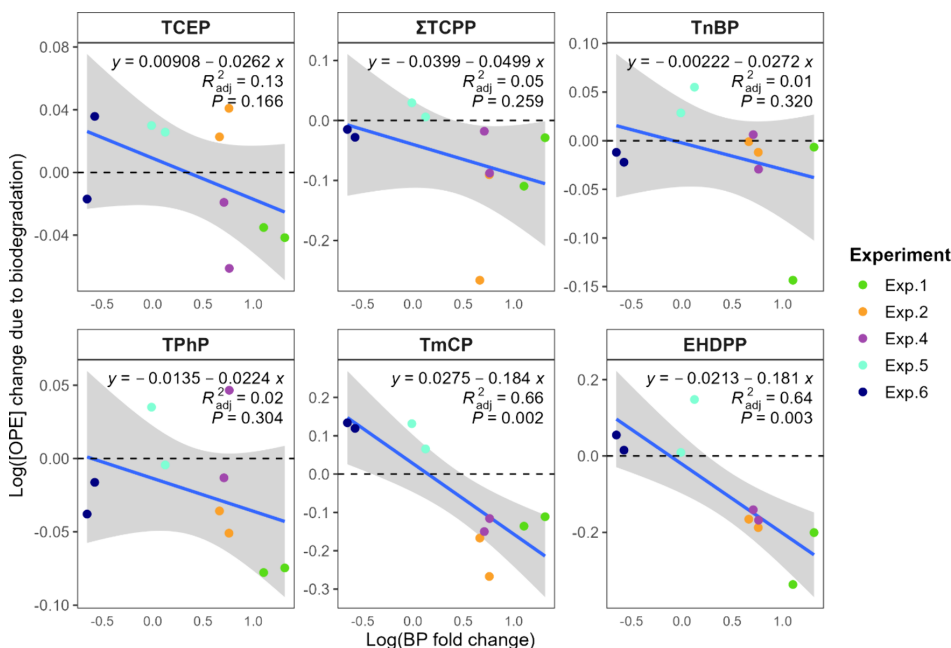


Figure 3. Scatter plots showing the relationship between changes in OPE concentrations due to biodegradation and changes in bacterial production (BP) levels after incubation (see Annex S4). The dashed line represents a log(1) ratio of 0. Adjusted R^2 and p values were calculated using Pearson correlation. Equations were derived from linear model fits to the data points.

ments showed no clear trend (Figures S12–S14). A NMDS analysis performed per ocean further confirmed a shift in bacterial communities over time (Figure S15), consistent with changes observed in the relative abundance of the main taxonomic groups (Figure S5). To identify the specific amplicon sequence variants (ASVs) driving these changes, the fold change in the relative abundances of individual ASVs was calculated, and the most relevant ASVs were selected (Annex S4). Up to 28 and 19 ASVs were selected for the Atlantic and Southern Ocean, respectively (Tables S5 and S6). In the Atlantic Ocean experiments, ASV1 and ASV3, both classified as *Alteromonas macleodii*, increased their abundance in all the experiments (Figure S16), while initially abundant ASVs annotated as *Prochlorococcus* decreased. This was further confirmed by their T48 relative abundances (Figure 2), where *A. macleodii* increased from 4 to 27% of the bacterial community, while *Prochlorococcus* decreased from 19 to 9%. *Alteromonas macleodii* is a potential OPE degrader that has already been shown to be important for organic matter cycling due to their fast response, metabolic versatility, and resistance.^{30,42,43}

In the Southern Ocean experiments, the decrease of cyanobacterial ASVs was followed by an increase of taxa classified in the *Enterobacteriales*, *Flavobacteriales*, and *Rhodobacteriales* orders, and generally associated with cold environments (Figure 2, Figure S17, and Table S6): *Moritella* sp., *Polaribacter* sp., *Polaribacter irgensii*, and *Yoonia* sp. Interestingly, these taxa have been reported as hydrocarbonoclastic bacteria in polar coastal waters.^{44–46} It could be possible that both the aromatic moiety and their sorption to particles facilitates aryl-OPEs biodegradation. The experimental setup

likely promoted heterotrophic bacterial growth while diminishing the primary producers' abundance.

Can Bacterial Metabolism Explain OPE Degradation?

Bacterial production, measured as Leucine Incorporation Rates (LIRs), increased in the Atlantic Ocean incubations. In contrast, no increase was observed in the Southern Ocean experiments (Figure S18). Bacterial abundances increased, including Antarctic waters, mostly thanks to the proliferation of high nucleic acid-containing prokaryotes (Figure S19B, and C), consistent with the proliferation of heterotrophic versatile fast-growing bacteria previously discussed, which usually have large genomes.^{43,47,48}

Significant negative correlations between the LIR fold change and the changes in TmCP and EHDPP concentrations due to biodegradation were found (Figure 3). Although the results for the other compounds were not statistically significant, a similar negative trend was observed. These findings suggest that the rates of OPE biodegradation increase when heterotrophic bacteria exhibit enhanced protein production activity. This could imply that OPEs were being used as a source of C or P. To investigate this hypothesis, OPEs were added as a nutrient together with N in the nutrient limitation experiment. Only experiment at station 1, showed an increase in bacterial production compared to the control treatment (Figure S3); however, it remained unclear whether OPEs served as a source of P, C, or if the response was solely attributable to N addition.

The results reported here show biodegradation of the more hydrophobic OPEs (containing aromatic moieties) in the Atlantic Ocean, consistent with previous works reporting preferential degradation of aryl-OPEs in comparison to alkyl- and halogenated-OPEs.^{49,50} Similarly, experiments performed

with coastal Mediterranean seawater reported a significant decrease of TmCP and EHDP. ²⁹ Longer incubation periods could have resulted in the observation of biodegradation for additional compounds, but this approach would have also led to a more pronounced shift in bacterial community composition, thereby making the results less representative of natural bacterial communities.

Further research is needed to assess if OPEs can serve as a P or C source, the relevance for marine biogeochemical cycles, and the persistence of OPEs. This work also shows that on-site experiments for biodegradation provide important information and are feasible, opening new ground for evaluating the persistence of organic contaminants in the ocean.

■ ASSOCIATED CONTENT

Supporting Information

The Supporting Information is available free of charge at <https://pubs.acs.org/doi/10.1021/acs.estlett.4c01128>.

Additional text on analytical methods, experimental setup, and statistical analyses, additional tables with ancillary data, details on OPE compounds, and ASV fold change values, and additional figures showing the experimental setup, OPE concentrations, changes in bacterial community, and bacterial production and bacterial abundance results (PDF)

■ AUTHOR INFORMATION

Corresponding Author

Maria Vila-Costa – Department of Environmental Chemistry, Institute of Environmental Assessment and Water Research (IDAEA-CSIC), 08034 Barcelona, Catalunya, Spain; maria.vila@idaea.csic.es; orcid.org/0000-0003-1730-8418; Email: maria.vila@idaea.csic.es

Authors

Jon Iriarte – Department of Environmental Chemistry, Institute of Environmental Assessment and Water Research (IDAEA-CSIC), 08034 Barcelona, Catalunya, Spain; Doctoral Program in Analytical Chemistry and the Environment, Department of Chemical Engineering and Analytical Chemistry, Faculty of Chemistry, Universitat de Barcelona, 08034 Barcelona, Catalunya, Spain; orcid.org/0000-0003-2315-1920

Núria Trilla-Prieto – Department of Environmental Chemistry, Institute of Environmental Assessment and Water Research (IDAEA-CSIC), 08034 Barcelona, Catalunya, Spain; Departament of Ecology, Faculty of Earth Sciences, Universitat de Barcelona, 08034 Barcelona, Catalunya, Spain; orcid.org/0000-0001-6973-9514

Naiara Berrojalbiz – Department of Environmental Chemistry, Institute of Environmental Assessment and Water Research (IDAEA-CSIC), 08034 Barcelona, Catalunya, Spain

Jordi Dachs – Department of Environmental Chemistry, Institute of Environmental Assessment and Water Research (IDAEA-CSIC), 08034 Barcelona, Catalunya, Spain; orcid.org/0000-0002-4237-169X

Complete contact information is available at: <https://pubs.acs.org/doi/10.1021/acs.estlett.4c01128>

Notes

The authors declare no competing financial interest.

■ ACKNOWLEDGMENTS

We thank the staff of the Marine Technology Unit (UTM-CSIC) and the crew of the research ships Sarmiento de Gamboa and Hespérides for their logistical support during the sampling campaigns. J.I. acknowledges the predoctoral FPU fellowship (FPU19/02782) funded by the Spanish Ministry of Science. This work was supported by the Spanish Research Agency through projects AN TOM (PGC2018-096612-B-I00), PANTOC (PID2021-127769NB-I00), and MIQAS (PID2021-128084OB-I00). The research group of Global Change and Genomic Biogeochemistry receives support from the Catalan Government (2021-SGR-00448).

■ REFERENCES

- (1) Cousins, I. T.; Ng, C. A.; Wang, Z.; Scheringer, M. Why Is High Persistence Alone a Major Cause of Concern? *Environ. Sci. Process Impacts* **2019**, *21* (5), 781–792.
- (2) Martin, T. J.; Snape, J. R.; Bartram, A.; Robson, A.; Acharya, K.; Davenport, R. J. Environmentally Relevant Inoculum Concentrations Improve the Reliability of Persistent Assessments in Biodegradation Screening Tests. *Environ. Sci. Technol.* **2017**, *51* (5), 3065–3073.
- (3) Kowalczyk, A.; Martin, T. J.; Price, O. R.; Snape, J. R.; van Egmond, R. A.; Finnegan, C. J.; Schäfer, H.; Davenport, R. J.; Bending, G. D. Refinement of Biodegradation Tests Methodologies and the Proposed Utility of New Microbial Ecology Techniques. *Ecotoxicol. Environ. Saf.* **2015**, *111*, 9–22.
- (4) Poursat, B. A. J.; van Spanning, R. J. M.; de Voogt, P.; Parsons, J. R. Implications of Microbial Adaptation for the Assessment of Environmental Persistence of Chemicals. *Crit. Rev. Environ. Sci. Technol.* **2019**, *49* (23), 2220–2255.
- (5) Martínez-Varela, A.; Casas, G.; Berrojalbiz, N.; Piña, B.; Dachs, J.; Vila-Costa, M. Polycyclic Aromatic Hydrocarbon Degradation in the Sea-Surface Microlayer at Coastal Antarctica. *Front. Microbiol.* **2022**, *13*, 1.
- (6) González-Gaya, B.; Martínez-Varela, A.; Vila-Costa, M.; Casal, P.; Cerro-Gálvez, E.; Berrojalbiz, N.; Lundin, D.; Vidal, M.; Mompeán, C.; Bode, A.; Jiménez, B.; Dachs, J. Biodegradation as an Important Sink of Aromatic Hydrocarbons in the Oceans. *Nature Geoscience* **2019**, *12* (2), 119–125.
- (7) Charalampous, G.; Fragkou, E.; Kormas, K. A.; Menezes, A. B. De; Polymenakou, P. N.; Pasadakis, N.; Kalogerakis, N.; Antoniou, E.; Gontikaki, E. Comparison of Hydrocarbon-Degrading Consortia from Surface and Deep Waters of the Eastern Mediterranean Sea: Characterization and Degradation Potential. *Energies (Basel)* **2021**, *14* (8), 2246.
- (8) Vila-Costa, M.; Lundin, D.; Fernández-Pinos, M.-C.; Iriarte, J.; Irigoien, X.; Piña, B.; Dachs, J. Responses to Organic Pollutants in the Tropical Pacific and Subtropical Atlantic Oceans by Pelagic Marine Bacteria. *Front. Environ. Sci.* **2023**, *11*, 1.
- (9) Martínez-Varela, A.; Casas, G.; Berrojalbiz, N.; Lundin, D.; Piña, B.; Dachs, J.; Vila-Costa, M. Metatranscriptomic Responses and Microbial Degradation of Background Polycyclic Aromatic Hydrocarbons in the Coastal Mediterranean and Antarctica. *Environmental Science and Pollution Research* **2023**, *30* (S7), 119988–119999.
- (10) Martínez-Varela, A.; Cerro-Gálvez, E.; Auladell, A.; Sharma, S.; Moran, M. A.; Kiene, R. P.; Piña, B.; Dachs, J.; Vila-Costa, M. Bacterial Responses to Background Organic Pollutants in the Northeast Subarctic Pacific Ocean. *Environ. Microbiol.* **2021**, *23*, 4532.
- (11) van der Veen, I.; de Boer, J. Phosphorus Flame Retardants: Properties, Production, Environmental Occurrence. *Toxicity and Analysis. Chemosphere* **2012**, *88* (10), 1119–1153.
- (12) Regulatory Strategy for Flame Retardants. 2023. DOI: [10.2823/854233](https://doi.org/10.2823/854233).
- (13) Xie, Z.; Wang, P.; Wang, X.; Castro-Jiménez, J.; Kallenborn, R.; Liao, C.; Mi, W.; Lohmann, R.; Vila-Costa, M.; Dachs, J. Organophosphate Ester Pollution in the Oceans. *Nat. Rev. Earth Environ.* **2022**, *3* (5), 309–322.

- (14) Wang, X.; Zhu, Q.; Yan, X.; Wang, Y.; Liao, C.; Jiang, G. A Review of Organophosphate Flame Retardants and Plasticizers in the Environment: Analysis, Occurrence and Risk Assessment. *Science of The Total Environment* **2020**, 731, No. 139071.
- (15) Mathieu-Denoncourt, J.; Wallace, S. J.; de Solla, S. R.; Langlois, V. S. Plasticizer Endocrine Disruption: Highlighting Developmental and Reproductive Effects in Mammals and Non-Mammalian Aquatic Species. *Gen. Comp. Endocrinol.* **2015**, 219, 74–88.
- (16) Zhu, K.; Sarvajayakesavalu, S.; Han, Y.; Zhang, H.; Gao, J.; Li, X.; Ma, M. Occurrence, Distribution and Risk Assessment of Organophosphate Esters (OPEs) in Water Sources from Northeast to Southeast China. *Environ. Pollut.* **2022**, 307, No. 119461.
- (17) Wei, G.-L.; Li, D.-Q.; Zhuo, M.-N.; Liao, Y.-S.; Xie, Z.-Y.; Guo, T.-L.; Li, J.-J.; Zhang, S.-Y.; Liang, Z.-Q. Organophosphorus Flame Retardants and Plasticizers: Sources, Occurrence Toxicity and Human Exposure. *Environ. Pollut.* **2015**, 196, 29–46.
- (18) Li, J.; Zhao, L.; Letcher, R. J.; Zhang, Y.; Jian, K.; Zhang, J.; Su, G. A Review on Organophosphate Ester (OPE) Flame Retardants and Plasticizers in Foodstuffs: Levels, Distribution, Human Dietary Exposure, and Future Directions. *Environ. Int.* **2019**, 127, 35–51.
- (19) Fu, J.; Fu, K.; Chen, Y.; Li, X.; Ye, T.; Gao, K.; Pan, W.; Zhang, A.; Fu, J. Long-Range Transport, Trophic Transfer, and Ecological Risks of Organophosphate Esters in Remote Areas. *Environ. Sci. Technol.* **2021**, 55 (15), 10192–10209.
- (20) ECHA. ECHA Screening Report: An Assessment of Whether the Use of TCEP, TCPP and TDCP in Articles Should Be Restricted, 2018.
- (21) Castro-Jiménez, J.; Cuny, P.; Militon, C.; Sylvi, L.; Royer, F.; Papillon, L.; Sempéré, R. Effective Degradation of Organophosphate Ester Flame Retardants and Plasticizers in Coastal Sediments under High Urban Pressure. *Sci. Rep.* **2022**, 12 (1), 20228.
- (22) Liu, J.; Lin, H.; Dong, Y.; Li, B. Elucidating the Biodegradation Mechanism of Tributyl Phosphate (TBP) by *Sphingomonas* Sp. Isolated from TBP-Contaminated Mine Tailings. *Environ. Pollut.* **2019**, 250, 284–291.
- (23) Wang, J.; Khokhar, I.; Ren, C.; Li, X.; Wang, J.; Fan, S.; Jia, Y.; Yan, Y. Characterization and 16S Metagenomic Analysis of Organophosphorus Flame Retardants Degrading Consortia. *J. Hazard Mater.* **2019**, 380, No. 120881.
- (24) Castro-Jiménez, J.; Berrojalbiz, N.; Pizarro, M.; Dachs, J. Organophosphate Ester (OPE) Flame Retardants and Plasticizers in the Open Mediterranean and Black Seas Atmosphere. *Environ. Sci. Technol.* **2014**, 48 (6), 3203–3209.
- (25) Castro-Jiménez, J.; González-Gaya, B.; Pizarro, M.; Casal, P.; Pizarro-Álvarez, C.; Dachs, J. Organophosphate Ester Flame Retardants and Plasticizers in the Global Oceanic Atmosphere. *Environ. Sci. Technol.* **2016**, 50 (23), 12831–12839.
- (26) Dyhrman, S.; Ammerman, J.; Van Mooy, B. Microbes and the Marine Phosphorus Cycle. *Oceanography* **2007**, 20 (2), 110–116.
- (27) Browning, T. J.; Moore, C. M. Global Analysis of Ocean Phytoplankton Nutrient Limitation Reveals High Prevalence of Co-Limitation. *Nat. Commun.* **2023**, 14 (1), 5014.
- (28) Sebastian, M.; Ammerman, J. W. The Alkaline Phosphatase PhoX Is More Widely Distributed in Marine Bacteria than the Classical PhoA. *ISME J.* **2009**, 3 (5), 563–572.
- (29) Vila-Costa, M.; Sebastián, M.; Pizarro, M.; Cerro-Gálvez, E.; Lundin, D.; Gasol, J. M.; Dachs, J. Microbial Consumption of Organophosphate Esters in Seawater under Phosphorus Limited Conditions. *Sci. Rep.* **2019**, 9 (1), 233.
- (30) Despotović, D.; Aharon, E.; Trofimuk, O.; Dubovetskyi, A.; Cherukuri, K. P.; Ashani, Y.; Eliason, O.; Sperfeld, M.; Leader, H.; Castelli, A.; Fumagalli, L.; Savidor, A.; Levin, Y.; Longo, L. M.; Segev, E.; Tawfik, D. S. Utilization of Diverse Organophosphorus Pollutants by Marine Bacteria. *Proc. Natl. Acad. Sci. U. S. A.* **2022**, 119 (32), e2203604119.
- (31) Ren, X.; Zeng, G.; Tang, L.; Wang, J.; Wan, J.; Liu, Y.; Yu, J.; Yi, H.; Ye, S.; Deng, R. Sorption, Transport and Biodegradation—An Insight into Bioavailability of Persistent Organic Pollutants in Soil. *Science of The Total Environment* **2018**, 610–611, 1154–1163.
- (32) Singh, A.; Kumar Mishra, V. Biodegradation of Organic Pollutants for Its Effective Remediation from the Environment and the Role of Various Factors Affecting the Biodegradation Process. In *Sustainable Environmental Clean-up*; Elsevier: 2021; pp 1–27. DOI: 10.1016/B978-0-12-823828-8.00001-3.
- (33) Tang, Y. J.; Qi, L.; Krieger-Brockett, B. Evaluating Factors That Influence Microbial Phenanthrene Biodegradation Rates by Regression with Categorical Variables. *Chemosphere* **2005**, 59 (5), 729–741.
- (34) Trilla-Prieto, N.; Iriarte, J.; Berrojalbiz, N.; Casas, G.; Sobrino, C.; Vila-Costa, M.; Jiménez, B.; Dachs, J. Enrichment of Organophosphate Esters in the Sea Surface Microlayer from the Atlantic and Southern Oceans. *Environ. Sci. Technol. Lett.* **2024**, 11, 1008.
- (35) Falcioni, T.; Papa, S.; Gasol, J. M. Evaluating the Flow-Cytometric Nucleic Acid Double-Staining Protocol in Realistic Situations of Planktonic Bacterial Death. *Appl. Environ. Microbiol.* **2008**, 74 (6), 1767–1779.
- (36) Aksu, Z. Application of Biosorption for the Removal of Organic Pollutants: A Review. *Process Biochemistry* **2005**, 40 (3–4), 997–1026.
- (37) Church, M. J.; Hutchins, D. A.; Ducklow, H. W. *Limitation of Bacterial Growth by Dissolved Organic Matter and Iron in the Southern Ocean*; 2000; Vol. 66. <https://journals.asm.org/journal/aem>.
- (38) Fuhrman, J. A.; Cram, J. A.; Needham, D. M. Marine Microbial Community Dynamics and Their Ecological Interpretation. *Nat. Rev. Microbiol.* **2015**, 13 (3), 133–146.
- (39) Sunagawa, S.; Coelho, L. P.; Chaffron, S.; Kultima, J. R.; Labadie, K.; Salazar, G.; Djahanschiri, B.; Zeller, G.; Mende, D. R.; Alberti, A.; Cornejo-Castillo, F. M.; Costea, P. I.; Cruaud, C.; d'Ovidio, F.; Engelen, S.; Ferrera, I.; Gasol, J. M.; Guidi, L.; Hildebrand, F.; Kokoszka, F.; et al. Structure and Function of the Global Ocean Microbiome. *Science* (1979) **2015**, 348 (6237), 1.
- (40) Li, R.; Gao, H.; Hou, C.; Fu, J.; Shi, T.; Wu, Z.; Jin, S.; Yao, Z.; Na, G.; Ma, X. Occurrence, Source, and Transfer Fluxes of Organophosphate Esters in the South Pacific and Fildes Peninsula, Antarctic. *Sci. Total Environ.* **2023**, 894, 164263.
- (41) Schmidt, N.; Fauvel, V.; Ody, A.; Castro-Jiménez, J.; Jouanno, J.; Changeux, T.; Thibaut, T.; Sempéré, R. The Amazon River: A Major Source of Organic Plastic Additives to the Tropical North Atlantic? *Environ. Sci. Technol.* **2019**, 53 (13), 7513–7521.
- (42) Pedler, B. E.; Aluwihare, L. I.; Azam, F. Single Bacterial Strain Capable of Significant Contribution to Carbon Cycling in the Surface Ocean. *Proc. Natl. Acad. Sci. U. S. A.* **2014**, 111 (20), 7202–7207.
- (43) Wietz, M.; López-Pérez, M.; Sher, D.; Biller, S. J.; Rodríguez-Valera, F. Microbe Profile: *Alteromonas Macleodii*—a Widespread, Fast-Responding, ‘Interactive’ Marine Bacterium. *Microbiology (N Y)* **2022**, 168 (11), 1.
- (44) Iriarte, J.; Dachs, J.; Casas, G.; Martínez-Varela, A.; Berrojalbiz, N.; Vila-Costa, M. Snow-Dependent Biogeochemical Cycling of Polycyclic Aromatic Hydrocarbons at Coastal Antarctica. *Environ. Sci. Technol.* **2023**, 57 (4), 1625–1636.
- (45) Garneau, M.-E.; Michel, C.; Meisterhans, G.; Fortin, N.; King, T. L.; Greer, C. W.; Lee, K. Hydrocarbon Biodegradation by Arctic Sea-Ice and Sub-Ice Microbial Communities during Microcosm Experiments, Northwest Passage (Nunavut, Canada). *FEMS Microbiol. Ecol.* **2016**, 92 (10), No. fiw130.
- (46) Freyria, N. J.; Góngora, E.; Greer, C. W.; Whyte, L. G. High Arctic Seawater and Coastal Soil Microbiome Co-Occurrence and Composition Structure and Their Potential Hydrocarbon Biodegradation. *ISME Communications* **2024**, 4 (1), ycae100.
- (47) Schattener, M.; Wulf, J.; Kostadinov, I.; Glöckner, F. O.; Zubkov, M. V.; Fuchs, B. M. Phylogenetic Characterisation of Picoplanktonic Populations with High and Low Nucleic Acid Content in the North Atlantic Ocean. *Syst. Appl. Microbiol.* **2011**, 34 (6), 470–475.
- (48) Vila-Costa, M.; Gasol, J. M.; Sharma, S.; Moran, M. A. Community Analysis of High- and Low-nucleic Acid-containing Bacteria in NW Mediterranean Coastal Waters Using 16S rDNA Pyrosequencing. *Environ. Microbiol.* **2012**, 14 (6), 1390–1402.

(49) Kawagoshi, Y.; Nakamura, S.; Fukunaga, I. Degradation of Organophosphoric Esters in Leachate from a Sea-Based Solid Waste Disposal Site. *Chemosphere* **2002**, *48* (2), 219–225.

(50) Kawai, S. Degradation of Organophosphoric Acid Triesters by the Aquatic Bacteria and Toxicity to Fish. *J. Jpn. Soc. Water Environ* **1996**, *19*, 700–707.

Bacterial Production Modulates the Persistence of Organophosphate Ester Flame Retardants and Plasticizers in the Ocean

Jon Iriarte^{1,2}, Núria Trilla-Prieto^{1,3}, Naiara Berrojalbiz¹, Maria Vila-Costa^{1*}, Jordi Dachs¹

¹Department of Environmental Chemistry, Institute of Environmental Assessment and Water Research, 08034, Barcelona, Catalunya, Spain.

²Doctoral program in Analytical Chemistry and the Environment, Department of Chemical Engineering and Analytical Chemistry, Faculty of Chemistry, Universitat de Barcelona, 08034, Barcelona, Catalunya, Spain.

³Departament of Ecology, Faculty of Earth Sciences, Universitat de Barcelona, 08034, Barcelona, Catalunya, Spain.

*E-mail contact: maria.vila@idaea.csic.es

Supporting Information

Table of contents

Annex S1: Analytical procedures for determining water ancillary and environmental data.

Annex S2: Additional details of the experimental setup.

Annex S3: Determination of OPE concentration; Quality Assurance and Quality Control.

Annex S4: Statistical analyses.

Table S1: Ancillary and other environmental data of the seawater samples.

Table S2: Chemical structures and acronyms of the OPE compounds in the study.

Table S3: Physicochemical properties and chemical safety warnings of the six OPEs used in the experiments.

Table S4: Grouped t-test results for the concentrations of each individual OPE compound for each experiment.

Table S5: Mass balance results of OPE losses taking as baseline the nominal concentration.

Table S6: List of ASVs with absolute fold change > 1, and their taxonomy, from the Atlantic Ocean experiments (ANTOM-1).

Table S7: List of ASVs with absolute fold change > 1, and their taxonomy, from the Southern Ocean experiments (ANTOM-2).

Figure S1: Experimental setup.

Figure S2: NADS results showing the percentage of viable and non-viable cells in the analyzed sorption controls.

Figure S3: Nutrient addition experiment results.

Figure S4: Results of the ancillary data PCA analysis.

Figure S5: Structure of the bacterial community for each experiment.

Figure S6: Boxplots showing individual OPE concentrations at each experiment.

Figure S7: Concentration ratios of OPE compounds between 48-hour biotic treatments (BT) and 0.2-filtered controls (FC) across different experiments.

Figure S8: Concentration ratios of OPE compounds between 48-hour biotic treatments (BT) and sorption controls (SC) across different experiments.

Figure S9: Percentage of individual OPE compound concentration loss in the Atlantic Ocean experiments.

Figure S10: Percentage of individual OPE compound concentration loss in the Southern Ocean experiments.

Figure S11: Ratios between sorption control (SC) and 0.2-filtered control (FC) OPE concentrations vs octanol-water partition coefficient.

Figure S12: Alpha diversity indexes per ocean and incubation time.

Figure S13: Chao1 indexes per experiment and incubation time.

Figure S14: Shannon indexes per experiment and incubation time.

Figure S15: NMDS analysis for dissimilarities in the microbial community composition at the different sampling times.

Figure S16: Heatmap showing the Log₂ fold change of the relative abundance of each of the ASVs selected to explain the microbial community shift in the Atlantic Ocean experiments.

Figure S17: Heatmap showing the Log₂ fold change of the relative abundance of each of the 19 ASVs selected to explain the microbial community shift in the Southern Ocean experiments.

Figure S18: Barplots of the bacterial production results as leucine incorporation rates.

Figure S19: Results of bacterial abundance and cell viability.

References

Annex S1: Analytical procedures for determining water ancillary and environmental data.

Measurement of water basic parameters

The rosette of Niskin bottles used to take water samples was mounted on a conductivity-temperature-depth (CTD) profiler (SeaBird SBE 911 plus). Water temperature, salinity, turbidity, dissolved oxygen, photosynthetically active radiation (PAR), and water's transparency as beam transmittance (Cstar) were recorded at each station with the CTD sensors installed in the rosette sampler.

Total Chlorophyll α concentration determination method

Total Chlorophyll α (Chl α) concentration was measured in surface water samples collected with a Niskin bottle attached to the boat oceanographic rosette. For each sample, 250 mL were gently filtered under dim light in triplicate through a size fraction cascade system with 20, 2 and 0.22 μm size pore 47-mm Filter-Lab polycarbonate filters, and immediately stored at -20°C until further analysis. Chl α extraction was carried out with 90% acetone and the concentration in each sample ($\mu\text{g/L}$) was estimated following the protocol in Strickland and Parsons (1972) ¹ using a Turner A10 fluorometer previously calibrated with a pure Chl α standard (SIGMA C5753-1mg). The final total Chl α concentration value is the result of the sum of Chl α concentration at each size fraction.

DNA extraction, sequencing and taxonomical identification of bacterial communities

Samples for 16S rRNA gene sequencing were collected after 30 min (T0) and 48 h (T48) of the beginning of the experiment. Seawater (2 L) from the incubation bottles was filtered through 47-mm-diameter, 0.2- μm pore-size PTFE filters (Omnipore, Millipore) under low vacuum pressure using a baked-glass filter holder. PTFE have been shown to be optimal in order to minimize sampling time, but allowing an optimum extraction efficiency of DNA ². After filtration, each filter was placed into lysis buffer (50 mM Tris HCl, 40 mM EDTA, 0.75 M Sucrose) at -20°C to preserve nucleic acids until analysis.

For DNA extraction, samples were incubated with lysozyme, proteinase K, and sodium dodecyl sulfate (SDS), and nucleic acids were extracted simultaneously with phenol/chloroform/isoamyl alcohol (25: 24: 1 vol: vol: vol) and with chloroform/isoamyl alcohol (24: 1, vol: vol). Aqueous phases were separated, nucleic acids were precipitated with ammonium acetate (4 M) and isopropanol, then washed with ethanol 70%, and finally dried using an Eppendorf Concentrator Plus (15 min, 30°C , V/AL mode) and redissolved in 50 μL of DNase/RNase free water (Water Molecular biology grade, PanReac Applichem).

Aliquots of the total DNA were sent to Novogene Europe (Cambridge, UK) for Bacterial 16S Amplicon Sequencing. Briefly, the region V4-V5 of the 16S rDNA was amplified with specific primers barcoding for amplicon generation (515F-Y/926R) ³. PCR products were quality-checked, pooled, end-paired, A-tailed, joined with Illumina adapters, and purified. Then,

libraries were prepared on a paired-end Illumina platform, generating 250 bp paired-end raw reads. No negative controls, from DNA extraction to sequencing, were assessed in this study.

Processing of the raw reads was performed following nf-core/ampliseq pipeline (v.2.11.0) within Nextflow (v.24.04.2) ^{4,5}, using pipeline default values for the parameters. Briefly, the pipeline performs quality checking, followed by primer trimming of the raw reads. MultiQC ⁶ reports showed good quality for the dataset, with mean sequence quality Phred scores across the reads to be above 35. Primers were trimmed using cutadapt ⁷ and all untrimmed sequences were discarded. Sequences that did not contain primer sequences were considered artifacts. Less than 4.8% of the sequences were discarded per sample and a mean of 99.4% of the sequences per sample passed the filtering. The pipeline then uses DADA2 (v.1.30.0) ⁸ to perform denoising, chimera removal, and inference of amplicon sequence variants (ASVs) total counts per sample. Quality filtering parameters used by DADA2 were the following: reads were trimmed to a specific length and the length cutoff was automatically determined by the median quality of all input reads. Reads were trimmed before median quality dropped below 25 and at least 75% of reads were retained, resulting in a trim of forward reads at 223 bp and reverse reads at 222 bp, reads shorter than this were discarded. Reads with more than 2 expected errors were discarded. Taxonomic classification was performed by DADA2 and the database 'SBDI-GTDB - Sativa curated 16S GTDB database - Release R09-RS220-1' ⁹.

Ultimately, 2476 unique ASVs were obtained across all samples. The final database contained 1,312,895 reads, at least 23,405 and at most 76,190 per sample (average 54,704). The complete nucleotide sequence data set generated and analyzed in this study was deposited in the European Nucleotide Archive (ENA) under the bioproject accession # PRJEB82241.

Flow cytometric determination of prokaryotic cell abundances and membrane-compromised cells (NADS)

Flow cytometric determination of prokaryotic cell abundances

Subsamples of 1.8 ml for quantification of abundances of prokaryotes were fixed with 1% buffered paraformaldehyde solution (pH 7.0) plus 0.05% glutaraldehyde, left at room temperature in the dark for 10 minutes, flash-frozen in liquid nitrogen and stored at -80 °C. Prokaryotic cell abundance was estimated by flow cytometry as described elsewhere ¹⁰. Briefly, 400 µL of the fixed samples were placed in flow cytometric tubes. Then, 4 µL of SYBR Green I working solution (previously diluted in DMSO) were added and tubes were let at room temperature for 10 minutes. Samples were run using a BD Accuri C6 Plus flow cytometer. The resulting cytograms were analyzed using FlowJo software to quantify the high-nucleic acid-containing (HNA) and the low-nucleic acid-containing (LNA) prokaryotes.

NADS (Nucleic Acid Double Staining) protocol

This protocol does not work with fixed samples; therefore, it was performed onboard. The protocol is described elsewhere ¹⁰. Briefly, 400 µL of water sample were dispensed in flow cytometric tubes. Then, 4 µL of SYBR Green I working solution (previously diluted in DMSO)

and 4 μL of PI solution (Propidium Iodide diluted in Mili-Q water) were added. Tubes were incubated for 15 minutes at room temperature before running the samples using a BD Accuri C6 Plus flow cytometer. The resulting cytograms were analyzed using FlowJo software to quantify the percentage of “viable” cells with intact membranes and “non-viable” cells with damaged membranes. It is generally accepted that bacterial permeability to exclusion stains, such as PI (with a molecular weight of 668.4), is associated with the presence of substantial and presumably irreparable breaches in the membrane ¹¹.

Heterotrophic bacterial production (as Leucine incorporation rates, LIR)

Bacterial production was estimated as the incorporation of ^3H -leucine into protein using the microcentrifuge method described by Smith and Azam (1992) ¹². Briefly, 1.2 ml triplicate live and one killed (5% trichloroacetic acid, TCA) subsamples were incubated with ^3H -leucine (40 nM) for 4-5 hours at *in situ* temperature in the dark. Incubations were stopped by addition of 120 μL of cold TCA 50% and then frozen (-20°C) until further processing by centrifugation and TCA rinsing. DPM counts were measured using a Tri-carb 3100TR liquid scintillation analyzer (Perkin Elmer), and converted to leucine incorporation rates.

Annex S2: Additional details of the experimental setup.

Processing of the sampled seawater

Two 12L Niskin bottles were filled per site at 5 m depth. This water was then filtered through a 200 μm nylon mesh into a pre-cleaned 20L carboy for homogenization, and subsequently filtered through 3 μm pore-size polycarbonate (PC) membrane filters (Isopore, Millipore) into a second pre-cleaned 20L carboy, using a peristaltic pump at 40 rpm. The water in this second carboy was used to fill all the different condition bottles and, also, the bottles of the nutrient addition experiment.

Preparation of the sorption controls

Using the 3 μm filtered water sorption controls (SC) were prepared by heating the water in a thermostatic bath at 70 °C during 10-15 min. The temperature was monitored with a thermometer. After the heat treatment, the water was let at room temperature to cool down and was finally used to fill the corresponding bottles with spiked OPEs.

These controls were mainly intended to assess a number of metabolism-independent processes (physical and chemical adsorption, electrostatic interaction, ion exchange, complexation, chelation, and microprecipitation) taking place essentially in the cell wall, which can be resumed as the passive uptake of pollutants from aqueous solutions by non-growing or non-living microbial mass, so-called bio-sorption¹³. At the same time, this control also accounts for the potential sorption of the OPEs to the 0.2 pore-size PTFE filters. Heat treatment was chosen as the best method to create a non-viable microbial population, in order to achieve as little physicochemical modification of the seawater as possible while preserving a minimum cell integrity rather than destroying the cells. Heat treatment at 70 °C for 5 minutes has been shown to cause membrane damage in marine microbes, resulting in 80% non-viable cells as assessed by the NADS protocol¹⁴, with no measurable leucine uptake. Other authors have reported similar trends in lake water samples that were heat-exposed¹⁵. In our case, NADS analysis of the heat-treated controls reported on average 95% of non-viable cells (Figure S2).

Preparation of the 0.2-filtered controls

To prepare the 0.2-filtered controls (FC), the 3 μm filtered water was further filtered using 0.2 μm pore-size polytetrafluoroethylene (PTFE) filters and the peristaltic pump at 40 rpm. The corresponding bottles where OPEs had already been spiked were filled with this water.

Sterile filtration using 0.2 μm pore-size filters was chosen to significantly reduce microbial biomass while minimizing disturbance to the chemical composition of natural seawater¹⁶. While pasteurization could increase sterility, it would also alter the original chemical properties, reducing comparability¹⁷. Although 0.2 μm filtration does not completely remove microbes, our flow cytometry counts from the 0.2-filtered controls showed 90% bacterial removal, consistent with previous studies that showed retention efficiencies typically

between 91–99% ^{18,19}. While small microbes were possibly present in the filtrate, these are predominantly the least active bacteria ²⁰. We hypothesize that this substantially reduced and less active microbial population had minimal impact on OPE concentrations compared to the fully biotic treatments.

Temperature control during incubations

For the Atlantic Ocean experiments, the temperature during incubations was controlled by incubating the bottles inside a thermoregulated laboratory using a Stulz Comptrol 1002 A/C system. The system was set to adjust the room temperature according to the seawater temperature measured by the in-built thermosalinograph (SBE21, Sea Bird Scientific) that measured the seawater that the oceanographic ship constantly pumped, which circulated to the labs or to the deck. This seawater was taken from below the ship, thus at 4-4.5 m depth. For the Southern Ocean experiments, the temperature was controlled by incubating the bottles inside a thermostatic incubator set at 4 °C (the minimum temperature available).

Annex S3: Determination of OPE concentration; Quality Assurance and Quality Control.

OPE analyses

The procedures followed for extraction, identification, and quantification are the ones described in Trilla-Prieto *et al.* (2024)²¹, with slight modifications. Briefly, after the experiment, samples were filtered with 0.2- μm pore-size PTFE filters (Omnipore, Millipore) to collect bacterial DNA. Then, they filtered water was loaded onto a solid-phase extraction cartridge (Oasis HLB, 6 cm^3 , 200 mg; Waters) using a vacuum manifold. Cartridges were conditioned with 6 mL of 2-propanol and 12 mL of HPLC-grade water, and then spiked with 50 ng of a mix of labelled recovery standards (D27-TNBP, D15-TPhP, D12-TCEP, D21-TPrP, D18-TCP and D51-TEHP). were washed with 6 mL of chromatographic-grade water at 5% of methanol, dried under vacuum for 10 to 15 minutes, and stored at -20°C in sealed bags before further treatment analysis in an ultraclean laboratory.

Once in the ultraclean laboratory, HLB cartridges were unfreeze for 3 hours at room temperature, centrifuged at 3500 rpm for 4' and eluted with 12 mL methyl tert-butyl ether:methanol (3:1; v/v). The residual water was removed by adding 3 g of pre-baked sodium sulfate. The final eluents were concentrated under N_2 and reconstituted in 100 μL of toluene. 50 ng of perdeuterated Internal standards (d15-TDCPP, M6TBEP and MTPHP) were added before the instrumental analysis.

OPEs were analyzed by gas chromatography-tandem mass spectrometry (GC-MS/MS) on an Agilent 7890A gas chromatograph coupled to an Agilent 7000B triple quadrupole analyzer (qQq). The chromatographic separation was carried out using a HP-5MS column (30m, 0.25 mm internal diameter, 0.25 μm film thickness). Methane was used as ionization gas and helium was used as carrier gas at a constant flow mode of 20 mL min^{-1} . Two μL of sample were injected in splitless mode and injection port temperature of 280°C . The column temperatures were: 90°C for 1 min, increased at $15^\circ\text{C min}^{-1}$ to 200°C held for 6 min, then at 5°C min^{-1} to 250°C , held for 6 min and then at $10^\circ\text{C min}^{-1}$ to 315°C , held for 10 min. The detection was carried out using electronic impact ionization (EI) mode in positive mode. The EI source, transfer line and quadrupole temperature were 230°C , 280°C and 300°C , respectively. Acquisition was performed in multiple reaction monitoring (MRM). Finally, concentrations of the six OPE compounds were determined using the MassHunter Quantitative Analysis Software (Agilent).

Quality Assurance/Quality Control

Quality Assurance/Quality Control used are described Trilla-Prieto *et al.* (2024)²¹. Briefly, Field blanks consisted of GF/F filters and Oasis HLB cartridges that followed the same procedure, transport, and analysis as the field samples. Laboratory blanks (procedural blanks) followed the same extraction and analysis as the samples. A procedural and field blank were analyzed for each batch of 10 samples to monitor potential contamination. Concentrations

were recovery and blank corrected. The limits of quantification (LOQs) were defined as the mean concentration of field and procedural blanks plus three times the standard deviation. All concentrations were above LOQs. The recoveries were monitored using TNBP-d27, TCEP-d12, TCPP-d18, TEHP-d51, and TPhP-d15 as surrogate standards prior to extraction. Surrogate recoveries averaged 70% and 73% for the samples from the Atlantic and Southern Ocean, respectively. Details about LOQs, blank concentrations and recovery values can be found in Trilla-Prieto *et al.* (2024) ²¹.

Annex S4: Statistical analyses

All the statistical analyses were performed using R v.4.4.1 software (<http://www.r-project.org/>). Principal Component Analysis of the environmental variables was conducted utilizing the *prcomp* function (with the parameters *scale* and *center* set as *TRUE*) from the *stats* v.4.1.1 package. The non-metric multidimensional Scaling (NMDS) analysis were done using the *metaMDS* function from *vegan* v.2.6-6.1 package on the AVS absolute count database ²². Alpha diversity was assessed by computing the Chao1 index and Shannon index with *estimateR* and *diversity* functions from *vegan* package on sub-sampled data rarefied to the minimum read count of all samples. Bacterial community composition was assessed by computing relative abundances using total sum scaling normalization for all the ASVs with taxonomic classification. T-test analysis were done using the *compare_means* and *stat_compare_means* functions from the *ggpubr* v.0.6.0 package. To study variations between treatments associated with specific taxa, log2 fold change of the ratio of the relative abundance between T48 and T0 of individual ASV was computed. First, those non-detected ASVs at T0 or T48 times were excluded. After calculating the fold change values, to assess which ASVs were actually driving the bacterial community shift, we excluded those ASV whose relative abundances were not at least a 1% of the total community at T48 for those that grew, or at T0 for those that decreased. This resulted in a list of 28 ASVs for the Atlantic Ocean experiments, and of 19 ASVs for the Southern Ocean. Fold change heatmaps of the selected ASVs were created using *pheatmap* function from *pheatmap* v.1.0.12 package. Linear regression plots were done using the *stat_smooth* and *stat_poly_eq* functions from *ggplot2* v.3.5.1 and *ggpmisc* v.0.6.0. packages, respectively.

To perform the linear regression analysis between changes in OPE concentrations and bacterial production rates, biotic treatment T48 replicate values were treated as individual data points. For the T0 bacterial production and sorption control concentration values, the mean of the two replicates was used. Each T48 value was then normalized to the corresponding mean value of the sorption control or T0, generating the data points shown in the plot.

Table S1: Ancillary data of the seawater samples used in this study. Bacterial abundance and bacterial production are written as BA and BP, respectively. PAR means photosynthetic active radiation, and Cstar stands for beam transmission as a measure of water clarity.

Campaign	Station	Date	Lat	Long	Max_Depth (m)	Longhurst	Exp_number
an1	6	23/12/2020	22.22	-26.63	5,382	NATR	Exp.1
an1	10	27/12/2020	7.35	-29.58	4,960	WTRA	Exp.2
an1	14	31/12/2020	-6.78	-31.33	5,187	SATL	Exp.3
an1	21	08/01/2021	-34.40	-45.63	4,827	SATL	Exp.4
an2	3	25/01/2022	-64.58	-62.57	253	APLR	Exp.5
an2	9	31/01/2022	-69.21	-78.84	250	APLR	Exp.6

Exp_number	Depth (m)	Temp. (°C)	Sal (psu)	Dis. O ₂ (mg/L)	PAR	Tot_Chla(µg/L)	Turb(NTU)	Cstar
Exp.1	5.26	23.59	36.96	6.70	49.75	0.15	0.21	98.79
Exp.2	5.14	27.46	34.98	6.33	472.05	0.17	0.23	97.86
Exp.3	5.28	27.48	36.46	6.26	203.53	0.13	0.20	98.74
Exp.4	4.74	23.88	37.00	6.70	491.70	0.11	0.22	97.95
Exp.5	5.15	1.01	34.02	10.11	243.51	1.16	0.19	90.17
Exp.6	5.45	-0.05	33.56	11.36	73.88	0.72	0.16	90.35
mean_an1	5.10	25.60	36.35	6.50	304.26	0.14	0.21	98.34
mean_an2	5.30	0.48	33.79	10.74	158.70	0.94	0.17	90.26

Exp_number	BA_mean (cells/mL)	BA_sd	BP(pmol leu L ⁻¹ h ⁻¹)	BP_sd
Exp.1	5.24E+05	1.49E+04	1.25E+01	2.03E+00
Exp.2	9.27E+05	7.06E+04	2.39E+01	4.98E+00
Exp.3	6.87E+05	3.13E+04	1.37E+01	7.83E-01
Exp.4	7.50E+05	2.24E+04	1.49E+01	2.88E+00
Exp.5	2.07E+05		5.29E+00	2.12E+00
Exp.6	2.44E+05		3.40E+01	2.20E+01
mean_an1	722196.24	34797.12	16.24	2.67
mean_an2	225545.91		19.63	12.08

Table S2: Chemical structures and acronyms of the OPEs present in this study. *TCP is a mixture of isomers, where Tris(1-chloro-2-propyl) phosphate is the main isomer, followed by bis(1-chloro-2-propyl)-2-chloropropyl phosphate, and bis(2-chloropropyl)-1-chloro-2-propyl phosphate. TCP results are presented as the sum of the three isomers.

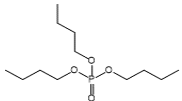
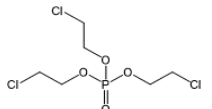
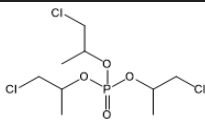
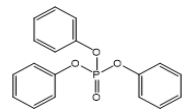
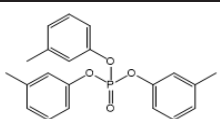
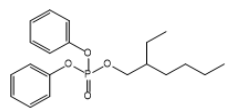
OPE compounds used in the experiments			
Name	Acronym	Group	Chemical structure
Tri-n-butyl phosphate	TnBP	Alkyl-OPE	
Tris (2-chloroethyl) phosphate	TCEP	Chlorinated-OPE	
*Tris(1-chloro-2-propyl) phosphate	Σ TCP	Chlorinated-OPE	
Triphenyl phosphate	TPhP	Aryl-OPE	
Tri-m-cresyl phosphate	TmCP	Aryl-OPE	
2-Ethylhexyl diphenyl phosphate	EHDPP	Aryl-OPE	

Table S3: Physicochemical properties and chemical safety warnings of the six OPEs used in the experiments.















Acronym	CAS No.	M.W.	Solubility (mg L ⁻¹)	logK _{ow}	V _p (Pa)	Chemical Safety	GHS hazard statements	Reference
TnBP	126-73-8	266.31	280	4.00	0.15	 	H302 (100%): Harmful if swallowed [Warning: Acute toxicity, oral] H315 (100%): Causes skin irritation [Warning: Skin corrosion/irritation] H351 (99.91%): Suspected of causing cancer [Warning: Carcinogenicity] H412 (88.23%): Harmful to aquatic life with long-lasting effects [Hazardous to the aquatic environment, long-term hazard]	National Center for Biotechnology Information (2024). PubChem Compound Summary for CID 31357, Triisobutylphosphate. Retrieved August 14, 2024 from https://pubchem.ncbi.nlm.nih.gov/compound/Triisobutylphosphate .
						  	H302 (97.19%): Harmful if swallowed [Warning: Acute toxicity, oral] H351 (100%): Suspected of causing cancer [Warning: Carcinogenicity] H360 (88.38%): May damage fertility or the unborn child [Danger: Reproductive toxicity] H360F (11.11%): May damage fertility [Danger: Reproductive toxicity] H411 (100%): Toxic to aquatic life with long-lasting effects [Hazardous to the aquatic environment, long-term hazard]	"European Union Risk Assessment Report: TRIS (2-CHLOROETHYL) PHOSPHATE, TCEP RISK ASSESSMENT" 2009 [Online]. Available: http://europa.eu.int National Center for Biotechnology Information (2024). PubChem Compound Summary for CID 82895, Triis(2-chloroethyl) phosphate. Retrieved August 14, 2024 from https://pubchem.ncbi.nlm.nih.gov/compound/Triis_2-chloroethyl_phosphate .
TCPP	115-96-8	285.49	7.82 x 10 ³	1.78	1.14 x 10 ⁻³	  	H302 (99.86%): Harmful if swallowed [Warning: Acute toxicity, oral] H412 (14.49%): Harmful to aquatic life with long-lasting effects [Hazardous to the aquatic environment, long-term hazard]	National Center for Biotechnology Information (2024). PubChem Compound Summary for CID 26176, Triis(1-chloro-2-propyl) phosphate. Retrieved August 14, 2024 from https://pubchem.ncbi.nlm.nih.gov/compound/Triis_1-chloro-2-propyl_phosphate .
							H412 (14.49%): Harmful to aquatic life with long-lasting effects [Hazardous to the aquatic environment, long-term hazard]	"European Union Risk Assessment Report: TRIS(2-CHLORO-1-METHYLETHYL) PHOSPHATE (TCPP) RISK ASSESSMENT" [Online]. Available: http://europa.eu.int National Center for Biotechnology Information (2024). PubChem Compound Summary for CID 82899, Triphenyl phosphate. Retrieved August 14, 2024 from https://pubchem.ncbi.nlm.nih.gov/compound/Triphenylphosphate .
TPhP	115-86-6	326.29	1.9	4.59	8.53 x 10 ⁻⁴		H400 (83.69%): Very toxic to aquatic life [Warning: Hazardous to the aquatic environment, acute hazard] H410 (86.36%): Very toxic to aquatic life with long-lasting effects [Warning: Hazardous to the aquatic environment, long-term hazard] H411 (88.78%): Toxic to aquatic life with long-lasting effects [Hazardous to the aquatic environment, long-term hazard]	"Substance Evaluation Conclusion Document: SUBSTANCE EVALUATION CONCLUSION as required by REACH Article 48 and EVALUATION REPORT for Substance name: Triphenyl phosphate (TPP)." [Online]. Available: http://echa.europa.eu/web/guest/information-on-chemicals/registered-substances
TmCP	563-04-2	368.37	0.36	5.11	9.9 x 10 ⁻⁵	 	H302+H312 (50%): Harmful if swallowed or in contact with skin [Warning: Acute toxicity, oral, acute toxicity, dermal] H302 (98.68%): Harmful if swallowed [Warning: Acute toxicity, oral] H312 (98.68%): Harmful in contact with skin [Warning: Acute toxicity, dermal] H400 (48.68%): Very toxic to aquatic life [Warning: Hazardous to the aquatic environment, acute hazard] H411 (98.68%): Toxic to aquatic life with long-lasting effects [Hazardous to the aquatic environment, long-term hazard]	National Center for Biotechnology Information (2024). PubChem Compound Summary for CID 11232, Tri-M-cresyl phosphate. Retrieved August 14, 2024 from https://pubchem.ncbi.nlm.nih.gov/compound/Tri-M-cresylphosphate .
								Environmental risk evaluation report: Tricresyl phosphate (CAS no. 1330-78-5) Report Product Code: SCH0080BQU-E-P https://www.gov.uk/government/publications/environmental-risk-evaluation-reports
EHDPP	1241-94-7	362.41	0.051	5.73	3.4 x 10 ⁻⁴	 	H331 (11.85%): Toxic if inhaled [Warning: Acute toxicity, inhalation] H400 (72.34%): Very toxic to aquatic life [Warning: Hazardous to the aquatic environment, acute hazard] H410 (66.35%): Very toxic to aquatic life with long-lasting effects [Warning: Hazardous to the aquatic environment, long-term hazard] H411 (28.88%): Toxic to aquatic life with long-lasting effects [Hazardous to the aquatic environment, long-term hazard]	National Center for Biotechnology Information (2024). PubChem Compound Summary for CID 14716, 2-Ethylhexyl diphenyl phosphate. Retrieved August 14, 2024 from https://pubchem.ncbi.nlm.nih.gov/compound/2-Ethylhexyldiphenylphosphate .
								Environmental risk evaluation report: 2-Ethylhexyl diphenyl phosphate (CAS no. 1241-94-7) Report Product Code: SCH0030BQFE-E-P https://www.gov.uk/government/publications/environmental-risk-evaluation-reports

Table S4: Results of the grouped t-test for the comparison of the concentrations of each individual OPE compound for each experiment. The groups are BT for 48-hour biotic treatment (viable bacteria 48-hour incubation treatment), SC for sorption control (non-viable heat-treated bacteria 48-hour treatment), and FC for 0.2-filtered control (3 and 0.2 μm filtered water 48-hour treatment).

experiment	compound	group1	group2	p	p.signi	method
1	TnBP	BT	SC	0.46	ns	T-test
1	TnBP	BT	FC	0.53	ns	T-test
1	TnBP	SC	FC	0.36	ns	T-test
1	TCEP	BT	SC	0.51	ns	T-test
1	TCEP	BT	FC	0.41	ns	T-test
1	TCEP	SC	FC	0.82	ns	T-test
1	TPhP	BT	SC	0.09	ns	T-test
1	TPhP	BT	FC	0.12	ns	T-test
1	TPhP	SC	FC	0.41	ns	T-test
1	TmCP	BT	SC	0.20	ns	T-test
1	TmCP	BT	FC	0.02	*	T-test
1	TmCP	SC	FC	0.02	*	T-test
1	EHDPP	BT	SC	0.06	ns	T-test
1	EHDPP	BT	FC	0.00	**	T-test
1	EHDPP	SC	FC	0.01	*	T-test
1	Σ TCPP	BT	SC	0.29	ns	T-test
1	Σ TCPP	BT	FC	0.14	ns	T-test
1	Σ TCPP	SC	FC	0.18	ns	T-test
2	TnBP	BT	SC	0.91	ns	T-test
2	TnBP	BT	FC	0.16	ns	T-test
2	TnBP	SC	FC	0.73	ns	T-test
2	TCEP	BT	SC	0.48	ns	T-test
2	TCEP	BT	FC	0.09	ns	T-test
2	TCEP	SC	FC	0.27	ns	T-test
2	TPhP	BT	SC	0.06	ns	T-test
2	TPhP	BT	FC	0.52	ns	T-test
2	TPhP	SC	FC	0.33	ns	T-test
2	TmCP	BT	SC	0.25	ns	T-test
2	TmCP	BT	FC	0.11	ns	T-test
2	TmCP	SC	FC	0.33	ns	T-test
2	EHDPP	BT	SC	0.00	**	T-test
2	EHDPP	BT	FC	0.01	*	T-test
2	EHDPP	SC	FC	0.04	*	T-test
2	Σ TCPP	BT	SC	0.32	ns	T-test
2	Σ TCPP	BT	FC	0.35	ns	T-test
2	Σ TCPP	SC	FC	0.73	ns	T-test
4	TnBP	BT	SC	0.71	ns	T-test
4	TnBP	BT	FC	0.41	ns	T-test
4	TnBP	SC	FC	0.30	ns	T-test
4	TCEP	BT	SC	0.52	ns	T-test
4	TCEP	BT	FC	0.03	*	T-test
4	TCEP	SC	FC	0.20	ns	T-test
4	TPhP	BT	SC	0.66	ns	T-test
4	TPhP	BT	FC	0.43	ns	T-test
4	TPhP	SC	FC	0.28	ns	T-test
4	TmCP	BT	SC	0.03	*	T-test
4	TmCP	BT	FC	0.04	*	T-test
4	TmCP	SC	FC	0.05	ns	T-test
4	EHDPP	BT	SC	0.02	*	T-test
4	EHDPP	BT	FC	0.05	ns	T-test
4	EHDPP	SC	FC	0.09	ns	T-test
4	Σ TCPP	BT	SC	0.52	ns	T-test

4	ΣTCPP	BT	FC	0.15	ns	T-test
4	ΣTCPP	SC	FC	0.47	ns	T-test
5	TnBP	BT	SC	0.17	ns	T-test
5	TnBP	BT	FC	0.14	ns	T-test
5	TnBP	SC	FC	0.90	ns	T-test
5	TCEP	BT	SC	0.01	*	T-test
5	TCEP	BT	FC	0.18	ns	T-test
5	TCEP	SC	FC	0.44	ns	T-test
5	TPhP	BT	SC	0.67	ns	T-test
5	TPhP	BT	FC	0.53	ns	T-test
5	TPhP	SC	FC	0.41	ns	T-test
5	TmCP	BT	SC	0.17	ns	T-test
5	TmCP	BT	FC	0.12	ns	T-test
5	TmCP	SC	FC	0.03	*	T-test
5	EHDPP	BT	SC	0.46	ns	T-test
5	EHDPP	BT	FC	0.81	ns	T-test
5	EHDPP	SC	FC	0.26	ns	T-test
5	ΣTCPP	BT	SC	0.39	ns	T-test
5	ΣTCPP	BT	FC	0.16	ns	T-test
5	ΣTCPP	SC	FC	0.35	ns	T-test
6	TnBP	BT	SC	0.67	ns	T-test
6	TnBP	BT	FC	0.47	ns	T-test
6	TnBP	SC	FC	0.87	ns	T-test
6	TCEP	BT	SC	0.83	ns	T-test
6	TCEP	BT	FC	0.71	ns	T-test
6	TCEP	SC	FC	0.92	ns	T-test
6	TPhP	BT	SC	0.38	ns	T-test
6	TPhP	BT	FC	0.34	ns	T-test
6	TPhP	SC	FC	0.98	ns	T-test
6	TmCP	BT	SC	0.01	*	T-test
6	TmCP	BT	FC	0.05	ns	T-test
6	TmCP	SC	FC	0.03	*	T-test
6	EHDPP	BT	SC	0.58	ns	T-test
6	EHDPP	BT	FC	0.04	*	T-test
6	EHDPP	SC	FC	0.12	ns	T-test
6	ΣTCPP	BT	SC	0.44	ns	T-test
6	ΣTCPP	BT	FC	0.13	ns	T-test
6	ΣTCPP	SC	FC	0.41	ns	T-test

Table S5: Mass balance results of OPE losses taking as baseline the nominal concentration of 200ng/L. These values are the mean of TmCP and EHDPP compounds. “n.d.” stands for non-detected losses. The losses between the nominal concentration and the 0.2-filtered control account for abiotic factors (sorption to wall, abiotic degradation). The differences between 0.2-filtered and sorption control account for sorption to cells and the PTFE filter (sorption loss), and the reaming losses are due to microbial degradation, here referred to as biotic loss.

experiment	mean_abiotic_loss	mean_sorption_loss	mean_biotic_loss
1	0.06	0.44	0.19
2	0.16	0.23	0.22
4	0.04	0.41	0.16
5	n.d.	0.33	n.d.
6	n.d.	0.27	n.d.

Table S6: List of 28 ASVs with absolute fold change > 1, and their taxonomy, from the Atlantic Ocean experiments (ANTOM-1).

ASV_number	log2 FC	Domain	Kingdom	Phylum	Class	Order	Family	Genus	Species
ASV70_Winogradskyella sp029624125	6.24	Bacteria	Bacteria	Bacteroidota	Bacteroidia	Flavobacteriales	Flavobacteriaceae	Winogradskyella	Winogradskyella sp029624125
ASV269_Mesoflavibacter zeaxanthinifaciens	5.11	Bacteria	Bacteria	Bacteroidota	Bacteroidia	Flavobacteriales	Flavobacteriaceae	Mesoflavibacter	Mesoflavibacter zeaxanthinifaciens
ASV165_UBA2705 sp002690045	4.66	Bacteria	Bacteria	Pseudomonadota	Alphaproteobacteria	Micavibrionales	Micavibrionaceae	UBA2705	UBA2705 sp002690045
ASV116_Sulfitobacter	3.40	Bacteria	Bacteria	Pseudomonadota	Alphaproteobacteria	Rhodobacterales	Rhodobacteraceae	Sulfitobacter	
ASV3_Alteromonas macleodii	2.76	Bacteria	Bacteria	Pseudomonadota	Gammaproteobacteria	Enterobacterales	Alteromonadaceae	Alteromonas	Alteromonas macleodii
ASV1_Alteromonas macleodii	2.61	Bacteria	Bacteria	Pseudomonadota	Gammaproteobacteria	Enterobacterales	Alteromonadaceae	Alteromonas	Alteromonas macleodii
ASV15_Alteromonas stellipolaris	2.02	Bacteria	Bacteria	Pseudomonadota	Gammaproteobacteria	Enterobacterales	Alteromonadaceae	Alteromonas	Alteromonas stellipolaris
ASV22_MED-G13	1.79	Bacteria	Bacteria	Bacteroidota	Bacteroidia	Flavobacteriales	Flavobacteriaceae	MED-G13	
ASV12_Alteromonas stellipolaris	1.79	Bacteria	Bacteria	Pseudomonadota	Gammaproteobacteria	Enterobacterales	Alteromonadaceae	Alteromonas	Alteromonas stellipolaris
ASV121_Halopseudomonas aestuansnigri	1.68	Bacteria	Bacteria	Pseudomonadota	Gammaproteobacteria	Pseudomonadales	Pseudomonadaceae	Halopseudomonas	Halopseudomonas aestuansnigri
ASV47_Alteromonas stellipolaris	1.53	Bacteria	Bacteria	Pseudomonadota	Gammaproteobacteria	Enterobacterales	Alteromonadaceae	Alteromonas	Alteromonas stellipolaris
ASV188_AAA300-D14 sp002715065	1.48	Bacteria	Bacteria	Pseudomonadota	Gammaproteobacteria	Pseudomonadales	Porticococcaceae	AAA300-D14	AAA300-D14 sp002715065
ASV69_MED-G13	1.45	Bacteria	Bacteria	Bacteroidota	Bacteroidia	Flavobacteriales	Flavobacteriaceae	MED-G13	
ASV281_Marinisoma sp028140795	1.00	Bacteria	Bacteria	Marinisomatota	Marinisomatia	Marinisomatales	Marinisomataceae	Marinisoma	Marinisoma sp028140795
ASV162_Acinetobacter junii	-1.01	Bacteria	Bacteria	Pseudomonadota	Gammaproteobacteria	Pseudomonadales	Moraxellaceae	Acinetobacter	Acinetobacter junii
ASV10_Prochlorococcus_A marinus_AD	-1.03	Bacteria	Bacteria	Cyanobacteriota	Cyanobacteriia	PCC-6307	Cyanobiaceae	Prochlorococcus_A	Prochlorococcus_A marinus_AD
ASV27_Actinomarina	-1.07	Bacteria	Bacteria	Actinomycetota	Acidimicrobia	Actinomarinales	Actinomarinaceae	Actinomarina	
ASV4_Prochlorococcus_A marinus_AB	-1.10	Bacteria	Bacteria	Cyanobacteriota	Cyanobacteriia	PCC-6307	Cyanobiaceae	Prochlorococcus_A	Prochlorococcus_A marinus_AB
ASV31_Parasynochococcus marenigrum	-1.14	Bacteria	Bacteria	Cyanobacteriota	Cyanobacteriia	PCC-6307	Cyanobiaceae	Parasynochococcus	Parasynochococcus marenigrum
ASV71_Pelagibacter_A sp003282965	-1.17	Bacteria	Bacteria	Pseudomonadota	Alphaproteobacteria	Pelagibacterales	Pelagibacteraceae	Pelagibacter_A	Pelagibacter_A sp003282965
ASV78_Pseudalteromonas sp002685175	-1.38	Bacteria	Bacteria	Pseudomonadota	Gammaproteobacteria	Enterobacterales	Alteromonadaceae	Pseudoalteromonas	Pseudoalteromonas sp002685175
ASV143_Actinomarina	-1.39	Bacteria	Bacteria	Actinomycetota	Acidimicrobia	Actinomarinales	Actinomarinaceae	Actinomarina	
ASV291_Cyanobacteriales	-1.50	Bacteria	Bacteria	Cyanobacteriota	Cyanobacteriia	Cyanobacteriales	Actinomarinaceae	Actinomarina	
ASV73_CACIUG01	-1.58	Bacteria	Bacteria	Pseudomonadota	Alphaproteobacteria	Rhodobacterales	Rhodobacteraceae	CACIUG01	
ASV65_Pelagibacter sp003213015	-1.62	Bacteria	Bacteria	Pseudomonadota	Alphaproteobacteria	Pelagibacterales	Pelagibacteraceae	Pelagibacter	Pelagibacter sp003213015
ASV330_Actinomarina sp02519845	-1.96	Bacteria	Bacteria	Actinomycetota	Acidimicrobia	Actinomarinales	Actinomarinaceae	Actinomarina	Actinomarina sp02519845
ASV49_HIMB59	-2.24	Bacteria	Bacteria	Pseudomonadota	Alphaproteobacteria	HIMB59	HIMB59	HIMB59	
ASV200_UBA1014 sp001469005	-2.67	Bacteria	Bacteria	SAR324	SAR324	SAR324	NAC60-12	UBA1014	UBA1014 sp001469005

Table S7: List of 19 ASVs with absolute fold change > 1, and their taxonomy, from the Sothern Ocean experiments (ANTOM-2).

ASV_number	log2 FC	Domain	Kingdom	Phylum	Class	Order	Family	Genus	Species
ASV428_Moritella sp018219455	5.41	Bacteria	Bacteria	Pseudomonadota	Gammaaproteobacteria	Enterobacterales	Moritellaceae	Moritella	Moritella sp018219455
ASV53_Polaribacter sp019278525	2.54	Bacteria	Bacteria	Bacteroidota	Bacteroidia	Flavobacteriales	Flavobacteriaceae	Polaribacter	Polaribacter sp019278525
ASV83_Polaribacter irgensii	2.43	Bacteria	Bacteria	Bacteroidota	Bacteroidia	Flavobacteriales	Flavobacteriaceae	Polaribacter	Polaribacter irgensii
ASV224_UBA6772 sp028110365	2.12	Bacteria	Bacteria	Bacteroidota	Bacteroidia	Flavobacteriales	UBA7430	UBA6772	UBA6772 sp028110365
ASV117_Rhodobacteriales	2.11	Bacteria	Bacteria	Pseudomonadota	Alphaproteobacteria	Rhodobacterales	Rhodobacteraceae	Patrisocius	Patrisocius sp913048215
ASV35_Patrisocius sp913048215	1.80	Bacteria	Bacteria	Bacteroidota	Bacteroidia	Flavobacteriales	Flavobacteriaceae	Polaribacter	
ASV60_Polaribacter	1.67	Bacteria	Bacteria	Bacteroidota	Bacteroidia	Flavobacteriales	Flavobacteriaceae		
ASV120_Yoonia sp905182645	1.66	Bacteria	Bacteria	Pseudomonadota	Alphaproteobacteria	Rhodobacterales	Rhodobacteraceae	Yoonia	Yoonia sp905182645
ASV204_HTC2207	1.60	Bacteria	Bacteria	Pseudomonadota	Gammaaproteobacteria	Pseudomonadales	Porticoccaceae	HTCC2207	
ASV118_Rhodobacteriales	1.59	Bacteria	Bacteria	Pseudomonadota	Alphaproteobacteria	Rhodobacterales	Rhodobacteraceae		
ASV97_UBA10364	1.00	Bacteria	Bacteria	Bacteroidota	Bacteroidia	Flavobacteriales	Schleiferiaceae	UBA10364	Planktomarina sp017856985
ASV66_Planktomarina sp017856985	-1.43	Bacteria	Bacteria	Pseudomonadota	Alphaproteobacteria	Rhodobacterales	Rhodobacteraceae	Planktomarina	
ASV88_Cyanobacteriales	-1.55	Bacteria	Bacteria	Cyanobacteriota	Cyanobacteriia	Cyanobacteriales			
ASV26_Cyanobacteriia	-2.93	Bacteria	Bacteria	Cyanobacteriota	Cyanobacteriia				
ASV38_Cyanobacteriia	-3.11	Bacteria	Bacteria	Cyanobacteriota	Cyanobacteriia				
ASV33_Cyanobacteriales	-3.23	Bacteria	Bacteria	Cyanobacteriota	Cyanobacteriia	Cyanobacteriales			
ASV39_Cyanobacteriia	-3.46	Bacteria	Bacteria	Cyanobacteriota	Cyanobacteriia				
ASV187_Cyanobacteriia	-3.47	Bacteria	Bacteria	Cyanobacteriota	Cyanobacteriia				
ASV448_Cyanobacteriales	-4.11	Bacteria	Bacteria	Cyanobacteriota	Cyanobacteriia	Cyanobacteriales			

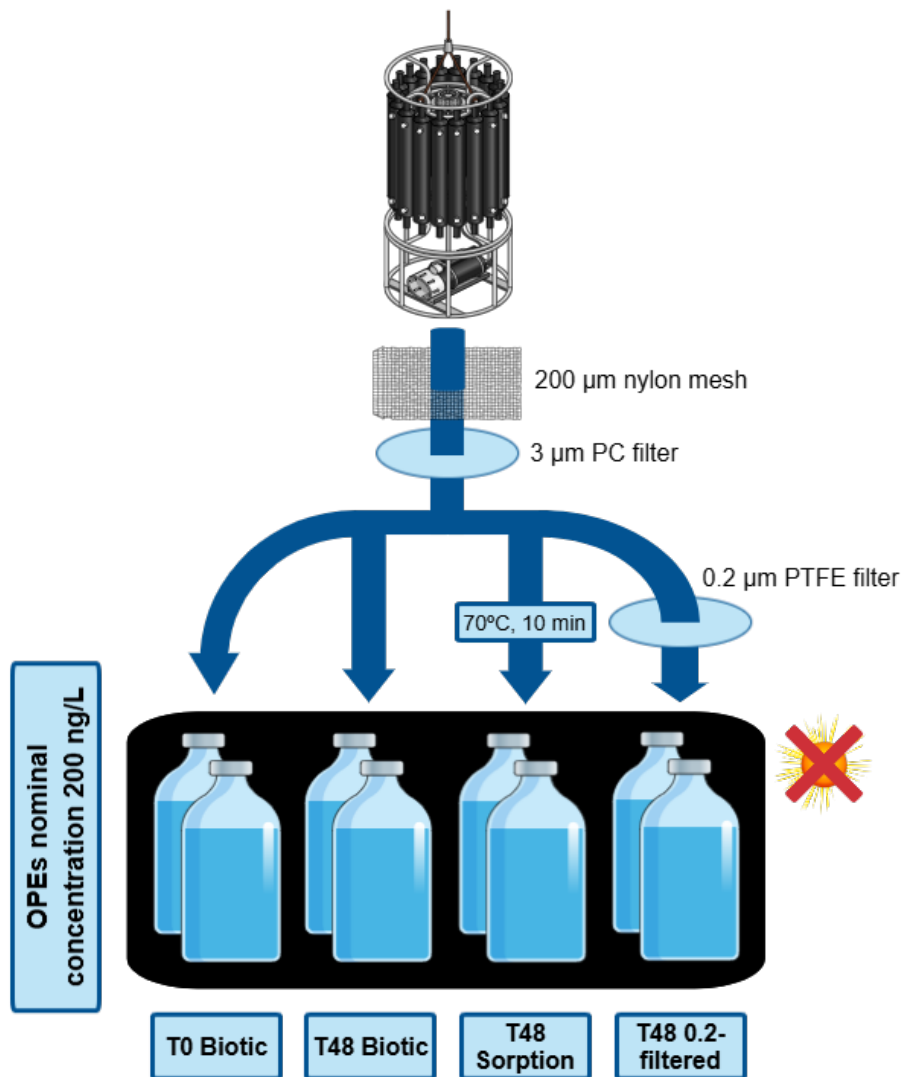


Figure S1: Experimental setup. Water was pre-filtered using a 3µm pore-size polycarbonate (PC) filter in order to exclude grazers and particles as potential sources of stochastic variability between replicates. PTFE stands for polytetrafluoroethylene.

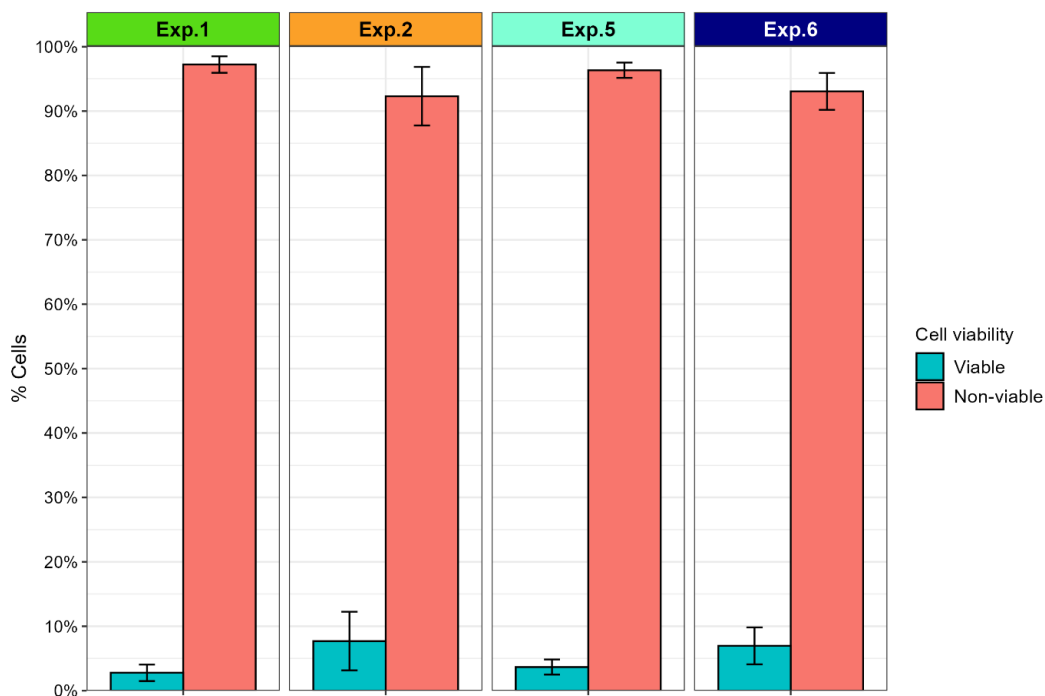


Figure S2: NADS results showing the percentage of viable and non-viable cells in the analyzed sorption controls.

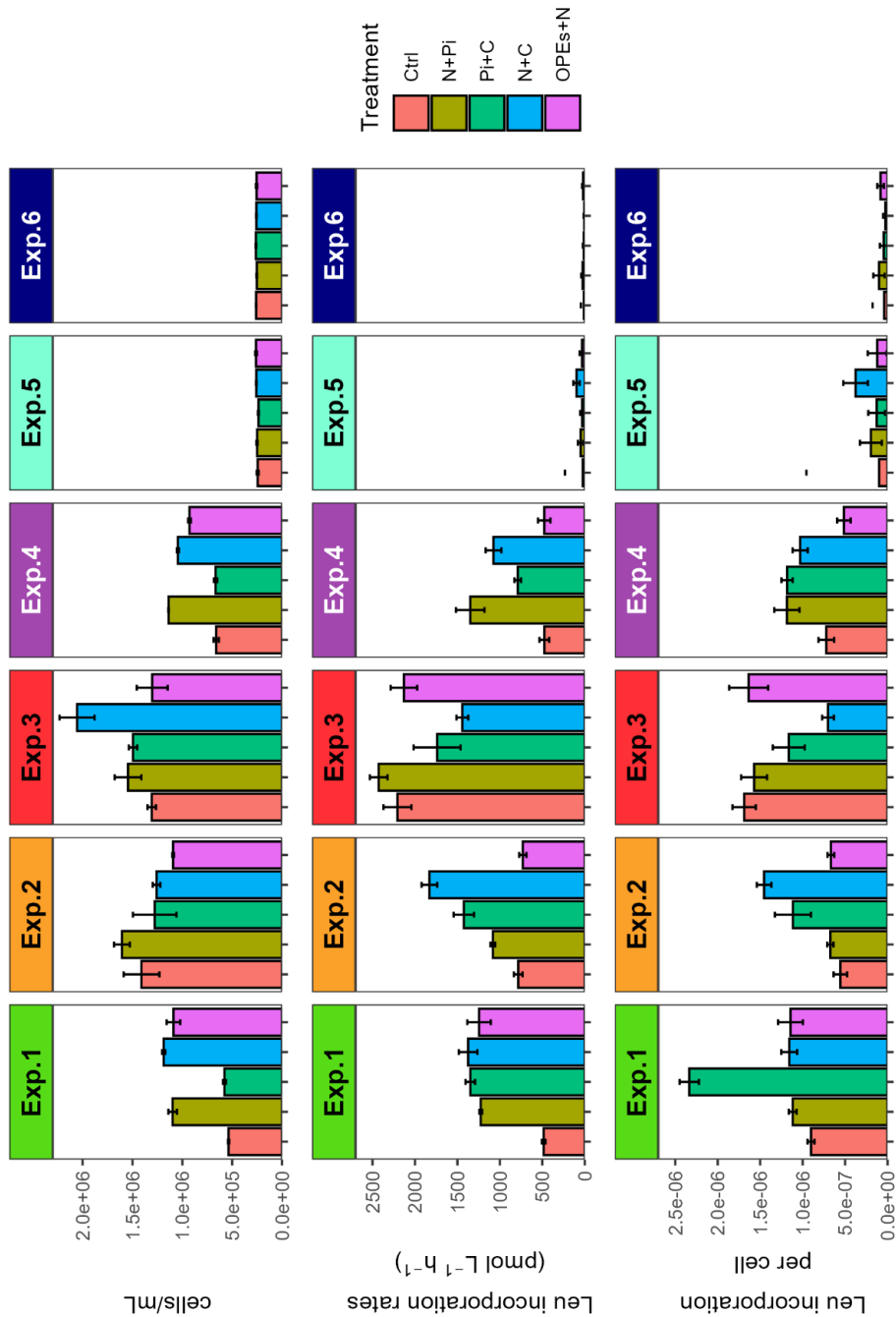


Figure S3: Nutrient limitation experiments. The upper plot shows bacterial abundance results, the middle plot shows bacterial production results as Leucine incorporation rates per liter, and the lower plot shows bacterial production results as Leucine incorporation rates per cell.

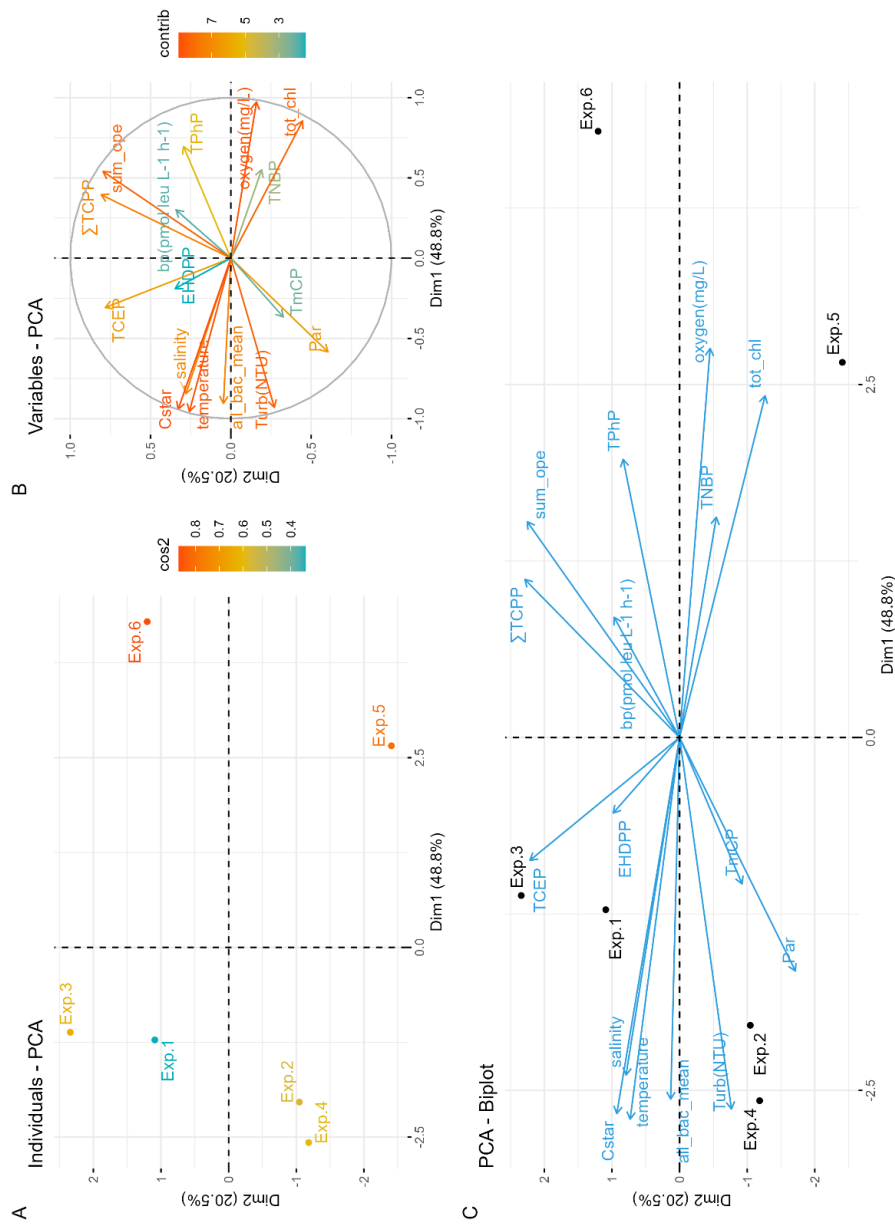


Figure S4: Results of the ancillary data PCA analysis. A) Graph of individuals, where individuals with a similar profile are grouped together. B) Graph of variables. Positive correlated variables point to the same side of the plot. Negative correlated variables point to opposite sides of the graph. C) Biplot of individuals and variables

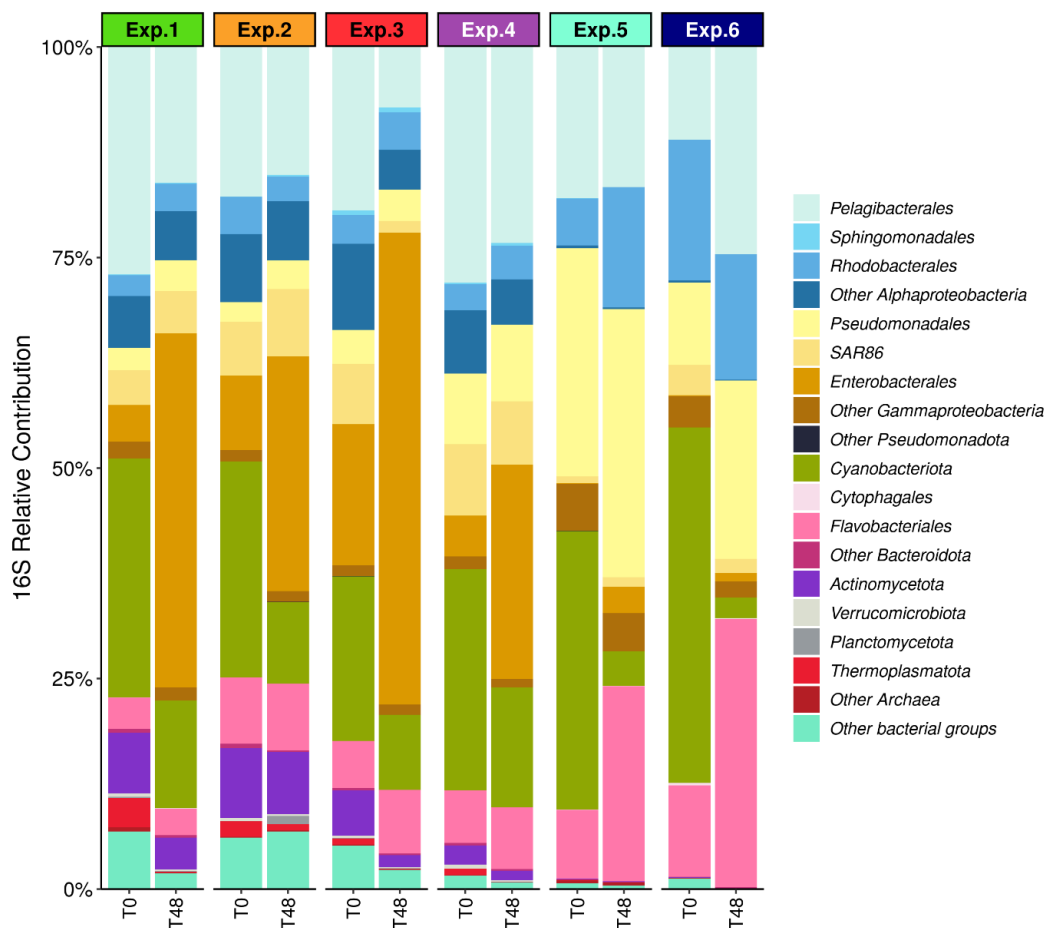


Figure S5: Structure of the bacterial community for each experiment at T0 (initial time biotic treatment) and T48 (48-hour incubation biotic treatment).

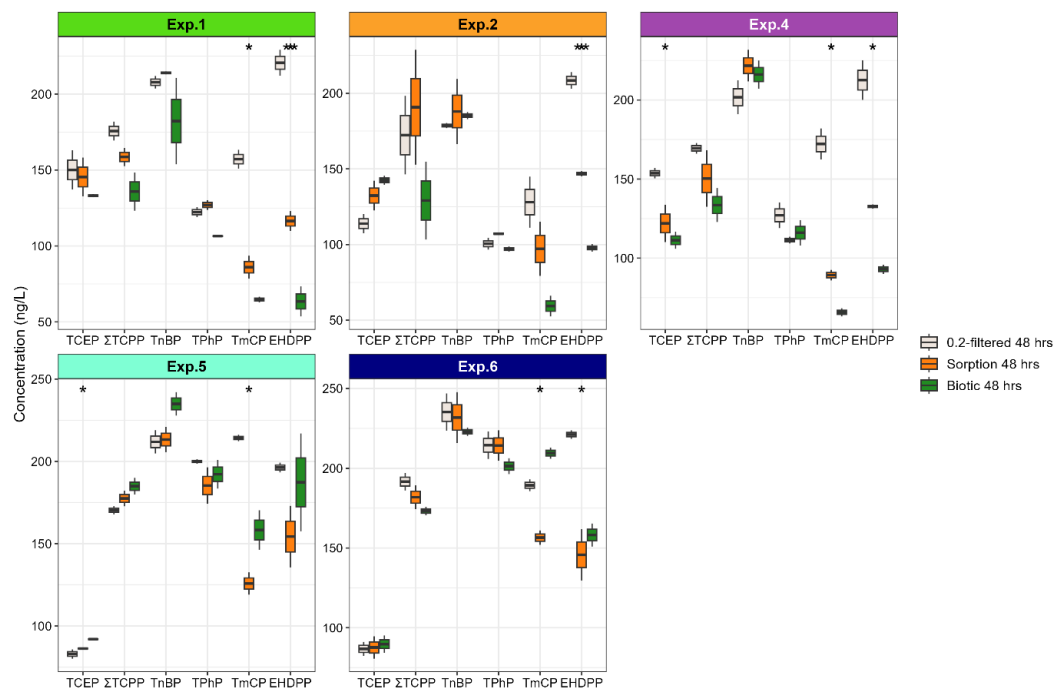


Figure S6: Boxplots showing individual OPE concentrations at each experiment. Green boxes represent 48-hour biotic treatments (viable bacteria 48-hour incubation treatment), orange boxes represent 48-hour sorption controls (non-viable heat-treated bacteria 48-hour treatment), and white boxes represent 48-hour 0.2-filtered controls (3 and 0.2 μm filtered water 48-hour treatment).

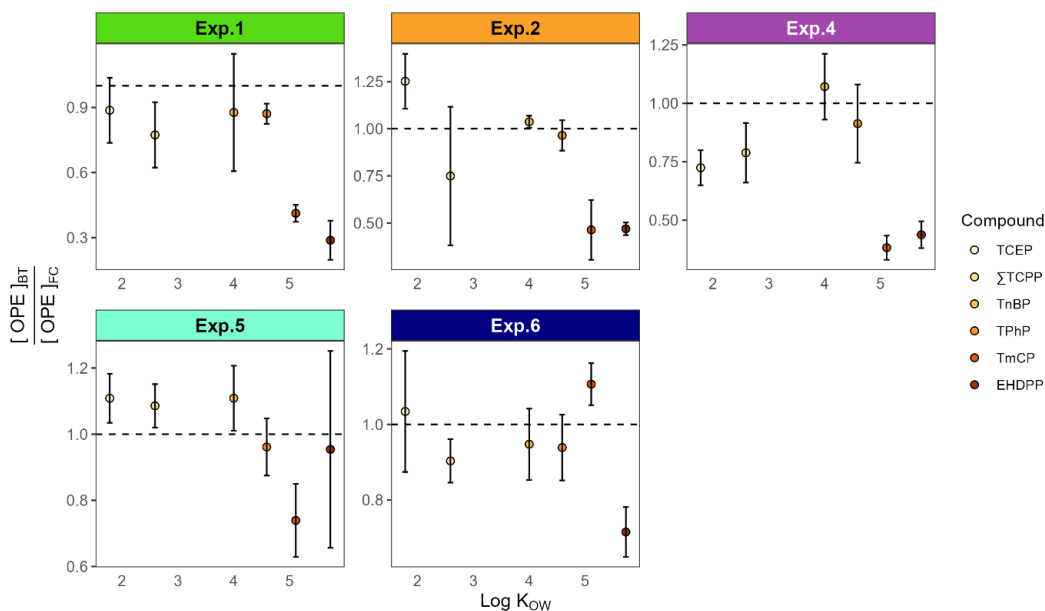


Figure S7: Concentration ratios of OPE compounds between 48-hour biotic treatments (BT) and 0.2-filtered controls (FC) across different experiments. The dashed line indicates a ratio of 1, and error bars represent the 95% confidence interval for each measurement.

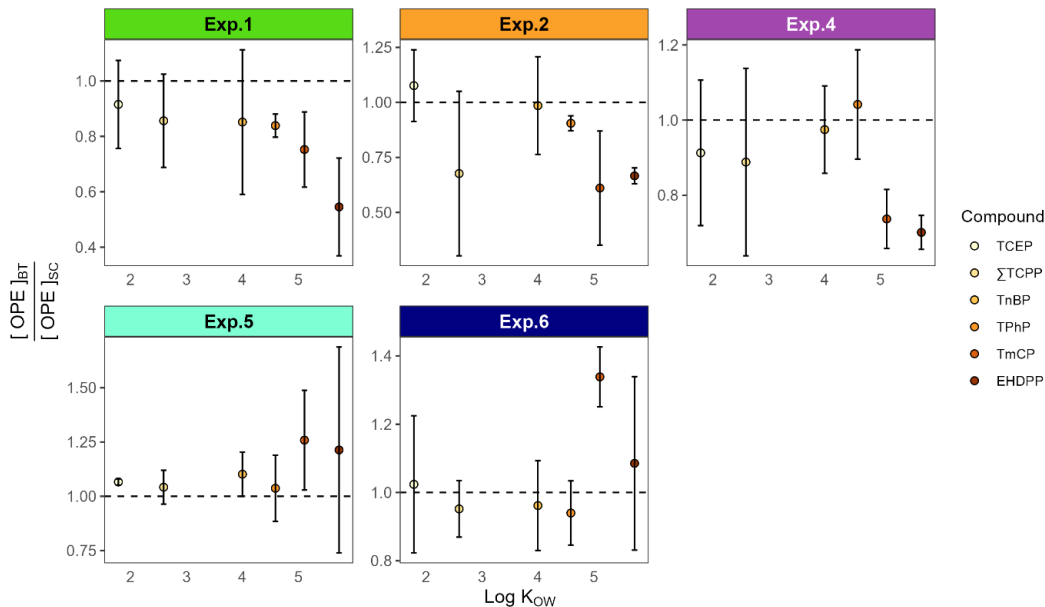


Figure S8: Concentration ratios of OPE compounds between 48-hour biotic treatments (BT) and sorption controls (SC) across different experiments. The dashed line indicates a ratio of 1, and error bars represent the 95% confidence interval for each measurement.

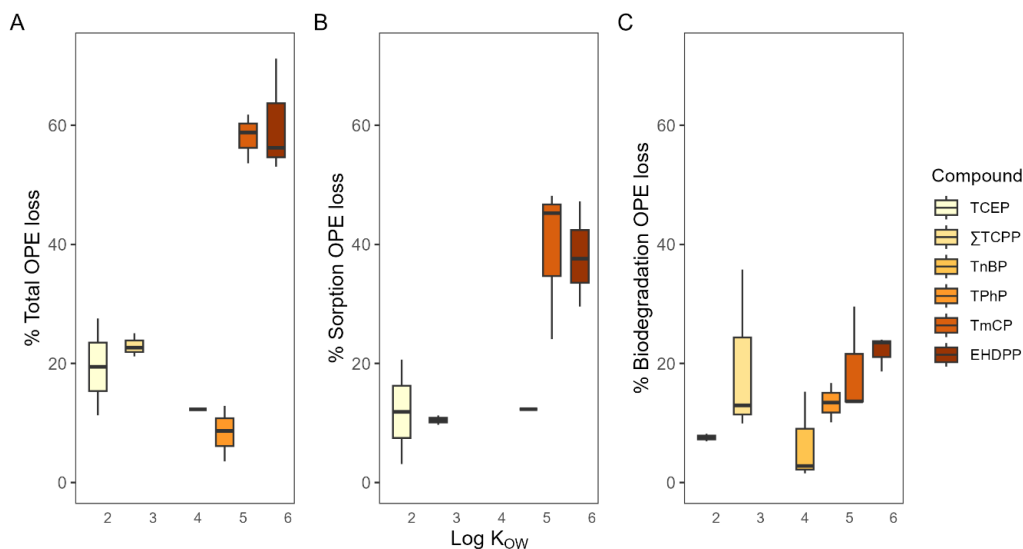


Figure S9: Percentage of individual OPE compound concentration loss in the Atlantic Ocean experiments (Exp.1, Exp.2 and Exp.4) due to: A) partitioning to bacteria cells and other particulate organic matter < 3 μm + biodegradation by bacteria; B) only partitioning to bacteria cells and other particulate organic matter < 3 μm ; C) only biodegradation by bacteria. All the percentages are calculated using the 0.2-filtered control concentrations as baseline measurements.

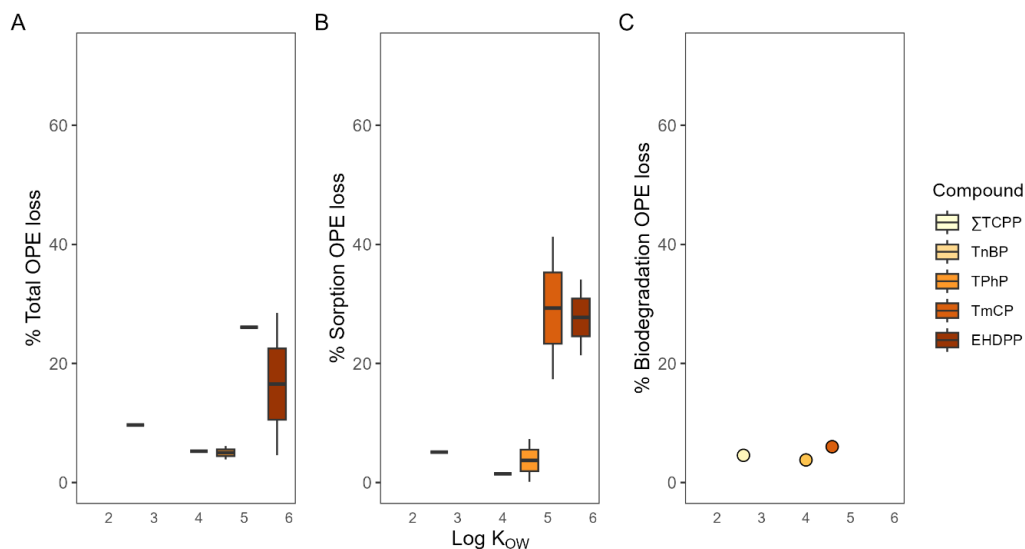


Figure S10: Percentage of individual OPE compound concentration loss in the Southern Ocean experiments (Exp.5 and Exp.6) due to: A) partitioning to bacteria cells and other particulate organic matter < 3 μm + biodegradation by bacteria; B) only partitioning to bacteria cells and other particulate organic matter < 3 μm; C) only biodegradation by bacteria. All the percentages are calculated using the 0.2-filtered control concentrations as baseline measurements.

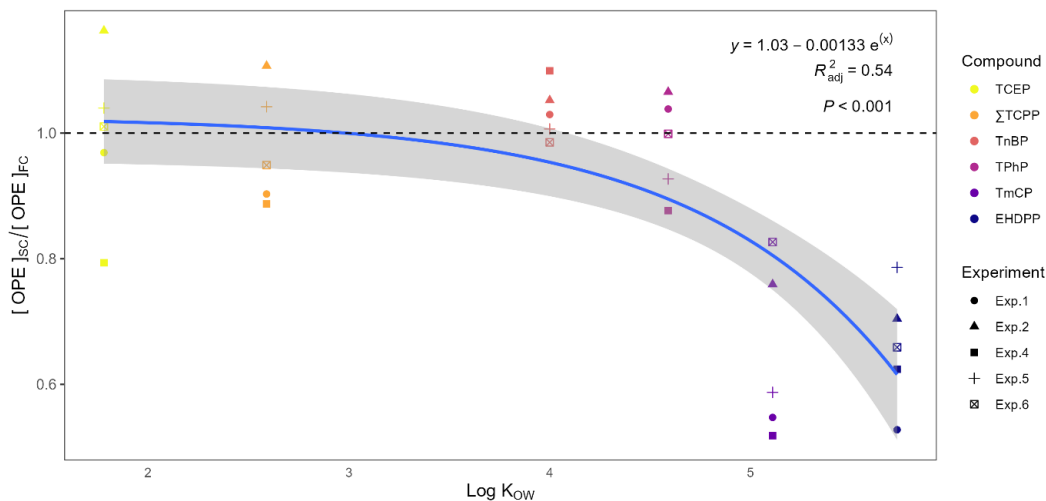


Figure S11: Ratios between sorption control (SC) and 0.2-filtered control (FC) OPE concentrations vs octanol-water partition coefficient (K_{OW}). As the hydrophobicity of the compound increases, the ratio decreases following an exponential curve.

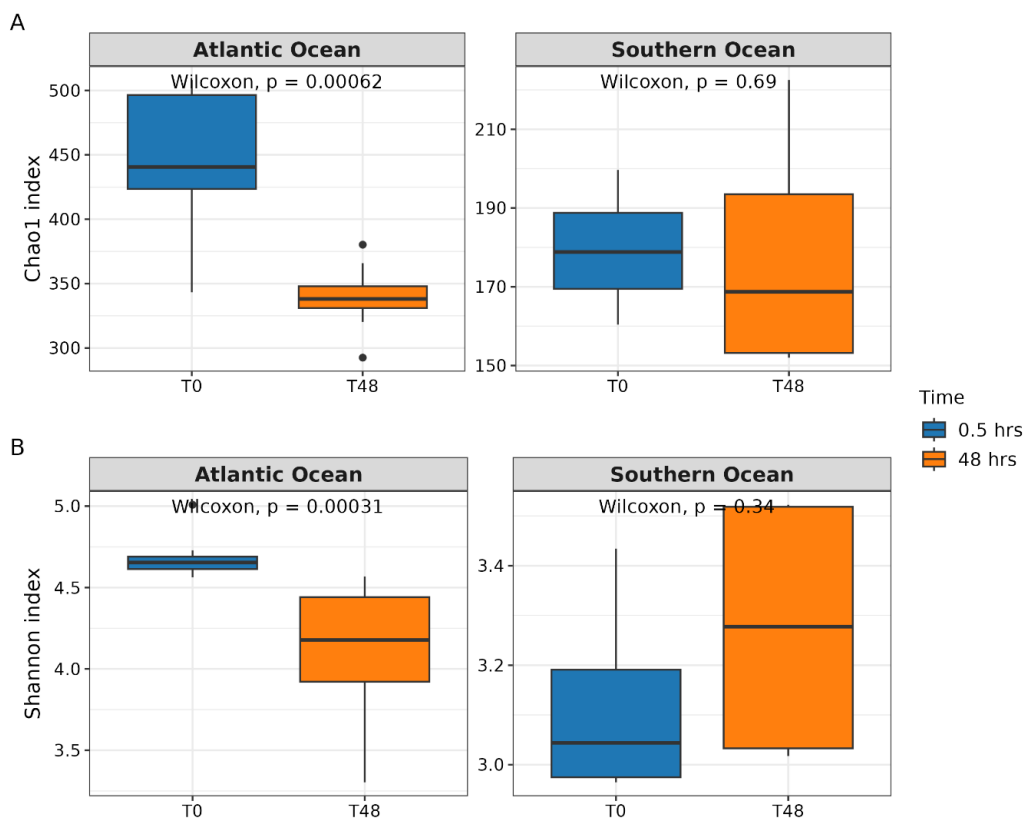


Figure S12: Alpha diversity indexes per ocean and incubation time (T0, initial time biotic treatment; T48, 48-hour incubation biotic treatment): A) Chao1 index, an indicator of species richness (total number of ASVs in a sample) that is sensitive to rare ASVs (singletons and doubletons). B) Shannon index, a measure of diversity that combines species richness and their relative abundance. Significant differences were addressed by a Wilcoxon test.

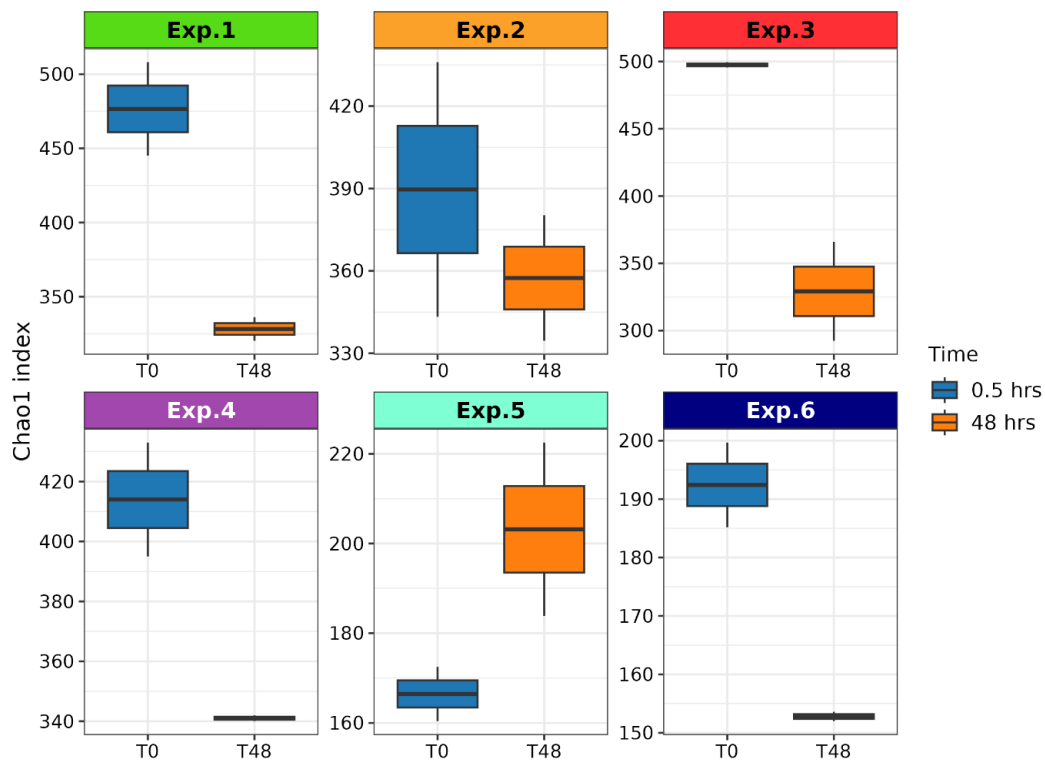


Figure S13: Chao1 indexes per experiment and incubation time (T0, initial time biotic treatment; T48 ,48-hour incubation biotic treatment).

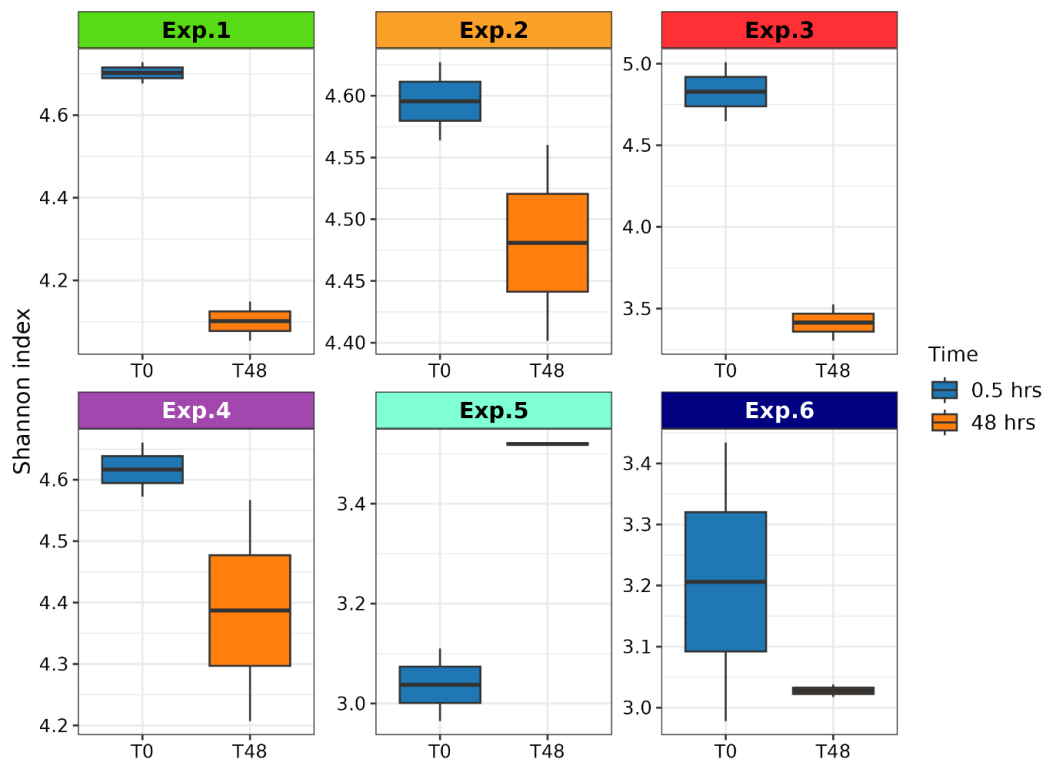


Figure S14: Shannon indexes per experiment and incubation time (T0, initial time biotic treatment; T48 ,48-hour incubation biotic treatment).

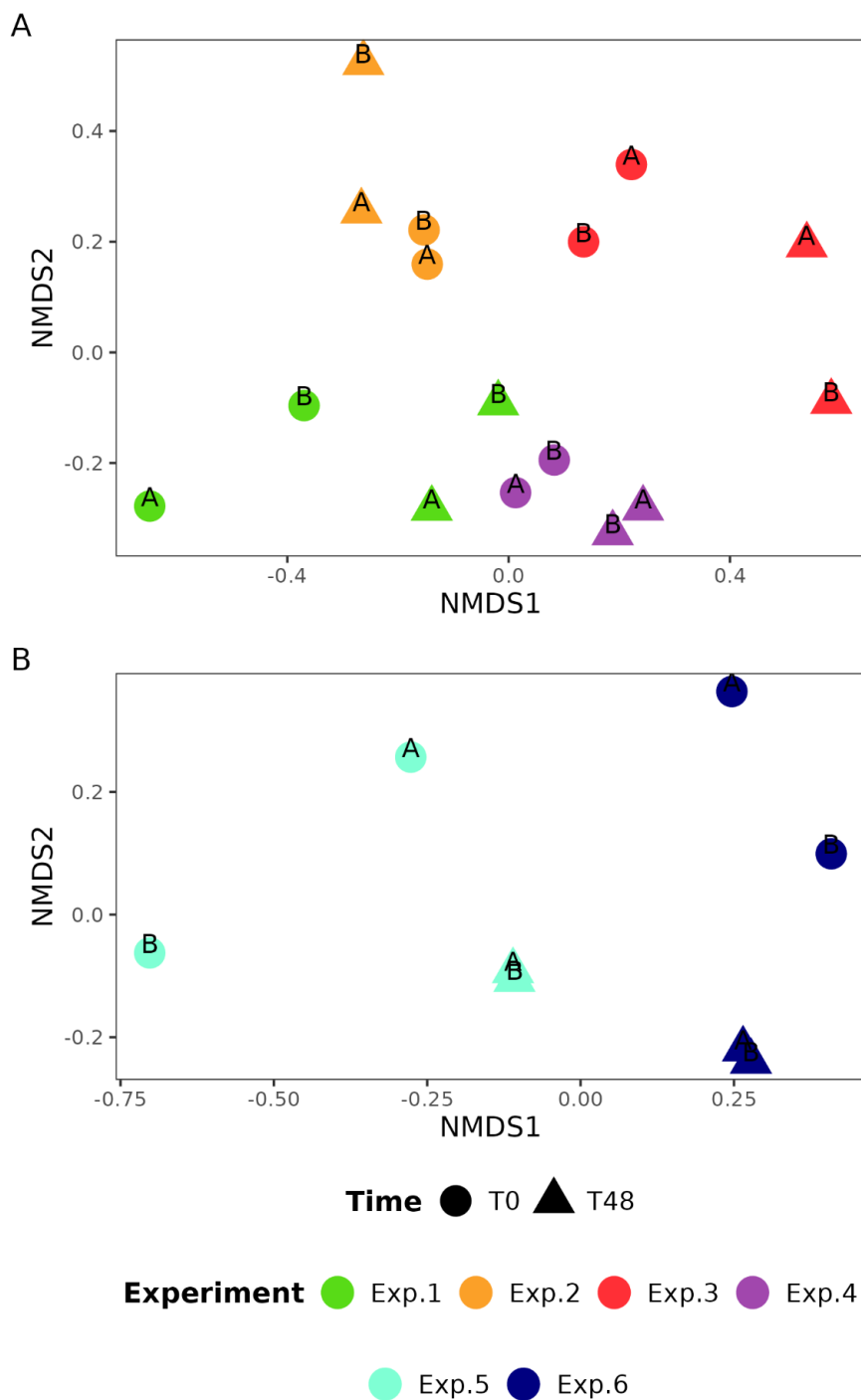


Figure S15: NMDS analysis for dissimilarities in the microbial community composition at the different sampling times (T0, initial time biotic treatment; T48 ,48-hour incubation biotic treatment) per ocean: A) Atlantic Ocean experiments, B) Southern Ocean experiments.

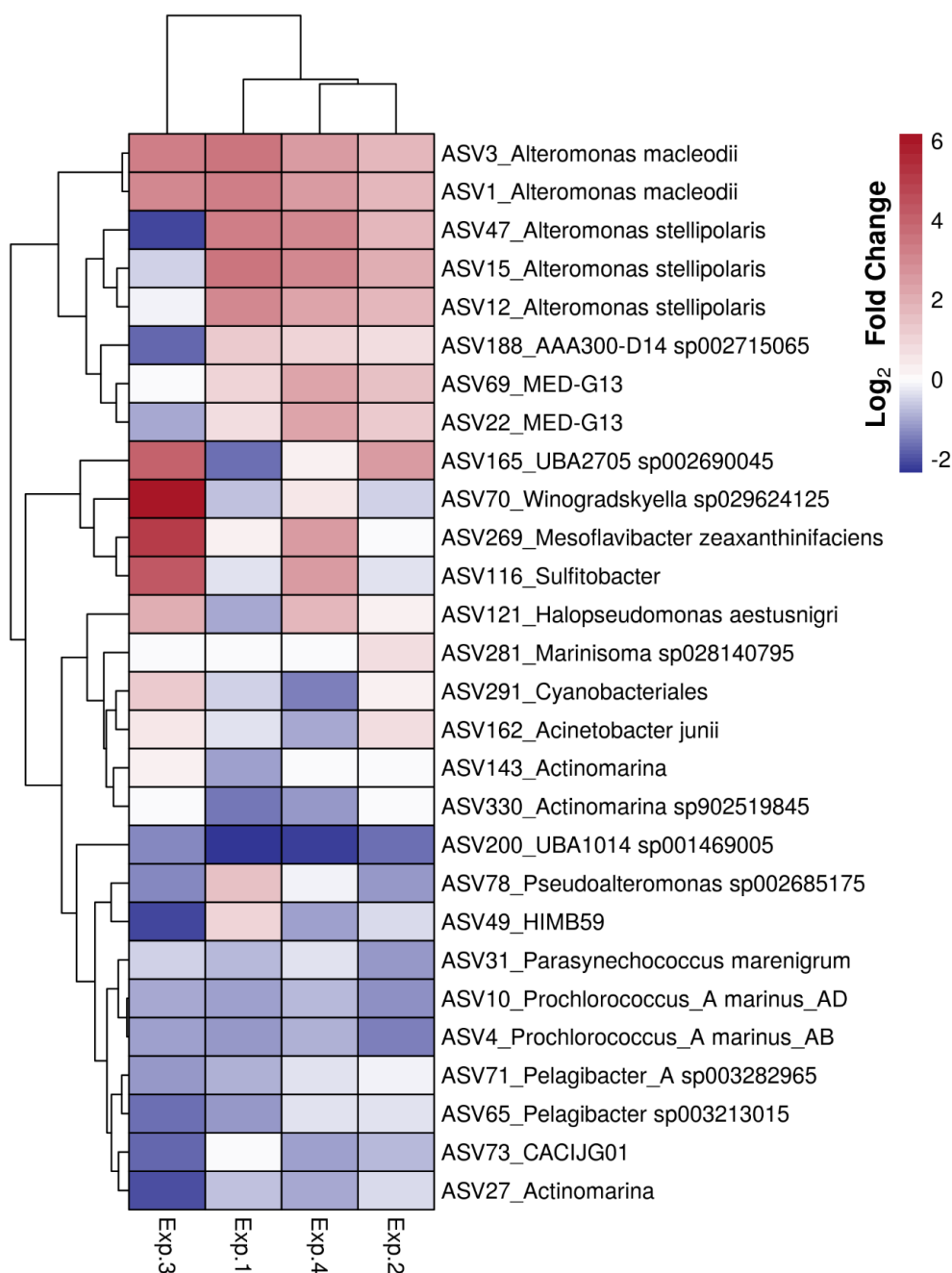


Figure S16: Heatmap showing the Log₂ fold change of the relative abundance of each of the 28 ASVs selected to explain the microbial community shift in the Atlantic Ocean experiments. The taxonomic label represents the most detailed classification available for that specific ASV.

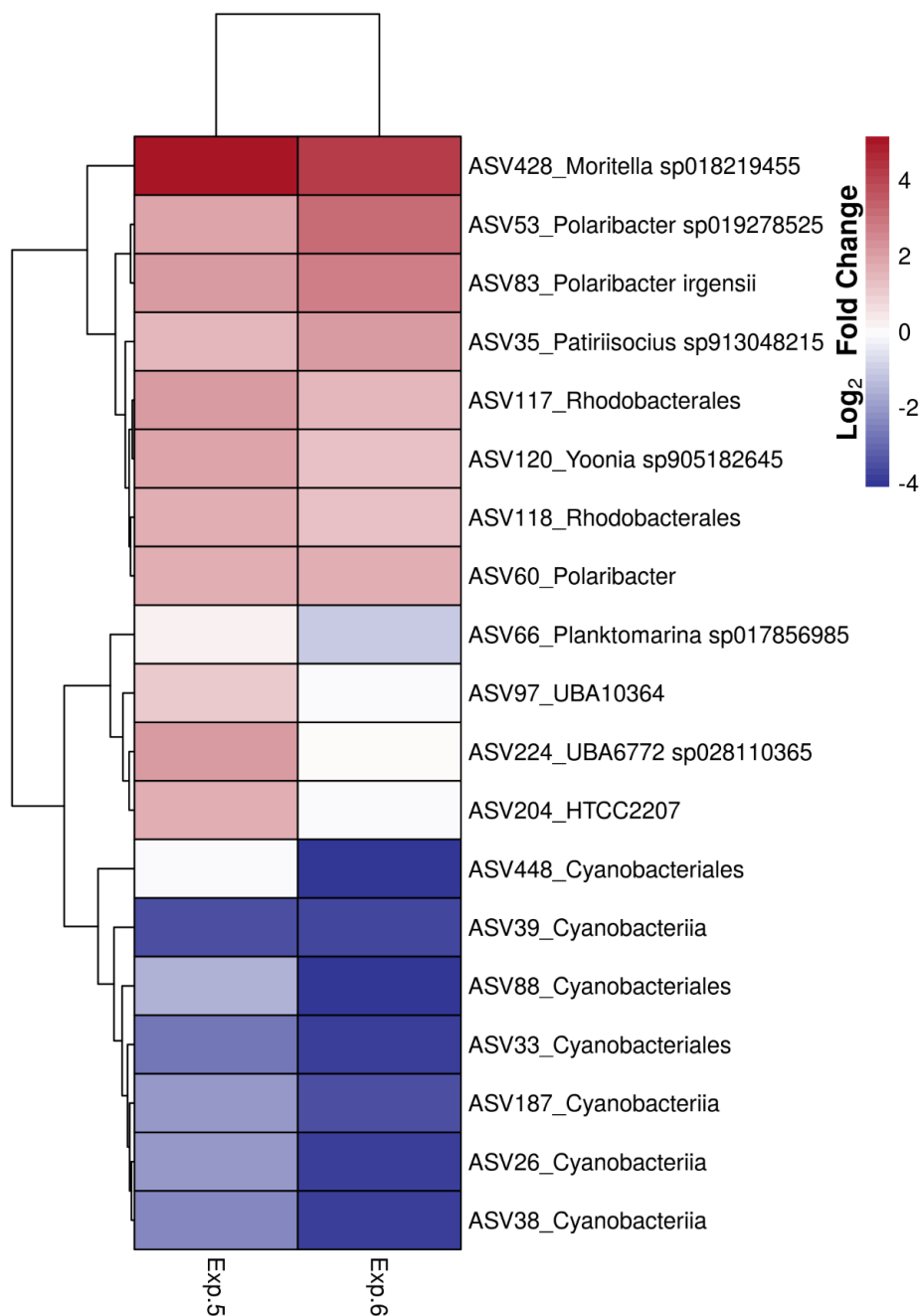


Figure S17: Heatmap showing the Log₂ fold change of the relative abundance of each of the 19 ASVs selected to explain the microbial community shift in the Southern Ocean experiments. The taxonomic label represents the most detailed classification available for that specific ASV.

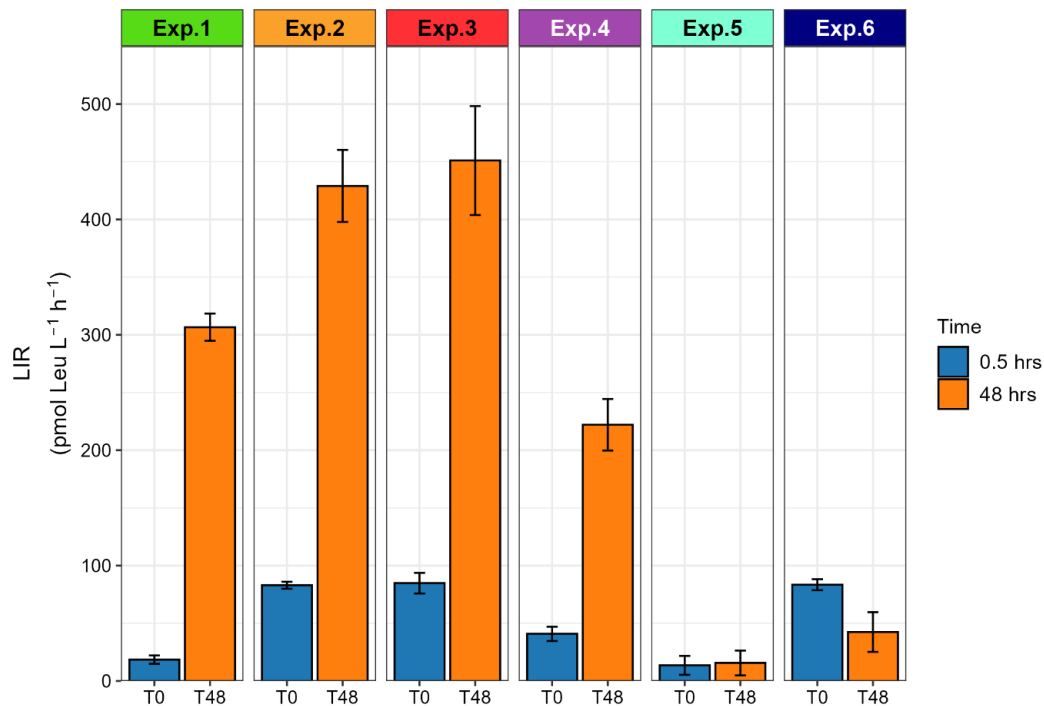


Figure S18: Barplots of the bacterial production results for each experiment and incubation time (T0, initial time biotic treatment; T48 ,48-hour incubation biotic treatment), expressed as the Leucine incorporation rates per liter.

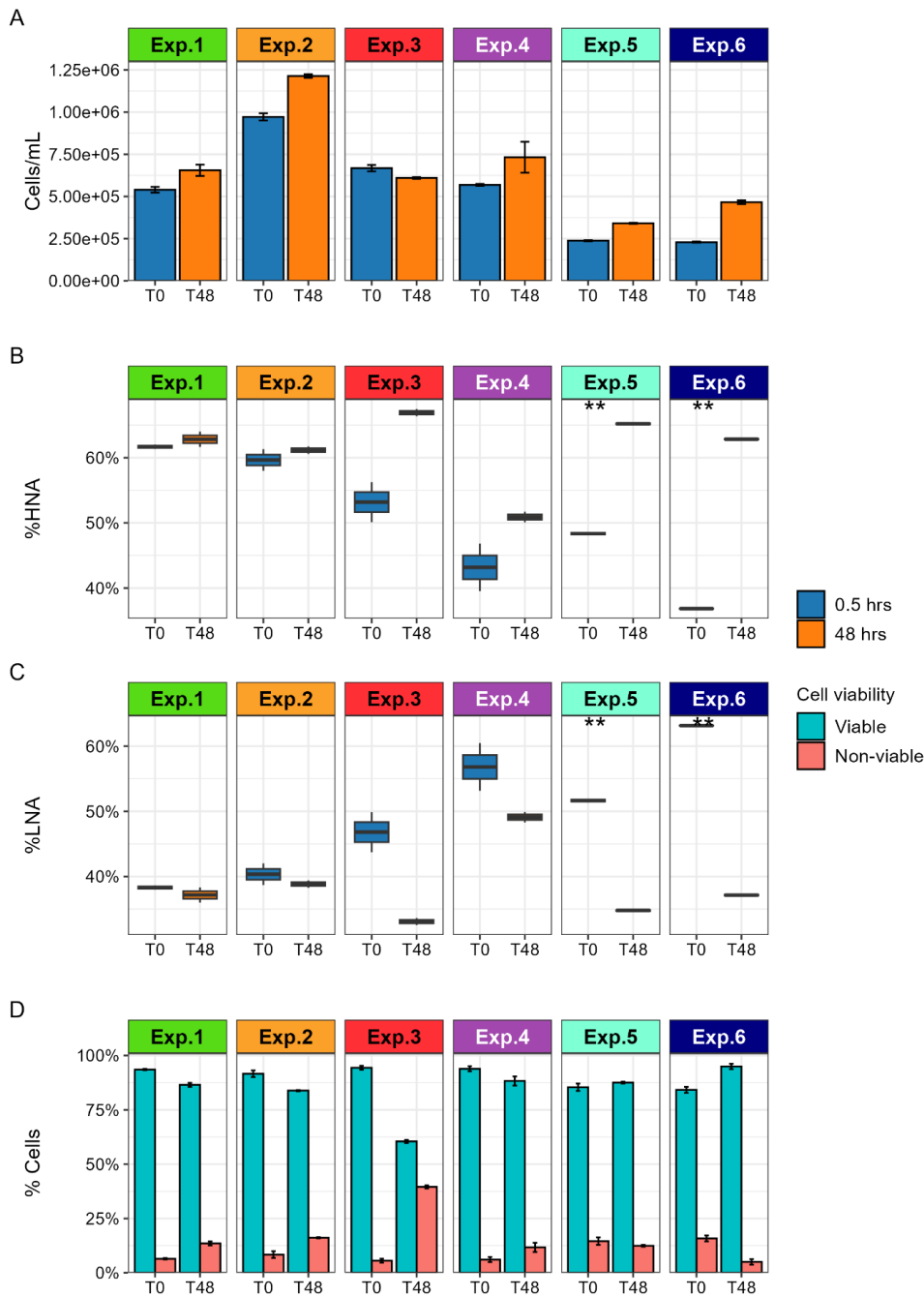


Figure S19: Results of bacterial abundance and cell viability for each experiment and incubation time (T0, initial time biotic treatment; T48, 48-hour incubation biotic treatment). A) Total heterotrophic bacterial abundance in cells/mL. B) Percentage of high-nucleic acid-containing cells. C) Percentage of low-nucleic acid-containing cells. D) Percentage of viable (blue) and non-viable (red) cells.

References

- (1) Strickland, J. D. H.; Parsons, T. R. Fluorometric Determination of Chlorophylls. In *A Practical Handbook of Seawater Analysis*.; Bulletin Fisheries Research Board of Canada, 1972; Vol. Nr. 167, pp 201–206.
- (2) Fernández-Pinos, M.-C.; Casado, M.; Caballero, G.; Zinser, E. R.; Dachs, J.; Piña, B. Clade-Specific Quantitative Analysis of Photosynthetic Gene Expression in *Prochlorococcus*. *PLoS One* **2015**, *10* (8), e0133207. <https://doi.org/10.1371/journal.pone.0133207>.
- (3) Parada, A. E.; Needham, D. M.; Fuhrman, J. A. Every Base Matters: Assessing Small Subunit rRNA Primers for Marine Microbiomes with Mock Communities, Time Series and Global Field Samples. *Environ Microbiol* **2016**, *18* (5), 1403–1414. <https://doi.org/10.1111/1462-2920.13023>.
- (4) Ewels, P. A.; Peltzer, A.; Fillinger, S.; Patel, H.; Alneberg, J.; Wilm, A.; Garcia, M. U.; Di Tommaso, P.; Nahnsen, S. The Nf-Core Framework for Community-Curated Bioinformatics Pipelines. *Nat Biotechnol* **2020**, *38* (3), 276–278. <https://doi.org/10.1038/s41587-020-0439-x>.
- (5) Straub, D.; Blackwell, N.; Langarica-Fuentes, A.; Peltzer, A.; Nahnsen, S.; Kleindienst, S. Interpretations of Environmental Microbial Community Studies Are Biased by the Selected 16S rRNA (Gene) Amplicon Sequencing Pipeline. *Front Microbiol* **2020**, *11*. <https://doi.org/10.3389/fmicb.2020.550420>.
- (6) Ewels, P.; Magnusson, M.; Lundin, S.; Käller, M. MultiQC: Summarize Analysis Results for Multiple Tools and Samples in a Single Report. *Bioinformatics* **2016**, *32* (19), 3047–3048. <https://doi.org/10.1093/bioinformatics/btw354>.
- (7) Martin, M. Cutadapt Removes Adapter Sequences from High-Throughput Sequencing Reads. *EMBnet J* **2011**, *17* (1), 10. <https://doi.org/10.14806/ej.17.1.200>.
- (8) Callahan, B. J.; McMurdie, P. J.; Rosen, M. J.; Han, A. W.; Johnson, A. J. A.; Holmes, S. P. DADA2: High-Resolution Sample Inference from Illumina Amplicon Data. *Nat Methods* **2016**, *13* (7), 581–583. <https://doi.org/10.1038/nmeth.3869>.
- (9) Lundin, D.; Andersson, A. SBDI Sativa Curated 16S GTDB Database. 2021. <https://doi.org/https://doi.org/10.17044/scilifelab.14869077.v7>.
- (10) Gasol, J. M.; Morán, X. A. G. Flow Cytometric Determination of Microbial Abundances and Its Use to Obtain Indices of Community Structure and Relative Activity; 2015; pp 159–187. https://doi.org/10.1007/8623_2015_139.
- (11) Novo, D. J.; Perlmutter, N. G.; Hunt, R. H.; Shapiro, H. M. Multiparameter Flow Cytometric Analysis of Antibiotic Effects on Membrane Potential, Membrane Permeability, and Bacterial Counts of *Staphylococcus Aureus* and *Micrococcus Luteus*. *Antimicrob Agents Chemother* **2000**, *44* (4), 827–834. <https://doi.org/10.1128/AAC.44.4.827-834.2000>.
- (12) Smith, D. C.; Azam, F. A Simple, Economical Method for Measuring Bacterial Protein Synthesis Rates in Seawater Using 3H-Leucine; 1992.
- (13) Aksu, Z. Application of Biosorption for the Removal of Organic Pollutants: A Review. *Process Biochemistry* **2005**, *40* (3–4), 997–1026. <https://doi.org/10.1016/j.procbio.2004.04.008>.

- (14) Falcioni, T.; Papa, S.; Gasol, J. M. Evaluating the Flow-Cytometric Nucleic Acid Double-Staining Protocol in Realistic Situations of Planktonic Bacterial Death. *Appl Environ Microbiol* **2008**, *74* (6), 1767–1779. <https://doi.org/10.1128/AEM.01668-07>.
- (15) Maranger, R.; del Giorgio, P.; Bird, D. Accumulation of Damaged Bacteria and Viruses in Lake Water Exposed to Solar Radiation. *Aquatic Microbial Ecology* **2002**, *28*, 213–227. <https://doi.org/10.3354/ame028213>.
- (16) Little, B.; Gerchakov, S.; Udey, L. A Method for Sterilization of Natural Seawater. *J Microbiol Methods* **1987**, *7* (4–5), 193–200. [https://doi.org/10.1016/0167-7012\(87\)90040-6](https://doi.org/10.1016/0167-7012(87)90040-6).
- (17) Enzinger, R. M.; Cooper, R. C. Role of Bacteria and Protozoa in the Removal of Escherichia Coli from Estuarine Waters. *Appl Environ Microbiol* **1976**, *31* (5), 758–763. <https://doi.org/10.1128/aem.31.5.758-763.1976>.
- (18) Gasol, J.; Morán, X. Effects of Filtration on Bacterial Activity and Picoplankton Community Structure as Assessed by Flow Cytometry. *Aquatic Microbial Ecology* **1999**, *16*, 251–264. <https://doi.org/10.3354/ame016251>.
- (19) Liu, J.; Li, B.; Wang, Y.; Zhang, G.; Jiang, X.; Li, X. Passage and Community Changes of Filterable Bacteria during Microfiltration of a Surface Water Supply. *Environ Int* **2019**, *131*, 104998. <https://doi.org/10.1016/j.envint.2019.104998>.
- (20) Gasol, J.; del Giorgio, P.; Massana, R.; Duarte, C. Active versus Inactive Bacteria: Size-Dependence in a Coastal Marine Plankton Community. *Mar Ecol Prog Ser* **1995**, *128*, 91–97. <https://doi.org/10.3354/meps128091>.
- (21) Trilla-Prieto, N.; Iriarte, J.; Berrojalbiz, N.; Casas, G.; Sobrino, C.; Vila-Costa, M.; Jiménez, B.; Dachs, J. Enrichment of Organophosphate Esters in the Sea Surface Microlayer from the Atlantic and Southern Oceans. *Environ Sci Technol Lett* **2024**. <https://doi.org/10.1021/acs.estlett.4c00636>.
- (22) Oksanen, J.; Simpson, G. L.; Blanchet, F. G.; Kindt, R.; Legendre, P.; Minchin, P. R.; O'Hara, R. B.; Solymos, P.; Stevens, M. H. H. *Vegan: Community Ecology Package*. 2020.





CHAPTER 6

Occurrence of Aromatic Hydrocarbon-Degrading Genes in the Temperate and Tropical Ocean

6.1 Publication IV: Entanglement of Hydrocarbon Degrading Bacteria and Polycyclic Aromatic Hydrocarbons in the Ocean





6.1 PUBLICATION IV

Entanglement of Hydrocarbon Degrading Bacteria and Polycyclic Aromatic Hydrocarbons in the Ocean

Jon Iriarte
Daniel Lundin
Alicia Martínez-Varela
José M. González
Jordi Dachs
Maria Vila-Costa

Submitted to Environmental Pollution

Entanglement of Hydrocarbon-Degrading Bacteria and Polycyclic Aromatic Hydrocarbons in the Ocean

Jon Iriarte^{1,2}, Daniel Lundin^{3,4}, Alicia Martínez-Varela¹, José M. González⁵, Jordi Dachs¹, and Maria Vila-Costa^{1*}

¹ Department of Environmental Chemistry, IDAEA-CSIC, Barcelona, Catalunya, Spain.

² Doctoral program in Analytical Chemistry and the Environment, Department of Chemical Engineering and Analytical Chemistry, Faculty of Chemistry, Universitat de Barcelona, Barcelona, Catalunya, Spain.

³ Centre for Ecology and Evolution in Microbial model Systems – EEMiS, Linnaeus University, SE-39182, Kalmar, Sweden;

⁴ Dept. of Biochemistry and Biophysics, Stockholm University, SE-10691, Stockholm, Sweden.

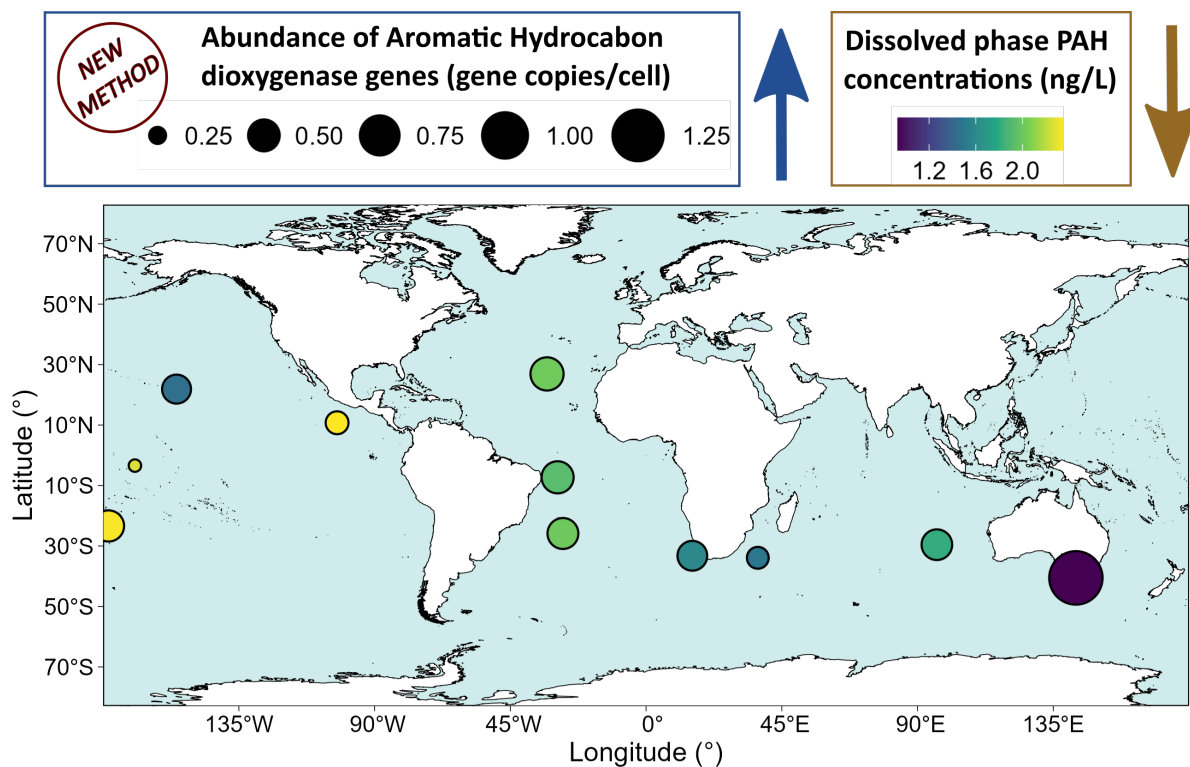
⁵ Department of Microbiology, University of La Laguna, La Laguna, Spain.

E-mail contact: maria.vila@idaea.csic.es

ABSTRACT

Knowledge of Earth's microbiomes capacity to degrade aromatic compounds is limited by the lack of precise tools for accurately targeting degrading genes and their associated taxa. Additionally, these estimates are hardly compared to in situ background concentrations of polycyclic aromatic hydrocarbons (PAHs), particularly in oceanic waters. This knowledge is important for assessing the persistence of the widespread and abundant PAHs in the environment, and their interactions with microbes. Here, we present a new tool to identify aromatic ring-hydroxylating dioxygenase α -subunit (*arhdA*) gene sequences by combining profile-based search with phylogenetic placement in a reference phylogeny. We identified *arhdA*-harboring taxa in the both the Genome Taxonomy Database and the Malaspina Vertical Profiles Gene Database, a gene catalog derived from metagenomes collected during the Malaspina expedition. We found that multiple ubiquitous taxa in tropical and temperate oceans harbor *arhdA*. The comparison of *arhdA* gene abundances in seawater metagenomes with the field PAH concentrations showed that higher abundances of *arhdA* gene copies per cell were negatively correlated with 2-4 ring PAHs, consistent with the known degradation of lighter PAHs. Gene abundances were significantly higher in the particle-associated fraction than in the free-living fraction, suggesting particulate matter as a relevant reservoir of PAH degraders. Finally, we show that PAHs modulate, with other environmental variables, the structure of oceanic microbial communities.

GRAPHICAL ABSTRACT



KEYWORDS

Organic pollutants, PAH, metagenomics, marine microbial communities, aromatic hydrocarbon degradation, marker gene, dioxygenase

HIGHLIGHTS

- A new protein identification method based on phylogenetic placement was developed.
- Aromatic ring hydroxylating dioxygenases (ARHDs) were identified in public data.
- Oil spill-related ARHD-harboring taxa were found in tropical and temperate oceans.
- ARHD abundance correlated with polycyclic aromatic hydrocarbon (PAH) concentrations.
- Background levels of PAHs influence microbial populations alongside other factors.

INTRODUCTION

Aromatic hydrocarbons (AHs) are among the most widespread organic contaminants in the environment. Among them, polycyclic aromatic hydrocarbons (PAHs) and other semi-volatile aromatic-like compounds (SALCs) have drawn particular attention, with several classified as priority pollutants by the U.S. Environmental Protection Agency. Although they can originate from natural sources (e.g., natural oil seeps, forest fires), anthropogenic combustion of oil, coal, and biomass and the subsequent fluvial run-off and atmospheric deposition are considered to be the primary source of PAHs in the global ocean (Duran and Cravo-Laureau, 2016; González-Gaya et al., 2016). The ubiquitous presence of these substances in marine ecosystems is evident even in pristine regions distant from anthropogenic sources, such as subtropical oceanic gyres and polar environments (Cai et al., 2016; González-Gaya et al., 2016; Liu et al., 2022; Zhang et al., 2023, 2022). Due to their chemical properties, PAHs are recalcitrant and can exert toxic effects on aquatic animals, microorganisms, and humans (Honda and Suzuki, 2020; Patel et al., 2020). PAHs interact with the microbial communities in a bidirectional manner, undergoing biodegradation through specific metabolic processes while simultaneously influencing microbial diversities, and potentially, activities. Both aspects have been mostly studied under high concentrations of PAHs, but hardly addressed under background concentrations.

This is especially true in the marine environment, where many studies have been devoted to the measurement of PAH concentrations, but few have assessed their large-scale distribution in the ocean (Cai et al., 2016; González-Gaya et al., 2019; Zhang et al., 2023). Biodegradation of hydrocarbons has been deeply characterized under oil spill conditions (Kimes et al., 2014), while the consumption of PAHs at background concentrations has barely been assessed. Biodegradation is key for understanding the sinks of marine PAHs since as much as 99% of airborne PAHs are microbially degraded in the photic water column (González-Gaya et al., 2019). However, significant gaps exist in the understanding of biodegradation potential, prevalence and importance in marine microbiomes under realistic conditions since it is also highly dependent on complex environmental conditions.

Identifying and quantifying bacteria capable of degrading PAH in the environment is the initial step to determine their persistence. Hydrocarbonoclastic bacteria (HCB), which can utilize hydrocarbons as a carbon or energy source either obligately or facultatively, have been extensively studied through culturing to identify their taxonomies and key degradation pathways and genes (Ghosal et al., 2016). The most common aerobic AH degradation route starts with the oxidative cleavage of an aromatic ring by aromatic ring-hydroxylating dioxygenases (ARHDs) (Mallick et al., 2011). The catalytic or oxygenase component of these multicomponent enzyme systems is composed of two subunits, α and β (ARHD α and ARHD β respectively, encoded by the *ardhA* and *ardhB* genes), where the ARHD α contains the catalytic center. It is highly conserved and has previously been used as a marker to study potential PAH-degrading organisms in environmental studies (González-Gaya et al., 2019; Li et al., 2022; Vilchez-Vargas et al., 2013).

Quantification errors and mismatches in *ardhA* and *ardhB* genes arising from the HCB detection methodology have been detected. Hidden Markov Models (HMMs) are widely used in bioinformatics for tasks such as protein sequence alignment and homology detection. Genomic data can be screened for *ardhA* occurrence and abundance, using the *hmmsearch* function from HMMER (Eddy, 2011) and HMMs such as the Pfam (Finn et al., 2007) model PF00848, which defines the catalytic domain of the ARHDα. Recent findings suggest this approach is inaccurate, causing ambiguous hits due to the ARHDα protein family's limited specificity (Love et al., 2021). In particular, genes coding for homologous enzymes lacking AH-oxidation capacity can reach high scores, complicating the identification of true ARHD enzymes. To address this limitation, more specific HMM profiles have been developed, such as the Calgary approach for ANnoTating HYDrocarbon degradation genes (CANT-HYD) (Khot et al., 2022). CANT-HYD is a database comprising 37 HMMs of marker genes associated with both anaerobic and aerobic degradation pathways of aliphatic and aromatic hydrocarbons that allows the analysis of high-throughput sequence data. While the curated CANT-HYD HMM database improves accuracy in annotating hydrocarbon degradation genes, a restrictive confidence threshold may exclude potential hits, limiting the discovery of new biomarker genes. Identifying novel genes is particularly relevant, as studies have shown that the diversity of *ardhA* genes in natural environments is poorly characterized (Iwai et al., 2011; Li et al., 2022). Further assessment and comparison of the CANT-HYD approach with alternative methods are therefore necessary, especially for analyzing AH biodegradation at background oceanic levels. An alternative to improve functional classification in metagenomic analyses is adding phylogenetic inference to *hmmsearch* results, as it is considered the gold standard for assigning function to sequences based on evolutionary relationships (Ohno, 1970). While estimating phylogenies for large sequence sets can be time-consuming, phylogenetic placement algorithms offer a scalable solution by integrating sequences into reference phylogenies (Czech et al., 2022). The main challenge is the lack of comprehensive reference phylogenies with functional annotations, but databases like Uniprot, especially its manually curated "SwissProt" section, provide a robust starting point for building such resources (Boutet et al., 2007).

The objective of this study was to explore the dual relationship between PAHs and microorganisms, studying how AH-degraders can influence PAH fate and how PAHs impact the structure of microbial communities. We aimed to develop a method for reliable identification of ARHDα sequences in large datasets and use this knowledge to assess AH degradation potential in open-ocean microbial communities, correlating it with the occurrence of PAHs at surface and deep chlorophyll maximum (DCM) depths in the temperate and subtropical ocean. The approach was based on phylogenetic classification of ARHDα sequences in genomes and metagenomes and overcomes previous limitations when identifying AH degraders. This reliable methodology of ARHDα sequences allows the quantification of the pollutant-bacteria interactions and paves the path to gene-centric biogeochemistry of pollutants.

MATERIAL AND METHODS

Construction and curation of reference tree for ring-hydroxylating dioxygenases, identification in Genome Taxonomy Database (GTDB) and Anvi'o tree construction

To identify ring-hydroxylating enzymes among species-representative GTDB genomes (R07-RS207) (Parks et al., 2022), we used HMMER (v.3.1b2) (Eddy, 2011) and the Pfam profile “Ring hydroxylating alpha subunit (catalytic domain)” (PF00848) (Finn et al., 2007) with gathering threshold (model-specific bit score threshold defined for each HMM profile). Since paralogs not involved in degradation of AHs have been described (Iwai et al., 2011), we estimated a reference phylogeny for the protein family in which we identified clans containing manually curated AH-degrading enzymes from SwissProt (Boutet et al., 2007) (see Lundin (2023a) for a full method description).

Sequences from GTDB genomes were subsequently placed and classified in the reference phylogeny with nf-core/phyloplace (v1.0, Lundin, 2023b) that uses EPA-NG (v.0.3.8; Barbera et al., 2019), which phylogenetically places the query sequences in the reference tree and uses GAPPa (v.0.8.0, Czech et al., 2020) to classify them and produce a tree with the query sequences placed among the references. The phylogenomic trees of Bacteria and Archaea from GTDB, subset to the class level, were used to create plots to illustrate the taxonomic distribution of the identified ARHD α proteins with Anvi'o (v.8, Eren et al., 2015).

To assess the CANT-HYD approach (Khot et al., 2022), the HMMs associated with the α -subunit of the ARHD involved in the aerobic degradation of AHs – MAH α , NdoB and non-NdoB – were used to query the same set of species-representative GTDB genomes. We used HMMER, with the noise cutoff threshold recommended by the CANT-HYD authors.

Data from Malaspina Expedition

Environmental ancillary data, PAH concentrations, 16S rRNA amplicon sequences, and metagenome data were obtained during the Malaspina 2010 circumnavigation expedition (from December 2010 to July 2011) and published in separate works (González-Gaya et al., 2019, 2016; Ruiz-González et al., 2019; Sánchez et al., 2024). See annexes S1 and S2 for details. Stations were located along a transect in the tropical and subtropical Atlantic, Indian, and Pacific oceans (Figure 1). Selected samples included those from surface waters (4 m) and, when available, from the Deep Chlorophyll Maximum, DCM, (48–150 m), in which PAH concentrations and DNA material were analyzed simultaneously.

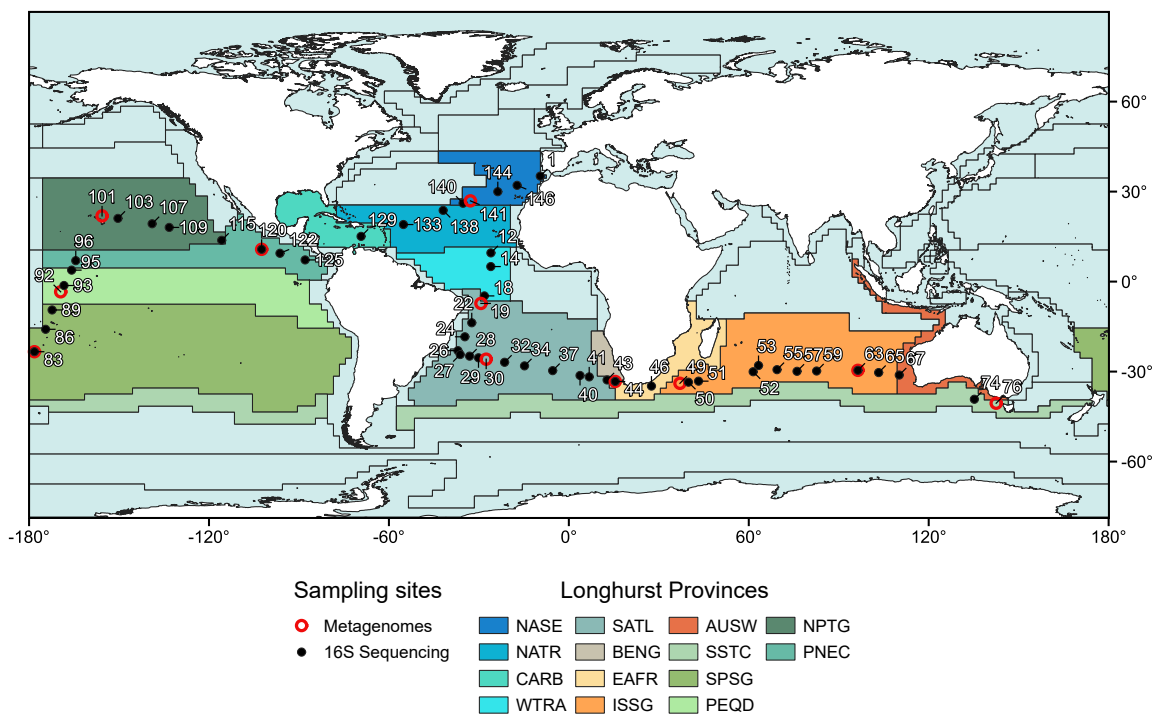


Figure 1. Location of the samples from the Malaspina circumnavigation expedition used in this study. The inclusion of sampling sites was based on the availability of physicochemical and genomic data, with the latter represented by 16S rRNA gene sequences (black dots), metagenomic sequences (red circles), or both (black dots with red outline). The limits of the oceanic biogeographical provinces have been incorporated. The provinces crossed during the Malaspina 2010 circumnavigation are colored. NASE, North Atlantic Subtropical Gyral; NATR, North Atlantic Tropical Gyral; CARB, Caribbean Province; WTRA, Western Tropical Atlantic; SATL, South Atlantic Gyral; BENG, Benguela Current Coastal Province; EAFR, East Africa Coastal; ISSG, Indian South Subtropical Gyre; AUSW, West Australian Coastal Province; SSTC, South Subtropical Convergence; SPSG, South Pacific Subtropical Gyre; PEQD, Pacific Equatorial Divergence; NPTG, North Pacific Tropical Gyre; PNEC, North Pacific Equatorial Countercurrent. Map created using the open-source application QGIS (v.3.20.0).

Identification of *arhdA*-genes in the Malaspina Vertical Profiles Gene Database data using phylogenetic placement

The identification of genes coding for proteins matching the Pfam PF00848 HMM in the Malaspina Vertical Profiles Gene Database (M-GeneDB-VP, Sánchez et al., 2024) was done following the same steps as described above for the GTDB database. Briefly, the PF00848 HMM was used to search all the protein sequences of the M-GeneDB-VP, a gene catalog constructed from the Malaspina Microbial Vertical Profiles metagenomes dataset (see Sánchez et al., 2024 for more details). The sequences were subsequently placed in the reference phylogeny described above with *nf-core/phyloplace*. The files containing the gene sequences, annotations for functional and taxonomic profiles, and counts of reads from each metagenome mapping to the gene catalog were downloaded from the European Bioinformatics Institute BioStudies repository (accession S-BSST1059). The protein sequences that compose this catalog correspond to samples taken at different depths and filter sizes (free-living fraction, FL, 0.22-3.0 μm ; particle-attached fraction, PA, 3.0-20 μm) at 11 stations during the Malaspina 2010 circumnavigation expedition. From this dataset we selected the samples corresponding to surface and DCM depths, for which we have concurrent PAH measurements, yielding a total of 39 samples.

Functional and taxonomic profiles of the identified candidate proteins, along with their abundances, were obtained from the M-GeneDB-VP annotation and read count files. We used the gene length single-copy marker gene normalized gene abundances provided by the authors. According to Sánchez et al. (2024), gene counts in the database were transformed to gene-length relative abundances by calculating the ratio between count and gene length in bp. Subsequently, gene length normalized abundances were normalized to relative cell numbers in the sample by dividing them by the geometric median abundance of 10 universal single-copy marker genes. Normalizing coverage-corrected read counts by the abundance of these marker genes acts as a proxy for the number of gene copies per cell (Salazar et al., 2019).

Statistical analyses

Bacterial ASV counts were Hellinger-transformed using the function *decostand* from the *vegan* package in R. Environmental data variables were log10-transformed and the values were subsequently transformed to z-scores by subtracting the mean of the variable and then dividing by its standard deviation. *arhdA* gene abundance values from the M-GeneDB-VP were log10-transformed for the Multiple Linear Regression (MLR) models. MLR models were computed using the *lm* function from the *stats* package. Explanatory or independent variables were manually selected by iteratively removing the variable with the highest p-value among the non-significant variables. Redundancy Analysis (RDAs) were performed with default settings, using the *rda* function from *vegan*. Forward selections with the double-stopping criterion to control for type-I error rate were performed to test which environmental factors had a significant influence on the bacterial community composition using the function *ordiR2step*. The significance and the marginal effects of the selected variables were assessed by a permutation test using the function *anova* (by = "mar"). The analyses were run with R version 4.3.3 (2024-02-29) in all cases. Versions of packages can be found in Table S1.

RESULTS AND DISCUSSION

Identification of ARHD α proteins and the phylogenetic diversity of *arhdA*-harboring genomes

To improve identification rates with better selectivity and accuracy, we applied phylogenetic placement of candidate proteins retrieved by HMM search with the PF00848 profile on a reference tree. After estimation of a reference phylogeny, we identified six clans (potential clades in an unrooted tree) (Wilkinson et al., 2007) in the tree (Figure 2) and identified proteins functionally annotated in SwissProt (Boutet et al., 2007). In “ClanA”, consisting of 85 sequences, we found proteins annotated as “naphthalene dioxygenase”, “benzene dioxygenase”, “biphenyl dioxygenase”, “chlorobenzene dioxygenase”, and “phenylpropionate/cinnamic acid dioxygenase”. “ClanB” contained proteins annotated in SwissProt as “p-cumate dioxygenase”, “terephthalate dioxygenase”, “anthranilate dioxygenase”, “salicylate hydroxylase”, “aminobenzenesulfonate dioxygenase”, “halobenzoate dioxygenase”, “benzoate dioxygenase” and “toluate dioxygenase”. In the other four, we only found two annotations among SwissProt proteins, “Carnitine monooxygenase” and “Choline monooxygenase” (Figure 2). Similarly, (Li et al., 2022) also found several gene names after collecting amino acid sequences annotated as ARHD α from public databases, highlighting the diversity of target AHs these genes interact with (Iwai et al., 2011). Only clanA and clanB hence appear to represent dioxygenases with aromatic substrates, and only proteins placed in these two clans were considered ARHD α s and used in the analyses below.

We applied this approach to all species-representative genomes in GTDB, which includes genomes from aquatic, terrestrial and atmospheric environments (R07-RS207, (Parks et al., 2022), and identified 43,171 unique candidate proteins, which were subsequently narrowed down to 11,956 following phylogenetic placement. These candidate proteins were encoded by 5,770 bacterial genomes containing 11,895 genes and 49 archaeal genomes containing 61 genes. As many as 72 genomes harbored 10 or more copies of the gene per genome (Table S2). These results were compared to the results from the CANT-HYD approach applied to the same set of GTDB genomes (Figure S1). This approach detected 4,383 candidate proteins associated with the ARHD α , which were divided between NdoB, MAH α , and non-NdoB HMMs, with 740, 404 and 3239, respectively. Interestingly, based on the phylogenetic placement of these candidate proteins, those annotated as NdoB or MAH α were assigned to either clan A (1,139 proteins) or clan B (5 proteins). In contrast, non-NdoB were assigned to clans F, E, and D, with 2,993, 244, and 2 proteins, respectively. Furthermore, most of the proteins identified as non-NdoB were phylogenetically annotated as Carnitine monooxygenase, which is not an aromatic compound, suggesting that they were likely not ARDH α s.

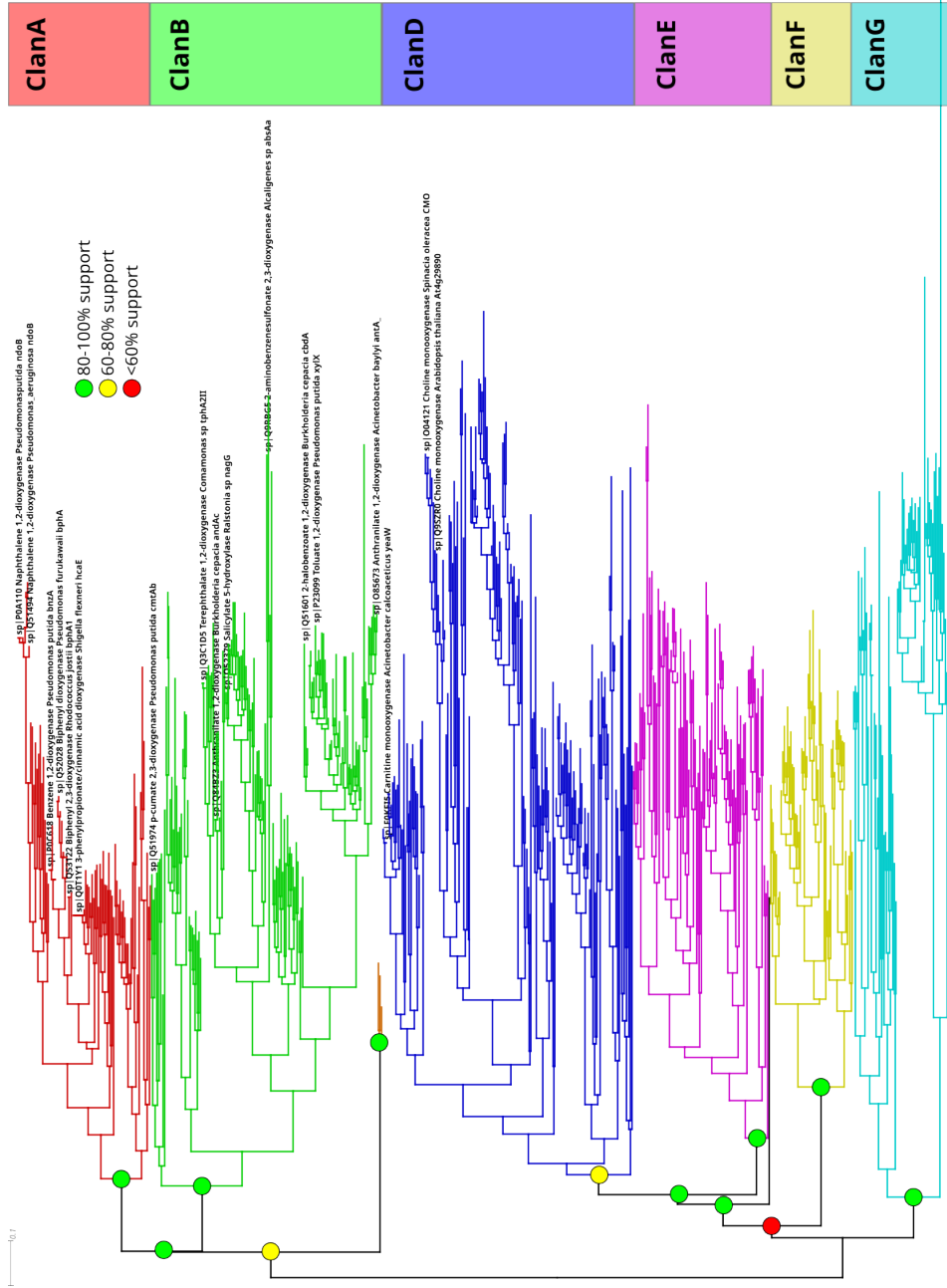


Figure 2. Unrooted maximum likelihood phylogeny of Pfam PF00848 proteins. Sequences were selected to represent the full diversity of proteins annotated with the Pfam PF00848 profile in Uniprot, and clans – possible clades in an unrooted tree – identified. Representative proteins from SwissProt are shown with labels. ClanA and ClanB contain sequences annotated as dioxygenases with aromatic substrates, ClanD contains monooxygenases, while the remaining clans do not contain any SwissProt proteins and were not functionally annotated.

In aggregate, NdoB and MAH_alpha candidate proteins resulted in less than 10% of the candidate proteins phylogenetically assigned to clans A or B (Table S2). It has previously been suggested that the reduced number of reference sequences used to create the HMMs in CANT-HYD could cause divergent sequences to go undetected (Góngora et al., 2024). Our analysis lends some support to this hypothesis, and phylogenetic placement in our reference tree provides a less conservative classification tool.

Bacterial *arhdA*-harboring genomes were widely distributed across different orders and classes, with the ratio between the number of species predicted to encode *arhdA* vs total number of species per class ranging from 0 to 0.75, and the number of *arhdA* copies per species ranging from 0 to 4.25 (Figure 3A, Table S3). In most of the classes, the presence of *arhdA* was low (< 0.15). Bacterial taxa with a higher number of copies were "*Candidatus* Entotheonella", "*Candidatus* Binatia", *Gammaproteobacteria*, *Alphaproteobacteria*, "*Candidatus* Methyloirabillia", *UBA9160*, *J058*, and *Actinomycetes*. Among them, *Gammaproteobacteria*, *Alphaproteobacteria*, and *Actinomycetes* had the highest number of *arhdA* copies per class (6111, 2813, and 1979, respectively), which is consistent with the high number of confirmed AH-degrading taxa they harbor (Ghosal et al., 2016; Lu et al., 2019). In general, the order *Burkholderiales* within *Gammaproteobacteria* accounted for the majority of *arhdA* copies, followed by *Pseudomonadales* (*Gammaproteobacteria*), *Mycobacteriales* (*Actinomycetota*), and *Sphingomonadales* (*Alphaproteobacteria*), consistent with previous studies that showed both the presence of genes and important roles of the four orders in the degradation of PAHs (Figure S2) (Bacosa et al., 2021; Lu et al., 2019; Pérez-Pantoja et al., 2012; Somee et al., 2022). Interestingly, "*Ca. Entotheonella*", the type genus, is a symbiont of the marine sponge *Theonella swinhoei* with the metabolic capacity to use a wide variety of carbon sources (Liu et al., 2016). Marine sponges, known for accumulating pollutants, host AH-degrading bacteria, suggesting "*Ca. Entotheonella*" spp. as potential AH degraders. (Marzuki et al., 2021). "*Candidatus* Methyloirabillia" (also known as *Rokubacteria*) is a bacterial genus with large genomes that encode genes for the oxidative degradation of aromatic compounds (Becraft et al., 2017). Members of the "*Ca. Binatia*" class (*Desulfobacterota*, formerly the *Deltaproteobacteria* class), have also been suggested as potential AH degraders (Somee et al., 2022).

Among the genomes harboring 10 or more copies, genera with high AH degradation potential appeared, such as *Cycloclasticus* (*Methylococcales*), *Pigmentiphaga* (*Burkholderiales*), *Mycobacterium* (*Mycobacteriales*), *Rugosibacter* (*Burkholderiales*), and *Immundisolibacter* (*Immundisolibacterales*). All of them have been described as efficient PAH degraders and found in oil-contaminated sites (Corteselli et al., 2017a; Jeon et al., 2024; Wang et al., 2018). They are facultative consumers of AHs that also consume other organic compounds in the environment (Liu et al., 2024). Surprisingly, a genome classified as *Immundisolibacter cernigliae*, isolated from a PAH-contaminated site (Corteselli et al., 2017b), harbored 46 copies. Somee et al. (2022) also found multiple copies of AH degrading genes in this genome. Furthermore, Góngora et al. (2024) found several copies of *arhdA* and other genes involved in AH degradation pathways in a metagenome-assembled genome (MAG) classified to the *Immundisolibacteraceae* family.

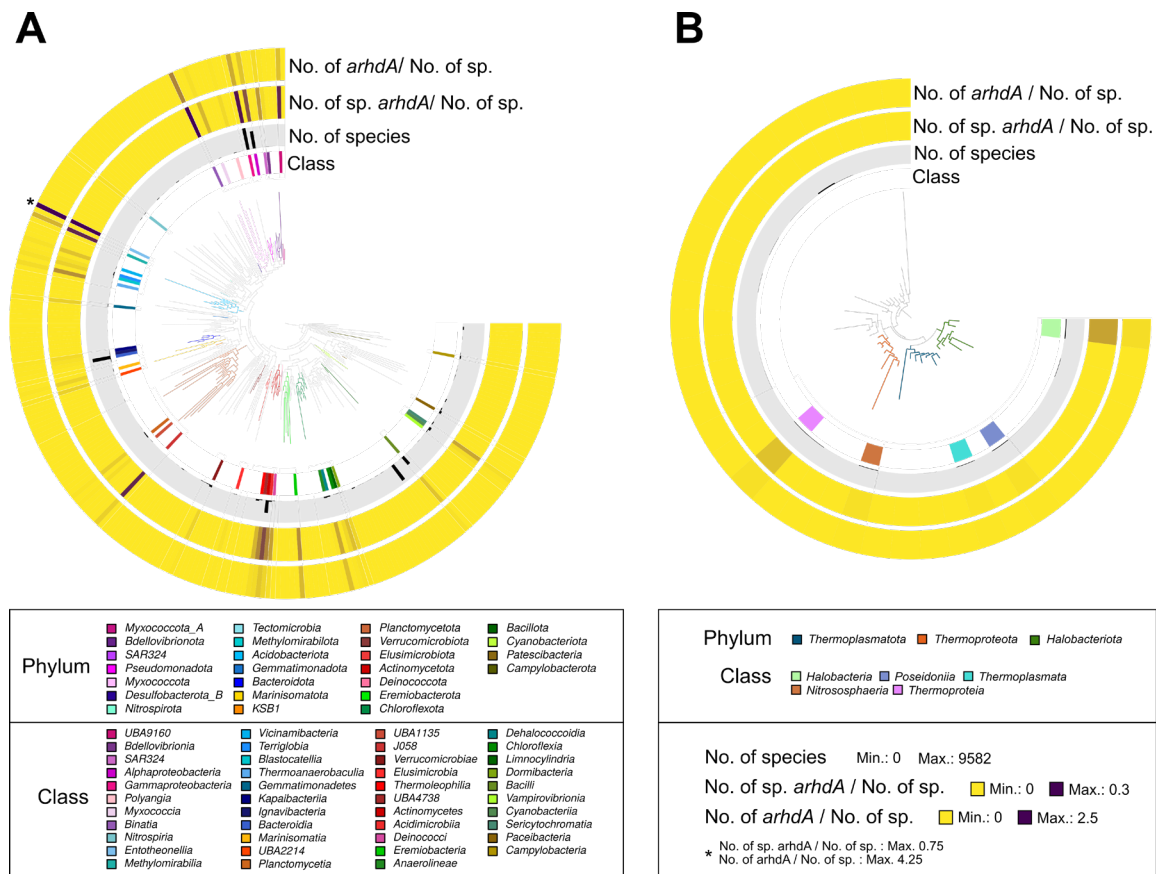


Figure 3. Phylogeny of all GTDB (release r207) species representative genomes at Class level. (A) bacteria, (B) archaea. Only taxonomic classes corresponding to the genomes where at least one *arhdA* gene has been identified are shown in colors (inner ring). The remaining rings, from inner to outer, display the following information per class: the number of species, the proportion of species with the *arhdA* gene to the total number of species (no. of sp. *arhdA* / no. of sp.), and the mean number of *arhdA* genes per species (no. of *arhdA* / no. of sp.). Branches are colored according to taxonomic phyla.

Only five classes of archaea with *arhdA* genes were found (Figure 3B). *Halobacteriota* (*Halobacteriota*) and *Thermoproteia* (*Thermoproteota*) had the highest number of copies per class (40 and 16, respectively), two orders of magnitude lower than those found in the bacterial genomes. Consistent with previous studies, *arhdA*-harboring archaea were found to contain few copies of the gene (Table S4). Somee et al. (2022) also noted that the enzymes for the initial degradation of hydrocarbons were rarely present in archaea. *Halobacteriales* and *Sulfolobales* were the orders that accounted for most of these (Figure S3). Previous studies have shown the capacity of archaea to degrade AH, although mostly in anaerobic environments so likely not using the ARDH enzyme (Zhang et al., 2021).

The presence of the gene encoding ARHDA across various branches of bacterial and archaeal phylogenomic trees indicates that the capacity for aerobic degradation of AHs is not restricted to specific taxa. Several studies support that horizontal gene transfer events between microbial groups contribute to the wide taxonomic distribution of this enzyme and the occurrence of multiple copies per genome (DeBruyn et al., 2012; Ma et al., 2006; Somee et al., 2022). Furthermore, individual genomes seldom contain all the genes necessary for the complete degradation (Góngora et al., 2024; Somee et al., 2022). Instead, bacterial consortia are generally more efficient at fully degrading AHs and crude oil (Pandolfo et al., 2023; Vaidya et al., 2017). These findings reiterate that microbial cooperation is typically essential for AH degradation, with gene transfer promoting this cooperative process.

Distribution of ARHDA in free-living (FL) and particle-attached (PA) bacterial communities in the tropical and subtropical oceans

ARHDA sequences are ubiquitous in the Earth microbiome, as demonstrated previously. The application of this novel methodology to detect ARHDA sequences was implemented in the analysis of results from the Malaspina circumnavigation, enabling the exploration of gene-chemical interactions in the ocean. More specifically, candidate protein sequences for 17 and 22 samples of surface and DCM DNA, respectively, were obtained from the Malaspina Vertical Profiles Gene Database (M-GeneDB-VP). The initial 21969 candidate proteins found by HMM search were narrowed down to 5339 unique sequences after phylogenetic placement among clanA and clanB in the reference tree. From these candidates, 2268 were present in the 39 samples for which we had concurrent PAH measurements. Taxonomic annotation of the M-GeneDB-VP genes restricted the results to marine organisms, revealing that 1966 corresponded to bacteria, 39 to archaea, 9 to eukaryotes, 1 to viruses, and 255 remained unclassified. For our analyses, we focused exclusively on bacterial and archaeal genes (Table S5). Unfortunately, a considerable portion of the bacterial and archaeal sequences were unclassified at the class level or lower.

Consistent with the focus on oceanic environment, up to 40% of the unique ARHDA sequences found were assigned to marine orders from the alphaproteobacterial class ("*Candidatus Pelagibacterales*", *Rhodospirillales*, *Hyphomicrobiales*, *Rhodobacterales*, and *Sphingomonadales*), while 6% were assigned to marine orders from the gammaproteobacterial class (*Cellvibrionales*, *Thiotrichales*, *Oceanospirillales*, and *Alteromonadales*, Figure S4). Surprisingly, a high number of sequences were assigned to the widespread marine genus "*Candidatus Pelagibacter*". Similarly, (Peeb et al., 2022) found AH degradation genes to be predominantly affiliated as "*Ca. Pelagibacter*" in an experiment with ice-encapsulated crude oil. However, the lack of evidence of hydrocarbon degradation by "*Ca. Pelagibacter*" places this association in question. Although "*Ca. Pelagibacter*" has previously been found to increase following the crude oil biodegradation period (Brakstad et al., 2015), further research is necessary to establish a direct correlation between this genus and hydrocarbon degradation. Relevant genera for AH degradation were found, such as *Pseudoalteromonas*, with experimentally characterized PAH degrading strains (Hedlund and Staley, 2006), and environmental studies showing their response to low and high doses of PAH

exposure (Krolicka et al., 2017; Martinez-Varela et al., 2022); or *Sulfitobacter*, whose relative abundances have been correlated with background concentrations of PAHs (Iriarte et al., 2023) (Table S5). The list of *arhdA*-harboring bacteria also included typical marine PAH degraders such as *Colwellia*, and to a lesser extent, *Cycloclasticus*. Both genera are considered potential biomarkers of PAH degradation in seawater due to typically being rare, but forming opportunistic blooms under high PAH concentrations (Kleindienst et al., 2016; Krolicka et al., 2019). To get a better picture of the taxa with AH degradation potential we computed the average number of annotated *arhdA* genes per order. The highest average number of genes was found in the orders *Alteromonadales*, *Oceanospirillales*, *Mycobacteriales*, and *Moraxellales* (Table S6). These marine orders have frequently been identified under exposure to high concentrations of AH in oil spill accidents (Bacosa et al., 2018; Mason et al., 2012).

In contrast, only two classes of environmental archaea were detected in the gene catalog, both exhibiting a low average number of *ahrdA* genes (Table S6). Within these, only the order “*Candidatus* Poseidoniales” could be identified. This taxon represents the most abundant archaeal group in surface seawaters (Rinke et al., 2019). Their genomes contain genes for medium-chain alkane degradation, and they have shown transcriptomic activity when exposed to low concentrations of hydrophobic pollutants, including alkanes and PAHs (Love et al., 2021; Vila-Costa et al., 2023).

Abundances of *arhdA* genes per cell in bacteria averaged 0.79 ± 0.34 at the 11 stations, ranging from 0.28 at station 49 to 1.45 at station 76 (Figure S5). These values are lower but still at the same order of magnitude as previously reported (González-Gaya et al., 2019). Regarding the water layers, DCM average abundance (0.47 ± 0.26) was higher than surface average (0.36 ± 0.22), but not statistically significant according to a paired t-test (p -value = 0.17). The comparison of abundances per filter-fraction, separating particle attached (PA) and free-living (FL) bacteria, showed significantly higher values in the PA fraction (mean 0.27) compared to the FL fractions (mean 0.15, paired t-test, p -value = 0.007), even after excluding station 76, which had a disproportionately high PA gene abundance due to a gene taxonomically annotated as *Rhodococcus* sp. CUA-806 (Figure S6, Table S7). That particular gene was also responsible for the high abundances found in the surface PA samples 63, 83, and 92, accounting on average for almost 30% of the gene copies per cell found in all the PA samples. *Rhodococcus* strains have previously shown strong hydrocarbon degradation potential and are being proposed for the bioremediation of organic and inorganic pollutants (Nazari et al., 2022). Regarding AH degradation, a study where 133 isolated *Rhodococcus* strains were tested demonstrated their capacity to oxidize AHs, and found 23 to 69 ARHD coding genes in their genomes (Krivoruchko et al., 2023). Another specific marine *Rhodococcus* strain has also been found to encode several PAH-degrading genes and is capable of utilizing PAHs, especially HMW ones (Peng et al., 2020). Similarly, various studies show the capacity of *Rhodococcus*, as well as other bacteria such as *Mycobacterium*, *Burkholderia*, *Cycloclasticus*, *Pseudomonas*, and *Sphingomonas*, to degrade the HMW PAH pyrene (DeBruyn et al., 2012; Vaidya et al., 2017; Zada et al., 2021). These results are consistent with recent studies in coastal Antarctica, where PA bacteria demonstrated a higher capacity for PAH degradation than FL bacteria (Martinez-Varela et al., 2022). Although AH concentrations account for less than 1%

of DOC (Liu et al., 2024), the taxa associated with background AH concentrations largely overlap with those previously reported in oil spills.

Correlation between *arhdA* gene abundances and PAH concentrations in the tropical and subtropical oceans

To test whether higher *arhdA* gene abundances correlate with PAH concentrations, we correlated the sum of LMW and HMW PAH concentrations in the dissolved, particulate, and planktonic phase with gene abundances in the two size fractions (FL and PA) at the two different depths (surface and DCM) (Figures 4, S7, and S8). Significant negative correlations (Figure S9) were found between LMW PAHs in the dissolved phase and gene abundances in the FL fraction in both surface (p-value = 0.01, $R^2_{\text{adj.}} = 0.51$) and DCM (p-value = 0.005, $R^2_{\text{adj.}} = 0.55$) layers, as well as in the PA fraction at DCM (p-value = 0.02, $R^2_{\text{adj.}} = 0.39$). The lowest concentration of LMW PAHs was observed off the southeastern Australian coast, where the highest *arhdA* abundances occurred (Figure 4). This aligns with the fact that LMW PAHs – typically those with 2-4 aromatic rings – are the most labile fraction of PAHs and are prone to biodegradation (Ghosal et al., 2016; González-Gaya et al., 2019). These compounds are also less hydrophobic, making them more likely to remain in the dissolved phase, which increases their encounter rate with marine degraders. These results suggest that a higher potential for PAH degradation (indicated by greater *arhdA* gene abundance) within the bacterial community correlates with lower PAH concentrations, likely due to microbial degradation.

The FL/PA ratios of *arhdA* gene abundances versus PAH concentrations were significantly negatively correlated with HMW dissolved water concentrations (p-value = 0.04, $R^2 = 0.32$) and positively correlated with LMW (p-value = 0.009, $R^2 = 0.51$) and HMW (p-value = 0.003, $R^2 = 0.60$) concentrations in plankton at the DCM (Figure S10). HMW PAHs, being more lipophilic than LMW PAHs, have a higher tendency to bioaccumulate in organic tissues, including plankton. A higher abundance of *arhdA* genes in the PA fraction (indicating a lower FL/PA ratio) was associated with lower PAH concentrations in plankton. This finding suggests that the PA fraction serves as a hotspot for PAH biodegradation in the oceans, as previously proposed (Martinez-Varela et al., 2022). PAH bioaccumulation in plankton could enhance the abundance of *arhdA* genes in PA, promoting degradation, which can eventually be detected in the dissolved phase as well by particle-water partitioning. Overall, the evidence from single linear correlations suggests that at sites with background PAH concentrations, bacteria influence PAH levels rather than the other way around (Iriarte et al., 2023). If PAH-driven shaping of bacterial communities does occur, it may be subtle and likely interacts with other environmental factors, such as temperature, nutrient concentrations, PAH bioavailability, and prior exposure to PAH, among others (Singh and Kumar Mishra, 2021; Varjani and Upasani, 2017).

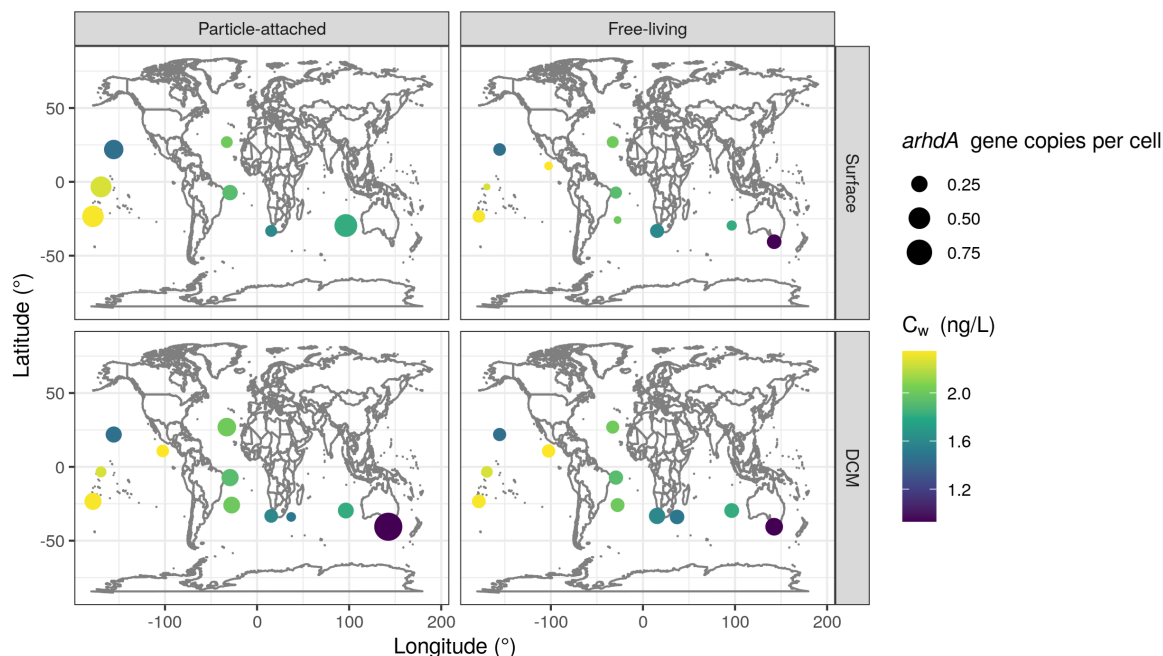


Figure 4. Geographic distribution and abundance (estimated gene copies per cell) of genes identified as *arhdA* in the M-GeneDB-VP database per size fraction (free-living fraction, 0.22-3.0 μm ; particle-attached fraction, 3.0-20 μm), concurrently with the sum of the PAH compounds in the seawater dissolved phase per water layer (surface water, 3 m; DCM, Deep Chlorophyll Maximum).

Environmental drivers of *arhdA* gene abundances in the tropical and subtropical oceans

In order to assess which environmental factors could explain the variability in the AH degrading potential across samples, Multiple Linear Regression (MLR) analysis was performed, using the *arhdA* gene abundance as a proxy of PAH degrading potential. Manual selection of variables on models trying to explain the variability of *arhdA* abundance (as copies per cell) resulted in the same simple linear correlation with LMW PAHs (Table S8) described above (Figure S9). Alternatively, seawater temperature showed a negative correlation with *arhdA* abundance ($p\text{-value} = 0.017$, $R^2 = 0.15$). Temperature has previously been described as the main environmental driver for microbial community composition in the epipelagic layer (Sunagawa et al., 2015).

Absolute abundance of *arhdA* gene (gene per liter) was also tested. This was obtained by multiplying *arhdA* gene abundance per cell by heterotrophic bacterial abundance (cell counts per liter). The model that best explained the variability ($p\text{-value} = 5 \times 10^{-4}$, $R^2 = 0.51$) included the nitrate+nitrite concentrations, total chlorophyll *a* concentrations, the concentrations of LMW PAH and HMW PAH in the particulate phase, as well the HMW PAH concentrations in the dissolved and planktonic phases, as explanatory variables (Table S8). Thus, microbial PAH degraders

(or their *arhdA* gene abundance) are modulated not only by PAH concentrations, but common environmental variables modulating microbial communities, such as nutrient concentrations (nitrogen) and planktonic biomass (as given by chlorophyll α). This regression model explains half of the variability in *arhdA* gene abundance and appears to depend on biogeochemical drivers such as nutrients and biomass, in addition to a complex function of the PAH concentrations across different phases. This is the first time that abundances of degradation genes in the marine environment for a contaminant have been correlated with concurrent pollutant concentrations. This finding implies that pollutants, while generally less influential than nutrients and other biogeochemical drivers (Bristow et al., 2017; Iriarte et al., 2023), can still significantly affect microbial communities capable of using PAHs as a carbon source.

Do AHs influence the structuring of microbial communities in the tropical and subtropical oceans?

Further exploration of the influence of PAHs, and generally AHs, on oceanic microbial communities (not limited to potential degraders), was performed by including PAH concentrations plus other relevant environmental factors influencing community structure (temperature, nutrients, etc.) in a Redundancy Analysis (RDA). Automated forward selection RDA identified water total chlorophyll α concentration, water temperature, water in vivo fluorescence, and LMW PAHs in water (dissolved concentrations) as significant in explaining a portion of the variation in the heterotrophic bacterial community composition (p-value = 0.001). These results are consistent with the ones obtained above for the *arhdA* gene abundance. Specifically, a permutation test on the automatically selected variables showed that total chlorophyll α concentration (p-value = 0.001), temperature (p-value = 0.003), LMW PAHs in water (p-value = 0.006), and in vivo fluorescence (p-value = 0.010) were significantly related to the variation in the bacterial community composition along the transect (Figure 5, Table S9). The cumulative variance of the species-environment relationship explained by the four RDAs was 17.39%. To evaluate the proportion of variance explained by these four variables, we compared this value to the variance explained by the first four Principal Components (PCs) of a Principal Component Analysis (PCA) model applied to the same dataset. This comparison was conducted because the variance explained by an unconstrained component in PCA represents the maximum amount of variance that any component can elucidate. The first four PCs of the unconstrained model explained 42.17%, meaning that the RDA forward-selected variables explained 41.24% of the maximum variance they could potentially explain (Table S9). These results suggest a significant impact of PAH on the heterotrophic fraction of microbial communities, which have been shown to respond to background concentrations of organic pollutants at transcriptomic and physiological levels. Often, this response includes taxon-specific stimulation of respiration and other heterotrophic activities, along with the activation of antioxidative mechanisms (Cerro-Gálvez et al., 2021; Martinez-Varela et al., 2021).

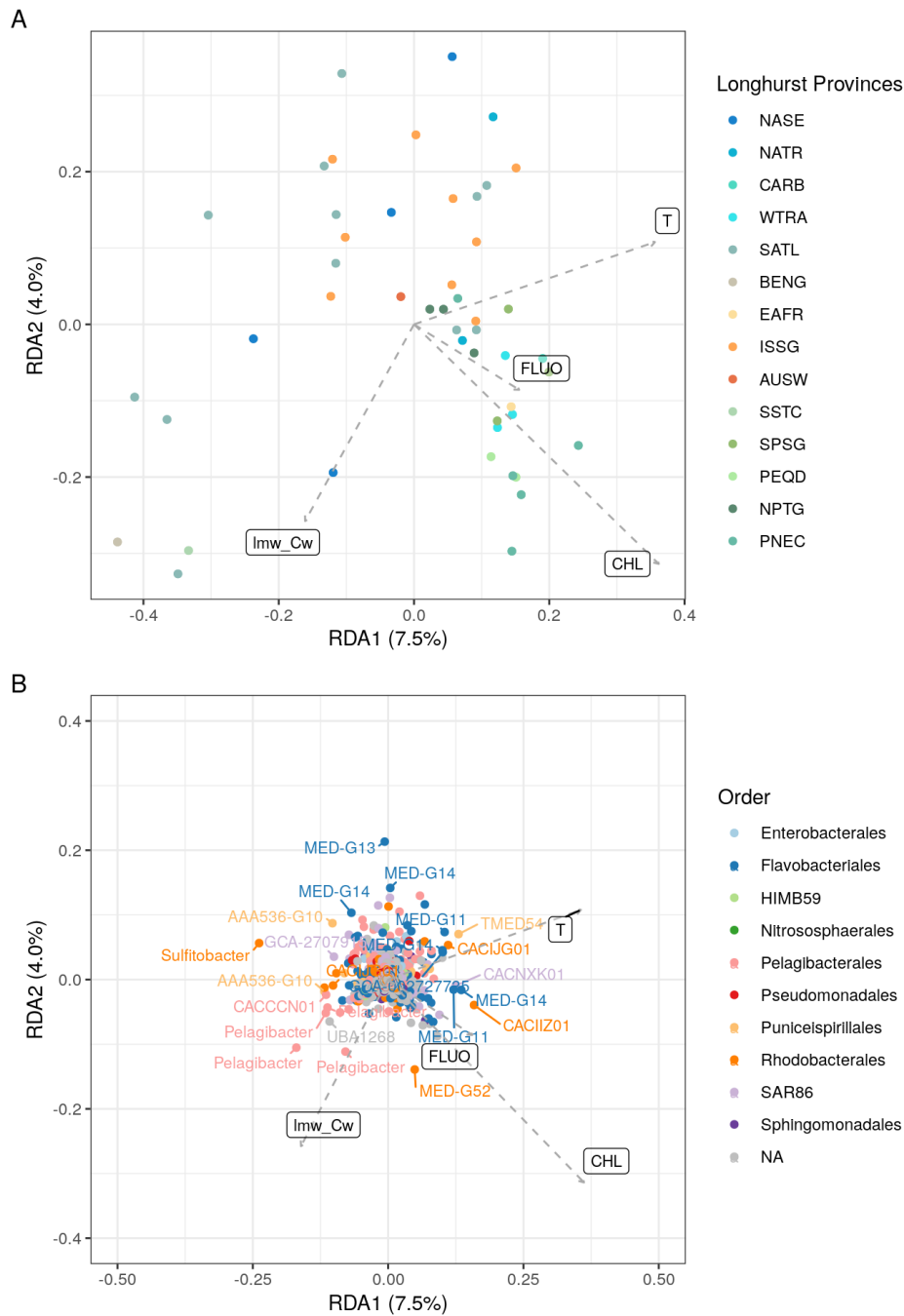


Figure 5. Redundancy Analysis (RDA) biplots (with symmetric scaling) showing the selected explanatory variables (as vectors) that significantly explained the variation in the heterotrophic bacterial community composition. A) Site scores and B) Species scores are represented as colored dots, showing the Longhurst Provinces of the sampling locations, and the taxonomy at order level, respectively.

When cyanobacteria were included in the analysis, not only obligate heterotrophic bacteria, temperature (p -value = 0.001), total chlorophyll α concentration (p -value = 0.005) and LMW PAHs in water (p -value = 0.002) were automatically selected as significant according to the permutation test (Figure S11, Table S9). The cumulative variance explained by the RDAs in this new model was 19.30%. The variance explained by the first three PCs in the unconstrained PCA model was 48.35%, meaning that the RDA forward-selected variables explained a 40.00% of the maximum variance they could potentially explain (Table S9). This is consistent with previous data indicating a higher sensitivity of the smallest phytoplanktonic cells to the negative effects of organic pollutants on populations and photosynthesis (Echeveste et al., 2016).

CONCLUSIONS

Using our methodology based on the phylogenetic placement of candidate protein sequences retrieved with HMMER into a reference phylogenetic tree, we identified ARHDA sequences in publicly available MAGs and metagenomes, and selected those query sequences that were phylogenetically placed in clans containing manually curated AH-degrading enzymes. Taxonomic annotation of these sequences from sites with background concentrations of PAHs revealed specific AH degrading taxa also found under oil spill conditions. Overall, the results of the statistical analyses suggest that background PAH concentrations may influence microbial populations, alongside known factors such as temperature and chlorophyll α , with already-known influence (Fuhrman et al., 2015; Ruiz-González et al., 2019). Although AHs represent a minor portion of DOC, they may significantly influence microbial communities due to their hydrophobic nature (Cerro-Gálvez et al., 2021). The methodology applied here for AHs could also be used for other organic contaminants. Nevertheless, the scarcity of field measurements for many contaminants, along with the large unknowns surrounding contaminant degradation genes, hampers their inclusion as a determinant factor modulating marine microbial communities and, eventually, influencing major biogeochemical cycles. In this study, we have provided unique evidence of the role of background pollution as a potential vector influencing global biodiversity, which further emphasizes the urgent need to assess the influence of pollution-microbial interactions on other vectors of the current environmental global change (Persson et al., 2022).

Funding sources

J. Iriarte acknowledges the predoctoral FPU fellowship (FPU19/02782) funded by the Spanish Ministry of Science. This work was supported by the Spanish Research Agency through projects PANTOC (PID2021-127769NB-I00) and MIQAS (PID2021-128084OB-I00). The research group of Global Change and Genomic Biogeochemistry receives support from the Catalan Government (2021-SGR-00448).

Appendix A. Supplementary data

The following are the Supplementary data to this article.

Multimedia component 1: Word document with Annexes S1 and S2, Figures S1-S11 and Tables S1, S4, S6, S8 and S9.

Multimedia component 2: Spreadsheet with Table S2.

Multimedia component 3: Spreadsheet with Table S3.

Multimedia component 5: Spreadsheet with Table S5.

Multimedia component 7: Spreadsheet with Table S7.

REFERENCES

- Bacosa HP, Erdner DL, Rosenheim BE, Shetty P, Seitz KW, Baker BJ, et al. Hydrocarbon degradation and response of seafloor sediment bacterial community in the northern Gulf of Mexico to light Louisiana sweet crude oil. *ISME J* 2018;12:2532–43. <https://doi.org/10.1038/s41396-018-0190-1>.
- Bacosa HP, Mabuhay-Omar JA, Balisco RAT, Omar DM, Inoue C. Biodegradation of binary mixtures of octane with benzene, toluene, ethylbenzene or xylene (BTEX): insights on the potential of Burkholderia, Pseudomonas and Cupriavidus isolates. *World J Microbiol Biotechnol* 2021;37:122. <https://doi.org/10.1007/s11274-021-03093-4>.
- Barbera P, Kozlov AM, Czech L, Morel B, Darriba D, Flouri T, et al. EPA-ng: Massively Parallel Evolutionary Placement of Genetic Sequences. *Syst Biol* 2019;68:365–9. <https://doi.org/10.1093/sysbio/syy054>.
- Becraft ED, Woyke T, Jarett J, Ivanova N, Godoy-Vitorino F, Poulton N, et al. Rokubacteria: Genomic Giants among the Uncultured Bacterial Phyla. *Front Microbiol* 2017;8. <https://doi.org/10.3389/fmicb.2017.02264>.
- Boutet E, Lieberherr D, Tognolli M, Schneider M, Bairoch A. UniProtKB/Swiss-Prot. *Plant Bioinformatics*, Totowa, NJ: Humana Press; 2007, p. 89–112. https://doi.org/10.1007/978-1-59745-535-0_4.
- Brakstad OG, Throne-Holst M, Netzer R, Stoeckel DM, Atlas RM. Microbial communities related to biodegradation of dispersed Macondo oil at low seawater temperature with Norwegian coastal seawater. *Microb Biotechnol* 2015;8:989–98. <https://doi.org/10.1111/1751-7915.12303>.
- Bristow LA, Mohr W, Ahmerkamp S, Kuypers MMM. Nutrients that limit growth in the ocean. *Curr Biol* 2017;27:R474–8. <https://doi.org/10.1016/j.cub.2017.03.030>.
- Cai Minggang, Liu M, Hong Q, Lin J, Huang P, Hong J, et al. Fate of polycyclic aromatic hydrocarbons in seawater from the western Pacific to the Southern Ocean (17.5°N to 69.2°S) and their inventories on the antarctic shelf. *Environ Sci Technol* 2016;50:9161–8. <https://doi.org/10.1021/acs.est.6b02766>.
- Cerro-Gálvez E, Dachs J, Lundin D, Fernández-Pinos M-C, Sebastián M, Vila-Costa M. Responses of Coastal Marine Microbiomes Exposed to Anthropogenic Dissolved Organic Carbon. *Environ Sci Technol* 2021;55:9609–21. <https://doi.org/10.1021/acs.est.0c07262>.
- Corteselli EM, Aitken MD, Singleton DR. *Rugosibacter aromaticivorans* gen. nov., sp. nov., a bacterium within the family Rhodocyclaceae, isolated from contaminated soil, capable of degrading aromatic compounds. *Int J Syst Evol Microbiol* 2017a;67:311–8. <https://doi.org/10.1099/ijsem.0.001622>.
- Corteselli EM, Aitken MD, Singleton DR. Description of *Immundisolibacter cernigliae* gen. nov., sp. nov., a high-molecular-weight polycyclic aromatic hydrocarbon-degrading bacterium within the class Gammaproteobacteria, and proposal of *Immundisolibacterales* ord. nov. and *Immundisolibacteraceae* fam. nov. *Int J Syst Evol Microbiol* 2017b;67:925–31. <https://doi.org/10.1099/ijsem.0.001714>.
- Czech L, Barbera P, Stamatakis A. Genesis and Gappa: processing, analyzing and visualizing phylogenetic (placement) data. *Bioinform* 2020;36:3263–5. <https://doi.org/10.1093/bioinformatics/btaa070>.
- Czech L, Stamatakis A, Dunthorn M, Barbera P. Metagenomic Analysis Using Phylogenetic Placement—A Review of the First Decade. *Front Bioinform* 2022;2. <https://doi.org/10.3389/fbinf.2022.871393>.
- DeBruyn JM, Mead TJ, Sayler GS. Horizontal Transfer of PAH Catabolism Genes in *Mycobacterium*: Evidence from Comparative Genomics and Isolated Pyrene-Degrading Bacteria. *Environ Sci Technol* 2012;46:99–106. <https://doi.org/10.1021/es201607y>.
- Duran R, Cravo-Laureau C. Role of environmental factors and microorganisms in determining the fate of polycyclic aromatic hydrocarbons in the marine environment. *FEMS Microbiol Rev* 2016;40:814–30. <https://doi.org/10.1093/femsre/fuw031>.
- Echeveste P, Galbán-Malagón C, Dachs J, Berrojalbiz N, Agustí S. Toxicity of natural mixtures of organic pollutants in temperate and polar marine phytoplankton. *Sci Total Environ* 2016;571:34–41. <https://doi.org/10.1016/j.scitotenv.2016.07.111>.

- Eddy SR. Accelerated Profile HMM Searches. *PLoS Comput Biol* 2011;7:e1002195. <https://doi.org/10.1371/journal.pcbi.1002195>.
- Eren AM, Esen ÖC, Quince C, Vineis JH, Morrison HG, Sogin ML, et al. Anvi'o: an advanced analysis and visualization platform for 'omics data. *PeerJ* 2015;3:e1319. <https://doi.org/10.7717/peerj.1319>.
- Finn RD, Tate J, Misty J, Coghill PC, Sammut SJ, Hotz H-R, et al. The Pfam protein families database. *Nucleic Acids Res* 2007;36:D281–8. <https://doi.org/10.1093/nar/gkm960>.
- Fuhrman JA, Cram JA, Needham DM. Marine microbial community dynamics and their ecological interpretation. *Nat Rev Microbiol* 2015;13:133–46. <https://doi.org/10.1038/nrmicro3417>.
- Ghosal D, Ghosh S, Dutta TK, Ahn Y. Current State of Knowledge in Microbial Degradation of Polycyclic Aromatic Hydrocarbons (PAHs): A Review. *Front Microbiol* 2016;7:1369. <https://doi.org/10.3389/fmicb.2016.01369>.
- Góngora E, Lirette A-O, Freyria NJ, Greer CW, Whyte LG. Metagenomic survey reveals hydrocarbon biodegradation potential of Canadian high Arctic beaches. *Environ Microbiome* 2024;19:72. <https://doi.org/10.1186/s40793-024-00616-y>.
- González-Gaya B, Fernández-Pinos M-C, Morales L, Méjanelle L, Abad E, Piña B, et al. High atmosphere–ocean exchange of semivolatile aromatic hydrocarbons. *Nat Geosci* 2016;9:438–42. <https://doi.org/10.1038/ngeo2714>.
- González-Gaya B, Martínez-Varela A, Vila-Costa M, Casal P, Cerro-Gálvez E, Berrojalbiz N, et al. Biodegradation as an important sink of aromatic hydrocarbons in the oceans. *Nat Geosci* 2019 12:2 2019;12:119–25. <https://doi.org/10.1038/s41561-018-0285-3>.
- Hedlund BP, Staley JT. Isolation and characterization of *Pseudoalteromonas* strains with divergent polycyclic aromatic hydrocarbon catabolic properties. *Environ Microbiol* 2006;8:178–82. <https://doi.org/10.1111/j.1462-2920.2005.00871.x>.
- Honda M, Suzuki N. Toxicities of Polycyclic Aromatic Hydrocarbons for Aquatic Animals. *Int J Environ Res Public Health* 2020;17:1363. <https://doi.org/10.3390/ijerph17041363>.
- Iriarte J, Dachs J, Casas G, Martínez-Varela A, Berrojalbiz N, Vila-Costa M. Snow-Dependent Biogeochemical Cycling of Polycyclic Aromatic Hydrocarbons at Coastal Antarctica. *Environ Sci Technol* 2023;57:1625–36. <https://doi.org/10.1021/acs.est.2c05583>.
- Iwai S, Johnson TA, Chai B, Hashsham SA, Tiedje JM. Comparison of the Specificities and Efficacies of Primers for Aromatic Dioxygenase Gene Analysis of Environmental Samples. *Appl Environ Microbiol* 2011;77:3551–7. <https://doi.org/10.1128/AEM.00331-11>.
- Jeon Y, Kwon YS, Noh YJ, Lee S-M, Song J, Kim J-H, et al. Unraveling the mechanisms of benzo[a]pyrene degradation by *Pigmentiphaga kullae* strain KIT-003 using a multi-omics approach. *Ecotoxicol Environ Saf* 2024;281:116665. <https://doi.org/10.1016/j.ecoenv.2024.116665>.
- Khot V, Zorz J, Gittins DA, Chakraborty A, Bell E, Bautista MA, et al. CANT-HYD: A Curated Database of Phylogeny-Derived Hidden Markov Models for Annotation of Marker Genes Involved in Hydrocarbon Degradation. *Front Microbiol* 2022;12. <https://doi.org/10.3389/fmicb.2021.764058>.
- Kimes NE, Callaghan A V., Suflita JM, Morris PJ. Microbial transformation of the Deepwater Horizon oil spill—past, present, and future perspectives. *Front Microbiol* 2014;5:603. <https://doi.org/10.3389/fmicb.2014.00603>.
- Kleindienst S, Grim S, Sogin M, Bracco A, Crespo-Medina M, Joye SB. Diverse, rare microbial taxa responded to the Deepwater Horizon deep-sea hydrocarbon plume. *ISME J* 2016;10:400–15. <https://doi.org/10.1038/ismej.2015.121>.
- Krivoruchko A, Kuyukina M, Peshkur T, Cunningham CJ, Ivshina I. *Rhodococcus* Strains from the Specialized Collection of Alkanotrophs for Biodegradation of Aromatic Compounds. *Molecules* 2023;28:2393. <https://doi.org/10.3390/molecules28052393>.
- Krolicka A, Boccadoro C, Nilsen MM, Baussant T. Capturing Early Changes in the Marine Bacterial Community as a Result of Crude Oil Pollution in a Mesocosm Experiment. *Microbes Environ* 2017;32:358–66. <https://doi.org/10.1264/jsme2.ME17082>.
- Krolicka A, Boccadoro C, Nilsen MM, Demir-Hilton E, Birch J, Preston C, et al. Identification of microbial key-indicators of oil contamination at sea through tracking of oil biotransformation: An Arctic field and laboratory study. *Sci Total Environ*

- 2019;696:133715. <https://doi.org/10.1016/j.scitotenv.2019.133715>.
- Li S, Shen W, Lian S, Wu Y, Qu Y, Deng Y. DARHD: A sequence database for aromatic ring-hydroxylating dioxygenase analysis and primer evaluation. *J Hazard Mater* 2022;436:129230. <https://doi.org/10.1016/j.jhazmat.2022.129230>.
- Liu F, Li J, Feng G, Li Z. New Genomic Insights into "Entotheonella" Symbionts in Theonella swinhoei: Mixotrophy, Anaerobic Adaptation, Resilience, and Interaction. *Front Microbiol* 2016;7. <https://doi.org/10.3389/fmicb.2016.01333>.
- Liu M, Cai M, Duan M, Chen M, Lohmann R, Lin Y, et al. PAHs in the North Atlantic Ocean and the Arctic Ocean: Spatial Distribution and Water Mass Transport. *J Geophys Res Oceans* 2022;127. <https://doi.org/10.1029/2021JC018389>.
- Liu Q, Peng Y, Liao J, Liu X, Peng J, Wang J-H, et al. Broad-spectrum hydrocarbon-degrading microbes in the global ocean metagenomes. *Sci Total Environ* 2024;926:171746. <https://doi.org/10.1016/j.scitotenv.2024.171746>.
- Love CR, Arrington EC, Gosselin KM, Reddy CM, Van Mooy BAS, Nelson RK, et al. Microbial production and consumption of hydrocarbons in the global ocean. *Nat Microbiol* 2021;6:489–98. <https://doi.org/10.1038/s41564-020-00859-8>.
- Lu C, Hong Y, Liu J, Gao Y, Ma Z, Yang B, et al. A PAH-degrading bacterial community enriched with contaminated agricultural soil and its utility for microbial bioremediation. *Environ Pollut* 2019;251:773–82. <https://doi.org/10.1016/j.envpol.2019.05.044>.
- Lundin D. Reference Phylogenies. GitHub Repository 2023a. https://github.com/LNUc-EEMiS/reference_phylogenies/blob/master/ring-hydroxylase_alpha/README.md (accessed November 20, 2024).
- Lundin D. nf-core/phyloplace: First release, v1.0 [software], 2023b. Zenodo. <https://doi.org/10.5281/zenodo.7643948>.
- Ma Y, Wang L, Shao Z. Pseudomonas, the dominant polycyclic aromatic hydrocarbon-degrading bacteria isolated from Antarctic soils and the role of large plasmids in horizontal gene transfer. *Environ Microbiol* 2006;8:455–65. <https://doi.org/10.1111/j.1462-2920.2005.00911.x>.
- Mallick S, Chakraborty J, Dutta TK. Role of oxygenases in guiding diverse metabolic pathways in the bacterial degradation of low-molecular-weight polycyclic aromatic hydrocarbons: A review. *Crit Rev Microbiol* 2011;37:64–90. <https://doi.org/10.3109/1040841X.2010.512268>.
- Martinez-Varela A, Casas G, Berrojalbiz N, Piña B, Dachs J, Vila-Costa M. Polycyclic Aromatic Hydrocarbon Degradation in the Sea-Surface Microlayer at Coastal Antarctica. *Front Microbiol* 2022;13. <https://doi.org/10.3389/fmicb.2022.907265>.
- Martinez-Varela A, Cerro-Gálvez E, Auladell A, Sharma S, Moran MA, Kiene RP, et al. Bacterial responses to background organic pollutants in the northeast subarctic Pacific Ocean. *Environ Microbiol* 2021;1462–2920.15646. <https://doi.org/10.1111/1462-2920.15646>.
- Marzuki I, Asaf R, Paena M, Athirah A, Nisaa K, Ahmad R, et al. Anthracene and Pyrene Biodegradation Performance of Marine Sponge Symbiont Bacteria Consortium. *Molecules* 2021;26:6851. <https://doi.org/10.3390/molecules26226851>.
- Mason OU, Hazen TC, Borglin S, Chain PSG, Dubinsky EA, Fortney JL, et al. Metagenome, metatranscriptome and single-cell sequencing reveal microbial response to Deepwater Horizon oil spill. *ISME J* 2012;6:1715–27. <https://doi.org/10.1038/ismej.2012.59>.
- Nazari MT, Simon V, Machado BS, Crestani L, Marchezi G, Concolato G, et al. Rhodococcus: A promising genus of actinomycetes for the bioremediation of organic and inorganic contaminants. *J Environ Manage* 2022;323:116220. <https://doi.org/10.1016/j.jenvman.2022.116220>.
- Ohno S. Evolution by gene duplication. Heidelberg: Springer-Verlag; 1970.
- Pandolfo E, Barra Caracciolo A, Rolando L. Recent Advances in Bacterial Degradation of Hydrocarbons. *Water (Basel)* 2023;15:375. <https://doi.org/10.3390/w15020375>.
- Parks DH, Chuvochina M, Rinke C, Mussig AJ, Chaumeil P-A, Hugenholtz P. GTDB: an ongoing census of bacterial and archaeal diversity through a phylogenetically consistent, rank normalized and complete genome-based taxonomy. *Nucleic Acids Res* 2022;50:D785–94. <https://doi.org/10.1093/nar/gkab776>.

- Patel AB, Shaikh S, Jain KR, Desai C, Madamwar D. Polycyclic Aromatic Hydrocarbons: Sources, Toxicity, and Remediation Approaches. *Front Microbiol* 2020;11. <https://doi.org/10.3389/fmicb.2020.562813>.
- Peeb A, Dang NP, Truu M, Nölvak H, Petrich C, Truu J. Assessment of Hydrocarbon Degradation Potential in Microbial Communities in Arctic Sea Ice. *Microorganisms* 2022;10:328. <https://doi.org/10.3390/microorganisms10020328>.
- Peng T, Kan J, Hu J, Hu Z. Genes and novel sRNAs involved in PAHs degradation in marine bacteria *Rhodococcus* sp. P14 revealed by the genome and transcriptome analysis. *3 Biotech* 2020;10:140. <https://doi.org/10.1007/s13205-020-2133-6>.
- Pérez-Pantoja D, Donoso R, Agulló L, Córdova M, Seeger M, Pieper DH, et al. Genomic analysis of the potential for aromatic compounds biodegradation in Burkholderiales. *Environ Microbiol* 2012;14:1091–117. <https://doi.org/10.1111/j.1462-2920.2011.02613.x>.
- Persson L, Carney Almroth BM, Collins CD, Cornell S, de Wit CA, Diamond ML, et al. Outside the Safe Operating Space of the Planetary Boundary for Novel Entities. *Environ Sci Technol* 2022;56:1510–21. <https://doi.org/10.1021/acs.est.1c04158>.
- Rinke C, Rubino F, Messer LF, Youssef N, Parks DH, Chuvochina M, et al. A phylogenomic and ecological analysis of the globally abundant Marine Group II archaea (Ca. Poseidoniales ord. nov.). *ISME J* 2019;13:663–75. <https://doi.org/10.1038/s41396-018-0282-y>.
- Ruiz-González C, Logares R, Sebastián M, Mestre M, Rodríguez-Martínez R, Galí M, et al. Higher contribution of globally rare bacterial taxa reflects environmental transitions across the surface ocean. *Mol Ecol* 2019;28:1930–45. <https://doi.org/10.1111/mec.15026>.
- Salazar G, Paoli L, Alberti A, Huerta-Cepas J, Ruscheweyh H-J, Cuenca M, et al. Gene Expression Changes and Community Turnover Differentially Shape the Global Ocean Metatranscriptome. *Cell* 2019;179:1068–1083.e21. <https://doi.org/10.1016/j.cell.2019.10.014>.
- Sánchez P, Coutinho FH, Sebastián M, Pernice MC, Rodríguez-Martínez R, Salazar G, et al. Marine picoplankton metagenomes and MAGs from eleven vertical profiles obtained by the Malaspina Expedition. *Sci Data* 2024;11:154. <https://doi.org/10.1038/s41597-024-02974-1>.
- Singh A, Kumar Mishra V. Biodegradation of organic pollutants for its effective remediation from the environment and the role of various factors affecting the biodegradation process. *Sustainable Environmental Clean-up*, Elsevier; 2021, p. 1–27. <https://doi.org/10.1016/B978-0-12-823828-8.00001-3>.
- Somee MR, Amoozegar MA, Dastgheib SMM, Shavandi M, Maman LG, Bertilsson S, et al. Genome-resolved analyses show an extensive diversification in key aerobic hydrocarbon-degrading enzymes across bacteria and archaea. *BMC Genomics* 2022;23:690. <https://doi.org/10.1186/s12864-022-08906-w>.
- Sunagawa S, Coelho LP, Chaffron S, Kultima JR, Labadie K, Salazar G, et al. Structure and function of the global ocean microbiome. *Science* (1979) 2015;348. <https://doi.org/10.1126/science.1261359>.
- Vaidya S, Jain K, Madamwar D. Metabolism of pyrene through phthalic acid pathway by enriched bacterial consortium composed of *Pseudomonas*, *Burkholderia*, and *Rhodococcus* (PBR). *3 Biotech* 2017;7:29. <https://doi.org/10.1007/s13205-017-0598-8>.
- Varjani SJ, Upasani VN. A new look on factors affecting microbial degradation of petroleum hydrocarbon pollutants. *Int Biodeterior Biodegradation* 2017;120:71–83. <https://doi.org/10.1016/j.ibiod.2017.02.006>.
- Vila-Costa M, Lundin D, Fernández-Pinos M-C, Iriarte J, Irigoien X, Piña B, et al. Responses to organic pollutants in the tropical Pacific and subtropical Atlantic Oceans by pelagic marine bacteria. *Front Environ Sci* 2023;11. <https://doi.org/10.3389/fenvs.2023.1110169>.
- Vilchez-Vargas R, Geffers R, Suárez-Diez M, Conte I, Waliczek A, Kaser VS, et al. Analysis of the microbial gene landscape and transcriptome for aromatic pollutants and alkane degradation using a novel internally calibrated microarray system. *Environ Microbiol* 2013;15:1016–39. <https://doi.org/10.1111/j.1462-2920.2012.02752.x>.
- Wang W, Wang L, Shao Z. Polycyclic Aromatic Hydrocarbon (PAH) Degradation Pathways of the Obligate Marine PAH Degradator *Cycloclasticus* sp. Strain P1. *Appl Environ Microbiol* 2018;84. <https://doi.org/10.1128/AEM.01261-18>.

Wilkinson M, McInerney JO, Hirt RP, Foster PG, Embley TM. Of clades and clans: terms for phylogenetic relationships in unrooted trees. *Trends Ecol Evol* 2007;22:114–5. <https://doi.org/10.1016/j.tree.2007.01.002>.

Zada S, Zhou H, Xie J, Hu Z, Ali S, Sajjad W, et al. Bacterial degradation of pyrene: Biochemical reactions and mechanisms. *Int Biodeterior Biodegradation* 2021;162:105233. <https://doi.org/10.1016/j.ibiod.2021.105233>.

Zhang C, Meckenstock RU, Weng S, Wei G, Hubert CRJ, Wang J-H, et al. Marine sediments harbor diverse archaea and bacteria with the potential for anaerobic hydrocarbon degradation via fumarate addition. *FEMS Microbiol Ecol* 2021;97. <https://doi.org/10.1093/femsec/fiab045>.

Zhang L, Ma Y, Vojta S, Morales-McDevitt M, Hoppmann M, Soltwedel T, et al. Presence, Sources and Transport of Polycyclic Aromatic Hydrocarbons in the Arctic Ocean. *Geophys Res Lett* 2023;50. <https://doi.org/10.1029/2022GL101496>.

Zhang Xue, Zhang Z-F, Zhang Xianming, Zhu F-J, Li Y-F, Cai M, et al. Polycyclic Aromatic Hydrocarbons in the Marine Atmosphere from the Western Pacific to the Southern Ocean: Spatial Variability, Gas/Particle Partitioning, and Source Apportionment. *Environ Sci Technol* 2022;56:6253–61. <https://doi.org/10.1021/acs.est.1c08429>.

SUPPLEMENTARY MATERIAL

Entanglement of Hydrocarbon-Degrading Bacteria and Polycyclic Aromatic Hydrocarbons in the Ocean

Jon Iriarte^{1,2}, Daniel Lundin^{3,4}, Alicia Martínez-Varela¹, José M. González⁵, Jordi Dachs¹, and Maria Vila-Costa^{1*}

¹ Department of Environmental Chemistry, IDAEA-CSIC, Barcelona, Catalunya, Spain.

² Doctoral program in Analytical Chemistry and the Environment, Department of Chemical Engineering and Analytical Chemistry, Faculty of Chemistry, Universitat de Barcelona, Barcelona, Catalunya, Spain.

³ Centre for Ecology and Evolution in Microbial model Systems – EEMiS, Linnaeus University, SE-39182, Kalmar, Sweden;

⁴ Dept. of Biochemistry and Biophysics, Stockholm University, SE-10691, Stockholm, Sweden.

⁵ Department of Microbiology, University of La Laguna, La Laguna, Spain.

E-mail contact: maria.vila@idaea.csic.es

Table of contents

Annex S1: 16S rRNA gene amplicon sequencing and taxonomic annotation using ampliseq pipeline.

Annex S2: PAH concentrations data from Malaspina expedition.

Table S1: Versions of R and packages used in this analysis.

Table S2*: Bacterial genomes with *arhdA* hits from GTDB (R07-RS207), genome taxonomy and number of hits per method.

Table S3*: Anvi'o bacterial tree data.

Table S4: Archaeal genomes with *arhdA* hits from GTDB (R07-RS207), genome taxonomy and number of hits per method.

Table S5*: Taxonomic annotation of unique *arhdA* hits from Malaspina Vertical Profiles Gene Database (M-GeneDB-VP) database.

Table S6: Average number of *arhdA* gene copies and taxonomic classification per order.

Table S7*: Individual gene abundance, taxonomy and phyloplace functional annotation of the hits found in each Malaspina sample.

Table S8: Multiple Linear Regression models summary table.

Table S9: RDAs summary table.

*Tables S2,S3,S5 and S7 are in separate excel file files.

Figure S1: Comparison of the ARHDa identification methods on GTDB.

Figure S2: Bacterial taxonomy of the *arhdA* gene hits from GTDB.

Figure S3: Archaeal taxonomy of the *arhdA* gene hits from GTDB.

Figure S4: Phylogenetic diversity of the *arhdA* unique genes from M-GeneDB-VP.

Figure S5: Geographic distribution of the *arhdA* gene abundances (gene copies per cell).

Figure S6: Barplot of *arhdA* abundance as gene copies per cell per station, water layer, and filter-fraction.

Figure S7: Geographic distribution of *arhdA* gene copies per cell and particulate phase PAH concentrations.

Figure S8: Geographic distribution of *arhdA* gene copies per cell and planktonic phase PAH concentrations.

Figure S9: Linear regression plots of *arhdA* gene copies per cell vs PAH concentrations.

Figure S10: Linear regression plots of ratio the of *arhdA* gene copies per cell between free-living and particle-attached size fraction vs PAH concentrations per sample matrix.

Figure S11: RDA sites and scores plot for bacterial communities including cyanobacteria.

Annex S1: 16S rRNA gene amplicon sequencing and taxonomic annotation using ampliseq pipeline

Sequencing of the 16S rRNA gene in the surface stations was done as described elsewhere (Ruiz-González et al., 2019). Briefly, the V4–V5 region of the 16S rRNA gene was amplified with the primers 515F and 926R (Parada et al., 2016) and sequenced in an Illumina MiSeq platform using 2 × 250 bp paired-end approach at the Research and Testing Laboratory facility (Lubbock, TX, USA; <http://www.researchandtesting.com>).

The raw 16S rRNA gene amplicon sequencing data were downloaded from the European Nucleotide Archive (acc. num. PRJEB25224) and were analyzed using the nf-core pipeline for amplicon sequencing called ampliseq (v.2.4.0) within Nextflow (v.22.04.5). Briefly, primer trimming was skipped (`—skip_cutadapt`) since the primer sequences had already been removed from the raw data. DADA2 (v.1.22.0) (Callahan et al., 2016) incorporated in the Ampliseq pipeline was used for denoising and quality control followed by inference of amplicon sequence variants (ASVs) and chimera removal (parameters: `maxN = 0`, `maxEE = 2,2`, `truncLen = 232, 218`). Taxonomic assignment of the ASVs used SBDI-GTDB (Sativa curated 16S GTDB database, R07-RS207-1; FigShare. doi: 10.17044/scilifelab.14869077.v49). ASVs annotated as mitochondria or chloroplast were filtered out by default by Ampliseq. The dataset accounted for a total of 7047 unique ASVs.

Annex S2: PAH concentrations data from Malaspina expedition

PAH concentrations were measured in the dissolved phase, particulated phase and plankton, and have been reported elsewhere (González-Gaya et al., 2016, 2019). This is the largest available dataset on oceanic PAHs, and as all samples have been analyzed by the same research group using the same methodology there is not bias between oceans. We use these concentrations in this work when needed. Briefly, water samples for the dissolved and particulate phases were taken at 4 m depth using the continuous seawater system of the ship, and during transects. In order to match the PAH concentrations with the other environmental variables measured at static stations, the initial coordinates of each transect have been considered as the sampling point, and only those sampling points for which physicochemical and genomic data were available have been included in this study. In the case of some metagenomic samples for which there was no data on PAH concentrations nor environmental variables we computed the mean of the data of the prior and posterior stations (stations 19, 49 and 141), or directly used the data of the closest station (stations 30, 76, 92 and 101). For the metagenomic samples obtained from the DCM, the in-situ pollutant concentrations were assumed to equal the one measured at surface. Concurrently, plankton samples were gathered from vertical trawls with a 50µm mesh size net from 20 m deeper than the deep chlorophyll maxima depth (DCM) to the surface (depths ranging from 20 to 160).

Table S1: Versions of R and packages used in this analysis.

Package	Version	Citation
DT	0.32	Xie, Cheng, and Tan (2024)
base	4.3.3	R Core Team (2024)
car	3.1.2	Fox and Weisberg (2019)
carData	3.0.5	Fox, Weisberg, and Price (2022)
colorspace	2.1.0	Zeileis, Hornik, and Murrell (2009); Stauffer et al. (2009); Zeileis et al. (2020)
corrplot	0.92	Wei and Simko (2021)
cowplot	1.1.3	Wilke (2024)
data.table	1.15.0	Barrett et al. (2024)
ggnewscale	0.4.10	Campitelli (2024)
ggpmisc	0.5.5	Aphalo (2023)
ggpp	0.5.6	Aphalo (2024)
ggrepel	0.9.5	Slowikowski (2024)
ggtree	3.6.2	Yu et al. (2017); Yu et al. (2018); Yu (2020); Yu (2022)
kfigr	1.2.1	Koohafkan (2021)
knitr	1.45	Xie (2014); Xie (2015); Xie (2023)
lattice	0.22.5	Sarkar (2008)
lemon	0.4.9	Edwards (2024)
patchwork	1.2.0	Pedersen (2024)
permute	0.9.7	Simpson (2022)
stats	4.4.1	R Core Team (2024)
tidyverse	2.0.0	Wickham et al. (2019)
treeio	1.22.0	Wang et al. (2020); Yu (2022b)
vegan	2.6.4	Oksanen et al. (2022)
viridis	0.6.5	Garnier et al. (2024)

Table S2: Bacterial genomes with *arhdA* hits from GTDB (R07-RS207), genome taxonomy and number of hits per method (phyloplace or CANT-HYD approach).

*This file is deposited in the CORA, Repositori de Dades de Recerca, and can be accessed in the following dataset: IRIARTE MARTINEZ, JON, 2025, "Table S2. Bacterial genomes with *arhdA* hits from GTDB (R07-RS207), genome taxonomy and number of hits per method", <https://doi.org/10.34810/data2017>.

Table S3: Anvi'o bacterial tree data.

*This file is deposited in the CORA, Repositori de Dades de Recerca, and can be accessed in the following dataset: IRIARTE MARTINEZ, JON, 2025, "Table S3. Anvi'o bacterial tree data", <https://doi.org/10.34810/data2019>.

Table S4: Archaeal genomes with *arhda* hits from GTDB (R07-RS207), genome taxonomy and number of hits per method (phyloplace or CANT-HYD approach).

Genome	checkm comple teness	checkm contam ination	genome size (bp)	Domain	Phylum	Class	Order	Family	Genus	Species	arhda copies phylo place	arhda copies cant_hyd
GCF_000_243315.1	100	0	2817452	Archaea	Thermo proteota	Thermoproteia	Sulfolobales	Sulfolobaceae	Metallosphaera	Metallosphaera yellowstonensis	3	0
GCF_009_601705.1	100	0	2543529	Archaea	Thermo proteota	Thermoproteia	Sulfolobales	Sulfolobaceae	Saccharolobus	Saccharolobus sp009601705	3	0
GCF_003_841465.1	99.3	1.27	4614480	Archaea	Halobacteriota	Halobacteriia	Halobacteriales	Natrialbaceae	Natrarchaeobius	Natrarchaeobius chitinivorans_A	3	0
GCA_000_508305.1	99.4	0	2061920	Archaea	Thermo proteota	Thermoproteia	Sulfolobales	Sulfolobaceae	Sulfolobus	Sulfolobus acidocaldarius_A	3	0
GCF_900_108505.1	98.41	0	3136824	Archaea	Halobacteriota	Halobacteriia	Halobacteriales	Haloferacaceae	Halopenitius	Halopenitius malekzadehii	2	0
GCF_900_107195.1	98.92	0.38	3754978	Archaea	Halobacteriota	Halobacteriia	Halobacteriales	Haloferacaceae	Halobellus	Halobellus clavatus	2	0
GCF_003_841485.1	99.35	0.86	3511219	Archaea	Halobacteriota	Halobacteriia	Halobacteriales	Natrialbaceae	Natrarchaeobius	Natrarchaeobius halalkaliphilus	2	0
GCF_008_245225.1	99.92	0.95	4201486	Archaea	Halobacteriota	Halobacteriia	Halobacteriales	Natrialbaceae	Natrarchaeobius	Natrarchaeobius swarupiae	2	0
GCF_000_012285.1	99.4	0	2225959	Archaea	Thermo proteota	Thermoproteia	Sulfolobales	Sulfolobaceae	Sulfolobus	Sulfolobus acidocaldarius	1	0
GCF_019_175345.1	99.4	0	2916875	Archaea	Thermo proteota	Thermoproteia	Sulfolobales	Sulfolobaceae	Saccharolobus	Saccharolobus shibatae	1	0
GCF_900_107205.1	98.11	0.51	3424491	Archaea	Halobacteriota	Halobacteriia	Halobacteriales	Haloferacaceae	Halopenitius	Halopenitius persicus	1	0
GCF_900_116205.1	99.2	0.4	4108147	Archaea	Halobacteriota	Halobacteriia	Halobacteriales	Natrialbaceae	Halostagnicola	Halostagnicola kamekurae	1	0
GCA_005_877185.1	89.81	5.5	1861687	Archaea	Thermo proteota	Nitrososphaeria	Nitrososphaerales	UBA183	TA-13	TA-13 sp005877185	1	0
GCF_000_306765.2	99.25	0	3904707	Archaea	Halobacteriota	Halobacteriia	Halobacteriales	Haloferacaceae	Haloferax	Haloferax mediterranei	1	0
GCF_000_739575.1	95.63	0.62	3852219	Archaea	Halobacteriota	Halobacteriia	Halobacteriales	Haloferacaceae	Halobellus	Halobellus rufus	1	0
GCF_009_831455.1	99.5	0	3369022	Archaea	Halobacteriota	Halobacteriia	Halobacteriales	Haloarculaceae	Salinirussus	Salinirussus salinus	1	0
GCA_005_877365.1	75.49	1.62	1792239	Archaea	Thermo proteota	Nitrososphaeria	Nitrososphaerales	UBA183	TA-13	TA-13 sp005877365	1	0
GCF_000_337215.1	98.92	0.46	4588634	Archaea	Halobacteriota	Halobacteriia	Halobacteriales	Natrialbaceae	Natronolimn	Natronolimnoba bitans	1	0
GCA_002_496635.1	72.23	1.52	1617893	Archaea	Thermo plasmata	Poseidonii	Poseidoniales	Poseidoniceae	MGLa-L2	inermongolicus MGLa-L2 sp002496635	1	0
GCA_005_954745.1	98.73	1.13	3942449	Archaea	Halobacteriota	Halobacteriia	Halobacteriales	QS-9-68-17	Halostella	Halostella pelagica	1	0
GCF_001_482285.1	99.44	0	3977555	Archaea	Halobacteriota	Halobacteriia	Halobacteriales	Haloferacaceae	Haloferax	Haloferax sp001482285	1	0

GCF_012_222305.1	99.4	0	2789526	Archaea	Thermo proteota	Thermoproteia	Sulfolobales	Sulfolobaceae	Sulfurisphaera	1	0
GCA_003_023195.1	88.72	3.2	3291641	Archaea	Halobact	Halobacteria	Halobact	SW-7-71-33	SW-7-71-33	1	0
GCF_003_967175.1	97.62	0.6	2353189	Archaea	Thermo proteota	Thermoproteia	Sulfolobales	Sulfolobaceae	Sulfodilicoccus	1	0
GCF_000_337695.1	99.92	0.4	4496185	Archaea	Halobact	Halobacteria	Halobact	Natrialbaceae	Natronococcus	1	0
GCF_003_665925.1	99.49	5.91	3871390	Archaea	Halobact	Halobacteria	Halobact	Haloferacaceae	Halobellus	1	0
GCF_004_118325.1	98.65	1.49	4087668	Archaea	Halobact	Halobacteria	Halobact	Halocarullaceae	Halorientalis	1	0
GCF_000_025325.1	99.49	0.95	5440782	Archaea	Halobact	Halobacteria	Halobact	Natrialbaceae	Haloterrigena	1	0
GCF_000_337135.1	99.74	0.76	4309274	Archaea	Halobact	Halobacteria	Halobact	Natrialbaceae	Natrialba	1	0
GCF_002_355635.1	98.22	0.13	3105937	Archaea	Halobact	Halobacteria	Halobact	Haloferacaceae	Halopenitus	1	0
GCA_017_857195.1	96.63	1.49	1781932	Archaea	Thermo proteota	Thermoproteia	Sulfolobales	Sulfolobaceae	Sulfodilicoccus	1	0
GCF_001_316045.1	93.21	0.63	2214633	Archaea	Thermo proteota	Thermoproteia	Sulfolobales	Sulfolobaceae	Sulfuracidifex	1	0
GCF_007_655485.1	98.47	1.14	3351536	Archaea	Halobact	Halobacteria	Halobact	Haloferacaceae	Halobellus	1	0
GCA_001_564255.1	74.3	1.4	2155803	Archaea	Halobact	Halobacteria	Halobact	Natrialbaceae	Tc-Br11-E2g1	1	0
GCA_003_602665.1	74.61	2.4	1764012	Archaea	Thermo plasmata	Poseidonila	Poseidoniales	Poseidonaceae	MGla-L2	1	0
GCA_004_116405.1	99.57	1.81	4891127	Archaea	Halobact	Halobacteria	Halobact	Haloferacaceae	Halogenicoccus	1	0
GCF_003_697845.1	98.92	0.48	3592980	Archaea	Halobact	Halobacteria	Halobact	Haloferacaceae	Halorubrum	1	0
GCF_002_156705.1	99.53	0.4	3930546	Archaea	Halobact	Halobacteria	Halobact	Natrialbaceae	Natrarchaeobaculum	1	0
GCF_002_906575.1	98.42	1.05	4973118	Archaea	Halobact	Halobacteria	Halobact	Haloferacaceae	Salinigranum	1	0
GCF_004_681185.1	99.45	0.53	5038561	Archaea	Halobact	Halobacteria	Halobact	Halocarullaceae	Halomicroarcula	1	0
GCF_003_665935.1	98.73	5.48	3548073	Archaea	Halobact	Halobacteria	Halobact	Haloferacaceae	Halobellus	1	0
GCF_009_729055.1	99.4	0	2803915	Archaea	Thermo proteota	Thermoproteia	Sulfolobales	Sulfolobaceae	Sulfurisphaera	1	0
GCF_900_102305.1	99.15	1.7	4032197	Archaea	Halobact	Halobacteria	Halobact	Halocarullaceae	Halorientalis	1	0
GCA_005_879045.1	80.46	3.2	1695803	Archaea	Thermo plasmata	Thermoplasma	RBG-16-68-12	RBG-16-68-12	RBG-16-68-12	1	0

GCF_000336755.1	99.57	0	3952136	Archaea	Halobact erota	Halobacteria	Halobact eriales	Haloferacaceae	Haloferax elongans	1	0
GCF_000336715.1	99.08	1.28	4052434	Archaea	Halobact erota	Halobacteria	Halobact eriales	Halococcaceae	Halococcus thailandensis	1	0
GCF_000691505.1	87.74	1.1	3178490	Archaea	Halobact erota	Halobacteria	Halobact eriales	Natrialbaceae	Halostagnicola sp000691505	1	0
GCF_004799685.1	99.55	0.95	3749890	Archaea	Halobact erota	Halobacteria	Halobact eriales	Haloferacaceae	Halobellus limi	1	0
GCF_900109065.1	99.19	2.76	3284590	Archaea	Halobact erota	Halobacteria	Halobact eriales	Haloferacaceae	Halohera litchfieldiae	1	0

Table S5: Taxonomic annotation of unique *arhdA* hits from Malaspina Vertical Profiles Gene Database (M-GeneDB-VP) database.

*This file is deposited in the CORA,Repositori de Dades de Recerca, and can be accessed in the following dataset: IRIARTE MARTINEZ, JON, 2025, "Table S5. Taxonomic annotation of unique *arhdA* hits from Malaspina Vertical Profiles Gene Database (M-GeneDB-VP) database.",<https://doi.org/10.34810/data2020>.

Table S6: Average number of *arhdA* gene copies and taxonomic classification per order.

Domain	Class	order	average_gene_copies
Bacteria	Gammaproteobacteria	Alteromonadales	7.25
Bacteria	Gammaproteobacteria	Oceanospirillales	6.67
Bacteria	Actinomycetes	Mycobacteriales	6.53
Bacteria	Gammaproteobacteria	Moraxellales	6.50
Bacteria	Gammaproteobacteria	Acidiferrobacterales	5.00
Bacteria	Nitriliruptoria	Euzebyales	5.00
Bacteria	Gammaproteobacteria	Pseudomonadales	4.50
Bacteria	Alphaproteobacteria	Hyphomonadales	4.40
Bacteria	Acidimicrobiia	Acidimicrobiales	4.20
Bacteria	Actinomycetes	Micrococcales	4.00
Bacteria	Flavobacteriia	Flavobacteriales	4.00
Bacteria	Oligoflexia	Bacteriovoracales	4.00
Bacteria	Verrucomicrobiia	Verrucomicrobiales	4.00
Bacteria	Gammaproteobacteria	unclassified	3.93
Bacteria	Alphaproteobacteria	Rhodospirillales	3.91
Bacteria	Gammaproteobacteria	Cellvibrionales	3.80
Bacteria	Alphaproteobacteria	unclassified	3.79
Bacteria	Actinomycetes	unclassified	3.79
Bacteria	unclassified	unclassified	3.76
Bacteria	Alphaproteobacteria	Rhodobacterales	3.55
Bacteria	Dehalococcoidia	unclassified	3.50
Archaea	unclassified	unclassified	3.42
Bacteria	Gammaproteobacteria	Xanthomonadales	3.33
Bacteria	Alphaproteobacteria	Sphingomonadales	3.25
Bacteria	Alphaproteobacteria	Pelagibacterales	3.04
Bacteria	Alphaproteobacteria	Hyphomicrobiales	3.03
Bacteria	Balneolia	Balneolales	3.00
Bacteria	Planctomycetia	Planctomycetales	3.00
Bacteria	Saprospiria	Saprospirales	3.00

Bacteria	Actinomycetes	Pseudonocardiales	2.86
Bacteria	Gammaproteobacteria	Chromatiales	2.75
Bacteria	Gammaproteobacteria	Nevskiales	2.50
Bacteria	Cytophagia	Cytophagales	2.25
Bacteria	Acidimicrobiia	unclassified	2.17
Bacteria	Gammaproteobacteria	Thiotrichales	2.15
Bacteria	Deltaproteobacteria	unclassified	2.04
Bacteria	Alphaproteobacteria	Rickettsiales	2.00
Bacteria	Betaproteobacteria	Nitrosomonadales	2.00
Bacteria	Deltaproteobacteria	Myxococcales	2.00
Bacteria	Gammaproteobacteria	Legionellales	2.00
Bacteria	Planctomycetia	Pirellulales	2.00
Archaea	Candidatus Poseidoniia	Candidatus Poseidoniales	1.67
Bacteria	Betaproteobacteria	Burkholderiales	1.56
Bacteria	Betaproteobacteria	unclassified	1.25
Bacteria	Actinomycetes	Propionibacteriales	1.00
Bacteria	Blastocatellia	Blastocatellales	1.00
Bacteria	Opitutia	Puniceococcales	1.00
Bacteria	unclassified	Oscillatoriales	1.00

Table S7: Individual gene abundance, taxonomy, and phyloplace functional annotation of the hits found in each Malaspina sample.

*This file is deposited in the CORA, Repositori de Dades de Recerca, and can be accessed in the following dataset: "Table S7. Individual gene abundance, taxonomy, and phyloplace functional annotation of aromatic ring hydroxylating dioxygenase alpha subunit gene hits found in Malaspina database samples.", <https://doi.org/10.34810/data2021>.

Table S8: Multiple Linear Regression models summary table. Abbreviations: hmw, high molecular weight; lmw, low molecular weight; Cw, seawater dissolved phase PAH concentrations; Cp, seawater particulate phase PAH concentrations; P, planktonic phase PAH concentrations; HBAC, heterotrophic bacterial abundance; T, temperature; NO₂+NO₃, nitrate plus nitrite concentrations; Tot_CHL, total chlorophyll a concentration.

PAH concentrations grouped by MW and sample fraction; volumetric concentrations (ng/L)								
Dependent variable	R ²	Adj R ²	Residual Standard Error	Model P value	Intercept	Independent variable	Coefficient estimate	P value
<i>arhdA</i> (copies/cell)	0.12	0.09	0.24	3.40E-02	-0.73	lmw_Cw	-0.084	0.034
	0.15	0.12	0.23	1.70E-02	-0.73	T	-0.094	0.017
<i>arhdA</i> * HBAC (copies/L)	0.51	0.41	0.29	5.40E-04	8.01	NO ₂ + NO ₃	0.12	0.09
						Tot_CHL	-0.18	9.00E-03
						hmw_Cw	-0.17	8.00E-03
						lmw_Cp	-0.15	1.00E-02
						hmw_Cp	0.26	6.30E-05
						hmw_P	-0.16	1.80E-02

Table S9: RDA analysis summary table. Abbreviations: lmw, low molecular weight; Cw, seawater dissolved phase PAH concentrations; T, temperature; Tot_CHL, total chlorophyll a concentration; FLUO, water in vivo fluorescence.

Dependent variable	Variance proportion explained by				Independent variable	F-statistics	P value
	R ²	Adj R ²	Model P value	Constrained variables	Unconstrained variables	Same number of PCs in a PCA model	
ASV without cyanobacteria (Hellinger transformed counts)	0.17	0.10	1.00E-03	17.39	82.60	42.17	3.00E-03
				RDA1: 7.51		PC1: 15.29	6.00E-03
				RDA2: 4.02		PC2: 11.87	1.00E-03
				RDA3: 3.56		PC3: 8.74	1.00E-02
ASV with cyanobacteria (Hellinger transformed counts)	0.19	0.14	1.00E-03	2.30		PC4: 6.27	
				19.30	80.70	48.35	2.00E-03
				RDA1: 12.16		PC1: 25.40	1.00E-03
				RDA2: 4.46		PC2: 14.14	5.00E-03
				RDA3: 2.68		PC3: 8.81	
						lmw_Cw	4.04
						T	3.58
						Tot_CHL	2.73
						FLUO	

HMM search of ARHD α sequences among species-representative GTDB genomes (R07-RS207)

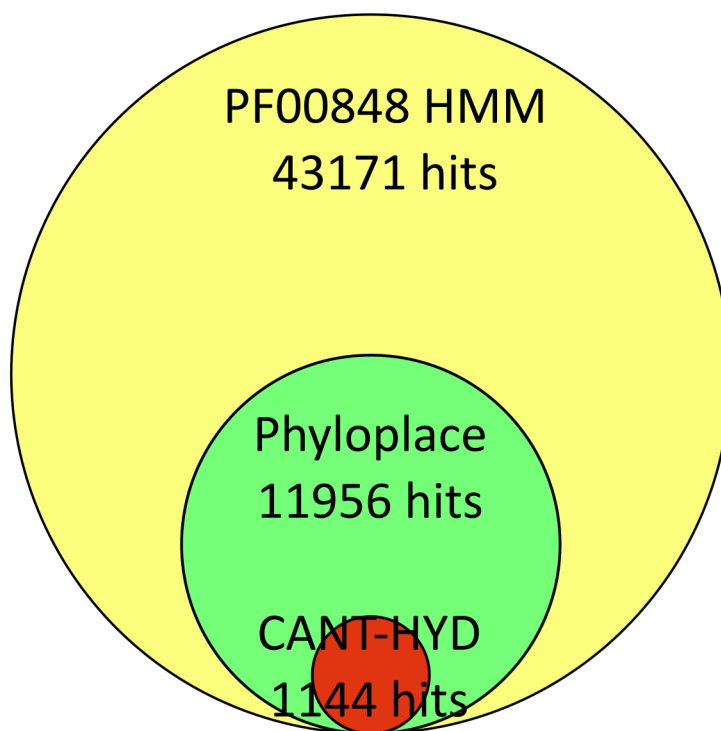


Figure S1: Comparison of the three methods used in this study to retrieve potential ARHD α -subunit sequences from GTDB species representative genomes. The yellow circle represents the HMM search using the HMM PF00848, the green circle represents the HMM search with PF00848 and the subsequent phylogenetic placement and selection of ARHD α sequences, and the red circle represents the HMM search using CANT-HYD HMMs (NdoB and MAH_alpha) with parameters recommended by the authors. The areas of the circles are proportional to the number of hits detected by each method.

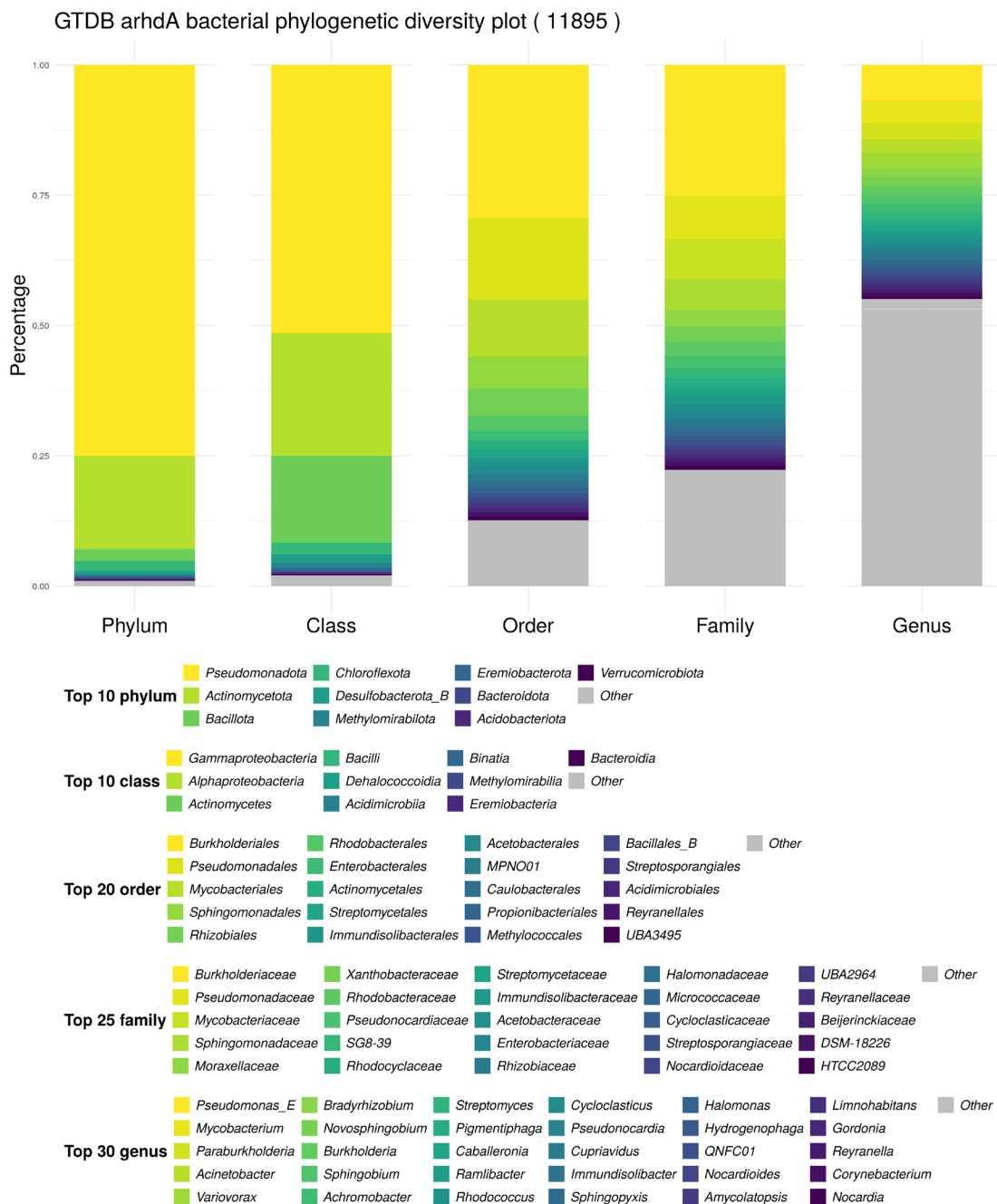


Figure S2: Taxonomy of the 11,895 unique potential *arhA* gene hits obtained from GTDB classified as bacteria, represented as the relative abundance of the main taxa at each taxonomic level, from phylum to family.

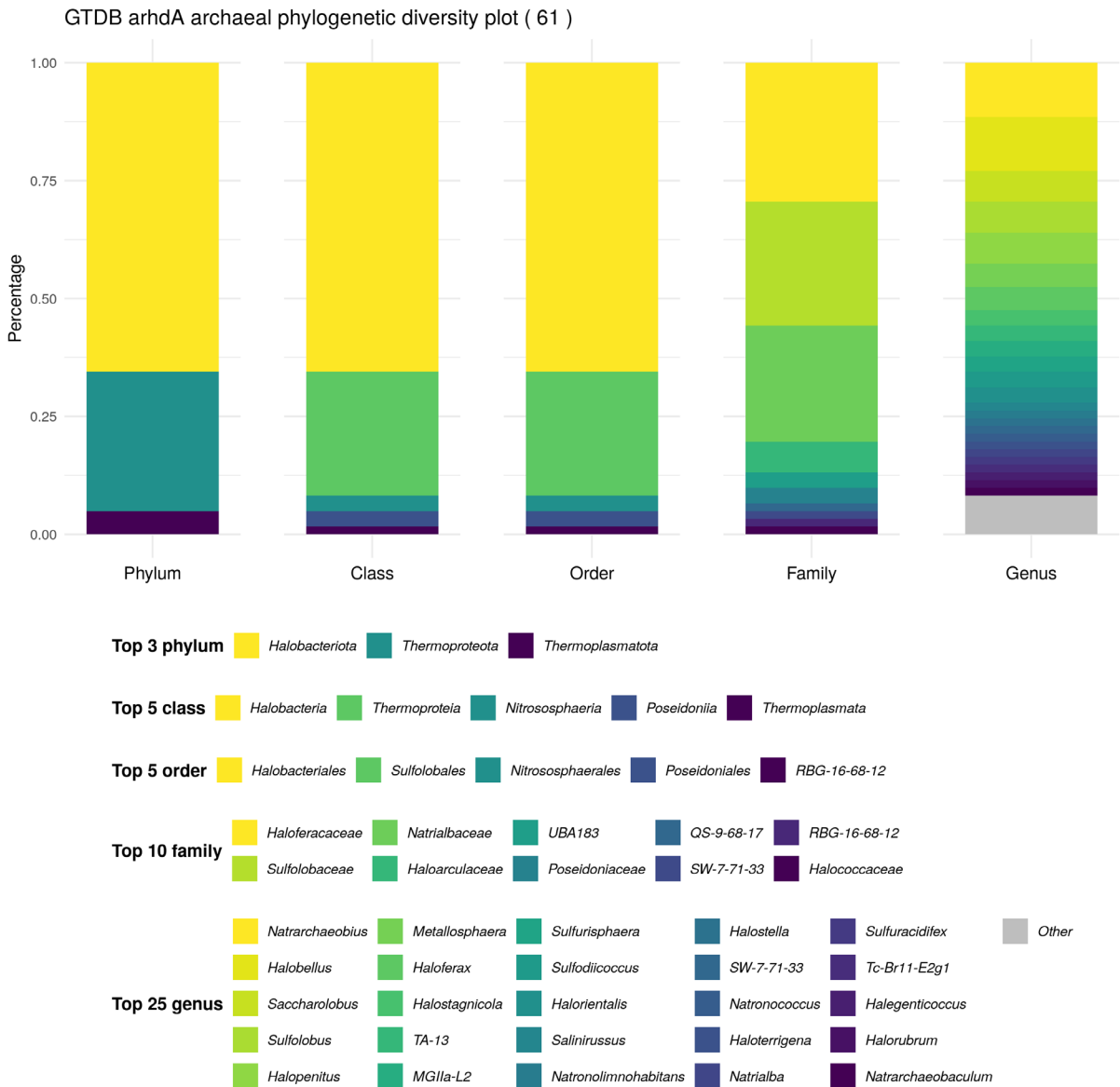


Figure S3: Taxonomy of the 61 unique potential *arhA* gene hits obtained from GTDB classified as archaea, represented as the relative abundance of the main taxa at each taxonomic level, from phylum to family.

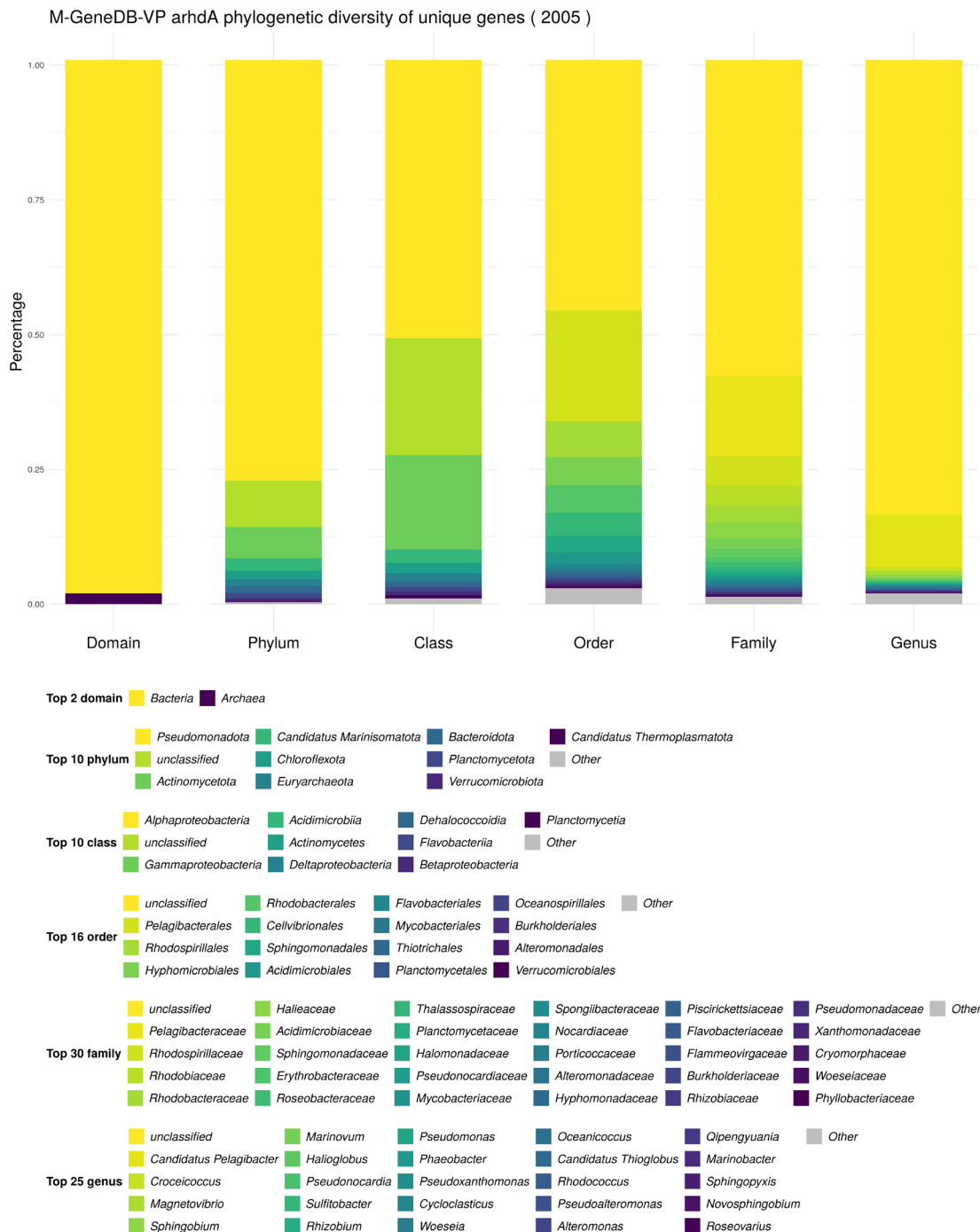


Figure S4: Taxonomy of the 2005 unique potential *arh*dA gene hits obtained from Malaspina Vertical Profiles Gene Database (M-GeneDB-VP), represented as the relative abundance of the main taxa at each taxonomic level, from domain to family.

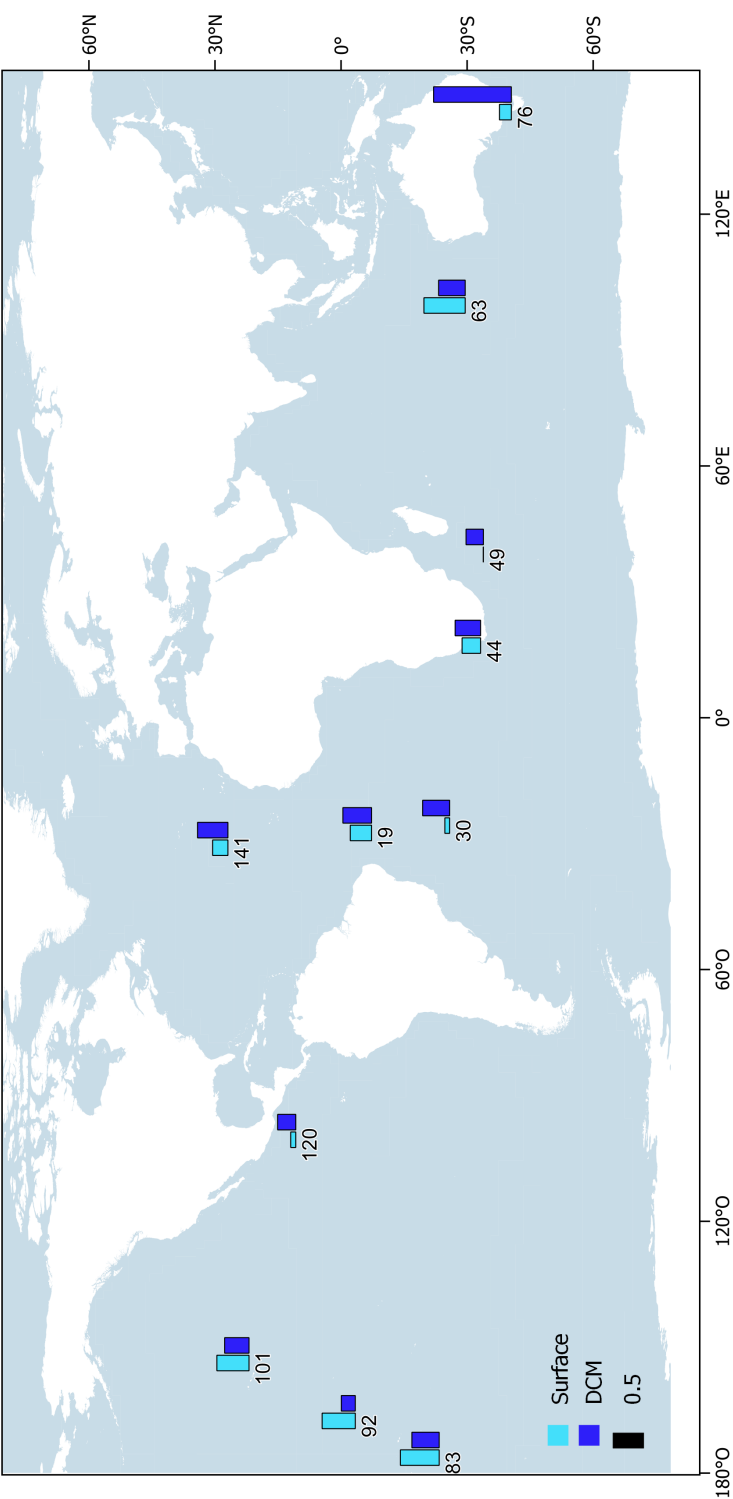


Figure S5: Geographic distribution of the *arhdA* gene abundances as gene copies per cell across the temperate and tropical ocean, represented by the 11 sampling locations from the Malaspina circumnavigation campaign. Water layers are represented by colors.

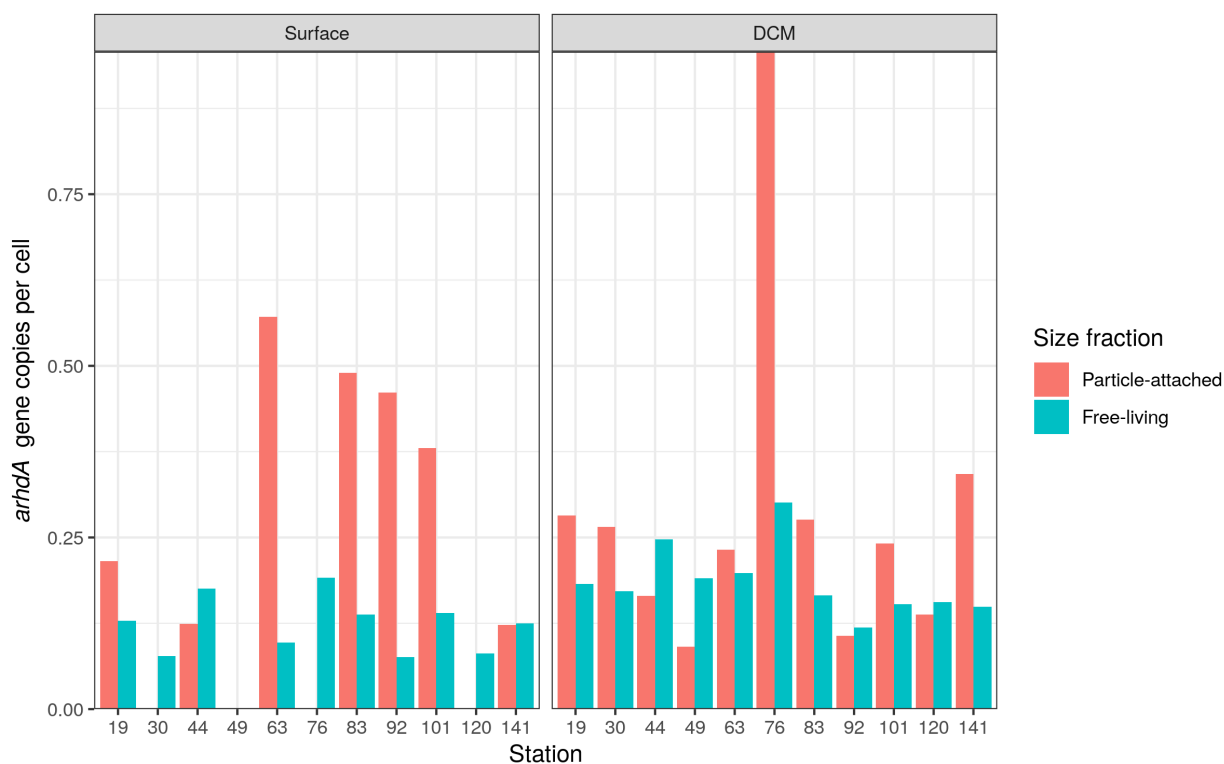


Figure S6: Barplot of *arhdA* abundance as gene copies per cell per station and water layer. Colors represent the bacterial size fraction (free-living fraction, 0.22-3.0 μm ; particle-attached fraction, 3.0-20 μm) from where the metagenomes were sequenced.

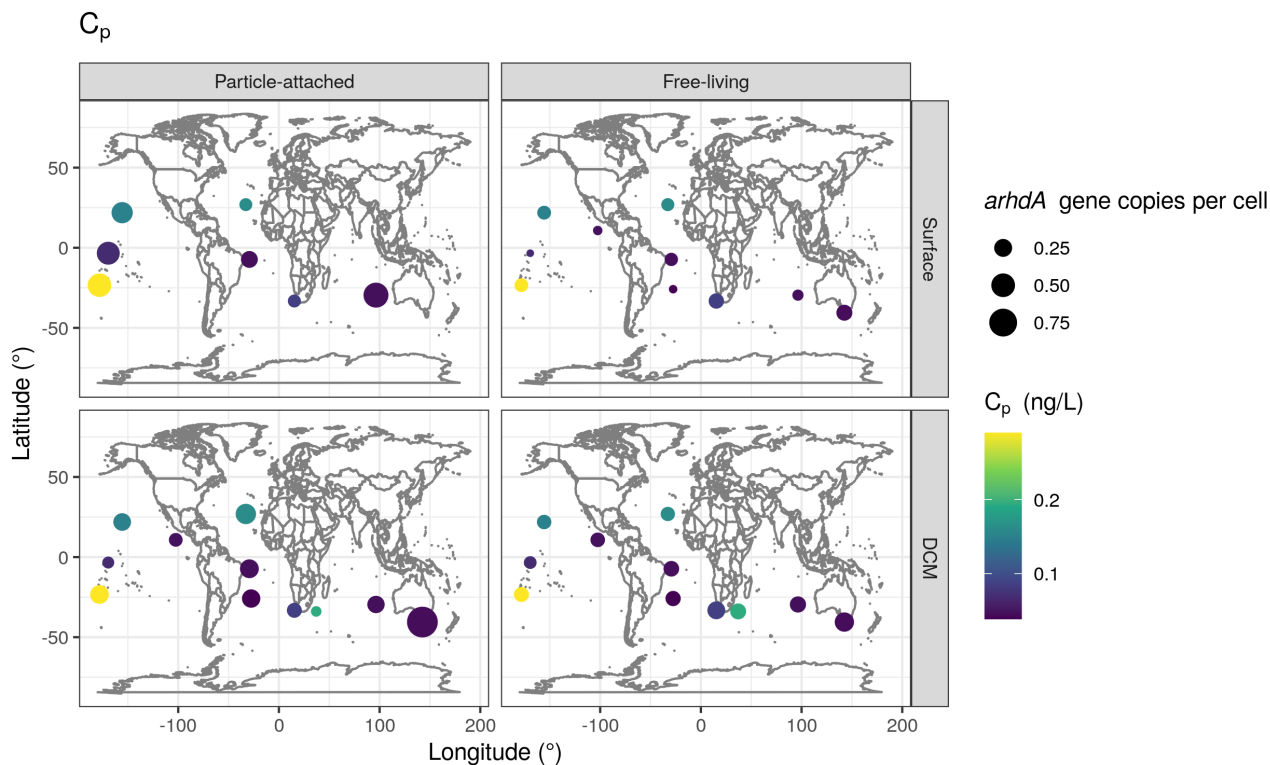


Figure S7: Geographic distribution and abundance (gene copies per cell) of genes identified as *arhdA* in the M-GeneDB-VP database per size fraction (free-living fraction, 0.22-3.0 μm ; particle-attached fraction, 3.0-20 μm), concurrently with the sum of the PAH compounds in the seawater particulate phase per water layer (Surface water, 3 m; Deep Chlorophyll Maximum, DCM).

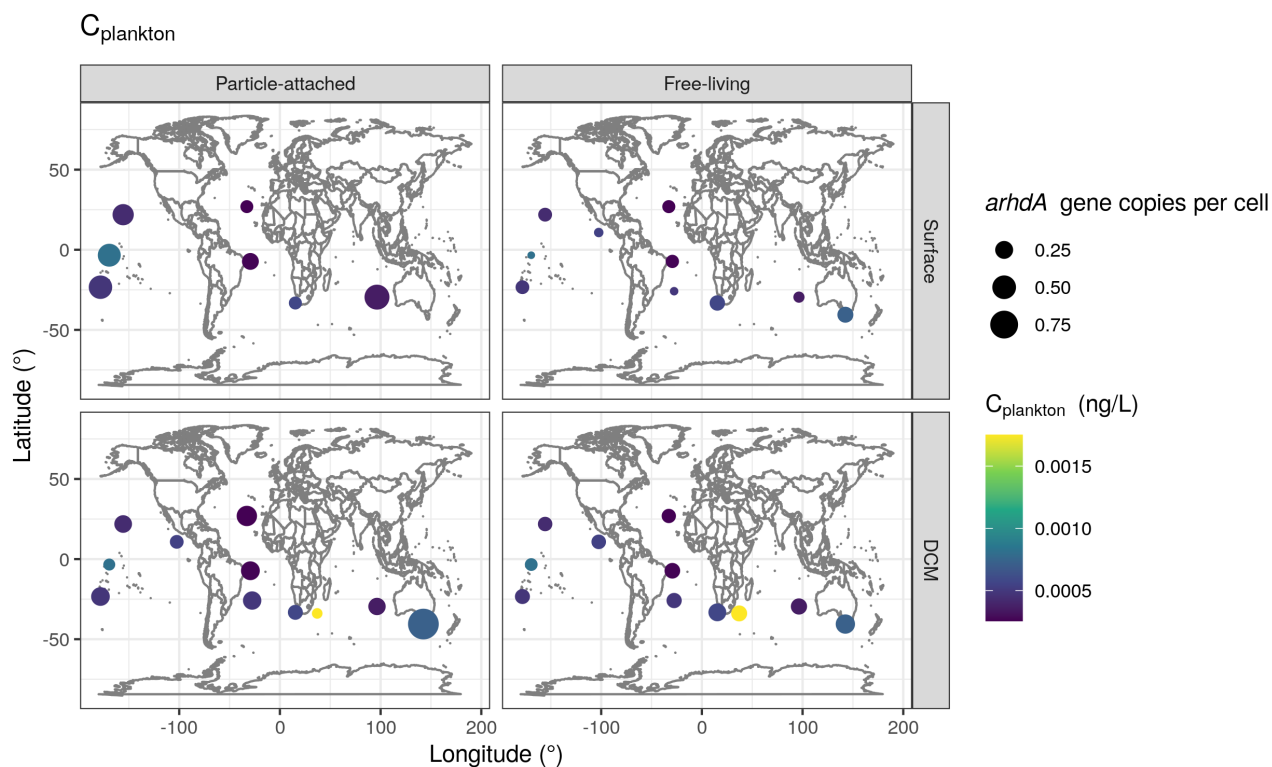


Figure S8: Geographic distribution and abundance (gene copies per cell) of genes identified as *arhdA* in the M-GeneDB-VP database per size fraction (free-living fraction, 0.22-3.0 μm ; particle-attached fraction, 3.0-20 μm), concurrently with the sum of the PAH compounds in the plankton phase per water layer (Surface water, 3 m; Deep Chlorophyll Maximum, DCM).

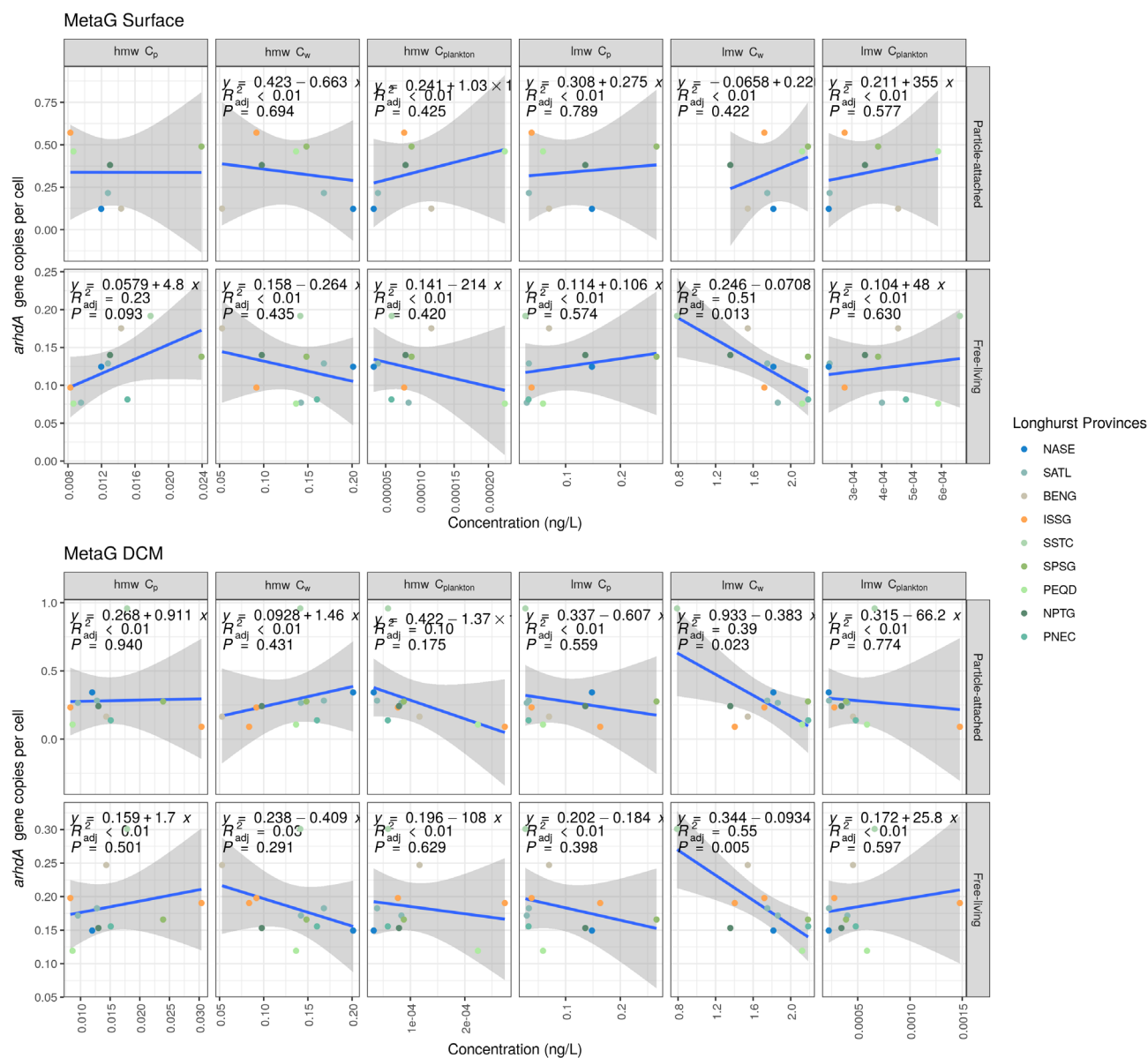


Figure S9: Linear regression plots of *arhda* gene copies per cell vs PAH concentrations. Individual plots are created per sample matrix where the PAHs are measured (Cw, seawater dissolved phase; Cp, seawater particulate phase; Cplankton, planktonic phase), per water layer (Surface water, 3 m; Deep Chlorophyll Maximum, DCM), and per metagenomic sample size fraction (free-living fraction, 0.22–3.0 μm ; particle-attached fraction, 3.0–20 μm). P value according to Pearson correlation.

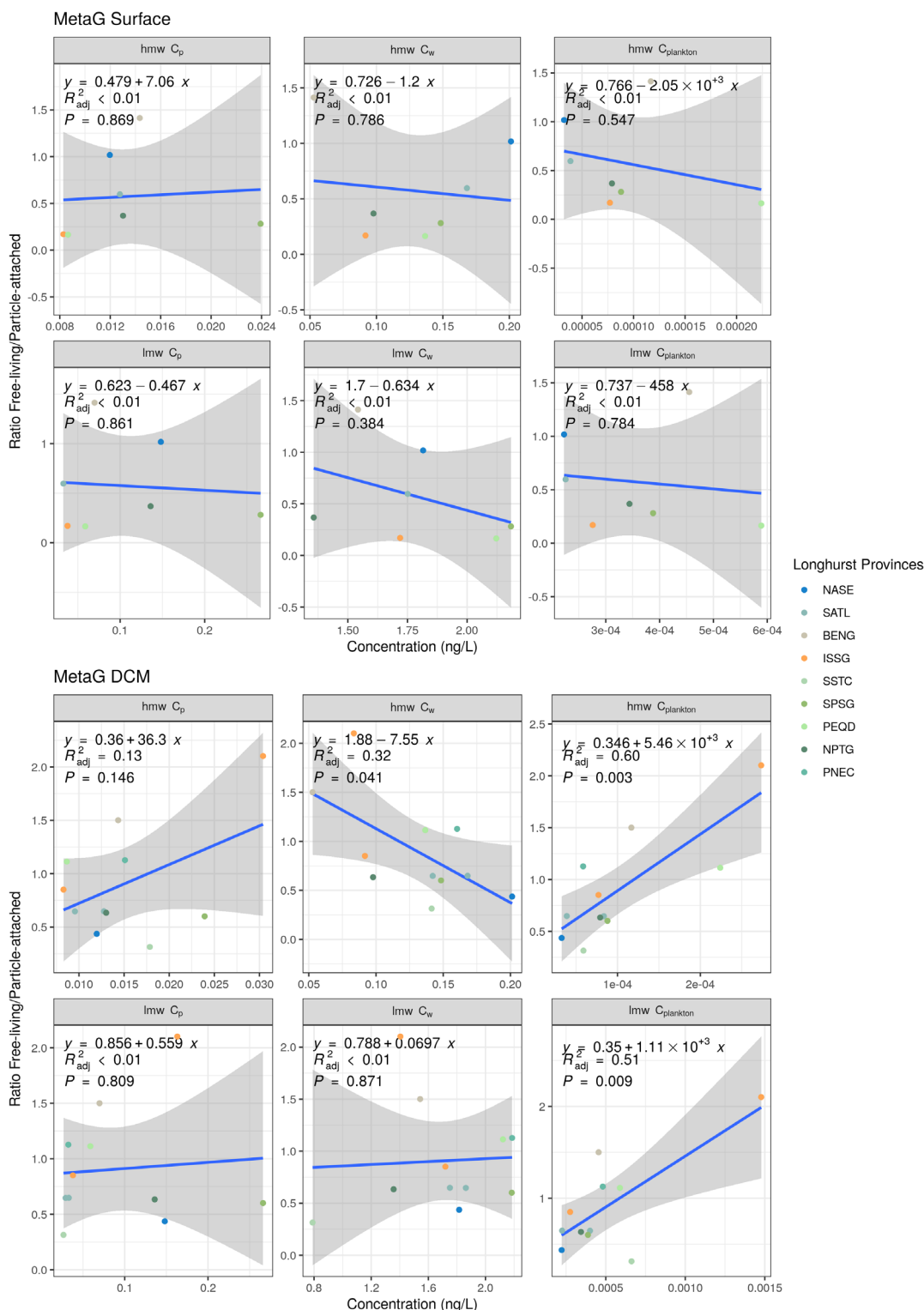


Figure S10: Linear regression plots of ratio the of *arhdA* gene copies per cell between free-living and particle-attached size fraction vs PAH concentrations per sample matrix (C_w , seawater dissolved phase; C_p , seawater particulate phase; $C_{plankton}$, planktonic phase). P value according to Pearson correlation.

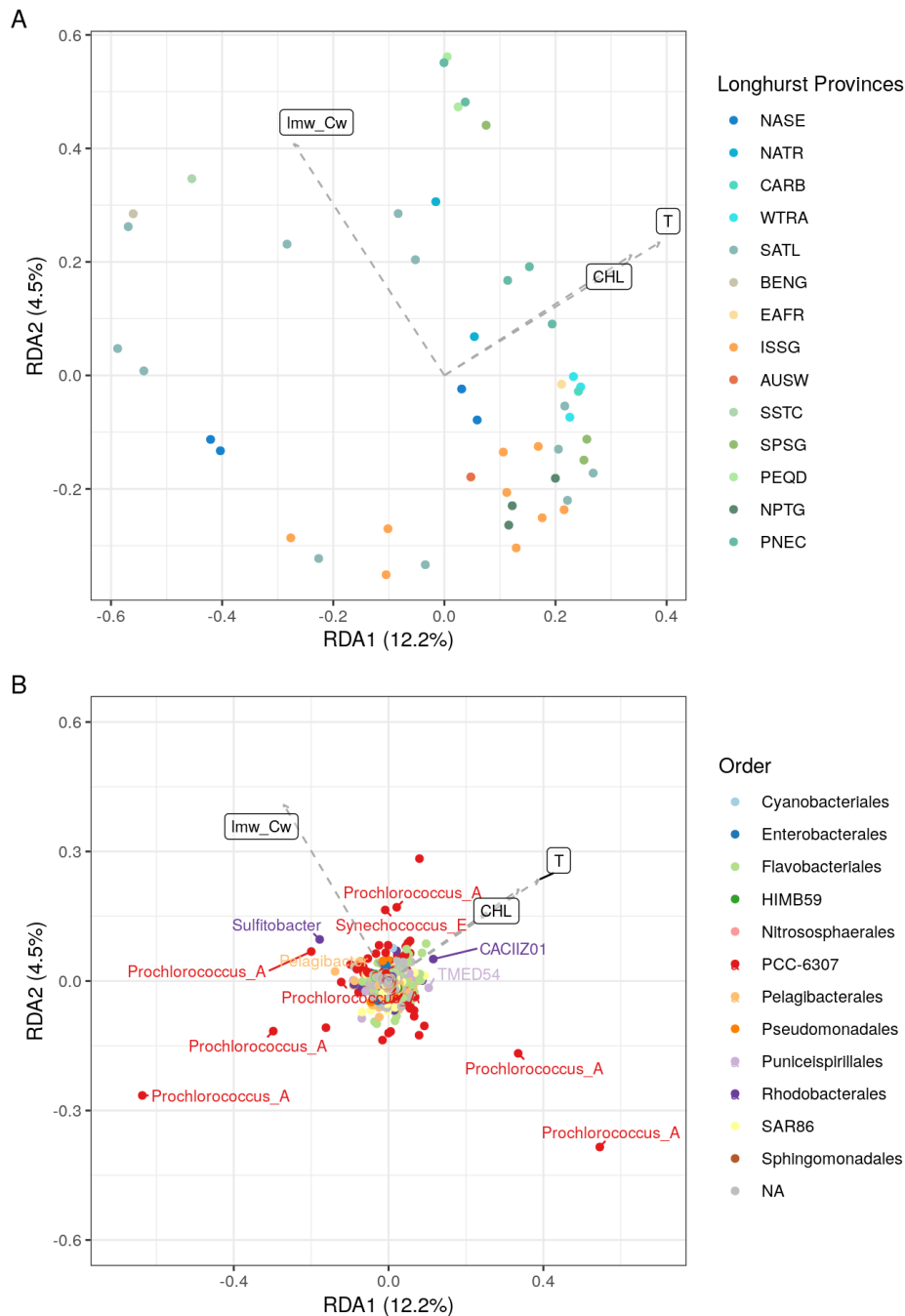


Figure S11: RDA biplots (with symmetric scaling) showing the selected explanatory variables (as vectors) that significantly explained the variation in the whole bacterial community composition. A) Site scores and B) Species scores are represented as colored dots, showing the Longhurst Provinces of the sampling locations, and the taxonomy at order level, respectively.

REFERENCES

Callahan, B. J., McMurdie, P. J., Rosen, M. J., Han, A. W., Johnson, A. J. A., & Holmes, S. P. (2016). DADA2: High-resolution sample inference from Illumina amplicon data. *Nature Methods*, 13(7), 581–583. <https://doi.org/10.1038/nmeth.3869>

González-Gaya, B., Fernández-Pinos, M.-C., Morales, L., Méjanelle, L., Abad, E., Piña, B., Duarte, C. M., Jiménez, B., & Dachs, J. (2016). High atmosphere–ocean exchange of semivolatile aromatic hydrocarbons. *Nature Geoscience*, 9(6), 438–442. <https://doi.org/10.1038/ngeo2714>

González-Gaya, B., Martínez-Varela, A., Vila-Costa, M., Casal, P., Cerro-Gálvez, E., Berrojalbiz, N., Lundin, D., Vidal, M., Mompeán, C., Bode, A., Jiménez, B., & Dachs, J. (2019). Biodegradation as an important sink of aromatic hydrocarbons in the oceans. *Nature Geoscience* 2019 12:2, 12(2), 119–125. <https://doi.org/10.1038/s41561-018-0285-3>

Parada, A. E., Needham, D. M., & Fuhrman, J. A. (2016). Every base matters: Assessing small subunit rRNA primers for marine microbiomes with mock communities, time series and global field samples. *Environmental Microbiology*, 18(5), 1403–1414. <https://doi.org/10.1111/1462-2920.13023>

Ruiz-González, C., Logares, R., Sebastián, M., Mestre, M., Rodríguez-Martínez, R., Galí, M., Sala, M. M., Acinas, S. G., Duarte, C. M., & Gasol, J. M. (2019). Higher contribution of globally rare bacterial taxa reflects environmental transitions across the surface ocean. *Molecular Ecology*, 28(8), 1930–1945. <https://doi.org/10.1111/mec.15026>





CHAPTER 7

General Discussion

7.1 Main discussion

7.1.1 Advancing knowledge on marine pollution

7.1.2 Integrating disciplines to explore microbial biogeochemistry

7.1.3 Methodological approaches: a comparative analysis of benefits and limitations

7.2 Unresolved questions and future research needs

7.3 Perspectives for future research

7.4 References

7.1 Main discussion

The research presented in this thesis contributes to the understanding of marine microbial community-mediated biogeochemical processes and their role in determining the fate of anthropogenic organic contaminants under the realistic conditions found in the oceans. To do so, this thesis integrates datasets from the traditionally distinct disciplines of environmental chemistry and marine microbiology, and utilizes different approaches, ranging from bioinformatics to field experiments, to assess microbial biogeochemistry.

7.1.1 Advancing knowledge on marine pollution

As stated throughout this thesis, chemical pollution is not a localized issue, but rather a first-order global threat comparable to climate change (Persson et al., 2022). Chemical pollution and its impact on the marine environment are of particular concern, considering that the global ocean covers approximately 70% of the planet's surface and plays a fundamental role in supporting life on Earth. Nevertheless, a significant knowledge gap persists regarding the relevance and impact of marine chemical pollution on a global scale, especially in remote areas. As the UNESCO Intergovernmental Oceanographic Commission stated in the *State of the Ocean Report* published in 2022 “Despite the global significance of ocean pollution, observations remain limited, geographically and thematically, being mainly concentrated at the ocean surface and in coastal areas” (Enevoldsen et al., 2022). Furthermore, in *The Zero-Pollution Ocean: A Call to Close the Evidence-Gap* report published by the Back to Blue initiative, the knowledge gaps concerning marine pollution are stated, including the scale gap, which refers to the inability to draw large-scale conclusions about the impact of pollution; the geography gap, referring to the imbalance between well-studied areas versus other that remain unexplored; and the long-term monitoring gap, which addresses how point-in-time studies hamper the discernment of trends (Back to Blue, 2022). The scientific community is drawing attention to the fragmented nature of current knowledge regarding chemical pollution and emphasizing the urgency of advancing toward a more comprehensive understanding of the global landscape of chemical pollution (Abessa et al., 2018; Hatje et al., 2022; Naidu et al., 2021). In line with this call, all the studies presented in this thesis aim to contribute to addressing one or more of the aforementioned knowledge gaps.

Publications I and II present data of PAHs and PFAAs concentrations in surface seawater and plankton samples from the Livingston and Deception Islands in the Antarctic Peninsula. Data on the occurrence of organic contaminants, particularly those of emerging concerns such as the PFAAs, in remote areas such as the poles are often limited, and these studies contribute to addressing the geographical knowledge gap. Furthermore, the polar regions, particularly Antarctica, function as sentinels of global pollution (Casas, 2022), facilitating the understanding of long-range contaminant transport mechanisms and persistence worldwide, thereby contributing to closing the scale gap. This is thanks to their remote location from primary pollution sources and their cold environments, which might act as sinks for contaminants (Bengtson Nash, 2011). The datasets presented in these studies also facilitated the analysis of concentration trends over time, not only within each austral summer but also between two austral summers on Livingston Island by complementing previously reported data of PAHs and PFAAs (Casal et al., 2017, 2018), thus contributing to the long-term monitoring of these contaminants in maritime Antarctica.

In the case of PFAAs, temporal comparisons showed a decrease in the concentrations of PFOS, PFOA, and PFHpA, whereas further confirmed the dominance of the short-chain PFBA already observed in the 2014-2015 campaign (Casal et al., 2017). PFBA has been previously shown to dominate snow and lake samples in the Antarctic Peninsula (Cai, Yang, et al., 2012), as well as in snow and surface seawater samples in the Arctic Ocean (Cai, Zhao, et al., 2012). The phase-out of PFOA and PFOS and their subsequent replacement with short-chain PFAS may account for this phenomenon (Renner, 2006), a trend that has been previously observed in the proximity to fluorochemical industry parks and in the global ocean (Muir & Miaz, 2021; Wang et al., 2016). The temporal comparison also highlighted a preferential decrease of PFOS over PFOA, which could not be attributed solely to settling fluxes or aerosolization, and suggested a potential role for microbial-mediated desulfurization, a process previously documented precisely in Deception Island (Cerro-Gálvez et al., 2020).

With respect to PAHs, the quantification of individual compounds extends the assessment beyond the initial determination of their occurrence. The use of the so-called diagnostic ratios based on isomer stability during PAH formation to identify their source (i.e., petrogenic, pyrogenic, mixed, ...) is quite extended (Biache et al., 2014; Stogiannidis & Laane, 2015). In the Antarctic Peninsula, according to the bibliography, the assessment of PAH diagnostic ratios reveals no discernible pattern, but rather a mixture of PAHs originated from local and global sources, where both natural and anthropogenic processes play a role (Cabrerizo et al., 2016; Szopińska et al., 2019). Nevertheless, in our investigation, we did not employ the diagnostic ratios to ascertain the PAH source; rather, we used them to evaluate the state of PAH biodegradation. Research has demonstrated that microbial degradation induces characteristic alterations in the relative distribution of PAHs, due to the accelerated degradation of PAHs with fewer aromatic rings or the preferential degradation of parent PAHs compared to alkylated variants (Wang et al., 1998). Consequently, specific isomer ratios were utilized as geochemical indicators of biodegradation, such as the parent-to-alkyl-PAHs ratios for selected compounds, and were compared inter-annually, revealing that the extent of PAH biodegradation varied between sampling campaigns. Increased snowmelt contributed to an increase in surface seawater PAH concentrations, but

could also potentially enhance PAH biodegradation mediated by increased microbial activities (Bunse & Pinhassi, 2017). This hypothesis is supported by the observation that maritime snow and snowmelt provide organic carbon and nutrients to seawater (Nowak et al., 2018).

Publications III and IV do not present new data on the marine occurrence of contaminants, only for the experiments performed, but instead try to assess the potential role of biodegradation as an oceanic sink of OPEs and PAHs using different methodological approaches. In an effort to approximate oceanic conditions and maximize representativeness, both publications have in common that are not limited to studying one specific area, but rather try to encompass multiple biogeochemical regimes and oceanic regions. This way, the conclusions derived from these studies apply to extensive regions of the global ocean, thereby mitigating the scale gap while contributing also to reduce the geographic gap concerning the biogeochemistry of organic contaminants in the open ocean. This is particularly relevant in the case of publication III, which, to the best of our knowledge, represents the first reports of OPE biodegradation rates, and of any contaminant of emerging concern, measured in situ using surface seawater in the open ocean.

7.1.2 Integrating disciplines to explore microbial biogeochemistry

One particularly relevant contribution of this thesis is that it explores the potential of concurrent field measurements of organic contaminant concentrations and microbial community parameters on the same samples as a method to infer the mutual interaction between contaminants' fate and microbial activities in the oceans under realistic scenarios. Understanding the factors that determine the persistence and fate of organic contaminants under realistic environmental conditions and the extent of microbial bioremediation is essential for a full risk assessment and consequent regulations of contaminants (Cousins et al., 2019). Unfortunately, the knowledge gathered mostly falls in the context of bioremediation under high contaminant concentrations, thus hampering the understanding of biodegradation at low background concentrations. Advanced methodological approaches involving interdisciplinary expertise are required to gather insights into how biotransformation works under low concentrations of contaminant mixtures and complex natural microbial communities (Fenner et al., 2021), in order to comprehensively include and characterize those factors influencing contaminant fate and microbial activity in field environmental settings (Nogales et al., 2011). However, this complexity and difficulties associated to field studies result in a scarcity of studies addressing this issue. Among the existing studies, most of them focus on highly impacted/polluted areas, such as oil spills or highly industrialized regions (Dubinsky et al., 2013; Lin et al., 2023). Since our goal is to understand the impact of background ubiquitous levels of organic contaminants, the focus is placed on remote areas far from the sources of pollution such as oceanic gyres and Antarctic sites.

Publications I and II combined data of PAHs and PFAS environmental concentrations with data on microbial community composition by 16S rRNA gene amplicon sequencing, as well as data on seawater physicochemical properties at coastal Antarctica. The statistical analyses and correlation tests conducted with these datasets enabled us to derive observations that would not have been attainable through alternative methods, such as significant correlations between relative abundances of certain Amplicon Sequence Variants (ASVs) and contaminant concentrations. In Publication I, negative correlations between dissolved phase LMW PAHs and ASVs of the *Pseudomonadales* and *Flavobacteriales* orders were found. These orders were preferentially correlated to concentrations during the 2014-2015 campaign, the one with chemical evidence of increased degradation of PAHs. The ASVs found to negatively correlate to LMW PAHs concentrations (that is, *Nitrospiraceae* and *SAR92* within the *Pseudomonadales* order, *Polaribacter* in the *Flavobacteriales* order) have been described as bloom-responsive taxa associated with organic matter availability in maritime Antarctica (Piontek et al., 2022). Furthermore, *Polaribacter* has been shown to play a role in hydrocarbon and oil degradation in cold and temperate environments, and some strains able to grow on hydrocarbons have been even isolated (Brakstad et al., 2017; Garneau et al., 2016; Kwon et al., 2019; Prabakaran et al., 2007; Zhou et al., 2024). In the aftermath of the Deepwater Horizon Oil spill, *Polaribacter* was found to be enriched in the late succession of hydrocarbon degrading bacteria, and *Flavobacteria* were suggested to take advantage of the organic residues derived from the decaying bloom of early hydrocarbon degraders, as well as of the recalcitrant components of crude oil, such as the PAHs (Dubinsky et al., 2013). In our investigation, it was not possible to determine whether

Polaribacter were directly responsible for low LMW PAH concentrations or served as biomarkers of oligotrophic bacteria responding to organic matter availability. Both hypotheses are plausible and not mutually exclusive. However, taking all the evidence into account, results suggest that snowmelt-driven bloom of bacterial activity promoted PAH biodegradation, probably through the action of facultative hydrocarbonoclastic bacteria (HCB), generalist microorganisms with the capacity to use hydrocarbons as well as a wide range of other carbon sources as growth substrates. Exposure to PAHs has been previously reported to promote the growth of facultative HCB, such as *Pseudoalteromonas*, while enriching the expression of PAH-degrading genes in the surface microlayer at coastal Antarctica (Martinez-Varela et al., 2022), supporting the role of PAH as growth substrates for marine HCB.

In Publication IV, PAH concentrations were correlated to both 16S amplicon sequencing data and physicochemical parameters obtained from samples collected during the Malaspina circumnavigation expedition (Duarte, 2015). Additionally, in this study, the potential for aromatic hydrocarbon degradation was also evaluated by using the abundance of aromatic ring hydroxylating dioxygenase alpha subunit gene as a proxy, measured from a gene catalogue constructed with selected sequenced metagenomes (Sánchez et al., 2024). Statistical analyses showed a negative correlation between the abundance of the gene and the occurrence of dissolved phase LMW PAHs concentrations, among others. This finding is in line with what was found in Publication I, where negative correlations were found between the abundance of oligotrophic potential facultative HCBs and concentrations of LMW PAHs.

Results from both publications suggest that at background environmental concentrations of PAHs, those sites exhibiting higher potential for aromatic hydrocarbon degradation report lower concentrations of the most labile fraction of PAHs. This phenomenon is not observed at sites with high PAH concentrations, where PAH-degrading bacterial genera are generally found to be significantly abundant (Lin et al., 2023; Zhou et al., 2023). However, it is important to note that biodegradation drivers may change fundamentally when shifting from high to low concentrations of contaminants, as environmental conditions become more significant than the selective pressure exerted by the contaminant (Fenner et al., 2021). Based on these findings, it seems appropriate to postulate that, at low background concentrations of PAHs, microbial communities shaped by environmental factors determine the fate and composition of the PAH pool.

However, the potential of anthropogenic organic compounds, such as PAHs, to modulate microbial communities should also be considered (see section 1.4.2 in the introduction). Experimental evidence for this was obtained in Publication IV, where dissolved phase LMW PAH concentration was a significant explanatory variable of microbial community composition in a redundancy analysis, along with other well-established environmental factors of bacterial community structures such as water temperature and chlorophyll α concentration (Sunagawa et al., 2015), suggesting a relevant yet neglected role of background PAH concentrations driving microbial community compositions (Martinez-Varela et al., 2023). In addition to the direct responses of bacteria, PAHs may also modulate microbial communities indirectly by exerting negative effects on phytoplankton and grazers (Almeda et al., 2013; Barata et al., 2005; Bellas &

Thor, 2007; Fernández-Pinos et al., 2017). Therefore, there is an entanglement of PAH pollution and microbial communities, which involves multiple biological players and physicochemical processes in a complex interplay. Furthermore, given the current estimates of increasing environmental contamination by anthropogenic organic compounds, the increasing stress from ocean warming and acidification caused by climate change, and the reduced capacity to cope with these stressors due to biodiversity loss in future global scenarios, the thresholds at which organic contaminants significantly affect ecosystems might change, most probably becoming lower. Therefore, results from this thesis call attention to organic contaminants as significant factors modulating microbial communities, as discussed further below.

Regarding Publication II, correlation analysis between the occurrence of PFAAs and the abundance of individual ASVs offered a way to explore if the observed preferential decrease of PFOS over PFOA could be related to the presence of certain microbial taxa. The PFSA/PFCA ratio showed only one significant negative correlation with the abundance of *Amylibacter* (*Rhodobacteraceae* family, in the order *Rhodobacterales*). *Amylibacter* has been previously related to the metabolism of organic sulfur compounds in temperate coastal waters (Li et al., 2024; O'Brien et al., 2022), and has been directly linked to the metabolism of DMSP, an organosulfur compound produced by phytoplankton (González et al., 2019). Furthermore, Priest et al. (2024) related an enrichment in sulfur metabolism, such as sulfur oxidation and sulfite reduction, found in an Arctic marine microbiome to an *Amylibacter* ASV dominating the prokaryotic community. Notably, among PFOS-degrading bacteria in coastal Antarctica, the order *Rhodobacterales* made the most significant contribution to the transcript pool and accounted for most of the desulfuring gene expression in microbial communities exposed to PFOS (Cerro-Gálvez et al., 2020). Therefore, the negative correlation found is consistent with the results reported by previous studies. However, further work supporting a mechanistic understanding of microbial degradation of PFOS is needed to confirm this observation. If confirmed, it would link PFOS desulfurization in the Antarctic marine environment to the cycle of dissolved organic and inorganic sulfur and biogenic organosulfur compounds.

While concurrent assessments of contaminant concentrations, microbial community structure and functionality, and environmental parameters provide a broader perspective for exploring contaminant interaction with microorganisms, the inferences drawn from these observations should be interpreted with caution, as the co-occurrence of certain factors does not necessarily imply causality between them. The statistical power of these comparisons is constricted by the limited number of observations, which, despite being unique, reflects the challenges associated with fieldwork. Nevertheless, such environmental studies are necessary, as they not only yield environmentally relevant data and observations that improve modeling capabilities, but also act as hypothesis generators (Figure 7.1), offering new research perspectives to explore. Derived from the results of this thesis, for example, it should be addressed under which circumstances PAHs are used as a growth substrate or transformed by co-metabolism. In the former case, the complete enzymatic machinery for biodegradation should be present within one degrader or small degrader consortium that covers its overall energy and nutrient needs from mixed substrate utilization (organisms referred to as facultative hydrocarbonoclastic

bacteria). In the case of PAHs co-metabolically (“fortuitously”) transformed, it still remains unclear which taxa are involved (Fenner et al., 2021). Regarding PFAAs, it would be interesting not only to experimentally confirm the link between the bacterial taxa in the *Rhodobacterales* order and sulfur-containing PFAAs, but also to isolate and characterize the enzyme(s) responsible for this transformation, as the current understanding of environmental biodegradation of PFAS is significantly less comprehensive compared to that of PAHs.

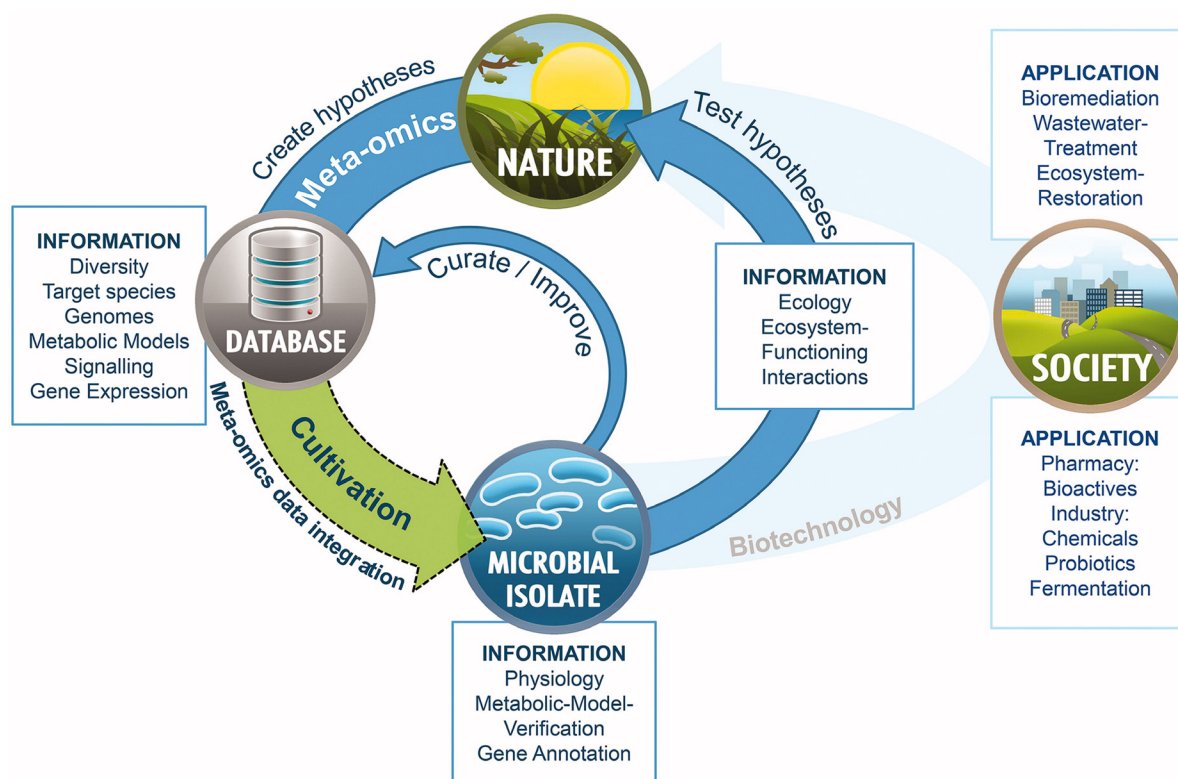


Figure 7.1 A model depicting the positive feedback loop between multi-omics data generation and isolation of as yet uncultured microorganisms. The culture-independent databases generated through meta-omics facilitate the formulation of hypotheses; however, they rely on cultivation of microbial isolates for mechanistic understanding. Integrating multi-omics data curated by physiological characterization of already available microbial isolates for the cultivation of novel environmental bacteria could potentially boost this feedback loop and promote biotechnological innovation. From Gutleben et al. (2018). Licensed under CC BY-NC-ND 4.0. <https://creativecommons.org/licenses/by-nc-nd/4.0/>

7.1.3 Methodological approaches: a comparative analysis of benefits and limitations

Assessing the overall complexity of organic contaminant biogeochemistry, associated microbial diversity, and environmental conditions in a way that yields environmentally meaningful results represents a challenge for which no standardized methodological approaches exist. The principal reason for that lies in the challenge environmental microbiologists face, which can be compared to their own version of the Heisenberg Uncertainty Principle: the closer a given process is examined, the more likely is that artifacts will be introduced into measurements of that process (Madsen, 1991). The results presented in this thesis take that into consideration and aim to improve the understanding of the processes that organic contaminants undergo in the surface open ocean, by generating and analyzing data obtained from the environment with minimal intervention/perturbation of the environmental conditions. To achieve this objective, two distinct methodological approaches have been employed: the first is based on data integration and statistical analyses of field-derived datasets covering temporal and/or spatial variability, utilizing available bioinformatic tools when feasible. Publications I, II and IV are representative of this approach. The second is based on obtaining direct experimental evidence of contaminant biodegradation by laboratory-based assays performed *in situ* trying to replicate environmental conditions. This approach is represented in Publication III.

Both approaches have their respective advantages and limitations (Table 7.1); however, they are necessary and often complementary for determining *in situ* biodegradation and obtaining a comprehensive understanding of the contaminant-microbiome interaction. Direct evidence of microbial metabolism can be obtained through laboratory assays, as they allow for the use of sterilized treatments as abiotic controls, while mass balances are made possible by performing the assay in a sealed vessel (Madsen, 1991). In addition, the capacity to control experimental conditions and design experimental setups provides a powerful way to test specific hypotheses. Nevertheless, the extent to which findings from controlled laboratory experiments accurately reflect environmental processes remains a subject of ongoing debate, due to the methodological artifacts inherent in experimental setups (Madsen, 1991). The fact that most marine bacteria remain uncultured and, importantly, the “bottle effect” -a change in community composition within a few hours caused by sample collection and containment- are examples of the current limitations (Massana et al., 2001). The handful of environmental factors and complex interactions among them render environmental conditions challenging to replicate. This becomes particularly relevant when assessing the persistence of chemical contaminants in the environment, crucial information required for conducting a reliable risk assessment and regulation (Cousins et al., 2019). While the results obtained from laboratory tests for hydrolysis can be reliably extrapolated to field conditions, the same level of confidence cannot be applied to photodegradation and biodegradation processes (McLachlan et al., 2017). Consequently, during the last decade, there has been a call to increase the environmental relevance of the gathered data, for example, by performing biodegradation tests under low spiking concentrations (Tian et al., 2023), or by quantifying field-based degradation rates (Ottosen et al., 2019).

In Publication III, an OPE exposure field experiment was designed to test the potential for OPE biodegradation in surface seawater of the Atlantic and Southern Oceans. The experimental design was intended to be as representative of the environmental conditions as possible, by conducting in situ quantification of OPE degradation under low spiking concentrations, controlled temperature conditions, and short-term incubations. However, due to technical restrictions implicit of the research carried out onboard a research vessel, some modifications were applied to reduce the variability and the complexity of the experimental design, such as filtering the water to exclude grazers or performing the incubations in the dark to block primary production. A significant decrease of aryl-OPEs, TmCP and EHDPP, was observed for the Atlantic Ocean experiments after 48 hours of incubation, related to sorption processes and potential biodegradation, whereas for those experiments performed in the Southern Ocean OPE losses could only be attributed to sorption. A preferential degradation of aryl-OPEs over other OPEs compounds has been previously reported. Kawai (1996) and Kawagoshi et al. (2002) reported rapid biodegradation of aryl-OPEs by aquatic bacteria, whereas alkyl-OPEs required extended periods to exhibit biodegradation, and chloroalkyl OPEs did not demonstrate discernible biodegradation. Similarly, Castro-Jiménez et al. (2022) observed that in marine sediments with OPE additions, the degradation of chlorinated OPEs under biotic and abiotic conditions was comparable. Finally, Vila-Costa et al. (2019) also reported a significant decrease of TmCP and EHDPP in OPE addition experiments after 24h of incubation, using surface seawater from the NW Mediterranean Sea.

This preferential decrease of TmCP and EHDPP relative to other OPEs raises some questions. It could be related to the presence of aromatic groups acting as better leaving groups than alkyl ones, due to their capacity to delocalize negative charges through resonance. In line with this, Despotović et al. (2022) reported higher growth rates for marine bacterial isolates when utilizing aromatic group-containing organophosphates. However, the existence of phosphotriesterases capable of cleaving these ester bonds in the open ocean has yet to be reported. Microbial reactions may be acting directly on the aromatic moieties, rather than on the ester bonds. Reactions occurring on the aromatic substituents of OPEs, such as hydroxylation or methylation, have been reported in soils (Yu et al., 2023), and the resulting transformation products have been detected in the environment (Gao et al., 2025). While these reactions have not yet been reported to occur in marine environments, given that the machinery to degrade aromatic hydrocarbons at background concentrations is available thanks to the widespread presence of facultative HCB (Chapter 6, Publication IV), it is plausible to suggest that aromatic compound-degrading microbes could interact with these aromatic groups present in TmCP and EHDPP, as well as in TPhP. While in the case of TPhP the decrease was not significant, a correlation analysis of field TPhP dissolved concentrations and bacterial production shows that TPhP concentrations are lower when bacterial production is larger (Trilla-Prieto et al., 2025).

Another factor that may be influencing this phenomenon is the hydrophobicity of the compounds. Both TmCP and EHDPP have log K_{ow} are higher than 5 (higher than the log K_{ow} of TPhP), which is considered the threshold to define a compound as bioaccumulative according to the UNEP (UNEP, 2023). The cell surface adherence to contaminants is of great importance for microorganisms as it is considered the initial step in the process of contaminant bioremediation (Turan et al., 2024; J. Zhang et al., 2009). Consequently, higher hydrophobicity of the compounds would facilitate this adhesion process, as well as potentially promote diffusion across membranes in case of organic contaminant utilization as nutrients (Despotović et al., 2022). Overall, a complex interplay between several physicochemical factors appears to be driving the fate of OPEs in the water column; however, further experimental design will be necessary to gain insights into these processes.

The percentage of TmCP and EHDPP decrease due to biodegradation correlated with the increase of heterotrophic bacterial production, further highlighting the role of some biological process behind this observation. As organic compounds with a phosphate group, OPEs could serve as C or P sources. Previous studies have described bacterial strains capable of growing on OPEs as the sole P or C source isolated from enrichment cultures of contaminated soils (Liu et al., 2019; Takahashi et al., 2012; Wang et al., 2019). Regarding the marine environment, bacteria from the Mediterranean Sea have been reported to use OPEs under phosphorus-limited conditions (Despotović et al., 2022; Vila-Costa et al., 2019). Unfortunately, our attempts to determine if OPEs were utilized as substrates or were being co-metabolized were inconclusive. This issue stems from the lack of knowledge regarding OPE degradation pathways, as well as the key enzymes and microorganisms responsible for this process in the open ocean and remote areas distant from human influence, thereby hindering the accurate assessment of biodegradation. Future research should address OPE transformation products in the open ocean water column to gain insights into OPE transformation pathways and their potential use as nutrient sources.

Indeed, the current state of knowledge regarding the biogeochemistry of a contaminant or family of contaminants constrains the feasible investigations that can be conducted. This is the case of the emerging contaminants, such as OPEs and PFAS, for which the environmental processes they undergo are not as well characterized as for other historic pollutants, such as PAHs, particularly with regard to their interaction with microorganisms and the microorganism-mediated biodegradation. PAHs have been extensively studied and consequently, PAH-degrading microbes have been identified, degradation pathways elucidated, and key enzymes characterized (Ghosal et al., 2016; Kaur et al., 2023). This comprehensive knowledge facilitates the assessment of PAH biogeochemistry directly from field-based data, through the utilization of diagnostic ratios, analysis of omics data for biomarker genes or specific microbial taxa, and other relevant methodologies. The use of field-based and culture independent methodologies not only provides environmental relevance to the assessment of the contaminant biogeochemistry, but also serves to reveal those processes involving unculturable microorganisms that are essential to the functioning of the naturally occurring microbial communities in the environment (Chakraborty & Das, 2016). Omics approaches can provide exemplary knowledge about microbial communities and their role in the bioremediation of environmental contaminants, especially when combined

in the often known as “multi-omics” research, which integrates data of the whole biological system (Hassan et al., 2022; Satya et al., 2024). Moreover, the availability of existing repositories containing publicly accessible genetic data enhances research accessibility by mitigating the constraints imposed by the costs associated with sequencing techniques.

Nevertheless, as stated in Fenner et al. (2021), “the identification of genes of interest in such large data sets may be all but trivial if the relevant catabolic pathways and reactions for a certain contaminant transformation have not been resolved a priori”, as is the case for OPEs and PFAS. There remains a necessity in the field of marine microbiology and biogeochemistry to isolate and characterize all those genes that are being discovered from metagenomic surveys, but about which the limited knowledge that we possess regarding their metabolic potential is solely derived from *in silico* predictions. Despite the latest advancements in the field of *in silico* functional predictions, the majority of the unknown genes are suggested to encode novel proteins distant from the known functional landscape (Rodríguez del Río et al., 2024). In this context, the cultivation of microorganisms emerges as a crucial methodology for the annotation and functional characterization of novel genes (Muller et al., 2013), as well as the currently most reliable approach to validate ecological hypotheses derived from multi-omics data (Figure 7.1, Gutleben et al., 2018). Using existing bacterial cultures, researchers can examine microbial metabolism at the biochemical level, uncovering previously unknown physiological characteristics under diverse incubation conditions (i.e., Sanz-Sáez et al., 2025). Additionally, experimental validation of complex ecological interactions, evolutionary processes, and population changes is only possible when isolates are available (Gutleben et al., 2018). Therefore, culture-dependent techniques will continue to play a crucial role in the understanding of the biogeochemistry of organic contaminants, and further advancements in cultivation techniques will be necessary to reduce the gap between the as-yet uncultivable microorganisms and the number of isolated species.

Table 7.1 Benefits and limitations of field-based measurements, field experiments, and experimental approaches with culturable isolates under laboratory-controlled conditions.

	Benefits	Limitations
Field-based measurements	<ul style="list-style-type: none"> • Observations and results directly reflect the processes occurring in the environment. • Data from remote and often underrepresented areas can be collected, providing valuable insights for the training and development of models. • Environmentally relevant in situ quantification of degradation rates can be performed. • Field-derived observations promote the creation of new hypotheses. 	<ul style="list-style-type: none"> • The vast number of factors and the complexity of their interactions hinder the identification of patterns and the formation of clear conclusions. • The high costs and complexity of fieldwork limit its feasibility and the sample size. • Determining field-based degradation rates requires multiple lines of evidence and a comprehensive understanding of the processes that the compound under study may undergo in the environment. • Testing the formulated hypothesis often requires further experimental work.
Field experiments	<ul style="list-style-type: none"> • The experimental setup enables the analysis of compound partitioning and the direct determination of degradation rates, ecotoxicology, and other measurements. • Allows the use of naturally occurring microbial communities and environmental conditions, making the results highly representative of real-world scenarios. 	<ul style="list-style-type: none"> • Even slight modifications or handling of environmental samples can introduce artifacts that may compromise the entire experiment if not properly assessed. • The complexity of environmental matrices makes it difficult to fully control experimental conditions, potentially hindering a comprehensive analysis of the results. • The high costs and complexity of fieldwork limit its feasibility, as well as its reproducibility.

Table 7.1 Benefits and limitations of field-based measurements, field experiments, and experimental approaches with culturable isolates under laboratory-controlled conditions (continued).

<p>Laboratory-controlled experiments with culturable isolates</p>	<ul style="list-style-type: none"> • Standardized and reproducible methodologies can be employed to determine degradation and/or toxicity in a reliable manner. • Reduced expenses make this type of research more accessible. • The ability to examine specific conditions enables the evaluation of previously proposed hypotheses. 	<ul style="list-style-type: none"> • The obtained results may be challenging to extrapolate to real-world scenarios, as laboratory conditions often fail to adequately represent the complexity of environmental conditions. • The scope of the research is constrained by the ability to simulate environmental-like conditions, such as access to seawater or the use of artificial seawater.
---	--	---

7.2 Unresolved questions and future research needs

After the results presented in this thesis, several aspects of the biogeochemistry of organic contaminants and their interactions with marine microbial communities remain to be answered. Some of the questions and recommendations for future research are:

Co-metabolism or growth substrates?

To comprehensively elucidate the potential effects of organic contaminants on microbial communities and marine biogeochemical cycles, future research should not be limited to addressing the removal of parent compounds, but should include an assessment of the mechanism of degradation. Organic contaminants, particularly those including heteroatoms such as the OPEs, are potential sources of energy and nutrients, and consequently, may offer a metabolic advantage to those microorganisms with the capacity to metabolically use them, especially within the context of nutrient limitation present in large areas of the open ocean (Browning & Moore, 2023). Although these anthropogenic organic compounds are usually not the preferred nutrient source, it might be a matter of time that some microorganisms will adapt to utilize these new sources of nutrients, thus producing an anthropogenic perturbation of the marine biogeochemical cycles. On the other side, if the transformation of the parent compound results from co-metabolism, complete degradation may not be achieved. Instead, the process could halt at a certain point, raising questions about the fate and effects of recalcitrant transformation products formed (Fenner et al., 2021). For instance, there is currently increasing concern regarding the degradation product of OPEs, namely di-OPEs, due to their enhanced hydrophilicity and potential increase in toxicity (Gao et al., 2025; Liang et al., 2024; Peng et al., 2023; L. Zhang et al., 2022). Regarding PAHs and similar aromatic-like compounds, González-Gaya et al. (2019) highlighted the need for future research to determine whether the microbial loop fully respire these compounds or transforms them into recalcitrant DOC, in order to understand the implications that these processes may have for the marine carbon cycle. The target analysis of certain transformation products, or the implementation of suspect and non-target screening techniques for the analysis of metabolites, could elucidate the nature of chemical transformations undergone by organic contaminants.

Need for isolation and characterization of new biomarker genes

The finding of biomarker genes associated with the biodegradation of specific compounds facilitates a multitude of research opportunities, including the evaluation of biodegradation potential through the analysis of metagenomic datasets. However, in the case of the contaminants of emerging concern, such as the OPEs, few degradation enzymes have been described to date, with the majority originating from highly polluted environments. There is a need for a more universally applicable biomarker of OPE degradation that could be used to evaluate OPE biodegradation potential in the global oceanic system through bioinformatic approaches, as well as for other anthropogenic organic compounds with biodegradation evidence. To accomplish this objective, additional research efforts are necessary to evaluate OPE biodegradation at sites with low background concentrations more representative of the global ocean, utilizing both field and laboratory-based experimental approaches, ultimately leading to the isolation of OPE-degrading microorganisms.

Optimization of techniques for marine isolates

In relation with the previous point, several molecular biology techniques are currently available that may prove beneficial for the identification and isolation of marine microorganisms capable of degrading anthropogenic organic compounds. One such technique is the gain-of-function approach, which facilitates high-throughput genetic screening of entire genomes (Fenner et al., 2021; Zimmermann et al., 2019). However, these techniques have predominantly been developed for use with human health-related cultures and are not suitable for environmental microorganisms, particularly marine species, where the high salt concentration typically introduces additional complexity to the system. In order to take advantage of the latest methods developed in the molecular biology field, more emphasis should be placed on the design and optimization of new techniques to facilitate the inclusion of environmental microbiology. In this regard, the development of single-cell or nano-sample approaches may offer new opportunities, but that will require extensive conceptual and methodological development (Dachs & Vila-Costa, 2022).

Need for characterizing pollution in remote areas to develop a global perspective on chemical pollution

Despite the efforts of this thesis to produce data and assess anthropogenic organic chemical pollution in remote areas, substantial work remains to address this knowledge deficit. The global picture of chemical pollution in the environment is often fragmented (Naidu et al., 2021), as highly polluted sites, or areas next to intense anthropogenic activities gather most of the scientific attention. Remote areas and other marine ecosystems should be addressed in future works in an effort to gather data and ultimately help reduce the scale and geographic gaps of marine chemical pollution (Back to Blue, 2022).

Understanding processes in the water column

Surface waters often gather most of the attention regarding environmental risk assessment of anthropogenic organic contaminants. However, chemical pollution threatens all the compartments across the water column. Further research should address less extensively studied ecosystems with globally important biogeochemical functions, such as the mesopelagic and deep sea (oceanic layer below 200m depths), to elucidate the ecological implications of organic contaminant occurrence and to determine the role these water compartments play in the cycling of organic contaminants, particularly with regard to contaminants of emerging concern (Sanganyado et al., 2021). Among the water compartments to be examined, the surface microlayer (SML) emerges as a particularly significant area of study due to its complex and unique physicochemical properties. This microenvironment at the surface of the ocean (a layer between 1 and 1000 μm thick) functions as the interphase between the atmosphere and the ocean, thereby playing an important role in the air-water exchange of organic contaminants. On top of that, the SML is enriched with organic matter with surfactant properties, which, together with other particular environmental factors, results in distinct microbial communities inhabiting this layer. The hydrophobic nature conferred by the accumulation of organic matter also results in the enrichment of other hydrophobic compounds, such as organic contaminants. This enrichment has already been reported for some of the families of contaminants that comprise the ADOC pool, and even the relevant role of the bacterial communities inhabiting the SML for the removal of PAHs in the oceans has been highlighted (Casas et al., 2020; Huang et al., 2020; Martinez-Varela et al., 2020, 2022; Trilla-Prieto et al., 2024). Further research should continue addressing the relationship between organic contaminants and the SML, in order to build a more comprehensive understanding of the role of SML in the fate of organic contaminants and perform adequate environmental risk assessment of the anthropogenic compounds present therein.

7.3 Perspectives for future research

Complexity of environmental sciences under the global change scenario

Vectors of global change do not act individually, and climate change, biodiversity loss and environmental pollution are no exception. The three are linked, and we are still learning how the chemical pollution, biodiversity loss, and the effects of climate change, such as warming water temperatures and increased acidification, interact to worsen each other's impacts (Carmichael & Brown, 2022). Biodiversity loss may affect the resilience of ecosystems to cope with climate change and pollution (Oliver et al., 2015; Pires et al., 2018). Meanwhile, acidification and warming affect the bioavailability and toxicity of various chemicals, leading to cumulative effects of multiple stressors on organisms and ecosystems (Bethke et al., 2023; Carmichael & Brown, 2022; Noyes et al., 2009). For instance, Coelho et al. (2015) reported that the interactive effect of acidification and oil pollution can affect the structure and functioning of sediment microbial communities, potentially exacerbating the toxicity of oil hydrocarbons in marine ecosystems. Marine microbial communities are already expected to suffer from the acidification and increase in seawater temperatures, as these phenomena will change the nutrient cycling and limit nutrient flux from sediments, together with the biodiversity, among other consequences (Abirami et al., 2021; Nogales et al., 2011).

Given the current rate of global warming, with the past two years exhibiting record-breaking surface global ocean temperatures (Bracco, 2025), and the anticipated increase in global synthetic chemical production and subsequent environmental release, this issue appears to be more pertinent than ever. While our understanding of the full extent of environmental impacts from compounds in the ADOC pool remains limited, the emerging paradigm of climate change threatens to alter the established principles of what was previously considered well-understood. The complex relationship between environmental pollution, climate change, biodiversity loss, and other global environmental vectors of change poses a significant challenge that requires a comprehensive, multi-stressor analysis to predict the impact of these changes on coastal and ocean ecosystems (Hatje et al., 2022). These environmental issues are deeply interconnected and can exacerbate one another, leading to far-reaching impacts on ecosystems, human well-being, and the entire planet (Wang et al., 2024). Therefore, addressing these challenges will require a coordinated effort that integrates marine microbiology and environmental chemistry, along with other branches of environmental sciences related to climate change.

The need for a new industrial paradigm

A significant disparity emerges when comparing the number of chemical compounds listed for regulation with the number of compounds in the market (even disregarding the growth rate of each). The increasing rate of production and releases of larger volumes and higher numbers of novel entities with diverse risk potentials exceed societies' ability to conduct safety related assessments and monitoring (Persson et al., 2022). Consequently, the observed discrepancy does not indicate that all unlisted chemicals are safe for use; rather, it suggests that sufficient evidence to demonstrate their detrimental effects on the environment is currently lacking. One may even argue whether the few regulations that apply are effective. For example, despite the global ban on chlorofluorocarbons (CFCs) in 2010, their atmospheric abundances increased between 2010 and 2020 (Western et al., 2023). Similarly, brominated flame-retardants (BFRs), besides being listed as POPs, remain commercially available in several countries, with at least 63 BFRs on the market and no signs of cessation (de Boer et al., 2024).

Overall, despite the introduction of the Green Chemistry Principles, the Stockholm Convention, and other regulations over two decades ago, humanity has far exceeded the planetary boundary for chemical pollution (Persson et al., 2022), with concentrations of hazardous compounds that may no longer be declining, and regrettable replacements of problematic substances that have proven ineffective or even aggravated risk (Blum et al., 2019; Fenner & Scheringer, 2021). The rate at which the global chemical market expands surpasses the capacities for chemical risk assessment, and the extensive complexity of interactions between numerous chemical compounds and biological targets renders the development of sufficiently robust predictive models an overwhelming challenge (Fenner et al., 2021). Meanwhile, "the chemical-related annual death toll is significantly greater than that of World War II and today constitutes the greatest preventable form of mortality" (Figure 7.2, Landrigan et al., 2018; Naidu et al., 2021). The dramatic increase in the release of chemicals suggests that current regulatory measures and risk assessment strategies are insufficient to mitigate or manage the environmental impact of the chemical industry.

Chemical pollutant: Global PICTURE

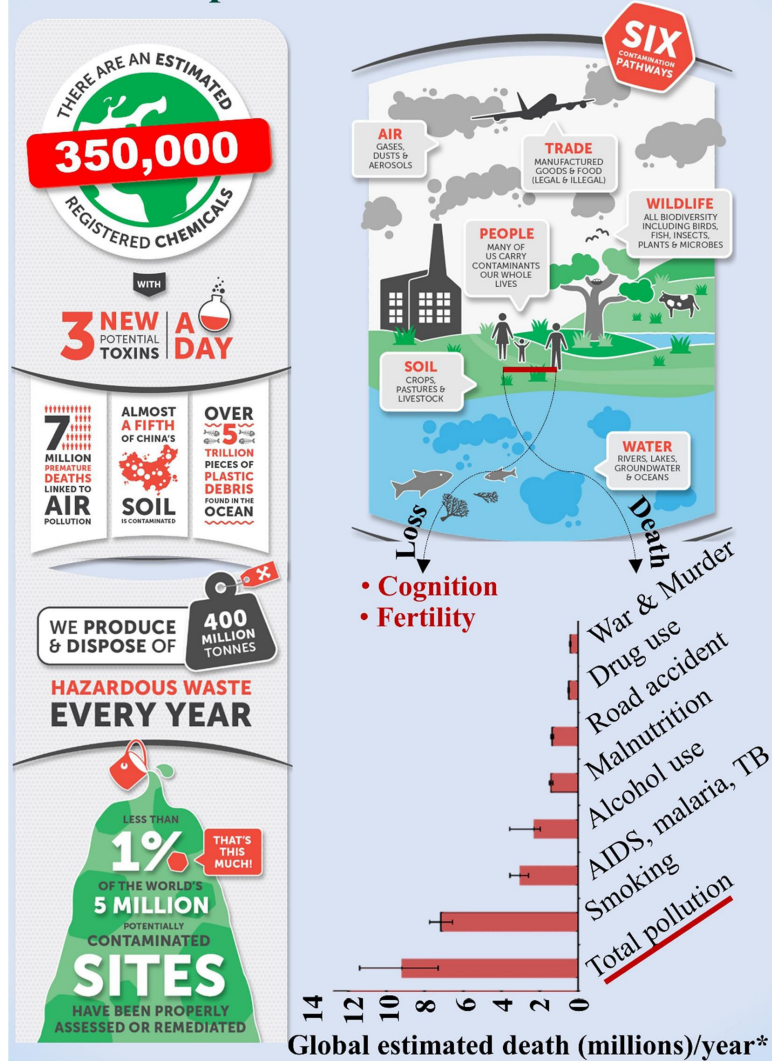


Figure 7.2 An overview of worldwide chemical pollution sources and routes, along with their potential effects on environmental systems and human well-being. The graphical component shows estimated deaths reported for the year 2015 (Landrigan et al., 2018). From Naidu et al. (2021). Licensed under CC BY 4.0. <https://creativecommons.org/licenses/by/4.0/>

As a result, many researchers are advocating for a fundamental shift in the chemical industry's approach. There is an immediate need to address the root cause of the issue, prioritize environmental and human health concerns, and set aside profit-driven motives (Lux, 2003). "Unless industry worldwide receives strong, clear economic and regulatory signals to produce clean, safe and healthy products it will continue with business as usual" (Hou & Ok, 2019; Naidu et al., 2021). Chemical simplification, both in the sense of reducing the number of chemicals in use and the chemical complexity of the compounds, has been proposed (Fenner & Scheringer, 2021). This simplification would come together with grouping approaches becoming an integral part of chemicals assessment, thus deprecating the current model of individual compound assessment. The combination of both would facilitate progress toward a simplified and reduced portfolio of chemicals, allowing resources and efforts to be allocated for thorough risk assessments of the chemicals remaining in commerce (Fenner & Scheringer, 2021).

Nevertheless, in the absence of coordinated global action, any proposed changes or interventions are unlikely to induce a significant alteration in this regard. To answer this need, the United Nations Environment Assembly (UNEA) mandated in 2022 the creation of a new Intergovernmental Panel on Chemicals, Waste and Pollution Prevention, an international Science-Policy Panel (SPP) equivalent to the Intergovernmental Panel on Climate Change (IPCC). While this SPP is in progress, several proposals have already been made about how this organization should conduct chemical assessments. Among them, one of the most revolutionary states that the SPP should be directed to conduct prospective assessments, as opposed retrospective impact-based assessments (Diamond et al., 2024). The assertion is grounded in two key observations. Firstly, taking preventive measures (proactive approaches) is significantly more efficient and economical than addressing issues after they occur (European Environment Agency, 2013). Secondly, instances of "false positives" (where anticipated problems do not materialize) are considerably less frequent than "false negatives" (situations where valid concerns were not acted upon preventively) (European Environment Agency, 2013). This underscores the importance of proactive risk management and the additional costs of inaction until an issue has grown to cause a major impact.

Scientific research will be essential to support the Intergovernmental Panel on Chemicals, Waste and Pollution Prevention in its mandate of coordinating global governmental action against chemical pollution, as well as to guide the industry to chemical simplification. However, immediate action is imperative, and policymakers should initiate proactive measures based on existing knowledge, rather than continuing to defer action while awaiting unprecedented scientific discoveries to rectify the environmental degradation human activities have caused.

7.4 References

- Abessa, D. M. S., Albuquerque, H. C., Morais, L. G., Araújo, G. S., Fonseca, T. G., Cruz, A. C. F., Campos, B. G., Camargo, J. B. D. A., Gusso-Choueri, P. K., Perina, F. C., Choueri, R. B., & Buruaem, L. M. (2018). Pollution status of marine protected areas worldwide and the consequent toxic effects are unknown. *Environmental Pollution*, 243, 1450–1459.
- Abirami, B., Radhakrishnan, M., Kumaran, S., & Wilson, A. (2021). Impacts of global warming on marine microbial communities. *Science of The Total Environment*, 791, 147905.
- Almeda, R., Wambaugh, Z., Wang, Z., Hyatt, C., Liu, Z., & Buskey, E. J. (2013). Interactions between Zooplankton and Crude Oil: Toxic Effects and Bioaccumulation of Polycyclic Aromatic Hydrocarbons. *PLoS One*, 8(6), e67212.
- Back to Blue. (2022). The zero-pollution ocean: A call to close the evidence gap.
- Barata, C., Calbet, A., Saiz, E., Ortiz, L., & Bayona, J. M. (2005). Predicting single and mixture toxicity of petrogenic polycyclic aromatic hydrocarbons to the copepod *Oithona davisae*. *Environ Toxicol Chem*, 24(11), 2992–2999.
- Bellas, J., & Thor, P. (2007). Effects of selected PAHs on reproduction and survival of the calanoid copepod *Acartia tonsa*. *Ecotoxicology*, 16(6), 465–474.
- Bengtson Nash, S. (2011). Persistent organic pollutants in Antarctica: current and future research priorities. *Journal of Environmental Monitoring*, 13(3), 497.
- Bethke, K., Kropidłowska, K., Stepnowski, P., & Caban, M. (2023). Review of warming and acidification effects to the ecotoxicity of pharmaceuticals on aquatic organisms in the era of climate change. *Science of The Total Environment*, 877, 162829.
- Biache, C., Mansuy-Huault, L., & Faure, P. (2014). Impact of oxidation and biodegradation on the most commonly used polycyclic aromatic hydrocarbon (PAH) diagnostic ratios: Implications for the source identifications. *J Hazard Mater*, 267, 31–39.
- Blum, A., Behl, M., Birnbaum, L. S., Diamond, M. L., Phillips, A., Singla, V., Sipes, N. S., Stapleton, H. M., & Venier, M. (2019). Organophosphate Ester Flame Retardants: Are They a Regrettable Substitution for Polybrominated Diphenyl Ethers? In *Environmental Science and Technology Letters* (Vol. 6, Issue 11, pp. 638–649). American Chemical Society.
- Bracco, A. (2025). 2024's extreme ocean heat breaks records again, leaving 2 mysteries to solve. <https://theconversation.com/2024s-extreme-ocean-heat-breaks-records-again-leaving-2-mysteries-to-solve-246843#:~:text=This%20past%20year%2C%202024%2C%20was,warmer%20than%20the%20previous%20one.>
- Brakstad, O. G., Lofthus, S., Ribicic, D., & Netzer, R. (2017). Biodegradation of Petroleum Oil in Cold Marine Environments. In *Psychrophiles: From Biodiversity to Biotechnology* (pp. 613–644). Springer International Publishing.
- Browning, T. J., & Moore, C. M. (2023). Global analysis of ocean phytoplankton nutrient limitation reveals high prevalence of co-limitation. *Nat Commun*, 14(1).
- Bunse, C., & Pinhassi, J. (2017). Marine Bacterioplankton Seasonal Succession Dynamics. *Trends Microbiol*, 25(6), 494–505.
- Cabrerizo, A., Tejedo, P., Dachs, J., & Benayas, J. (2016). Anthropogenic and biogenic hydrocarbons in soils and vegetation from the South Shetland Islands (Antarctica). *Science of The Total Environment*, 569–570, 1500–1509.
- Cai, M., Yang, H., Xie, Z., Zhao, Z., Wang, F., Lu, Z., Sturm, R., & Ebinghaus, R. (2012). Per- and polyfluoroalkyl substances in snow, lake, surface runoff water and coastal seawater in Fildes Peninsula, King George Island, Antarctica. *J Hazard Mater*, 209–210, 335–342.
- Cai, M., Zhao, Z., Yin, Z., Ahrens, L., Huang, P., Cai, M., Yang, H., He, J., Sturm, R., Ebinghaus, R., & Xie, Z. (2012). Occurrence of Perfluoroalkyl Compounds in Surface Waters from the North Pacific to the Arctic Ocean. *Environ Sci Technol*, 46(2), 661–668.
- Carmichael, R., & Brown, J. (2022). The Invisible Wave: Getting to zero chemical pollution in the ocean. <https://backtoblueinitiative.com/>
- Casal, P., Cabrerizo, A., Vila-Costa, M., Pizarro, M., Jiménez, B., & Dachs, J. (2018). Pivotal

Role of Snow Deposition and Melting Driving Fluxes of Polycyclic Aromatic Hydrocarbons at Coastal Livingston Island (Antarctica). *Environ Sci Technol*, 52(21), 12327–12337.

Casal, P., Zhang, Y., Martin, J. W., Pizarro, M., Jiménez, B., & Dachs, J. (2017). Role of Snow Deposition of Perfluoroalkylated Substances at Coastal Livingston Island (Maritime Antarctica). *Environ Sci Technol*, 51(15), 8460–8470.

Casas, G. (2022). The Antarctic as Sentinel of Global Pollution [Universitat de Barcelona]. <http://hdl.handle.net/2445/188128>

Casas, G., Martínez-Varela, A., Roscales, J. L., Vila-Costa, M., Dachs, J., & Jiménez, B. (2020). Enrichment of perfluoroalkyl substances in the sea-surface microlayer and sea-spray aerosols in the Southern Ocean. *Environmental Pollution*, 267, 115512.

Castro-Jiménez, J., Cuny, P., Milton, C., Sylvi, L., Royer, F., Papillon, L., & Sempéré, R. (2022). Effective degradation of organophosphate ester flame retardants and plasticizers in coastal sediments under high urban pressure. *Sci Rep*, 12(1), 20228.

Cerro-Gálvez, E., Roscales, J. L., Jiménez, B., Sala, M. M., Dachs, J., & Vila-Costa, M. (2020). Microbial responses to perfluoroalkyl substances and perfluorooctanesulfonate (PFOS) desulfurization in the Antarctic marine environment. *Water Res*, 171, 115434.

Chakraborty, J., & Das, S. (2016). Molecular perspectives and recent advances in microbial remediation of persistent organic pollutants. *Environmental Science and Pollution Research*, 23(17), 16883–16903.

Coelho, F. J. R. C., Cleary, D. F. R., Rocha, R. J. M., Calado, R., Castanheira, J. M., Rocha, S. M., Silva, A. M. S., Simões, M. M. Q., Oliveira, V., Lillebø, A. I., Almeida, A., Cunha, Â., Lopes, I., Ribeiro, R., Moreira-Santos, M., Marques, C. R., Costa, R., Pereira, R., & Gomes, N. C. M. (2015). Unraveling the interactive effects of climate change and oil contamination on laboratory-simulated estuarine benthic communities. *Glob Chang Biol*, 21(5), 1871–1886.

Cousins, I. T., Ng, C. A., Wang, Z., & Scheringer, M. (2019). Why is high persistence alone a major cause of concern? *Environ Sci Process Impacts*, 21(5), 781–792.

Dachs, J., & Vila-Costa, M. (2022). Toward a Multi-Omics-Based Single-Cell Environmental Chemistry and Toxicology. *Environ Sci Technol*, 56(15), 10550–10552.

de Boer, J., Harrad, S., & Sharkey, M. (2024). The European Regulatory Strategy for flame retardants – The right direction but still a risk of getting lost. *Chemosphere*, 347, 140638.

Despotović, D., Aharon, E., Trofimiyuk, O., Dubovetskyi, A., Cherukuri, K. P., Ashani, Y., Eliason, O., Sperfeld, M., Leader, H., Castelli, A., Fumagalli, L., Savidor, A., Levin, Y., Longo, L. M., Segev, E., & Tawfik, D. S. (2022). Utilization of diverse organophosphorus pollutants by marine bacteria. *Proceedings of the National Academy of Sciences*, 119(32).

Diamond, M. L., Sigmund, G., Bertram, M. G., Ford, A. T., Ågerstrand, M., Carlini, G., Lohmann, R., Šebková, K., Soehl, A., Starling, M. C. V. M., Suzuki, N., Venier, M., Vlahos, P., & Scheringer, M. (2024). Exploring Outputs of the Intergovernmental Science-Policy Panel on Chemicals, Waste, and Pollution Prevention. *Environ Sci Technol Lett*, 11(7), 664–672.

Duarte, C. M. (2015). Seafaring in the 21st Century: The Malaspina 2010 Circumnavigation Expedition. *Limnol Oceanogr Bull*, 24(1), 11–14.

Dubinsky, E. A., Conrad, M. E., Chakraborty, R., Bill, M., Borglin, S. E., Hollibaugh, J. T., Mason, O. U., M. Piceno, Y., Reid, F. C., Stringfellow, W. T., Tom, L. M., Hazen, T. C., & Andersen, G. L. (2013). Succession of Hydrocarbon-Degrading Bacteria in the Aftermath of the Deepwater Horizon Oil Spill in the Gulf of Mexico. *Environ Sci Technol*, 47(19), 10860–10867.

Enevoldsen, H., Isensee, K., & Yoon, I. (2022). State of the Ocean Report 2022 Pilot edition. <https://unesdoc.unesco.org/ark:/48223/pf0000381921.locale=en>

European Environment Agency. (2013). Late lessons from early warnings: science, precaution, innovation. <https://www.eea.europa.eu/en/analysis/publications/late-lessons-2>

Fenner, K., Elsner, M., Lueders, T., McLachlan, M. S., Wackett, L. P., Zimmermann, M., & Drewes, J. E. (2021). Methodological Advances to Study Contaminant Biotransformation: New Prospects for Understanding and Reducing Environmental Persistence? *ACS ES&T Water*, 1(7), 1541–1554.

Fenner, K., & Scheringer, M. (2021). The

Need for Chemical Simplification As a Logical Consequence of Ever-Increasing Chemical Pollution. *Environ Sci Technol*, 55(21), 14470–14472.

Fernández-Pinos, M.-C., Vila-Costa, M., Arrieta, J. M., Morales, L., González-Gaya, B., Piña, B., & Dachs, J. (2017). Dysregulation of photosynthetic genes in oceanic *Prochlorococcus* populations exposed to organic pollutants. *Sci Rep*, 7(1), 8029.

Gao, M., Wang, Y., Wei, L., Li, S., Zhang, Q., Yang, Z., Bai, M., Yao, Y., Wang, L., & Sun, H. (2025). Novel organophosphate esters and their transformation products in offshore sediment from Eastern China: Occurrence, temporal trend, and risk assessment. *Environ Int*, 195, 109205.

Garneau, M.-È., Michel, C., Meisterhans, G., Fortin, N., King, T. L., Greer, C. W., & Lee, K. (2016). Hydrocarbon biodegradation by Arctic sea-ice and sub-ice microbial communities during microcosm experiments, Northwest Passage (Nunavut, Canada). *FEMS Microbiol Ecol*, 92(10), fiw130.

Ghosal, D., Ghosh, S., Dutta, T. K., & Ahn, Y. (2016). Current State of Knowledge in Microbial Degradation of Polycyclic Aromatic Hydrocarbons (PAHs): A Review. *Front Microbiol*, 7(AUG), 1369.

González, J. M., Hernández, L., Manzano, I., & Pedrós-Alió, C. (2019). Functional annotation of orthologs in metagenomes: a case study of genes for the transformation of oceanic dimethylsulfoniopropionate. *ISME J*, 13(5), 1183–1197.

González-Gaya, B., Martínez-Varela, A., Vila-Costa, M., Casal, P., Cerro-Gálvez, E., Berrojalbiz, N., Lundin, D., Vidal, M., Mompeán, C., Bode, A., Jiménez, B., & Dachs, J. (2019). Biodegradation as an important sink of aromatic hydrocarbons in the oceans. *Nature Geoscience* 2019 12:2, 12(2), 119–125.

Gutleben, J., Chaib De Mares, M., van Elsas, J. D., Smidt, H., Overmann, J., & Sipkema, D. (2018). The multi-omics promise in context: from sequence to microbial isolate. *Crit Rev Microbiol*, 44(2), 212–229.

Hassan, S., Sabreena, Khurshid, Z., Bhat, S. A., Kumar, V., Ameen, F., & Ganai, B. A. (2022). Marine bacteria and omic approaches: A novel and potential repository for bioremediation assessment. *J Appl Microbiol*, 133(4), 2299–2313.

Hatje, V., Sarin, M., Sander, S. G., Omanović,

D., Ramachandran, P., Völker, C., Barra, R. O., & Tagliabue, A. (2022). Emergent interactive effects of climate change and contaminants in coastal and ocean ecosystems. *Front Mar Sci*, 9.

Hou, D., & Ok, Y. S. (2019). Soil pollution -- speed up global mapping. *Nature*, 566, 455.

Huang, Y. J., Lin, B. S., Lee, C. L., & Brimblecombe, P. (2020). Enrichment behavior of contemporary PAHs and legacy PCBs at the sea-surface microlayer in harbor water. *Chemosphere*, 245, 125647.

Kaur, T., Lakhawat, S. S., Kumar, V., Sharma, V., Neeraj, R. R. K., & Sharma, P. K. (2023). Polyaromatic Hydrocarbon Specific Ring Hydroxylating Dioxygenases: Diversity, Structure, Function, and Protein Engineering. *Curr Protein Pept Sci*, 24(1), 7–21.

Kawagoshi, Y., Nakamura, S., & Fukunaga, I. (2002). Degradation of organophosphoric esters in leachate from a sea-based solid waste disposal site. *Chemosphere*, 48(2), 219–225.

Kawai, S. (1996). Degradation of organophosphoric acid triesters by the aquatic bacteria and toxicity to fish. *J Jpn Soc Water Environ*, 19, 700–707. <https://cir.nii.ac.jp/crid/1571980074132818944.bib?lang=en>

Kristiansson, E., Coria, J., Gunnarsson, L., & Gustavsson, M. (2021). Does the scientific knowledge reflect the chemical diversity of environmental pollution? – A twenty-year perspective. *Environ Sci Policy*, 126, 90–98.

Kwon, K., Kwon, Y. M., & Kim, S.-J. (2019). Aerobic Hydrocarbon-Degrading Bacteroidetes. In *Taxonomy, Genomics and Ecophysiology of Hydrocarbon-Degrading Microbes* (pp. 73–91). Springer International Publishing.

Landrigan, P. J., Fuller, R., Acosta, N. J. R., Adeyi, O., Arnold, R., Basu, N. (Nil), Baldé, A. B., Bertollini, R., Bose-O'Reilly, S., Boufford, J. I., Breyse, P. N., Chiles, T., Mahidol, C., Coll-Seck, A. M., Cropper, M. L., Fobil, J., Fuster, V., Greenstone, M., Haines, A., ... Zhong, M. (2018). The Lancet Commission on pollution and health. *The Lancet*, 391(10119), 462–512.

Li, Y., Hablützel, P. I., Liu, Z., Van Acker, E., Janssen, C. R., Asselman, J., & De Rijcke, M. (2024). Seasonal dynamics of bacterial community structure and function in the surf zone seawater of a recreational beach in Ostend, Belgium. *Environ*

Microbiol Rep, 16(6).

Liang, C., He, Y., Mo, X.-J., Guan, H.-X., & Liu, L.-Y. (2024). Universal occurrence of organophosphate tri-esters and di-esters in marine sediments: Evidence from the Okinawa Trough in the East China Sea. *Environ Res*, 248, 118308.

Lin, W., Fan, F., Xu, G., Gong, K., Cheng, X., Yuan, X., Zhang, C., Gao, Y., Wang, S., Ng, H. Y., & Dong, Y. (2023). Microbial community assembly responses to polycyclic aromatic hydrocarbon contamination across water and sediment habitats in the Pearl River Estuary. *J Hazard Mater*, 457, 131762.

Liu, J., Lin, H., Dong, Y., & Li, B. (2019). Elucidating the biodegradation mechanism of tributyl phosphate (TBP) by *Sphingomonas* sp. isolated from TBP-contaminated mine tailings. *Environmental Pollution*, 250, 284–291.

Lux, K. (2003). The failure of the profit motive. *Ecological Economics*, 44(1), 1–9.

Madsen, E. L. (1991). Determining in situ biodegradation. *Environ Sci Technol*, 25(10), 1662–1673.

Martinez-Varela, A., Casas, G., Berrojalbiz, N., Lundin, D., Piña, B., Dachs, J., & Vila-Costa, M. (2023). Metatranscriptomic responses and microbial degradation of background polycyclic aromatic hydrocarbons in the coastal Mediterranean and Antarctica. *Environmental Science and Pollution Research*, 30(57), 119988–119999.

Martinez-Varela, A., Casas, G., Berrojalbiz, N., Piña, B., Dachs, J., & Vila-Costa, M. (2022). Polycyclic Aromatic Hydrocarbon Degradation in the Sea-Surface Microlayer at Coastal Antarctica. *Front Microbiol*, 13.

Martinez-Varela, A., Casas, G., Piña, B., Dachs, J., & Vila-Costa, M. (2020). Large Enrichment of Anthropogenic Organic Matter Degrading Bacteria in the Sea-Surface Microlayer at Coastal Livingston Island (Antarctica). *Front Microbiol*, 11(September), 1–13.

Massana, R., Pedrós-Alió, C., Casamayor, E. O., & Gasol, J. M. (2001). Changes in marine bacterioplankton phylogenetic composition during incubations designed to measure biogeochemically significant parameters. *Limnol Oceanogr*, 46(5), 1181–1188.

McLachlan, M. S., Zou, H., & Gouin, T. (2017).

Using Benchmarking To Strengthen the Assessment of Persistence. *Environ Sci Technol*, 51(1), 4–11.

Muir, D., & Miaz, L. T. (2021). Spatial and Temporal Trends of Perfluoroalkyl Substances in Global Ocean and Coastal Waters. *Environ Sci Technol*, 55(14), 9527–9537.

Muller, E. E. L., Glaab, E., May, P., Vlassis, N., & Wilmes, P. (2013). Condensing the omics fog of microbial communities. *Trends Microbiol*, 21(7), 325–333.

Naidu, R., Biswas, B., Willett, I. R., Cribb, J., Kumar Singh, B., Paul Nathanail, C., Coulon, F., Semple, K. T., Jones, K. C., Barclay, A., & Aitken, R. J. (2021). Chemical pollution: A growing peril and potential catastrophic risk to humanity. *Environ Int*, 156, 106616.

Nogales, B., Lanfranconi, M. P., Piña-Villalonga, J. M., & Bosch, R. (2011). Anthropogenic perturbations in marine microbial communities. *FEMS Microbiol Rev*, 35(2), 275–298.

Nowak, A., Hodson, A., & Turchyn, A. V. (2018). Spatial and Temporal Dynamics of Dissolved Organic Carbon, Chlorophyll, Nutrients, and Trace Metals in Maritime Antarctic Snow and Snowmelt. *Front Earth Sci (Lausanne)*, 6.

Noyes, P. D., McElwee, M. K., Miller, H. D., Clark, B. W., Van Tiem, L. A., Walcott, K. C., Erwin, K. N., & Levin, E. D. (2009). The toxicology of climate change: Environmental contaminants in a warming world. *Environ Int*, 35(6), 971–986.

O'Brien, J., McParland, E. L., Bramucci, A. R., Ostrowski, M., Siboni, N., Ingleton, T., Brown, M. V., Levine, N. M., Laverock, B., Petrou, K., & Seymour, J. (2022). The Microbiological Drivers of Temporally Dynamic Dimethylsulfoniopropionate Cycling Processes in Australian Coastal Shelf Waters. *Front Microbiol*, 13.

Oliver, T. H., Isaac, N. J. B., August, T. A., Woodcock, B. A., Roy, D. B., & Bullock, J. M. (2015). Declining resilience of ecosystem functions under biodiversity loss. *Nat Commun*, 6(1), 10122.

Ottosen, C. B., Murray, A. M., Broholm, M. M., & Bjerg, P. L. (2019). In Situ Quantification of Degradation Is Needed for Reliable Risk Assessments and Site-Specific Monitored Natural Attenuation. *Environ Sci Technol*, 53(1), 1–3.

Peng, Y., Shi, C., Wang, C., Li, Y., Zeng, L., Zhang, J., Huang, M., Zheng, Y., Chen, H., Chen, C.,

& Li, H. (2023). Review on typical organophosphate diesters (di-OPEs) requiring priority attention: Formation, occurrence, toxicological, and epidemiological studies. *J Hazard Mater*, 460, 132426.

Persson, L., Carney Almroth, B. M., Collins, C. D., Cornell, S., de Wit, C. A., Diamond, M. L., Fantke, P., Hassellöv, M., MacLeod, M., Ryberg, M. W., Søgaard Jørgensen, P., Villarrubia-Gómez, P., Wang, Z., & Hauschild, M. Z. (2022). Outside the Safe Operating Space of the Planetary Boundary for Novel Entities. *Environ Sci Technol*, 56(3), 1510–1521.

Piontek, J., Meeske, C., Hassenrück, C., Engel, A., & Jürgens, K. (2022). Organic matter availability drives the spatial variation in the community composition and activity of Antarctic marine bacterioplankton. *Environ Microbiol*, 24(9), 4030–4048.

Pires, A. P. F., Srivastava, D. S., Marino, N. A. C., MacDonald, A. A. M., Figueiredo-Barros, M. P., & Farjalla, V. F. (2018). Interactive effects of climate change and biodiversity loss on ecosystem functioning. *Ecology*, 99(5), 1203–1213.

Posthuma, L., Zijp, M. C., De Zwart, D., Van de Meent, D., Globevnik, L., Koprivsek, M., Focks, A., Van Gils, J., & Birk, S. (2020). Chemical pollution imposes limitations to the ecological status of European surface waters. *Sci Rep*, 10(1), 14825.

Prabakaran, S. R., Manorama, R., Delille, D., & Shivaji, S. (2007). Predominance of *Roseobacter*, *Sulfitobacter*, *Glaciecola* and *Psychrobacter* in seawater collected off Ushuaia, Argentina, Sub-Antarctica. *FEMS Microbiol Ecol*, 59(2), 342–355.

Priest, T., Oldenburg, E., Popa, O., Dede, B., Metfies, K., von Appen, W.-J., Torres-Valdés, S., Bienhold, C., Fuchs, B. M., Amann, R., Boetius, A., & Wietz, M. (2024). Seasonal recurrence and modular assembly of an Arctic pelagic marine microbiome.

Renner, R. (2006). The long and the short of perfluorinated replacements. *Environ Sci Technol*, 40(1), 12–13.

Rodríguez del Río, Á., Giner-Lamia, J., Cantalapiedra, C. P., Botas, J., Deng, Z., Hernández-Plaza, A., Munar-Palmer, M., Santamaría-Hernando, S., Rodríguez-Herva, J. J., Ruscheweyh, H.-J., Paoli, L., Schmidt, T. S. B., Sunagawa, S., Bork, P., López-Solanilla, E., Coelho, L. P., & Huerta-Cepas, J. (2024). Functional and evolutionary significance of unknown genes from uncultivated taxa. *Nature*,

626(7998), 377–384.

Sánchez, P., Coutinho, F. H., Sebastián, M., Pernice, M. C., Rodríguez-Martínez, R., Salazar, G., Cornejo-Castillo, F. M., Pesant, S., López-Alforja, X., López-García, E. M., Agustí, S., Gojobori, T., Logares, R., Sala, M. M., Vaqué, D., Massana, R., Duarte, C. M., Acinas, S. G., & Gasol, J. M. (2024). Marine picoplankton metagenomes and MAGs from eleven vertical profiles obtained by the Malaspina Expedition. *Sci Data*, 11(1), 154.

Sanganyado, E., Chingono, K. E., Gwenzi, W., Chaukura, N., & Liu, W. (2021). Organic pollutants in deep sea: Occurrence, fate, and ecological implications. *Water Res*, 205, 117658.

Sanz-Sáez, I., Berrojalbiz, N., Dachs, J., & Vila-Costa, M. (2025). A framework for assessing microbial degradation of organophosphate ester plasticizers in seawater. *Chemosphere*, 371, 144025.

Satya, S., Sharma, S., Choudhary, G., & Kaushik, G. (2024). Advances in Environmental Microbiology: A Multi-omic Perspective. In *Microbial Omics in Environment and Health* (pp. 175–204). Springer Nature Singapore.

Stogiannidis, E., & Laane, R. (2015). Source Characterization of Polycyclic Aromatic Hydrocarbons by Using Their Molecular Indices: An Overview of Possibilities (pp. 49–133).

Sunagawa, S., Coelho, L. P., Chaffron, S., Kultima, J. R., Labadie, K., Salazar, G., Djahanschiri, B., Zeller, G., Mende, D. R., Alberti, A., Cornejo-Castillo, F. M., Costea, P. I., Cruaud, C., d'Ovidio, F., Engelen, S., Ferrera, I., Gasol, J. M., Guidi, L., Hildebrand, F., ... Velayoudon, D. (2015). Structure and function of the global ocean microbiome. *Science* (1979), 348(6237).

Szopińska, M., Szumińska, D., Bialik, R. J., Dymerski, T., Rosenberg, E., & Polkowska, Ż. (2019). Determination of polycyclic aromatic hydrocarbons (PAHs) and other organic pollutants in freshwaters on the western shore of Admiralty Bay (King George Island, Maritime Antarctica). *Environmental Science and Pollution Research*, 26(18), 18143–18161.

Takahashi, S., Miura, K., Abe, K., & Kera, Y. (2012). Complete detoxification of tris(2-chloroethyl) phosphate by two bacterial strains: *Sphingobium* sp. strain TCM1 and *Xanthobacter autotrophicus* strain GJ10. *J Biosci Bioeng*, 114(3), 306–311.

Tian, R., Posselt, M., Fenner, K., & McLachlan,

- M. S. (2023). Increasing the Environmental Relevance of Biodegradation Testing by Focusing on Initial Biodegradation Kinetics and Employing Low-Level Spiking. *Environ Sci Technol Lett*, 10(1), 40–45.
- Trilla-Prieto, N., Berrojalbiz, N., Iriarte, J., Fuentes, A., Sobrino, C., Vila-Costa, M., Jiménez, B., & Dachs, J. (2025). Biogeochemical Controls on Latitudinal (42°N to 70°S) and Depth Distribution of Organophosphate Esters in the Atlantic and Southern Oceans. Submitted to *Environmental Science & Technology*.
- Trilla-Prieto, N., Iriarte, J., Berrojalbiz, N., Casas, G., Sobrino, C., Vila-Costa, M., Jiménez, B., & Dachs, J. (2024). Enrichment of Organophosphate Esters in the Sea Surface Microlayer from the Atlantic and Southern Oceans. *Environ Sci Technol Lett*, 11(9), 1008–1015.
- Turan, H., Khalfaoui-Hassani, B., Godino-Sanchez, A., Naimah, Z., Sebilo, M., Guyoneaud, R., & Monperrus, M. (2024). Insights into bacterial resistance to contaminants of emerging concerns and their biodegradation by marine bacteria. *Emerg Contam*, 10(3), 100332.
- UNEP. (2023). Stockholm Convention on Persistent Organic Pollutants (POPs). Text and Annexes (Revised in 2023). <https://www.pops.int/TheConvention/Overview/TextoftheConvention/tabid/2232>
- Vila-Costa, M., Sebastián, M., Pizarro, M., Cerro-Gálvez, E., Lundin, D., Gasol, J. M., & Dachs, J. (2019). Microbial consumption of organophosphate esters in seawater under phosphorus limited conditions. *Sci Rep*, 9(1), 233.
- Wang, F., Xiang, L., Sze-Yin Leung, K., Elsner, M., Zhang, Y., Guo, Y., Pan, B., Sun, H., An, T., Ying, G., Brooks, B. W., Hou, D., Helbling, D. E., Sun, J., Qiu, H., Vogel, T. M., Zhang, W., Gao, Y., Simpson, M. J., ... Tiedje, J. M. (2024). Emerging contaminants: A One Health perspective. *The Innovation*, 5(4), 100612.
- Wang, J., Khokhar, I., Ren, C., Li, X., Wang, J., Fan, S., Jia, Y., & Yan, Y. (2019). Characterization and 16S metagenomic analysis of organophosphorus flame retardants degrading consortia. *J Hazard Mater*, 380, 120881.
- Wang, P., Lu, Y., Wang, T., Zhu, Z., Li, Q., Meng, J., Su, H., Johnson, A. C., & Sweetman, A. J. (2016). Coupled production and emission of short chain perfluoroalkyl acids from a fast developing fluorochemical industry: Evidence from yearly and seasonal monitoring in Daling River Basin, China. *Environmental Pollution*, 218, 1234–1244.
- Wang, Z., Fingas, M., Blenkinsopp, S., Sergy, G., Landriault, M., Sigouin, L., Foght, J., Semple, K., & Westlake, D. W. S. (1998). Comparison of oil composition changes due to biodegradation and physical weathering in different oils. *J Chromatogr A*, 809(1–2), 89–107.
- Western, L. M., Vollmer, M. K., Krummel, P. B., Adcock, K. E., Crotwell, M., Fraser, P. J., Harth, C. M., Langenfelds, R. L., Montzka, S. A., Mühle, J., O'Doherty, S., Oram, D. E., Reimann, S., Rigby, M., Vimont, I., Weiss, R. F., Young, D., & Laube, J. C. (2023). Global increase of ozone-depleting chlorofluorocarbons from 2010 to 2020. *Nat Geosci*, 16(4), 309–313.
- Yu, Y., Yu, X., Zhang, D., Jin, L., Huang, J., Zhu, X., Sun, J., Yu, M., & Zhu, L. (2023). Biotransformation of Organophosphate Esters by Rice and Rhizosphere Microbiome: Multiple Metabolic Pathways, Mechanism, and Toxicity Assessment. *Environ Sci Technol*, 57(4), 1776–1787.
- Zhang, J., Sun, Z., Li, Y., Peng, X., Li, W., & Yan, Y. (2009). Biodegradation of p-nitrophenol by *Rhodococcus* sp. CN6 with high cell surface hydrophobicity. *J Hazard Mater*, 163(2–3), 723–728.
- Zhang, L., Meng, L., Wang, H., Lu, D., & Luo, X. (2022). Development and validation of a liquid chromatography-tandem mass spectrometry method for comprehensive detection of organophosphate esters and their degradation products in sediment. *J Chromatogr A*, 1665, 462826.
- Zhou, Y., Wang, Y., Yang, L., Kong, Q., & Zhang, H. (2023). Microbial degradation mechanisms of surface petroleum contaminated seawater in a typical oil trading port. *Environmental Pollution*, 324, 121420.
- Zhou, Y., Wang, Y., Yao, S., Zhao, X., Kong, Q., Cui, L., & Zhang, H. (2024). Driving mechanisms for the adaptation and degradation of petroleum hydrocarbons by native microbiota from seas prone to oil spills. *J Hazard Mater*, 476, 135060.
- Zimmermann, M., Zimmermann-Kogadeeva, M., Wegmann, R., & Goodman, A. L. (2019). Mapping human microbiome drug metabolism by gut bacteria and their genes. *Nature*, 570(7762), 462–467.



CHAPTER 8

Conclusions



Conclusions

The main conclusions of this thesis are summarized below:

The concurrent characterization of organic contaminants and microbial communities in field-derived time series of measurements is a powerful approach that provides essential tools to elucidate the complexity of biogeochemical controls of contaminant occurrence and dynamics. Utilizing this approach, the following conclusions were derived from the research conducted in coastal Antarctica:

- Organic contaminants, such as polycyclic aromatic hydrocarbons (PAHs) and perfluoroalkyl acids (PFAAs), were ubiquitous in coastal maritime Antarctica, and their concentrations showed a large temporal variability that could be partially attributed to inputs from snowmelt and the geographical features of the Livingston and Deception Islands.
- PAH biodegradation was found to be maximal in the year with large snowmelt inputs, suggesting that organic and inorganic nutrient inputs triggered the response of the microbial loop/pump, resulting in higher biodegradation of PAHs.
- Significant correlations between specific hydrocarbon-degrading taxa and PAH concentrations were found, although the potential for biodegradation could not be solely attributed to the presence of these bacteria, indicating a complex interplay between bacterial communities and environmental factors in the biogeochemical cycling of PAHs.
- Evaluating potential PFAA sinks suggests that, besides the biological pump-derived removal of PFAAs associated with plankton, the depletion of PFSA through microbial degradation linked to the organic sulfur cycle is feasible, and should receive further attention in future research efforts.

Field experiments enable the testing of specific hypotheses under controlled conditions while ensuring that the results closely reflect real environmental conditions. This is particularly relevant when the biogeochemical processes affecting organic contaminants are still unknown, limiting the use of analyses such as diagnostic ratios. In this context, the following conclusions were derived from Organophosphate Ester (OPE) flame retardant and plasticizers exposure experiments with naturally occurring microbial communities to assess potential biodegradation:

- Dissolved phase OPE removal related to biotic processes was found for the two most hydrophobic compounds of the targeted OPEs in the Atlantic Ocean after 48h of incubations.

- Abiotic sorption controls are mandatory in OPEs biodegradation assessment experiments to account for the passive sorption to microbial cells. This process accounted for a significant depletion of dissolved phase OPEs in both the Atlantic and Southern Oceans, and was correlated with the octanol-water partition coefficient of the OPE compounds. This conclusion is relevant for all hydrophobic organic pollutants.
- Greater OPE depletion due to biotic processes was found to correlate with increased fold change in bacterial production rates, suggesting a direct link between OPE biodegradation and protein production activity of heterotrophic bacteria.

Advances in omic techniques and bioinformatic tools offer new possibilities for using marine microbial communities' compositional, functional, and/or transcriptional data as biomarkers of biodegradation potential for organic contaminants. This approach provides valuable information for more accurately assessing the persistence of these compounds and enhancing the predictive power of current models. In line with this, the following conclusions were drawn from our bioinformatic approach to assessing PAH biodegradation using field measurements of chemicals and metagenomic datasets:

- The developed phylogenetic placement methodology identified aromatic ring hydroxylating dioxygenase alpha subunit (*arhdA*) genes across various branches of bacterial and archaeal phylogenomic trees and in a marine metagenomic dataset.
- Across temperate and subtropical seawaters, the lowest concentrations of the low-molecular-weight fraction of the PAHs were observed in regions with the highest abundances of *arhdA* gene.
- A higher abundance of *arhdA* genes in the particle-attached fraction was associated with lower PAH concentrations in plankton, suggesting the potential role of the particle-attached fraction as a hotspot for PAH biodegradation in the oceans.
- Background concentration levels of PAHs were found to be significant factors in explaining both the abundance of *arhdA* genes and the variation in the bacterial community composition, together with other previously described environmental factors such as temperature, nutrient concentrations, and planktonic biomass.

To summarize, the findings of this thesis lead to several conclusions and suggestions regarding potential directions for future research:

- Although background environmental levels of organic pollutants may not possess the capacity to modulate microbial communities to the same extent as other environmental factors such as nutrients, our findings suggest they should be considered as a relevant factor still significantly influencing marine microbial communities.
- Assessment of OPEs and PFAAs biodegradation from field-derived measurements in marine environments is limited due to current uncertainties regarding the main

bacterial players, their metabolic pathways, and key genes. Emphasis should be placed on culture-based approaches to identify and characterize these unknown factors.

- In light of projected increases in environmental stressors (acidification, elevated temperatures, altered oceanic circulation) and the anticipated rise in anthropogenic organic compounds, it is imperative to emphasize the potential disruption of microbial community functioning and biogeochemical cycles due to complex interactions with the Anthropogenic Dissolved Organic Carbon (ADOC) pool within this emerging scenario.
- The different approaches available for assessing microbial degradation of organic pollutants provide key and complementary information on chemical persistence, a key property when evaluating chemical risk, and such approaches will need further development to cover an increasing number of contaminants of emerging concern.



Acknowledgements

No tenía nada claro si este momento llegaría y, sin embargo, aquí estoy. Lo que sí tengo claro es que solo no habría llegado muy lejos, así que trataré de agradecer como corresponde a todas aquellas personas que me han acompañado en este trayecto. Han sido 5 años, largos por momentos, muy breves en otros. Muchas horas junto a esa ventana con vistas a Collserola, pero también una pandemia mundial y tres campañas de por medio. Un camino de altibajos y contrastes, lleno de experiencias y lecciones de vida. Y también lleno de amistades y personas que, sin duda, son las que dan valor a todo lo vivido en este tramo de mi vida.

Empiezo por la base, los dos pilares fundamentales, que no son otros que mis directores de tesis. Por un lado, Jordi, con su saber estar y su sabiduría, siempre aportando esa serenidad tan necesaria por momentos y esas grandes ideas y comentarios que mejoran todo lo que tocan. Por otro, Maria, inquieta y brillante también, llena de una energía y entusiasmo de los que es difícil no contagiarse. Una combinación, la de ambos, que marida muy bien, a mi juicio. A vosotros os estoy agradecido por haberme dado esta oportunidad, a aquel chico indeciso que allá por 2019 apareció por vuestro despacho y que, sin saberlo, encontró el mejor lugar donde crecer como científico y como persona. Gracias por la oportunidad de participar en las campañas, de visitar el continente helado... Vosotros, mejor que nadie, sabéis que ese lugar es capaz de cambiar a las personas, y es de alabar la generosidad que mostráis al dar la oportunidad a los más jóvenes de participar en la investigación polar. Pero no todo es la Antártida. Quisiera daros las gracias también por haber estado siempre dispuestos a ayudar, por tener siempre la puerta abierta para resolver cualquier duda, por saber que estáis al lado... pero también por haberme dado cierto espacio cuando ha sido necesario. Todas estas son cualidades fundamentales para ser un buen mentor o mentora, pero no son tan comunes como deberían, por lo que es justo reconocerlas.

A Anna, mi tutora de la UB, gracias por la disponibilidad y amabilidad con la que siempre me has atendido, resolviendo mis dudas siempre que te he requerido. Sin tu apoyo todo habría sido más difícil.

Por supuesto, tras cualquier resultado existe todo un equipo detrás. Personas que van y vienen, con las cuales he tenido la fortuna de compartir buenos y malos momentos, y a las cuales me gustaría dar las gracias. Personas que te acogen cuando aún estás aterrizando y le dan sentido al día a día. Como Alicia. Seguramente la mejor mentora que pude tener. Me enseñaste a ver las cosas de otra manera, que cualquier momento es bueno para hacer la vida un poco más entretenida e interesante. Solo tú podías conseguir ponerme de mote "Jonsito" y que acabara echándolo de menos. Gemma, una gran referente en muchos momentos. Fue un placer cada una de las cervezas que nos tomamos juntos. Contigo he aprendido que los catalanes y los vascos nos parecemos mucho... ¡es la única explicación que tengo para tu imitación inmejorable de Olasagasti y sus bueyes bañados en "Neuco"! Naiara, tú me has arropado, me has echado una mano cuando más la necesitaba y me has ayudado a crecer, y te estaré eternamente agradecido. Tu labor es fundamental para muchos de nosotros, pero muchas veces no recibe el reconocimiento que

merece. Te diré una cosa. ¡Ya queda menos para la jubilación! Y cuando llegue nos apuntaremos a un curso de acuarela juntos. Claudia, siempre dispuesta a escucharme... la cantidad de veces que debí bajar a la quinta planta para hablar contigo. Tu amabilidad y tu cariño hacían que cualquier día malo mejorara al momento. Se podría decir que le dabas color al día a día. Y yo me pregunto... ¿Qué color de pelo sorprendente tendrás ahora? Berta, siempre llena de energía. Desde el principio trataste de integrarme y es algo que valoro mucho. Qué difícil se me hacía tu acento catalán... puedo decir sin miedo a equivocarme que con Gemma y contigo he aprendido este idioma, así que gracias por eso también. Núria, compañera de viaje inseparable. Visto en perspectiva, creo que no hay nada mejor que tener alguien que te acompañe en este largo viaje que es el doctorado, y contigo me tocó el gordo de la lotería. Con esa determinación, capacidad de superación y fuerza que desprendes, llegarás donde te lo propongas, no me cabe la menor duda. Tan solo espero haber sido la mitad de buen compañero de lo que tú has sido para mí.

El tiempo pasa, y con él las personas. Así llegaron las nuevas incorporaciones. Clara, con esa mezcla tan maravillosa de espíritu aventurero y serenidad. He disfrutado mucho cada una de las experiencias que hemos compartido, pero sin duda me quedo con aquel fin de semana en la Selva de Oza. Todavía necesito que tu padre me firme su libro, así que no te vas a librar de mí tan fácilmente. Mapis, combinación sorprendente de espiritualidad y pensamiento crítico. Podría aprender tantas cosas de ti que necesitaría otros 5 años. Por suerte me quedan Youtube y la newsletter. Y quién sabe, tal vez nos veamos por Euskadi. Jessica, gran trabajadora y con un sentido del humor del que me declaro abiertamente fan. De ti he aprendido que es importante respetar los tiempos de cocción, no importa que sea para una sopa. Y también que debo ir a Bagnoli Irpino a probar sus recetas con castañas y trufas (high-priority). Isa, tan colmada de experiencia como de amabilidad, siempre dispuesta a compartir su conocimiento con los demás. Fuiste un gran apoyo en todo lo relacionado con los cultivos, especialmente para mi estancia, y te estoy muy agradecido. ¡Me alegro de haber tenido la oportunidad de trabajar contigo y espero que las bacterias se porten bien contigo! Mar, entusiasmo en estado puro. Tu estancia fue algo más breve pero a mí me marcó. Disfruté mucho de las salidas al monte que hicimos y espero poder repetirlas en el futuro. Marta Gual, tu ayuda ha sido muy importante para sacar adelante la cantidad ingente de muestras que tenía, y te estoy agradecido por ello. Las últimas incorporaciones, María y Júlia. Me hubiera gustado tener tiempo para conocerlos más, pero al menos marchó tranquilo porque sé que con vosotras el grupo queda en muy buenas manos.

Uno de los grandes momentos de esta tesis ha sido, sin duda, sus campañas y todas las personas maravillosas que participaron en ellas, quienes, al fin y al cabo, son las que realmente otorgan a estas experiencias su profundo valor. Mención especial merece ANATOM. Una campaña rodeada de incertidumbre, pero que conseguimos sacar adelante con esfuerzo y dedicación. Fue una campaña intensa en muchos sentidos, pero que me ha dejado grandes recuerdos. Albert, gran compañero de camarote. Claudia, Marta y Paulo, compañeras del club de cine aquellas noches que pasamos viendo "La Veneno". Toño, también conocido como Dj Gominola, y su gran selección de música. También Andrea, Massimo, Dani, Natalia, Sílvia, María y Begoña. A todos vosotros, muchas gracias. Y para quien lea esto, creo que deberíamos repetir el viajecito por la Patagonia. Escrito queda.

Más tarde vino PANTOC, cuando ya pensaba que no había tiempo para más. Conocí al que sería mi compañero de camarote recurrente, Juan. ¡Y gran rival al backgammon! Y también a todas aquellas personas que dan vida a la base antártica y que hacen que aquel pequeño rincón en la isla Livingston sea lo más parecido que he visto al paraíso en la Tierra. Gracias en especial a Joan, por todo el apoyo que nos diste. Gracias también a todo el resto de miembros de la BAE, fue un placer compartir comidas y caminatas con vosotros. No sé qué echo más de menos, si el walkie-talkie o las subidas al monte Sofía...

Para cerrar con las campañas, me gustaría agradecer la gran labor que llevan a cabo todas las personas que hacen que nuestro trabajo sea posible. La tripulación del Sarmiento, del Hespérides, equipo de las BAEs, ... gracias a todos porque sin vosotros nada de esto sería posible.

I would especially like to thank Daniel, probably the most unexpected and enriching person I have had the good fortune to meet. Before meeting you, I saw myself as someone who would never be able to work on anything related to coding. But then you came along, once a year, to share your light with us. I can now say that the command prompt no longer intimidates me. But it wasn't all about science—Pedraforca, Palau de la Música, Montserrat... It has been a pleasure to share those moments and enjoy the wonderful conversations we had together.

I would also like to thank the entire team at the Zimmermann lab at EMBL, especially Michael, who made it possible for me to spend some time with them. The circumstances didn't turn out to be the best for me, but even so, it was a wonderful experience where I shared many great moments with all of you.

Oierri ere eskerrak eman nahi nizkioke. Nire ibilbide zientifikoa zurekin hasi zen duela urte batzuk, eta oraingoz harrotasunez esan dezaket honaino ekarri nauela. Askotan gogoratu zaitut urte hauetan zehar, eta tesi honen zati txiki bat dagokizu. Mila esker ibilbide honen lehen urratsetan nire ondoan egoteagatik eta irakatsi zenizkidan ikasgai guztiengatik.

También me gustaría dedicar este trabajo a todas esas personas que me llevan acompañando (y aguantando mis quejas) prácticamente toda la vida. A mi cuadrilla, Pablo, Haritz, Mendi, Belzu, Ibarra y Etxarri. Pese a la distancia y a que todo lo que digo suene a chino, siempre me habéis apoyado y animado, y os he tenido muy presentes en todo este proceso. A Ane, gracias por todas las visitas, por todas las charlas, por todos esos momentos que has compartido conmigo y en los que siempre consigues animarme. A Alaitz y Maider, por estar siempre dispuestas a dar un paseo, charlar de la vida, por más que pasen los años. Qué mejor regalo que saber que voy a poder seguir contando con vuestro apoyo en esta nueva etapa.

Otros nombres me vienen a la mente, a los que también me gustaría por lo menos mencionar. Marta, Aina y Tamara, mis valencianas de referencia; Jon, Yuri, Maria, Silvia, Aitor, Simon; los compañeros perfectos para ir al monte y pasarlo en grande; Fernando, gran mentor y mejor persona, ... gracias a todos por haberme ayudado a desconectar cuando más lo necesitaba.

Gracias a Elisabet, porque, aunque me costó tomar la decisión, acudir a ti fue un gran acierto, el cual me ha permitido llegar hasta este momento.

Por supuesto, dar las gracias a mi familia, a mis primas, a mis tíos, a mi abuela (a la que espero poder decirle que por fin he aprobado el doctorado). Pero sobre todo a mi ama y a mi aita. Me habéis dado los medios, me habéis apoyado en todas las decisiones que he tomado y habéis ayudado en todo lo que estaba en vuestras manos. No os ha importado hacer los kilómetros que hiciera falta para venir a visitarme. Gracias, porque si he llegado hasta aquí y a ser la persona que soy hoy en día, es por vosotros.

Por último, gracias a Saioa. Compañera de vida. Hace tiempo decidimos recorrer nuestros caminos juntos, a pesar de la distancia, a pesar del tiempo. Porque si algo tenemos claro es que dentro de toda la incertidumbre que rodea nuestras profesiones, la vida es un poco mejor cuando estamos juntos. Tú más que nadie sabes todo lo que he vivido para llegar hasta aquí, lo has sufrido y, por si fuera poco, has luchado incansablemente para sacarme una sonrisa en cualquier circunstancia. Te estaré eternamente agradecido. Ahora se abre una nueva etapa. Nuevas decisiones que tomar. Que venga lo que tenga que venir, porque sabiendo que te tengo a mi lado estoy tranquilo.

Mila esker denoi!

